



U.S. Department
of Transportation
**National Highway
Traffic Safety
Administration**



DOT HS 813 431

July 2023

Vehicle Simulation Process to Support the Analysis for MY 2027 and Beyond CAFE and MY 2030 and Beyond HDPUV FE Standards

DISCLAIMER

This publication is distributed by the U.S. Department of Transportation, National Highway Traffic Safety Administration, in the interest of information exchange. The opinions, findings, and conclusions expressed in this publication are those of the authors and not necessarily those of the Department of Transportation or the National Highway Traffic Safety Administration. The United States Government assumes no liability for its contents or use thereof. If trade or manufacturers' names or products are mentioned, it is because they are considered essential to the object of the publication and should not be construed as an endorsement. The United States Government does not endorse products or manufacturers.

Suggested APA Format Citation:

Islam, E. S., Kim, N., Vijayagopal, R., & Rousseau, A. (2023, July) *Vehicle simulation process to support the analysis for MY 2027 and beyond CAFE and MY 2030 and beyond HDPUV FE standards* (Report No. DOT HS 813 431). National Highway Traffic Safety Administration.

Technical Report Documentation Page

1. Report No. DOT HS 813 431	2. Government Accession No.	3. Recipient's Catalog No.	
4. Title and Subtitle Vehicle Simulation Process to Support the Analysis for MY 2027 and Beyond CAFE and MY 2030 and Beyond HDPUV FE Standards		5. Report Date July 2023	
		6. Performing Organization Code	
7. Authors Ehsan Sabri Islam, Namdoo Kim, Ram Vijayagopal, Aymeric Rousseau Transportation and Power Systems Division, Argonne National Laboratory		8. Performing Organization Report No. ANL/TAPS-23/2 DE-AC02-06CH11357	
9. Performing Organization Name and Address Argonne National Laboratory 9700 South Cass Avenue Lemont, IL, 60439		10. Work Unit No. (TRAIS)	
		11. Contract or Grant No.	
12. Sponsoring Agency Name and Address National Highway Traffic Safety Administration 1200 New Jersey Avenue SE Washington, DC 20590		13. Type of Report and Period Covered	
		14. Sponsoring Agency Code	
15. Supplementary Notes			
16. Abstract Congress passed the Energy Policy and Conservation Act in 1975 to require standards for Corporate Average Fuel Economy and told the U.S. Department of Transportation (and NHTSA by delegation) to establish and enforce these standards. In 2007 Congress gave NHTSA additional authority to set standards for medium- and heavy-duty vehicles in the Energy Independence and Security Act. NHTSA currently (and for the last several years) has analyzed the effects of different levels of CAFE, and now heavy-duty pickup truck and van fuel efficiency standards, using the CAFE model. The Volpe Center helps NHTSA develop engineering and economic inputs to the CAFE model by analyzing the application of potential technologies to the current automotive industry vehicle fleet to determine the feasibility of future standards, the associated costs, and the benefits of the standards. This typically involves accounting for more than 1,000 distinct vehicle models and variants, many more than can be examined in a practical way using full vehicle simulation or other techniques mentioned above. Instead, the model estimates effectiveness of specific technologies for a representative vehicle in each vehicle class and arranges technologies in decision trees defining logical progressions from lower to higher levels of cost, complexity, development requirements, or implementation challenges. Full vehicle simulation tools use physics-based mathematical equations, engineering characteristics (e.g., engine maps, transmission shift points, and hybrid vehicle control strategies), and explicit drive cycles to predict the effectiveness of individual fuel-saving technologies as well as their combinations. Argonne National Laboratory developed a full vehicle simulation tool called Autonomie, which has become one of the industry's standard tools for analyzing vehicle performance, energy consumption, and technology effectiveness. This report describes the process Argonne used to conduct full vehicle simulation for the MY 2027 and beyond CAFE and MY 2030 and beyond HDPUV FE notice of proposed rulemaking.			
17. Key Words CAFE, Corporate Average Fuel Economy, Autonomie, MY 2027–2032 CAFE, notice of proposed rulemaking		18. Distribution Statement Document is available to the public from the DOT, BTS, National Transportation Library, Repository & Open Science Access Portal, https://rosap.ntl.bts.gov .	
19 Security Classif. (of this report) Unclassified	20. Security Classif. (of this page) Unclassified	21 No. of Pages 323	22. Price

Form DOT F 1700.7 (8-72)

Reproduction of completed page authorized

Table of Contents

List of Figures	vii
List of Tables	xiv
Introduction	1
Project Statement	3
Autonomie Simulation Process	6
Autonomie	7
Overview	7
Structure	8
Engine Model.....	11
Model Description	11
Engine Technologies Evaluated	16
Friction Reduction	16
Turbocharged Engines	16
Cylinder Deactivation and Advanced Cylinder Deactivation	17
Engine Cylinder Deactivation Methodology	17
Fuel Cutoff.....	19
Transmission Model.....	20
Automatic Transmission.....	20
Manual Transmission	24
Continuously Variable Transmission	27
Dual-Clutch Transmission.....	30
Transmission Shifting.....	36
Engine Start Control for Pre-Transmission HEVs	45
Torque Converter	46
Plant Model	47
Operational Modes	47
Steady-State Calculation	48
Transient Calculation.....	48
Idle Calculation	49
Energy Storage Model	49
High-Power Battery Model (Used for HEVs)	51
High Energy Battery Model (Used for PHEVs and BEVs)	53
Electric Machine Models	54
Electrical Accessories Model.....	57
Driver Model.....	58
Wheel Model.....	59
Chassis Model.....	62
Final Drive Model.....	65
Vehicle-Level Control Algorithms	67
Micro- and Mild HEV	67
Power-Split HEV	67
Single-Mode Power-Split PHEV	68

Engine-ON Condition.....	68
SOC Control in CS Mode.....	69
Engine Operation.....	70
Multi-Mode E-REV (E-REV PHEV50).....	71
Parallel HEV.....	73
Engine Operation.....	73
Fuel Cell HEV.....	74
High-Level Overview of Autonomie Controllers.....	75
Supervisory Controller.....	75
Component Controllers.....	77
The Demand Block—dmd.....	78
The Transient Block—trs.....	79
The Constraint Block—cstr.....	79
The Command Block—cmd.....	80
Low-Level Controller Summary for Engine and Transmission Models.....	80
Autonomie Validation.....	88
Conventional Vehicles.....	88
Power-Split HEV.....	91
Pre-Transmission HEV.....	92
Range-Extender PHEV.....	93
Battery Performance and Cost Model.....	94
Process.....	94
Cathode/Anode Combination Selection.....	94
Vehicle Pack Specifications Selection.....	95
BatPaC Examples From Existing Vehicles in the Market.....	96
Full HEV.....	96
PHEVs.....	98
EVs.....	100
Use of BatPaC in Autonomie.....	101
Setting Assumptions in BatPaC for This Analysis.....	105
Inputs to BatPaC From Autonomie.....	108
Outputs From BatPaC Into Autonomie.....	108
BatPaC Lookup Tables.....	109
Micro HEV for Micro-HEVs.....	109
Mild Hybrid BISG.....	110
Full Hybrid HEV.....	112
PHEV 20 AER (Power-Split/Parallel).....	116
PHEV50 AER (Voltec Extended Range Electric Vehicle [EREV]/Parallel).....	119
BEV 150/200/250 AER.....	122
BEV300 AER.....	127
BEV400 AER.....	132
Vehicle and Component Assumptions.....	137
Light-Duty Vehicle Specifications.....	137
HDPUV Specifications.....	137

Vehicle-Level Attributes Selection.....	139
Light-Duty Vehicles	139
HDPUVs.....	142
Vehicle Component Weight Selection.....	144
Light-Duty Vehicles	144
Heavy-Duty Pickups and Vans.....	154
Transmission Assumptions	156
Transmission Technology Definitions	156
Transmission Attributes.....	159
Transmission Weights	164
Transmission Performance Data.....	167
Transmission Gear-Shifting Maps.....	173
Torque Converter Assumptions	176
Engine Technologies.....	177
Light-Duty Vehicles	177
Heavy-Duty Pickups and Vans.....	205
Electric Machines.....	213
Electric Machine Efficiency Maps	214
Electric Machine Peak Efficiency Scaling	215
Fuel Cell System.....	216
Energy Storage System.....	217
Accessory Loads (LDV)	217
Lightweighting Technologies	218
Light-Duty Vehicles	218
Heavy-Duty Pickups and Vans.....	218
Aerodynamic Drag Reduction Technologies.....	218
Rolling Resistance Reduction Technologies	219
Test Procedure and Energy Consumption Calculations.....	220
Conventional Vehicles	220
Hybrid EVs	221
Fuel Consumption	222
Combined Fuel Consumption.....	223
Plug-in HEVs.....	223
Charge Sustaining on the UDDS Cycle.....	223
Charge Sustaining on the HWFET Cycle.....	224
Charge Depleting on the UDDS and HWFET Cycles.....	224
Battery Electric Vehicles	226
Cold-Start Penalty.....	227
Vehicle Simulation Setup Process.....	230
Powertrain Template (LDV).....	230
Vehicle Tab	230
Parameter Tab.....	231
Control Tab.....	232
Sizing Tab.....	233

Run Tab	234
Translation Tab.....	235
Vehicle Assumption Template (HDPUV)	235
Baseline Specs Tab.....	236
Sizing Tab.....	236
Engine Tab.....	236
Reference Vehicles Tab.....	237
Translation Tab.....	238
Multi-Vehicle Template Expansion and Duplication	238
Vehicle Assumptions Definition.....	239
Vehicle Sizing Process.....	241
Inheritance.....	241
Conventional Powertrain (Conventional/Micro-12V/Mild Hybrid BISG)	241
Hybrid Powertrains (Split HEV/Split PHEV/EREV PHEV/Fuel Cell HEV/BEV).....	242
Parallel Hybrid Powertrains	244
Vehicle Technical Specifications.....	246
Light-Duty Vehicles	246
Heavy-Duty Pickups and Vans.....	247
Vehicle Powertrain Sizing Algorithms	248
Light-Duty Vehicles	248
Heavy-Duty Pickups and Vans.....	257
Determining the Relationship Between Engine Displacement and Number of Cylinders (LDV)	262
Distributed Computing Process.....	264
Setup	264
Distributed Computing Flexibility.....	265
Vehicle Simulation Process	266
Data.mat File.....	267
XML Results File.....	268
Simulation Results Analysis and Detailed Validation Processes	269
Engine Operating Points Across Transmissions	269
Light-Duty Vehicle.....	269
Automatic Transmission.....	269
Dual-Clutch Transmissions	273
CVT Transmission.....	274
Heavy-Duty Pickups and Vans.....	274
Powertrain Efficiency Analysis	276
Light-Duty Vehicle.....	276
Heavy-Duty Pickups and Vans.....	282
Total Number of Shifting Events With Different Transmission Types and Numbers of Gears	284
Light-Duty Vehicle.....	284
Automatic Transmission Types	285

Dual-Clutch Transmission Types	287
Heavy-Duty Pickups and Vans	288
Engine Power Inheritance Validation	289
Light-Duty Vehicle	289
Heavy-Duty Pickups and Vans	294
Machine Learning for Outlier Detection	297
Statistical Methods	298
References	299

List of Figures

Figure 1. Technologies considered for the Autonomie light-duty vehicle analysis	4
Figure 2. Technologies considered for the Autonomie heavy-duty pickup and van analysis	5
Figure 3. Simulation management concepts	9
Figure 4. Class diagram of container and terminating systems	9
Figure 5. Top-level vehicle layout	10
Figure 6. Models automatically built	11
Figure 7. Autonomie spark-ignition engine model diagram	12
Figure 8. Engine model Block A: Engine torque calculation	13
Figure 9. Engine model Block B: Thermal model	14
Figure 10. Engine model Block C: Fuel rate model	15
Figure 11. BMEP response of turbo-charged engine to a step command	16
Figure 12. Stateflow diagram for cylinder deactivation regulator	17
Figure 13. Engine plant model with cylinder deactivation	18
Figure 14. Stateflow diagram showing the ability to switch cylinder deactivation fuel maps	18
Figure 15. Engine operating regions for throttled engines (WOT = wide-open throttle)	19
Figure 16. Engine operating region for unthrottled engines	19
Figure 17. Engine fuel cutoff analysis based on test data	20
Figure 18. Autonomie automatic gearbox model I/O	20
Figure 19. Top level of the automatic gearbox model	21
Figure 20. Block A: Speed calculation of the AU	21
Figure 21. Block A1: Speed calculation when the gearbox is not in neutral	22
Figure 22. Block A2: Speed calculation when the gearbox is in neutral	22
Figure 23. Block A2-1: When gearbox not in neutral, with free-wheeling input shaft losses	23
Figure 24. Block B: Output torque calculation	23
Figure 25. Block C: Output inertia calculation	24
Figure 26. Autonomie DM model I/O	24
Figure 27. Top level of the manual gearbox model	25
Figure 28. Block A: Gearbox input shaft speed calculation	25
Figure 29. Block A1: Torque loss calculation when the gearbox is in neutral	26
Figure 30. Block B: Speed calculation when the gearbox is in neutral	26
Figure 31. Block C: Output inertia calculation	27
Figure 32. Hydraulic pump loss and mechanical loss for metal V-belt CVT	28
Figure 33. F _p F _s ratio map (CVT)	29
Figure 34. CVT system block diagram	30
Figure 35. Stick diagram of a DCT	30
Figure 36. DCT operating conditions	31
Figure 37. Pre-selection mode bond graph	32
Figure 38. Gearbox plant model for DCT	32
Figure 39. Model and governing equations for clutch	33
Figure 40. Gearbox plant model for DCT	33
Figure 41. DCT controller	34
Figure 42. State diagram representation of the control strategy for a DCT	35
Figure 43. Clutch controller for DCT	35
Figure 44. Engine operating points for 2017 Ford F150 (UDDS)	37

Figure 45. Example of engine operating conditions for 5-speed and 10-speed transmissions on UDDS cycle for NA engine	38
Figure 46. Upshifting gear map (left) and upshifting vehicle speeds (right).....	38
Figure 47. Example of engine speed range in economical driving and economical shift	39
Figure 48. Maximum engine torque at wheels and performance upshift speeds.....	40
Figure 49. Design of upshifting and downshifting speed curves for two adjacent gears	41
Figure 50. Shifting controller schematic in Autonomie.....	41
Figure 51. Shifting calculations in Autonomie.....	43
Figure 52. Shift process for AU.....	43
Figure 53. Torque hole in Autonomie during shifting event	44
Figure 54. Engine start transient control using electric machine.....	45
Figure 55. Typical torque converter efficiency.....	46
Figure 56. Torque converter lockup control algorithm.....	47
Figure 57. Autonomie torque converter model I/O	47
Figure 58. Steady-state mode calculation	48
Figure 59. Transient mode calculation.....	48
Figure 60. Idle mode calculation	49
Figure 61. Initialization parameters	49
Figure 62. Autonomie energy storage model I/O	50
Figure 63. High-power battery model diagram in Autonomie	51
Figure 64. Block A: High-power battery model output voltage calculation.....	52
Figure 65. Block B: High-power battery model current calculation	53
Figure 66. Block C: High-power energy model SOC calculation	53
Figure 67. High-energy battery model diagram in Autonomie.....	54
Figure 68. Autonomie electric machine model I/O	54
Figure 69. Autonomie electric machine model in Simulink.....	55
Figure 70. Block A: Electric machine model max torque calculation.....	56
Figure 71. Block A1: Heat index	57
Figure 72. Autonomie electrical accessories model I/O	57
Figure 73. Top-level Simulink diagram of electrical accessories model.....	58
Figure 74. Autonomie driver model.....	58
Figure 75. Top-level Simulink diagram of the look-ahead driver model	59
Figure 76. Equations for the look-ahead driver model	59
Figure 77. Autonomie wheel model I/O	59
Figure 78. Autonomie wheel model Simulink diagram.....	60
Figure 79. Block B: Force calculation	61
Figure 80. Block C: Mass calculation.....	62
Figure 81. Autonomie chassis model I/O	62
Figure 82. Simulink diagram of chassis model in Autonomie.....	63
Figure 83. Block A: Chassis losses.....	64
Figure 84. Autonomie final drive model I/O	65
Figure 85. Simulink diagram of the final drive model in Autonomie	65
Figure 86. Block A: Final drive model speed calculation	66
Figure 87. Block B: Torque calculation.....	66
Figure 88. Block C: Inertia calculation.....	67
Figure 89. Power-split HEV	68

Figure 90. Engine-ON condition—2017 Prius Prime example based on 25 test cycles	69
Figure 91. SOC regulation algorithm—2017 Prius Prime example based on 25 test cycles.....	70
Figure 92. Example of engine operating target—2017 Prius Prime example based on 25 test cycles.....	70
Figure 93. Configuration of the Chevrolet Volt 2016 powertrain system	71
Figure 94. Summary of control analysis for the second-generation Voltec system	72
Figure 95. Wheel torque versus vehicle speed of 2013 VW Jetta HEV	74
Figure 96. Component operating conditions of a fuel-cell vehicle on the urban European drive cycle using dynamic programming.....	75
Figure 97. Autonomie supervisory controller.....	76
Figure 98. Autonomie nested-level controllers.....	76
Figure 99. Autonomie component model layout	77
Figure 100. Battery controller composed of a single control model.....	77
Figure 101. Engine controller composed of four sub-models.....	78
Figure 102. Demand block.....	78
Figure 103. Transient block	79
Figure 104. Constraint block.....	79
Figure 105. Command block.....	80
Figure 106. Low-level control for engine	81
Figure 107. Low-level control for transmission	82
Figure 108. Simulation and testing results on UDDS cycle (0–505 s) for 2013 Hyundai Sonata conventional 6ATX.....	89
Figure 109. Shifting algorithm validation for 2013 Hyundai Sonata conventional 6ATX (left) and 2013 Chrysler 300 8ATX (right) on the UDDS cycle (0-505 s).....	89
Figure 110. Shifting algorithm validation for 2012 Ford Fusion conventional 6ATX (left) and 2013 Chrysler 300 8ATX (right) on the NEDC cycle	90
Figure 111. Comparison of simulation and test data for 2012 Honda Civic CVT HEV on UDDS (left) and HWFET (right) cycles.....	90
Figure 112. Results of simulation and testing on UDDS cycle for 2010 Toyota Prius HEV.....	91
Figure 113. Results of simulation and testing on UDDS cycle for 2013 Jetta DCT hybrid.....	92
Figure 114. Results of simulation and testing on UDDS cycle for 2012 Chevrolet Volt PHEV .	93
Figure 115. BatPaC cathode/anode pair selection	94
Figure 116. BatPaC Battery Design tab.....	95
Figure 117. BatPaC Fast Charging tab	95
Figure 118. Setting vehicle type	105
Figure 119. Cell chemistry for BEV200	106
Figure 120. Battery design information.....	107
Figure 121. Setting maximum thickness.....	107
Figure 122. Battery systems manufactured per year.....	108
Figure 123. Autonomie inputs to BatPaC	108
Figure 124. BatPaC Outputs to Autonomie	109
Figure 125. Overview of the performance parameters	139
Figure 126. Distribution of drag coefficient values of compact (base) vehicle class	139
Figure 127. Average frontal area for the vehicle models that account for about 50 percent of sales in the market.....	142
Figure 128. Body weight selection for compact (base) vehicles	144

Figure 129. Chassis weight selection for compact (base) vehicles.....	145
Figure 130. Interior weight selection for compact (base) vehicles.....	146
Figure 131. Safety system weight selection for compact (base) vehicle	147
Figure 132. Thermal system weight selection for compact (base) vehicle.....	148
Figure 133. Brake mechanism weight selection for compact (base) vehicle.....	149
Figure 134. Steering system weight selection for compact (base) vehicle	150
Figure 135. Electrical accessories weight selection for compact (base) vehicle	151
Figure 136. Engine weight (kg) versus engine power (kW) of gasoline engines across different aspiration methods	152
Figure 137. Engine weight (kg) versus engine power (kW) of diesel engines.....	153
Figure 138. Electric machine weight versus peak power output	154
Figure 139. Average curb weight for the vehicle models that account for about 50 percent of sales in the market.....	155
Figure 140. Engine weight (kg) versus engine peak torque (Nm) of diesel engines	156
Figure 141. Efficiency for direct drive, for the range of temperatures and speeds considered ..	158
Figure 142. Vehicle attribute analysis for gear span of 6AU (Source: Argonne Vehicle Database).....	159
Figure 143. Vehicle attribute analysis for final drive ratio of 6AU (Source: Argonne Vehicle Database).....	160
Figure 144. Final drive weight selection for 6AU	164
Figure 145. Gearbox weight selection for 6AU for midsize vehicles.....	165
Figure 146. Transmission weight (kg) versus gearbox peak torque (Nm) of automatic transmission	167
Figure 147. Automatic (AU/AU+/AU++) transmission efficiency maps for different numbers of gears.....	169
Figure 148. DCT efficiency maps for different numbers of gears.....	170
Figure 149. CVT oil pump and mechanical efficiency maps	171
Figure 150. CVT+ oil pump and mechanical efficiency maps	172
Figure 151. Maps of transmission upshifting (solid lines) and downshifting (dotted lines)	175
Figure 152. Maps of transmission upshifting (solid lines) and downshifting (dotted lines)	176
Figure 153. Autonomie torque converter characteristic map (LDV).....	176
Figure 154. Autonomie torque converter characteristic map (HDPUV)	177
Figure 155. Engine 1 BSFC map	180
Figure 156. Engine 2 BSFC map	181
Figure 157. Engine 3 BSFC map	181
Figure 158. Engine 4 BSFC map	182
Figure 159. Engine 5b BSFC map	183
Figure 160. Engine 6a BSFC map	183
Figure 161. Engine 7a BSFC map	184
Figure 162. Engine 8a BSFC map	184
Figure 163. Engine 12 BSFC map	185
Figure 164. Engine 13 BSFC map	186
Figure 165. Engine 14 BSFC map	187
Figure 166. Engine 18 BSFC map	187
Figure 167. Engine 19 BSFC map	188
Figure 168. Engine 20 BSFC map	189

Figure 169. Engine 21 BSFC map	189
Figure 170. Engine 23b BSFC map	190
Figure 171. Engine 23c BSFC map	191
Figure 172. Engine 26 BSFC map	191
Figure 173. Engine 26a BSFC map	192
Figure 174. Engine 32 BSFC map	192
Figure 175. Engine 33 BSFC Map.....	193
Figure 176. Engine 34 BSFC map	193
Figure 177. Engine 36 BSFC map	194
Figure 178. Engine 37 BSFC map	194
Figure 179. Engine 38 BSFC map	195
Figure 180. Engine 39 BSFC maps.....	195
Figure 181. Engine 40 BSFC map	196
Figure 182. Engine 45 BSFC map	196
Figure 183. Engine 46 BSFC map	197
Figure 184. Incremental BSFC and efficiency differences among engines.....	203
Figure 185. Engine 4a BSFC map	207
Figure 186. Engine 4b BSFC map	207
Figure 187. Engine 4c BSFC map	208
Figure 188. Engine 4d BSFC map	209
Figure 189. Engine 3a BSFC map	209
Figure 190. Engine 3c BSFC map	210
Figure 191. Engine 1a BSFC map	211
Figure 192. Engine 1c BSFC map	211
Figure 193. Incremental BSFC and efficiency differences among engines.....	213
Figure 194. Electric machines efficiency maps for different powertrains.....	215
Figure 195. Fuel cell efficiency versus power	216
Figure 196. Urban cycle for a non-hybrid vehicle	220
Figure 197. Highway cycle for a non-hybrid vehicle	221
Figure 198. Urban cycle for a hybrid vehicle	221
Figure 199. Highway cycle for a hybrid vehicle (only the results from the second cycle were used).....	222
Figure 200. Multi-cycle test.....	227
Figure 201. Cold-start penalty on Bag 1 across different engine types	228
Figure 202. Cold-start penalty on Bag 2 across engine types.....	228
Figure 203. Vehicle tab of conventional template	230
Figure 204. Parameter tab of conventional template	231
Figure 205. Control tab of hybrid template	232
Figure 206. Sizing tab of hybrid template	233
Figure 207. Run tab of hybrid template	234
Figure 208. Translation tab of template.....	235
Figure 209. Baseline specs tab of assumption template	236
Figure 210. Sizing tab of assumption template.....	236
Figure 211. Engine tab of assumption template.....	237
Figure 212. Reference Vehicle tab of assumption template	237
Figure 213. Translation tab of assumption template.....	238

Figure 214. Multiple vehicle template files	239
Figure 215. Main vehicle assumption inputs	240
Figure 216. Conventional powertrain inheritance flowchart for eng01	241
Figure 217. Inheritance algorithm for conventional vehicle.....	242
Figure 218. Hybrid powertrain vehicle inheritance flowchart.....	242
Figure 219. Inheritance algorithm for BEVs	243
Figure 220. Inheritance algorithm for fuel cell HEVs	243
Figure 221. Inheritance algorithm for EREVs.....	243
Figure 222. Inheritance algorithm for split PHEVs.....	244
Figure 223. Inheritance algorithm for split HEVs	244
Figure 224. Parallel HEVs: Inheritance from reference baseline vehicles	244
Figure 225. Inheritance algorithm for parallel HEVs	245
Figure 226. Parallel PHEVs: Inheritance from reference baseline vehicles	245
Figure 227. Inheritance algorithm for parallel PHEVs.....	245
Figure 228. Curb weight versus GVWR.....	247
Figure 229. Conventional powertrain sizing algorithm	249
Figure 230. Split hybrid electric powertrain sizing algorithm.....	250
Figure 231. Parallel hybrid electric powertrain sizing algorithm	251
Figure 232. Parallel plug-in hybrid (Par PHEV20) EV powertrain sizing	252
Figure 233. Parallel plug-in hybrid (Par PHEV50) EV powertrain sizing	252
Figure 234. Split PHEV sizing algorithm	253
Figure 235. Voltec PHEV vehicle sizing algorithm	254
Figure 236. BEV sizing algorithm.....	255
Figure 237. Fuel cell series HEV sizing algorithm.....	256
Figure 238. Conventional powertrain sizing algorithm	257
Figure 239. Parallel hybrid electric powertrain sizing algorithm	258
Figure 240. Parallel plug-in hybrid electric powertrain sizing algorithm.....	259
Figure 241. Parallel plug-in hybrid electric powertrain sizing algorithm.....	260
Figure 242. BEV sizing algorithm.....	261
Figure 243. Relationship between engine displacement and number of engine cylinders	262
Figure 244. Method for computing engine displacement and number of cylinders	263
Figure 245. Distributed computing process	264
Figure 246. Vehicle simulation folder organization	266
Figure 247. Sample Autonomie result (data.mat).....	267
Figure 248. XML Autonomie results file (simulation.a_result)	268
Figure 249. Engine operating points for automatic transmissions.....	272
Figure 250. Engine operating points for 6- and 8-speed DCT transmissions.....	273
Figure 251. Engine operating points for CVTs.....	274
Figure 252. Engine operating points for automatic transmissions.....	276
Figure 253. Powertrain efficiency values of different engine types with automatic transmissions and different numbers of gears.....	277
Figure 254. Powertrain efficiency values of different engine types with AU+ transmissions with different numbers of gears	278
Figure 255. Powertrain efficiency values of different engine types with AU++ transmissions with different numbers of gears	279

Figure 256. Powertrain efficiency values of different engine types with DCTs with different numbers of gears	280
Figure 257. Powertrain efficiency values of different engine types with CVT	281
Figure 258. Powertrain efficiency values of different engine types with CVT+.....	282
Figure 259. Powertrain efficiency values of different engine types with automatic transmissions and different numbers of gears.....	283
Figure 260. Powertrain efficiency values of different engine types with AU+ transmissions and different numbers of gears.....	284
Figure 261. Total number of shifting events for AU/AU+/AU++ transmissions during UDDS cycle	285
Figure 262. Total number of shifting events for AU/AU+/AU++ transmissions during US06 cycle.....	286
Figure 263. Total number of shifting events for DCTs during UDDS cycle.....	287
Figure 264. Total number of shifting events for DCTs during US06 cycle	288
Figure 265. Total number of shifting events for AU/AU+ transmission during UDDS cycle ...	289
Figure 266. Engine power versus MR step (compact, non-performance)	289
Figure 267. Engine power versus MR step (compact, performance)	290
Figure 268. Engine power versus MR step (midsize, non-performance)	290
Figure 269. Engine power versus MR step (midsize, performance).....	291
Figure 270. Engine power versus MR step (small SUV, non-performance)	291
Figure 271. Engine power versus MR step (small SUV, performance)	292
Figure 272. Engine power versus MR step (midsize SUV, non-performance)	292
Figure 273. Engine power versus MR step (midsize SUV, performance).....	293
Figure 274. Engine power versus MR step (pickup, non-performance).....	293
Figure 275. Engine power versus MR step (pickup, performance)	294
Figure 276. Engine power versus powertrain type (HDV Class 2b van).....	294
Figure 277. Engine power versus powertrain type (HDPU Class 2b pickup)	295
Figure 278. Engine power versus powertrain type (HDV Class 3 van).....	296
Figure 279. Engine power versus powertrain type (HDPU Class 3 pickup)	296
Figure 280. Confidence interval bands of simulation results	297
Figure 281. RANSAC validation method.....	298
Figure 282. QQ plot to confirm the normal distribution of results	298

List of Tables

Table 1. Engine lugging limits for different transmissions (NA engines).....	36
Table 2. Engine lugging limits for different transmissions (turbo engines).....	37
Table 3. Detailed gear-shifting events for Ford F-150.	44
Table 4. Argonne simulated gear-shifting events for 10-speed transmission.....	45
Table 5. Engine control—low-level demand models	83
Table 6. Engine control—low-level constraint models	83
Table 7. Engine control—low-level transient models	84
Table 8. BatPaC input details for BatPaC 4.0 October 1, 2020.....	94
Table 9. BatPaC output performance metric.....	96
Table 10. HEV battery pack details	97
Table 11. BatPaC HEV prediction.....	98
Table 12. PHEV battery pack details.....	99
Table 13. BatPaC PHEV predictions	99
Table 14. Battery pack details for EVs	100
Table 15. BatPaC EVs prediction	101
Table 16. BatPaC assumptions for mild hybrid BISG.....	102
Table 17. BatPaC assumptions for full HEVs	102
Table 18. BatPaC assumptions for PHEV20 AER	103
Table 19. BatPaC assumptions for PHEV50 AER	103
Table 20. BatPaC assumptions for BEV 150/200/250 AERs.....	104
Table 21. BatPaC assumptions for BEV300 AERs	104
Table 22. BatPaC assumptions for BE4300 AERs	105
Table 23. Battery cost table for micro-HEVs	109
Table 24. Mass assumptions for micro-HEVs	110
Table 25. BatPaC lookup table for mild hybrid BISG.....	111
Table 26. BatPaC lookup table for full hybrids (compact/midsize).....	112
Table 27. BatPaC lookup table for full hybrids (SUVs/pickups/HDPUVs).....	114
Table 28. BatPaC lookup table for PHEV20 AERs (compact/midsize).....	116
Table 29. BatPaC lookup table for PHEV20 AERs (SUVs/pickups/HDPUVs)	117
Table 30. BatPaC lookup table for PHEV50 AERs (compact/midsize).....	119
Table 31. BatPaC lookup table for PHEV50 AERs (SUVs/pickups/HDPUVs)	121
Table 32. BatPaC lookup table for BEV200-250 AERs (compact/midsize).....	122
Table 33. BatPaC lookup table for BEV150-250 AERs (SUVs/pickup).....	124
Table 34. BatPaC lookup table for BEV300 AERs (compact/midsize)	127
Table 35. BatPaC lookup table for BEV300 AERs (SUVs/pickups/HDPUVs).....	129
Table 36. BatPaC lookup table for BEV400 AERs (compact/midsize)	132
Table 37. BatPaC lookup table for BEV400 AERs (SUVs/pickups)	134
Table 38. Vehicle classification and performance categories.....	137
Table 39. Summary of HD vehicle classes and purposes and their performance requirements	138
Table 40. Drag coefficient ratio summary table	140
Table 41. Frontal Area Summary Table	140
Table 42. Effective tire radius analysis of MY 2020 vehicles.....	141
Table 43. Effective wheel radius used in the FY22 vehicle simulations.....	141
Table 44. Frontal area summary	142

Table 45. Drag coefficient ratio summary	143
Table 46. Effective tire radius summary table	143
Table 47. Body weight summary	144
Table 48. Chassis weight selection summary	145
Table 49. Interior weight selection summary	146
Table 50. Safety system weight selection summary	147
Table 51. Thermal system weight selection summary	148
Table 52. Brake mechanism weight selection summary	149
Table 53. Steering system weight selection summary	150
Table 54. Electrical accessories weight selection summary	151
Table 55. Glider weight selection summary	155
Table 56. Transmission technologies	156
Table 57. Final drive ratios for NA engines	162
Table 58. Final drive ratios for turbocharged engines	162
Table 59. Gear ratios, gear span and final drive ratio selected for different transmissions	163
Table 60. Gear span and final drive ratio selected for different transmissions	163
Table 61. Gear ratios, gear span and final drive ratio selected for different transmissions	164
Table 62. Final drive weight summary for all transmission types	166
Table 63. Gearbox weight summary for all transmission types	166
Table 64. Engine technologies with reference peak power and reference displacement	177
Table 65. Characteristics of Fuel Used for Modeling Engines	180
Table 66. IAV idle fuel rate for all engines	204
Table 67. Engine technologies with reference peak power and reference displacement	205
Table 68. Electric machine efficiency map sources for different powertrain configurations	213
Table 69. Efficiency scaling of electric machines	215
Table 70. Efficiency scaling of electric machines	216
Table 71. Base accessory load assumptions	217
Table 72. Cold-start penalty combinations	229
Table 73. Vehicle class performance times	246
Table 74. Cold-start penalty combinations	247
Table 75. Thresholds for engine displacement versus number of engine cylinders	263

Acronyms and Abbreviations

Argonne	Argonne National Laboratory
AMTL	Advanced Mobility Technology Laboratory
AU	automatic transmission
BEV	battery electric vehicle
BISG	belt-integrated starter generator
BMEP	brake mean effective pressure
BSFC	brake-specific fuel consumption
CAFE	Corporate Average Fuel Economy
CAFE model	CAFE Compliance and Effects Modeling System
CAN	controller area network
CD	charge-depleting
CDA	cylinder deactivation
CS	charge-sustaining
CVT	continuously variable transmission
DCT	dual-clutch transmission
DEAC	cylinder deactivation
DI	direct injection
DM	manual transmission
DOHC	dual overhead camshaft valvetrain
EGR	exhaust gas recirculation
EPCA	Energy Policy and Conservation Act
EREV	extended range electric vehicle
EV	electric vehicle
FE	fuel economy
FMEP	friction mean effective pressure
FTP	Federal Test Procedure
GDI	gasoline direct injection
GVW	gross vehicle weight
GVWR	gross vehicle weight rating
HD	heavy-duty
HDPU	heavy-duty pickup
HDPUV	heavy-duty pickup and van
HDV	heavy-duty van
HEV	hybrid electric vehicle
HFTO	DOE Hydrogen and Fuel Cell Technologies Office
HIL	hardware-in-the-loop
HWFET	Highway Fuel Economy Test
ICE	internal combustion engine
IMEP	indicated mean effective pressure
I/O	input/output
LHV	lower heating value
MR	mass reduction
NA	naturally aspirated
NEDC	New European Driving Cycle
NVH	noise, vibration, and harness

PEV	plug-in electrified vehicle
PFI	port fuel injection
PHEV	plug-in hybrid electric vehicle
PMEP	pumping mean effective pressure
QQ	quantile-quantile
RANSAC	random sample consensus algorithm
RCP	rapid-control prototyping
RC	resistor capacitor
SAE	Society of Automotive Engineers changed its formal name to SAE International in 2006
SIL	software-in-the-loop
SOC	state-of-charge
SPP	Strategic Partnership Project
TAR	technical assessment report
UDDS	urban dynamometer driving schedule
VPA	vehicle propulsion architecture
Volpe Center	Volpe National Transportation Systems Center
VVL	variable valve lift
VTs	vehicle technology specifications
VVT	variable valve timing
XML	extensible markup language

Introduction

In 1975 Congress passed the Energy Policy and Conservation Act that required standards for Corporate Average Fuel Economy and charged the U.S. Department of Transportation with the establishment and enforcement of these standards. The Secretary of Transportation delegated these responsibilities to the National Highway Traffic Safety Administration. In 2007 Congress gave NHTSA additional authority to set fuel efficiency standards for medium- and heavy-duty vehicles in the Energy Independence and Security Act. In this notice of proposed rulemaking associated with this analysis, NHTSA is proposing to set CAFE standards for light-duty vehicles and fuel efficiency standards for heavy-duty pickup trucks and vans.

NHTSA contracted the Volpe National Transportation Systems Center to provide analytical support for NHTSA's regulatory and analytical activities related to fuel economy and fuel efficiency standards. In developing the standards NHTSA made use of the CAFE Compliance and Effects Modeling System (CAFE model) developed by the Volpe Center for the 2005–2007 CAFE rulemaking and has been continually updated. NHTSA uses it to evaluate potential CAFE and HDPUV FE stringency levels by applying technologies incrementally to each manufacturer's fleet until the requirements under consideration are met.

The CAFE model relies on technology-related and economic inputs, such as market forecasts, technology cost, and effectiveness estimates. These inputs are categorized by vehicle classification, technology synergies, phase-in rates, cost learning curve adjustments, and technology decision trees. The Volpe Center helps NHTSA develop engineering and economic inputs to the CAFE model by analyzing the application of potential technologies to the current automotive industry vehicle fleet to determine the feasibility of future CAFE and HDPUV FE standards, the associated costs, and the benefits of the standards.

Part of the CAFE model analysis includes estimating improvements that a given manufacturer could achieve by applying additional technologies to specific vehicles. Because CAFE and HDPUV FE standards apply across the manufacturers' entire fleets rather than to individual vehicles, the model considers the entire range of each product line when simulating technology applications. This typically involves accounting for more than 1,000 distinct vehicle models and variants, many more than can be examined in a practical way using full vehicle simulation or other techniques mentioned above. Instead, the model estimates the effectiveness of specific technologies for a representative vehicle in each vehicle class and arranges technologies in decision trees defining logical progressions from lower to higher levels of cost, complexity, development requirements, or implementation challenges.

The CAFE model's decisionmaking algorithm includes evaluating the effectiveness (fuel consumption reduction) of each fuel-saving technology. Although vehicle testing could be used to estimate these factors, vehicle testing spanning many vehicle types and technology combinations could be prohibitively resource-intensive. Another alternative, either as a substitute for or as a complement to vehicle testing, is to make greater use of vehicle simulation. Full vehicle simulation tools use physics-based mathematical equations, engineering characteristics (e.g., engine maps, transmission shift points, and hybrid vehicle control strategies), and explicit drive cycles to predict the effectiveness of individual fuel-saving technologies as well as combinations of fuel-saving technologies.

The U.S. Department of Energy's Argonne National Laboratory developed a full vehicle simulation tool called Autonomie, which has become one of the industry's standard tools for

analyzing vehicle performance, energy consumption, and technology effectiveness. Through an inter-agency agreement, the DOE Argonne Site Office and Argonne were tasked with conducting full vehicle simulation to support NHTSA's current rulemaking. This report describes the process Argonne used to conduct full vehicle simulation for the current CAFE and HDPUV FE notice of proposed rulemaking.

Project Statement

Through an inter-agency agreement, the DOE Argonne Site Office and Argonne will perform full vehicle simulation through the Strategic Partnership Project program to support NHTSA's regulatory and analytic activities related to fuel economy. NHTSA's Office of International Policy, Fuel Economy and Consumer Programs oversees this project, which includes the following tasks.

1. Performing a full suite of full-vehicle simulation of light-duty and heavy-duty vehicles, including a wide variety of technologies and vehicle classes, to generate effectiveness inputs for the CAFE model.
2. Developing a comprehensive database of all full vehicle simulation outputs that could be referenced by the CAFE model.
3. Performing full vehicle simulation to support research for rulemaking related to light-duty vehicles.

The CAFE model currently relies on multiple decision trees to represent the following component technology options.

- Powertrain
- Engine
- Transmission
- Lightweighting
- Aerodynamics
- Rolling resistance

Figure 1 shows the variety of technology combinations adapted to represent current and potential future technologies that are simulated for the rulemaking for light-duty vehicle simulations, and Figure 2 shows the variety of technology combinations adapted to represent the current and potential future technologies that are simulated for the rulemaking for heavy-duty pickups and vans.

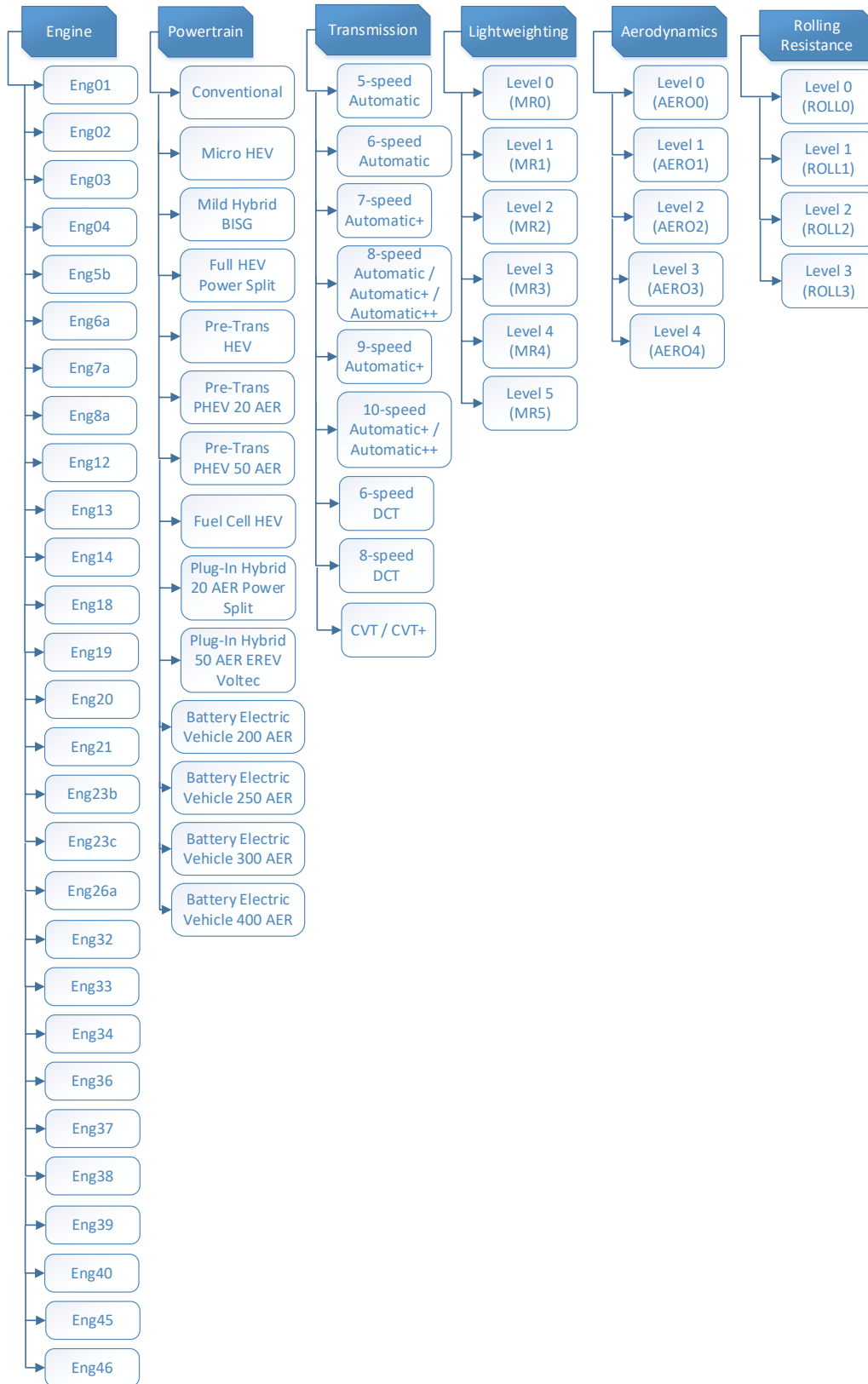


Figure 1. Technologies considered for the Autonomie light-duty vehicle analysis

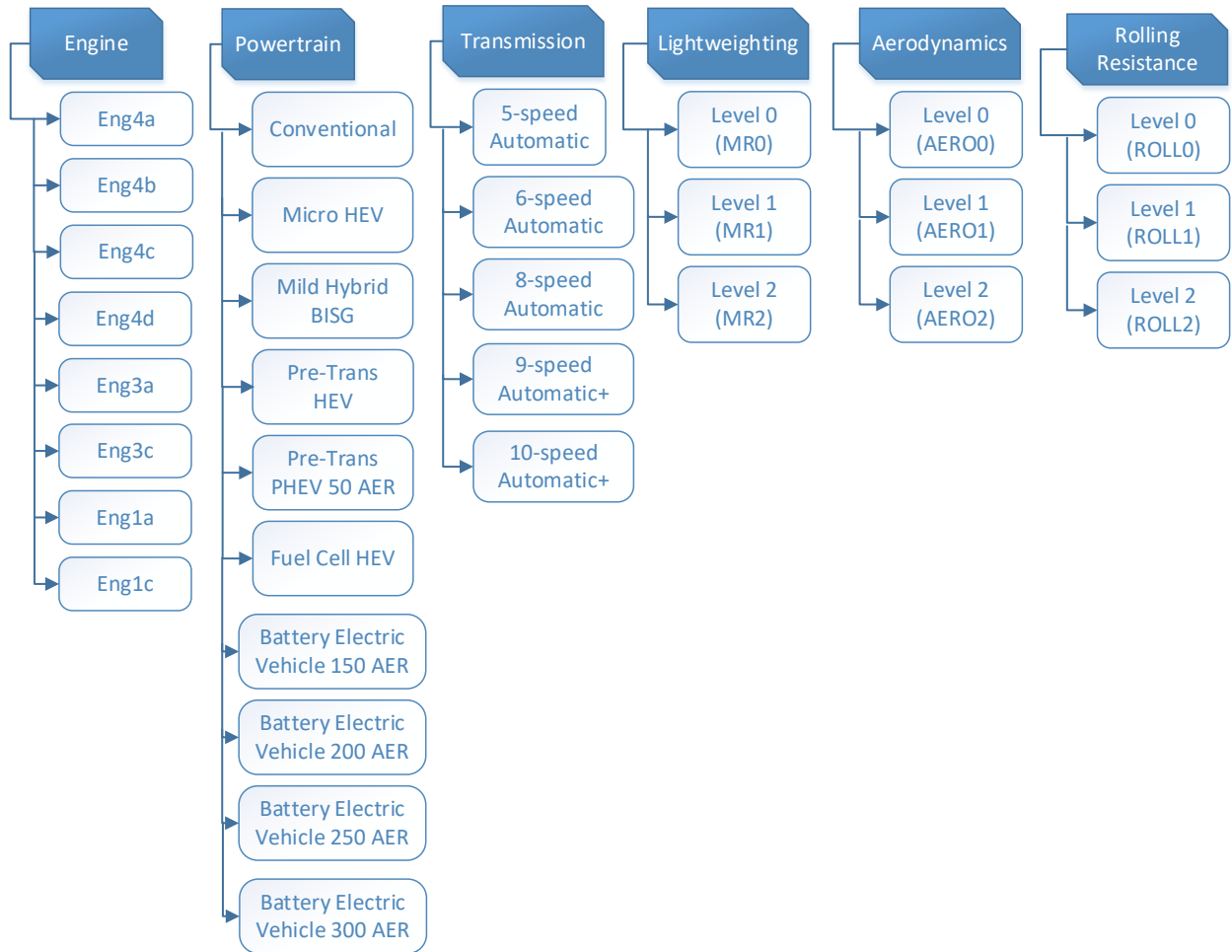


Figure 2. Technologies considered for the Autonomie heavy-duty pickup and van analysis

Autonomie Simulation Process

NHTSA directed the Argonne simulation team to update inputs and processes based on an extensive review of technical publications and meetings with stakeholders. Individual classes and performance categories have been simulated for every combination of vehicle, powertrain, and component technology. The LDV combinations include the following.

- 5 vehicle classes (i.e., compact, midsize, small SUV, midsize SUV, and pickup),
- 2 performance categories for each vehicle class: non-performance (base) and performance (premium)
- 22 engine technologies
- 16 transmission technologies
- 7 lightweighting levels
- 5 aerodynamic drag reduction levels
- 3 rolling resistance reduction levels
- 4 battery electric vehicle (BEV) ranges

The HDPUV combinations:

- 2 vehicle classes: HD gross vehicle weight rating (GVWR) of 8,501 lb to 10,000 lb (HD class 2b) and 10,001 lb to 14,000 lb (HD class 3)
- 2 vehicle purposes for each vehicle class: heavy-duty pickup and heavy-duty van
- 8 engine technologies
- 5 transmission technologies
- 3 lightweighting levels
- 3 aerodynamic drag reduction levels
- 3 rolling resistance reduction levels
- 4 BEV ranges

Along with the increased number of technology combinations, vehicle models were updated. Changes in the process also included technology inheritance (platform-sharing) for engines and transmissions.

The Autonomie simulation process includes the following steps:

1. Specify the vehicle technology specifications.
2. Select component assumptions.
3. Build the vehicle models.
4. Size the reference powertrains to meet the desired performance.
5. Build all the different vehicle combinations, including “inheritance.”
6. Simulate individual vehicles on U.S. standard driving cycles.
7. Perform QA/QC checks on the simulation results.
8. Create the CAFE model database.

Autonomie

Overview

Autonomie is a Mathworks-based software environment and framework for automotive control system design, simulation, and analysis. The tool, sponsored by the DOE Vehicle Technologies Office, is designed for rapid and easy integration of models with varying levels of detail (low to high fidelity), abstraction (from subsystems to systems to entire architectures), and processes (e.g., calibration, and validation). Developed by Argonne in collaboration with General Motors, Autonomie serves as a single tool that can be used to meet the requirements of automotive engineers throughout the development process—from modeling to control. Autonomie was built to do the following.

- Estimate the energy, performance, and cost impact of advanced vehicle and powertrain technologies
- Support proper methods, from model-in-the-loop, software-in-the-loop, and hardware-in-the-loop, to rapid-control prototyping
- Integrate math-based engineering activities through all stages of development—from feasibility studies to production release
- Promote re-use and exchange of models industry-wide through its modeling architecture and framework
- Support users' customization of the entire software package, including system architecture, processes, and post-processing
- Mix and match models with different levels of abstraction to facilitate execution efficiency with higher-fidelity models, for which analysis and high-detail understanding are critical
- Link with commercial off-the-shelf software applications, including GT-POWER, AMESim, and CarSim, for detailed, physically based models
- Protect proprietary models and processes

By building models automatically, Autonomie enables simulation of an unparalleled number of component technologies and powertrain configurations that offer the following capabilities.

- Simulate subsystems, systems, or entire vehicles
- Predict and analyze energy efficiency and performance
- Perform analyses and tests for virtual calibration, verification, and validation of hardware models and algorithms
- Support system hardware and software requirements
- Link to optimization algorithms
- Supply libraries of models for propulsion architectures of conventional powertrains, as well as electric-drive vehicles

In this study, Autonomie is used to assess the energy consumption of advanced powertrain technologies across vehicle classes and configurations. Autonomie has been validated for all powertrain configurations on multiple vehicles currently in the market, using dynamometer test data from Argonne's Advanced Mobility Technology Laboratory, formerly known as Argonne Research Powertrain Facility.

With hundreds of pre-defined powertrain configurations and controllers, Autonomie is a unique tool for analyzing the impact of different technologies (e.g., powertrains, components, controls, etc.) across different vehicle classes. Autonomie allows users to evaluate the impact of component sizing on energy consumption for different technologies, as well as to define the component requirements (e.g., power, and energy) to maximize fuel displacement for a specific application. This is important for the current study because the use of validated plant models, vehicle controls, and complete vehicle models is critical to properly evaluating the benefit of any specific technology. The vehicle-level control algorithms (e.g., engine ON/OFF logic and component operating conditions algorithm) are crucial for properly quantifying technology impact, especially for electric drives. Argonne has been developing shifting algorithms for conventional vehicles based on different component characteristics (e.g., engine fuel flow rate and gear ratios), as well as developing vehicle-level controls for electrified powertrains, for more than 20 years.

The ability to simulate most powertrain configurations, component technologies, and vehicle-level controls over numerous drive cycles has been used to support many studies focusing on energy efficiency, cost-benefit analysis, or greenhouse gases (Lee et al., 2017; Vijayagopal et al., 2013; Jeong et al., 2019; Kim et al., 2015; Kim et al., 2014; Lee et al., 2014; Kim et al., 2013; Kim et al., 2012; Karbowski et al., 2006). More than 250 companies and research entities, including major automotive companies, suppliers, and research organizations, have licensed Autonomie to support advanced vehicle development programs.

Structure

Autonomie was designed for full plug-and-play support. Models in the standard format create building blocks, which are assembled at run time into a simulation model of a vehicle, system, or subsystem. All parts of the user interface are designed to be flexible to support architectures, systems, subsystems, and processes not yet envisioned. The software can be molded to individual uses, so it can grow as requirements increase and technical knowledge expands. This flexibility also allows for implementation of legacy models, including plant and controls.

Autonomie is based on standardized modeling architecture, on-demand model building, associated extensible markup language definition files, and user interfaces for managing models, including a file-versioning database, as seen in Figure 3.

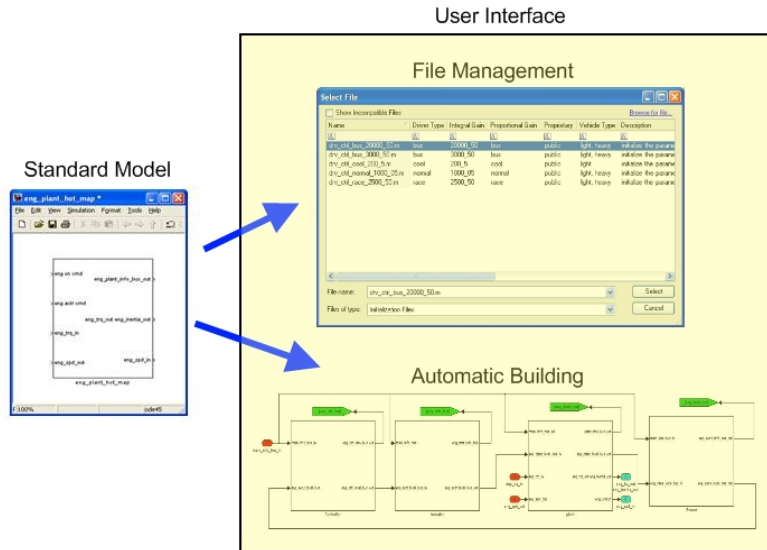


Figure 3. Simulation management concepts

All systems in the vehicle architecture can be logically categorized as either “containing systems” or “terminating systems” (Figure 4). Containing systems consist of one or more subsystems, as well as optional files to define that system. They do not contain models; they only describe the structure of the interconnections among systems and subsystems. Terminating systems consist of a model that defines the behavior of the system and any files needed to provide inputs or calculate outputs. Terminating system models contain the equations that describe the mathematical functions of a system or subsystem.

Both types of systems are arranged in a hierarchical fashion to define the vehicle to be simulated. To avoid confusion, it is a best practice to mimic the structure of the hardware as much as possible. For example, low-level component controllers should be grouped with the components that they control, at different levels of the hierarchy (where applicable). Only systems that appear in the vehicle should be represented; in other words, there is no need for unused components or empty controllers. In addition to simplifying the architecture, this philosophy will allow for easy transfer of systems among users and will fully support HIL, SIL, and RCP.

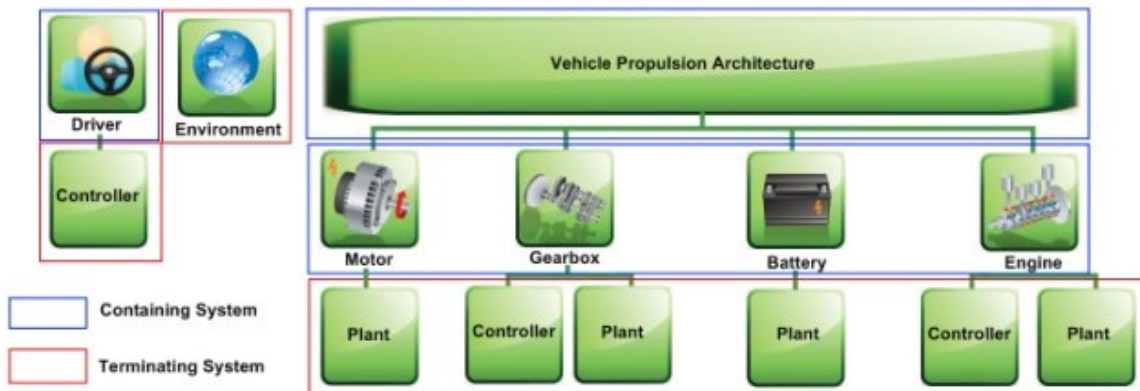


Figure 4. Class diagram of container and terminating systems

At the top level is a vehicle system containing the following systems: environment, driver, vehicle propulsion controller for advanced powertrain vehicles—such as hybrid electric vehicles or plug-in hybrid electric vehicles that require a vehicle level controller—and vehicle propulsion architecture (Figure 5). The VPA system will contain the powertrain components required to simulate the vehicle, such as engine, battery, and wheels.

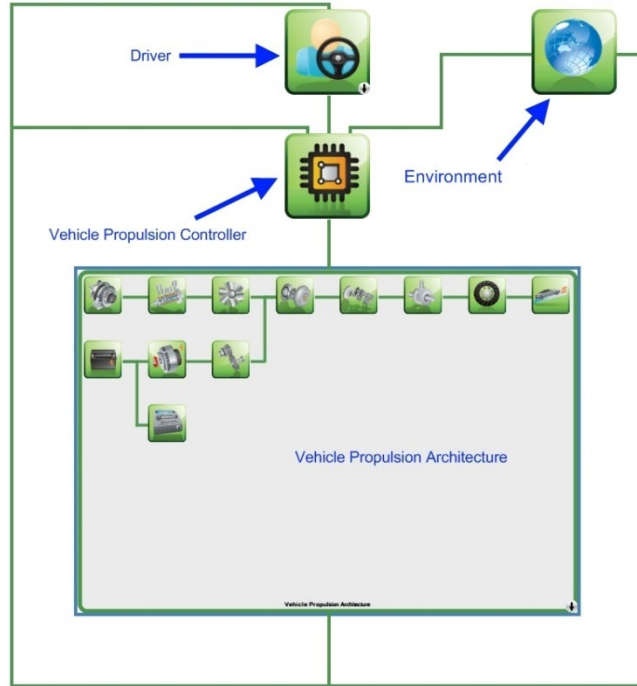


Figure 5. Top-level vehicle layout

The model files created for the terminating systems are combined to allow simulation in Simulink[®]. One option is to create every possible combination of the systems and save each complete vehicle as a separate model file. Because of the staggering number of possible combinations, this option is not feasible. Combinations involve not only many different components, but also different levels of fidelity and model versions for each component. Changing the version of a single component model would result in a new version of the entire vehicle. This method is clearly storage-intensive and impractical.

A second option is to save every model in its own file and manage a library. This would be an improvement over the first option; however, it still presents some difficulties. When users wish to create a new vehicle, they must select all the appropriate models from the library and connect them by hand into a vehicle context. Not only is this manual process time-consuming, but it introduces many opportunities for error. Consider an engine control unit model for auto code generation that can have more than 2,000 inputs and outputs. Manually connecting all I/Os almost guarantees errors. It also requires some outside solution for model library management (e.g., searching, versioning, and ensuring compatibility).

Autonomie uses a patented approach that combines the second option with an automated building process, giving the user the flexibility of saving and versioning models independently without the potential pitfalls of manual connections. Users select the desired files in a user

interface, and the automatic building process uses metadata associated with the models to create the correct connections, as shown in Figure 6.

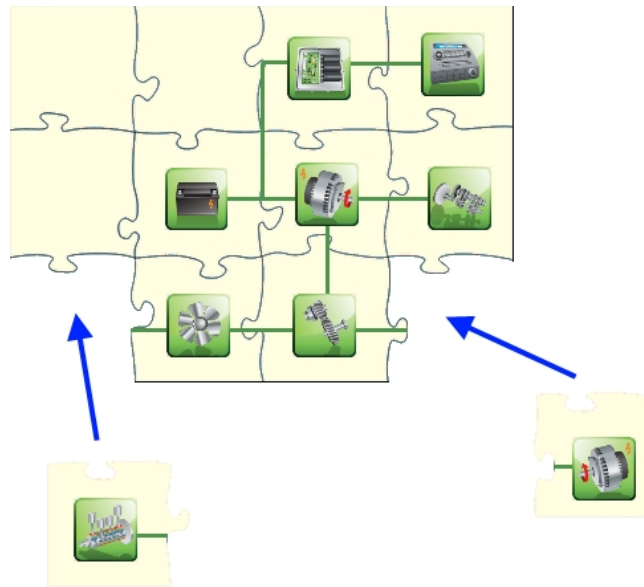


Figure 6. Models automatically built

The ability to automatically build entire vehicle models is critical to the current study, as more than 1.5 million different vehicle models are considered.

Engine Model

Autonomie uses different engine models to support specific technologies (e.g., cylinder deactivation, turbocharging, etc.). For this study, five different engine models are used.

- gasoline engine model
- diesel engine model
- gasoline turbocharged engine model
- cylinder deactivation engine model
- gasoline turbocharged engine with cylinder deactivation model

This section describes the baseline Autonomie engine model.

Model Description

The engine model simulates engine torque production, fuel consumption, etc. In this model the fuel rate is expressed as a function of the engine's brake torque and speed.

The engine model is divided into three blocks: engine torque calculation, engine thermal calculation, and engine fuel rate calculation.

Figure 7 shows the Autonomie spark-ignition engine model diagram, with these blocks outlined in red.

Block A (Figure 8) calculates the engine torque by interpolating between the maximum and minimum torque curves, using the engine command from the controller.

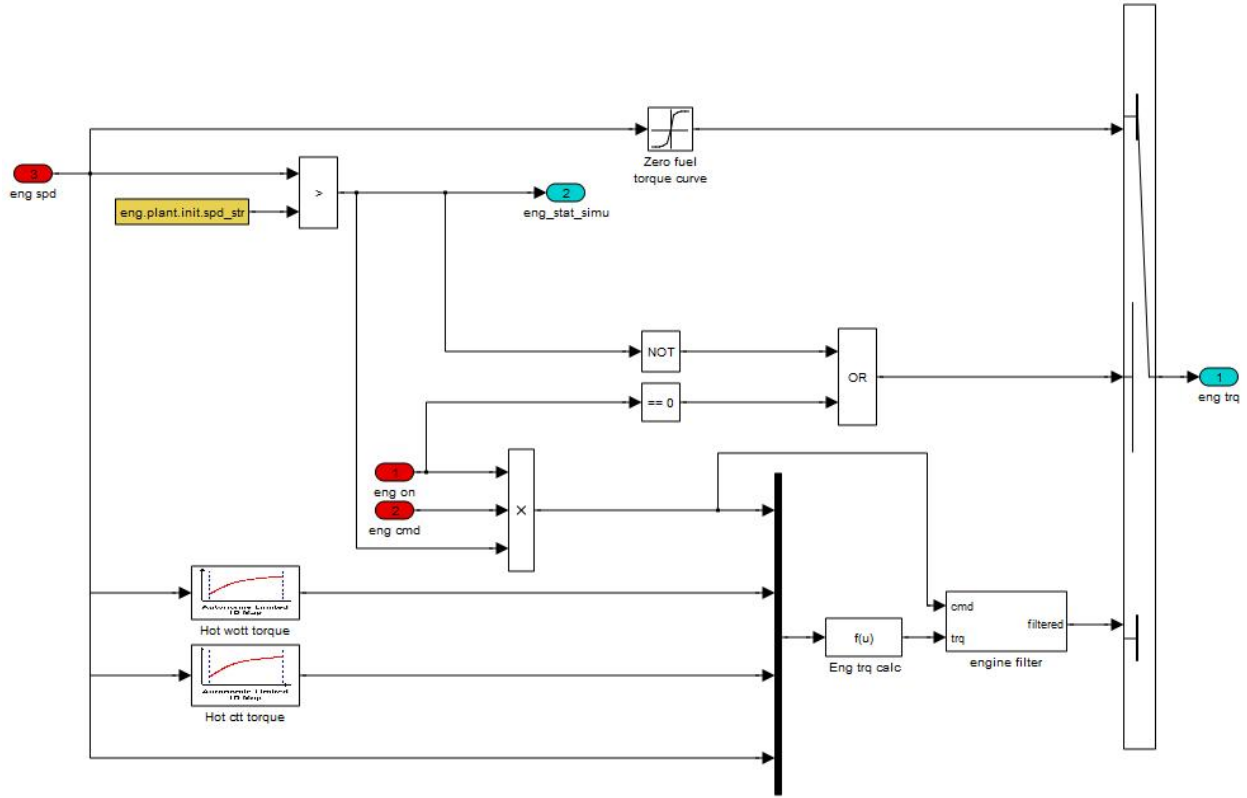


Figure 8. Engine model Block A: Engine torque calculation

If $T_{cmd} > 0$ and $\omega_{eng} > 0$ or T_{cmd} equals 0 and $\omega_{eng} > 0$, then

$$(1) T_{out} = (1 - T_{cmd}) \times T_{CTT} + (T_{cmd} \times T_{WOT})$$

Otherwise, if T_{cmd} equals 0 and ω_{eng} equals 0, then

$$(1a) T_{out} = 0$$

$$(2) T_{cmd} = PWM_cmd \times Eng_ON \times (W_{eng} > W_{starting})$$

where:

T_{CTT} = minimum torque curve of the engine as a function of speed (closed-throttle torque curve).

T_{WOT} = maximum torque curve of the engine as a function of speed (wide-open-throttle torque curve).

PWM_cmd = engine command from controller, not modified by any other signals.

$W_{starting}$ = engine starting speed threshold (if the engine speed is above this value, combustion is assumed to be stable, and the engine could be consuming fuel and capable of producing torque).

As this engine model is only for hot operation, the engine temperature, exhaust gas temperature, and warm-up coefficient are all set to constant values, as shown in Block B (Figure 9). The engine cold-start penalties are considered after the simulations, using adjustment factors developed from the Environmental Protection Agency test data.

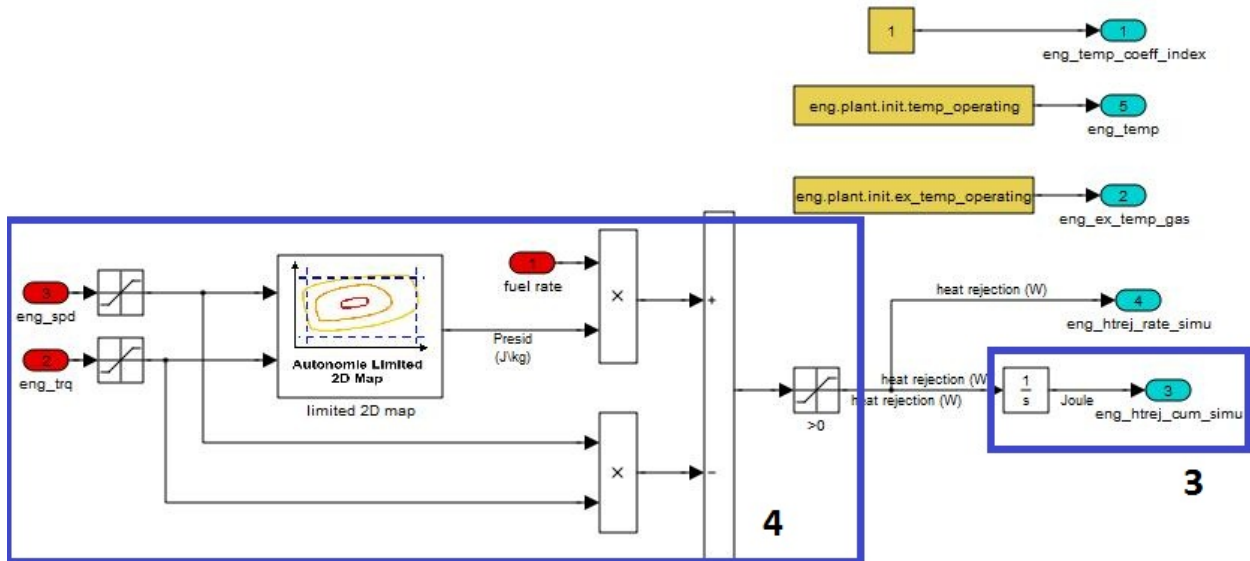


Figure 9. Engine model Block B: Thermal model

$$(3) \text{ Instantaneous_Heat_Rejection} = (\text{Fuel_rate} \times \text{Heat_rejected_per_unit_mass}) - (W_{eng} \times T_{eng})$$

$$(4) \text{ Cumulative_heat_rejection} = \int \text{Instantaneous_heat_rejection} \times dt$$

where:

Fuel_rate = mass flow rate of the engine fuel

Heat_rejected_per_unit_mass = total energy released from the fuel by combustion per unit mass of fuel

Block C (Figure 10) calculates the fuel rate. Block C1 calculates the instantaneous fuel rate by using Equations 5 and 6.

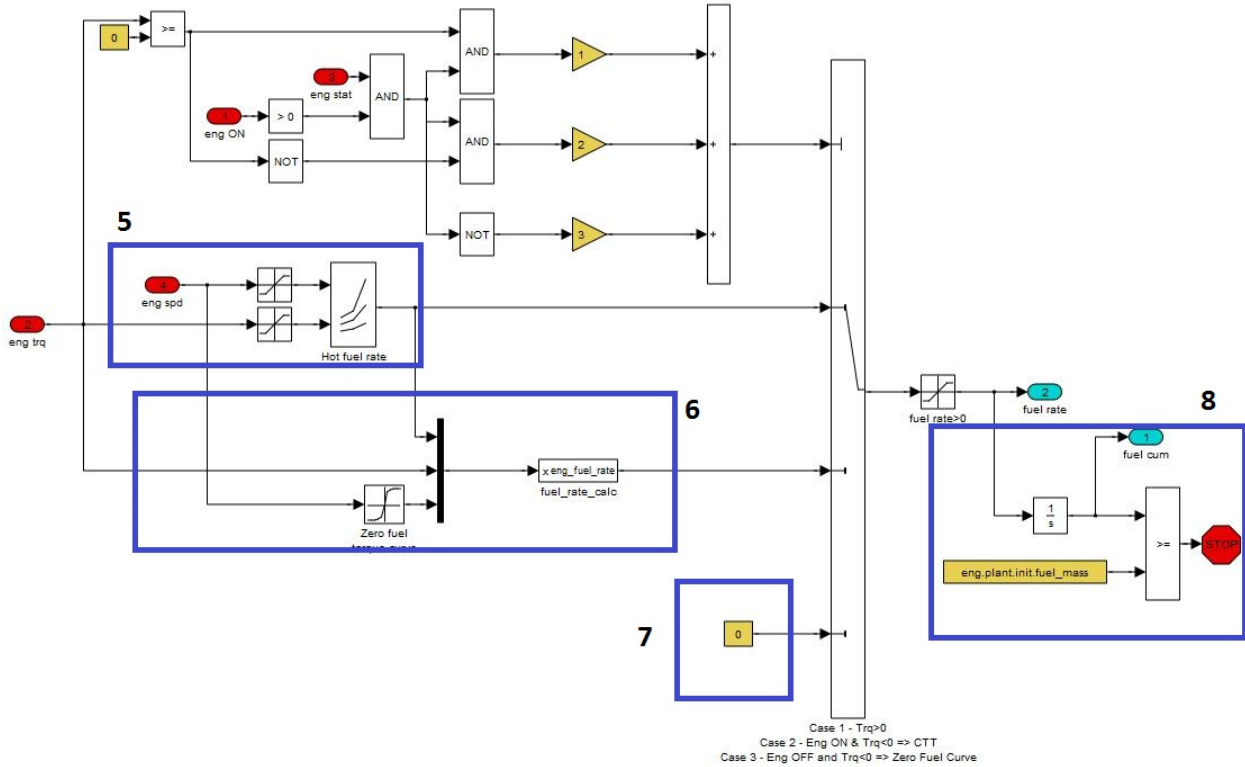


Figure 10. Engine model Block C: Fuel rate model

Equation 6 interpolates the fuel rate when the engine is on, and the torque delivered by the engine is below the torque boundary of the fuel rate map. Since no data are usually available in this region, the fuel rate is interpolated. When $T_{eng} = T_{min_map}$, the fuel rate at T_{min_map} is requested. When $T_{eng} = T_{CTT}$, the fuel rate is zero. The fuel rate is proportional to the engine torque fraction. Equation 7 ensures that no fuel is consumed when the engine is below its starting speed; the engine speed must be increased to starting speed by the starter motor before fuel can be injected. Note that the starting speed is lower than the engine idle speed.

If the engine is started and $T_{eng} > T_{min_map}$

$$(5) \quad \text{Instantaneous_fuel_rate} = \text{function}(W_{eng}, T_{eng})$$

If the engine is started and $T_{eng} < T_{min_map}$

$$(6) \quad \text{Instantaneous_fuel_rate} = \frac{\text{Fuelrate} \times (T_{eng} - T_{CTT}) \times (T_{eng} \times T_{CTT})}{R_{min_map} - T_{CTT}}$$

T_{min_map} = minimum torque index (minimum value in the vector eng.init.trq_fuel_hot_index).

This is the torque boundary for the fuel rate map. If it is below this value, unless data are available, the map must be interpolated.

Otherwise:

$$(7) \quad \text{Instantaneous_fuel_rate} = 0$$

Equation 8 calculates the total mass of fuel that went into the engine:

$$(8) \text{ Cumulative_fuel_rate} = \int \text{Instantaneous_fuel_rate} \times dt$$

Engine Technologies Evaluated

This section provides detail on the different engine technologies modeled in the gasoline and diesel engines.

Friction Reduction

Friction reduction has been shown to offer significant improvements in vehicle fuel consumption. Therefore, to evaluate the potential of friction reduction, engines can potentially be subjected to two levels of reduction in friction mean effective pressure.

- A reduction in FMEP by 0.1 bar across the entire engine speed range
- An extreme friction reduction (25% FMEP) across the entire speed range

For the current study, only the first level of friction reduction has been considered. A predictive FMEP equation was calibrated from test data to allow for a smooth and systemic friction study, but it may under-predict FMEP at high loads with late combustion phasing.

Turbocharged Engines

In addition to the naturally aspirated engines, turbo engines were mapped using GT-POWER, a commercially available engine simulation tool with detailed cylinder modeling and combustion analysis. With turbo engines, there is a lag in torque delivery because of the operation of the turbo charger. This lag impacts vehicle performance and vehicle shifting on aggressive cycles. Turbo lag has been modeled in Autonomie for turbo systems based on principles of a first order delay, where the turbo lag kicks in after the NA torque limit of the turbo engines has been reached.

Figure 11 shows the brake mean effective pressure response of the turbo engine model to a step command.

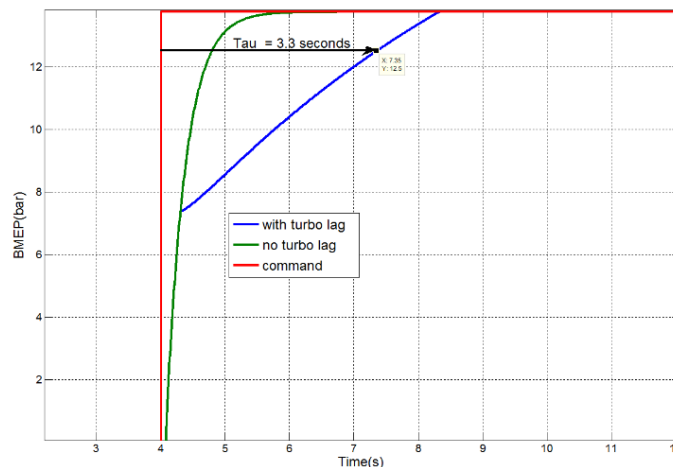


Figure 11. BMEP response of turbo-charged engine to a step command

The turbo response varies with engine speed, i.e., at higher speeds, the turbo response is faster because of higher exhaust flow rates. Note that the baseline engine maps for the NA and the

turbo engines were validated with test data. Maximum torque line on boosted engines is adjustable basis on boost pressure.

Cylinder Deactivation and Advanced Cylinder Deactivation

Autonomie uses a specific engine model for cylinder deactivation, as this model uses an advanced fuel calculation subsystem with different maps. Due to noise, vibration, and harness (NVH) considerations in production vehicles, cylinder deactivation operation is not performed during several vehicle operation modes: vehicle warm-up, lower-gear operation, idle, and low engine speed. As a result, cylinder deactivation is disabled under the following conditions.

- If the engine has not warmed up with the appropriate engine warm-up time
- If the engine idles or its speed is below 1,000 rpm or above 3,000 rpm
- If the vehicle is in first or second gear
- If the engine load is above half the maximum BMEP of the engine (and a certain hysteresis is maintained to prevent constant activation and deactivation)
- If the fuel rate of the CDA condition is lower than that of the non-CDA condition

As noted above, cylinder deactivation is not typically performed during the vehicle warm-up phase, i.e., for a cold start. Since all the simulations considered in this study assume a “hot start,” where the engine coolant temperature is steady at around 95° C, the cold start condition was not considered for the simulations. In addition, changes in the transmission shifting calibration (like lugging speed limits) and additional torque converter slippage during cylinder deactivation have not been considered.

Engine Cylinder Deactivation Methodology

The cylinder deactivation state is implemented in a Stateflow diagram as shown in Figure 12.

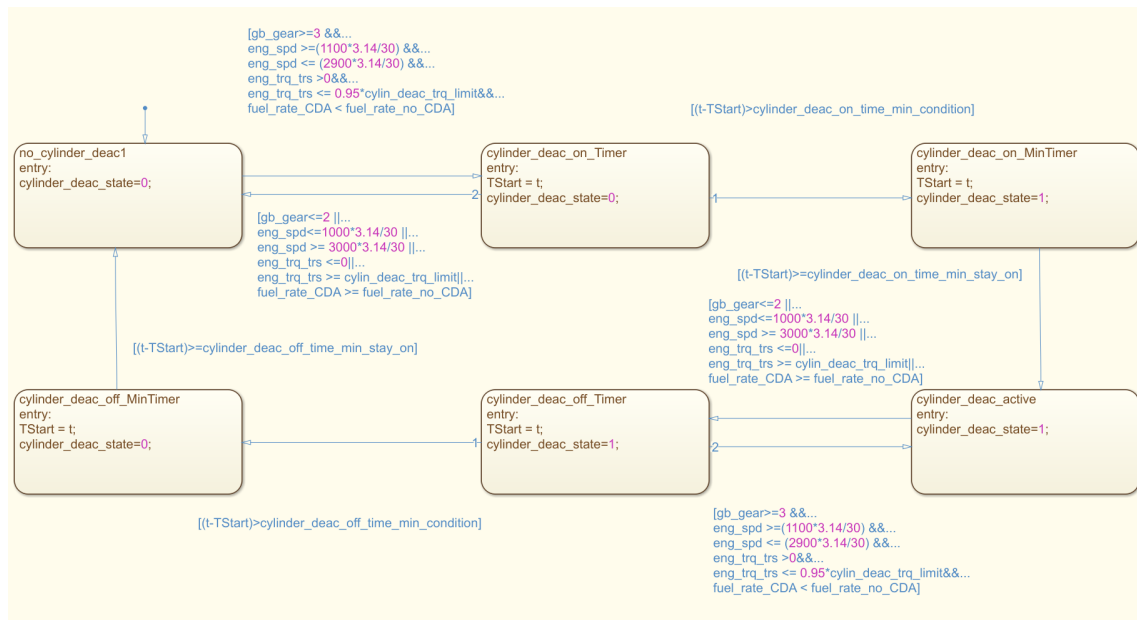


Figure 12. Stateflow diagram for cylinder deactivation regulator

In the engine plant model, the fuel rate maps for both cylinder deactivation and no cylinder deactivation are used by the Stateflow logic. Figure 13 shows the engine plant model with cylinder deactivation and shows how both fuel maps (with and without cylinder deactivation) are used by the Stateflow logic in the engine plant model.

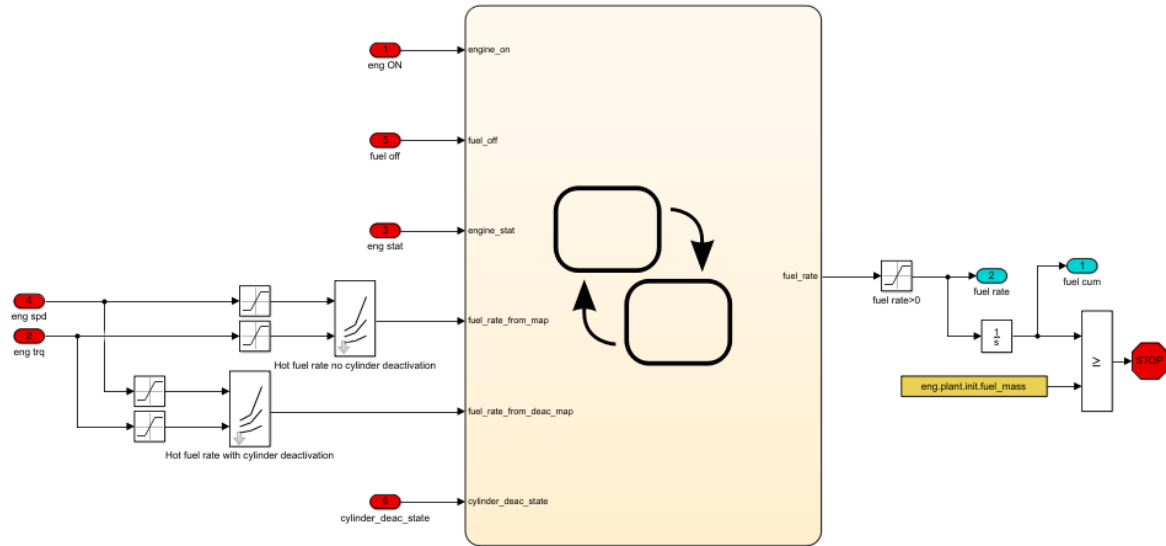


Figure 13. Engine plant model with cylinder deactivation

Figure 14 shows the Stateflow control that switches the fuel maps for the cylinder deactivation and no cylinder deactivation conditions are based on the cylinder deactivation signal.

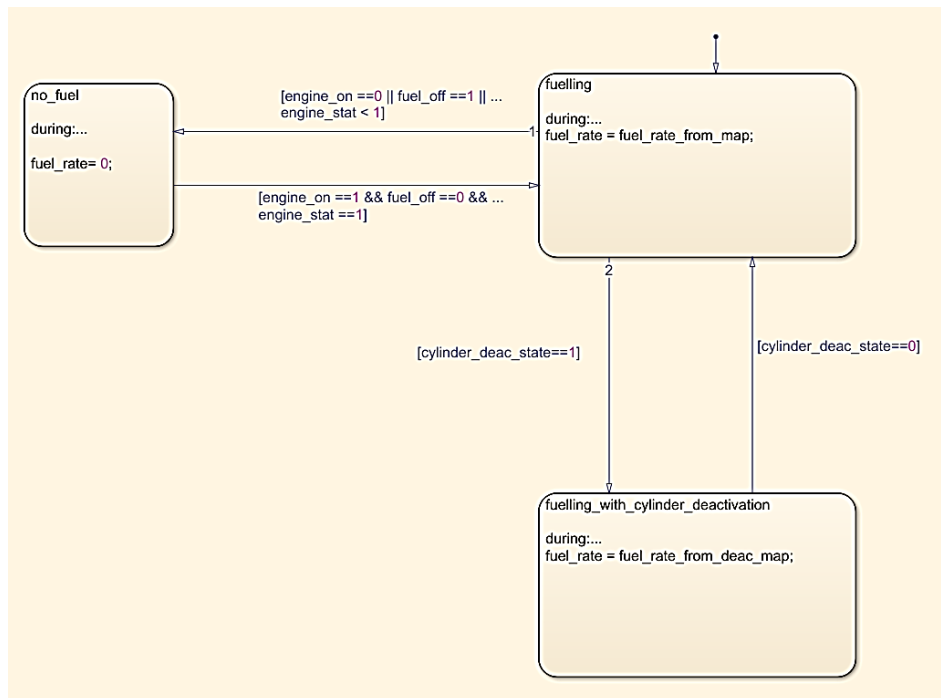


Figure 14. Stateflow diagram showing the ability to switch cylinder deactivation fuel maps

As shown in Figure 14, a state diagram is used to switch between the two different engine maps (state fueling versus fueling with cylinder deactivation) based on whether the cylinder deactivation state is active (cylinder_deac_state).

Fuel Cutoff

Autonomie’s fuel cutoff model uses a specific torque calculation to calculate the torque loss when fuel is cut off during deceleration events. In general, engine models in Autonomie are of two types: throttled engines and unthrottled engines. As shown in Figure 15 and Figure 16, both types of models provide motoring torque when fuel to the engine is cut (e.g., when fuel is cut off during deceleration). With throttled engines, the motoring torque is a function of throttle position. Figure 15 shows the engine operating regions for throttled engines, and Figure 16 shows the engine operating regions for unthrottled engines.

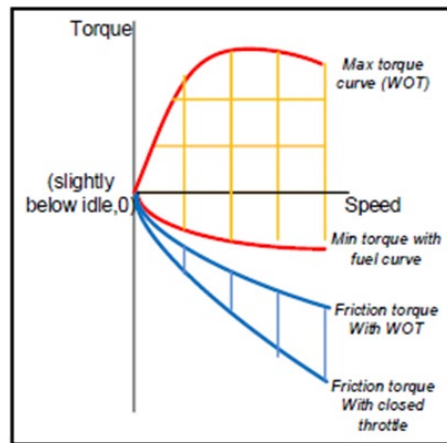


Figure 15. Engine operating regions for throttled engines (WOT = wide-open throttle)

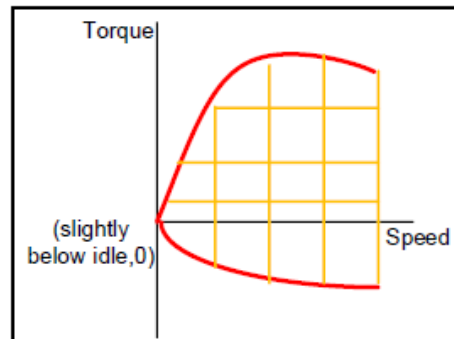


Figure 16. Engine operating region for unthrottled engines

Engine fuel cutoff control algorithms used in the study have been developed based on vehicle test data collected at AMTL.* The fuel cutoff controller is implemented for gasoline and diesel engines through analysis, as shown in Figure 17. In Autonomie, engine control and plant blocks

* 2017 Ford F150, 2016 Mazda CX9, 2014 Chevrolet Cruze Diesel, 2014 Mazda 3 iEloop, 2013 Dodge Ram 1500 HFE, 2013 Hyundai Sonata, 2013 Nissan Altima, 2013 Volkswagen Jetta TDI, 2012 Chrysler 300, 2012 Fiat 500 Sport, 2012 Ford F150 Ecoboost, 2012 Ford Focus, 2012 Ford Fusion V6, 2009 Volkswagen Jetta TDI. (Argonne National Laboratory, n.d.) www.anl.gov/taps/conventional-vehicle-testing

are organized for idle fuel rate and fuel-off conditions. Engine fuel is cut off under the following conditions.

- Vehicle is actively braking for a certain minimum time.
- Engine speed is above a minimum threshold (e.g., 1,000 rpm).

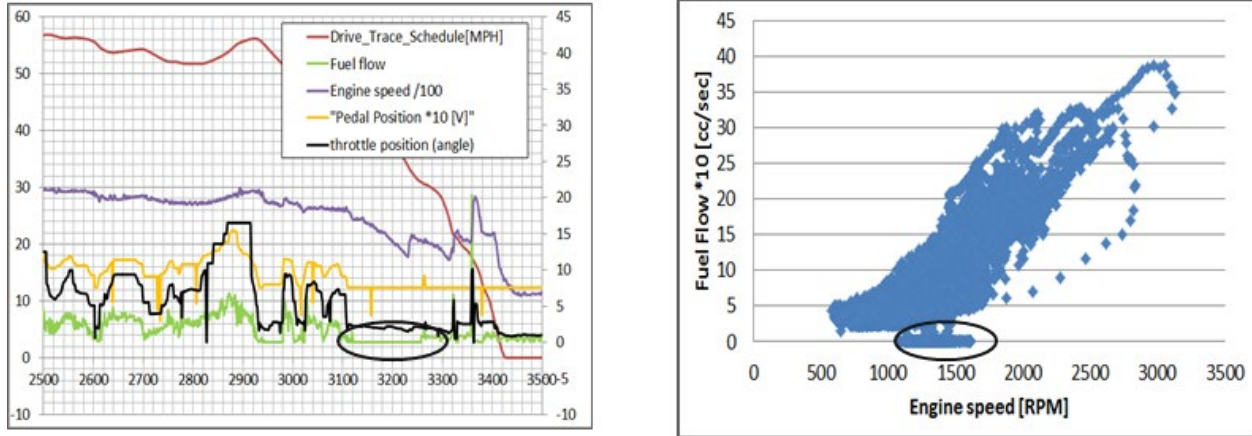


Figure 17. Engine fuel cutoff analysis based on test data

Transmission Model

The drivetrain is assumed to be rigidly attached to the wheels. Since the wheel speed and acceleration are calculated in the wheel model and propagated backward throughout the rest of the drivetrain model, the gearbox unit is modeled as a sequence of mechanical torque gains. The torque and speed are multiplied and divided, respectively, by the current ratio for the selected gear. Torque losses corresponding to the torque/speed operating point are subtracted from the torque input. Torque losses are defined as a three-dimensional efficiency lookup table (input shaft rotational speed, input shaft torque, and gear number). When a gear is selected, the input inertia is fed forward to the next component after being reflected to the output shaft using the square of the gear ratio. When the neutral gear is engaged, the input gearbox rotational speed is calculated based on the input shaft inertia.

Automatic Transmission

For automatic transmissions, gear shifting occurs without having to pass through neutral and without a complete torque interruption at its output. The torque converter model is separate from the automatic gearbox model. Figure 18 shows the I/O of the AU model.



Figure 18. Autonomie automatic gearbox model I/O

The top-level diagram of the automatic gearbox is composed of three main subsystems: speed calculation (Block A), torque calculation (Block B), and inertia calculation (Block C). Figure 19 shows the top-level diagram of the automatic gearbox model.

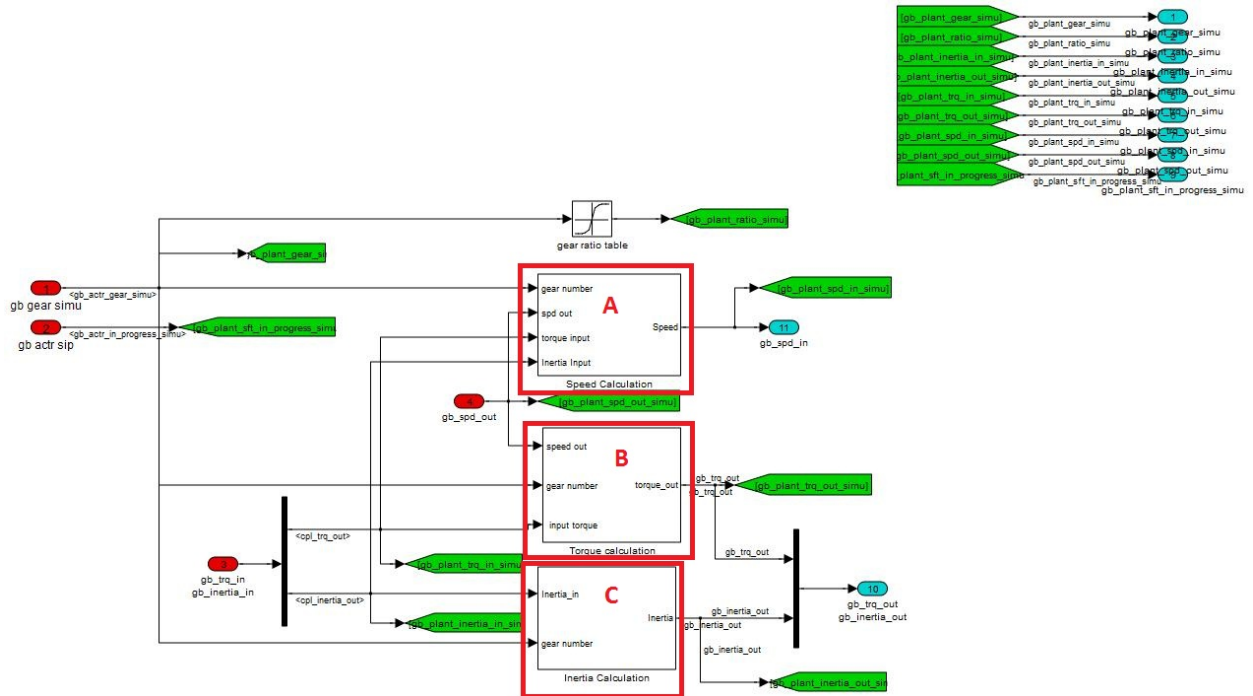


Figure 19. Top level of the automatic gearbox model

Block A (Figure 20) calculates the gearbox shaft input speed based on the output speed, gear ratio, and whether the gearbox is in neutral. If the gearbox is in first gear, Equation 9 is used to calculate the input speed of the gearbox.

$$(9) W_{in} = K_{Ratio} \times W_{out}$$

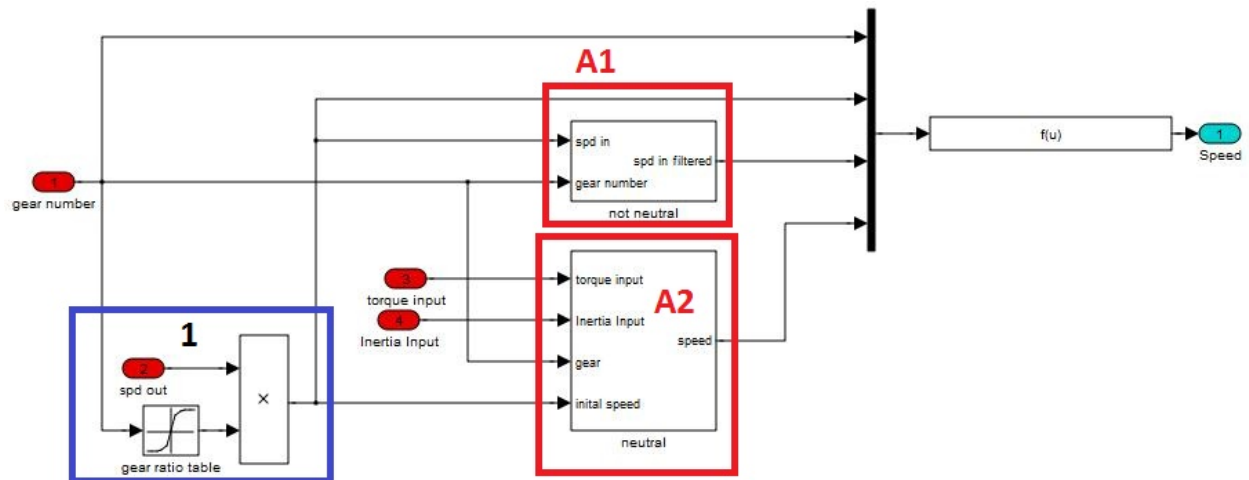


Figure 20. Block A: Speed calculation of the AU

Between gear choices during an AU shift, the output shaft speed lags the input shaft speed as one set of wet clutches opens and another closes, allowing for a smooth gear shift and no interruption in torque output. This speed characteristic of the automatic gearbox is modeled in Block A1 using a low-pass filter. However, this low-pass filter cannot be used during a shift from neutral into first gear, a shift that occurs during the performance test for a limited subset of hybrid configurations that are in neutral when the vehicle is stopped instead of being in first gear, as a stopped conventional vehicle. The low-pass filter interferes with the performance test, slowing the vehicle down and leading to exaggerated 0-to-60 mph times. To address this issue, the filter is not used during performance to ensure that when the vehicle is shifting from neutral into first, the input speed is proportional to the output speed.

Block A1 (Figure 21) calculates the input speed when the gearbox is not in neutral. Any gear changes will result in the input speed lagging the output speed. Equation 10 implements the phase difference between input and output speeds.

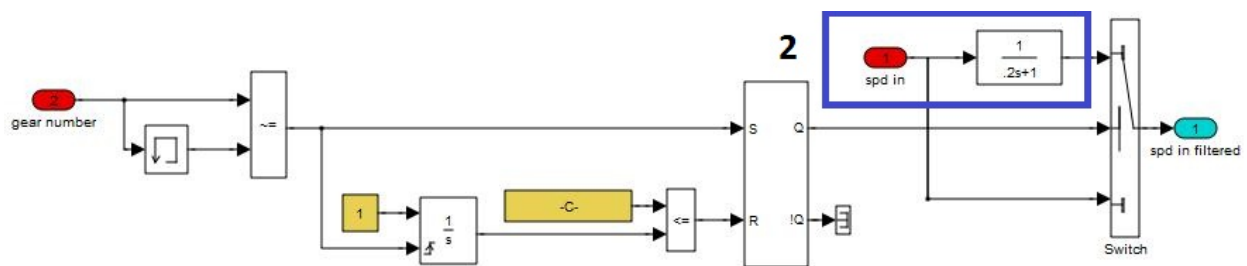


Figure 21. Block A1: Speed calculation when the gearbox is not in neutral

Equation 10 shows the calculation of the input speed when the gear number is higher than first:

$$(10) \quad W_{in} = \frac{1}{1 + \tau S} \times (K_{Ratio} \times W_{out})$$

Block A2 (Figure 22) calculates the input speed when the gearbox is in neutral.

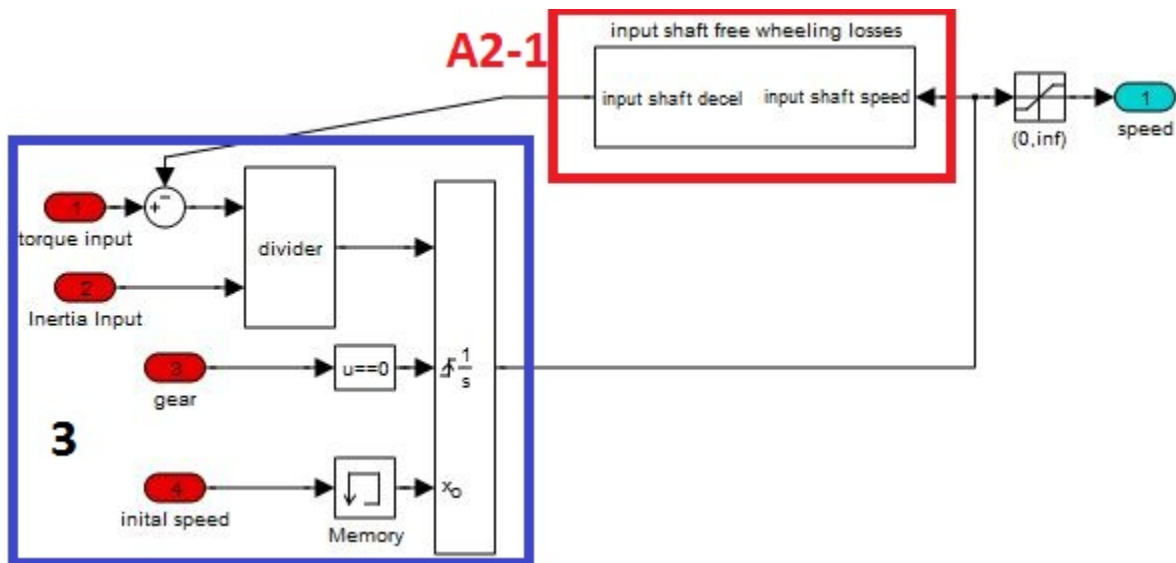


Figure 22. Block A2: Speed calculation when the gearbox is in neutral

When the gearbox is in neutral, the input shaft speed is calculated by using the first-order differential equation shown (Equation 11). If the input torque goes to 0, the shaft will continue to spin until the drag torque brings it to rest.

$$(11) \quad W_{in} = \int \frac{T_{in} - T_{loss}}{J_{in}}$$

Block A2-1 (Figure 23) calculates the torque loss of the free-wheeling input shaft. The torque loss is proportional to the shaft speed, per Equation 12.

$$(12) \quad T_{loss} = K_{coeff} \times W_{in}$$

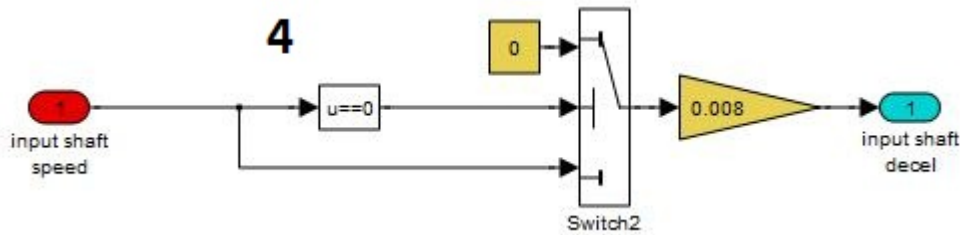


Figure 23. Block A2-1: When gearbox not in neutral, with free-wheeling input shaft losses

Block B (Figure 24) calculates the gearbox output torque using the gearbox ratio and torque loss.

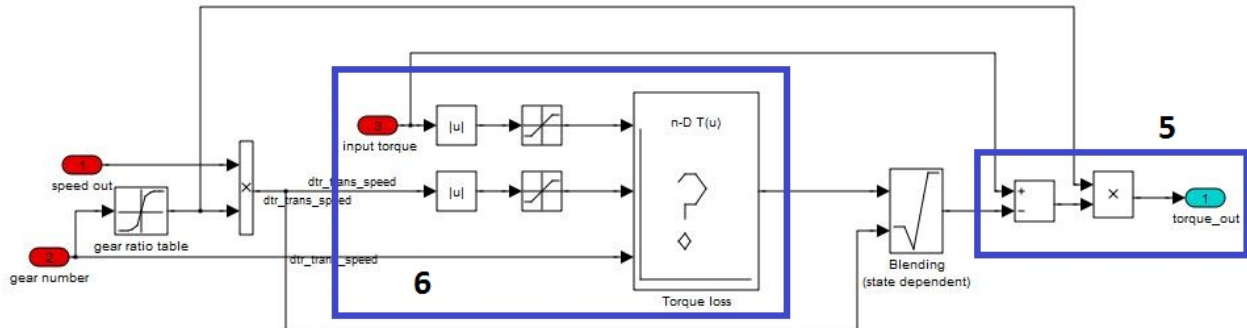


Figure 24. Block B: Output torque calculation

Equation 13 shows the output torque calculation based on input torque minus torque loss.

$$(13) \quad T_{out} = T_{in} - T_{loss}$$

Torque loss is a function of the gearbox input torque, speed, and ratio.

$$(14) \quad T_{loss} = f(T_{in}, W_{in}, K_{Ratio})$$

When the gearbox is in neutral, the torque output is forced to 0.

$$(15) \quad T_{loss} = 0$$

Block C (Figure 25) gives the output inertia of the gearbox.

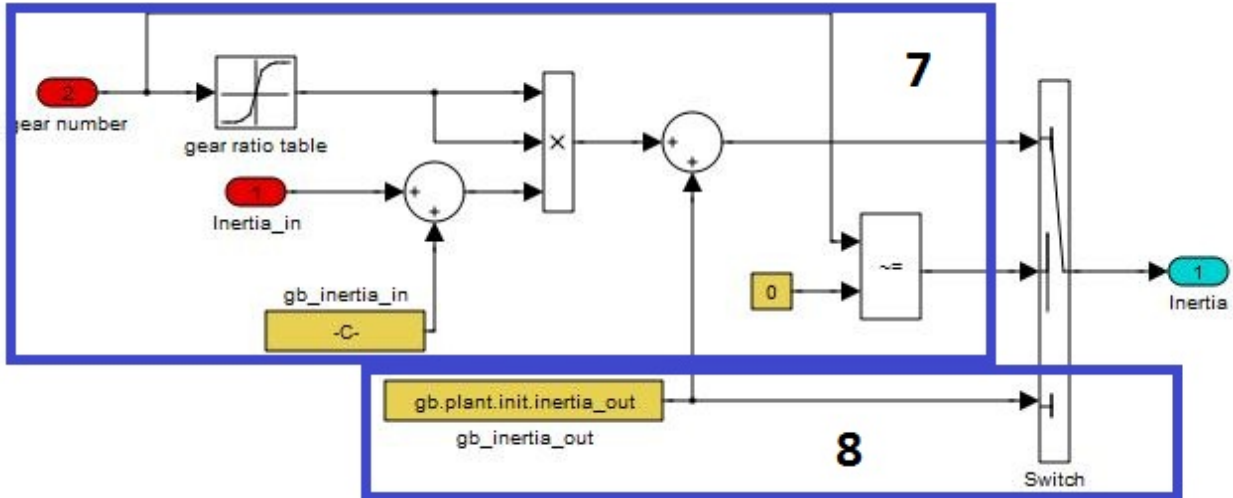


Figure 25. Block C: Output inertia calculation

The output inertia equals the upstream inertia reflected to the output shaft of the gearbox through the gear ratio plus the output shaft inertia of the gearbox.

$$(16) \quad J_{out} = (J_{in} + J_{input_shaft_tx}) \times K_{ratio}^2 + J_{output_shaft_tx}$$

When the gearbox is in neutral, Equation 17 demonstrates that the output inertia of the gearbox is the inertia of the output shaft.

$$(17) \quad J_{out} = J_{output_shaft_tx}$$

Manual Transmission

Figure 26 shows the main I/O of the manual transmission (DM) model. Although we do not model manual transmissions in the current analysis, we kept the description of this model in the documentation for possible inclusion in future analyses.



Figure 26. Autonomie DM model I/O

The top-level diagram of the manual gearbox is composed of three main subsystems: speed calculation (Block A), torque calculation (Block B), and inertia calculation (Block C). Figure 27 shows the top-level diagram of the manual gearbox model.

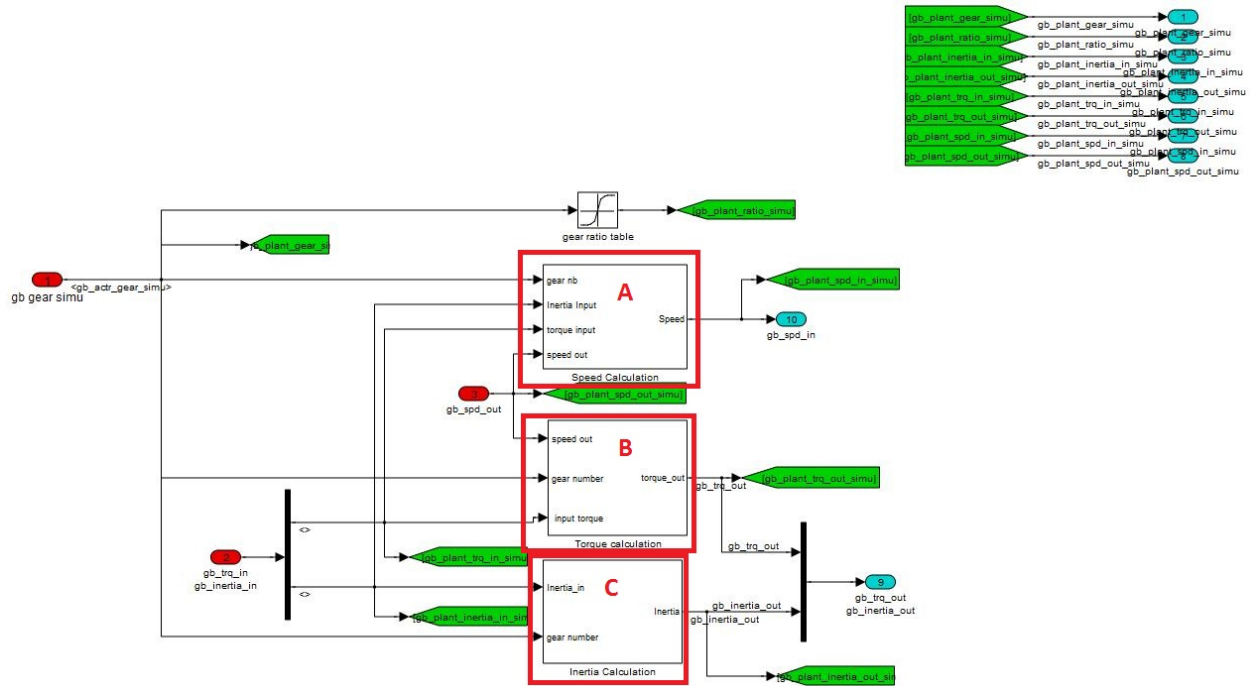


Figure 27. Top level of the manual gearbox model

Block A (Figure 28) calculates the input shaft speed of the gearbox on the basis of the current output shaft speed, the current gear ratio, and whether the gearbox is in neutral.

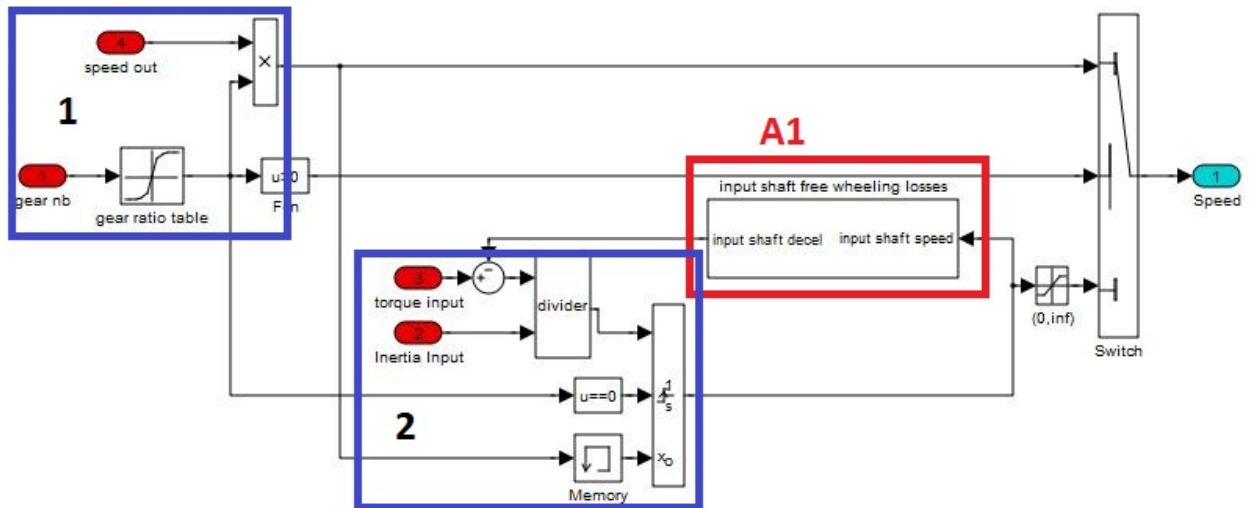


Figure 28. Block A: Gearbox input shaft speed calculation

If the gearbox is in gear, the input shaft speed is proportional to the output shaft speed. If the gearbox is in neutral, the input shaft is free to spin. The spinning shaft produces drag losses that are proportional to its speed. Equation 18 shows the speed calculation when the gearbox is in gear.

$$(18) \quad W_{in} = K_{Ratio} \times W_{out}$$

When the gearbox is in neutral, the input shaft speed is calculated by using the first-order differential equation shown below (Equation 19). If the input torque goes to 0, the shaft will continue to spin until the drag torque brings it to rest.

$$(19) \quad W_{in} = \int \frac{T_{in} - T_{loss}}{J_{in}}$$

Block A1 (Figure 29) shows the torque loss calculation when the gearbox is in neutral.

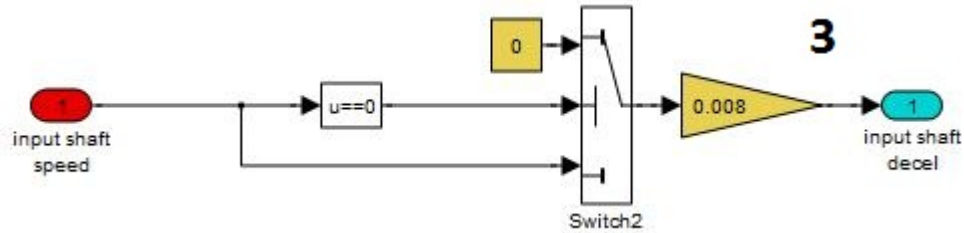


Figure 29. Block A1: Torque loss calculation when the gearbox is in neutral

The torque losses are proportional to the input speed, as shown in Equation 20.

$$(20) \quad T_{loss} = K_{coeff} \times W_{in}$$

Block B (Figure 30) calculates the torque output of the gearbox, accounting for the torque gain due to the ratio and the torque loss in the gearbox.

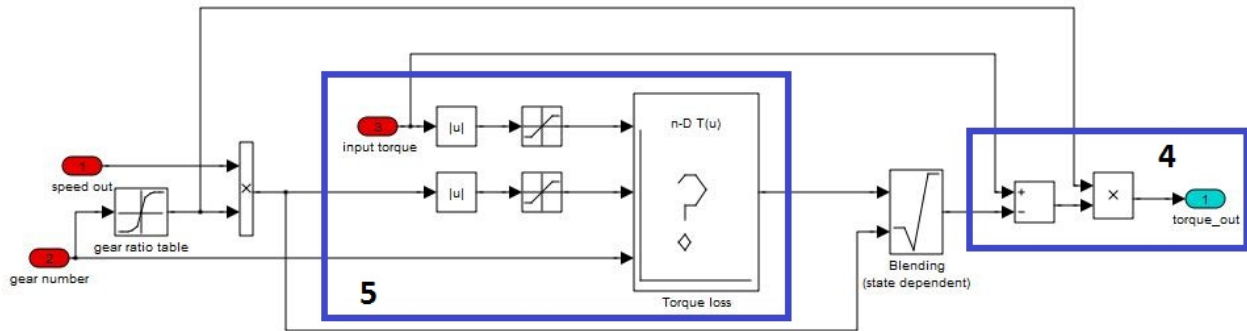


Figure 30. Block B: Speed calculation when the gearbox is in neutral

Equation 21 shows that the output torque before applying the ratio gain is the output torque minus the torque loss.

$$(21) \quad T_{out} = T_{in} - T_{loss}$$

When the gearbox is in neutral, the torque output is forced to 0.

$$(22) \quad T_{out} = 0$$

The torque loss is a function of the gearbox input torque, speed, and ratio.

$$(23) \quad T_{loss} = f(T_{in}, W_{in}, K_{ratio})$$

Block C (Figure 31) gives the output inertia of the gearbox.

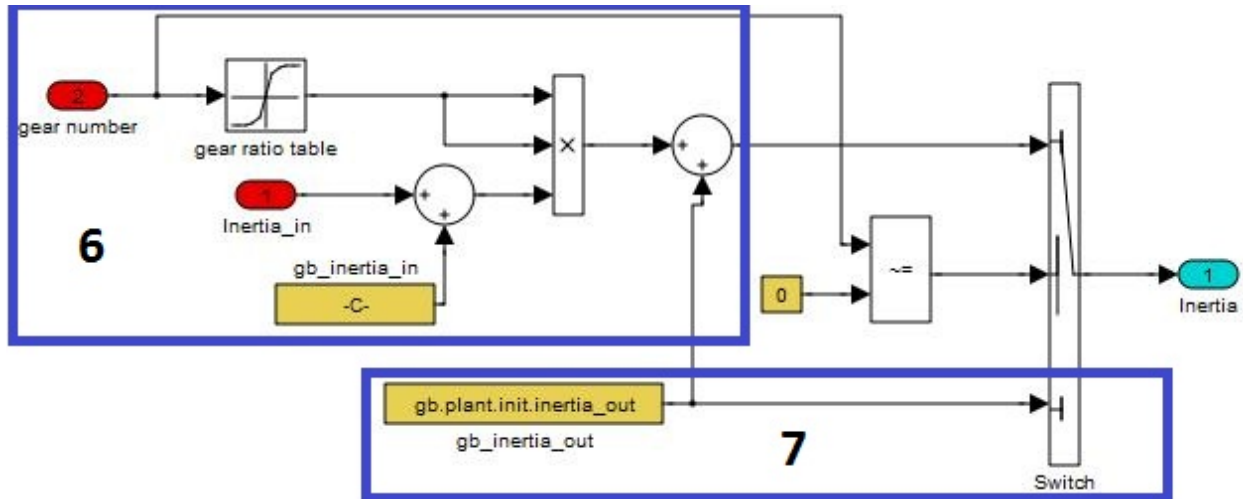


Figure 31. Block C: Output inertia calculation

The output inertia equals the upstream inertia reflected to the output shaft of the gearbox through the gear ratio plus the output shaft inertia of the gearbox.

$$(24) \quad J_{out} = (J_{in} + J_{input_shaft_tx}) \times K_{ratio}^2 + J_{output_shaft_tx}$$

When the gearbox is in neutral, Equation 25 demonstrates that the output inertia of the gearbox is the inertia of the output shaft.

$$(25) \quad J_{out} = J_{output_shaft_tx}$$

Continuously Variable Transmission

Plant Model

The metal V-belt continuously variable transmission model is based on the concepts of hydraulic and mechanical loss. Hydraulic loss constitutes most of the total loss at low vehicle speeds, while mechanical loss is the main source of inefficiency at high speed, as shown in Figure 32. The CVT model treats oil pump efficiency as a function of the line pressure and input speed. The mechanical loss map, collected from experimental data, is also taken to be a function of the speed ratio, input torque, and vehicle speed.

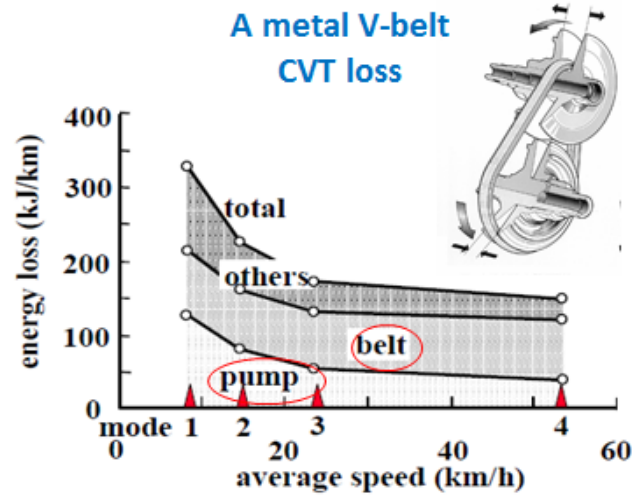


Figure 32. Hydraulic pump loss and mechanical loss for metal V-belt CVT (van der Sluis et al, 2007)

Generally, the operating conditions of the metal V-belt CVT system can be described by the following five parameters.

- Primary clamping force (F_p) or primary pressure (P_p)
- Secondary clamping force (F_s) or secondary pressure (P_s)
- Primary revolution speed (ω_p),
- Input torque (T_{in})
- Pulley ratio (i)

On both the primary and the secondary pulleys, the belt is clamped by the forces produced by the hydraulic pressures in the cylinders. These two clamping forces, F_p and F_s , counteract each other. Therefore, when the pulley ratio is constant, F_p and F_s are balanced. A ratio change occurs when their balance is lost. In the next subsection, the relation between F_p and F_s in a state of balance is discussed, and a discussion of rate-of-change (di/dt) follows.

Variator Clamping Force Model

In the CVT system, the pulley ratio is controlled by the primary pulley; therefore, the state of balance is produced by the primary clamping force F_p . The necessary primary clamping force for counterbalance is denoted by F_p^* , and the corresponding primary pressure is denoted by P_p^* .

The secondary actuator pressure P_s can be obtained for the given input torque T_{in} and CVT ratio i from Fuji's formula.

$$(26) \quad F_s = \frac{T_{IN}}{2\mu R_P} \cos \frac{\alpha}{2}$$

where μ is the friction coefficient between the belt and the pulley, and R_P is the pitch radius of the primary pulley. In the CVT system design, F_s should be controlled to prevent slippage between the belt and the pulley.

The thrust ratio map determines the primary pressure P_p at a steady state. The thrust ratio shows the relationship between the steady-state primary force F_p and the secondary force F_s with respect to the speed ratio i and the torque ratio. The thrust ratio $F_p F_s$ is represented as follows.

$$(27) \quad F_P F_S = \frac{F_P}{F_S} = f\left(i_{CVT}, \frac{T_{IN}}{T_{max}}\right)$$

For a given speed ratio i and the input torque T_{in} , the secondary pressure P_S is calculated from Equation 26. The primary actuator force F_S is determined from the thrust ratio map for the given i and the ratio $F_P F_S$. The primary pressure can be calculated from Equation 27. Figure 33 shows the $F_P F_S$ ratio map of the CVT.

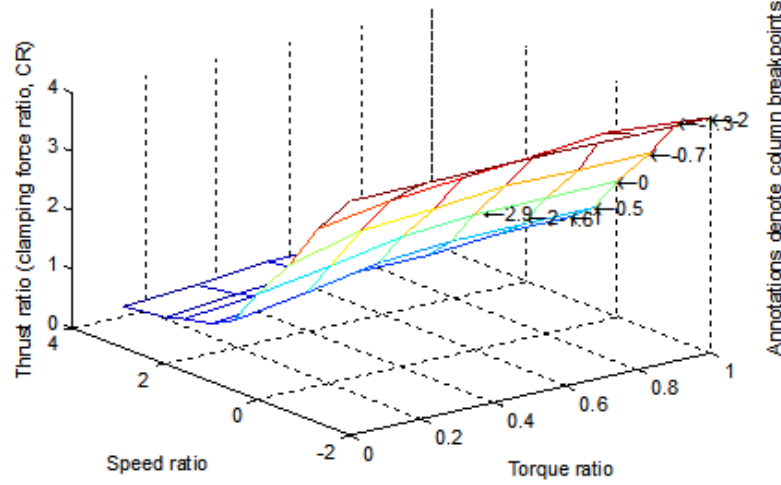


Figure 33. $F_P F_S$ ratio map (CVT)

CVT Shift Dynamics Model

To obtain the dependency of the rate of changing speed di/dt on the five parameters mentioned above, we use Ide's formula (Ide et al., 1995), which is based on a test rig using only the belt and pulley set.

The deviation of P_P from P_P^* is denoted by ΔP_P , and di/dt is expressed by the following equation.

$$(28) \quad \frac{di}{dt} = \beta(i) \times \omega_p \times (P_P - P_P^*)$$

The parameters of Ide's formula were determined from experiments reported in the literature. The linear relation is also obtained for all pulley ratios. The effect of P_P on di/dt is obtained from the five parameters P_P , P_S , ω_p , T_{in} , and i . This formula shows that di/dt is in a proportional relation with ΔP_P under loaded conditions as well, and the slope β barely changes even if T_{in} changes.

Controller

The CVT ratio control and clamping force control strategies, including the CVT shift dynamics, focus on the following.

- The engine best-efficiency line determines the demanded CVT ratio.
- The secondary pressure is determined for the given input torque and CVT ratio.
- The primary pressure needs to be controlled to meet the demanded CVT ratio.

Figure 34 shows a block diagram of the model-based ratio control and plan.

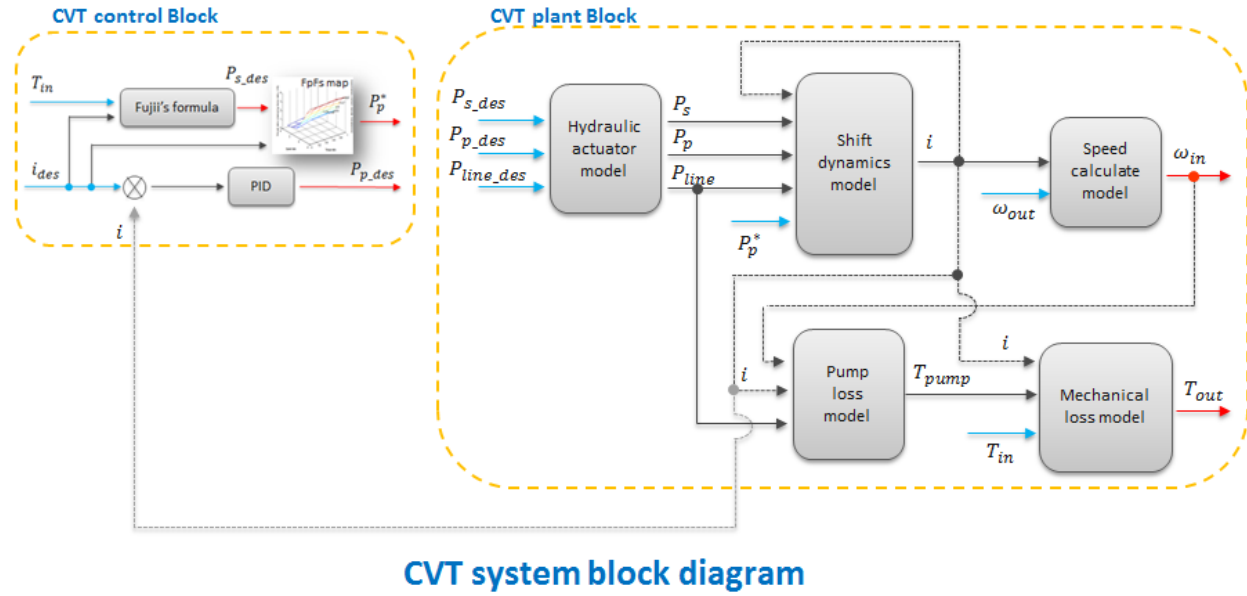


Figure 34. CVT system block diagram

Dual-Clutch Transmission

Plant Model

Dual-clutch transmission dynamic models include the clutch and gear train, as shown in Figure 35.

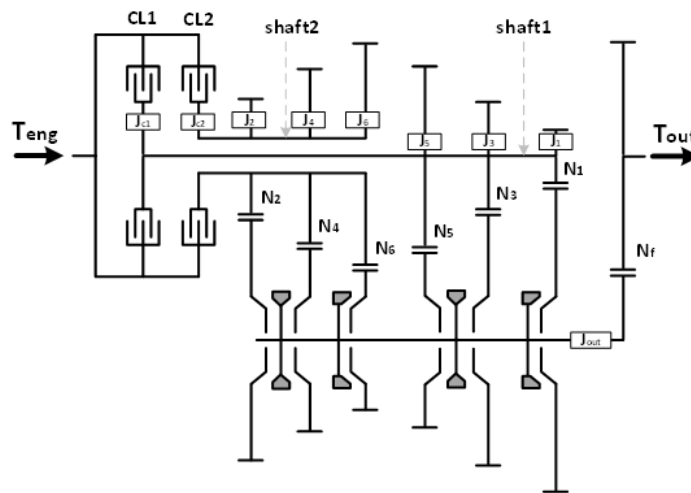


Figure 35. Stick diagram of a DCT (Kim et al., 2014)

The following assumptions are made in the model development of the shifting process.

- All shafts in the powertrain are assumed to be rigid.
- The synchronization transition process of the synchronizer is ignored.
- The inertia of shaft1 is combined with that of clutch1 (CL1), and the inertia of shaft2 is combined with that of clutch2 (CL2).

System Operating Conditions

Gear pre-selection can be implemented based on the DCT operating conditions, as shown in Figure 36. For example, if the first synchronizer is at the first gear position, and the third through fifth synchronizers are at the neutral position (as they must be), then the gear ratio between shaft1 and the output shaft is first gear. At the same time, the gear ratio between shaft2 and the output shaft can be selected in the same manner for the pre-selection mode. To achieve a desired I/O gear ratio, the corresponding synchronizer and clutch must be applied.

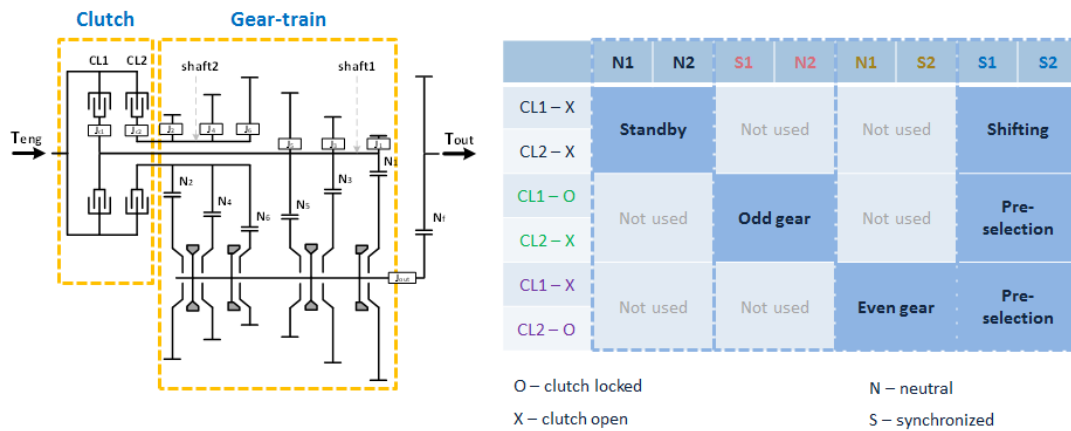


Figure 36. DCT operating conditions

Dynamic Modeling

The schematic diagram in Figure 37 and the operating conditions in Figure 36 were used to generate the equations for each mode, as described below.

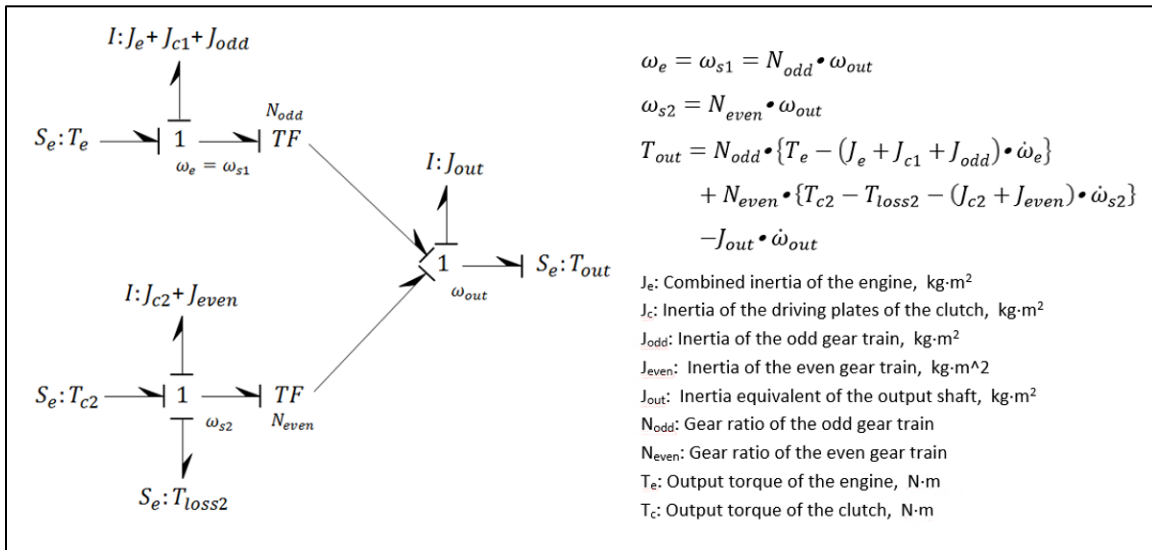


Figure 37. Pre-selection mode bond graph

The synchronizer of shaft1 is at an odd gear position, and the synchronizer of shaft2 is at an even gear position for the pre-selection. CL1 or CL2 is applied to connect the input power path into shaft1 or shaft2. Figure 37 shows the bond graph representation of the pre-selection mode when only CL1 is locked.

Figure 38 shows the details of the Autonomie gearbox plant model for the DCT.

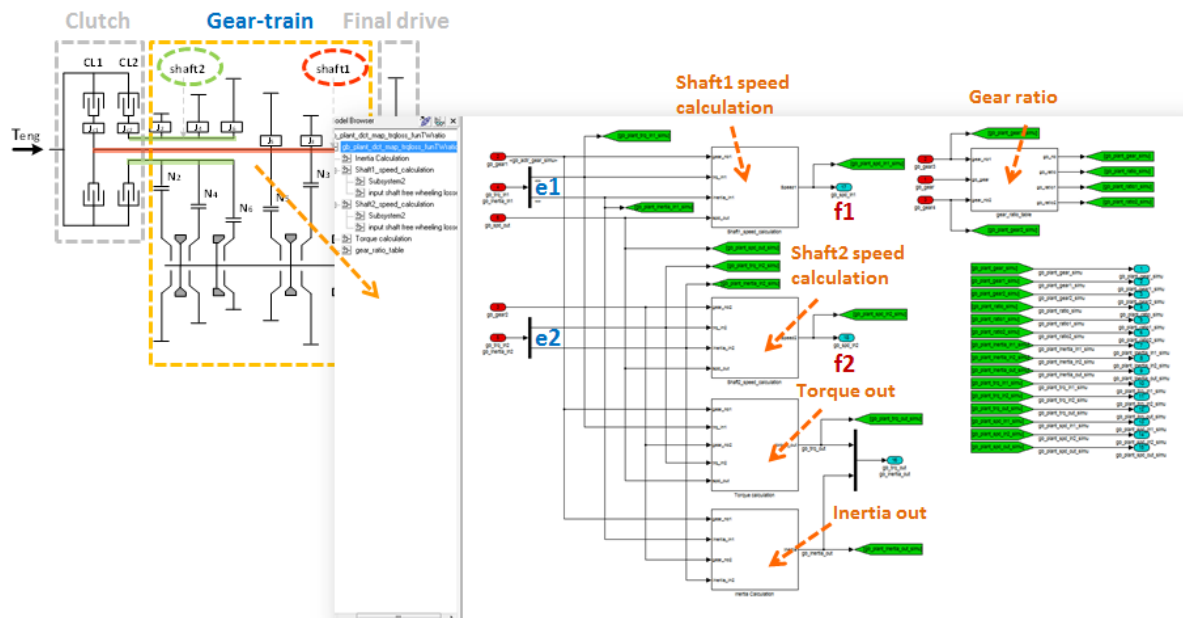


Figure 38. Gearbox plant model for DCT

Figure 39 describes the model and the governing equations for the clutch:

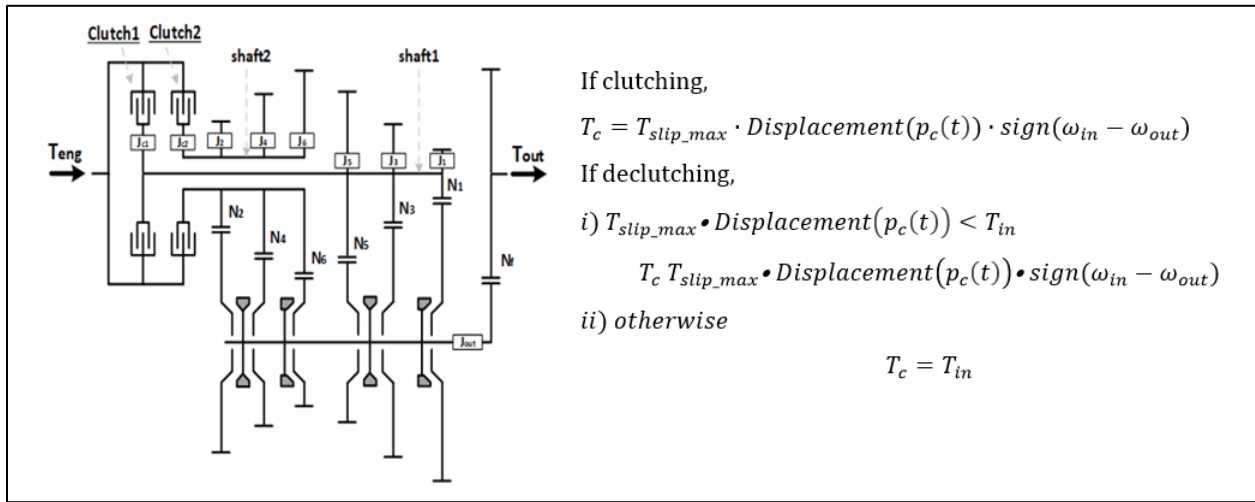


Figure 39. Model and governing equations for clutch

Figure 40 shows the high-level DCT model in Autonomie.

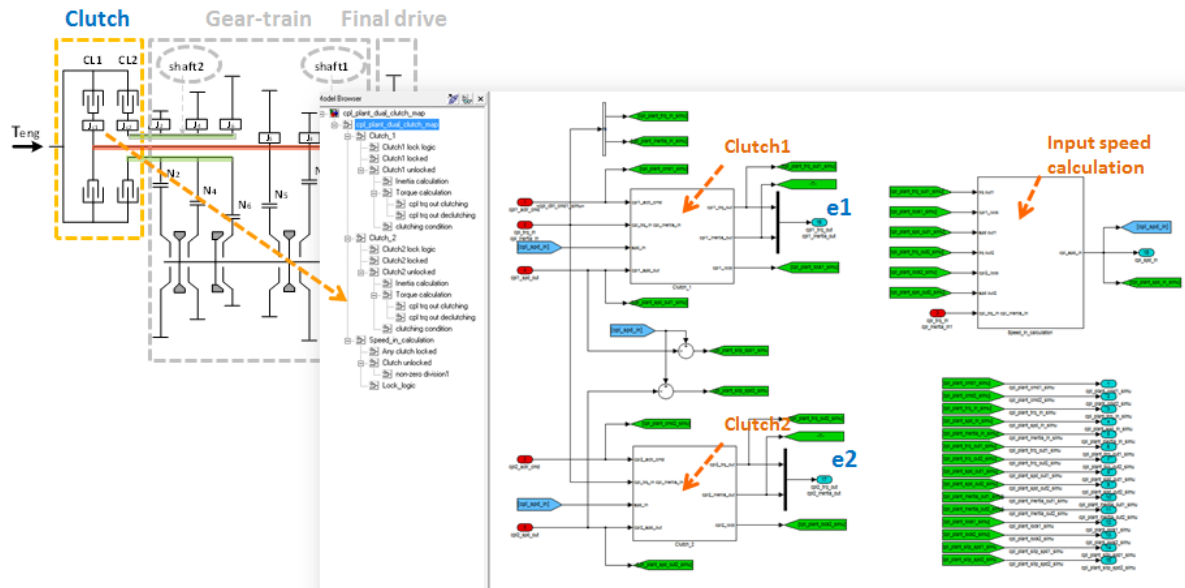


Figure 40. Gearbox plant model for DCT

Controller

The controller operating logic was defined based on the principle of DCT operation. The gearbox transient block coordinates all components during transient phases, as shown in Figure 41.

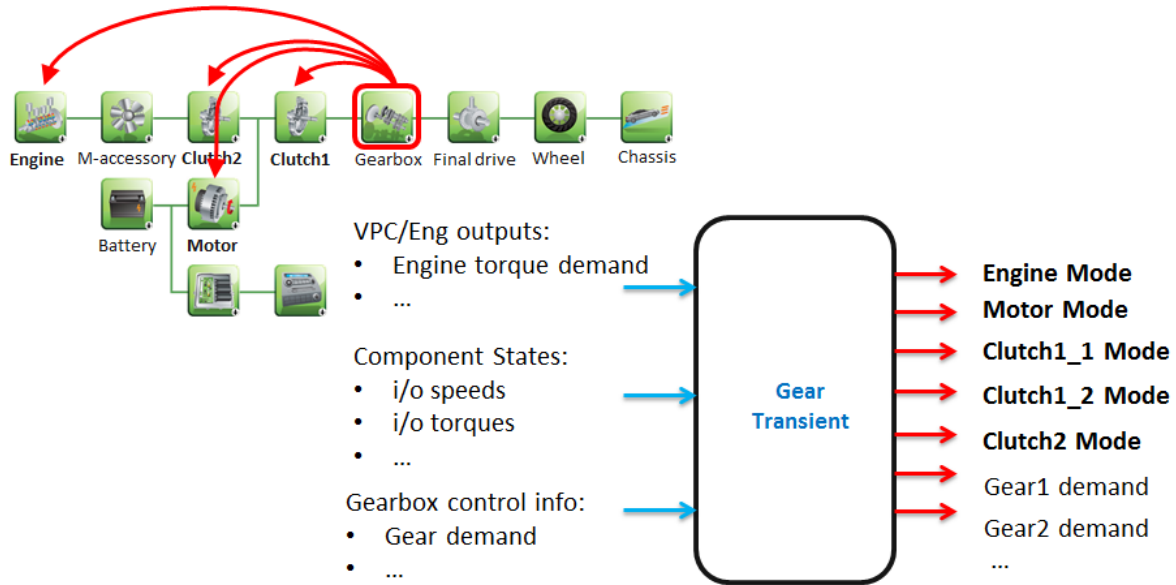


Figure 41. DCT controller

Gearbox Transient Controller

The component modes (i.e., engine mode, clutch mode, and electric motor mode) and signals of gear demand (odd/even) are generated when a gear shift is required, or the engine turns on. The gear selection control (synchronizer control) algorithm is unique to DCT systems (Figure 42). Once the gearshift schedule algorithm generates a new desired gear command, the gear selection control algorithm controls the synchronizer actuators to select the desired gear.

Example of gear shifting : 2nd → 3rd

- Check gear dmd if odd or even?
EV driving or HEV driving?
- Pre-selection : synchronizing 3rd in shaft1
- CL1 clutching / CL2 declutching
- CL1 locked / neutral of shaft2
- Finishing

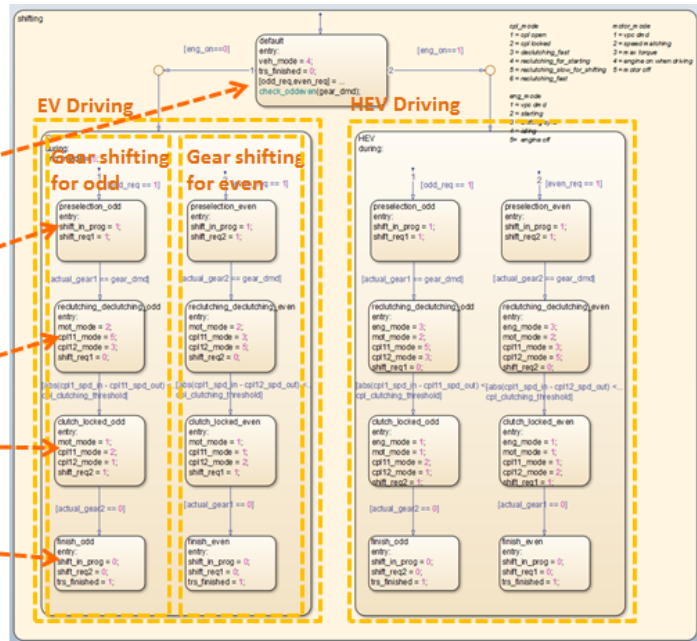


Figure 42. State diagram representation of the control strategy for a DCT

Clutch Controller

The clutch controls use time-based clutch position maps, as shown in Figure 43.

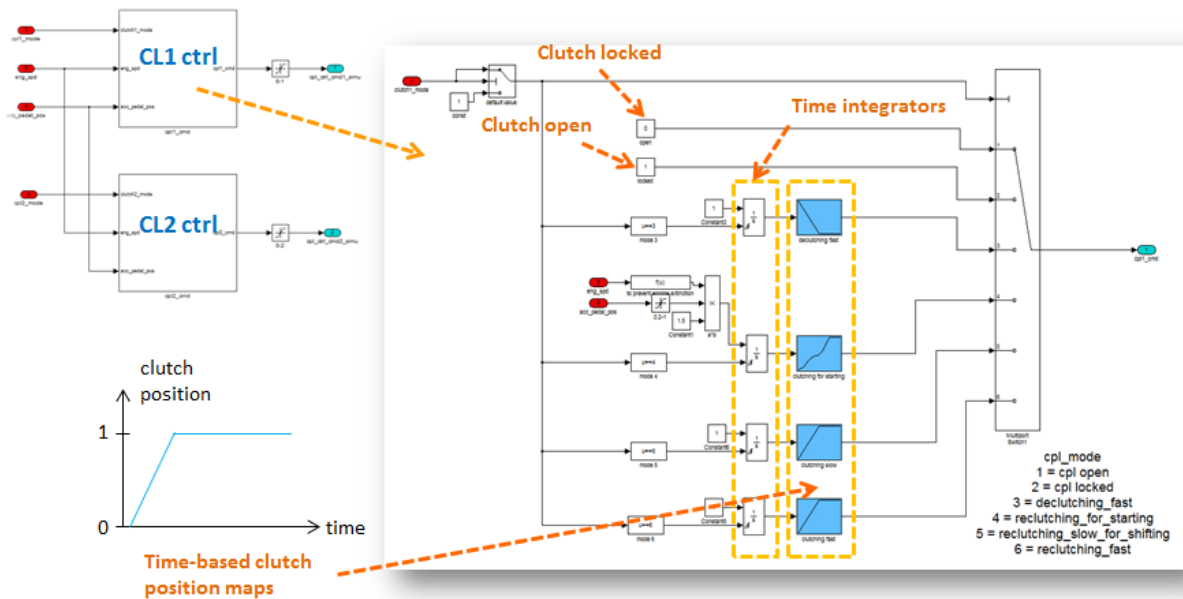


Figure 43. Clutch controller for DCT

Transmission Shifting

There are two parts to transmission shifting logic.

- Shift initializer
 - The shift initializer logic, implemented in the vehicle model, decides when to change gears. In addition to the shift maps, there are different thresholds in place (i.e., gear upshift demand validation) to ensure proper drive quality. One of the key parameters of the shifting logic is the shift map. For a given transmission, the shifting logic is the same in all vehicles.
- Shift controller

The shift controller consists of the following.

 - The shift map: There are two separate maps, one for upshift and one for downshift, which use vehicle speed and pedal position as inputs. Shift maps are developed for each individual vehicle/powertrain/component combination using a generic shifting algorithm.
 - The shifting algorithm: The shifting algorithm uses the component characteristics (e.g., engine brake-specific fuel consumption (BSFC), gear ratios, final drive ratio, wheel radius, etc.) to develop the shift maps. While energy consumption is very important, other drive quality metrics are also considered (e.g., avoiding low/high vehicle speeds, high torque demands, etc.)

Transmission shifting has a significant impact on vehicle energy consumption and should be carefully designed to maximize the powertrain efficiency while maintaining acceptable drive quality. The logic used in the simulated conventional light-duty vehicle models relies on two components: (1) the shifting controller, which provides the logic to select the appropriate gear during the simulation, and (2) the shifting initializer, the algorithm that defines the shift maps (i.e., the values of the parameters of the shifting controller) specific to a selected set of component assumptions. While the algorithm used to develop shift maps is similar across all vehicles, the shift maps are specific to each individual vehicle, as they are designed using component information such as gear and final drive ratios, BSFC, and so on.

Engine Lugging Limits

Engine lugging limit is a critical NVH parameter. The assumptions shown in Table 1 and Table 2 below describe the logic implemented in Autonomie to prevent lugging. The logic and values were developed based on AMTL vehicle test data analysis.

To ensure consistency with the different engine technologies using the vehicle test data, engine lugging limits for different geared transmissions are shown separately for NA and turbo-charged engines. Shift parameters are selected such that low-speed, high-torque operation is avoided. The selected shifting limits are based on test data observations relative to the number of gears available.

Table 1. Engine lugging limits for different transmissions (NA engines)

	5-speed	6-speed	7-speed	8-speed	9-speed	10-speed
Lugging speed (rad/s)	140	130	120	110	110	110
Lugging speed (rpm)	1337	1241	1241	1050	1050	1050

Table 2. Engine lugging limits for different transmissions (turbo engines)

	5-speed	6-speed	7-speed	8-speed	9-speed	10-speed
Lugging speed (rad/s)	140	130	130	130	130	130
Lugging speed (rpm)	1337	1241	1241	1241	1241	1241

Figure 44 shows the engine operating points for a 2017 Ford F-150 during a UDDS cycle (Lohse-Busch et al., 2018).

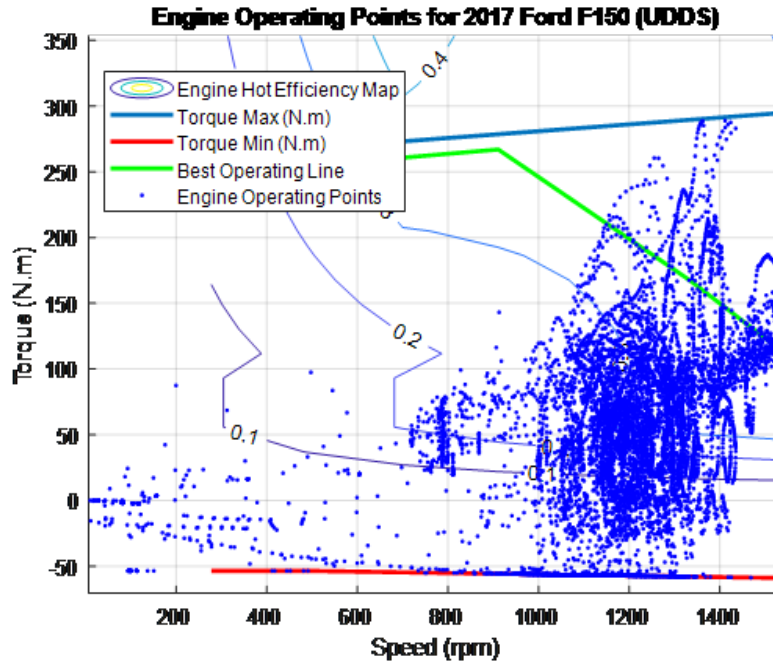


Figure 44. Engine operating points for 2017 Ford F150 (UDDS)

Figure 45 shows an example of how engine operating conditions are restricted to prevent lugging for 5-speed and 10-speed AUs on the UDDS cycle for an NA engine.

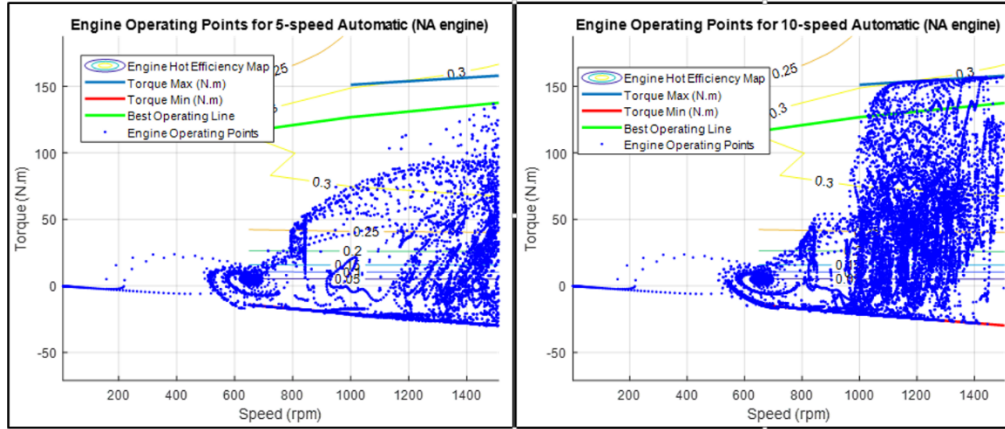


Figure 45. Example of engine operating conditions for 5-speed and 10-speed transmissions on UDDS cycle for NA engine

Shifting Initializer

The shifting controller uses shifting maps to compute the gear command. In the controller, the shift map is a two-dimensional lookup table indexed by vehicle speed and accelerator pedal position. Defining such a map is equivalent to defining the boundaries of each gear area; those boundaries are the shifting speeds. Figure 46 illustrates that equivalence.

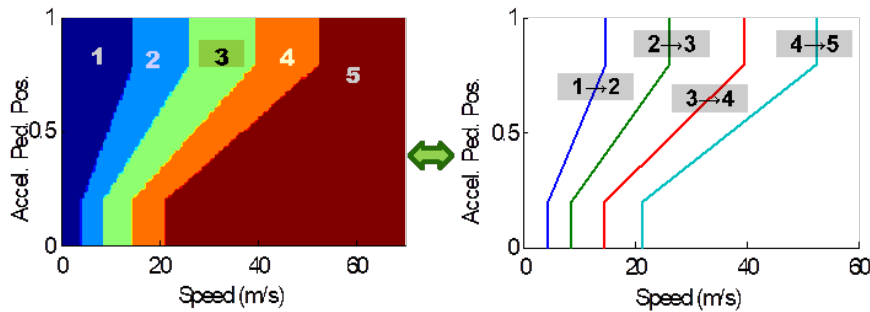


Figure 46. Upshifting gear map (left) and upshifting vehicle speeds (right)

For each shifting curve, there are two key points: the “economical” shifting speed (at very low pedal position) and the “performance” shifting speed (at high pedal position). The objective of the control engineer is to combine both goals of the shifting control to fulfill the driver’s expectations: minimization of energy consumption on the one hand and maximization of vehicle performance on the other.

The economical shifting speed for an upshift or a downshift is the speed at which the upshift/downshift occurs when the accelerator pedal is very lightly pressed: $V_{eco}^{k \rightarrow k+1}$ is the economical vehicle speed for upshifting from gear k to gear $k+1$, and $V_{eco}^{k+1 \rightarrow k}$ is the downshifting speed for this same set of gears. The vehicle speed shift points are computed from the engine shift points $\omega_{eco}^{k \rightarrow k+1}$ and $\omega_{eco}^{k+1 \rightarrow k}$. Figure 47 shows the engine speed shift points for an engine associated with a 5-speed transmission.

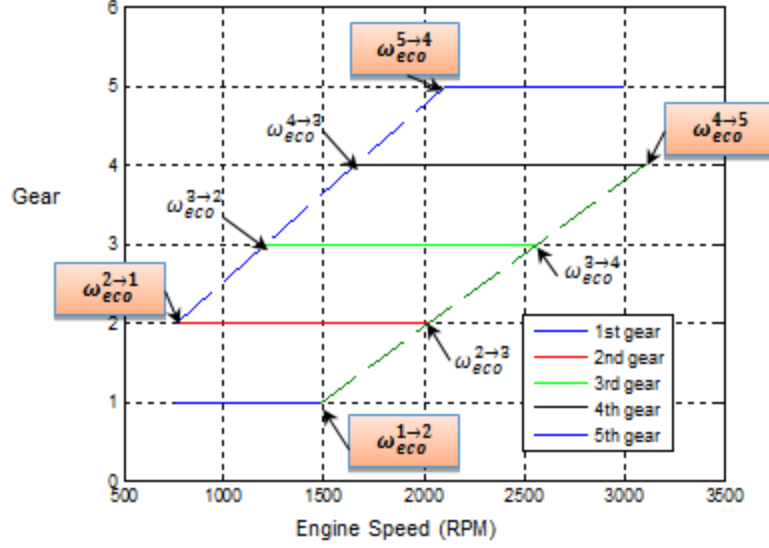


Figure 47. Example of engine speed range in economical driving and economical shift

The initializing algorithm for the shifting controller computes the upshifting and downshifting speeds at zero pedal position based on the four “extreme” shift points: upshifting from lowest gear ($\omega_{eco}^{1 \rightarrow 2}$), upshifting into highest gear ($\omega_{eco}^{N-1 \rightarrow N}$), downshifting into lowest gear ($\omega_{eco}^{2 \rightarrow 1}$), and downshifting from highest gear ($\omega_{eco}^{N \rightarrow N-1}$), where N is the number of gears. The speeds can be set by the user or left at their default values.

Below is a description of their default values in Autonomie.

$\omega_{eco}^{2 \rightarrow 1} = \omega_{idle} + \omega_{margin}$ where ω_{idle} is the engine idle speed, and ω_{margin} is the speed margin of $\approx 50-100$ rpm.

$\omega_{eco}^{1 \rightarrow 2} = \omega_{idle} \frac{k_1}{k_2} (1 + \epsilon_{ud})$ where k_1 and k_2 are gear ratios for gears 1 and 2, and ϵ_{ud} is the margin to avoid overlap, $\approx 0.05-0.1$.

$\omega_{eco}^{N-1 \rightarrow N}$ is the engine speed at which best efficiency can be achieved.

$\omega_{eco}^{N \rightarrow N-1} = \omega_{eco}^{N-1 \rightarrow N} - \omega_{\Delta}$ where $\omega_{\Delta} \approx 1,000$ rpm.

Once those four speeds are computed, the remaining ones are computed by linear interpolation to allow consistent shifting patterns that are acceptable to the driver. For example, any upshifting speed is given by Equation 29.

$$(29) \quad \omega_{eco}^{i \rightarrow i+1} = \frac{\omega_{eco}^{N-1 \rightarrow N} - \omega_{eco}^{1 \rightarrow 2}}{N-2} \times (i-1) + \omega_{eco}^{1 \rightarrow 2} \text{ where } 1 \leq i \leq N-1$$

In a shifting map, the vehicle upshifting speed from gear i to $i+1$ must be higher than the downshifting speed from gear $i+1$ to i . Otherwise, the downshifting speed will always request gear i while gear $i+1$ is engaged and vice versa, resulting in oscillations between gears that would be unacceptable to the driver. For this study, the algorithm in the initialization file prevents that by making sure the following relation is true.

$$(30) \quad \omega_{eco}^{i \rightarrow i+1} > \omega_{eco}^{i+1 \rightarrow i} \times \frac{k_1}{k_2} (1 + \epsilon_{ud}) \text{ where } 1 \leq i \leq N-1$$

The values of the engine economical shifting speeds at lowest and highest gears are automatically defined based on the engine and transmission characteristics.

Finally, the vehicle economical up- and downshifting speeds can be computed using the engine up- and downshifting speeds, the gear ratio, the final drive ratio, and the wheel radius.

$$(31) \quad V_{eco}^{i \rightarrow i+1} = \frac{\omega_{eco}^{i \rightarrow i+1}}{k_i k_{FD}} \times R_{wh} \text{ where } k_{FD} \text{ is the final drive ratio and } R_{wh} \text{ is the wheel radius}$$

During performance, the gears are automatically selected to maximize the torque at the wheel. Figure 48 illustrates that gear selection, which consists of finding the point at which the curve of engine peak torque (reported at the wheels) at gear k falls under the curve at gear $k+1$.

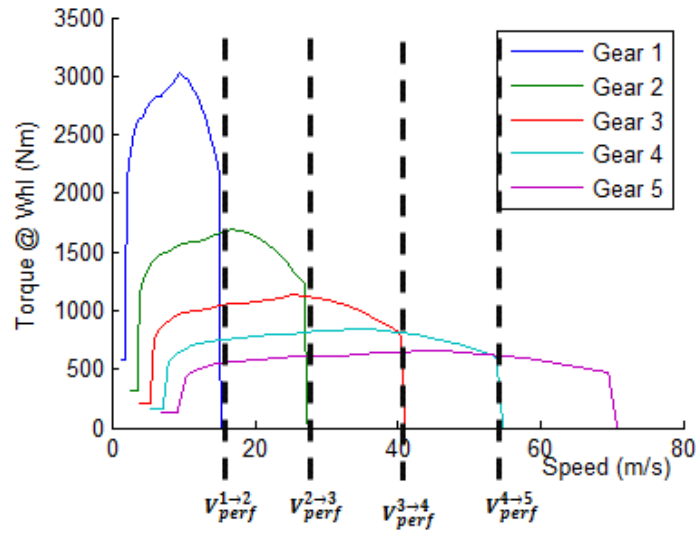


Figure 48. Maximum engine torque at wheels and performance upshift speeds

The performance downshifting speed is given by the performance upshifting speed and the difference between the economical shifting speeds.

$$(32) \quad \Delta V_{perf}^i = \alpha_{pf,ec} \times \Delta V_{eco}^i \Leftrightarrow V_{perf}^{i \rightarrow i+1} - V_{perf}^{i+1 \rightarrow i} = \alpha_{pf,ec} \times (V_{perf}^{i \rightarrow i+1} - V_{perf}^{i+1 \rightarrow i})$$

The definition of the final shifting curves is critical to properly evaluating the benefits of technologies while maintaining acceptable performance. Figure 49 shows how a set of upshifting and downshifting curves for two adjacent gears is built, based on selected vehicle speeds and accelerator pedal positions. At low pedal positions (i.e., below a_{eco}^{up}), the upshifting speed is the economical upshifting speed. Similarly, below a_{eco}^{dn} , the downshifting speed is the economical downshifting speed. This approach ensures optimal engine operating conditions under gentle driving conditions. At high pedal positions (i.e., above a_{perf}), the shifting speed is the performance shifting speed, ensuring maximum torque at the wheels under aggressive driving conditions.

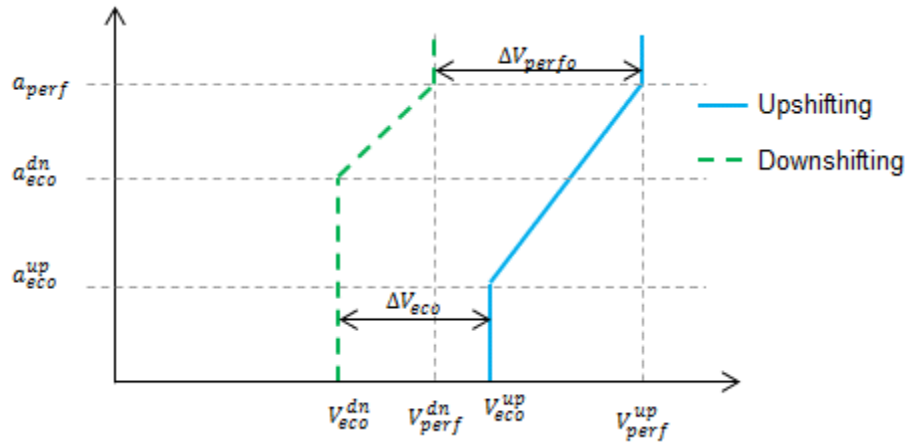


Figure 49. Design of upshifting and downshifting speed curves for two adjacent gears

Traditional Gear Shifting Controller

The shifting controller determines the appropriate gear command at each simulation step using the shifting maps developed by the shifting initializer. A simplified schematic of the controller is shown in Figure 50. The letters and numbers in the discussion that follows correspond to those shown in circles in Figure 50.

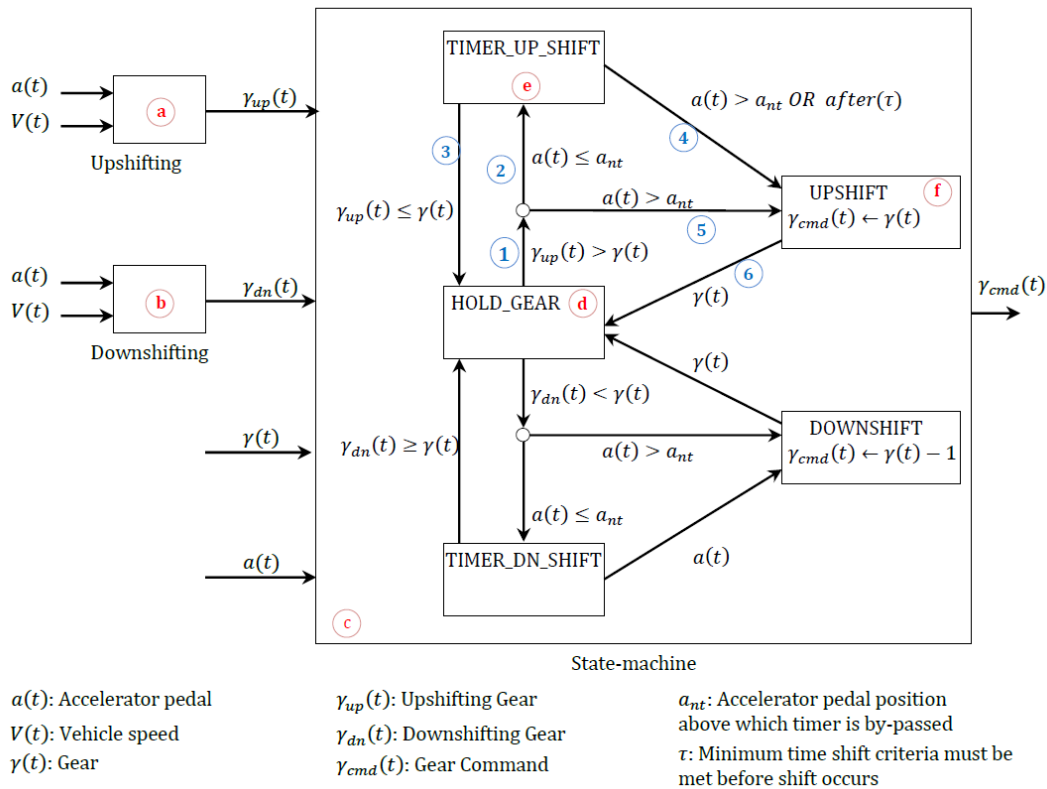


Figure 50. Shifting controller schematic in Autonomie

The controller is based on two main shifting maps—one for upshifting (a) or moving from a lower gear to a higher gear, and another one for downshifting (b) or moving from a higher gear to a lower gear—as well as a state machine (c) that defines the status of the system (e.g., no shifting, and upshifting). Each shifting map outputs a next-gear command $\gamma_{dn}(t)$ and $\gamma_{up}(t)$ based on the current accelerator pedal position $a(t)$ and vehicle speed $V(t)$. The state machine is composed of different states, of which only one is active at any time step; a change in state occurs whenever a transition condition from the active state becomes true (i.e., an upshift will occur only if a set of conditions is true).

The state that is active most of the time is the hold-gear state (d), which makes sense because most of the time, for drivability reasons, the vehicle should be in gear and not shifting. An upshift occurs when the upshifting gear $\gamma_{up}(t)$ is strictly higher than the current gear $\gamma(t)$ by 1 (e.g., $\gamma_{up}(t) = 5$ and $\gamma(t) = 4$).

For all vehicles, the shift does not necessarily happen instantly when the command to shift is given; it depends on the current pedal position. In aggressive driving, i.e., at high accelerator pedal positions (5), the shift happens as soon as the gear transition (1) becomes true, ensuring optimal performance. In contrast, in “normal” driving, i.e., at low pedal positions (2), there is an intermediate state (e) that allows the shift only when the gear condition (1) is true for a minimum time τ . This constraint is imposed to avoid an excessive number of shifting events, which would lead to unacceptable drive quality and increased energy consumption. The upshifting itself is executed in state (f), in which the shift command $\gamma_{cmd}(t)$ is incremented (i.e., the next upper gear is selected); once the shifting is completed (6), the state machine comes back to the hold-gear state (d). Downshifting occurs in a similar way.

As an additional level of robustness in the Autonomie control algorithm, an upshift or downshift cannot occur if the resulting engine speed would be too low or too high, respectively. This approach ensures that the engine is not operated below idle or above its maximum rotational speed, as shown in Figure 51.

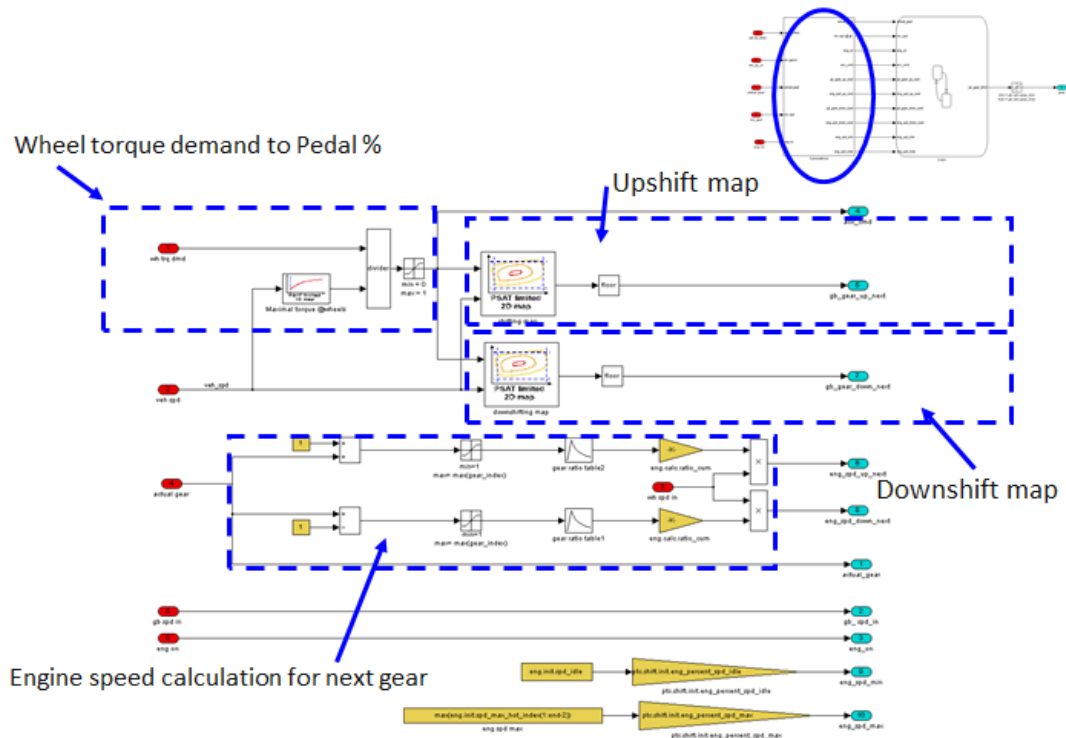


Figure 51. Shifting calculations in Autonomie

Torque Control During Shifting Events for Automatic Transmission

Figure 52 shows the transmission clutch pressure, output torque, and engine speed curves during a change from first to second gear. The output torque experiences both a trough period (lower than the torque in the original gear) and a crest period (higher than the torque in the original gear). The trough period is called a torque hole, while the crest period is called a torque overshoot. The torque hole is defined by depth and width, where the depth is the difference between minimum torque and the torque in previous gear, and the width is the half value of the maximum width of the torque hole.

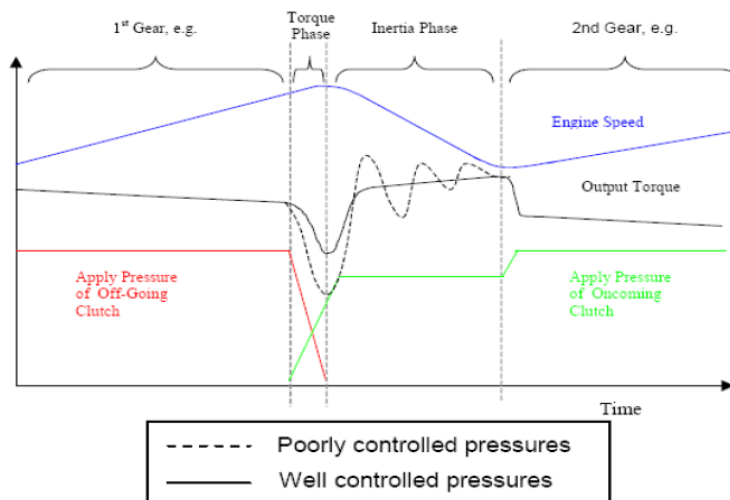


Figure 52. Shift process for AU

The bigger the torque hole, the larger the decrease of torque in torque phase, resulting in a more significant reduction in acceleration. Because the decrease in acceleration causes discomfort for both the driver and passengers, the torque hole should be as shallow and narrow as possible. Torque reduction behavior is a well-known phenomenon, observed during vehicle testing and referenced in several papers and presentations.

Autonomie integrates a low-level control algorithm that reproduces the torque hole phenomenon. Figure 53 illustrates the behavior of the vehicle model for a short period of time (205 to 205.8 s). The area highlighted by the oval outline indicates the torque hole during a shifting event.

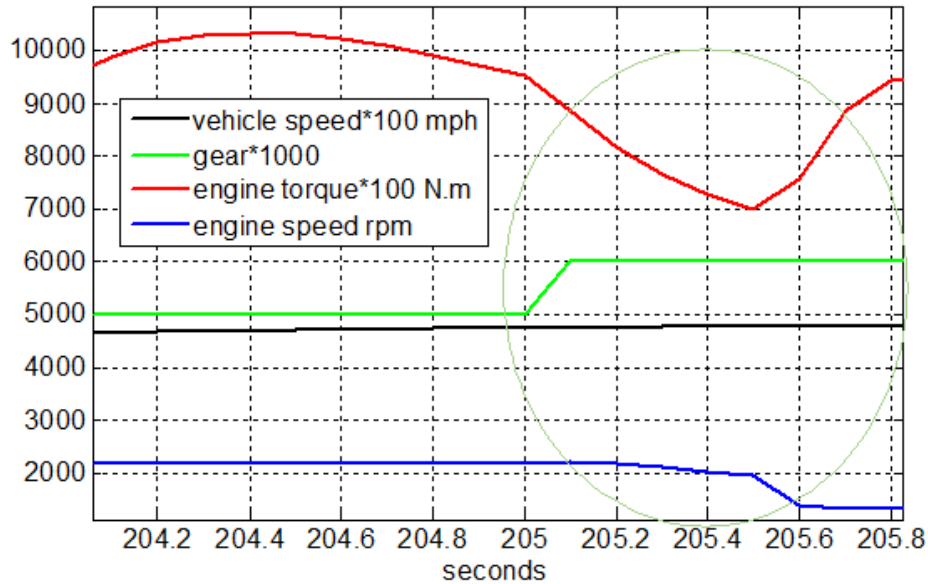


Figure 53. Torque hole in Autonomie during shifting event

Gear Skip-Shifting Strategy

For the current set of runs, a gear skip-shifting strategy was developed and implemented for 10-speed transmissions using the Ford F-150 10-speed benchmarking report (Lohse-Busch et al., 2018). It is shown in Table 3.

Table 3. Detailed gear-shifting events for Ford F-150.

# of Shifts	1-2	1-3	2-3	2-4	3-4	3-5	4-5	4-6	5-6	6-7	7-8	8-9	9-10	Total
UDDS		18			14	5	16	1	21	12	4	1	2	94
Highway		1			1		1		1	2	2	5	5	18
US06	1	6		1		7	1		9	5	7	5	11	53

From the table, a consistent gear-skipping can be observed for the drive cycles covered in the study. A similar gear-skipping method was implemented for this analysis. Table 4 details the shifting events for the different cycles in simulation of pickup-nonperfo/micro hybrid/eng12/MR0/AERO0/ROLL0.

Table 4. Argonne simulated gear-shifting events for 10-speed transmission

Cycles	1-2	1-3	2-3	3-4	3-5	4-5	5-6	6-7	7-8	8-9	9-10	Total
UDDS		18			18		21	12	1	1	2	73
Highway		1			1		1	2	2	4	3	13
US06		7			8		8	7	5	6	4	46

Engine Start Control for Pre-Transmission HEVs

The vehicle speed, engine speed, and electric motor torque for engine start-up are compared with the vehicle test results for $t = 21-24$ sec in Figure 54. The single clutch (CPL2) is located inside the electric machine, between the engine and the electric machine. The clutch is engaged when starting the internal combustion engine.

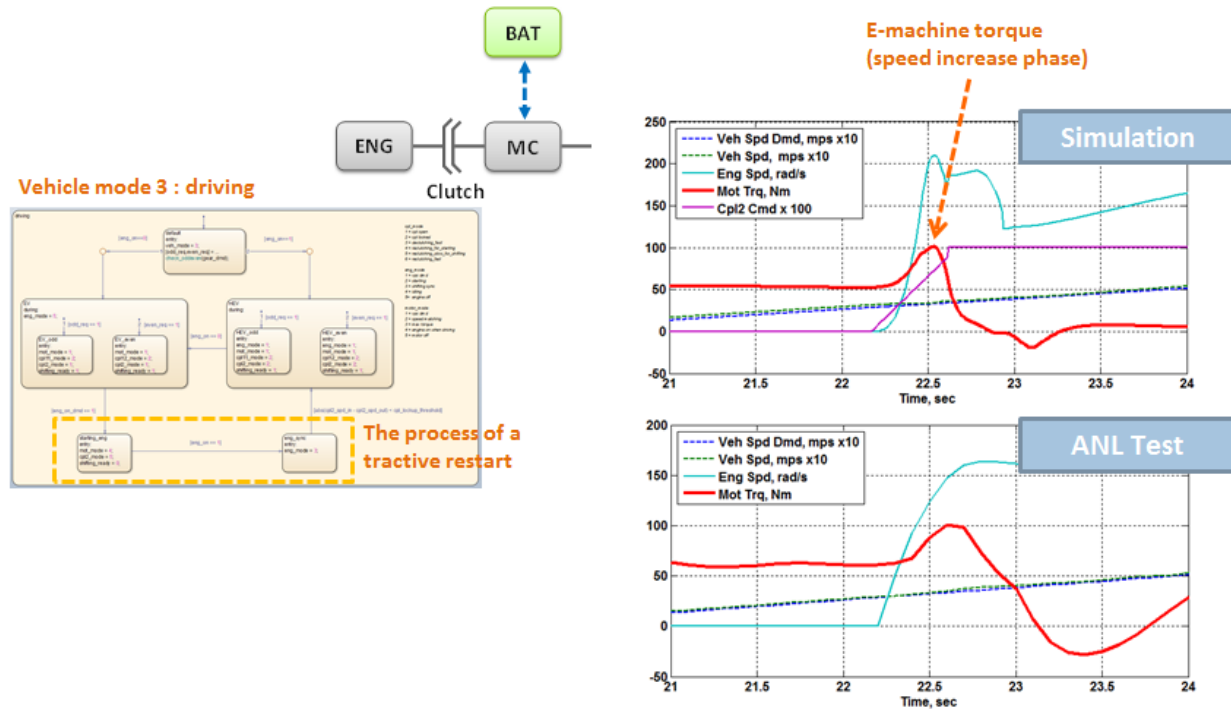


Figure 54. Engine start transient control using electric machine

The electric machine torque is also controlled to quickly synchronize the clutch I/O speed. The controller reacts by setting a torque-increasing intervention that is added to the torque of the electric machine in the speed increase phase.

Torque Converter

A torque converter is a hydrodynamic fluid coupling used to transfer rotating power from a prime mover, such as an ICE, to a rotating driven load. It consists of an impeller (drive element), a turbine (driven component), and a stator (a set of stationary windings that generate a magnetic field) that assists the torque converter function. The torque converter is filled with oil and transmits the engine torque by means of the flowing force of the oil. The device compensates for speed differences between the engine and the other drivetrain components and is ideally suited to the start-up function.

The torque converter is modeled as two separate rigid bodies when the coupling is unlocked and as one rigid body when the coupling is locked. The downstream portion of the torque converter unit is treated as being rigidly connected to the drivetrain. Therefore, there is only one degree of dynamic freedom, and the model has only one integrator. This integrator is reset when the coupling is locked, which corresponds to the loss of the degree of dynamic freedom. Figure 55 shows the efficiency of the torque converter used for the study.

The effective inertias are distributed downstream until actual integration takes place. When the coupling is unlocked, the engine inertia is dispersed up to the coupling input, where it is used for calculating the rate of change of the input speed of the coupling. When the coupling is locked, the engine inertia is scattered all the way to the wheels.

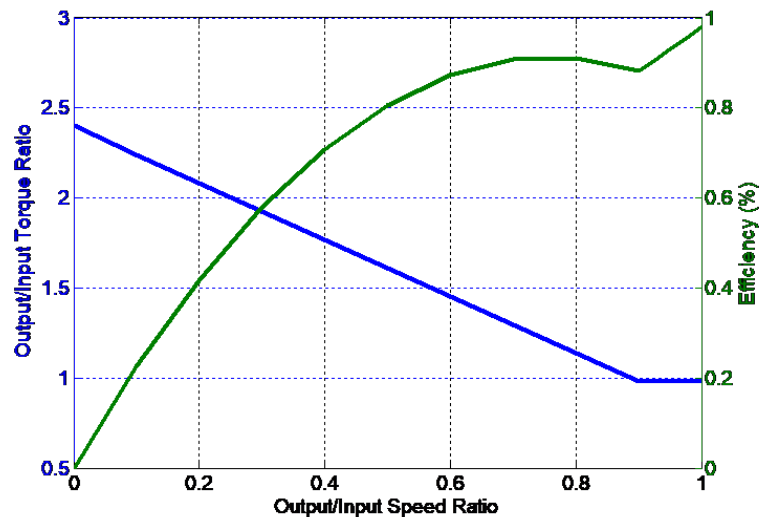


Figure 55. Typical torque converter efficiency

Figure 56 describes the conditions under which the torque converter will be locked. The same algorithm is used to represent current torque converter lockup logic as well as future aggressive lockup logic. The torque converter is used as a start-up device in first gear, with very low slip (torque ratio of 0.95) at higher speeds in first gear. Recent trends in torque-converter technology suggest operation in locked or controlled-slip mode in second and higher gears. In general, the torque converter is in controlled slip mode or mechanically locked, depending on vehicle speed and pedal position, for each gear apart from the first. To suggest advances in torque converter technology, it was assumed that the torque converter would be in a mechanically locked state for the second and higher gears. This approach has been applied to all transmissions with six gears or more. The logic does not change between different AUs types (AU/AU+/AU++).

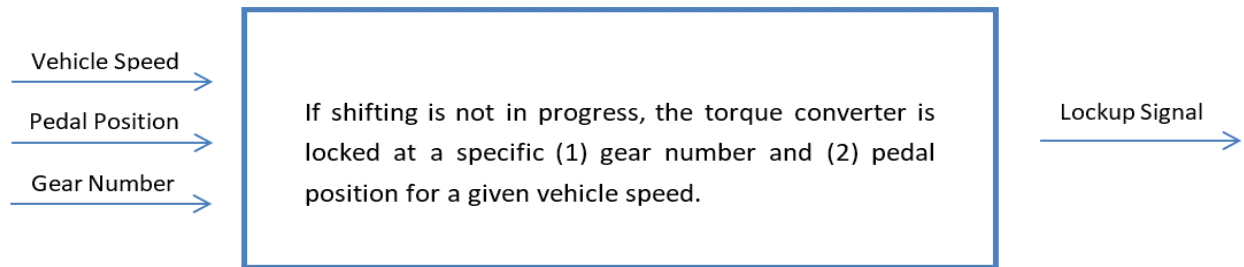


Figure 56. Torque converter lockup control algorithm

Plant Model

Figure 57 shows the main I/O of the torque converter model. The torque converter model is based on a lookup table, which determines the output torque depending on the lockup command. The upstream acceleration during slip and the downstream acceleration are considered in calculating the output speed.



Figure 57. Autonomie torque converter model I/O

Operational Modes

The different operational modes are described below.

- Mode 1: Idle
We enter this mode if $W_{in} < W_{eng_idle} + \text{Threshold}$. We quit the mode if $W_{in} > W_{eng_idle} + \text{Threshold}$ and T_{in} is increasing and positive.
- Mode 2: Acceleration (transient calculation)
We are in this mode if $T_{in} > 0$ and $\text{Speed_Ratio} < 0.1$ (meaning $W_{in} \gg W_{out}$).
- Mode 3: Steady state
We are in this mode if $W_{in} > W_{eng_idle} + \text{Threshold}$ and W_{in} is close to W_{out}
OR $\text{Speed_Ratio} > 0.8$ (W_{in} close to W_{out})
OR $T_{in} < 0$.
- Mode 4: Locked
We enter this mode if the torque converter command is 1.

Steady-State Calculation

Figure 58 details the steady-state operational mode calculation of the torque converter model.

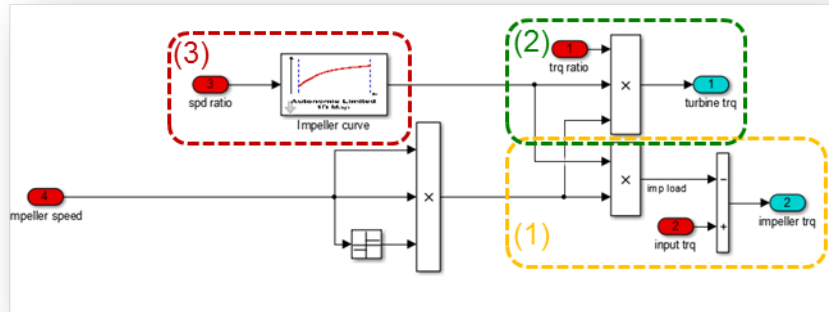


Figure 58. Steady-state mode calculation

$$(33) \quad T_{impeller} = T_{in} - [K_{in} \times \omega_{impeller}^2 \times \text{sign}(\omega_{impeller})]$$

$$(34) \quad T_{turbine} = T_{ratio} \times K_{in} \times \omega_{impeller}^2 \times \text{sign}(\omega_{impeller})$$

$$(35) \quad K_{in} = \frac{1}{\text{capacity_factor}^2} = f(\omega_{ratio})$$

$$T_{ratio} = f(\omega_{ratio})$$

$$\omega_{impeller} = \int \frac{T_{impeller}}{J_{impeller}}$$

$$\omega_{ratio} = \frac{\omega_{turbine}}{\omega_{impeller}}$$

Transient Calculation

Figure 59 details the transient operational mode calculation of the torque converter model.

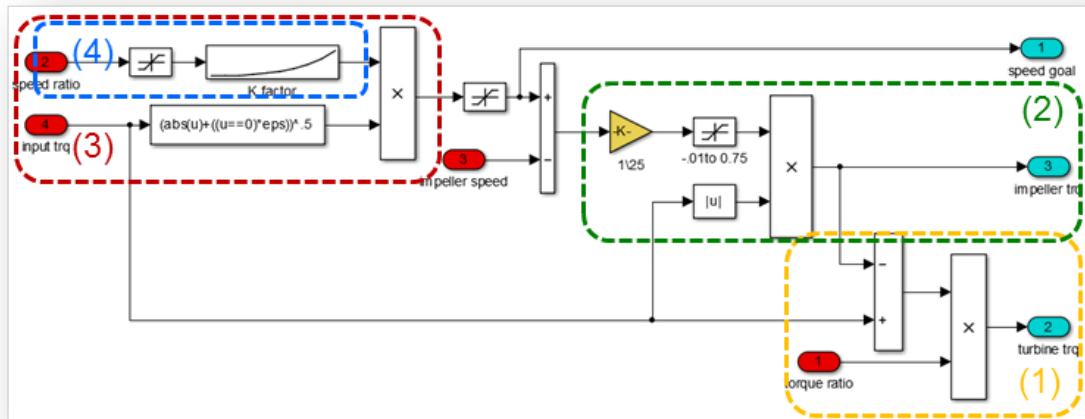


Figure 59. Transient mode calculation

$$(36) \quad T_{turbine} = (T_{in} - T_{impeller}) \times T_{ratio}$$

$$(37) \quad T_{impeller} = |T_{in}| \times \frac{\omega_{goal} - \omega_{impeller}}{gain}$$

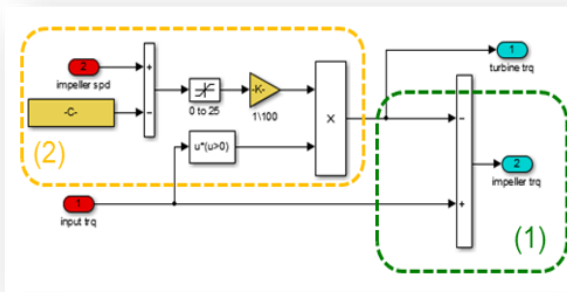
$$(38) \quad \omega_{goal} = capacity_factor \times T_{in}^{0.5}$$

$$(39) \quad capacity_factor = \frac{\omega_{impeller}}{\sqrt{T_{impeller}}} = f(\omega_{ratio})$$

$$\omega_{impeller} = \int \frac{T_{impeller}}{J_{impeller}}$$

Idle Calculation

Figure 60 details the idle operational mode calculation of the torque converter model. Figure 61 illustrates the list of initialization parameters for the torque converter model in Autonomie.



$$(1) \quad T_{impeller} = T_{in} - T_{turbine}$$

$$(2) \quad T_{turbine} = T_{in} \cdot \frac{\omega_{impeller} - \omega_{engine_idle}}{gain}$$

$$\omega_{impeller} = \int \frac{T_{impeller}}{J_{impeller}}$$

Figure 60. Idle mode calculation

$$capacity_factor(k) = \frac{\omega_{impeller}}{\sqrt{T_{impeller}}} = f(\omega_{ratio})$$

Name	Unit	Description	Size
cpl.plant.init.trq_impeller.idx1_spd	rad/s	Impeller speed index used to index impeller torque map; used in calculating the "k" factor	1*n
cpl.plant.init.trq_impeller.map	Nm	Impeller torque map indexed by impeller speed index; used in calculating the "k" factor	1*n
cpl.plant.init.k_factor.idx1_spd_ratio	-	Speed ratio vector used to index the torque ratio map or k factor	1*n
cpl.plant.init.k_factor.map	(rad/s)/sqrt(Nm)	Torque converter "k" value calculated from impeller speed index and impeller torque map used in the transient calculation block to calculate the desired impeller speed	1*n

Figure 61. Initialization parameters

Energy Storage Model

The energy storage system block models the battery pack as a charge reservoir and an equivalent circuit. The equivalent circuit accounts for the circuit parameters of the battery pack as if it were a perfect open-circuit voltage source in series with an internal resistance and two resistor-capacitor (RC) circuits that represent the polarization time constants. Figure 62 shows the main I/O of the energy storage model.



Figure 62. Autonomie energy storage model I/O

Autonomie includes several energy storage models for use in various high power and high energy applications:

- High-power application: One battery model is used as a charge reservoir. An equivalent circuit, the parameters of which are a function of the remaining charge in the reservoir (also known as the state-of-charge), accounts for circuit parameters of the battery pack as if it were a perfect open-circuit voltage source in series with an internal resistance.
- High-energy application: Another battery model in Autonomie, used for high-energy batteries, uses two-time constants to represent the polarization behavior of the battery pack. This lumped parameter model can represent internal resistance, capacitance, and open-circuit voltage—all maps based on SOC and in some cases temperature—for many different battery chemistries.

The pulse power limits of the battery pack are another important aspect to consider for sizing. There are several different options to represent the maximum power of the battery. The main one represents maximum power as a function of SOC. Other models introduce a time constraint for the maximum power. These battery packs have different power limits for 10-second, 2-second, and continuous power. The model accounts for the duration of the pulse and limits power accordingly. This aspect is not necessarily a feature of the plant, but rather is handled by the low-level control and is dependent on the battery chemistry and the plant's performance characteristics.

High-Power Battery Model (Used for HEVs)

Figure 63 shows the top-level diagram of the high-power battery model.

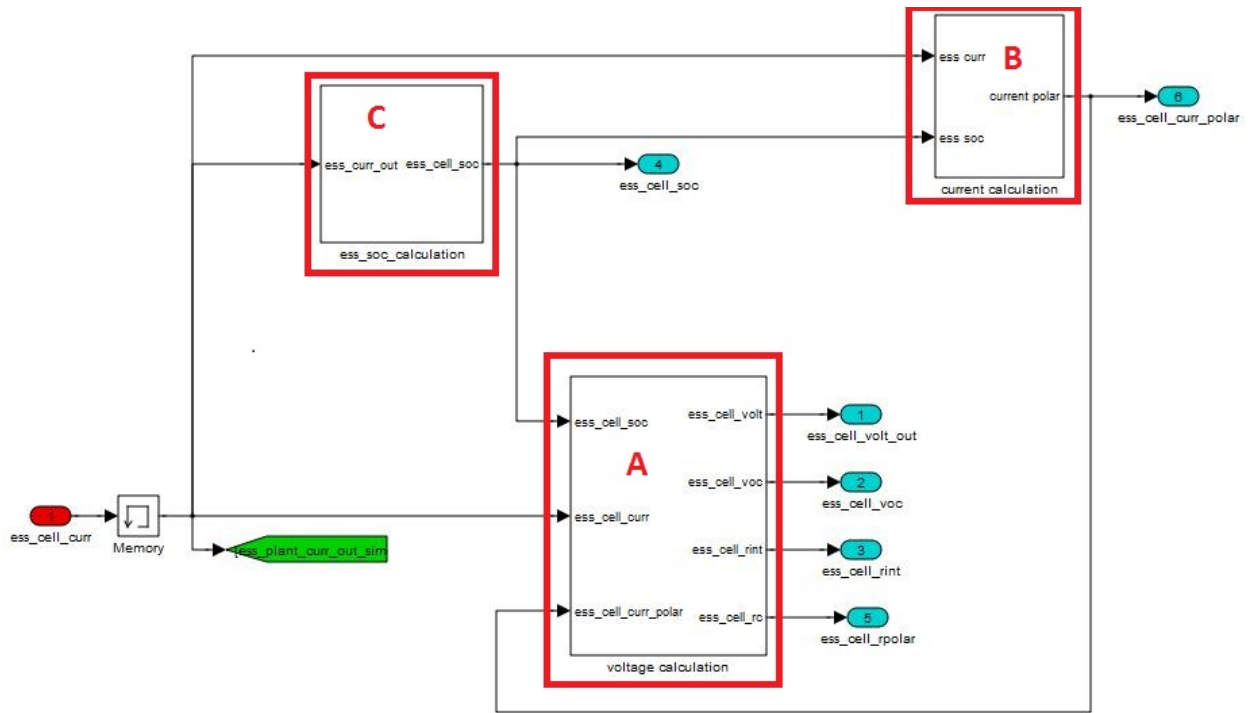


Figure 63. High-power battery model diagram in Autonomie

The top-level diagram of the high-power model consists of three main blocks: the voltage calculation (Block A), the current calculation (Block B), and the SOC calculation (Block C).

Block A (Figure 64) calculates the output voltage by taking the open-circuit voltage, which depends on SOC, and subtracting three terms: the voltage drop due to the internal resistance of each cell, the voltage drop due to the polarization resistance of each cell, and the voltage drop due to an effective series, modeling the variation of output voltage with the time essential of the current.

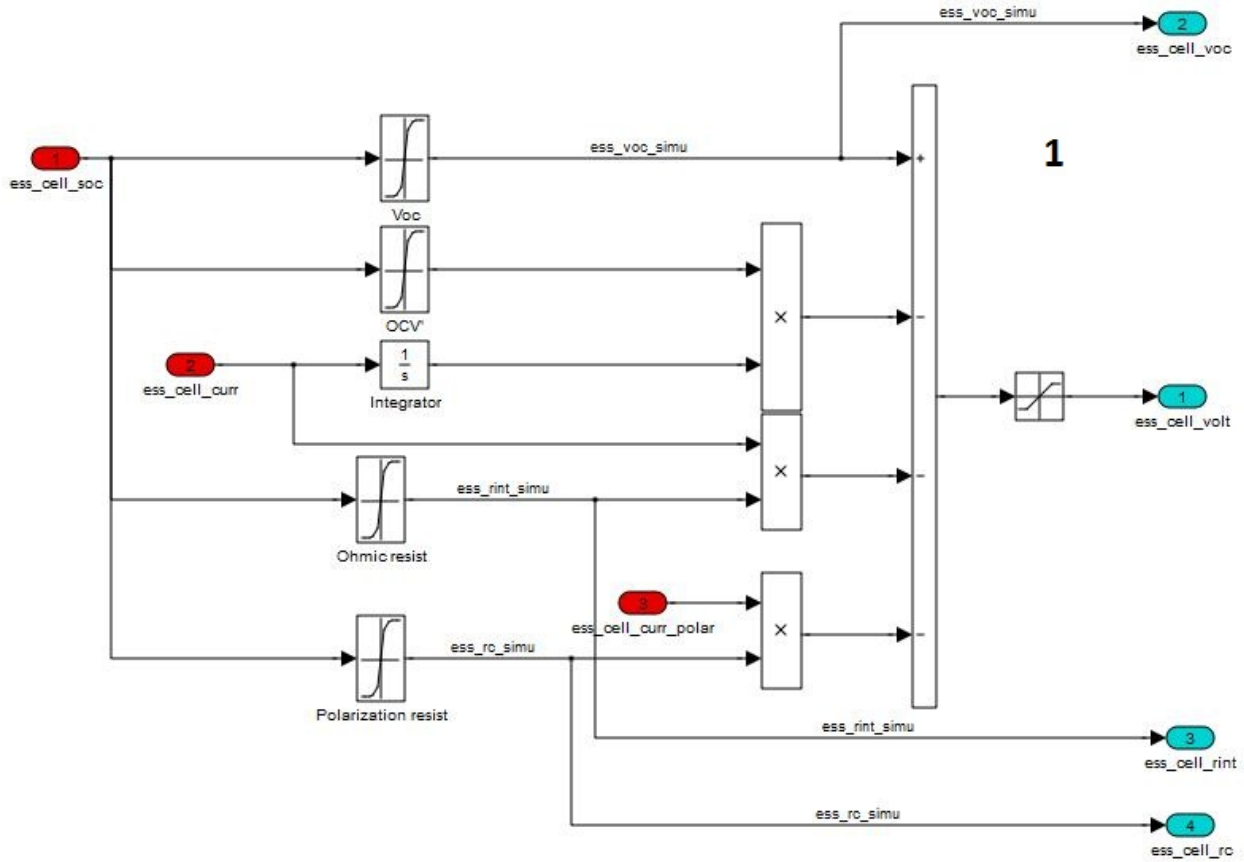


Figure 64. Block A: High-power battery model output voltage calculation

The polarization current causes an additional voltage drop at the terminals of the battery. As the current continues to flow in one direction through the cell, this voltage drop increases. As the ions migrate in a lithium-ion cell, it takes more work to keep the current flowing in the same direction. However, when the current reverses, the migrated ions facilitate current flow in the reverse direction.

$$(40) \quad V_{out} = V_{oc} - OCV \times \int I_{load} \times dt - R_0 \times I_{load} - R_p \times I_p$$

where:

I_{load} = current flowing into the load, that is, the input current from the voltage bus

OCV = series capacitance of the battery modeling the variation of output voltage with the time integral of the current

R_0 = series internal resistance of a cell

R_p = polar resistance of a cell

I_p = polar current in a cell

In Block B (Figure 65), the polarization current is calculated by solving differential Equation 41.

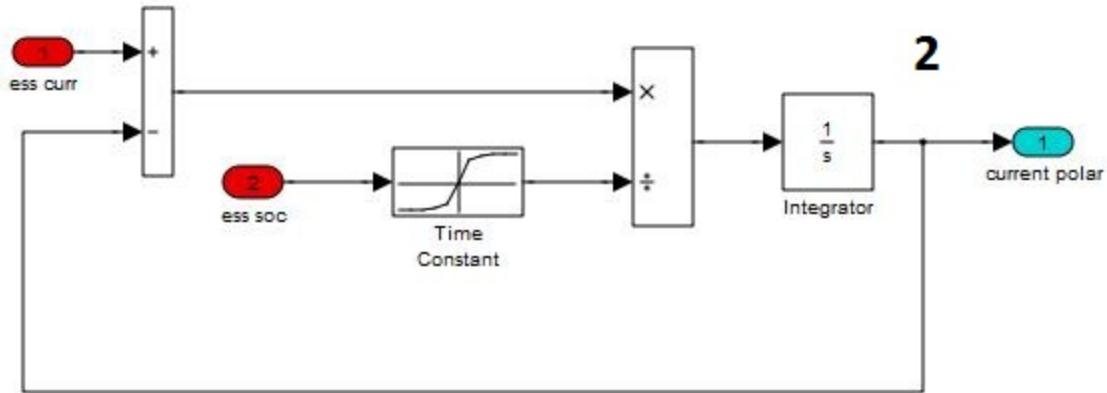


Figure 65. Block B: High-power battery model current calculation

$$(41) \quad \tau_p(SOC) \times \frac{dI_p}{dt} + I_p = I_{load}$$

In Block C (Figure 66), the SOC for the battery is calculated. If the SOC drops too low, the stop block automatically stops the simulation.

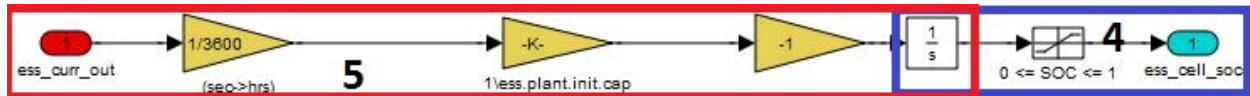


Figure 66. Block C: High-power energy model SOC calculation

$$(42) \quad SOC = SOC_{init} + \Delta SOC$$

$$(43) \quad \Delta SOC = - \int \frac{I_{in}}{Capacity_{max}}$$

where:

SOC_{init} = initial SOC (initial value of the integrator)

I_{in} = input current into the battery from the bus

$Capacity_{max}$ = maximum charge capacity

The SOC is calculated by determining the variation of charge in the battery and dividing it by the maximum coulombs the battery can store. A value of 0 is the unattainable state of having no charge remaining in the battery, while a value of 1 is the unattainable state of having a perfectly charged battery. Attempting to reach either of these values in practice would damage the battery and result in a short lifespan.

In practice, different values of minimum and maximum SOC values are used, depending on the battery chemistry and applications.

High Energy Battery Model (Used for PHEVs and BEVs)

Unlike the high-power battery model, the high-energy battery model uses two polarization resistances. The top-level diagram of the high-energy battery model in Figure 67 comprises three main blocks: the voltage calculation (Block A), the current calculation (the two B blocks correspond to the two current polarizations), and the SOC calculation (Block C).

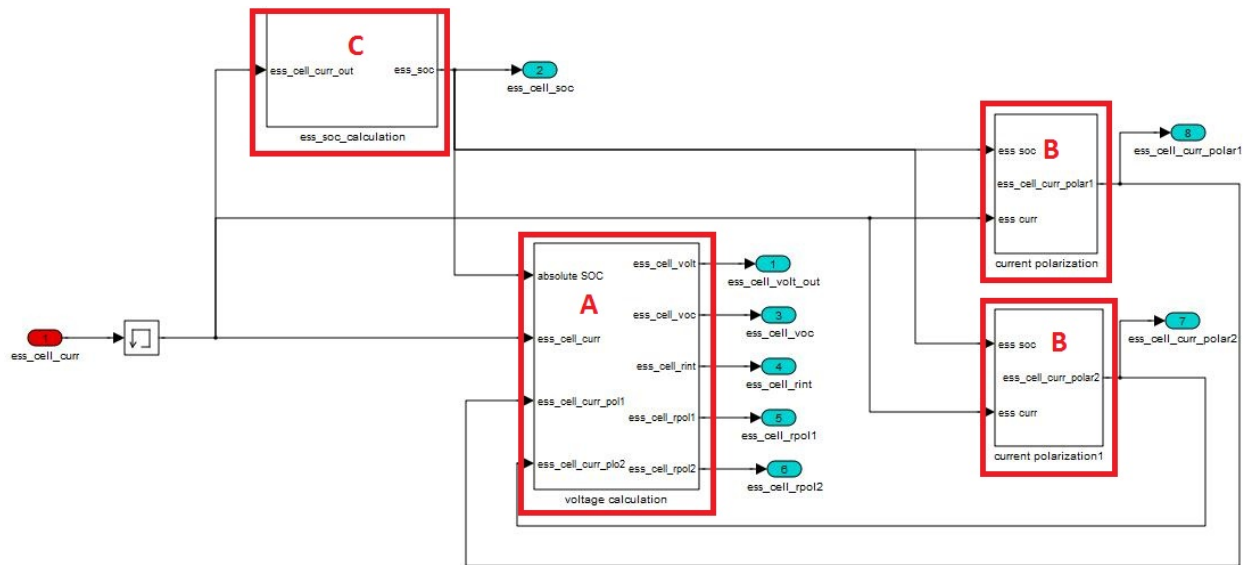


Figure 67. High-energy battery model diagram in Autonomie

Electric Machine Models

The electric machine transforms electrical power into mechanical power by creating a magnetic field that applies a force to current-carrying conductors. Electric machines that operate on this principle can be divided into two main categories: DC electric machines and AC electric machines. DC electric machines can be further divided into electric machines with and without brushes. AC electric machines can also be divided into two main categories: synchronous and asynchronous. The AC electric machine categories can be even further subdivided based on the number of phases. Figure 68 shows the main I/O of the electric machine model in Autonomie.

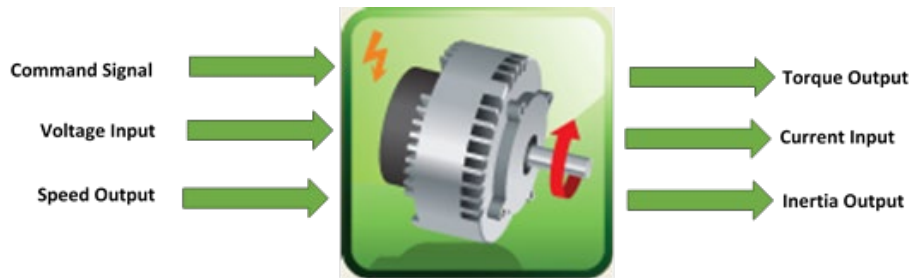


Figure 68. Autonomie electric machine model I/O

All electric machines consist of two major parts: the stator, a set of stationary windings that generate a magnetic field that encompasses the rotor or armature, and the second part, the rotor or armature, which is the rotating part.

Electric machine plant models in Autonomie use torque or power as the command and produce a torque output. The electric machine operating speed is determined by components connected to the electric machine. In a vehicle, the vehicle speed and gear ratios determine the electric machine operating speed. The lookup table used in an electric machine model estimates operational losses over the entire operating region.

An electric machine typically has a continuous operating region (under the continuous torque curve) and a transient region in which the electric machine can operate for a short period of time.

The peak torque capability of an electric machine is defined for a specific duration, such as 30 seconds. The maximum torque output gets de-rated to continuous torque levels when the electric machine's temperature increases. The electric machine model in Autonomie has this general logic built into it.

Figure 69 shows the general map-based electric machine model used in Autonomie. It has three essential maps that include:

- continuous torque as a function of speed,
- maximum torque as a function of speed, and
- a four-quadrant efficiency map as a function of speed and torque.

A warm-up time constant is used to interpolate between the maximum and continuous torque curves of the electric machine. The maximum-torque curve and efficiency map do not depend on the electric machine input voltage. Except for the fuel-cell-only configuration, this is the default electric machine model used in all configurations.

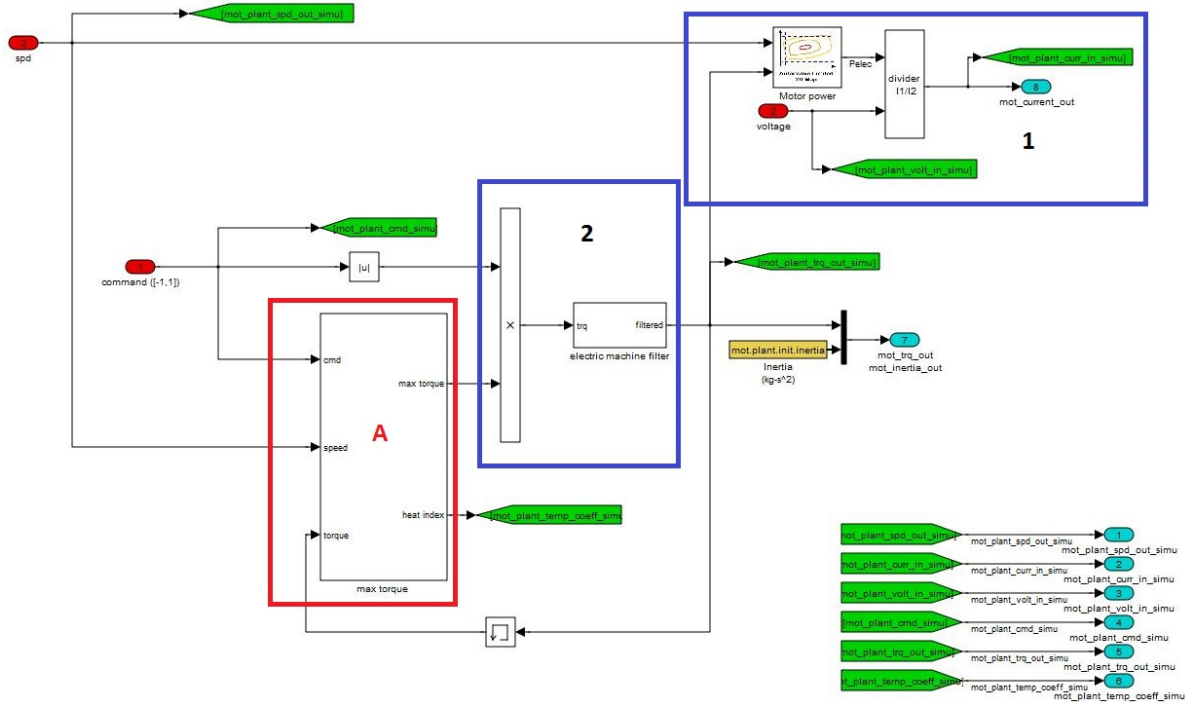


Figure 69. Autonomie electric machine model in Simulink

Equation 44 calculates the electric machine current:

$$(44) \quad I_{in} = \frac{P_{electrical}}{V_{in}}$$

Equation 45 computes the electric machine output torque by using the electric machine command and the maximum available torque of the electric machine at a given temperature and speed.

$$(45) \quad T_{out} = T_{max} \times PWM_{cmd}$$

Figure 70 shows the diagram of Block A for the max torque calculation of the electric machine model.

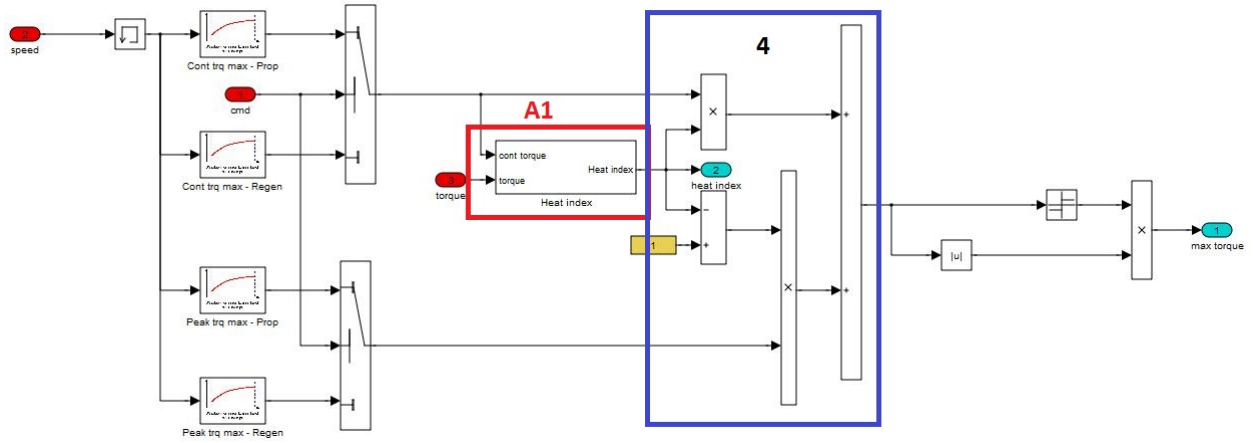


Figure 70. Block A: Electric machine model max torque calculation

Equation 46 interpolates between the continuous-torque curve and the maximum-torque curve by using the heat index. If the electric machine is hot, then the continuous-torque curve is used (i.e., the heat index is 1). If the electric machine is at its operating temperature, then the maximum-torque curve is used.

$$(46) \quad T_{max_{mechanical}} = T_{cont} \times PWM_{heatindex} + T_{peak} \times (1 - PWM_{heatindex})$$

Equations 47 through 51 show the dependence of the electric machine torque curves on the electric machine speed.

$$(47) \quad T_{cont} = T_{cont_{prop}} = function(W_{in})$$

$$(48) \quad T_{peak} = T_{peak_{prop}} = function(W_{in})$$

$$(49) \quad T_{cont} = T_{cont_{regen}} = function(W_{in})$$

$$(50) \quad T_{peak} = T_{peak_{regen}} = function(W_{in})$$

$$(51) \quad T_{max_{electrical}} = function(W_{in}, P_{electrical})$$

Figure 71 shows Block A1 for the heat index calculation of the electric machine model.

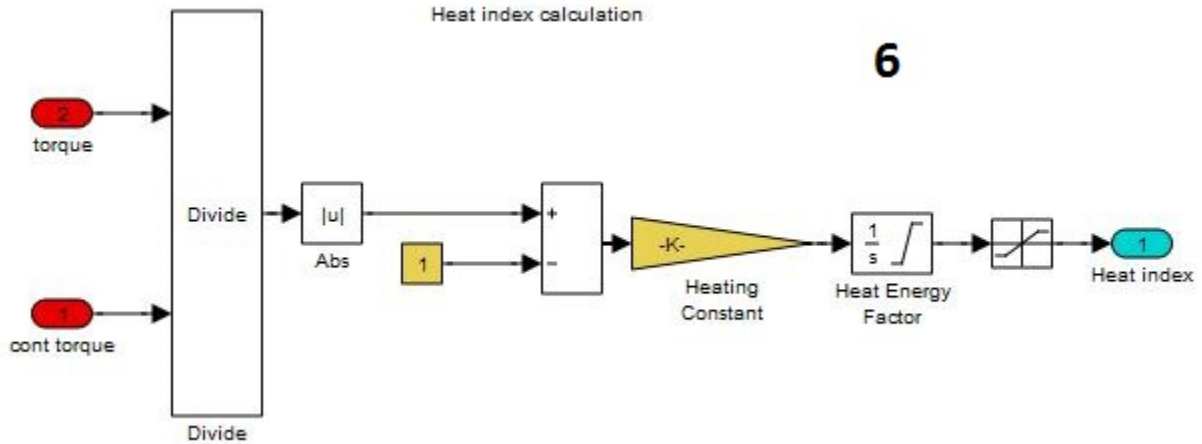


Figure 71. Block A1: Heat index

Equation 52 computes the heat index of the electric machine.

$$(52) \quad PWM_{Heatindex} = -0.3 + \int \frac{0.3}{\tau} \times \left(\frac{T_{out}}{T_{cont}} - 1 \right) \times dt$$

Electrical Accessories Model

Electrical accessories, such as lamps, radiator fans, and wipers, obtain their energy from an electrical source. They represent dedicated auxiliary load systems.

The plant model of an electrical accessory loss uses a constant power draw. The model considers the electrical losses associated with the powertrain. The current losses are taken from the energy storage. While the accessory load varies under real-world driving conditions, it is fairly constant during standard driving cycles. Therefore, the approach of constant power draw is valid for the study. Figure 72 shows the main I/O of the electrical accessories model.



Figure 72. Autonomie electrical accessories model I/O

Figure 73 shows the Simulink diagram for the electrical accessories model.

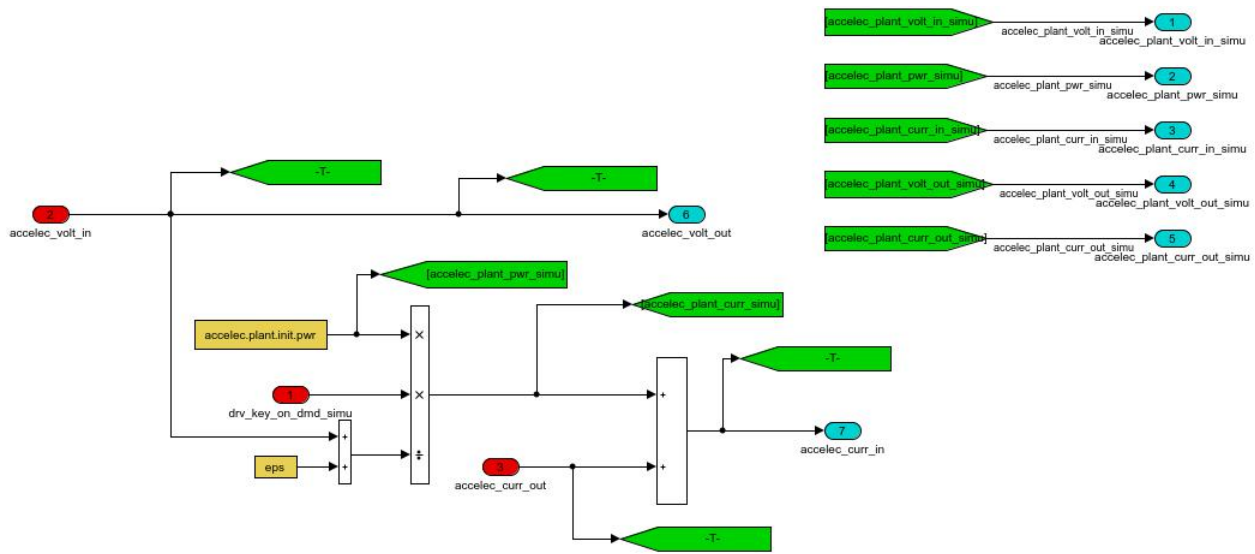


Figure 73. Top-level Simulink diagram of electrical accessories model

Two equations govern the electrical-accessories plant model:

$$(53) \quad I_{in} = I_{out} + \frac{P_{loss}}{V_{in}}$$

$$(54) \quad V_{out} = V_{in}$$

The current drawn by the accessory load is the constant power loss constant divided by the bus voltage. As shown in Equation 53, the total current flowing in is the sum of the current sunk by the accessory load and the output current distributed back to this model.

Driver Model

The driver model uses a look-ahead controller to model the accelerator and brake pedals. The desired vehicle speed is compared with the current speed, and a controller is used to request more or less torque to the vehicle. Figure 74 shows the main I/O of the driver model.



Figure 74. Autonomie driver model

The look-ahead model estimates the additional torque needed to meet the speed trace in the next Δ seconds to provide a more realistic model of driver behavior. This approach avoids unrealistic high torque demands during acceleration. Figure 75 shows the top-level diagram of the driver model in Autonomie.

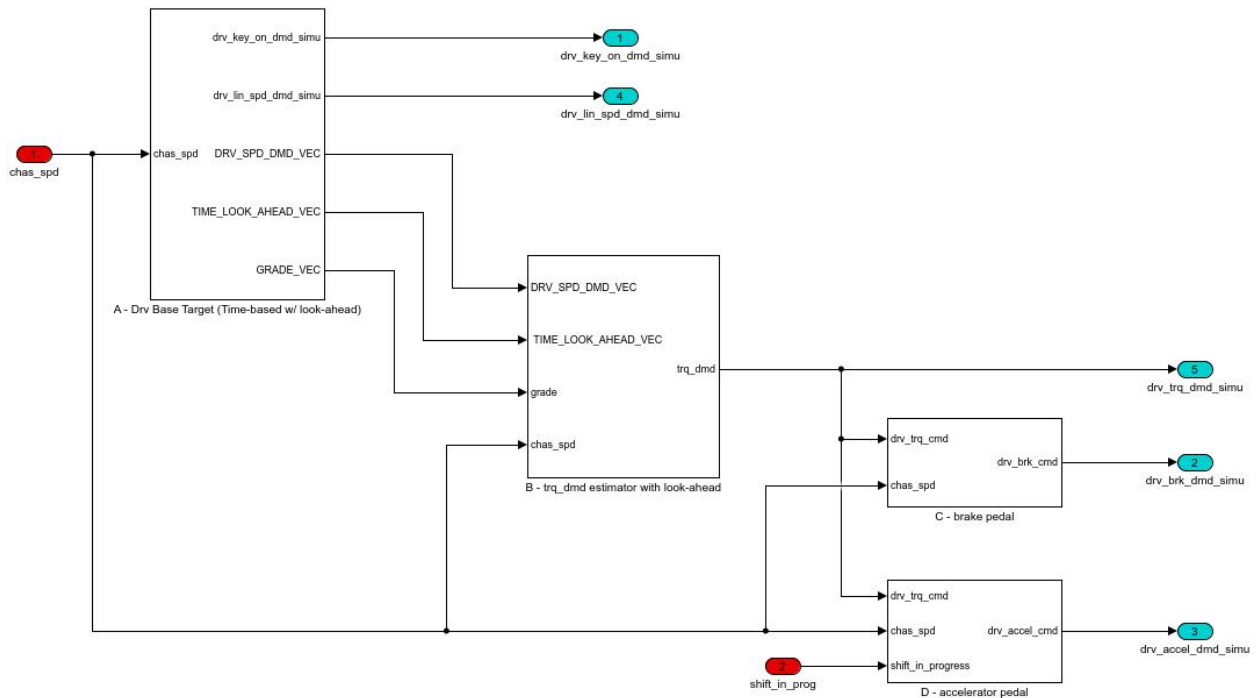


Figure 75. Top-level Simulink diagram of the look-ahead driver model

Figure 76 shows the equations involved in the look-ahead driver model.

$$T_{\Delta t}(t) = m \cdot \frac{r(t + \Delta t) - \omega(t)}{\Delta t} + m \cdot \dot{r}(t + \Delta t) + L(r(t + \Delta t))$$

ω : actual wheel speed
 r : reference wheel speed (trace)

↑ Torque demand ↑ Estimation of additional torque needed to reach $r(t+\Delta t)$ ↑ Acceleration ↑ Vehicle losses
 Needed to meet trace @ $(t+\Delta t)$

Figure 76. Equations for the look-ahead driver model

Wheel Model

The wheel model accounts for the braking force at each wheel and the inertia of all the wheels added to the drivetrain. Figure 77 shows the main I/O of the Autonomie wheel model.



Figure 77. Autonomie wheel model I/O

As shown in Figure 78, the wheel model can be divided into three subsystems: wheel angular speed calculation (Block A), output force calculation (Block B), and wheel mass calculation (Block C).

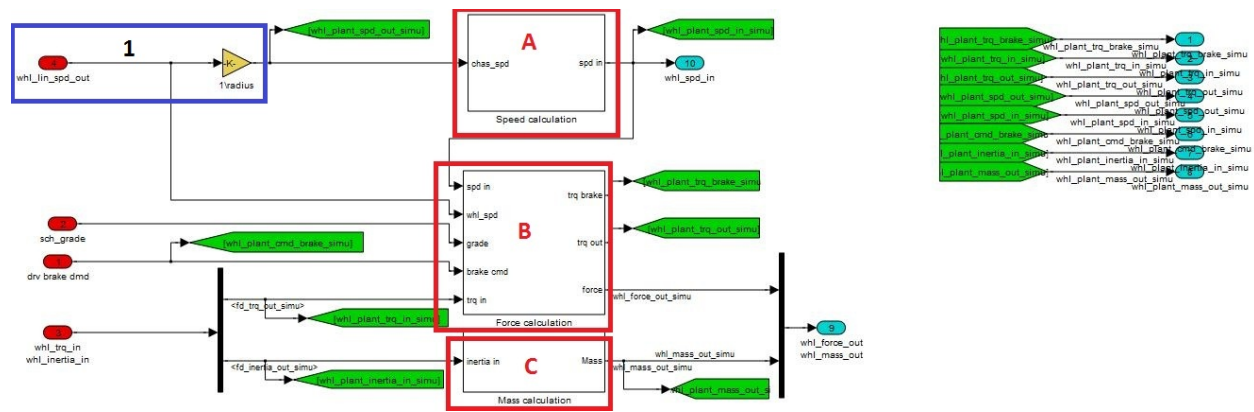


Figure 78. Autonomie wheel model Simulink diagram

The wheel angular speed is calculated by dividing the linear speed of the vehicle by the radius of the wheel.

$$(55) \quad W_{in} = \frac{V_{veh}}{K_{Radius}}$$

There is no slip calculation in the wheel model.

Block B (Figure 79) implements the wheel-force calculation.

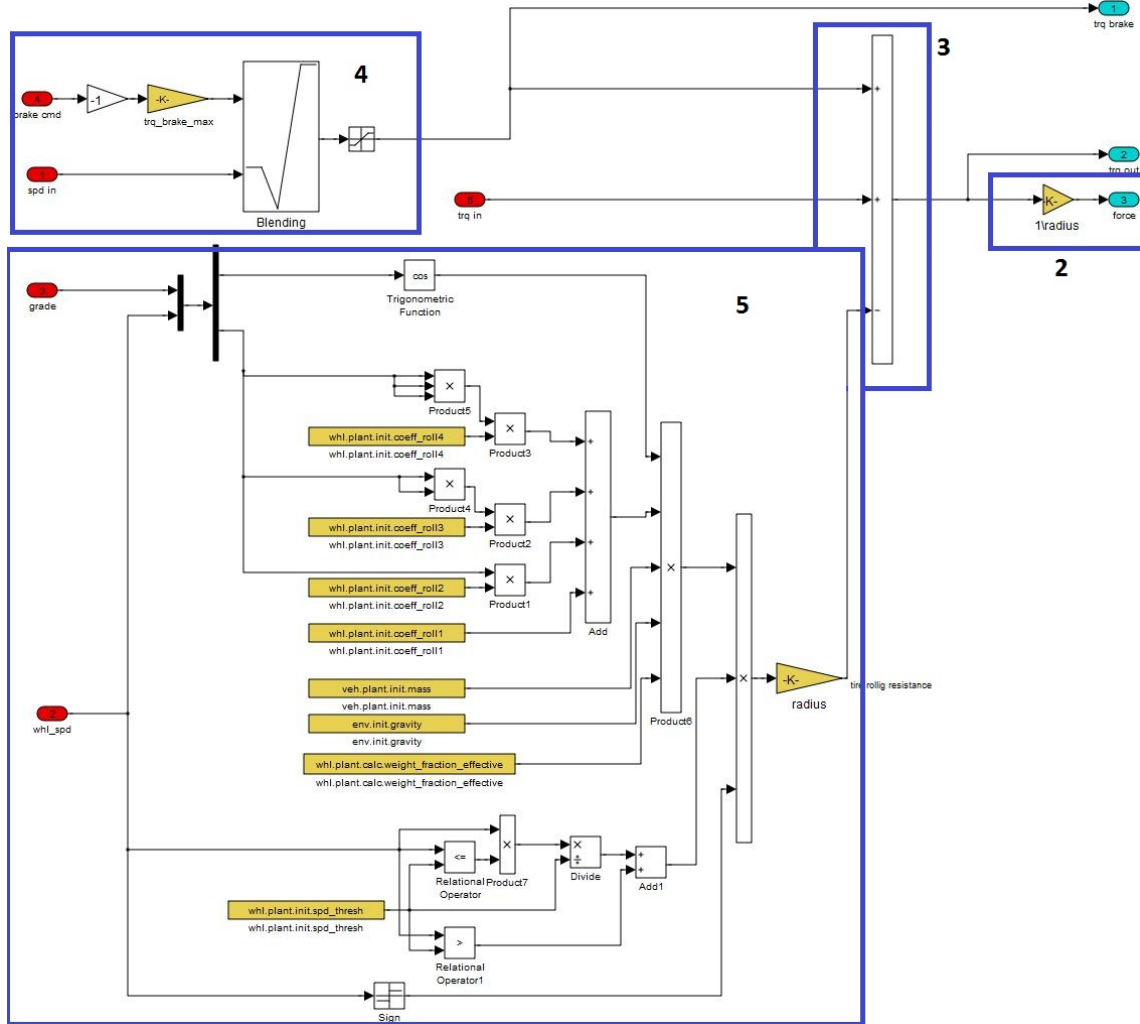


Figure 79. Block B: Force calculation

The wheel net torque is converted into a force by dividing by the wheel radius.

$$(56) \quad F_{out} = \frac{T_{out}}{K_{Radius}}$$

The wheel net torque equals the torque in from the drive axle minus the brake torque minus the rolling resistance losses.

$$(57) \quad T_{out} = T_{in} - T_{lossbrakes} - T_{lossstire}$$

The maximum brake torque is calculated by multiplying the brake command from the controller by the maximum available brake torque. The maximum available brake torque is assumed to be a constant and is unchanged across different vehicle powertrains and classes.

$$(58) \quad T_{lossbrake} = PWM_{brake} \times T_{maxbrake}$$

The wheel losses are modeled by a fourth-degree polynomial that is a function of vehicle speed.

$$(59) \quad T_{loss_{tire}} = \left[\cos(\alpha_{grade}) \times (C_1 + C_2 \times V_{veh} + C_3 \times V_{veh}^2 + C_4 \times V_{veh}^3) \times M_{veh} \times g \times \eta_{weight_{traction}} \times f\left(\frac{\omega}{\omega_{threshold}}\right) \right] \times R_{wheel}$$

The powertrain rotating inertia is converted into an equivalent mass using the wheel radius, as seen in Figure 80.

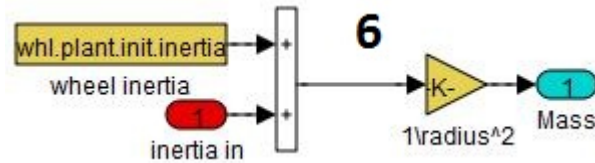


Figure 80. Block C: Mass calculation

The powertrain upstream inertia is added to the wheels inertia and then divided by the wheel radius squared to yield the equivalent powertrain mass.

$$(60) \quad Mass_{inertia} = \frac{J_{in} + J_{wh}}{K_{Radius}^2}$$

Chassis Model

The chassis model calculates speed based on the fed-forward upstream inertia of the drivetrain, the chassis mass, and the drag and grade losses. Figure 81 shows the main chassis model I/O.



Figure 81. Autonomie chassis model I/O

This model uses the frontal area, drag coefficient, and grade to calculate the losses. Since actual drag coefficient and frontal area values are used instead of the costdown coefficients, rolling resistance is accounted for in the wheel model.

Figure 82 shows the chassis model Simulink diagram.

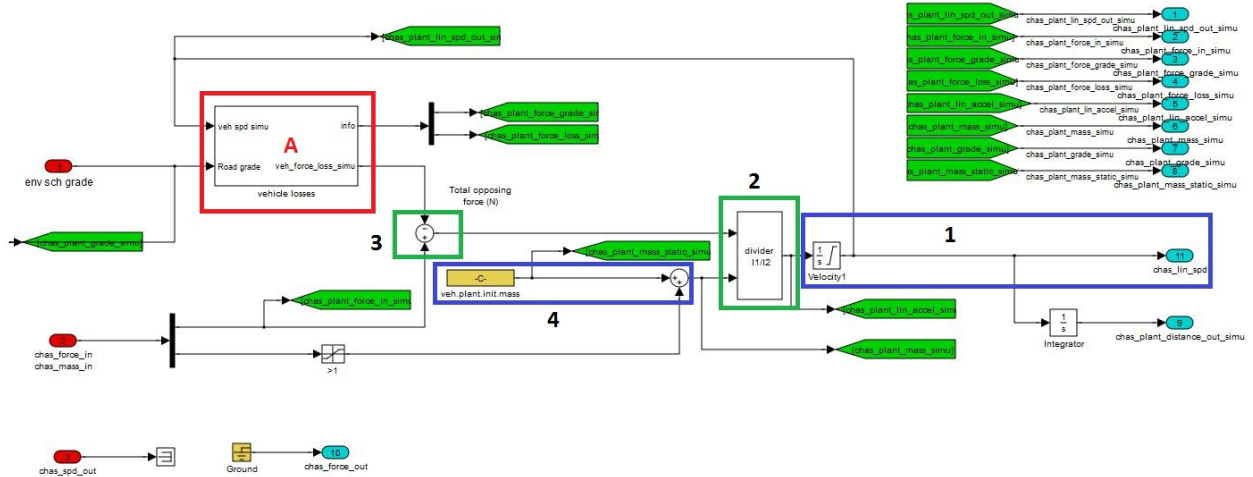


Figure 82. Simulink diagram of chassis model in Autonomie

The vehicle speed is calculated by this formula.

$$(61) \quad V_{veh} = \int Acceleration \times dt$$

The acceleration is calculated by dividing the net chassis force at the wheels by the chassis equivalent mass. This equivalent mass accounts for the translation acceleration of the chassis and the powertrain rotational acceleration.

$$(62) \quad Acceleration = \frac{F_{vehicle}}{Mass_{vehicle}}$$

The net chassis force is the total force coming from the upstream powertrain components minus the chassis-level losses due to aerodynamic drag and grade.

$$(63) \quad F_{vehicle} = F_{in} - F_{loss}$$

The equivalent chassis mass is the sum of the static chassis mass and the equivalent powertrain mass. The powertrain inertia is converted into an equivalent mass in the wheel model by dividing by the square of the wheel radius.

$$(64) \quad Mass_{vehicle} = Mass_{staticframe} + \sum J$$

Block A (Figure 83) calculates the aerodynamic drag and grade loss.

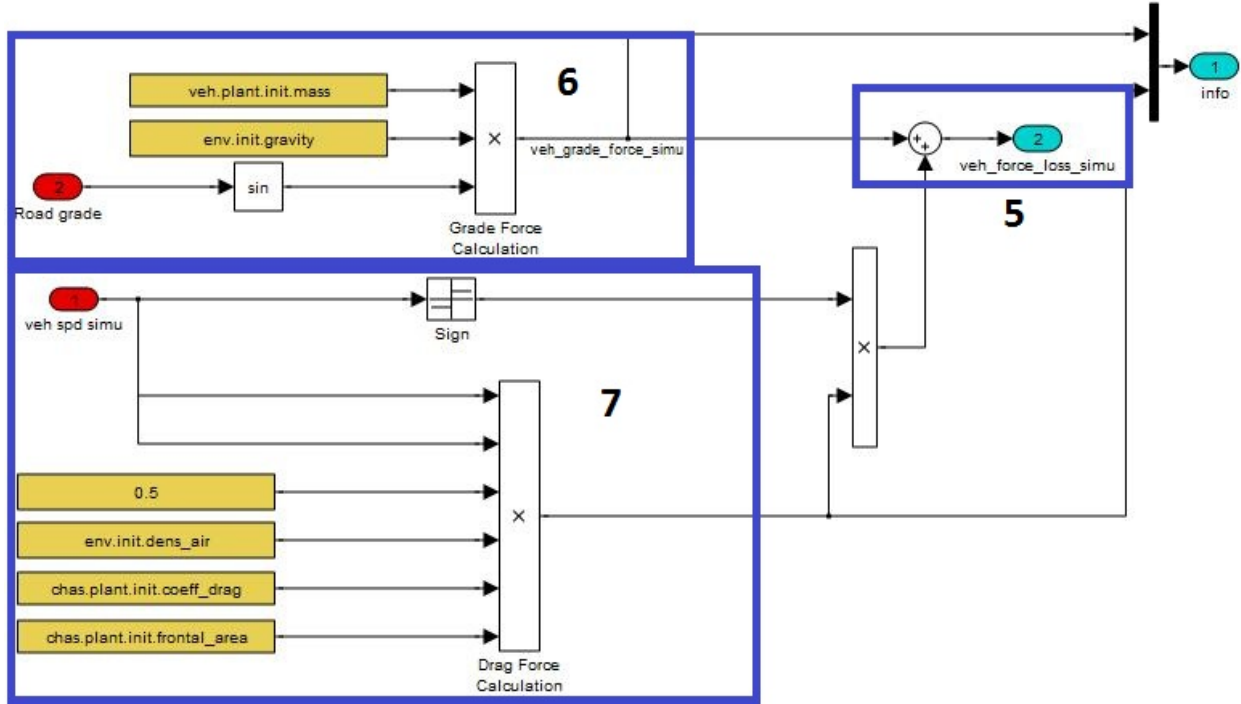


Figure 83. Block A: Chassis losses

The total chassis losses are the sum of the aerodynamic losses and the grade losses.

$$(65) \quad F_{loss} = F_{aerodynamics} + F_{grade}$$

The grade loss is computed when the grade angle and the weight of the chassis are known. The grade angle is the inclination that the chassis makes with the horizontal (parallel to the ground).

$$(66) \quad F_{grade} = Mass_{vehicle} \times g \times \sin(grade)$$

The standard equation for aerodynamic drag is used. The sine function is used to ensure that the aerodynamic drag opposes chassis movement. The chassis should never move backwards in simulations, so this function is not necessarily needed.

$$(67) \quad F_{aerodynamics} = -Kh \times \rho_{air} \times c_d \times f_a \times V_{veh}^2 \times \text{sign}(V_{veh})$$

Equation 68 shows the variation of air density with altitude, due to the compressibility of air. This equation is not currently implemented in the chassis model.

$$(68) \quad Kh = \frac{\rho}{2 \times g} = \begin{cases} 0.6 @ 200 \text{ meters} \\ 0.57 @ 500 \text{ meters} \\ 0.5 @ 1,500 \text{ meters} \end{cases}$$

Equation 69 expresses air density as a function of air pressure and temperature. Like Equation 68, it is not currently implemented in the chassis model.

$$(69) \quad \rho_{air} = 1.225 \times \frac{Pr}{101.325} \times \frac{288.16}{273.16 + T_r}$$

To estimate the frontal area of a chassis from track width and chassis height, Equation 70 is used.

$$(70) \quad f_a = 0.9 \times Width_{veh} \times Height_{veh}$$

Final Drive Model

Final drive gears are incorporated into vehicle driving axles and transaxles for the following reasons.

- To provide a right-angled drive from either the propeller shaft or the gearbox layshaft to the driven wheels
- Alternatively, to provide a parallel drive from the gearbox layshaft to the driven wheels
- To permit an additional and constant gear reduction in the transmission system

The second requirement applies only in the case of passenger cars with transversely mounted engines (i.e., one lying parallel to the axle of the driven front or rear wheels).

Two basic types of final drive reduction gearing have generally been used in vehicles with longitudinally mounted engines: bevel drive and worm drive. In the modern vehicle, the bevel drive has proven to be lighter, more efficient, less expensive, and equally quiet-running. For cars with transversely mounted engines, the final drive reduction gears are of the helical pinion type.

Figure 84 shows the main final drive model I/O.



Figure 84. Autonomie final drive model I/O

Figure 85 shows the top-level Simulink diagram of the final drive model in Autonomie.

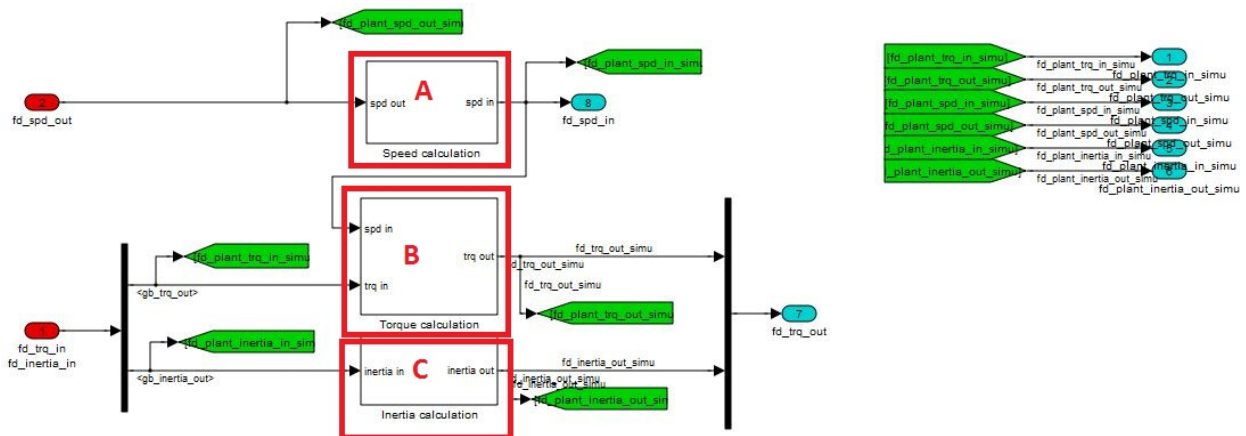


Figure 85. Simulink diagram of the final drive model in Autonomie

The top-level diagram of the final drive model is divided into three blocks, highlighted in red in Figure 85. Block A calculates the input and output speeds of the final drive, as shown in Figure 86. Block B calculates the output torque, as shown in Figure 87, and Block C calculates the inertia that is fed forward, as shown in Figure 88.

The input speed is the product of the final drive ratio and the output speed of the final drive. The output speed of the final drive is calculated downstream and fed back.

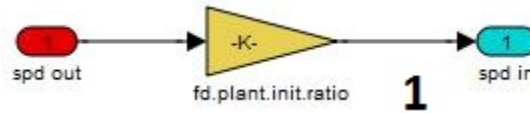


Figure 86. Block A: Final drive model speed calculation

$$(71) \quad W_{in} = W_{out} \times K_{finaldrive}$$

where:

W_{in} = final drive speed in

W_{out} = final drive speed out

K_{final_drive} = reduction gear ratio for the final drive

Block B (Figure 87) determines the torque output of the final drive by first subtracting the torque loss, which is a function of input torque and input speed, and then multiplying the remainder by the final drive ratio. The blending block ensures that at zero speed the torque loss is zero; otherwise, a negative torque at zero vehicle speed would lead the vehicle model to give the erroneous result of a negative vehicle acceleration and, consequently, a negative vehicle speed. Essentially, the vehicle model cannot discriminate between negative loss torque and negative propulsive torque.

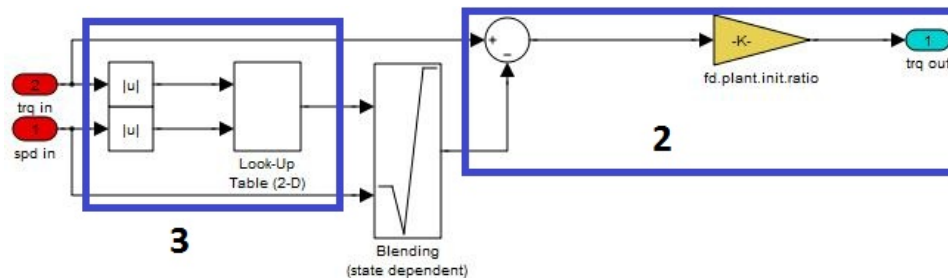


Figure 87. Block B: Torque calculation

$$(72) \quad T_{out} = K_{finaldrive}(T_{in} - T_{loss})$$

$$(73) \quad T_{loss} = function(W_{in}, T_{in})$$

where:

T_{out} = final drive output torque speed

W_{in} = final drive input shaft speed

T_{in} = final drive input shaft torque

T_{loss} = final drive input torque loss

K_{final_drive} = reduction gear ratio of the final drive

Block C (Figure 88) and Equation 74 reflect the product of multiplying the drivetrain inertia upstream of the final drive by the final drive ratio and adding its equivalent inertia at the output of the final drive. This equivalent inertia is fed forward on a path to the vehicle model, where the

combined drivetrain inertia is used to calculate the vehicle speed. Drivetrain speeds are then fed back through the drivetrain model.

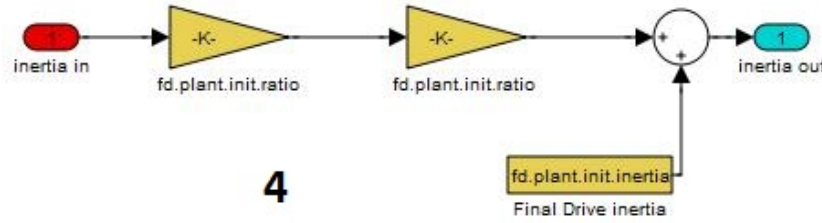


Figure 88. Block C: Inertia calculation

$$(74) \quad J_{out} = J_{in} \times K_{finaldrive}^2 + J_{FD}$$

where:

J_{in} = final drive input inertia from upstream components

J_{out} = final drive output inertia fed forward to downstream components

J_{FD} = inertia of the final drive

K_{final_drive} = reduction gear ratio of the final drive

Vehicle-Level Control Algorithms

All the vehicle-level control algorithms used in this study have been developed from vehicle test data collected at AMTL. Note that while the logic for the vehicle-level control algorithms was developed based on test data, only the logic has been used for the present study, since the calibration parameters have been adapted for each vehicle to ensure fuel consumption minimization with acceptable drive quality (i.e., acceptable number of engine on/off conditions).

Micro- and Mild HEV

The vehicle-level control strategies of the micro- and mild (i.e., belt-integrated starter generator) HEVs are similar in many aspects because of the low peak power and energy available from the energy storage system.

For the micro-HEV case, the engine is turned off as soon as the vehicle is fully stopped and restarted as soon as the brake pedal is released. No regenerative braking is considered in this controller.

For the mild HEV cases, the engine is also turned off as soon as the vehicle is fully stopped. However, since some regenerative braking energy can be recovered, the vehicle is propelled by the electric machine during vehicle launch, allowing the engine to be restarted later. The electric machine also provides some limited assist during propelling to improve engine efficiency.

Power-Split HEV

As shown in Figure 89, power-split hybrids combine aspects of series and parallel hybrids to create an extremely efficient system. The most common configuration, called an input split, is composed of a power-split device (planetary gear transmission), two electric machines, and an engine. All these elements can operate separately. The engine is not always ON, and the

electricity from the generator may go directly to the wheels to help propel the vehicle or go through an inverter to be stored in the battery. The operational phases for an input split configuration are the following.

- During vehicle launch, when driving, or when the SOC of the battery is high enough, the ICE is not as efficient as electric drive, so the ICE is turned off and the electric machine alone propels the vehicle.
- During normal operation, the ICE output power is split, with part going to drive the vehicle and part used to generate electricity. The electricity goes either to the electric machine, which assists in propelling the vehicle, or to charge the energy storage system. The generator also acts as a starter for the engine.
- During full-throttle acceleration, the ICE and electric machine both power the vehicle, with the energy storage device (e.g., battery) providing extra energy.

During deceleration or braking, the electric machine acts as a generator, transforming the kinetic energy of the wheels into electricity to charge the energy storage system.

The vehicle control algorithms were based on both the Toyota and Ford implementations.

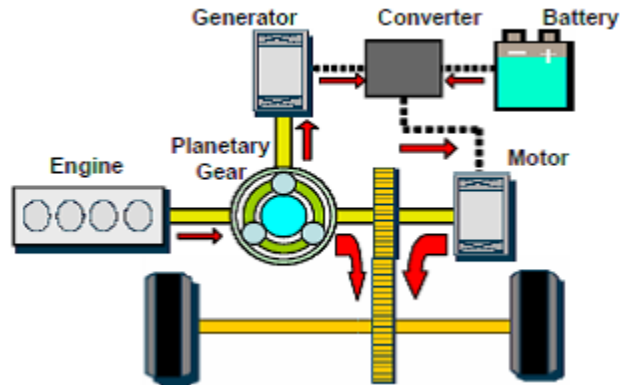


Figure 89. Power-split HEV

Single-Mode Power-Split PHEV

The vehicle-level control strategy of a single-mode power-split PHEV was based on the Toyota Prius Prime (Jeong et al., 2019). The implemented control can be divided into three areas: engine-ON condition, battery SOC control, and engine operating condition.

Engine-ON Condition

The engine operation determines the mode: plug-in electric vehicle mode or HEV mode. The engine is turned ON when the driver's power demand exceeds a predefined threshold. As shown in Figure 90, the engine is ON only when the battery SOC is under 17 percent. This means that only electric energy is used when the battery SOC is over 17 percent, i.e., in charge-sustaining mode. Once the operating mode, based on SOC, is determined, the engine is turned ON early if the driver's torque demand exceeds a predefined threshold, which means that the system changes from PEV mode to HEV mode to meet the power demand.

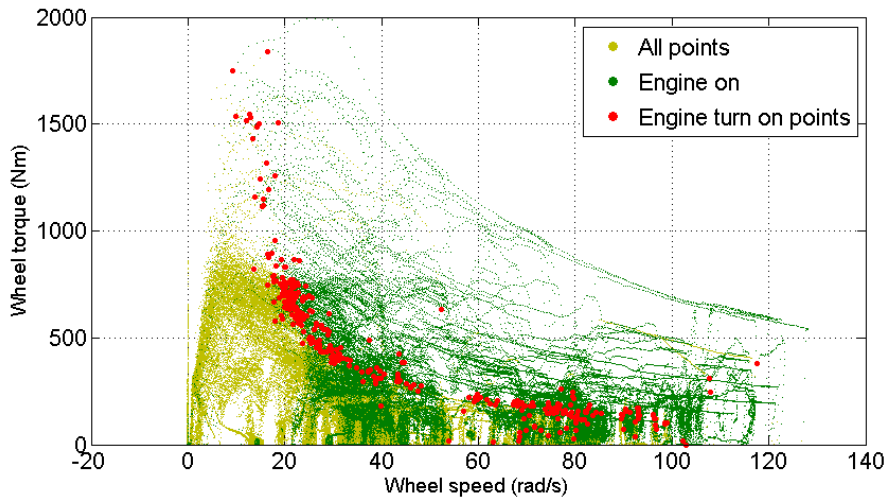
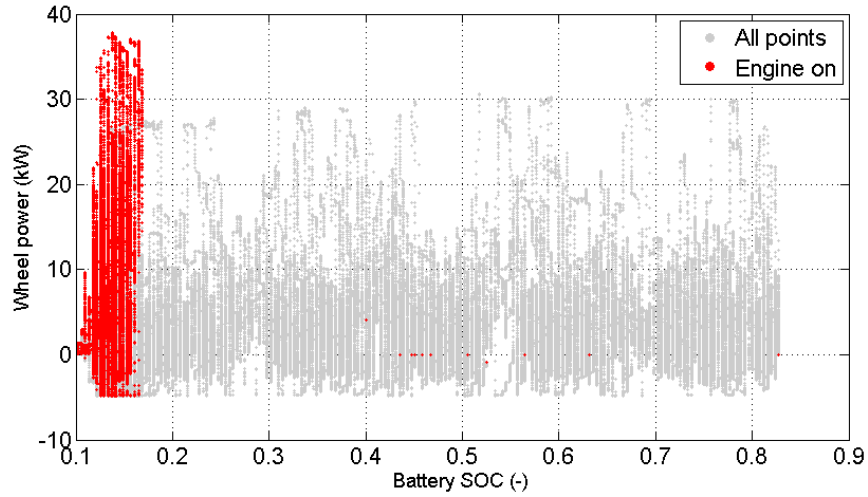


Figure 90. Engine-ON condition—2017 Prius Prime example based on 25 test cycles

SOC Control in CS Mode

The desired output power of the battery is closely related to the energy management strategy. When the vehicle is in HEV mode, the battery power is determined by the current SOC, as shown in Figure 91. The overall trend shows that the energy management strategy consists of bringing the SOC back to a regular value close to 14 percent. When the battery SOC decreases to under 13.5 percent, the battery is charged to 10 kW to sustain the battery SOC. As battery SOC is increasing, the charging power is decreasing, and the battery is discharged when the battery SOC is over 14.5 percent. If the battery output power is determined, engine output power can be calculated.

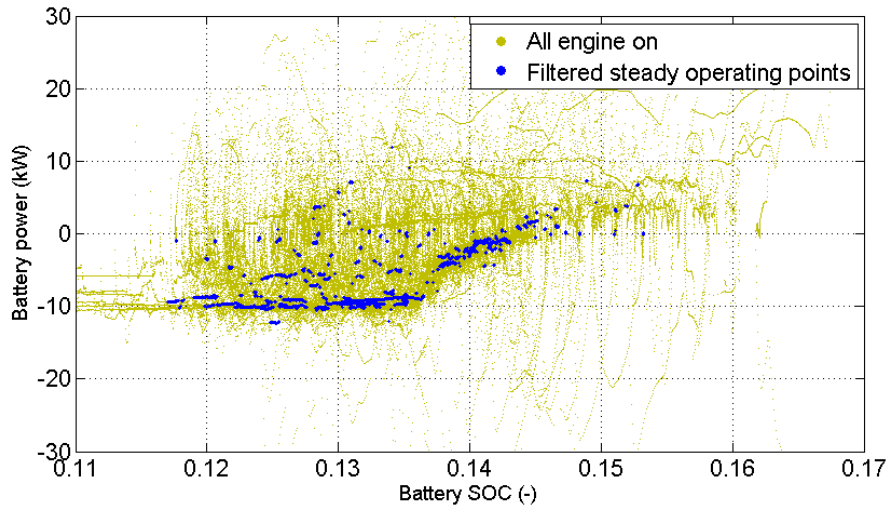


Figure 91. SOC regulation algorithm—2017 Prius Prime example based on 25 test cycles

Engine Operation

The two previously described control concepts determine the power-split ratio. The concepts do not, however, generate the target speed or torque of the engine, because the power-split system could have infinite control targets that produce the same power. Therefore, an additional algorithm determines the engine torque operating points according to the engine speed, as shown in Figure 92. An engine operating line is defined based on the best efficiency curve to select the optimum engine speed for a specific engine power demand.

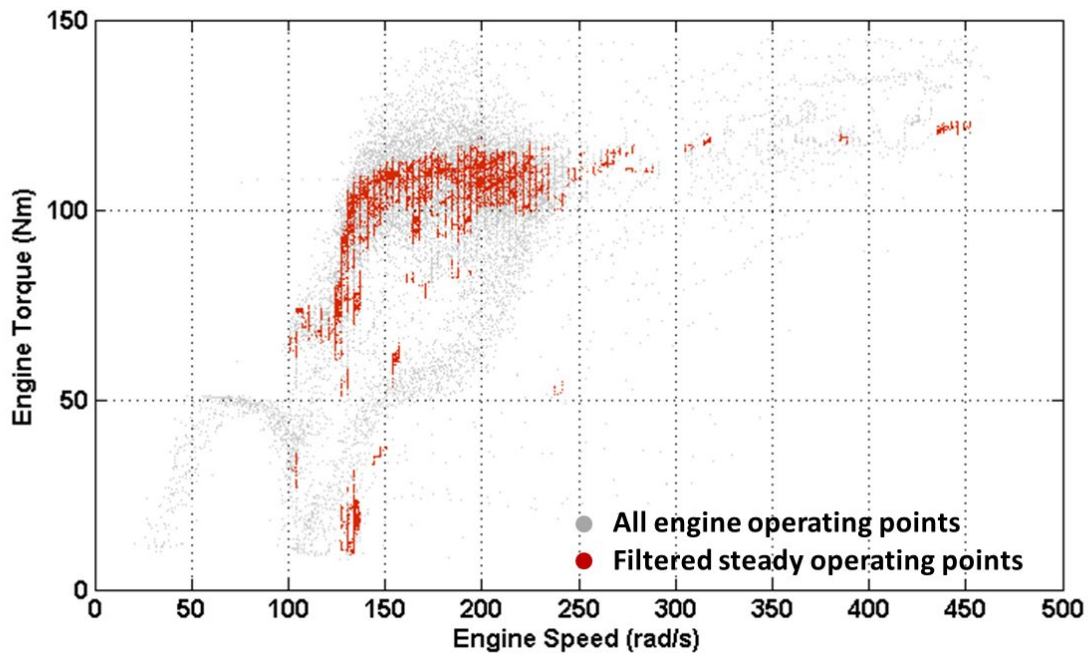


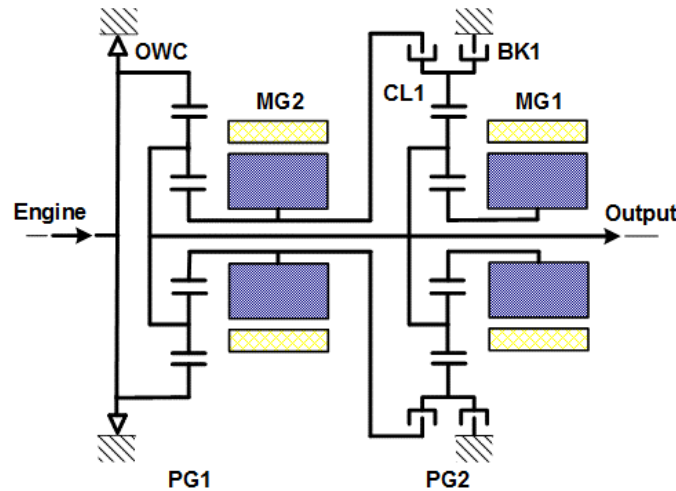
Figure 92. Example of engine operating target—2017 Prius Prime example based on 25 test cycles

In summary, the engine is turned ON based on the power demand at the wheel and the battery SOC. If the engine is turned on, the desired output power of the battery is determined based on the current SOC, and the engine should provide appropriate power to drive the vehicle. The engine operating targets are determined by a predefined line, so the controller can produce required torque values for the motor and the generator based on the engine speed and torque target.

Multi-Mode E-REV (E-REV PHEV50)

The multi-mode E-REV control is based on the Voltec powertrain from General Motors (GM Authority, n.d.; Miller et al., 2011).

The second-generation Voltec PHEV has one engine, two motor-generators, and one battery. The two electric machines are connected to a main transmission shaft using an individual planetary gear set, as shown in Figure 93. By activating the brake and clutches, the vehicle can be driven in various modes. Normally, electric machine 1 (MG1) drives the vehicle only by holding the BK. When the BK and one-way clutch are locked, both electric machines can provide the maximum torque, putting the vehicle into two-motor electric vehicle mode. An additional planetary gear set is used for a compound power-split mode in extended-range operation. The clutch position or the BK activation status determines whether the mode is the input-split or the compound-split. The input-split mode is activated by the BK by holding the ring gear of the second planetary gear set. The compound-split mode is activated by the CL when it connects the sun gear of the first planetary gear set to the ring gear of the second gear set.



Mode	BK1	CL1	OWC
EV1	closed	open	open
EV2	closed	open	closed
Low extended range	closed	open	open
Fixed ratio	closed	closed	open
High extended range	open	closed	open

Figure 93. Configuration of the Chevrolet Volt 2016 powertrain system

Although many sophisticated control concepts were added to the supervisory control concepts, the main control flow of the vehicle, based on test data, can be summarized as shown in Figure 94. First, the engine ON/OFF control is determined by the battery SOC and the driver's power demand. During EV driving, the use of two electric machines allows for two EV driving modes to provide either maximum output torque or increased efficiency by torque distribution. If the engine is ON after most of the battery energy has been depleted by EV driving, the operational state of the clutch or brakes is defined to select the extended-range mode. Energy management between the engine and the battery is controlled based on the powertrain operation mode.

Once the operation mode is chosen, the battery power demand is determined by the proportional control power, which also determines the engine power demand by subtracting the battery power demand from the driver power demand. Then, each component operates according to an optimal target based on engine target and battery power demand. The entire powertrain model, including the vehicle-level controller, was implemented in Autonomie.

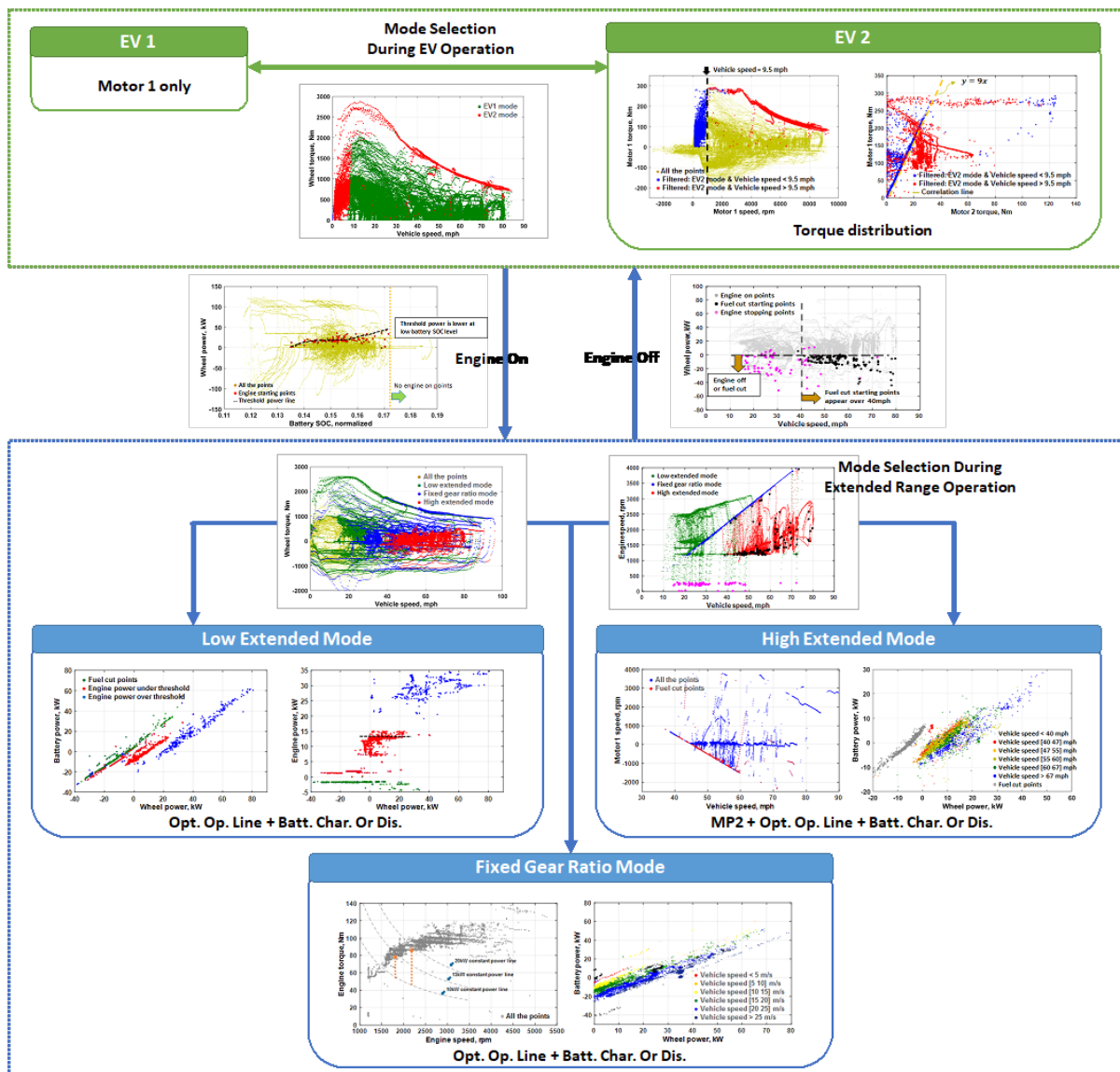


Figure 94. Summary of control analysis for the second-generation Voltec system

Parallel HEV

In a parallel configuration, the vehicle can be directly propelled by either electrical or mechanical power. Direct connection between the power sources and the wheels leads to lower powertrain losses compared to the pure series configuration. However, since all the components' speeds are linked to the vehicle's speed, the engine cannot consistently be operated close to its best efficiency curve. The pre-transmission configuration used in this study has an electric machine between the engine and the transmission. The electric machine peak power usually ranges from 19 to 45 kW for light-duty applications, allowing the driver to propel the vehicle in electric-only mode as well as recover energy through regenerative braking.

The pre-transmission parallel HEV configuration can take advantage of different gear ratios that allow the electric machine to operate at higher efficiency and provide high torque for a longer operating range. This configuration allows operation in electric mode during low and medium power demands in addition to the ICE ON/OFF operation. The main challenge for these configurations is being able to maintain good drive quality given the engine ON/OFF feature and the high component inertia during shifting events.

The vehicle-level control strategy for a parallel HEV is based on the 2013 Volkswagen Jetta HEV (Kim, Lohse-Busch, et al., 2014). Vehicle control behaviors are interpreted based on the analyzed results to understand the overall control behaviors.

Engine Operation

The upper panel in Figure 95 shows the vehicle speed and wheel demand torque when the engine is ON. The lower panel shows the operating area of pure electric driving in the same index.

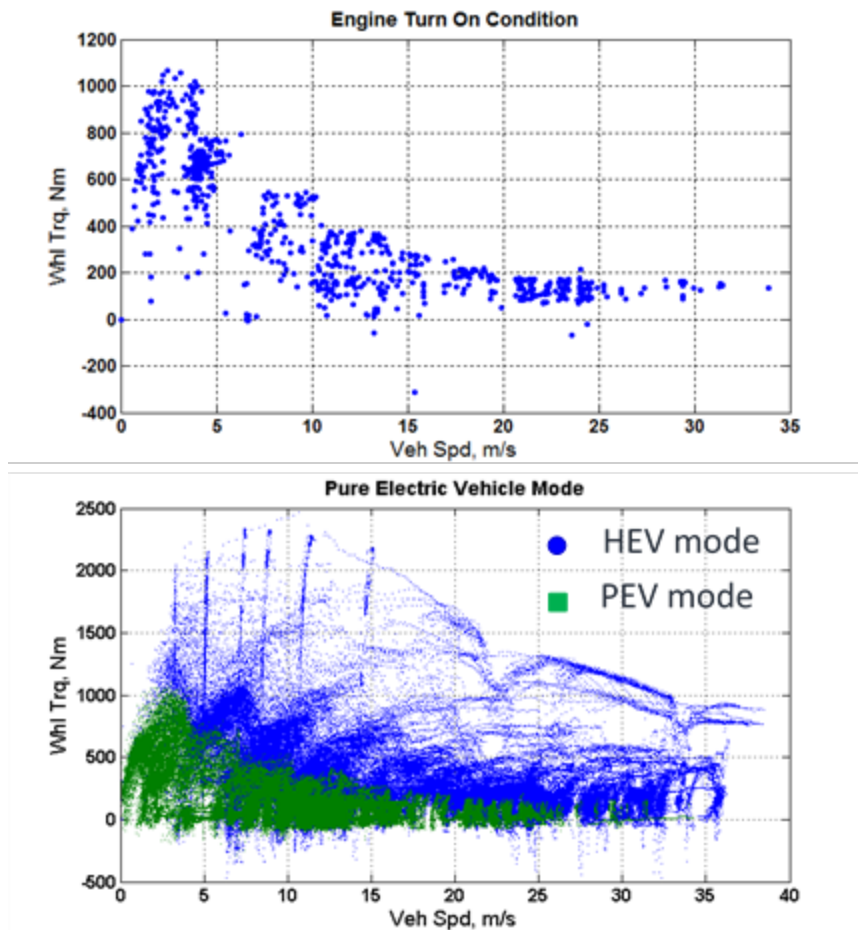


Figure 95. Wheel torque versus vehicle speed of 2013 VW Jetta HEV

Fuel Cell HEV

Unlike the other vehicle-level control algorithms previously discussed, the algorithm for fuel cell HEVs is not derived from test data, owing to the lack of test vehicles. Instead, dynamic programming was used to define the optimum vehicle-level control algorithms for a fuel cell vehicle. A rule-based control is then implemented to represent the rules issued from the dynamic programming.

Overall, owing to the high efficiency of the fuel cell system, energy storage only regains energy during deceleration and propels the vehicle under low-load operations; the fuel cell system does not recharge the battery. Unlike in electric-drive powertrains with an engine, the battery does not smooth the transient demands. An example of fuel cell hybrid operations is shown in Figure 96.

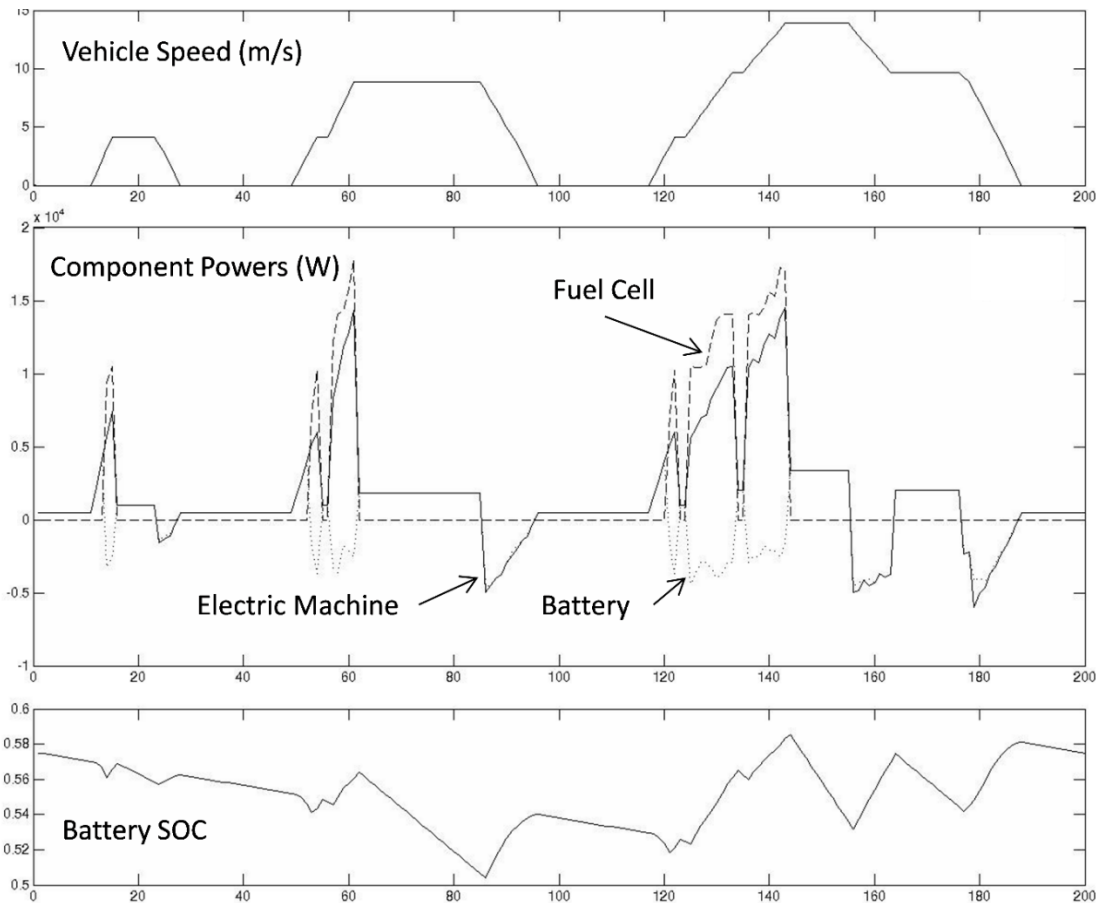


Figure 96. Component operating conditions of a fuel-cell vehicle on the urban European drive cycle using dynamic programming

High-Level Overview of Autonomie Controllers

Supervisory Controller

In Autonomie the supervisory controller manages the vehicle-level decision-making. The main control decisions (e.g., gear shift demand, etc.) are sent to the VPA. The lower-level controls within the VPA execute the demands, such as different steps to perform a shifting event coordinated between the engine, gearbox, etc. The split of the control logic between the supervisory controller and component controllers depends on the vehicle configuration.

For conventional vehicles, all decisions are made at the component (including the driver) level.

For electrified vehicles, the supervisory controller manages most decisions, including engine ON/OFF strategy, engine demand, electric machine demand, and others, while the transients (e.g., how to shift a gear) are handled at the component level.

Figure 97 shows the Autonomie supervisory controller. The individual component controllers are part of the VPA.

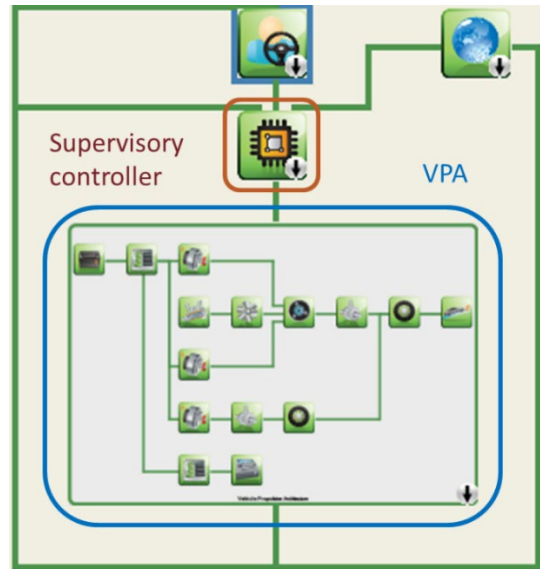


Figure 97. Autonomie supervisory controller

Figure 98 shows the structure inside the VPA.

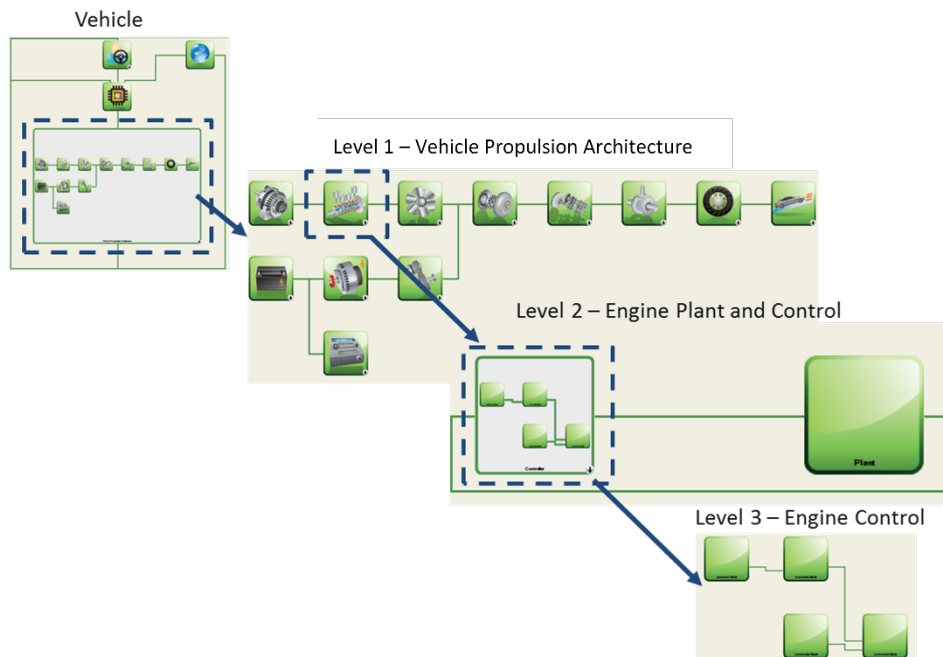


Figure 98. Autonomie nested-level controllers

Each of the component models in Autonomie may contain several subsystems, consisting of either plant model only or plant and controller models. Figure 99 shows the component model layout in Autonomie.

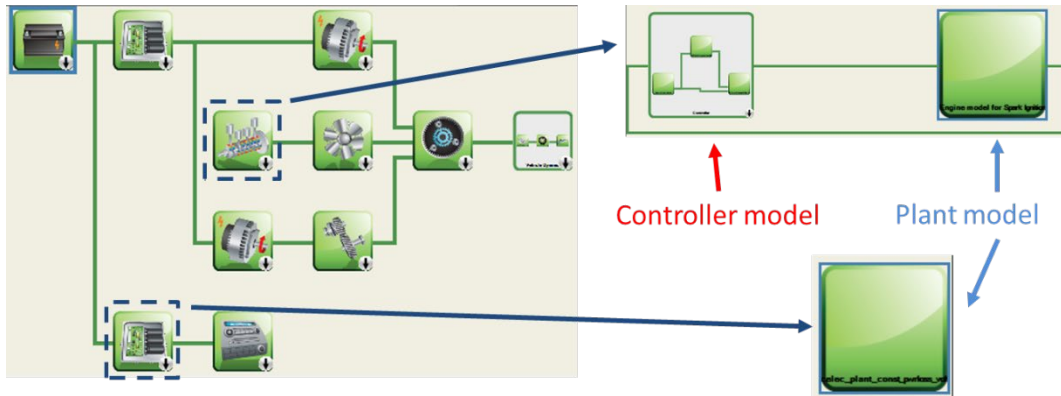


Figure 99. Autonomie component model layout

Component Controllers

A component controller can contain a single control model (ctrl) or a combination of two, three, or four of the following sub-models.

- demand model (dmd)
- transient model (trs)
- constraint model (cstr)
- command model (cmd)

For example, the battery controller in Figure 100 consists of a single control model (ctrl).

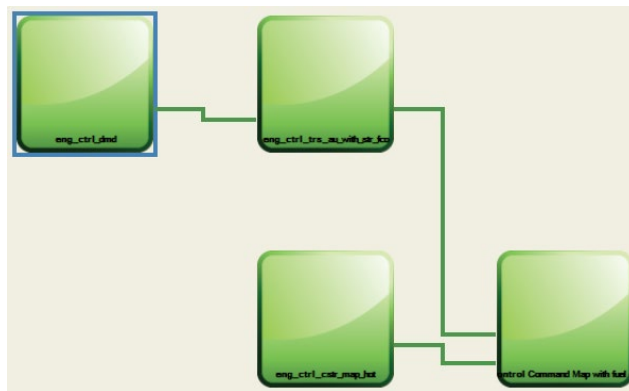


Figure 100. Battery controller composed of a single control model

In contrast, the engine controller in Figure 101 consists of four sub-models: dmd, trs, cstr, and cmd.

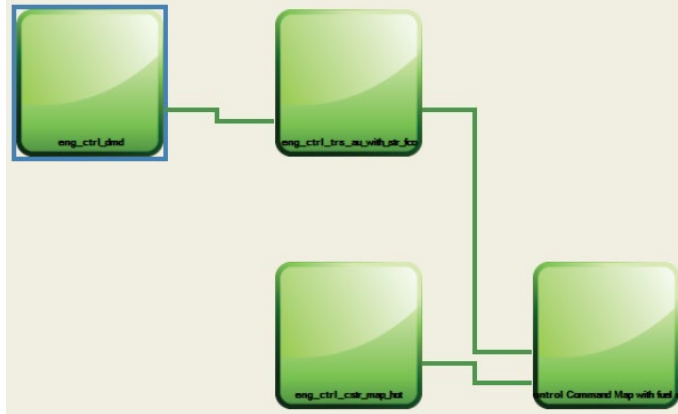


Figure 101. Engine controller composed of four sub-models

The Demand Block—dmd

The demand block in Figure 102 is the usual entry point of the low-level controllers. The request coming from the vehicle controller is translated into a request at the component level—for example, torque demand to pulse-width modulation (0–1). The request then feeds into the transient block.

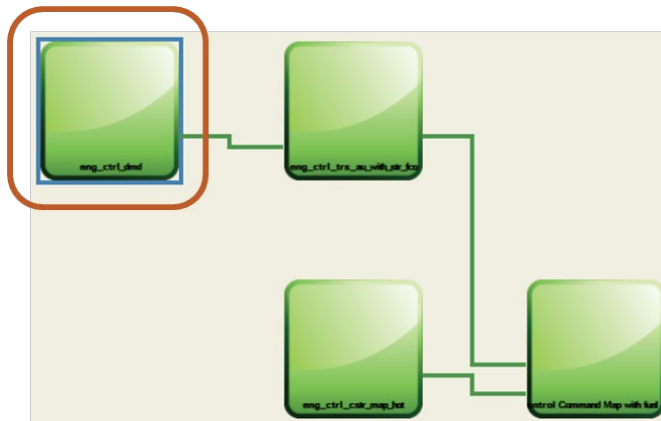


Figure 102. Demand block

The Transient Block—*trs*

The transient block in Figure 103 checks for conditions that may impact the request coming from prior blocks. For instance, if a shift is in progress, the engine torque may need to be reduced for the duration of the shift.

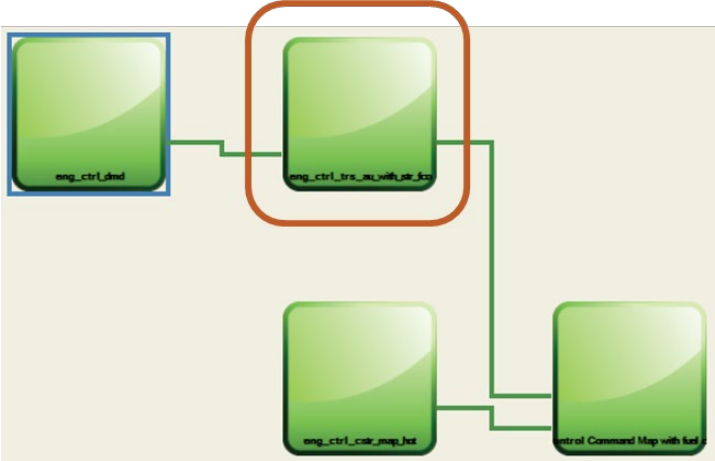


Figure 103. Transient block

The Constraint Block—*cstr*

The constraint block, shown in Figure 104, checks component limits at any given time. For example.

- The maximum engine torque available, given the current engine speed and engine condition
- The maximum battery charge and discharge current, given the current conditions (e.g., voltage, temperature, etc.)

The constraints are fed into the command block.

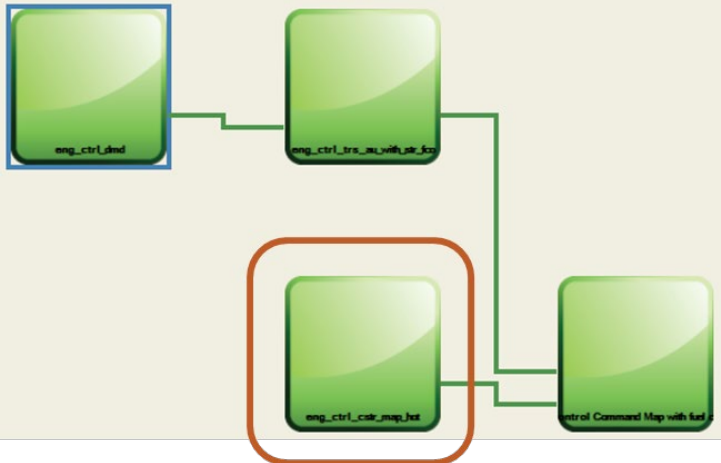


Figure 104. Constraint block

The Command Block—cmd

The command block, shown in Figure 105, receives inputs from the transient and constraint blocks and determines the final request that will be sent to the plant model.

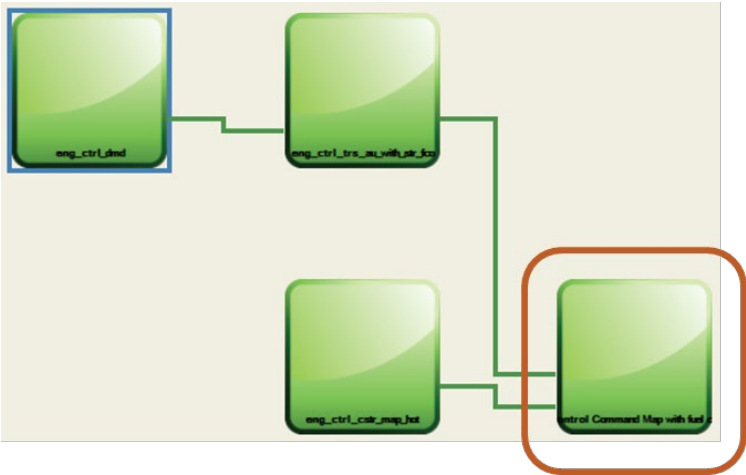


Figure 105. Command block

Low-Level Controller Summary for Engine and Transmission Models

Autonomie allows for the simulation of hundreds of powertrains and technology combinations. Many control functionalities are common across architectures. The following section describes the list of low-level controller options for both engine and transmission and how some are shared across multiple vehicle powertrains.

Figure 106 shows how the engine low-level controls are organized by functionality (i.e., transient, command, constraint, and demand) and reused across transmissions and powertrains.



Figure 106. Low-level control for engine

Figure 107 shows how the transmission low-level controls are organized by functionality (i.e., transient, demand, and command) and reused across transmission types and powertrains.

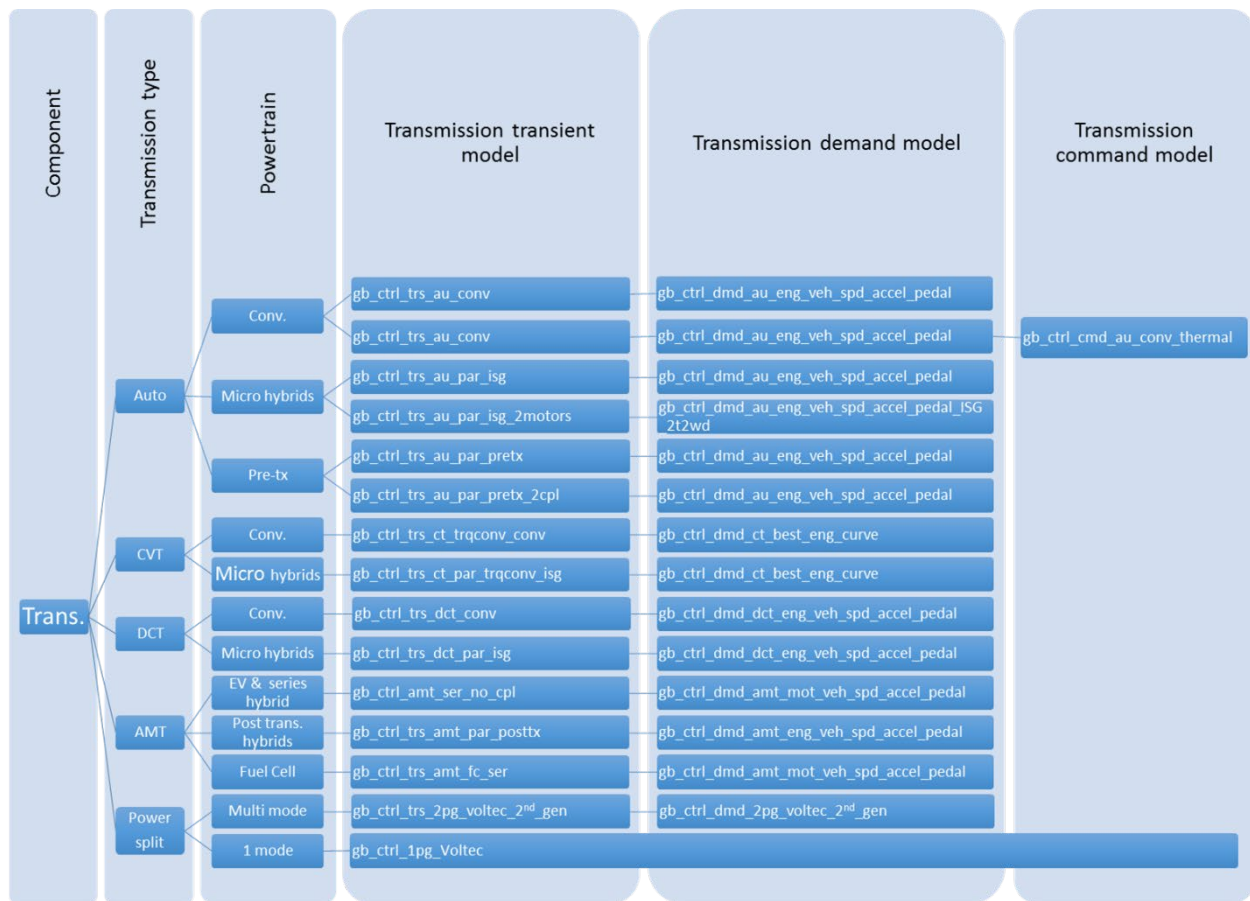


Figure 107. Low-level control for transmission

Table 5 through Table 7 provide short descriptions of the component control blocks and their I/O, as well as lists of compatible plant models.

Table 5. Engine control—low-level demand models

Model Name	Description	Powertrains Used	Compatible Plant Models	Inputs	Outputs
eng_ctrl_dmd	Translates the driver pedal position into a torque demand	Light-duty conventional powertrains with any transmission	eng_plant_hot_map_si_fuel_cut_off eng_plant_hot_map_si_thermal eng_plant_hot_map_ci eng_plant_hot_map_si_fuel_cut_off_with_cylinder_deac	drv_accel_dmd_simu gb_plant_ratio_simu chas_plant_lin_spd_out_simu eng_ctrl_cstr_trq_hot_max_simu eng_ctrl_cstr_trq_hot_min_simu eng_plant_spd_out_simu	eng_ctrl_trq_dmd_simu

Table 6. Engine control—low-level constraint models

Model Name	Description	Powertrains Used	Compatible Plant Models	Inputs	Outputs
eng_ctrl_cstr_map_hot	Provides min and max torque capabilities based on engine speed	Used in all powertrain configurations	eng_plant_hot_map_si_fuel_cut_off eng_plant_hot_map_si_thermal eng_plant_hot_map_ci eng_plant_hot_map_si_fuel_cut_off_with_cylinder_deac eng_plant_hot_map_si eng_plant_hot_map eng_plant_hot_map_CS	eng_plant_spd_out_simu	eng_ctrl_cstr_trq_hot_max_simu eng_ctrl_cstr_trq_hot_min_simu

Table 7. Engine control—low-level transient models

Model Name	Description	Powertrains Used	Compatible Plant Models	Inputs	Outputs
eng_ctrl_trs_au	Determines appropriate engine torque based on the engine mode (idling, shift in progress, engine starting, etc.)	Conventional and hybrid powertrain with AU	eng_plant_hot_map_ci eng_plant_hot_map_si eng_plant_hot_map_CS	gb_ctrl_trs_eng_mode_simu eng_ctrl_dmd_trq_simu eng_ctrl_cmd_on_simu eng_plant_spd_out_simu accmech_plant_trq_simu cpl_plant_cmd_simu drv_accel_dmd_simu gb_ctrl_trs_previous_gear_simu gb_ctrl_dmd_gear_simu gb_ctrl_trs_sit_in_progress_simu	eng_ctrl_trs_trq_simu eng_ctrl_trs_on_simu
eng_ctrl_trs_au_with_str_fco	Determines appropriate engine torque based on the engine mode (idling, shift in progress, engine starting, etc.)	Conventional powertrain with AU with fuel cut-off	eng_plant_hot_map_si_fuel_cut_off	gb_ctrl_trs_eng_mode_simu eng_ctrl_dmd_trq_simu eng_ctrl_cmd_on_simu eng_plant_spd_out_simu accmech_plant_trq_simu cpl_plant_cmd_simu drv_accel_dmd_simu gb_plant_gear_simu gb_ctrl_dmd_gear_simu gb_ctrl_trs_sft_in_progress_simu drv_brk_dmd_simu gen_plant_trq_out_simu chas_plant_lin_spd_out_simu	eng_ctrl_trs_trq_simu eng_ctrl_trs_on_simu eng_ctrl_trs_fuel_cut_off_simu
eng_ctrl_trs_au_with_str_fco_with_vpc	Determines appropriate engine torque based on the engine mode (idling, shift in progress, engine starting, etc.)	Hybrid powertrain with AU with fuel cut-off	eng_plant_hot_map_si_fuel_cut_off	eng_mode vpc_eng_trq_dmd vpc_eng_on_dmd eng_spd accmech_trq cpl_position drv_acc_pedal previous_gear gb_gear_dmd shift_in_progress drv_brk_dmd	eng_ctrl_trs_trq_simu eng_ctrl_trs_on_simu eng_ctrl_trs_fuel_cut_off_simu

Model Name	Description	Powertrains Used	Compatible Plant Models	Inputs	Outputs
eng_ctrl_trs_au_with_str_fco_with_vpc_cyldeac	Determines appropriate engine torque based on the engine mode (idling, shift in progress, engine starting, etc.)	Hybrid powertrain with AU with fuel cut-off and cylinder deactivation	eng_plant_hot_map_si_fuel_cut_off_with_cylinder_deac	eng_mode vpc_eng_trq_dmd vpc_eng_on_dmd eng_spd accmech_trq cpl_position drv_acc_pedal previous_gear gb_gear_dmd shift_in_progress drv_brk_dmd	eng_ctrl_trs_trq_simu eng_ctrl_trs_on_simu eng_ctrl_trs_fuel_cut_off_simu eng_ctrl_trs_cylin_deac_state_simu
eng_ctrl_trs_au_with_str_fco_thermal	Determines appropriate engine torque based on the engine mode (idling, shift in progress, engine starting, etc.)	Conventional powertrain with AU and an engine with a temperature model	eng_plant_hot_map_si_thermal	gb_ctrl_trs_eng_mode_simu eng_ctrl_dmd_trq_simu eng_ctrl_cmd_on_simu eng_plant_spd_out_simu accmeh_plant_trq_simu cpl_plant_cmd_simu drv_accel_dmd_simu gb_plant_gear_simu gb_ctrl_dmd_gear_simu gb_ctrl_trs_sft_in_progress_simu drv_brk_dmd_simu gen_plant_trq_out_simu chas_plant_lin_spd_out_simu eng_plant_temp_simu	eng_ctrl_trs_trq_simu eng_ctrl_trs_on_simu eng_ctrl_trs_fuel_cut_off_simu
eng_ctrl_trs_fuel_cut_off_dm	Determines appropriate engine torque on the basis of engine mode (idling, shift in progress, engine starting, etc.)	Conventional powertrain with DM with fuel cut-off	eng_plant_hot_map_si_fuel_cut_off	gb_ctrl_trs_eng_mode_simu eng_ctrl_dmd_trq_simu drv_key_on_dmd_simu eng_plant_spd_out_simu accmeh_plant_trq_simu gb_plant_gear_simu cpl_plant_cmd_simu gb_ctrl_dmd_gear_simu drv_accel_dmd_simu drv_brk_dmd_simu cpl_plant_spd_out_simu	eng_ctrl_trs_trq_simu eng_ctrl_trs_on_simu eng_ctrl_trs_fuel_cut_off_simu

Model Name	Description	Powertrains Used	Compatible Plant Models	Inputs	Outputs
eng_ctrl_trs_ct_with_str_fco	Determines appropriate engine torque on the basis of engine mode (idling, shift in progress, engine starting, etc.)	Conventional powertrain with a CVT and with fuel cut-off	eng_plant_hot_map_si_fuel_cut_off	gb_ctrl_trs_eng_mode_simu eng_ctrl_dmd_trq_simu eng_ctrl_cmd_on_simu eng_plant_spd_out_simu accmeh_plant_trq_simu cpl_plant_cmd_simu drv_accel_dmd_simu gb_ctrl_trs_cpl_mode_simu drv_brk_dmd gen_trq_out veh_speed	eng_ctrl_trs_trq_simu eng_ctrl_trs_on_simu eng_ctrl_trs_fuel_cut_off_simu
eng_ctrl_trs_dct_with_str_fco	Determines appropriate engine torque on the basis of engine mode (idling, shift in progress, engine starting, etc.)	Conventional powertrain with a DCT and with fuel cut-off	eng_plant_hot_map_si_fuel_cut_off	gb_ctrl_trs_eng_mode_simu eng_ctrl_dmd_trq_simu eng_ctrl_cmd_on_simu eng_plant_spd_out_simu accmeh_plant_trq_simu cpl_plant_cmd1_simu cpl_plant_cmd2_simu drv_accel_dmd_simu gb_plant_spd_out_simu gb_ctrl_dmd_gear_simu gb_ctrl_trs_sft_in_progress_simu gen_plant_gear_simu drv_brk_dmd_simu	eng_ctrl_trs_trq_simu eng_ctrl_trs_on_simu eng_ctrl_trs_fuel_cut_off_simu
eng_ctrl_trs_split	Limits engine torque to the max engine capability	Hybrid configuration with a power-split powertrain, including 2 times 2-wheel drive, extended range, and multi mode vehicles	eng_plant_hot_map_si eng_plant_hot_map_ci eng_plant_hot_map_si_thermal	vpc_eng_trq_dmd_simu eng_ctrl_cstr_trq_hot_max_simu vpc_eng_on_dmd_simu	eng_ctrl_trs_trq_simu eng_ctrl_trs_on_simu
eng_ctrl_trs_amt	Determines appropriate engine torque on the basis of	HEV and PHEV powertrain with an automated DM	eng_plant_hot_map_si	gb_ctrl_trs_eng_mode_simu eng_ctrl_dmd_trq_simu eng_ctrl_cmd_on_simu	eng_ctrl_trs_trq_simu eng_ctrl_trs_on_simu

Model Name	Description	Powertrains Used	Compatible Plant Models	Inputs	Outputs
	engine mode (idling, shift in progress, engine starting, etc.)			eng_plant_spd_out_simu accmech_plant_trq_simu cpl_plant_cmd_simu drv_accel_dmd_simu gb_plant_spd_out_simu gb_ctrl_dmd_gear_simu gb_ctrl_trs_sft_in_progress_simu gb_plant_gear_simu	
eng_ctrl_trs_ct	Determines appropriate engine torque on the basis of engine mode (idling, shift in progress, engine starting, etc.)	Parallel hybrid powertrain with CVT	eng_plant_hot_map_si	eng_ctrl_trs_eng_mode_simu eng_ctrl_dmd_trq_simu eng_ctrl_cmd_on_simu eng_plant_spd_out_simu accmech_plant_trq_simu cpl_plant_cmd_simu drv_accel_dmd_simu gb_ctrl_trs_cpl_mode_simu	eng_ctrl_trs_trq_simu eng_ctrl_trs_on_simu
eng_ctrl_trs_au_cylinder_deac_with_str_fco	Determines appropriate engine torque based on the engine mode (idling, shift in progress, engine starting, etc.)	Conventional powertrain with an AU, fuel cut-off, and cylinder deactivation	eng_plant_hot_map_si_fuel_cut_off_with_cylinder_deac	eng_mode vpc_eng_trq_dmd vpc_eng_on_dmd eng_spd accmech_trq cpl_position drv_acc_pedal previous_gear gb_gear_dmd shift_in_progress drv_brk_dmd gen_trq_out veh_speed	eng_ctrl_trs_trq_simu eng_ctrl_trs_on_simu eng_ctrl_trs_fuel_cut_off_simu u eng_ctrl_trs_cylin_deac_state_simu

Autonomie Validation

Argonne has been validating vehicle models for almost 30 years, leveraging vehicle dynamometer test data from the AMTL. Argonne collected test data from more than 60 vehicles, ranging from MY 2000 to the present. Signals were collected on each vehicle for specific control analysis: component efforts (e.g., torque, current, etc.) and flow (e.g., rotational speed, linear speed, etc.), as well as temperatures and direct fuel-flow measurement collected using sensors and high-speed controller area networks (CANs). These measurements were integrated and aligned into a single data acquisition system. Some additional parameters were estimated based on the measured data and other advanced vehicle technology (e.g., electric machine current as estimated from measured speed, torque, and voltage). Each individual model was then independently validated. Vehicle system model validation was quantified using normalized cross-correlation power (Miller et al., 2011), over many cycles.

As a result, most Autonomie vehicle models have been validated within test-to-test repeatability for a wide range of technologies and powertrain configurations. The following section provides some validation examples, using AMTL data.

Conventional Vehicles

The focus of conventional vehicle validation is the shifting algorithm, torque converter lockup, and fuel cutoff. First, the simulated vehicle speed, engine speed, and engine torque are compared with test results. For example, Figure 108 shows this comparison for an automatic transmission on the UDDS cycle.

- Initial calibration (simulation 1)
- Calibrated algorithm using test data (simulation 2)

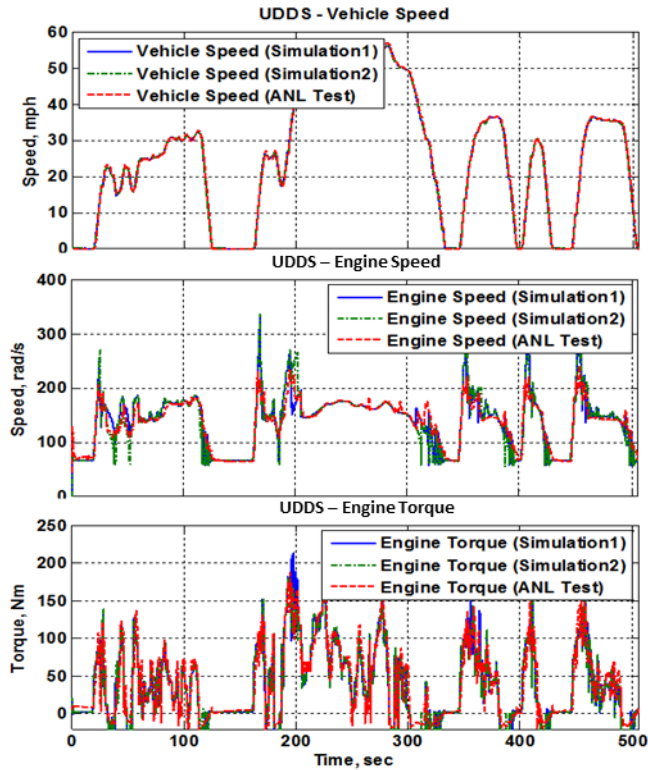


Figure 108. Simulation and testing results on UDDS cycle (0–505 s) for 2013 Hyundai Sonata conventional 6ATX

In Figure 109 the gear numbers on the UDDS cycle are compared with the test results for both 6- and 8-speed transmissions. Shifting performance in both simulations is close to the test results. Figure 110 demonstrates the robust calibration of the shifting algorithm in the new European driving cycle.

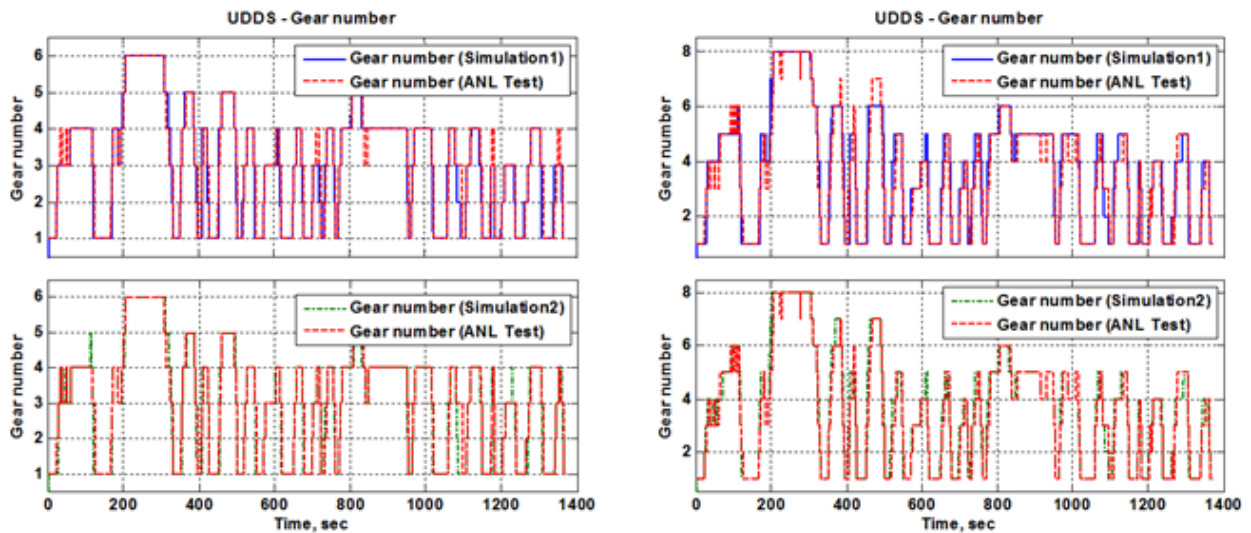


Figure 109. Shifting algorithm validation for 2013 Hyundai Sonata conventional 6ATX (left) and 2013 Chrysler 300 8ATX (right) on the UDDS cycle (0-505 s)

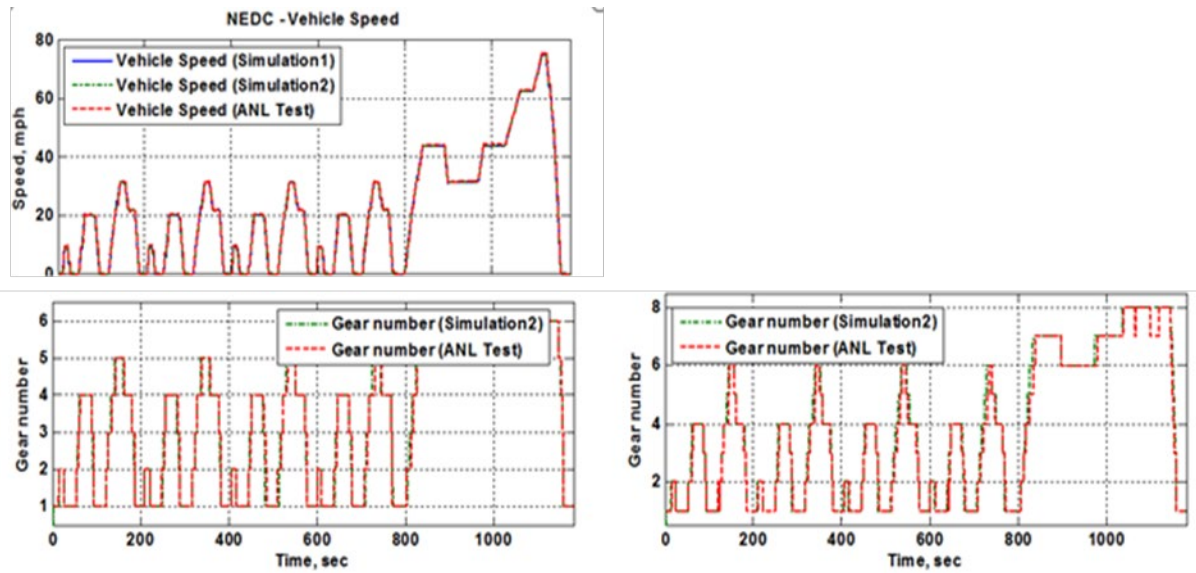


Figure 110. Shifting algorithm validation for 2012 Ford Fusion conventional 6ATX (left) and 2013 Chrysler 300 8ATX (right) on the NEDC cycle

The CVT model and shifting control strategy developed in Autonomie were also validated by comparing the simulation results with the experimental results from Argonne’s AMTL. Figure 111 shows the validation results for the 2012 Honda Civic HEV system on the UDDS and HWFET cycles. The simulated vehicle speed, gear ratio, engine torque and battery SOC behave like the experimental results, demonstrating the validity of the simulation model and control strategy.

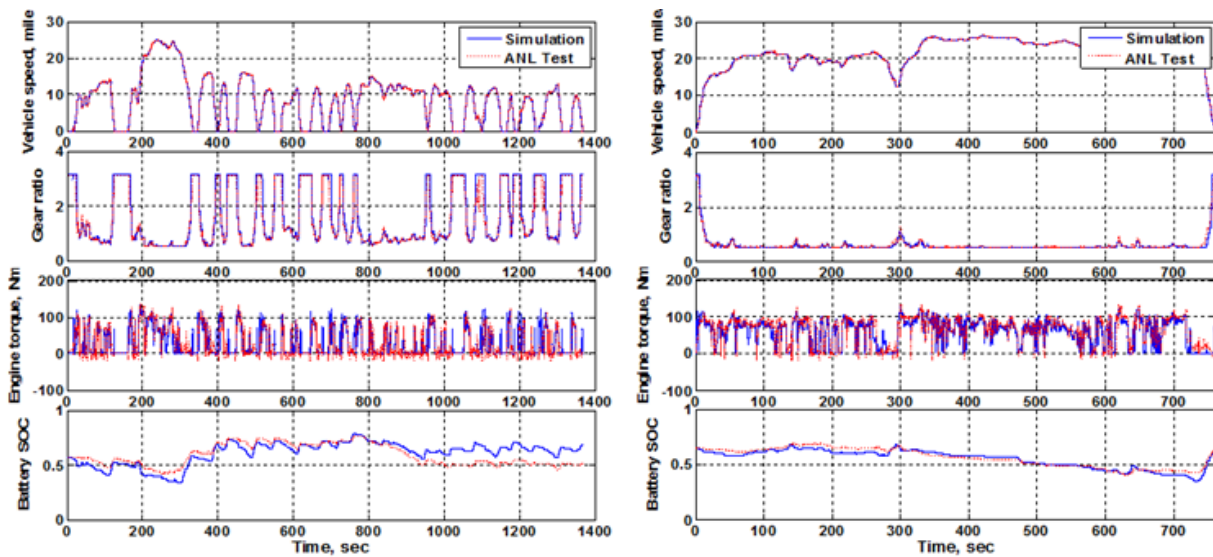


Figure 111. Comparison of simulation and test data for 2012 Honda Civic CVT HEV on UDDS (left) and HWFET (right) cycles

Power-Split HEV

Multiple versions of the power-split HEV have been tested and validated since early 2000. As with the other powertrains, the focus is first on validating the component operating conditions throughout the driving cycles. For example, Figure 112 shows consistent engine ON/OFF, SOC control and component operating conditions (e.g., engine torque, and speed) for the 2010 Toyota Prius on the UDDS cycle. The latest Toyota Prius HEV has been similarly validated.

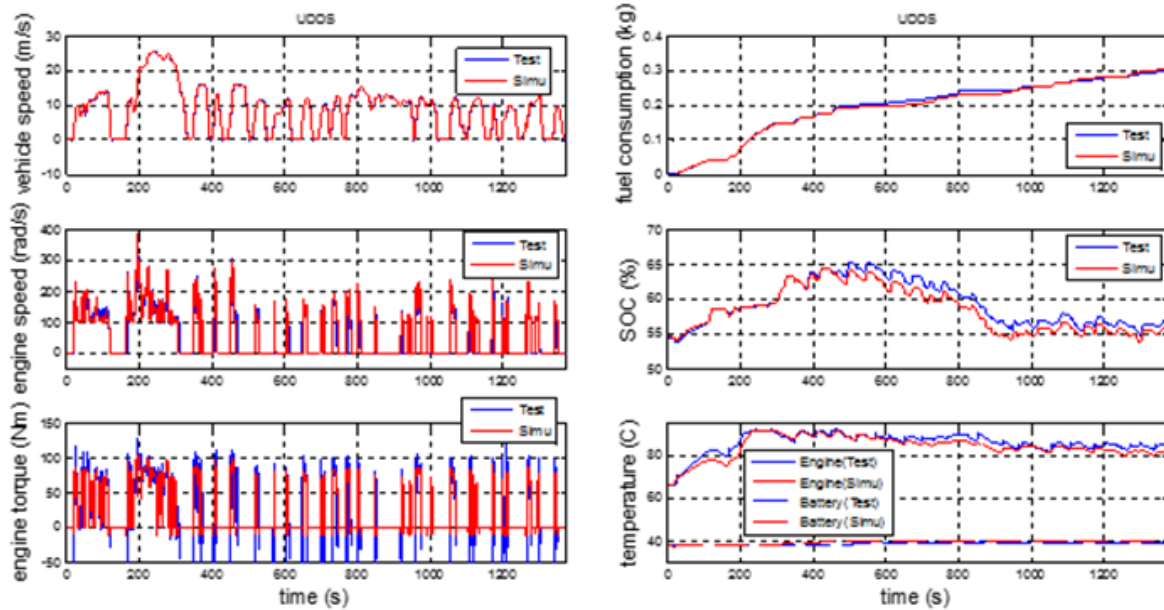


Figure 112. Results of simulation and testing on UDDS cycle for 2010 Toyota Prius HEV

Pre-Transmission HEV

Argonne used AMTL test data from the 2013 Jetta DCT hybrid to validate the pre-transmission HEV control logic. The simulation results for the vehicle speed, gear number, and battery SOC on the UDDS cycle, shown in Figure 113, showed good correlation with the test data.

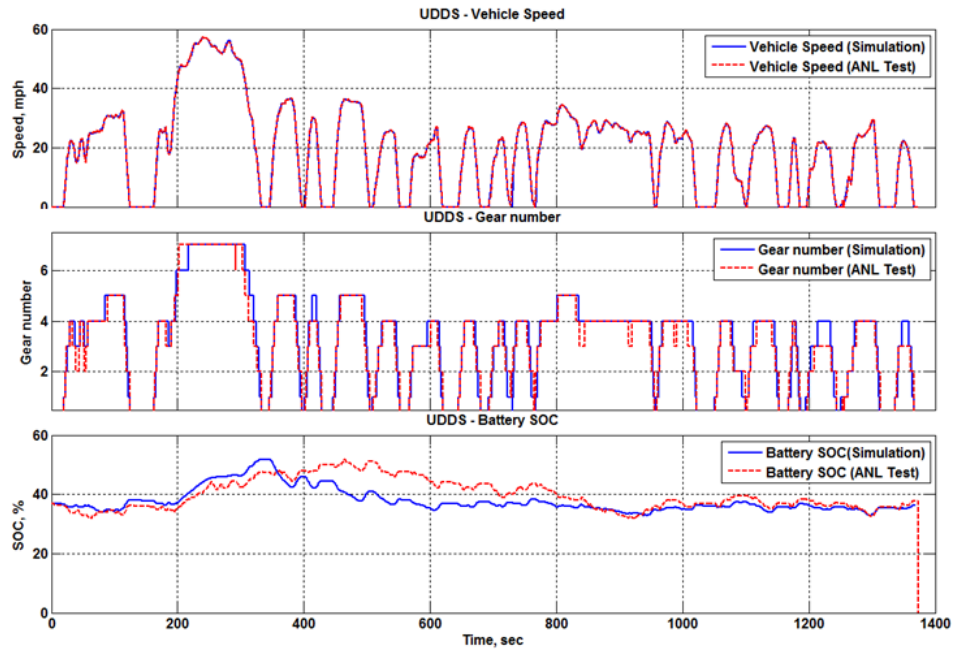


Figure 113. Results of simulation and testing on UDDS cycle for 2013 Jetta DCT hybrid

Range-Extender PHEV

Argonne used AMTL test data from the second-generation Chevrolet Volt to validate the range-extender PHEV model in different thermal conditions. The vehicle operating behavior, including vehicle speed, battery SOC, fuel consumption, and engine speed, torque, and temperature under ambient temperature were successfully compared with the testing results shown in Figure 114.

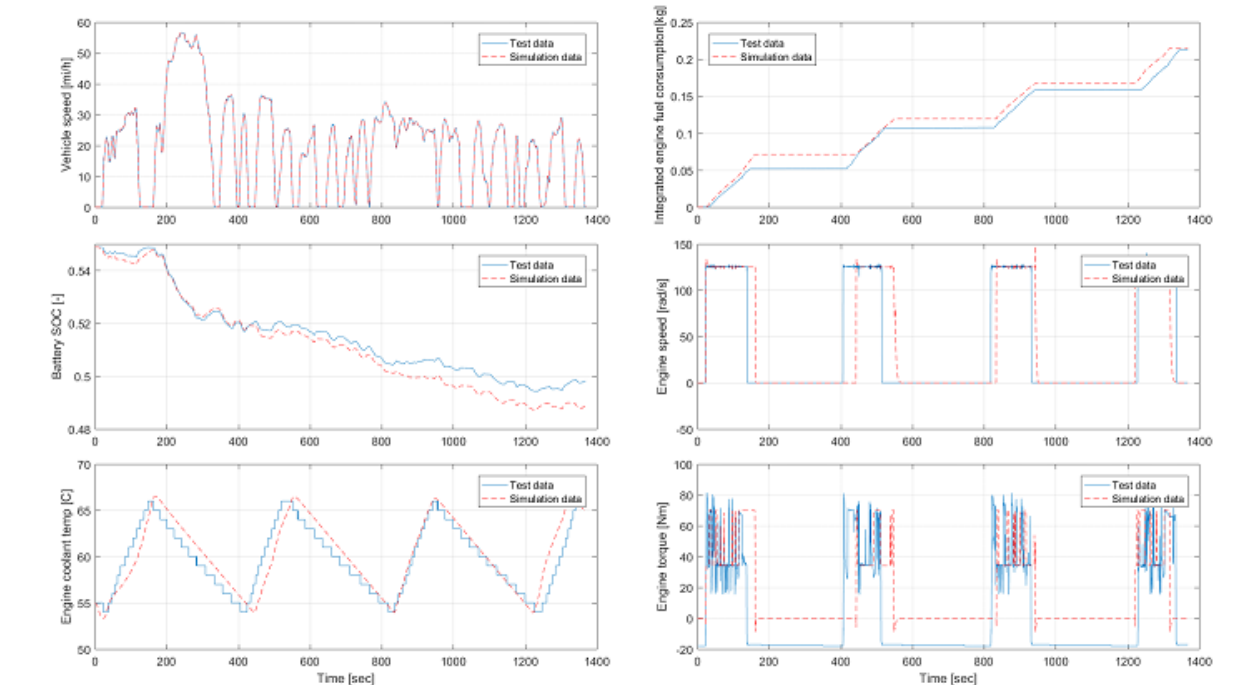


Figure 114. Results of simulation and testing on UDDS cycle for 2012 Chevrolet Volt PHEV

Additional configurations including start-stop, blended PHEV, and BEVs have also been validated.

Battery Performance and Cost Model

Argonne’s Chemical Sciences and Engineering division developed a lithium-ion battery performance and cost (BatPaC) model software for EVs (www.anl.gov/cse/batpac-model-software).

To accelerate the large-scale simulation process, a lookup table replaces the traditional BatPaC model initially developed in Microsoft Excel. The lookup table is dependent on powertrain options and consists of two dimensions—pack power and pack energy. The battery pack designs, including number of cells, modules, cell chemistry and heat transfer fluid, are fixed for each powertrain. Additional lookup tables for other BatPaC parameters (e.g., positive electrode thickness, negative electrode thickness, battery open circuit voltage, and battery pack volume) are also generated as constraints.

Process

The BatPaC model spreadsheet comes with a set of default specifications comparing seven different batteries for HEVs, PHEVs, and BEVs (Table 8). For the current set of runs, BatPaC v5.0 (March 2022) was used.

Table 8. BatPaC input details for BatPaC 4.0 October 1, 2020

Key Inputs	Tab/Sheet	Row No.
Vehicle type (micro-HEV, HEV-HP, PHEV, EV)	Dashboard	E28
Battery energy storage, kWh	Dashboard	42-44
Pulse power requirement, kW	Dashboard	33
Production volume, packs per year	Dashboard	39
Cathode/anode combination	Dashboard	D9

Cathode/Anode Combination Selection

A specific electrode combination is selected from the dropdown menu on Dashboard E9 in the Chem tab. The default values used in the calculations associated with the selected electrode are listed in Columns D and H. The user can override the default material property or price by entering new values in Columns E and I. Figure 115 shows the BatPaC model input for cathode/anode selection.

Chemistry		Current Selection	Choose
Electrode Pair	NMC622-G	NMC622-G	▼

Figure 115. BatPaC cathode/anode pair selection

Table 9. BatPaC output performance metric

Performance Metrics	Cost Parameters
Cell, Module, and Pack Level	Cell, Module, and Pack
Dimensions Mass Volume Voltage Wh/kg, Wh/liter Material inventory	Cost of production Cost breakdown

BatPaC Examples From Existing Vehicles in the Market

To validate BatPaC predictions, we referenced A2Mac1 benchmarking data using battery packs from current production vehicles across multiple vehicle classes and powertrains. The A2Mac1 data was then compared with the predicted battery pack designs from BatPaC, using the default assumptions (except the pack configuration).

Full HEV

The A2MAC1 battery cell teardown analysis for the following vehicles were used to evaluate the assumptions for full HEV.

- 2014–2018 Infiniti QX60
- 2016–2019 Prius Gen4
- 2016–2018 Toyota Rav4 Hybrid
- 2019 Toyota Camry Hybrid
- 2013–2016 Volkswagen (VW) Jetta Hybrid
- 2011–2019 Toyota Highlander Hybrid
- 2016–2019 Acura RLX Hybrid

The battery pack characteristics from HEV production vehicles and BatPaC are shown in Table 10 and Table 11.

Table 10. HEV battery pack details

Parameter	2014–2018 Infiniti QX60	2016–2019 Prius Gen4	2016–2018 Toyota Rav4 Hybrid	2019 Toyota Camry Hybrid	2013–2016 VW Jetta Hybrid	2011–2019 Toyota Highlander Hybrid	2014 Acura RLX Hybrid
Power (kW)	17	37.8	45.9	45.9	20	54	59
Energy (kWh)	0.63	0.75	1.59	1.59	1.1	1.87	1.3
Cells/module	40	28	34	34	15	30	12
Modules/pack	1	2	1	1	4	1	6
Number of modules in parallel	1	1	1	1	1	1	1
Total number of cells	40	56	34	34	60	30	72
Cathode type	NMC333-G	NMC333-G	NMC333-G	NMC333-G	NMC333-G	NMC333-G	NMC333-G
Cooling medium	Air	Air	Air	Air	Air	Air	Air
Cell mass (g)	260	201	-	216	253	-	-
Specific energy (Wh/kg) at pack	22.4	32	34.2	34.2	20.8	27.5	33.2
Battery pack mass (kg)	28.3	33.44	46.5	46.5	53	68	39
Battery cell capacity (Ah)	4.4	3.62	-	4.32	5	-	-
Battery pack nominal voltage (V)	144	204.4	244.8	244.8	220	288	260

Table 11. BatPaC HEV prediction

Parameter	2014–2018 Infiniti QX60	2016–2019 Prius Gen4	2016–2018 Toyota Rav4 Hybrid	2019 Toyota Camry Hybrid	2013–2016 VW Jetta Hybrid	2011–2019 Toyota Highlander Hybrid	2016–2019 Acura RLX Hybrid
Cell mass (g)	144	176	416	416	144	544	224
Specific energy (Wh/kg)	28.13	31.875	48.125	48.125	37.5	52.5	31.875
Battery pack mfr. cost (\$)	1,492	1,839	1,669	1,669	1,863	1,674	2,233
Total cost of packs (\$/kwh)	2,368.25	2,452	1,049.7	1,049.7	1,693.64	895.2	1,717.7
Battery pack mass (kg)	22.4	28.8	33.6	33.6	28.8	35.2	41.6
Battery pack volume	13	16	15	15	18	16	22
Battery cell capacity (Ah)	4	4	13	13	5	17	5
Battery pack nominal voltage (v)	147	206	125	125	220	110	264

PHEVs

The battery cell teardown analysis from A2MAC1 and Total Battery Consulting (<https://totalbatteryconsulting.com>) were used to evaluate the assumptions for plug-in hybrids.

- 2016–2018 BMW X5 xDrive40e
- 2019 BMW i8
- 2016–2017 Mercedes GLE550e
- 2017–2018 Fusion Energi
- 2012–2015 Toyota Prius Plug-In
- 2016–2018 Audi A3 e-tron

The battery pack characteristics from PHEV production vehicles and BatPaC are shown in Table 12 and Table 13.

Table 12. PHEV battery pack details

Parameter	2016–2018 BMW X5 xDrive40e	2019 BMW i8	2016– 2017 Mercedes GLE550e	2017–2018 Fusion Energi	2012–2015 Toyota Prius Plug-In	2016–2018 Audi A3 e-tron
Power (kw)	83	105	90	68	60	75
Energy (kWh)	9.2	11.6	8.7	7.6	4.4	8.7
Cell/ module	16	96	20	21	14	96
Modules/pack	6	1	6	4	4	1
Number of modules in parallel	1	1	1	1	1	1
Total number of cells	96	96	120	84	56	96
Cathode type	NMC333-G	NMC333-G	LFP-G	NMC333-G	NMC333-G	NMC333-G
Cooling medium	EG-W	EG-W	EG-W	CoolA	CoolA	Liquid
Cell mass (g)	703	824	631	690	720	690
Specific energy (Wh/kg) at pack	85.7	102.6	76.3	65	58	74.4
Battery pack mass (kg)	105	113	133.67	123	76	117
Battery cell capacity (Ah)	26	34	22	25	21	25
Battery pack nominal voltage (v)	355	355	396	309.1	206	360

Table 13. BatPaC PHEV predictions

Parameter	2016– 2018 BMW X5 xDrive40e	2019 BMW i8	2016–2017 Mercedes GLE550e	2017–2018 Fusion Energi	2012–2015 Toyota Prius Plug-In	2016– 2018 Audi A3 e-tron
Cell mass (g)	528	660	528	492	444	492
Specific energy at pack (Wh/kg)	97.5	101.67	73.33	104.17	90.83	102.5
Battery pack mfr. cost (\$)	3842	4122	4331	3328	2488	3663
Total cost of packs (\$/kwh)	417.61	355.34	497.82	437.9	565.45	421.03
Battery pack mass (kg)	94.8	114	118.8	73.2	48	85.2
Battery pack volume (l)	42	50	54	41	30	42

Parameter	2016–2018 BMW X5 xDrive40e	2019 BMW i8	2016–2017 Mercedes GLE550e	2017–2018 Fusion Energi	2012–2015 Toyota Prius Plug-In	2016– 2018 Audi A3 e-tron
Battery cell capacity (Ah)	26	33	22	25	21	25
Battery pack nominal voltage (v)	352	352	394	308	206	352

EVs

The battery cell teardown analysis from A2MAC1 and TBS for the following vehicles were used to evaluate the assumptions used for EVs.

- 2019 BMW i3
- 2017–2019 Chevrolet Bolt
- 2019 Hyundai Kona Standard Range
- 2020 Nissan Leaf
- 2019 Audi e-Tron

The battery pack characteristics from BEV production vehicles and BatPaC are shown in Table 14 and Table 15.

Table 14. Battery pack details for EVs

Parameter	2019 BMW i3	2017–2019 Chevrolet Bolt	2019 Hyundai Kona Standard Range	2020 Nissan Leaf	2019 Audi e-Tron
Power (kW)	125	160	100	110	300
Energy (kWh)	42.2	60	39.2	40	95
Number cells/module	12	32	90	8	12
Number modules/pack	8	9	2	24	36
Number of modules in parallel	1	3	2	2	4
Total number of cells	96	288	180	192	432
Cell chemistry	NMC622-G	NMC622-G	NMC622-G	NMC532-G	NMC622-G
Cooling medium	EG-W	EG-W	EG-W	EG-W	EG-W
Cell Mass (g)	2212	832	965	908	877
Specific energy (Wh/kg) at pack	160	140.63	123.7	135.6	142
Battery pack mass (kg)	275	426.64	317	295	681
Battery cell capacity (Ah)	120	56	63	56.3	61.2

Parameter	2019 BMW i3	2017–2019 Chevrolet Bolt	2019 Hyundai Kona Standard Range	2020 Nissan Leaf	2019 Audi e-Tron
Battery pack nominal voltage (V)	360	355	327	350	396

Table 15. BatPaC EVs prediction

Parameter	2019 BMW i3	2017–2019 Chevrolet Bolt	2019 Hyundai Kona Standard Range	2020 Nissan Leaf	2019 Audi e-Tron
Cell mass (g)	1,730	840	880	910	890
Specific energy at pack (Wh/kg)	172	167	138	150	166
Battery pack mfr. cost (\$)	8,023	11,949	8,707	9,119	17,583
Total cost of packs (\$/kWh)	190.12	199.15	222.12	227.98	185.08
Battery pack mass (kg)	246	358	284	267	572
Battery pack volume (L)	113	165	122	130	268
Battery cell capacity (Ah)	118	56	58	57	59
Battery pack nom. voltage (V)	360	360	338	351	405

Use of BatPaC in Autonomie

For the current study, significant changes were made to the BatPaC inputs to Autonomie, as different battery pack configurations were selected for different vehicle classes and powertrains, including numbers of the following.

- cells per module
- cells in parallel
- modules in row
- rows of modules per pack
- modules per battery pack
- modules in parallel

BatPaC provides Autonomie with the battery pack weight and cost as well as the cell capacity in ampere hours for different battery total energy and power requirements. These requirements and sets of configurations had been implemented for both LDV and HDPVs.

Table 16 provides the BatPaC assumptions for mild hybrid BISG for the different vehicle classes.

Table 16. BatPaC assumptions for mild hybrid BISG

Vehicle Class	Compact, Midsize	Small SUV, Midsize SUV, Pickup	HDPUVs
Cell chemistry	LFP-G	LFP-G	LFP-G
Numbers of cells per module	14	14	14
Number of cells in parallel	1	1	1
Number of modules in row	1	1	1
Number of rows of modules per pack	1	1	1
Number of modules per battery pack	1	1	1
Number of modules in parallel	1	1	1
Cells per battery pack	14	14	14
Maximum thickness limit, um	70	70	70
Number of batteries produced per year	200,000	200,000	200,000
Cell plant capacity, GWh	35	35	35
Nominal pack voltage	47	47	47

Table 17 provides the BatPaC assumptions for full HEVs for the different vehicle classes.

Table 17. BatPaC assumptions for full HEVs

Vehicle Class	Compact, Midsize	Small SUV, Midsize SUV, Pickup	HDPUVs
Cell chemistry	NMC622-G-Power	NMC622-G-Power	NMC622-G-Power
Numbers of cells per module	40	60	60
Number of cells in parallel	1	1	1
Number of modules in row	1	1	1
Number of rows of modules per pack	1	2	2
Number of modules per battery pack	1	2	2
Number of modules in parallel	1	1	1
Cells per battery pack	40	60	60
Maximum thickness limit, um	70	70	70
Number of batteries produced per year	200,000	200,000	200,000
Cell plant capacity, GWh	35	35	35
Nominal pack voltage	159	239	239

Table 18 provides the BatPaC assumptions for power-split PHEV 20 AER/par PHEV 20 AER for the different vehicle classes.

Table 18. BatPaC assumptions for PHEV20 AER

Vehicle Class	Compact, Midsize	Small SUV, Midsize SUV, Pickup	HDPUVs
Cell chemistry	NMC622-G-Power	NMC622-G-Power	NMC622-G-Power
Numbers of cells per module	20	24	24
Number of cells in parallel	1	1	1
Number of modules in row	2	2	2
Number of rows of modules per pack	2	2	2
Number of modules per battery pack	4	4	4
Number of modules in parallel	1	1	1
Cells per battery pack	80	96	96
Maximum thickness limit, um	70	70	70
Number of batteries produced per year	20,000	20,000	20,000
Cell plant capacity, GWh	35	35	35
Nominal pack voltage	295	354	354

Table 19 provides the BatPaC assumptions for PHEV 50 AERs for the different vehicle classes.

Table 19. BatPaC assumptions for PHEV50 AER

Vehicle Class	Compact, Midsize	Small SUV, Midsize SUV, Pickup	HDPUVs
Cell chemistry	NMC622-G-Energy	NMC622-G-Energy	NMC622-G-Energy
Numbers of cells per module	24	26	26
Number of cells in parallel	2	2	2
Number of modules in row	2	2	2
Number of rows of modules per pack	4	4	4
Number of modules per battery pack	8	8	8
Number of modules in parallel	1	1	1
Cells per battery pack	192	208	208
Maximum thickness limit, um	70	70	70
Number of batteries produced per year	20,000	20,000	20,000
Cell plant capacity, GWh	35	35	35
Nominal pack voltage	353	382	382

Table 20 provides the BatPaC assumptions for BEV 150/200/250 AERs for the different vehicle classes.

Table 20. BatPaC assumptions for BEV 150/200/250 AERs

Vehicle Class	Compact, Midsize	Small SUV, Midsize SUV, Pickup	HDPUVs
Cell chemistry	NMC622-G-Energy	NMC622-G-Energy	NMC622-G-Energy
Numbers of cells per module	16	20	20
Number of cells in parallel	4	4	4
Number of modules in row	5	5	5
Number of rows of modules per pack	4	4	4
Number of modules per battery pack	20	20	20
number of modules in parallel	1	1	1
Cells per battery pack	320	400	400
Maximum thickness limit, um	70	70	70
Number of batteries produced per year	60,000	60,000	60,000
Cell plant capacity, GWh	35	35	35
Nominal pack voltage	295	368	368

Table 21 provides the BatPaC assumptions for BEV 300 AERs for the different vehicle classes.

Table 21. BatPaC assumptions for BEV300 AERs

Vehicle Class	Compact, Midsize	Small SUV, Midsize SUV, Pickup	HDPUVs
Cell chemistry	NMC622-G-Energy	NMC622-G-Energy	NMC622-G-Energy
Numbers of cells per module	20	25	25
Number of cells in parallel	4	5	5
Number of modules in row	5	5	5
Number of rows of modules per pack	4	4	4
Number of modules per battery pack	20	20	20
number of modules in parallel	1	1	1
Cells per battery pack	400	500	500
Maximum thickness limit, um	70	70	70
Number of batteries produced per year	60,000	60,000	60,000
Cell plant capacity, GWh	35	35	35
Nominal pack voltage	368	368	368

Table 21 provides the BatPaC assumptions for BEV 400 AERs for the different vehicle classes.

Table 22. BatPaC assumptions for BE4300 AERs

Vehicle Class	Compact, Midsize	Small SUV, Midsize SUV, Pickup	HDPUVs
Cell chemistry	NMC622-G-Energy	NMC622-G-Energy	NMC622-G-Energy
Numbers of cells per module	30	30	30
Number of cells in parallel	5	6	6
Number of modules in row	4	5	5
Number of rows of modules per pack	4	4	4
Number of modules per battery pack	16	20	20
number of modules in parallel	1	1	1
Cells per battery pack	480	600	600
Maximum thickness limit, um	70	70	70
Number of batteries produced per year	60,000	60,000	60,000
Cell plant capacity, GWh	35	35	35
Nominal pack voltage	353	368	368

Setting Assumptions in BatPaC for This Analysis

This section details how the BatPaC files are set up for different powertrains. There are different spreadsheets for different powertrains, and in each spreadsheet, the different columns correspond to different vehicle classes.

Vehicle Type

In the Dashboard tab of the BatPaC file, the vehicle powertrain type (e.g., micro-HEV, HEV-HP, PHEV, and EV) is selected from the dropdown menu in cell E32.



Figure 118. Setting vehicle type

Battery Cell Manufactured at Scale

For this analysis, Argonne evaluated different battery cell plant manufacturing factors and implemented a cell manufacturing assumption at scale of 35 GWh. Therefore, for the different battery packs manufactured for different production volumes, the battery cells are being manufactured at 35 GWh.

Cell Chemistry

In the Dashboard tab, users can select the cell chemistry from the dropdown menu in cell E13. The default cell chemistry values can then be viewed in column D of the Chem tab. For example, Figure 119 shows the cell chemistry selection for BEV200. For this analysis, NMC622 was selected for full HEVs, PHEVs, and BEVs, as the cell chemistry is applicable to a wide range of vehicles based on the benchmarking details provided later in this report.

System ID	NMC622-G (Energy)	Column #	38	
Description				
Property	Applied Value	BatPaC Default	Override	Notes
Couple Name	Li(Ni0.5Mn0.3Co0.2)O2 / Graphite			
Positive Electrode Composition, Weight %				
Positive electrode active material weight %	96.0	96.0		
Positive electrode carbon additive weight %	2.0	2.0		
Positive electrode binder weight %	2.0	2.0		
Binder solvent for positive electrode	NMP	NMP		
Positive Material Density, g/cm³				
Positive electrode active material density, g/cm ³	4.65	4.65		
Positive electrode carbon additive density, g/cm ³	1.83	1.83		
Positive electrode binder density, g/cm ³	1.77	1.77		
Positive Electrode Structural/Kinetic Properties				
Positive electrode porosity, volume % of void space	25.0	25.00		
Positive electrode active material particle radius, μm	2.0	2.00		
Positive electrode specific particle area "a", cm ² /cm ³	10,155	10155		
Positive electrode active material exchange current, i ₀ , mA/cm ²	0.6	0.60		
Maximum thickness limit for positive electrode, mm	70	120		
Minimum thickness limit for positive electrode, mm	15	15		
Positive Foil Properties				
Positive foil material	Aluminum	Aluminum		
Positive foil thickness, μm	15	15		
Negative Electrode				
Add 5% silicon to negative electrode?	No	No		
Negative Electrode Active Material	G	G		
Negative-to-positive capacity ratio after formation	1.10	1.10		
Negative electrode active material capacity, mAh/g:	360	360		
Negative Electrode Composition, Weight %				
Negative electrode active weight %	98.0	98.0		
Negative electrode carbon additive weight %	0.0	0.0		
Negative electrode binder weight %	2.0	2.0		
Binder solvent for negative electrode	Water	Water		
Negative Material Density, g/cm³				
Negative electrode active material density, g/cm ³	2.24	2.24		
Negative electrode carbon additive density, g/cm ³	1.95	1.95		
Negative electrode binder density, g/cm ³	1.10	1.10		
Negative Electrode Structural/Kinetic Properties				
Negative electrode porosity, volume % of void space	25	25.0		
Negative electrode active material particle radius, μm	6	6.0		
Negative electrode specific area "a", cm ² /cm ³	3,600	3600.4		
Negative electrode active material exchange current, i ₀ , mA/cm ²	0.50	0.5		

Figure 119. Cell chemistry for BEV200

Battery Design

In the Dashboard tab, the battery design information (i.e., number of cells per module, number of cells in parallel, number of modules in row, number of rows of modules per pack, and number of modules in parallel) is set in cells D67:J71. The number of modules per battery pack and the cells per battery pack can be found in the Battery Design tab, in rows 29 and 32.

Dashboard									
EV with NMC622-G (Energy) Electrodes									
Applied input (can only be changed using overrides)			Default input values (may be changed)			Required input by user		Optional override input	
Reset Calculation									
Restart (0/1)			1		OR		CTRL+ SHIFT + R if Macro Enabled to Reconverge Calculation		
Pack Configuration									
		Battery 1	Battery 2	Battery 3	Battery 4	Battery 5	Battery 6	Battery 7	
67	Number of cells per module	16	16	20	20	20	16	20	
68	Number of cells in parallel	4	4	4	4	2	4	4	
69	Number of modules in row	5	5	5	5	5	5	5	
70	Number of rows of modules per pack	4	4	4	4	4	4	4	
71	Number of modules in parallel	1	1	1	1	2	1	1	
Add set of default pack designs (power, energy, pack configurations)									
Battery Pack Parameters									
20	Vehicle type		EV	EV	EV	EV	EV	EV	EV
21	Designated duration of power pulse		10	10	10	10	10	10	10
22	Target pack power, kW		100	100	100	100	100	100	100
23	Estimated pack power at target % OCV, kW		538	538	874	874	871	538	874
24	Target pack energy, kWh		60.00	60.00	100.00	100.00	100.00	60.00	100.00
25	Number of cells per module		16	16	20	20	20	16	20
26	Number of cells in parallel		4	4	4	4	2	4	4
27	Number of modules in row		5	5	5	5	5	5	5
28	Number of rows of modules per pack		4	4	4	4	4	4	4
29	Number of modules per pack		20	20	20	20	20	20	20
30	Number of modules in parallel		1	1	1	1	2	1	1
31	Cells per pack		320	320	400	400	400	320	400
32	Total cells per battery system		320	320	400	400	400	320	400

Figure 120. Battery design information

Maximum Thickness Limit

Based on the current status of the industry and feedback from the developers of the BatPaC model, a maximum thickness limit of 70 μm is specified for all batteries. In the Dashboard tab, the maximum thickness value is placed in cell E18.

Dashboard			
EV with NMC622-G (Energy) Electrodes			
Applied input (can only be changed using overrides)		Default input values (may be changed)	
Reset Calculation			
Restart (0/1)		1	OR CTRL+ SHIFT + F
Inputs			
Chemistry			
		Current Selection	Choose
	Electrode Couple	NMC622-G (Energy)	NMC622-G (Energy)
	Positive Electrode: Li(Ni _{0.5} Mn _{0.3} Co _{0.2})O ₂		Override
	Positive active material specific capacity, mAh/g	191	
	Void volume fraction, % of positive electrode	25	
	Positive foil thickness, μm	15	
	Maximum positive electrode thickness, μm	70	70

Figure 121. Setting maximum thickness

Number of Battery Systems Manufactured per Year

In the Dashboard tab, the number of battery systems manufactured per year is entered in row 105. A constant production volume of 60,000 battery systems is assumed for BEVs, a production volume of 20,000 for PHEVs, and a production volume of 200,000 battery systems for all HEVs, including mild hybrid BISG.

Plant Specifications							
		Battery 1	Battery 2	Battery 3	Battery 4	Battery 5	
102							
103							
104							
105	Number of packs manufactured per year	60,000	60,000	60,000	60,000	60,000	

Figure 122. Battery systems manufactured per year

Inputs to BatPaC From Autonomie

The following inputs are sent to BatPaC for Autonomie simulations.

- battery pack power (kW)
- total battery pack energy (kWh)

Power and Storage Requirements								
Power								
	Battery 1	Battery 2	Battery 3	Battery 4	Battery 5	Battery 6	Battery 7	
35								
36								
37								
38	Target rated peak power of pack, kW	100	100	100	100	100	100	100
39								
40								
41								
42								
43								
44								
45								
46								
47								
48								
49								
50	Fill in value for either capacity or energy							
51	Total pack capacity, 0-100% SOC (Ah)							
52	Total pack energy, 0-100% SOC (kWh)	60.0	60.0	100.0	100.0	100.0	60	100
53								

Figure 123. Autonomie inputs to BatPaC

Outputs From BatPaC Into Autonomie

The following outputs are sent to Autonomie from BatPaC.

- estimated total battery cost (\$)
- total battery mass (kg)
- battery pack capacity (Ah)
- nominal battery system voltage (v)

Dashboard								
EV with NMC622-G (Energy) Electrodes								
Applied input (can only be changed using overrides)			Default input values (may be changed)			Required input by user		Optional override input
Reset Calculation								
Restart (0/1)			1	OR	CTRL+ SHIFT + R if Macro Enabled to Reconverge Calculation			
System	EV Vehicle with NMC622-G (Energy) Electrodes	Battery 1	Battery 2	Battery 3	Battery 4	Battery 5	Battery 6	Battery 7
88	Configuration Errors	None	None	None	None	None	None	None
89	Configuration Warnings	None	None	None	None	None	None	None
90	1 Battery system total energy, kWh	60	60	100	100	100	60	100
91	2 Battery system capacity, Ah	204	204	272	272	272	204	272
92	3 Battery system rated power, kW	100	100	100	100	100	100	100
93	4 Battery system nominal operating voltage, V	294	295	368	368	368	295	368
94	5 Pack power to energy ratio (with respect to rated power)	1.7	1.7	1.0	1.0	1.0	1.7	1.0
95	6 Pack energy density, Wh/L	274	274	310	310	310	274	310
96	7 Pack specific energy, Wh/kg	161	161	178	178	178	161	178
97	8 Number of modules per pack	20	20	20	20	20	20	20
98	9 Number of cells per pack	320	320	400	400	400	320	400
99	10 Pack volume, L	219	219	322	322	322	219	322
200	11 Pack total mass, kg	373	373	563	563	561	373	563
201	12 Cell capacity, Ah	50.9	50.9	67.9	68	68	51	68
202	13 Cell nominal operating voltage, V	3.68	3.68	3.68	3.68	3.68	3.68	3.68
203	14 Positive electrode thickness, μm	70.0	70	70	70	70	70	70
204	15 Positive electrode areal capacity, mAh/cm ²	4.4	4.4	4.4	4.4	4.4	4.4	4.4
205	16 Negative electrode thickness, μm	80	80	80	80	80	80	80
206	17 Negative electrode areal capacity, mAh/cm ²	4.7	4.7	4.7	4.7	4.7	4.7	4.7
207	18 Cell energy density, Wh/L	558	558	585	585	585	558	585
208	19 Cell specific energy, Wh/kg	289	289	292	292	292	289	292
209	20 Pack cost, \$/pack	8,436	8,436	12,726	12,726	12,810	7,868	12,111
210	21 Pack cost, \$/kWh	141	141	127	127	128	131	121
211	22 Pack cost, \$/kWh(Useable)	165	165	150	150	151	154	142
212	23 Cell cost, \$/kWh	98	98	95	95	95	92	91
213	24 Plant Size, GWh	4	4	6	6	6	35	35
214	25 Packs manufactured per year (packs/year)	60,000	60,000	60,000	60,000	60,000	583,333	350,000
215	26 Savings for producing cells at scale	-344	-344	-394	-394	0	0	0

Figure 124. BatPaC Outputs to Autonomie

BatPaC Lookup Tables

Micro HEV

Table 23 summarizes the battery pack costs for micro-HEVs.

Table 23. Battery cost table for micro-HEVs

Vehicle Class	Performance Category	Battery cost (\$)
Compact	Base	113
Compact	Premium	113
Midsize	Base	113
Midsize	Premium	113
Small SUV	Base	113
Small SUV	Premium	113
Midsize SUV	Base	113
Midsize SUV	Premium	113
Pickup	Base	113
Pickup	Premium	113

The battery mass of micro-HEVs differs across classes and performance categories. It is defined in the assumptions sheet shown in Table 24.

Table 24. Mass assumptions for micro-HEVs

Vehicle Class	Performance Category	Battery Mass (kg)	
		Gasoline	Diesel
Compact	Base	15	20
Compact	Premium	25	30
Midsize	Base	18	20
Midsize	Premium	28	30
Small SUV	Base	18	20
Small SUV	Premium	28	30
Midsize SUV	Base	20	25
Midsize SUV	Premium	30	35
Pickup	Base	20	20
Pickup	Premium	30	35

Mild Hybrid BISG

For mild hybrid BISGs, mass and costs of additional pack level components (e.g., pack hardware, TMS, high voltage wiring, and BMU) are subtracted.

Table 25 summarizes the final lookup tables generated from BatPaC for mild hybrid BISG battery packs for cost, mass, and cell capacity.

Table 25. BatPaC lookup table for mild hybrid BISG

BatPac Cost: Mild BISG						
Power, kW	Energy, kWh					
	0.30	0.40	0.60	0.81	1.00	1.20
5.00	\$280	\$294	\$318	\$342	\$365	\$388
6.00	\$281	\$294	\$318	\$343	\$365	\$388
7.69	\$285	\$294	\$319	\$343	\$366	\$389
8.00	\$286	\$295	\$319	\$343	\$366	\$389
9.00	\$288	\$297	\$319	\$343	\$366	\$389
10.00	\$291	\$300	\$319	\$344	\$366	\$389
BatPac Mass (kg): Mild BISG						
Power, kW	Energy, kWh					
	0.30	0.40	0.60	0.81	1.00	1.20
5.00	8.2	9.3	11.3	13.3	15.1	16.9
6.00	8.2	9.3	11.3	13.3	15.1	16.9
7.69	8.5	9.4	11.4	13.3	15.1	17.0
8.00	8.6	9.4	11.4	13.4	15.2	17.0
9.00	8.8	9.6	11.4	13.4	15.2	17.0
10.00	9.0	9.8	11.4	13.4	15.2	17.0
BatPac Cell Capacity (Ah): Mild BISG						
Power, kW	Energy, kWh					
	0.30	0.40	0.60	0.81	1.00	1.20
5.00	6.40	8.59	12.80	17.19	21.33	25.60
6.00	6.40	8.59	12.80	17.19	21.33	25.60
7.69	6.39	8.59	12.80	17.19	21.33	25.60
8.00	6.39	8.59	12.80	17.19	21.33	25.60
9.00	6.39	8.59	12.80	17.19	21.33	25.60
10.00	6.39	8.59	12.80	17.19	21.33	25.60

The mild hybrid BISGs battery packs considered in the current analysis consist of 0.403 kWh total energy with 7.69 kW power output. As a result, BatPaC provides a manufacturing cost of \$294 with a pack mass value of 9.4 kg.

Full Hybrid HEV

Table 26 summarizes the cost, mass, and cell capacities generated for compact and midsize full hybrids from BatPaC, using the assumptions specified in Table 17.

Table 26. BatPaC lookup table for full hybrids (compact/midsize)

BatPac Cost: HEV															
Power, kW	Energy, kWh														
	0.3	0.5	0.7	0.9	1.0	1.2	1.4	1.6	1.8	2.0	2.2	2.4	2.6	2.8	3.0
10.0	\$ 488	\$509	\$ 529	\$ 551	\$562	\$585	\$607	\$ 628	\$650	\$671	\$693	\$ 714	\$ 735	\$ 755	\$776
20.0		\$527	\$547	\$566	\$575	\$594	\$612	\$630	\$651	\$673	\$694	\$715	\$736	\$757	\$777
30.0			\$565	\$584	\$593	\$611	\$629	\$647	\$664	\$682	\$699	\$716	\$737	\$758	\$778
40.0			\$582	\$601	\$611	\$629	\$647	\$664	\$682	\$700	\$716	\$734	\$750	\$767	\$784
60.0						\$664	\$682	\$700	\$717	\$734	\$752	\$769	\$786	\$803	\$820
80.0								\$735	\$752	\$770	\$787	\$804	\$821	\$838	\$855
100.0											\$823	\$840	\$857	\$874	\$892
BatPac Mass (kg): HEV															
Power, kW	Energy, kWh														
	0.3	0.5	0.7	0.9	1.0	1.2	1.4	1.6	1.8	2.0	2.2	2.4	2.6	2.8	3.0
10.0	11.28	12.40	13.49	14.65	15.29	16.54	17.75	18.93	20.09	21.22	22.34	23.44	24.53	25.61	26.68
20.0		13.81	14.88	15.79	16.34	17.26	18.27	19.06	20.22	21.36	22.47	23.58	24.67	25.75	26.82
30.0			16.09	17.08	17.57	18.49	19.34	20.29	21.13	22.01	22.99	23.71	24.80	25.88	26.95
40.0			17.37	18.29	18.79	19.66	20.56	21.44	22.34	23.28	24.02	24.97	25.71	26.56	27.37
60.0						22.09	22.92	23.84	24.68	25.55	26.35	27.22	28.03	28.93	29.67
80.0								26.21	27.05	27.84	28.67	29.55	30.39	31.19	31.97
100.0									29.39	30.18	31.01	31.88	32.64	33.45	34.34

BatPac Cell Capacity (Ah): HEV															
Power, kW	Energy, kWh														
	0.3	0.5	0.7	0.9	1.0	1.2	1.4	1.6	1.8	2.0	2.2	2.4	2.6	2.8	3.0
10.0	1.88	3.14	4.40	5.66	6.29	7.54	8.80	10.06	11.31	12.57	13.83	15.09	16.34	17.60	18.86
20.0		3.13	4.39	5.65	6.28	7.54	8.80	10.06	11.31	12.57	13.83	15.09	16.34	17.60	18.86
30.0			4.39	5.64	6.27	7.53	8.79	10.04	11.30	12.56	13.82	15.09	16.34	17.60	18.86
40.0			4.39	5.64	6.27	7.52	8.78	10.04	11.30	12.55	13.81	15.07	16.33	17.59	18.85
60.0						7.52	8.78	10.03	11.29	12.54	13.80	15.06	16.31	17.57	18.83
80.0								10.03	11.28	12.54	13.79	15.05	16.31	17.56	18.82
100.0									11.28	12.53	13.79	15.04	16.30	17.56	18.81

Table 27 summarizes the cost, mass, and cell capacities generated for full hybrid SUVs, pickups, and HDPUVs from BatPaC, using the assumptions specified.

Table 27. BatPaC lookup table for full hybrids (SUVs/pickups/HDPUVs)

BatPac Cost: HEV															
Power, kW	Energy, kWh														
	0.9	1.0	1.2	1.4	1.6	1.8	2.0	2.2	2.4	2.6	2.8	3.0	3.4	3.8	4.0
10.0	\$652	\$664	\$687	\$710	\$732	\$755	\$776	\$798	\$820	\$841	\$862	\$884	\$926	\$967	\$988
20.0	\$667	\$677	\$696	\$714	\$733	\$755	\$777	\$799	\$821	\$842	\$863	\$885	\$927	\$968	\$989
30.0	\$685	\$694	\$713	\$732	\$750	\$768	\$786	\$804	\$822	\$843	\$864	\$886	\$928	\$969	\$990
40.0	\$702	\$712	\$731	\$749	\$768	\$786	\$803	\$821	\$838	\$856	\$873	\$890	\$929	\$970	\$991
60.0			\$765	\$784	\$802	\$820	\$838	\$855	\$873	\$890	\$908	\$925	\$959	\$993	\$1,010
80.0				\$818	\$837	\$855	\$872	\$890	\$908	\$925	\$942	\$959	\$994	\$1,028	\$1,044
100.0						\$889	\$907	\$924	\$942	\$959	\$977	\$994	\$1,028	\$1,062	\$1,079
150.0											\$1,064	\$1,082	\$1,116	\$1,150	\$1,167
200.0														\$1,244	\$1,261

BatPac Mass (kg): HEV															
Power, kW	Energy, kWh														
	0.9	1.0	1.2	1.4	1.6	1.8	2.0	2.2	2.4	2.6	2.8	3.0	3.4	3.8	4.0
10.0	17.32	17.99	19.28	20.53	21.75	22.94	24.11	25.26	26.39	27.51	28.61	29.71	31.86	33.98	35.03
20.0	18.53	18.95	20.08	20.91	21.86	23.05	24.22	25.37	26.50	27.62	28.72	29.82	31.97	34.09	35.14
30.0	19.87	20.24	21.17	22.18	23.19	24.03	24.95	25.74	26.61	27.73	28.84	29.93	32.08	34.20	35.25
40.0	21.08	21.49	22.49	23.42	24.34	25.27	26.08	26.97	27.77	28.71	29.59	30.40	32.19	34.31	35.36
60.0			24.81	25.78	26.61	27.45	28.34	29.14	30.02	30.85	31.80	32.49	34.14	35.85	36.79
80.0				28.01	28.96	29.82	30.60	31.43	32.35	33.21	34.02	34.78	36.52	38.12	38.87
100.0						32.10	32.88	33.72	34.51	35.37	36.20	36.98	38.59	40.23	41.01
150.0											41.78	42.57	44.20	45.73	46.53
200.0														51.47	52.27
BatPac Cell Capacity (Ah): HEV															
Power, kW	Energy, kWh														
	0.9	1.0	1.2	1.4	1.6	1.8	2.0	2.2	2.4	2.6	2.8	3.0	3.4	3.8	4.0
10.0	3.77	4.19	5.03	5.87	6.70	7.54	8.38	9.22	10.06	10.90	11.73	12.57	14.25	15.93	16.76
20.0	3.76	4.18	5.02	5.86	6.70	7.54	8.38	9.22	10.06	10.90	11.73	12.57	14.25	15.92	16.76
30.0	3.76	4.18	5.02	5.86	6.70	7.54	8.38	9.22	10.06	10.90	11.73	12.57	14.25	15.92	16.76
40.0	3.76	4.18	5.02	5.85	6.69	7.53	8.37	9.21	10.05	10.89	11.73	12.57	14.25	15.92	16.76
60.0			5.01	5.85	6.69	7.52	8.36	9.20	10.04	10.88	11.71	12.55	14.23	15.91	16.75
80.0				5.85	6.68	7.52	8.36	9.20	10.03	10.87	11.71	12.55	14.22	15.90	16.74
100.0						7.52	8.36	9.19	10.03	10.87	11.70	12.54	14.22	15.89	16.73
150.0											11.70	12.53	14.21	15.88	16.72
200.0														15.88	16.71

PHEV 20 AER (Power-Split/Parallel)

Table 28 summarizes the cost, mass, and cell capacities generated for compact and midsize PHEV20 AERs from BatPaC, using the assumptions specified.

Table 28. BatPaC lookup table for PHEV20 AERs (compact/midsize)

BatPac Cost: PHEV20			
Power, kW	Energy, kWh		
	5.0	10.0	20.0
30.0	\$1,570	\$2,120	\$3,193
40.0	\$1,578	\$2,128	\$3,202
60.0	\$1,596	\$2,146	\$3,219
80.0	\$1,613	\$2,163	\$3,237
100.0	\$1,631	\$2,181	\$3,254
120.0	\$1,658	\$2,198	\$3,271
140.0	\$1,703	\$2,215	\$3,289
160.0	\$1,750	\$2,233	\$3,306
200.0	\$1,854	\$2,268	\$3,341
240.0	\$1,975	\$2,341	\$3,376
280.0	\$2,124	\$2,436	\$3,411
BatPac Mass (kg): PHEV20			
Power, kW	Energy, kWh		
	5.0	10.0	20.0
30.0	53.2	80.8	135.2
40.0	53.2	80.8	135.2
60.0	53.4	81.0	135.4
80.0	53.5	81.1	135.5
100.0	53.6	81.2	135.6
120.0	54.3	81.4	135.8
140.0	56.1	81.5	135.9
160.0	58.1	81.6	136.1
200.0	62.7	81.9	136.3
240.0	68.0	84.3	136.6
280.0	74.9	88.1	136.9

BatPac Cell Capacity (Ah): PHEV20			
Power, kW	Energy, kWh		
	5.0	10.0	20.0
30.0	16.9	33.9	67.8
40.0	16.9	33.9	67.8
60.0	16.9	33.9	67.8
80.0	16.9	33.9	67.8
100.0	16.9	33.9	67.8
120.0	16.9	33.9	67.8
140.0	16.9	33.9	67.8
160.0	16.9	33.9	67.8
200.0	16.9	33.9	67.7
240.0	16.9	33.8	67.7
280.0	16.9	33.8	67.7

Table 29 summarizes the cost, mass, and cell capacities generated for SUV, pickup, and HDPUV PHEV20 AERs from BatPaC, using the assumptions specified.

Table 29. BatPaC lookup table for PHEV20 AERs (SUVs/pickups/HDPUVs)

BatPac Cost: PHEV20			
Power, kW	Energy, kWh		
	5.0	10.0	20.0
30.0	\$1,662	\$2,216	\$3,290
40.0	\$1,670	\$2,224	\$3,297
60.0	\$1,684	\$2,238	\$3,312
80.0	\$1,699	\$2,253	\$3,326
100.0	\$1,713	\$2,267	\$3,341
120.0	\$1,737	\$2,282	\$3,355
140.0	\$1,779	\$2,296	\$3,370
160.0	\$1,822	\$2,311	\$3,384
200.0	\$1,919	\$2,340	\$3,413
240.0	\$2,030	\$2,401	\$3,442
280.0	\$2,167	\$2,488	\$3,472

BatPac Mass (kg): PHEV20			
Power, kW	Energy, kWh		
	5.0	10.0	20.0
30.0	55.9	83.8	138.3
40.0	55.9	83.8	138.4
60.0	56.1	84.0	138.5
80.0	56.2	84.1	138.6
100.0	56.3	84.2	138.7
120.0	57.0	84.3	138.8
140.0	58.8	84.4	138.9
160.0	60.8	84.5	139.0
200.0	65.1	84.7	139.3
240.0	70.3	86.8	139.5
280.0	76.8	90.5	139.7
BatPac Cell Capacity (Ah): PHEV20			
Power, kW	Energy, kWh		
	5.0	10.0	20.0
30.0	14.1	28.2	56.5
40.0	14.1	28.2	56.5
60.0	14.1	28.2	56.5
80.0	14.1	28.2	56.5
100.0	14.1	28.2	56.5
120.0	14.1	28.2	56.5
140.0	14.1	28.2	56.5
160.0	14.1	28.2	56.5
200.0	14.1	28.2	56.5
240.0	14.1	28.2	56.5
280.0	14.1	28.2	56.5

PHEV50 AER (Voltec EREV/Parallel)

Table 30 summarizes the cost, mass, and cell capacities generated for compact and midsize PHEV50 AERs from BatPaC using the assumptions specified.

Table 30. BatPaC lookup table for PHEV50 AERs (compact/midsize)

BatPac Cost: PHEV50						
Power, kW	Energy, kWh					
	10.0	20.0	30.0	40.0	50.0	60.0
60.0	\$2,487	\$3,533	\$4,545	\$5,541	\$6,533	\$7,552
80.0	\$2,502	\$3,549	\$4,560	\$5,557	\$6,549	\$7,568
100.0	\$2,518	\$3,564	\$4,576	\$5,573	\$6,565	\$7,584
120.0	\$2,533	\$3,580	\$4,591	\$5,588	\$6,580	\$7,599
140.0	\$2,553	\$3,595	\$4,607	\$5,604	\$6,596	\$7,615
160.0	\$2,601	\$3,611	\$4,623	\$5,620	\$6,612	\$7,631
200.0	\$2,709	\$3,642	\$4,654	\$5,651	\$6,643	\$7,662
240.0	\$2,827	\$3,673	\$4,685	\$5,682	\$6,675	\$7,694
280.0	\$2,960	\$3,727	\$4,716	\$5,714	\$6,706	\$7,725
BatPac Mass (kg): PHEV50						
Power, kW	Energy, kWh					
	10.0	20.0	30.0	40.0	50.0	60.0
60.0	94.1	144.7	188.9	231.6	273.4	315.4
80.0	94.3	144.9	189.1	231.9	273.6	315.6
100.0	94.5	145.1	189.4	232.1	273.9	315.9
120.0	94.7	145.4	189.6	232.3	274.1	316.2
140.0	95.4	145.6	189.9	232.6	274.3	316.4
160.0	96.8	145.8	190.1	232.8	274.6	316.7
200.0	101.1	146.3	190.6	233.3	275.1	317.2
240.0	105.4	146.7	191.1	233.8	275.6	317.7
280.0	110.6	147.9	191.5	234.3	276.1	318.3

BatPac Cell Capacity (Ah): PHEV50						
Power, kW	Energy, kWh					
	10.0	20.0	30.0	40.0	50.0	60.0
60.0	14.14	28.29	42.44	56.60	70.77	84.93
80.0	14.14	28.29	42.44	56.60	70.76	84.93
100.0	14.14	28.29	42.44	56.60	70.76	84.93
120.0	14.14	28.29	42.44	56.60	70.76	84.92
140.0	14.14	28.29	42.44	56.60	70.76	84.92
160.0	14.13	28.29	42.44	56.60	70.76	84.92
200.0	14.11	28.29	42.44	56.60	70.76	84.92
240.0	14.10	28.29	42.44	56.60	70.76	84.92
280.0	14.09	28.28	42.44	56.60	70.76	84.92

Table 31 summarizes the cost, mass, and cell capacities generated for SUV, pickup, and HDPUV PHEV50 AERs from BatPaC using the assumptions specified.

Table 31. BatPaC lookup table for PHEV50 AERs (SUVs/pickups/HDPUVs)

BatPac Cost: PHEV50							
Power, kW	Energy, kWh						
	10.0	20.0	30.0	40.0	50.0	60.0	80.0
60.0	\$2,550	\$3,600	\$4,613	\$5,612	\$6,603	\$7,600	\$9,590
80.0	\$2,564	\$3,614	\$4,628	\$5,626	\$6,617	\$7,615	\$9,605
100.0	\$2,578	\$3,629	\$4,642	\$5,641	\$6,632	\$7,629	\$9,619
120.0	\$2,593	\$3,643	\$4,657	\$5,655	\$6,646	\$7,644	\$9,634
140.0	\$2,608	\$3,657	\$4,671	\$5,669	\$6,661	\$7,658	\$9,648
160.0	\$2,658	\$3,672	\$4,685	\$5,684	\$6,675	\$7,673	\$9,663
200.0	\$2,762	\$3,700	\$4,714	\$5,713	\$6,704	\$7,702	\$9,692
240.0	\$2,878	\$3,729	\$4,743	\$5,742	\$6,733	\$7,731	\$9,721
280.0	\$3,008	\$3,778	\$4,772	\$5,771	\$6,762	\$7,760	\$9,750
BatPac Mass (kg): PHEV50							
Power, kW	Energy, kWh						
	10.0	20.0	30.0	40.0	50.0	60.0	80.0
60.0	96.5	147.4	191.8	234.6	276.4	318.6	399.3
80.0	96.7	147.6	192.0	234.8	276.7	318.8	399.6
100.0	96.9	147.8	192.2	235.1	276.9	319.1	399.8
120.0	97.1	148.0	192.5	235.3	277.1	319.3	400.1
140.0	97.1	148.3	192.7	235.5	277.3	319.6	400.3
160.0	99.2	148.5	192.9	235.7	277.6	319.8	400.6
200.0	103.0	148.9	193.3	236.2	278.0	320.3	401.1
240.0	107.7	149.3	193.8	236.6	278.5	320.8	401.6
280.0	113.0	150.6	194.2	237.1	278.9	321.3	402.1
BatPac Cell Capacity (Ah): PHEV50							
Power, kW	Energy, kWh						
	10.0	20.0	30.0	40.0	50.0	60.0	80.0
60.0	13.05	26.11	39.18	52.24	65.32	78.39	104.55
80.0	13.05	26.11	39.18	52.24	65.32	78.39	104.55
100.0	13.05	26.11	39.18	52.24	65.31	78.39	104.55
120.0	13.05	26.11	39.18	52.24	65.31	78.38	104.55
140.0	13.05	26.11	39.18	52.24	65.31	78.38	104.54
160.0	13.04	26.11	39.18	52.24	65.31	78.38	104.54
200.0	13.02	26.11	39.18	52.24	65.31	78.38	104.54
240.0	13.01	26.11	39.18	52.24	65.31	78.38	104.54
280.0	13.01	26.10	39.18	52.24	65.31	78.38	104.54

BEV 150/200/250 AER

Table 32 summarizes the cost, mass, and cell capacities generated for compact and midsize BEV200-250 AERs from BatPaC using the assumptions specified.

Table 32. BatPaC lookup table for BEV200-250 AERs (compact/midsize)

BatPac Cost: BEV200				
Power, kW	Energy, kWh			
	30.0	50.0	70.0	90.0
20.0	\$4,954	\$6,998	\$9,006	\$11,005
40.0	\$4,976	\$7,020	\$9,028	\$11,026
60.0	\$4,998	\$7,042	\$9,049	\$11,048
80.0	\$5,019	\$7,064	\$9,071	\$11,070
100.0	\$5,041	\$7,086	\$9,093	\$11,092
120.0	\$5,063	\$7,108	\$9,115	\$11,114
140.0	\$5,085	\$7,129	\$9,137	\$11,136
160.0	\$5,107	\$7,151	\$9,159	\$11,158
180.0	\$5,129	\$7,173	\$9,181	\$11,180
200.0	\$5,151	\$7,195	\$9,203	\$11,202
240.0	\$5,194	\$7,239	\$9,247	\$11,247
280.0	\$5,309	\$7,283	\$9,291	\$11,291
320.0	\$5,477	\$7,327	\$9,335	\$11,335
400.0	\$5,844	\$7,415	\$9,423	\$11,423
BatPac Mass (kg): BEV200				
Power, kW	Energy, kWh			
	30.0	50.0	70.0	90.0
20.0	238.54	327.99	413.32	496.23
40.0	239.13	328.58	413.90	496.80
60.0	239.72	329.18	414.51	497.41
80.0	240.31	329.78	415.11	498.02
100.0	240.91	330.39	415.72	498.63
120.0	241.50	330.99	416.33	499.25
140.0	242.09	331.59	416.95	499.87
160.0	242.69	332.20	417.56	500.49
180.0	243.28	332.80	418.17	501.11
200.0	243.88	333.41	418.78	501.73
240.0	245.06	334.62	420.01	502.97

280.0	249.64	335.82	421.23	504.21
320.0	256.68	337.03	422.46	505.45
400.0	271.67	339.45	424.91	507.93
BatPac Cell Capacity (Ah): BEV200				
Power, kW	Energy, kWh			
	30.0	50.0	70.0	90.0
20.0	25.46	42.45	59.44	76.44
40.0	25.46	42.44	59.43	76.43
60.0	25.46	42.44	59.43	76.43
80.0	25.46	42.44	59.43	76.43
100.0	25.46	42.44	59.43	76.42
120.0	25.46	42.44	59.43	76.42
140.0	25.46	42.44	59.43	76.42
160.0	25.46	42.44	59.43	76.42
180.0	25.46	42.44	59.43	76.42
200.0	25.46	42.44	59.43	76.42
240.0	25.46	42.44	59.43	76.42
280.0	25.44	42.44	59.43	76.42
320.0	25.42	42.44	59.43	76.42
400.0	25.39	42.44	59.43	76.42

Table 33 summarizes the cost, mass, and cell capacities generated for SUV, pickup, and HDPUV BEV150/200/250 AERs from BatPaC using the assumptions specified.

Table 33. BatPaC lookup table for BEV150-250 AERs (SUVs/pickup)

BatPac Cost: BEV150-250											
Power, kW	Energy, kWh										
	30.0	50.0	70.0	90.0	120.0	140.0	160.0	180.0	200.0	220.0	240.0
20.0	\$5,208	\$7,263	\$9,277	\$11,268	\$14,292	\$16,267	\$18,255	\$20,217	\$22,174	\$24,126	\$26,076
40.0	\$5,225	\$7,280	\$9,294	\$11,284	\$14,308	\$16,283	\$18,271	\$20,232	\$22,188	\$24,140	\$26,089
60.0	\$5,243	\$7,298	\$9,311	\$11,302	\$14,325	\$16,300	\$18,288	\$20,249	\$22,205	\$24,156	\$26,105
80.0	\$5,260	\$7,315	\$9,329	\$11,319	\$14,343	\$16,317	\$18,305	\$20,266	\$22,222	\$24,174	\$26,122
100.0	\$5,278	\$7,333	\$9,346	\$11,337	\$14,360	\$16,335	\$18,323	\$20,284	\$22,239	\$24,191	\$26,139
120.0	\$5,295	\$7,350	\$9,364	\$11,354	\$14,378	\$16,353	\$18,341	\$20,301	\$22,257	\$24,209	\$26,157
140.0	\$5,313	\$7,368	\$9,381	\$11,372	\$14,396	\$16,370	\$18,358	\$20,319	\$22,275	\$24,226	\$26,174
160.0	\$5,330	\$7,385	\$9,399	\$11,390	\$14,413	\$16,388	\$18,376	\$20,337	\$22,292	\$24,244	\$26,192
180.0	\$5,348	\$7,403	\$9,416	\$11,407	\$14,431	\$16,406	\$18,394	\$20,354	\$22,310	\$24,262	\$26,210
200.0	\$5,365	\$7,420	\$9,434	\$11,425	\$14,449	\$16,423	\$18,411	\$20,372	\$22,328	\$24,279	\$26,227
240.0	\$5,400	\$7,455	\$9,469	\$11,460	\$14,484	\$16,459	\$18,447	\$20,407	\$22,363	\$24,315	\$26,263
280.0	\$5,497	\$7,490	\$9,504	\$11,495	\$14,519	\$16,494	\$18,482	\$20,443	\$22,399	\$24,351	\$26,299
320.0	\$5,656	\$7,525	\$9,539	\$11,531	\$14,555	\$16,529	\$18,518	\$20,479	\$22,434	\$24,386	\$26,334
400.0	\$6,006	\$7,595	\$9,610	\$11,601	\$14,625	\$16,600	\$18,589	\$20,550	\$22,506	\$24,457	\$26,406
BatPac Mass (kg): BEV150-250											

Power, kW	Energy, kWh										
	30.0	50.0	70.0	90.0	120.0	140.0	160.0	180.0	200.0	220.0	240.0
20.0	257.9	349.1	435.8	519.9	642.8	723.2	805.2	883.9	962.1	1039.7	1116.9
40.0	258.4	349.6	436.3	520.3	643.2	723.6	805.6	884.3	962.5	1040.1	1117.2
60.0	258.8	350.1	436.8	520.8	643.7	724.1	806.1	884.8	962.9	1040.5	1117.7
80.0	259.3	350.5	437.3	521.3	644.2	724.6	806.6	885.3	963.5	1041.1	1118.2
100.0	259.8	351.0	437.7	521.8	644.7	725.1	807.1	885.9	964.0	1041.6	1118.7
120.0	260.2	351.5	438.2	522.3	645.2	725.6	807.6	886.4	964.5	1042.1	1119.2
140.0	260.7	352.0	438.7	522.8	645.7	726.1	808.2	886.9	965.0	1042.6	1119.8
160.0	261.2	352.5	439.2	523.3	646.2	726.6	808.7	887.4	965.6	1043.2	1120.3
180.0	261.7	352.9	439.7	523.8	646.6	727.1	809.2	888.0	966.1	1043.7	1120.8
200.0	262.1	353.4	440.2	524.2	647.1	727.6	809.7	888.5	966.6	1044.2	1121.4
240.0	263.1	354.4	441.1	525.2	648.1	728.6	810.8	889.5	967.7	1045.3	1122.5
280.0	266.6	355.3	442.1	526.2	649.1	729.6	811.8	890.6	968.7	1046.4	1123.5
320.0	273.7	356.3	443.1	527.2	650.1	730.6	812.9	891.7	969.8	1047.4	1124.6
400.0	288.7	358.2	445.0	529.2	652.1	732.6	815.0	893.8	971.9	1049.6	1126.8
BatPac Cell Capacity (Ah): BEV150-250											
Power, kW	Energy, kWh										
	30.0	50.0	70.0	90.0	120.0	140.0	160.0	180.0	200.0	220.0	240.0
20.0	20.37	33.95	47.54	61.14	81.54	95.15	108.75	122.37	135.99	149.62	163.25
40.0	20.37	33.95	47.54	61.13	81.53	95.14	108.73	122.35	135.96	149.58	163.21
60.0	20.37	33.95	47.54	61.13	81.53	95.13	108.73	122.34	135.95	149.57	163.19
80.0	20.37	33.95	47.54	61.13	81.53	95.13	108.72	122.33	135.95	149.56	163.19
100.0	20.37	33.95	47.54	61.13	81.52	95.13	108.72	122.33	135.94	149.56	163.18
120.0	20.37	33.95	47.54	61.13	81.52	95.13	108.72	122.33	135.94	149.56	163.18

140.0	20.37	33.95	47.54	61.13	81.52	95.13	108.72	122.33	135.94	149.56	163.18
160.0	20.37	33.95	47.54	61.13	81.52	95.13	108.72	122.33	135.94	149.56	163.18
180.0	20.37	33.95	47.54	61.13	81.52	95.12	108.72	122.33	135.94	149.55	163.17
200.0	20.37	33.95	47.54	61.13	81.52	95.12	108.72	122.33	135.94	149.55	163.17
240.0	20.37	33.95	47.54	61.13	81.52	95.12	108.72	122.33	135.94	149.55	163.17
280.0	20.35	33.95	47.54	61.13	81.52	95.12	108.72	122.33	135.94	149.55	163.17
320.0	20.33	33.95	47.54	61.13	81.52	95.12	108.72	122.33	135.94	149.55	163.17
400.0	20.31	33.95	47.54	61.13	81.52	95.12	108.72	122.32	135.94	149.55	163.17

BEV300 AER

Table 34 summarizes the cost, mass, and cell capacities generated for compact and midsize BEV300 AERs from BatPaC, using the assumptions specified.

Table 34. BatPaC lookup table for BEV300 AERs (compact/midsize)

BatPac Cost: BEV300					
Power, kW	Energy, kWh				
	30.0	50.0	70.0	90.0	120.0
20.0	\$5,208	\$7,263	\$9,277	\$11,268	\$14,292
40.0	\$5,225	\$7,280	\$9,294	\$11,284	\$14,308
60.0	\$5,243	\$7,298	\$9,311	\$11,302	\$14,325
80.0	\$5,260	\$7,315	\$9,329	\$11,319	\$14,343
100.0	\$5,278	\$7,333	\$9,346	\$11,337	\$14,360
120.0	\$5,295	\$7,350	\$9,364	\$11,354	\$14,378
140.0	\$5,313	\$7,368	\$9,381	\$11,372	\$14,396
160.0	\$5,330	\$7,385	\$9,399	\$11,390	\$14,413
180.0	\$5,348	\$7,403	\$9,416	\$11,407	\$14,431
200.0	\$5,365	\$7,420	\$9,434	\$11,425	\$14,449
240.0	\$5,400	\$7,455	\$9,469	\$11,460	\$14,484
280.0	\$5,497	\$7,490	\$9,504	\$11,495	\$14,519
320.0	\$5,656	\$7,525	\$9,539	\$11,531	\$14,555
400.0	\$6,006	\$7,595	\$9,610	\$11,601	\$14,625
BatPac Mass (kg): BEV300					
Power, kW	Energy, kWh				
	30.0	50.0	70.0	90.0	120.0
20.0	257.88	349.12	435.83	519.89	642.78
40.0	258.35	349.59	436.30	520.35	643.21
60.0	258.82	350.07	436.77	520.82	643.69
80.0	259.29	350.54	437.26	521.31	644.17
100.0	259.76	351.02	437.74	521.79	644.67
120.0	260.23	351.50	438.22	522.28	645.16
140.0	260.71	351.98	438.71	522.77	645.65
160.0	261.18	352.46	439.19	523.26	646.15
180.0	261.65	352.94	439.68	523.75	646.64
200.0	262.12	353.42	440.16	524.24	647.14
240.0	263.07	354.38	441.13	525.22	648.13

280.0	266.55	355.34	442.11	526.20	649.13
320.0	273.73	356.30	443.08	527.19	650.12
400.0	288.72	358.22	445.02	529.15	652.11
BatPac Cell Capacity (Ah): BEV300					
Power, kW	Energy, kWh				
	30.0	50.0	70.0	90.0	120.0
20.0	20.37	33.95	47.54	61.14	81.54
40.0	20.37	33.95	47.54	61.13	81.53
60.0	20.37	33.95	47.54	61.13	81.53
80.0	20.37	33.95	47.54	61.13	81.53
100.0	20.37	33.95	47.54	61.13	81.53
120.0	20.37	33.95	47.54	61.13	81.52
140.0	20.37	33.95	47.54	61.13	81.52
160.0	20.37	33.95	47.54	61.13	81.52
180.0	20.37	33.95	47.54	61.13	81.52
200.0	20.37	33.95	47.54	61.13	81.52
240.0	20.37	33.95	47.54	61.13	81.52
280.0	20.35	33.95	47.54	61.13	81.52
320.0	20.33	33.95	47.54	61.13	81.52
400.0	20.31	33.95	47.54	61.13	81.52

Table 35 summarizes the cost, mass, and cell capacities generated for SUV, pickup, and HDPUV BEV300 AERs from BatPaC using the assumptions specified.

Table 35. BatPaC lookup table for BEV300 AERs (SUVs/pickups/HDPUVs)

BatPac Cost: BEV300												
Power, kW	Energy, kWh											
	30.0	50.0	70.0	90.0	120.0	140.0	160.0	180.0	200.0	250.0	300.0	350.0
20.0	\$5,458	\$7,536	\$9,567	\$11,571	\$14,552	\$16,534	\$18,568	\$20,565	\$22,529	\$27,420	\$32,290	\$37,146
40.0	\$5,476	\$7,553	\$9,584	\$11,588	\$14,569	\$16,551	\$18,584	\$20,581	\$22,544	\$27,434	\$32,303	\$37,157
60.0	\$5,493	\$7,571	\$9,601	\$11,606	\$14,586	\$16,568	\$18,601	\$20,598	\$22,561	\$27,450	\$32,319	\$37,173
80.0	\$5,510	\$7,588	\$9,619	\$11,623	\$14,604	\$16,586	\$18,619	\$20,615	\$22,579	\$27,468	\$32,336	\$37,189
100.0	\$5,528	\$7,606	\$9,636	\$11,641	\$14,621	\$16,603	\$18,636	\$20,633	\$22,596	\$27,485	\$32,353	\$37,207
120.0	\$5,545	\$7,623	\$9,654	\$11,658	\$14,639	\$16,621	\$18,654	\$20,651	\$22,614	\$27,503	\$32,371	\$37,224
140.0	\$5,563	\$7,641	\$9,671	\$11,676	\$14,657	\$16,639	\$18,672	\$20,668	\$22,632	\$27,520	\$32,389	\$37,242
160.0	\$5,580	\$7,658	\$9,689	\$11,693	\$14,674	\$16,656	\$18,689	\$20,686	\$22,649	\$27,538	\$32,406	\$37,259
180.0	\$5,598	\$7,675	\$9,706	\$11,711	\$14,692	\$16,674	\$18,707	\$20,704	\$22,667	\$27,556	\$32,424	\$37,277
200.0	\$5,615	\$7,693	\$9,724	\$11,728	\$14,710	\$16,692	\$18,725	\$20,721	\$22,685	\$27,574	\$32,442	\$37,295
240.0	\$5,650	\$7,728	\$9,759	\$11,764	\$14,745	\$16,727	\$18,760	\$20,757	\$22,720	\$27,609	\$32,477	\$37,331
280.0	\$5,744	\$7,763	\$9,794	\$11,799	\$14,780	\$16,762	\$18,795	\$20,792	\$22,756	\$27,645	\$32,513	\$37,366
320.0	\$5,899	\$7,798	\$9,829	\$11,834	\$14,815	\$16,798	\$18,831	\$20,827	\$22,791	\$27,680	\$32,549	\$37,402
400.0	\$6,249	\$7,868	\$9,899	\$11,904	\$14,886	\$16,868	\$18,902	\$20,898	\$22,862	\$27,751	\$32,620	\$37,474
BatPac Mass (kg): BEV300												
Power, kW	Energy, kWh											
	30.0	50.0	70.0	90.0	120.0	140.0	160.0	180.0	200.0	250.0	300.0	350.0
20.0	281.93	375.33	463.74	549.21	673.90	755.35	835.81	918.65	997.60	1192.60	1385.10	1575.60
40.0	282.40	375.80	464.20	549.68	674.35	755.80	836.24	919.09	998.02	1193.00	1385.40	1575.80

60.0	282.87	376.27	464.68	550.16	674.83	756.28	836.72	919.58	998.52	1193.50	1385.90	1576.30
80.0	283.34	376.75	465.16	550.64	675.32	756.77	837.21	920.10	999.03	1194.00	1386.40	1576.80
100.0	283.81	377.23	465.64	551.13	675.81	757.26	837.71	920.61	999.54	1194.50	1386.90	1577.30
120.0	284.28	377.70	466.12	551.61	676.30	757.75	838.20	921.13	1000.10	1195.00	1387.40	1577.80
140.0	284.75	378.18	466.60	552.10	676.79	758.25	838.70	921.65	1000.60	1195.60	1387.90	1578.40
160.0	285.22	378.65	467.08	552.58	677.28	758.74	839.19	922.17	1001.10	1196.10	1388.50	1578.90
180.0	285.69	379.13	467.57	553.07	677.77	759.24	839.69	922.70	1001.60	1196.60	1389.00	1579.40
200.0	286.16	379.61	468.05	553.55	678.26	759.73	840.19	923.22	1002.20	1197.10	1389.50	1580.00
240.0	287.09	380.56	469.01	554.53	679.25	760.72	841.19	924.27	1003.20	1198.20	1390.60	1581.10
280.0	291.45	381.51	469.97	555.50	680.23	761.71	842.18	925.31	1004.30	1199.30	1391.70	1582.10
320.0	297.02	382.46	470.94	556.47	681.22	762.70	843.18	926.36	1005.30	1200.30	1392.80	1583.20
400.0	312.73	384.37	472.86	558.42	683.19	764.69	845.18	928.46	1007.40	1202.50	1394.90	1585.40
BatPac Cell Capacity (Ah): BEV300												
Power, kW	Energy, kWh											
	30.0	50.0	70.0	90.0	120.0	140.0	160.0	180.0	200.0	250.0	300.0	350.0
20.0	16.29	27.16	38.03	48.90	65.21	76.09	86.98	97.86	108.74	135.98	163.23	190.50
40.0	16.29	27.16	38.03	48.90	65.21	76.09	86.97	97.85	108.73	135.96	163.20	190.46
60.0	16.29	27.16	38.03	48.90	65.21	76.09	86.97	97.84	108.73	135.95	163.19	190.44
80.0	16.29	27.16	38.02	48.90	65.21	76.08	86.97	97.84	108.72	135.94	163.18	190.43
100.0	16.29	27.16	38.02	48.90	65.21	76.08	86.96	97.84	108.72	135.94	163.18	190.43
120.0	16.29	27.16	38.02	48.90	65.21	76.08	86.96	97.84	108.72	135.94	163.18	190.43
140.0	16.29	27.16	38.02	48.89	65.21	76.08	86.96	97.84	108.72	135.94	163.17	190.42
160.0	16.29	27.16	38.02	48.89	65.21	76.08	86.96	97.84	108.72	135.94	163.17	190.42
180.0	16.29	27.16	38.02	48.89	65.21	76.08	86.96	97.84	108.72	135.94	163.17	190.42
200.0	16.29	27.16	38.02	48.89	65.21	76.08	86.96	97.84	108.72	135.94	163.17	190.42
240.0	16.29	27.16	38.02	48.89	65.21	76.08	86.96	97.84	108.72	135.94	163.17	190.42

280.0	16.28	27.16	38.02	48.89	65.21	76.08	86.96	97.84	108.72	135.94	163.17	190.42
320.0	16.27	27.16	38.02	48.89	65.21	76.08	86.96	97.84	108.72	135.94	163.17	190.42
400.0	16.25	27.16	38.02	48.89	65.20	76.08	86.96	97.83	108.72	135.94	163.17	190.42

BEV400 AER

Table 36 summarizes the cost, mass, and cell capacities generated for compact and midsize BEV400 AERs from BatPaC, using the assumptions specified.

Table 36. BatPaC lookup table for BEV400 AERs (compact/midsize)

BEV400								
Power, kW	Energy, kWh							
	70.0	90.0	110.0	130.0	150.0	170.0	190.0	210.0
20.0	\$9,427	\$11,421	\$13,400	\$15,378	\$17,403	\$19,394	\$21,352	\$23,305
50.0	\$9,453	\$11,447	\$13,426	\$15,404	\$17,429	\$19,419	\$21,377	\$23,329
80.0	\$9,480	\$11,474	\$13,453	\$15,431	\$17,456	\$19,446	\$21,403	\$23,356
110.0	\$9,507	\$11,500	\$13,480	\$15,457	\$17,482	\$19,472	\$21,430	\$23,382
140.0	\$9,533	\$11,527	\$13,506	\$15,484	\$17,509	\$19,499	\$21,457	\$23,409
170.0	\$9,560	\$11,554	\$13,533	\$15,511	\$17,536	\$19,526	\$21,484	\$23,436
200.0	\$9,587	\$11,581	\$13,560	\$15,538	\$17,563	\$19,553	\$21,511	\$23,463
230.0	\$9,613	\$11,607	\$13,587	\$15,565	\$17,590	\$19,580	\$21,538	\$23,490
260.0	\$9,640	\$11,634	\$13,613	\$15,591	\$17,617	\$19,607	\$21,565	\$23,517
290.0	\$9,667	\$11,661	\$13,640	\$15,618	\$17,644	\$19,634	\$21,592	\$23,544
320.0	\$9,693	\$11,688	\$13,667	\$15,645	\$17,671	\$19,661	\$21,619	\$23,571
350.0	\$9,720	\$11,714	\$13,694	\$15,672	\$17,697	\$19,688	\$21,646	\$23,598
380.0	\$9,747	\$11,741	\$13,721	\$15,699	\$17,724	\$19,715	\$21,673	\$23,625
410.0	\$9,773	\$11,768	\$13,748	\$15,726	\$17,751	\$19,742	\$21,700	\$23,652
440.0	\$9,800	\$11,795	\$13,774	\$15,753	\$17,778	\$19,769	\$21,727	\$23,679
BEV400								
Power, kW	Energy, kWh							
	70.0	90.0	110.0	130.0	150.0	170.0	190.0	210.0
20.0	453.5	538.1	620.8	702.1	782.3	864.8	943.5	1021.6
50.0	454.1	538.7	621.4	702.7	782.9	865.4	944.1	1022.1
80.0	454.7	539.3	622.0	703.3	783.6	866.1	944.8	1022.8
110.0	455.3	539.9	622.7	704.0	784.2	866.8	945.4	1023.5
140.0	456.0	540.6	623.3	704.6	784.9	867.5	946.1	1024.2
170.0	456.6	541.2	623.9	705.3	785.5	868.1	946.8	1024.9
200.0	457.2	541.9	624.6	705.9	786.2	868.8	947.5	1025.6
230.0	457.9	542.5	625.2	706.6	786.9	869.5	948.2	1026.3
260.0	458.5	543.1	625.9	707.2	787.5	870.2	948.9	1027.0
290.0	459.1	543.8	626.5	707.9	788.2	870.9	949.6	1027.7

320.0	459.8	544.4	627.2	708.5	788.8	871.6	950.3	1028.4
350.0	460.4	545.1	627.8	709.2	789.5	872.3	951.0	1029.1
380.0	461.0	545.7	628.5	709.9	790.2	873.0	951.7	1029.8
410.0	461.7	546.4	629.1	710.5	790.8	873.7	952.4	1030.5
440.0	462.3	547.0	629.8	711.2	791.5	874.4	953.1	1031.2
	BEV400							
Power, kW	Energy, kWh							
	70.0	90.0	110.0	130.0	150.0	170.0	190.0	210.0
20.0	39.61	50.94	62.27	73.60	84.94	96.27	107.61	118.95
50.0	39.61	50.94	62.26	73.59	84.93	96.26	107.59	118.93
80.0	39.61	50.93	62.26	73.59	84.92	96.25	107.59	118.93
110.0	39.61	50.93	62.26	73.59	84.92	96.25	107.59	118.93
140.0	39.61	50.93	62.26	73.59	84.92	96.25	107.59	118.93
170.0	39.61	50.93	62.26	73.59	84.92	96.25	107.59	118.92
200.0	39.61	50.93	62.26	73.59	84.92	96.25	107.59	118.92
230.0	39.61	50.93	62.26	73.59	84.92	96.25	107.58	118.92
260.0	39.61	50.93	62.26	73.59	84.92	96.25	107.58	118.92
290.0	39.61	50.93	62.26	73.59	84.92	96.25	107.58	118.92
320.0	39.61	50.93	62.26	73.59	84.92	96.25	107.58	118.92
350.0	39.61	50.93	62.26	73.59	84.92	96.25	107.58	118.92
380.0	39.61	50.93	62.26	73.59	84.92	96.25	107.58	118.92
410.0	39.61	50.93	62.26	73.59	84.92	96.25	107.58	118.92
440.0	39.61	50.93	62.26	73.59	84.92	96.25	107.58	118.92

Table 37 summarizes the cost, mass, and cell capacities generated for SUVs, pickups, and HDPUVs BEV400 AERs from BatPaC using the assumptions specified.

Table 37. BatPaC lookup table for BEV400 AERs (SUVs/pickups)

BatPac Cost: BEV400														
Power, kW	Energy, kWh													
	70.0	90.0	110.0	130.0	150.0	170.0	190.0	210.0	230.0	250.0	270.0	290.0	310.0	330.0
20.0	\$9,846	\$11,863	\$13,862	\$15,846	\$17,831	\$19,809	\$21,852	\$23,821	\$ 25,818	\$ 27,777	\$ 29,733	\$ 31,685	\$ 33,635	\$ 35,582
50.0	\$9,872	\$11,889	\$13,888	\$15,872	\$17,856	\$19,835	\$21,877	\$23,845	\$ 25,842	\$ 27,801	\$ 29,756	\$ 31,708	\$ 33,657	\$ 35,604
80.0	\$9,898	\$11,915	\$13,914	\$15,898	\$17,883	\$19,861	\$21,903	\$23,871	\$ 25,868	\$ 27,827	\$ 29,782	\$ 31,734	\$ 33,683	\$ 35,629
110.0	\$9,924	\$11,942	\$13,940	\$15,924	\$17,909	\$19,887	\$21,929	\$23,898	\$ 25,894	\$ 27,853	\$ 29,808	\$ 31,760	\$ 33,709	\$ 35,655
140.0	\$9,950	\$11,968	\$13,966	\$15,951	\$17,935	\$19,914	\$21,956	\$23,924	\$ 25,921	\$ 27,879	\$ 29,834	\$ 31,786	\$ 33,735	\$ 35,682
170.0	\$9,977	\$11,994	\$13,993	\$15,977	\$17,962	\$19,940	\$21,982	\$23,951	\$ 25,947	\$ 27,906	\$ 29,861	\$ 31,813	\$ 33,762	\$ 35,708
200.0	\$10,003	\$12,021	\$14,019	\$16,004	\$17,988	\$19,967	\$22,009	\$23,977	\$ 25,974	\$ 27,932	\$ 29,888	\$ 31,839	\$ 33,788	\$ 35,735
230.0	\$10,029	\$12,047	\$14,046	\$16,030	\$18,015	\$19,993	\$22,035	\$24,004	\$ 26,000	\$ 27,959	\$ 29,914	\$ 31,866	\$ 33,815	\$ 35,762
260.0	\$10,055	\$12,073	\$14,072	\$16,056	\$18,041	\$20,019	\$22,062	\$24,030	\$ 26,027	\$ 27,986	\$ 29,941	\$ 31,893	\$ 33,842	\$ 35,788
290.0	\$10,082	\$12,100	\$14,098	\$16,083	\$18,068	\$20,046	\$22,088	\$24,057	\$ 26,053	\$ 28,012	\$ 29,967	\$ 31,919	\$ 33,869	\$ 35,815
320.0	\$10,108	\$12,126	\$14,125	\$16,109	\$18,094	\$20,072	\$22,115	\$24,083	\$ 26,080	\$ 28,039	\$ 29,994	\$ 31,946	\$ 33,895	\$ 35,842
350.0	\$10,134	\$12,152	\$14,151	\$16,136	\$18,120	\$20,099	\$22,141	\$24,110	\$ 26,107	\$ 28,066	\$ 30,021	\$ 31,973	\$ 33,922	\$ 35,868
380.0	\$10,160	\$12,179	\$14,177	\$16,162	\$18,147	\$20,125	\$22,168	\$24,136	\$ 26,133	\$ 28,092	\$ 30,047	\$ 31,999	\$ 33,949	\$ 35,895
410.0	\$10,187	\$12,205	\$14,204	\$16,189	\$18,173	\$20,152	\$22,194	\$24,163	\$ 26,160	\$ 28,119	\$ 30,074	\$ 32,026	\$ 33,975	\$ 35,922
440.0	\$10,213	\$12,231	\$14,230	\$16,215	\$18,200	\$20,178	\$22,221	\$24,190	\$ 26,186	\$ 28,145	\$ 30,101	\$ 32,053	\$ 34,002	\$ 35,949
BatPac Mass (kg): BEV400														
Power, kW	Energy, kWh													
	70.0	90.0	110.0	130.0	150.0	170.0	190.0	210.0	230.0	250.0	270.0	290.0	310.0	330.0
20.0	491	578	662	746	828	908	989	1068	1151	1229	1307	1385	1462	1539
50.0	492	578	663	746	828	909	989	1069	1152	1230	1308	1385	1462	1539
80.0	492	579	664	747	829	910	990	1069	1152	1231	1308	1386	1463	1540

110.0	493	580	665	748	830	911	991	1070	1153	1231	1309	1387	1464	1541
140.0	494	581	665	749	830	911	991	1071	1154	1232	1310	1388	1465	1541
170.0	494	581	666	749	831	912	992	1072	1155	1233	1311	1388	1465	1542
200.0	495	582	667	750	832	913	993	1072	1155	1234	1312	1389	1466	1543
230.0	496	583	668	751	833	914	994	1073	1156	1235	1312	1390	1467	1544
260.0	497	584	668	751	833	914	994	1074	1157	1235	1313	1391	1468	1545
290.0	497	584	669	752	834	915	995	1075	1158	1236	1314	1392	1469	1545
320.0	498	585	670	753	835	916	996	1075	1159	1237	1315	1392	1469	1546
350.0	499	586	670	754	836	917	997	1076	1159	1238	1316	1393	1470	1547
380.0	500	586	671	754	836	917	997	1077	1160	1239	1316	1394	1471	1548
410.0	500	587	672	755	837	918	998	1078	1161	1239	1317	1395	1472	1549
440.0	501	588	673	756	838	919	999	1078	1162	1240	1318	1396	1473	1549

BatPac Cell Capacity (Ah): BEV400

Power, kW	Energy, kWh													
	70.0	90.0	110.0	130.0	150.0	170.0	190.0	210.0	230.0	250.0	270.0	290.0	310.0	330.0
20.0	31.7	40.7	49.8	58.9	67.9	77.0	86.1	95.1	104.2	113.3	122.4	131.4	140.5	149.6
50.0	31.7	40.7	49.8	58.9	67.9	77.0	86.1	95.1	104.2	113.3	122.3	131.4	140.5	149.6
80.0	31.7	40.7	49.8	58.9	67.9	77.0	86.1	95.1	104.2	113.3	122.3	131.4	140.5	149.6
110.0	31.7	40.7	49.8	58.9	67.9	77.0	86.1	95.1	104.2	113.3	122.3	131.4	140.5	149.6
140.0	31.7	40.7	49.8	58.9	67.9	77.0	86.1	95.1	104.2	113.3	122.3	131.4	140.5	149.6
170.0	31.7	40.7	49.8	58.9	67.9	77.0	86.1	95.1	104.2	113.3	122.3	131.4	140.5	149.6
200.0	31.7	40.7	49.8	58.9	67.9	77.0	86.1	95.1	104.2	113.3	122.3	131.4	140.5	149.6
230.0	31.7	40.7	49.8	58.9	67.9	77.0	86.1	95.1	104.2	113.3	122.3	131.4	140.5	149.6
260.0	31.7	40.7	49.8	58.9	67.9	77.0	86.1	95.1	104.2	113.3	122.3	131.4	140.5	149.6
290.0	31.7	40.7	49.8	58.9	67.9	77.0	86.1	95.1	104.2	113.3	122.3	131.4	140.5	149.6
320.0	31.7	40.7	49.8	58.9	67.9	77.0	86.1	95.1	104.2	113.3	122.3	131.4	140.5	149.6
350.0	31.7	40.7	49.8	58.9	67.9	77.0	86.1	95.1	104.2	113.3	122.3	131.4	140.5	149.6
380.0	31.7	40.7	49.8	58.9	67.9	77.0	86.1	95.1	104.2	113.3	122.3	131.4	140.5	149.6

410.0	31.7	40.7	49.8	58.9	67.9	77.0	86.1	95.1	104.2	113.3	122.3	131.4	140.5	149.6
440.0	31.7	40.7	49.8	58.9	67.9	77.0	86.1	95.1	104.2	113.3	122.3	131.4	140.5	149.6

Vehicle and Component Assumptions

Light-Duty Vehicle Specifications

Per NHTSA and the feedback received from reviewers of the previous analysis, many steps were taken to improve the overall vehicle simulation process and consider additional vehicles to better replicate fleets in both existing and future markets.

The primary focus was to update the vehicle and component assumptions to represent the latest vehicles in the market. An extensive analysis was carried out on the existing vehicles in the market to evaluate vehicle parameters and component weights across the vehicle classifications considered. In addition to vehicle parameters (frontal area, drag coefficient, etc.), individual component weight assumptions (body, chassis, interior, etc.) have been analyzed. The vehicle attribute parameters have been updated using Argonne’s internal vehicle technical database. Finally, the vehicle component weights have been updated using A2Mac1 teardown analysis of different representative vehicles.

This section elaborates on the method used to select each attribute. The attributes were defined across different vehicle classes and performance categories, with different transmission types and numbers of gears. Table 38 shows the different vehicle classifications and the definition of the different performance categories for LDV combinations.

Table 38. Vehicle classification and performance categories

Vehicle Class	Performance Category	0–60 mph Time (s)
Compact	Base/Premium	9/7
Midsize	Base/Premium	8/6
Small SUV	Base/Premium	8/7
Midsize SUV	Base/Premium	8/7
Pickup	Base/Premium	7/7

The following are additional performance metrics.

- Gradeability: 6% grade at 65 mph
- Payload: 650 kg (pickup base) and 900 kg (pickup premium) only
- Towing: 3,000 kg (pickup base) and 4,500 kg (pickup premium) only

HDPUV Specifications

Assumptions made in vehicle simulations were established with inputs from NHTSA, VTO, and HFTO analysts. Additional information and review of some assumptions were provided by industry experts, including industrial partners in the 21st Century Truck Partnership and representatives from truck manufacturers and fleet operators.

Each truck is unique in its functional requirements. The performance capabilities that determine the engine power requirements are rarely advertised for these types of vehicles. However, the engine power rating, transmission ratios, and curb weight are all available from original equipment manufacturers. Performance capabilities were estimated through simulations for each

category of vehicle. Based on feedback from many of the industry partners, we have identified the following parameters for enforcing performance parity between conventional and more advanced powertrains.

- 0 to 30 mph acceleration time
- 0 to 60 mph acceleration time
- Sustainable maximum speed at 6-percent grade
- Driving range between refueling/recharging
- Maximum cruising speed
- Start/launch capability on grade
- Maximum sustainable grade at highway cruising speed
- Towing weight

By simulating the conventional vehicle models over various test cycles, the performance requirements for various types of vehicles were determined, as shown in Table 39. This performance is measured for the maximum gross vehicle weight allowed for each class of truck. Although the targets vary depending on size class, all powertrain variants of a given type of truck should meet or exceed these minimum requirements. Please see the EPA rulemaking documents for the cargo mass used for sizing and fuel economy evaluations (EPA & NHTSA, 2016).

Table 39. Summary of HD vehicle classes and purposes and their performance requirements

Class	Purpose	0–30 mph time (s)	0–60 mph time (s)	6% grade speed (mph)	Cruise speed (mph)	Cruise grade (%)	Max. speed (mph)	Start-ability (%)	Towing weight (lb)
HD (2b)	Van	7	16	50	70	1.5	75	20	6,000
HD (2b)	Pickup	7	13	65	70	1.5	75	20	15,000
HD (3)	Van	7	20	50	65	1.5	70	20	6,500
HD (3)	Pickup	7	16	65	70	1.5	75	20	18,000

The following are additional performance metrics.

- Test weight for sizing: 10,000 lb (HDPUV Class 2b) and 14,000 lb (HDPUV Class 3)
- Payload: Calculated as 50 percent of the maximum loading of baseline vehicle
- EV range (miles): BEV1 ranges of 150 and 250 (van) and BEV2 ranges of 200 and 300 (pickup)

Performance capabilities for vehicles included both transient and continuous power requirements, as shown in Figure 125. While a motor might meet the acceleration requirement with its peak power rating, the motor power output over a prolonged grade will be reduced to roughly half of the peak power rating (depending on the motor characteristics). This factor is important enough to be considered specifically while sizing the components for commercial trucks with electric drivetrains.

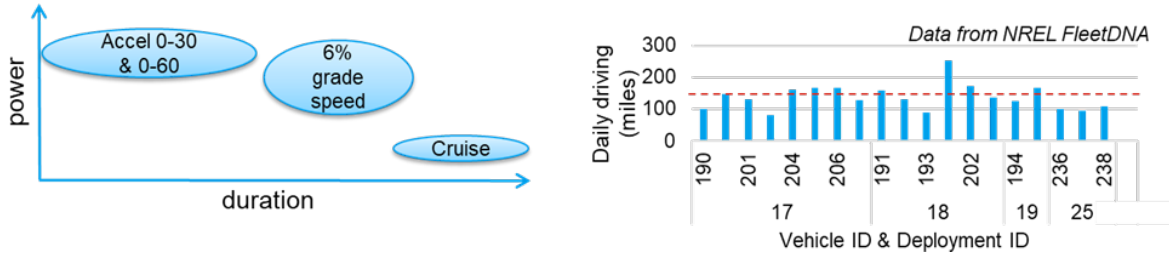


Figure 125. Overview of the performance parameters

Vehicle-Level Attributes Selection

Light-Duty Vehicles

The assumptions for each vehicle class and performance category have been defined individually.

Drag Coefficient

The following section shows the distribution of the drag coefficient using the Argonne internal vehicle technology database. “ANL value” represents the parameter value selected for the reference vehicle in Autonomie. Figure 126 shows the distribution of drag coefficient values for the compact (base) vehicle class.

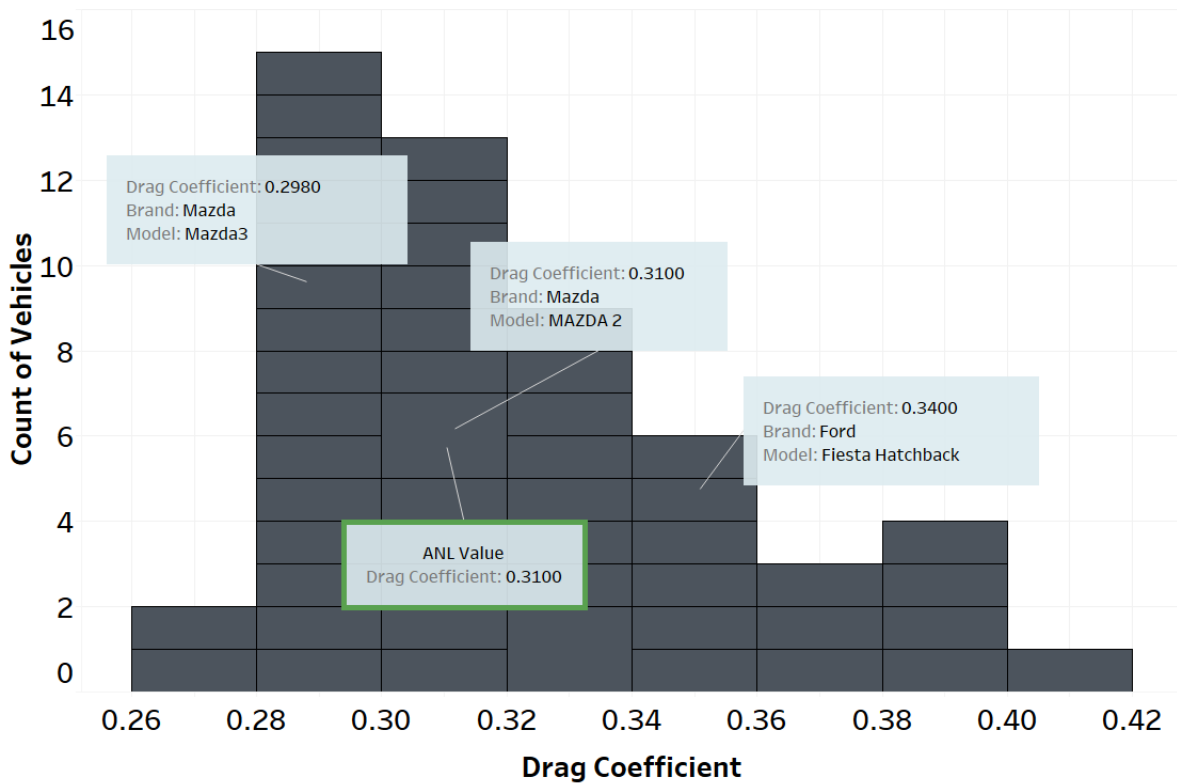


Figure 126. Distribution of drag coefficient values of compact (base) vehicle class

Similar analyses were performed across the different vehicle classes and performance categories and the reference values selected. Table 40 summarizes the values defined for the drag coefficient of the reference vehicles for each vehicle class and performance category.

Table 40. Drag coefficient ratio summary table

Vehicle Class	Performance Category	Reference Value
Compact	Base/Premium	0.31
Midsize	Base/Premium	0.30
Small SUV	Base/Premium	0.36
Midsize SUV	Base/Premium	0.38
Pickup	Base/Premium	0.42

Frontal Area

A similar detailed analysis determined the frontal area values for the reference vehicle across different vehicle classifications and performance categories.

Table 41 summarizes the values defined for the frontal area of the reference vehicles for the different vehicle classes and performance categories.

Table 41. Frontal Area Summary Table

Vehicle Class	Performance Category	Reference Value (m²)
Compact	Base/Premium	2.3
Midsize	Base/Premium	2.35
Small SUV	Base/Premium	2.65
Midsize SUV	Base/Premium	2.85
Pickup	Base/Premium	3.25

Rolling Resistance

A constant value of 0.009 is used as the first coefficient term of the wheel rolling resistance for all classes and performance categories. The overall rolling resistance of the wheel is, however, speed-dependent, with a factor of 0.00012.

Effective Tire Radius

Argonne evaluated the trends in effective tire radius, which is used in the effective rolling radius calculation. Table 42 shows the database analysis of MY 2020 vehicles.

Table 42. Effective tire radius analysis of MY 2020 vehicles

Vehicle Class	Premium	Cnt	Avg	Std	Min	25th	50th	75th	Max	95% CI (lower)	95% CI (upper)
Compact	No	4	0.2931	0.0161	0.2851	0.2851	0.2851	0.2931	0.3172	0.2693	0.3009
	Yes	217	0.3245	0.0131	0.2851	0.3178	0.3262	0.3306	0.3688	0.3245	0.3279
Midsize	No	68	0.3320	0.0119	0.3108	0.3253	0.3342	0.3365	0.3733	0.3314	0.3370
	Yes	445	0.3412	0.0151	0.3108	0.3322	0.3388	0.3538	0.3814	0.3374	0.3402
Midsize SUV	No	44	0.3784	0.0163	0.3468	0.3636	0.3814	0.3893	0.4014	0.3766	0.3862
	Yes	351	0.3899	0.0150	0.3468	0.3801	0.3926	0.4014	0.4190	0.3910	0.3942
Pickup	No	163	0.3963	0.0113	0.3756	0.3870	0.4014	0.4071	0.4211	0.3997	0.4031
	Yes	135	0.4005	0.0133	0.3756	0.3887	0.4014	0.4014	0.4364	0.3992	0.4036
Small SUV	No	151	0.3578	0.0131	0.3184	0.3509	0.3560	0.3686	0.3832	0.3539	0.3581
	Yes	458	0.3697	0.0146	0.3262	0.3622	0.3706	0.3814	0.4154	0.3693	0.3719
Two-Seater	No	86	0.3339	0.0151	0.3007	0.3270	0.3386	0.3442	0.3700	0.3354	0.3418
	Yes	8	0.3257	0.0161	0.3007	0.3205	0.3323	0.3376	0.3376	0.3211	0.3435

Using the analysis above, Argonne determined the following effective wheel radius to be used across the different vehicle and performance technology classes (shown in Table 43).

Table 43. Effective wheel radius used in the FY22 vehicle simulations

Vehicle Class	Performance Category	Effective Wheel Radius (in)
Compact	Base	0.3173
	Premium	0.3262
Midsize	Base	0.3342
	Premium	0.3388
Small SUV	Base	0.3686
	Premium	0.3814
Midsize SUV	Base	0.3814
	Premium	0.3926
Pickup	Base	0.4014
	Premium	0.4014

HDPUVs

The assumptions for each HD vehicle class and purpose category have been defined individually.

Frontal Area

The following section shows the distribution of the drag coefficient using the Argonne internal vehicle technology database. “ANL Value” represents the parameter value selected for the reference vehicle in Autonomie. Figure 127 shows the average of the minimum frontal area and maximum frontal area values for each trim of each vehicle model.

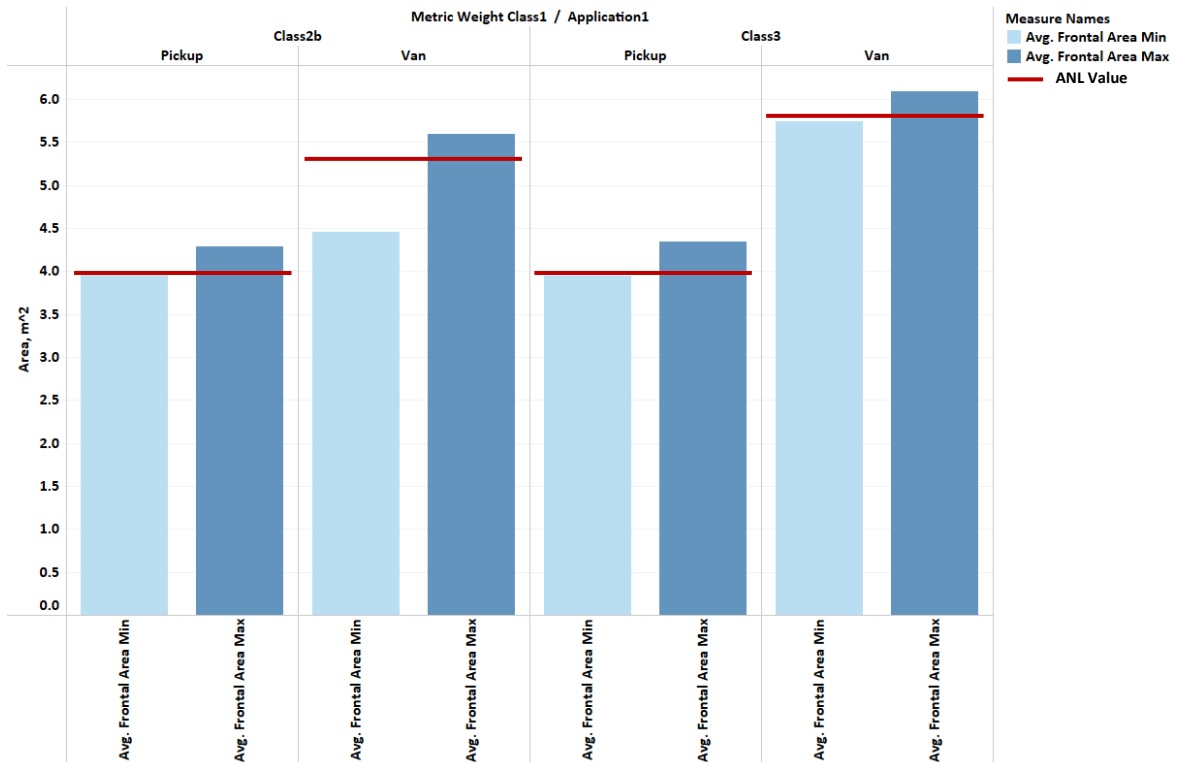


Figure 127. Average frontal area for the vehicle models that account for about 50 percent of sales in the market

Table 47 summarizes the values defined for the drag coefficient of the reference vehicles for each vehicle class and purpose category.

Table 44. Frontal area summary

Vehicle Class	Purpose Category	Reference Value
HD (2b)	Van	5.38
HD (2b)	Pickup	3.95
HD (3)	Van	5.60
HD (3)	Pickup	3.95

Drag Coefficient

A similar analysis determined the drag coefficient values for the reference vehicle across different vehicle classifications and purpose categories. Table 45 summarizes values defined for the drag coefficient of the reference vehicles for the different vehicle classes and purpose categories.

Table 45. Drag coefficient ratio summary

Vehicle Class	Purpose Category	Reference Value
HD (2b)	Van	0.50
HD (2b)	Pickup	0.50
HD (3)	Van	0.60
HD (3)	Pickup	0.50

Rolling Resistance

A constant value of 0.009 is used as the first coefficient term of the wheel rolling resistance for all classes and purpose categories. The overall rolling resistance of the wheel is, however, speed-dependent, with a factor of 0.00012.

Effective Tire Radius

As part of this analysis, Argonne evaluated the trends in effective tire radius, which is used in the effective rolling radius calculation. Using an analysis of vehicle models that accounts for about 50 percent of sales in the market, Argonne determined the following effective wheel radius to be used across the different vehicle and purpose technology classes.

Table 46. Effective tire radius summary table

Vehicle Class	Purpose Category	Effective Wheel Radius (m)	Width (mm)	Aspect Ratio	Rim Diameter (in)
HD (2b)	Van	0.349	235	65	16
HD (2b)	Pickup	0.393	265	70	17
HD (3)	Van	0.349	235	65	16
HD (3)	Pickup	0.393	265	70	17

Vehicle Component Weight Selection

Light-Duty Vehicles

The vehicles in Autonomie are built from the ground up using individual component weights. Powertrain-dependent component weights (e.g., engine, motor, fuel cell system, high-power/energy battery, etc.) are updated as part of the sizing procedure. The following sections describe the process of selecting the non-powertrain weights based on an analysis using the A2Mac1 database.

Body Weight

Figure 128 shows the distribution of body weights for the compact (base) vehicle class.

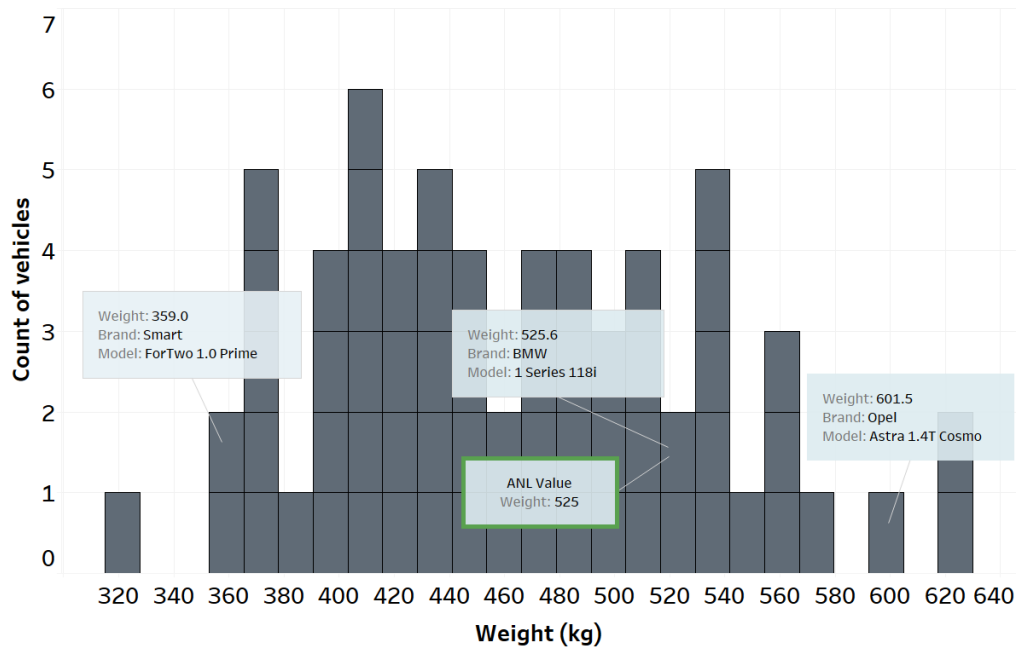


Figure 128. Body weight selection for compact (base) vehicles

Similar analyses are performed across the different vehicle classes and performance categories and the reference values are selected. Table 47 summarizes the values defined for the body weight of the reference vehicles for the different vehicle classes and performance categories.

Table 47. Body weight summary

Vehicle Class	Performance Category	Reference Value (kg)
Compact	Base/Premium	525
Midsize	Base/Premium	650
Small SUV	Base/Premium	650
Midsize SUV	Base/Premium	650/750
Pickup	Base/Premium	650/800

Chassis Weight

Figure 129 shows the distribution of chassis weights for the compact (base) vehicle class.

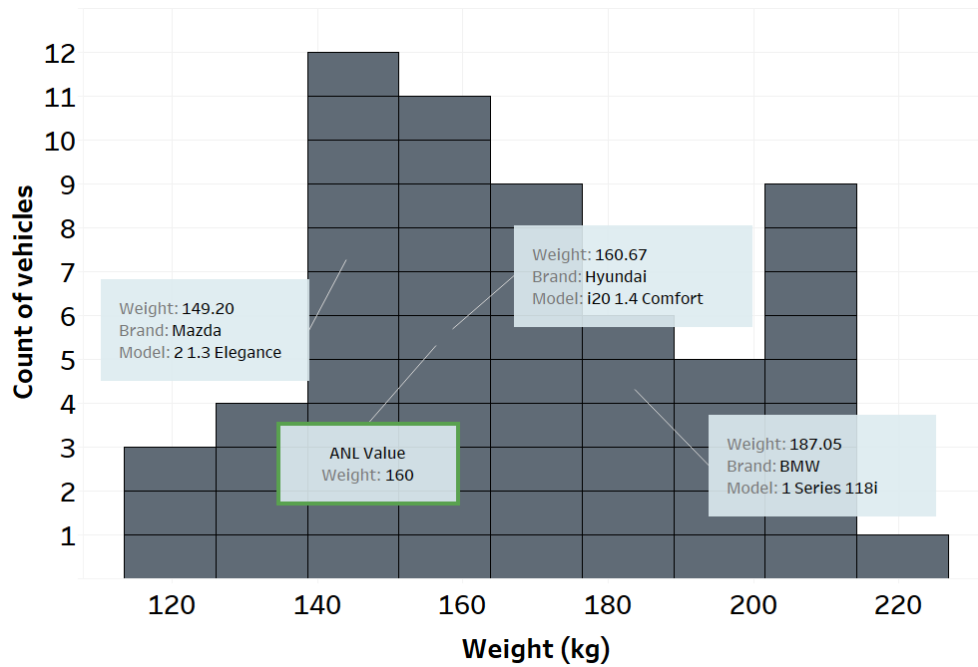


Figure 129. Chassis weight selection for compact (base) vehicles

Similar analyses are performed across the different vehicle classes and performance categories, and the reference values are selected.

Table 48 summarizes the values defined for the chassis weights of the reference vehicles for the different vehicle classes and performance categories.

Table 48. Chassis weight selection summary

Vehicle Class	Performance Category	Reference Value (kg)
Compact	Base/Premium	160
Midsized	Base/Premium	200
Small SUV	Base/Premium	200
Midsized SUV	Base/Premium	200/225
Pickup	Base/Premium	300/350

Interior Weight

Figure 130 shows the distribution of interior weights for the compact (base) vehicle class.

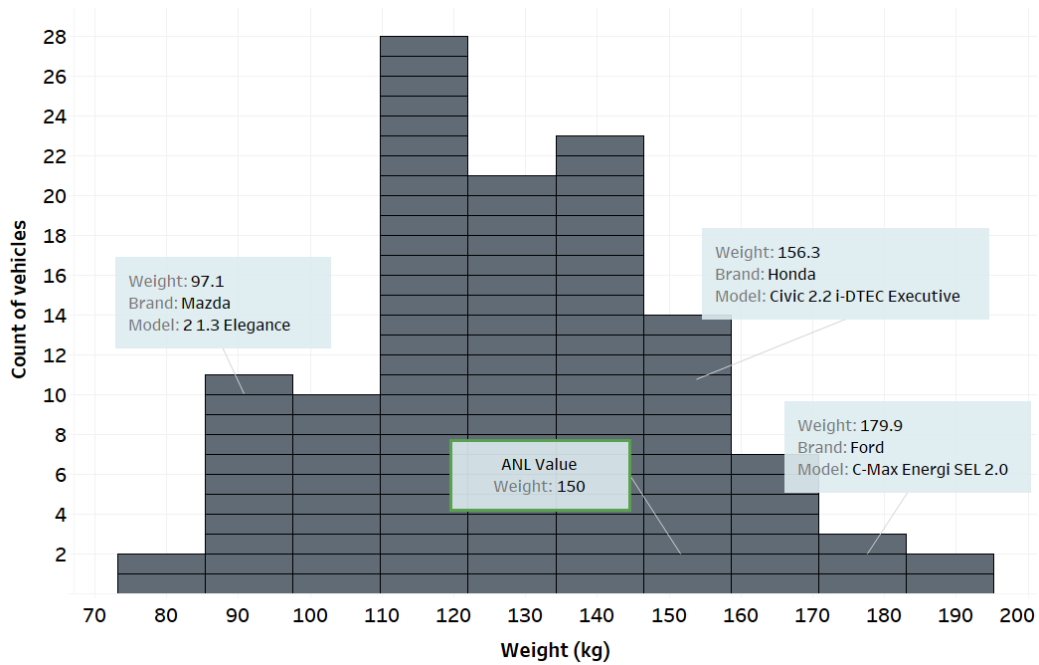


Figure 130. Interior weight selection for compact (base) vehicles

These analyses are performed across the different vehicle classes and performance categories, and the reference values are selected. Table 49 summarizes the values defined for the interior weights of the reference vehicles for the different vehicle classes and performance categories.

Table 49. Interior weight selection summary

Vehicle Class	Performance Category	Reference Value (kg)
Compact	Base/Premium	150/200
Midsize	Base/Premium	175/200
Small SUV	Base/Premium	180/220
Midsize SUV	Base/Premium	200/240
Pickup	Base/Premium	160/200

Safety System Weight

Figure 131 shows the distribution of safety system weights for the compact (base) vehicle class.

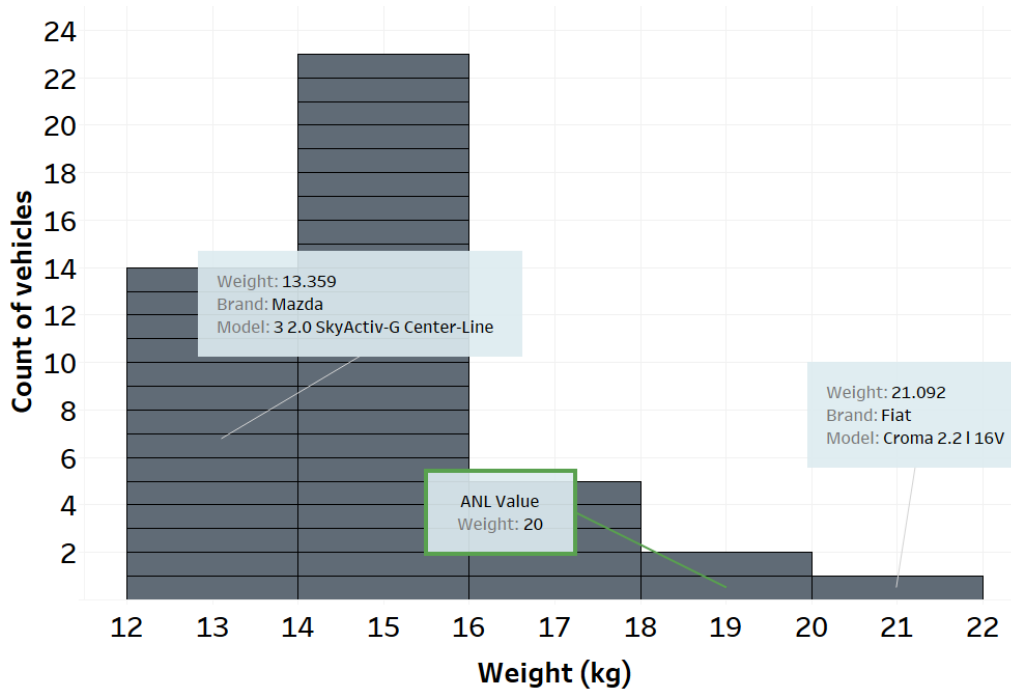


Figure 131. Safety system weight selection for compact (base) vehicle

Similar analyses are performed across the different vehicle classes and performance categories, and the reference values are selected. Table 50 summarizes the values defined for the safety system weights of the reference vehicles for the different vehicle classes and performance categories.

Table 50. Safety system weight selection summary

Vehicle Class	Performance Category	Reference Value (kg)
Compact	Base/Premium	20/22
Midsized	Base/Premium	25/28
Small SUV	Base/Premium	25/28
Midsized SUV	Base/Premium	30
Pickup	Base/Premium	30

Thermal System Weight

Figure 132 shows the distribution of thermal system weights for the compact (base) vehicle class.

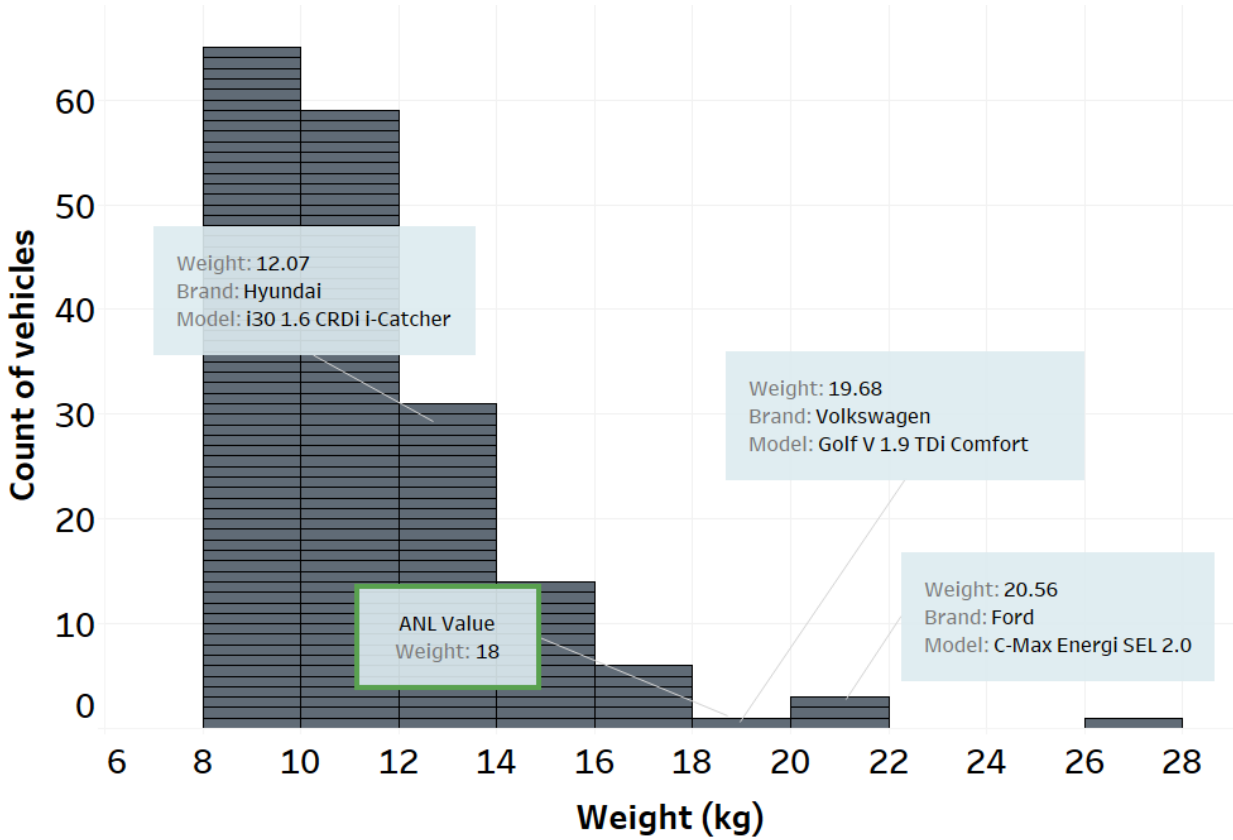


Figure 132. Thermal system weight selection for compact (base) vehicle

Similar analyses are performed across the different vehicle classes and performance categories, and the reference values are selected. Table 51 summarizes the values defined for the thermal system weights of the reference vehicles for the different vehicle classes and performance categories.

Table 51. Thermal system weight selection summary

Vehicle Class	Performance Category	Reference Value (kg)
Compact	Base/Premium	18/20
Midsized	Base/Premium	25/28
Small SUV	Base/Premium	25/28
Midsized SUV	Base/Premium	30
Pickup	Base/Premium	30

Brake Mechanism Weight

Figure 133 shows the distribution of brake mechanism weights for the compact (base) vehicle class.

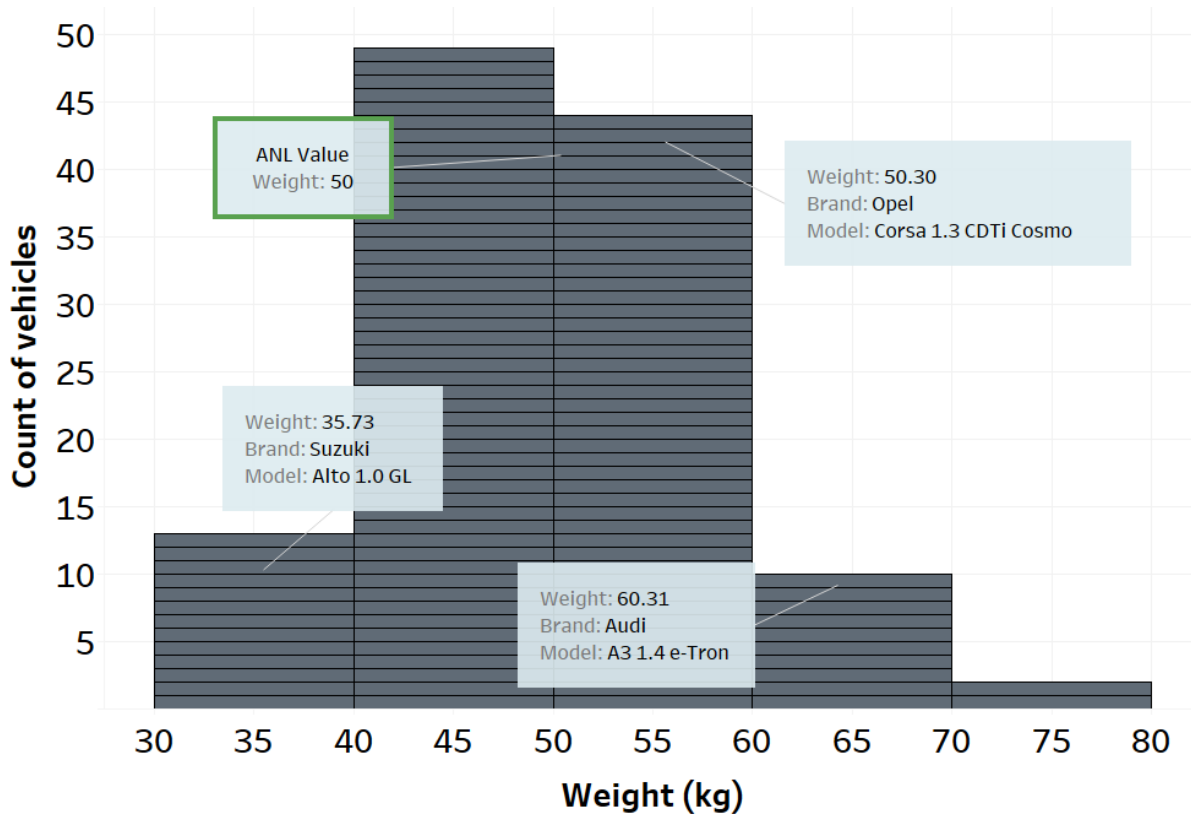


Figure 133. Brake mechanism weight selection for compact (base) vehicle

These analyses are performed across the different vehicle classes and performance categories, and the reference values are selected. Table 52 summarizes the values defined for the brake mechanism weights of the reference vehicles for the different vehicle classes and performance categories.

Table 52. Brake mechanism weight selection summary

Vehicle Class	Performance Category	Reference Value (kg)
Compact	Base/Premium	50/55
Midsize	Base/Premium	60/65
Small SUV	Base/Premium	60/75
Midsize SUV	Base/Premium	70/75
Pickup	Base/Premium	90/95

Steering System Weight

Figure 134 shows the distribution of steering system weights for the compact (base) vehicle class.

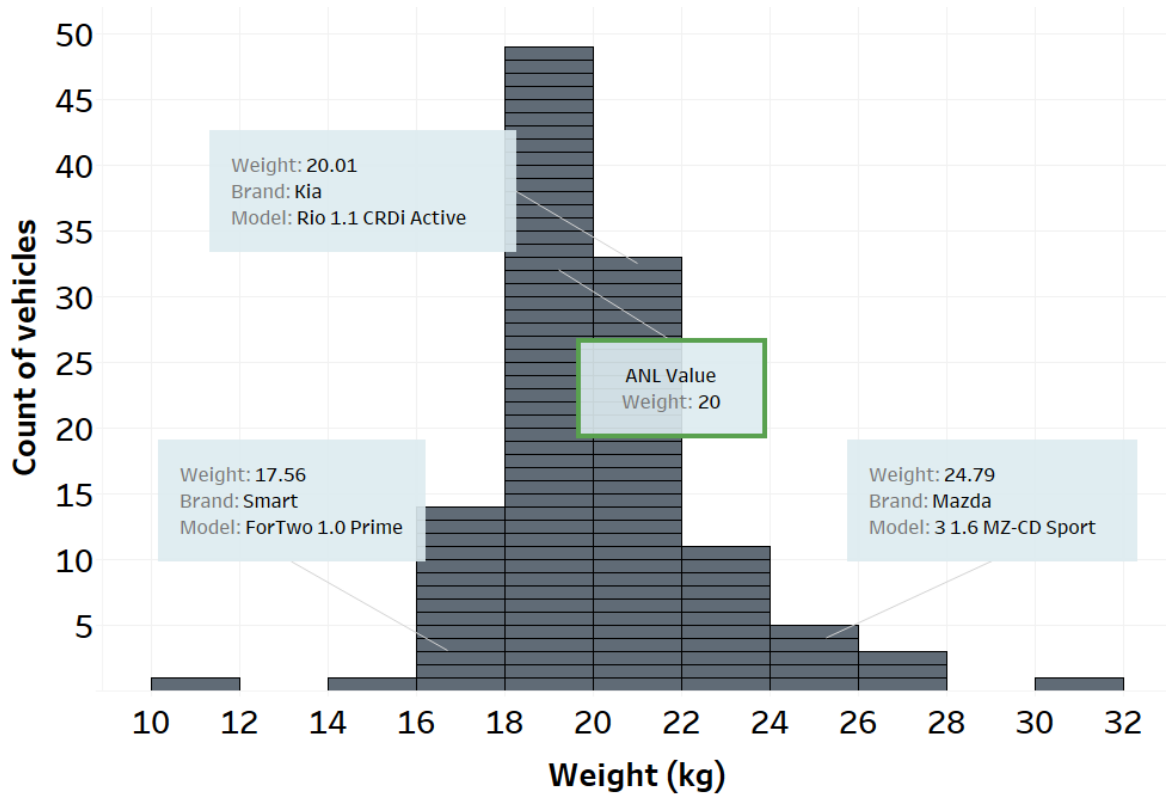


Figure 134. Steering system weight selection for compact (base) vehicle

Similar analyses are performed across the different vehicle classes and performance categories, and the reference values are selected. Table 53 summarizes the values defined for the steering system weights of the reference vehicles for the different vehicle classes and performance categories.

Table 53. Steering system weight selection summary

Vehicle Class	Performance Category	Reference Value (kg)
Compact	Base/Premium	20/22
Midsize	Base/Premium	25/28
Small SUV	Base/Premium	25/28
Midsize SUV	Base/Premium	30
Pickup	Base/Premium	30

Electrical Accessories Weight

Figure 135 shows the distribution of electrical accessories weights for the compact (base) vehicle class.

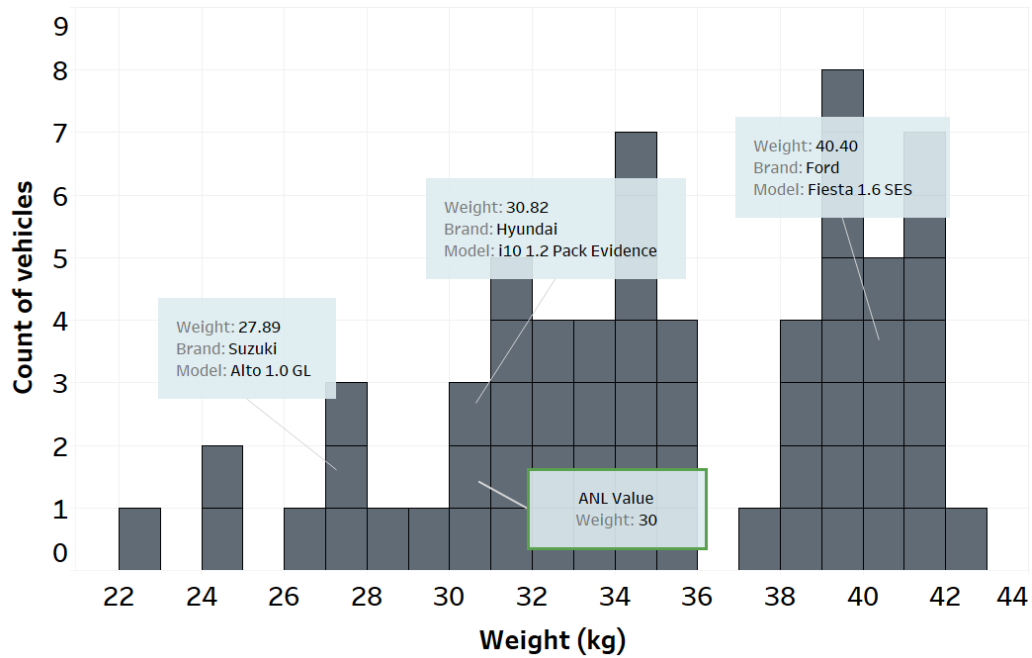


Figure 135. Electrical accessories weight selection for compact (base) vehicle

Similar analyses are performed across the different vehicle classes and performance categories, and the reference values are selected. Table 54 summarizes the values defined for the electrical accessories weights of the reference vehicles for the different vehicle classes and performance categories.

Table 54. Electrical accessories weight selection summary

Vehicle Class	Performance Category	Reference Value (kg)
Compact	Base/Premium	30/35
Midsized	Base/Premium	30/40
Small SUV	Base/Premium	30/40
Midsized SUV	Base/Premium	30/50
Pickup	Base/Premium	80/100

Engine Weight Determination

For the current set of runs, a detailed analysis of engine weight was conducted using A2mac1. The analysis consisted of different engine technologies for the North American market in A2Mac1. Figure 136 shows the updated regression analysis performed across MY 2015–2020 in A2Mac1 for gasoline engines.

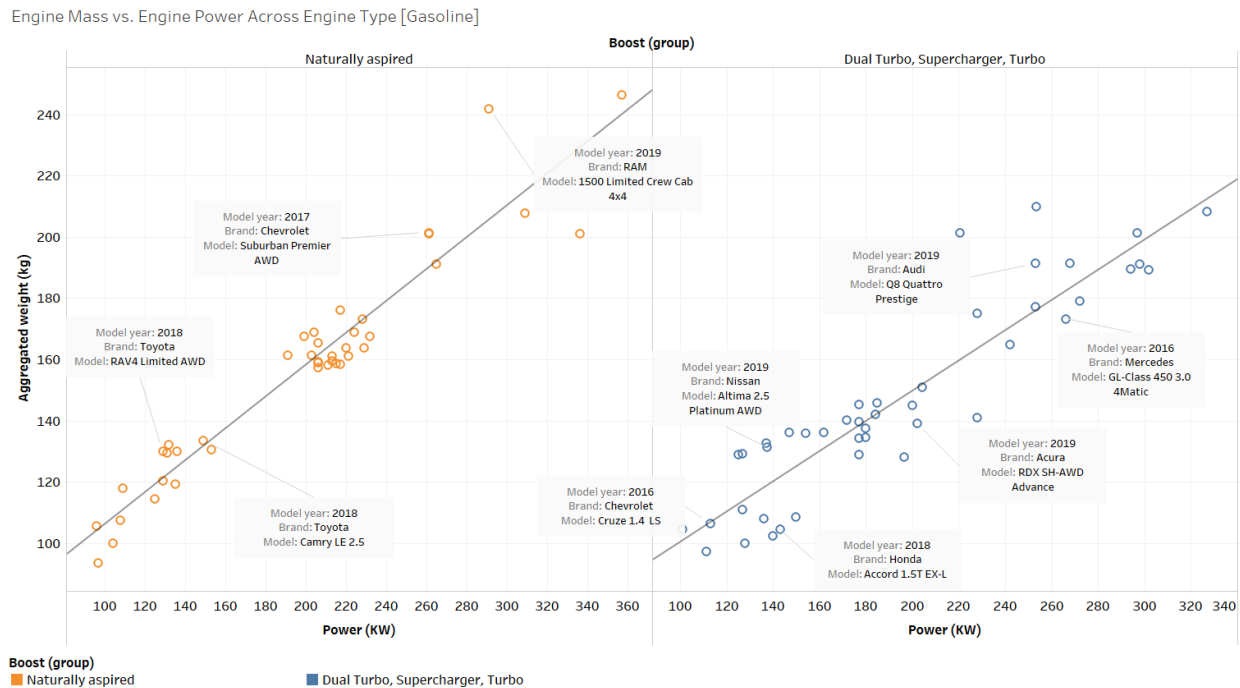


Figure 136. Engine weight (kg) versus engine power (kW) of gasoline engines across different aspiration methods

Figure 137 shows the updated regression analysis performed for diesel engines of vehicles across MY 2007–2022 from North America in A2Mac1. Using the updated regression analyses performed for vehicles in A2Mac1, Argonne uses the following equations for the current set of runs.

- Naturally aspirated, gasoline:
Weight (kg) = $0.494526 \times (\text{Engine Power [kW]}) + 58.7248$
- Turbocharged engine, gasoline:
Weight (kg) = $0.494828 \times (\text{Engine Power [kW]}) + 50.1853$
- Diesel engine:
Weight (kg) = $1.04559 \times (\text{Engine Power [kW]}) + 95.2388$

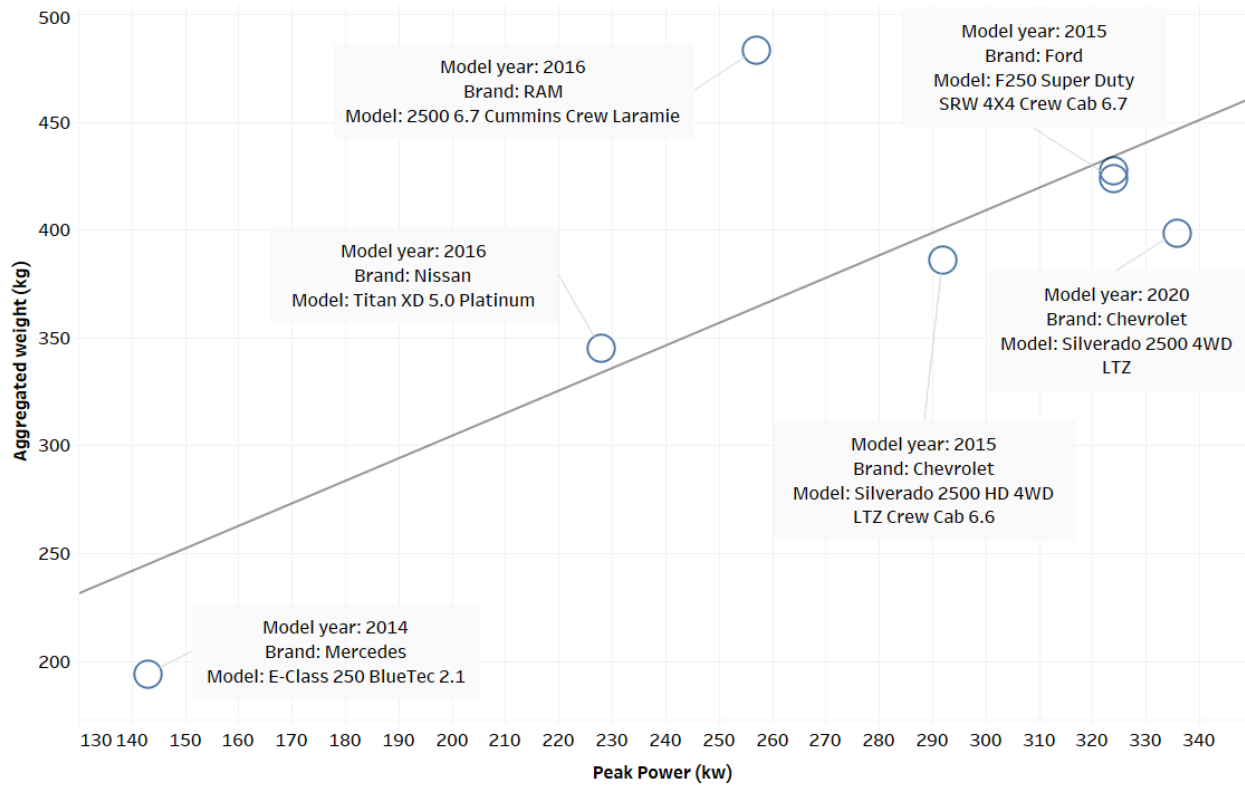


Figure 137. Engine weight (kg) versus engine power (kW) of diesel engines

Electric Drive System Weight Determination

For the current set of runs, the electric machine weight computation was updated by analyzing the existing electric machine component and controller weights against the electric machine peak power output from A2mac1.

Figure 138 shows the updated regression analysis performed from A2Mac1 data across different EVs.

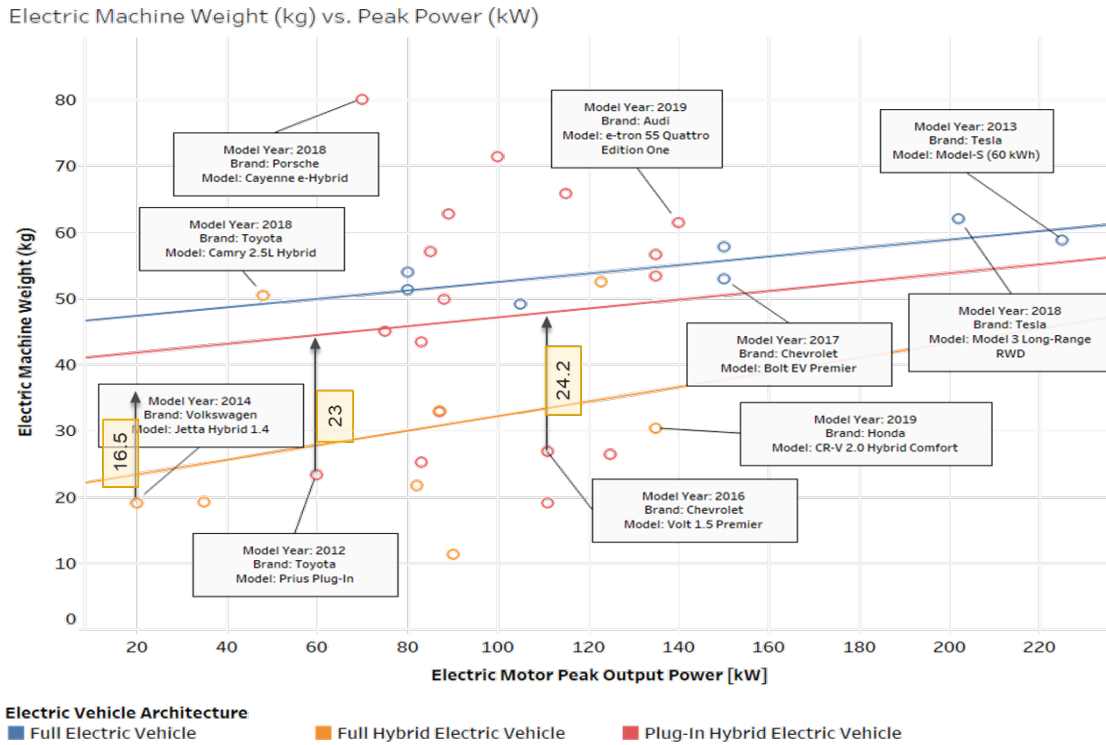


Figure 138. Electric machine weight versus peak power output

Per the figure, while accounting for the enclosure masses for the HEVs and PHEVs, the values are close to the EV trend line observed. Therefore, from the analysis above, Argonne recommended using the regression analysis performed for the EVs to develop a generalized equation.

$$Weight (kg) = 0.0639176 \times Electric\ Motor\ Peak\ Output\ Power (kW) + 46.0497$$

Heavy-Duty Pickups and Vans

The vehicles in Autonomie are built from the ground up using individual component weights. Powertrain-dependent component weights (e.g., engine, motor, fuel cell system, high-power/energy battery, etc.) are updated as part of the sizing procedure. The following sections describe the process of selecting the component weights based on an analysis using the Autonomie database.

Glider Weight

Figure 139 shows the average curb weights for the vehicle models that account for about 50 percent of sales in the market. These analyses are performed across the different vehicle classes and purpose categories. The curb weight after sizing plus the powertrain weight is shown as the ANL value.

Table 55 summarizes the values defined for the glider weights of the reference vehicles for the different vehicle classes and purpose categories.

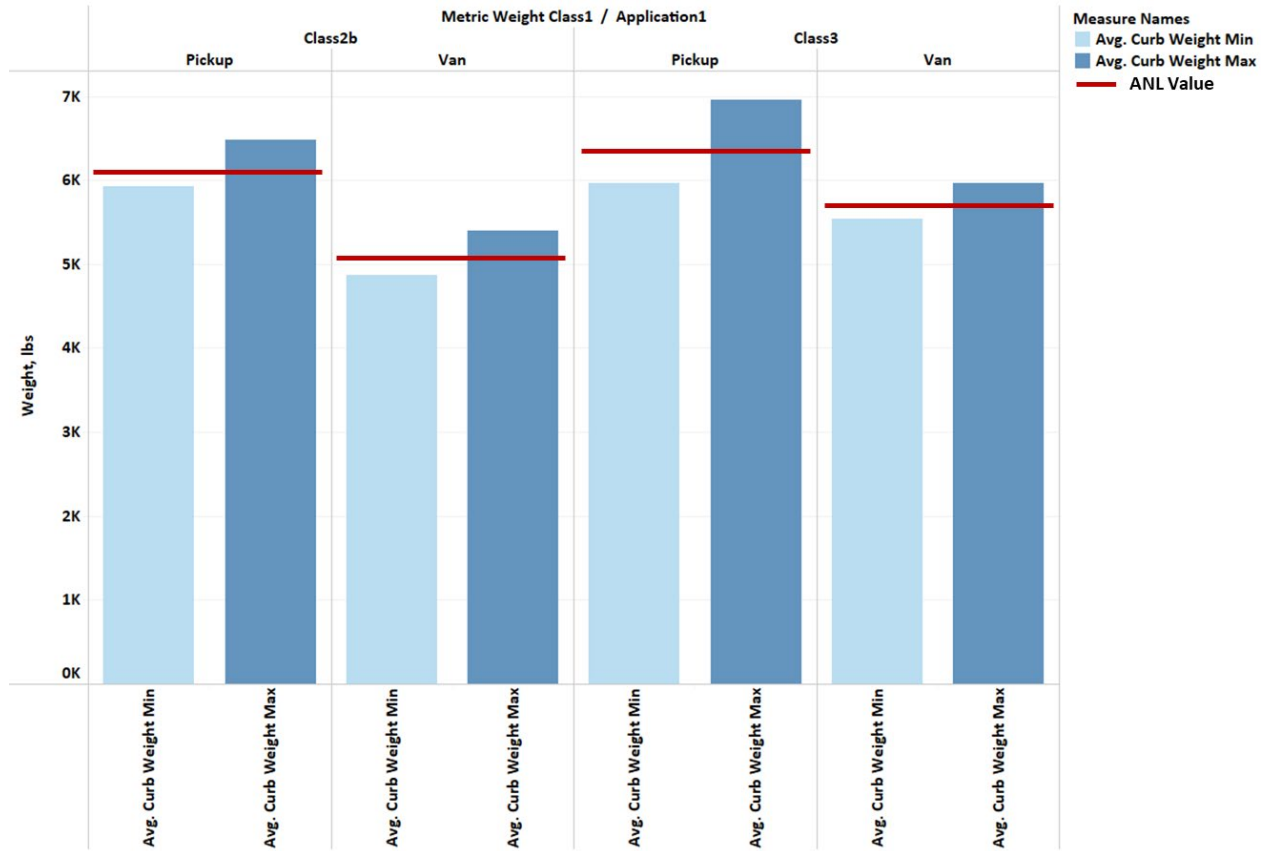


Figure 139. Average curb weight for the vehicle models that account for about 50 percent of sales in the market

Table 55. Glider weight selection summary

Vehicle Class	Purpose Category	Reference Value (kg)
HD (2b)	Van	1,600
HD (2b)	Pickup	2,000
HD (3)	Van	1,900
HD (3)	Pickup	2,100

Engine Weight Determination

For the current set of runs, a detailed analysis of engine weight was conducted on Autonomie data. The analysis included different engine technologies for the North American market. Figure 140 shows the updated regression analysis performed across Cummins diesel engines.

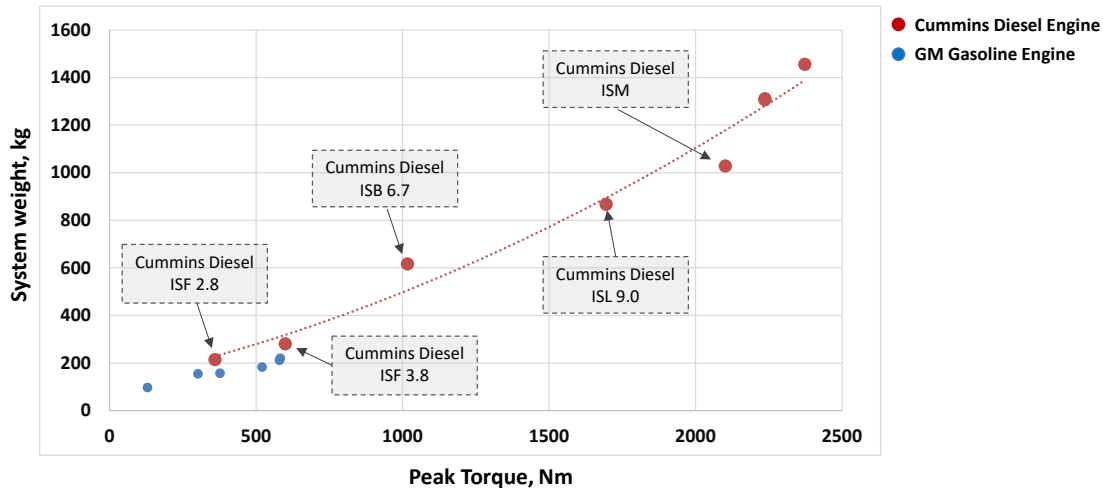


Figure 140. Engine weight (kg) versus engine peak torque (Nm) of diesel engines

Argonne used the following equations for the current set of runs. For gasoline engines, the same assumptions for LD vehicles are used.

- Naturally aspirated, gasoline:
Weight (kg) = $0.494526 \times (\text{Engine Power [kW]}) + 58.7248$
- Turbocharged engine, gasoline:
Weight (kg) = $0.494828 \times (\text{Engine Power [kW]}) + 50.1853$
- Diesel engine:
Weight (kg) = $0.001 \times (\text{Engine Torque [Nm]})^2 + 0.2897 \times (\text{Engine Torque [Nm]}) + 51.493$

Transmission Assumptions

Transmission Technology Definitions

Table 56 details the different transmission technologies used in the study.

Table 56. Transmission technologies

Simulation Name	Transmission Type	Description/Source
5AU	5-speed automatic (base class)	1:1 ratio efficiency from 6AU (base) and used rule to generate the efficiency for other ratios
5AU	5-speed automatic (premium class)	1:1 ratio efficiency from 6AU (premium) and used rule to generate the efficiency for other ratios

Simulation Name	Transmission Type	Description/Source
6AU	6-speed automatic (base class)	Transmission used for low-torque engines (EPA, 2019a)
6AU	6-speed automatic (premium class)	Transmission used for high-torque engines [(NHTSA, 2016)
7AUp	7-speed automatic+	1:1 ratio efficiency from 8AU+ and used rule to generate the efficiency for other ratios
8AU	8-speed automatic	(EPA, 2019b)
8AUp	8-speed automatic+	845RE (8AU) with improved efficiency (NHTSA, 2016)
8AUpp	8-speed automatic++	845RE (8AU) with improved efficiency (NHTSA, 2016)
9AUp	9-speed automatic+	1:1 ratio efficiency from 8AU+ and used rule to generate the efficiency for other ratios
10AUp	10-speed automatic+	MY 2017 Ford F-150 10R80 (Wileman, 2021)
10AUpp	10-speed automatic++	10R80 (10AUp) with improved efficiency
6DCT	6-speed DCT	(Kim et al., 2014)
8DCT	8-speed DCT	1:1 ratio efficiency from 6DCT and used rule to generate the efficiency for other ratios
CVT	CVT	(Son et al., 2015)
CVTp	CVT+	CVT with improved efficiency (NHTSA, 2016)

Like engines, transmissions in the market always include multiple improvements from one generation to the next (such as increased gear number and efficiency). The objective of the transmission selection process was to separate the benefits of increased gear number from those of improved efficiency. For example, simulations 6AU to 8AU quantify the effectiveness of increased gear span and gear number, while 8AU to 8AU+ quantify the impact of efficiency. As a result, while the test data were used to model several transmissions, a rule was used to develop some transmission models to ensure appropriate effectiveness value.

Automatic Transmission Efficiency Rule (USCAR, 2015)

In the equations below, τ is the normalized torque (torque/max rated input torque). In the specific data set that was used to generate these equations, the maximum torque was taken to be 450 Nm.

The maximum efficiency is given by:

$$(1) \eta = 100 - 1.385 \times \tau^{-1.0127}$$

The temperature dependence is considered as a function of torque for temperatures ranging from $T=38^\circ \text{C}$ to $T=93^\circ \text{C}$.

$$(2) \Delta\eta = 0.3612 \times \tau^{-0.9238}$$

The speed dependence is a function of input torque for speeds ranging from 500 to 5,000 rpm.

$$(3) \Delta\eta = 0.6394 \times \tau^{-1.3068}$$

The efficiency data is generated using the following steps.

- Start with the “maximum efficiency curve,” which essentially represents the efficiency for direct drive (1:1 ratio) at 93° C.
- The temperature offset is applied when calculating efficiency at 38° C.
- The speed offset is applied.
- The gear ratio other than the direct drive is scaled.

Figure 141 shows the plot of direct drive efficiency for the range of temperatures and speeds considered. For other gears, the results are scaled down by a factor ranging between 0.97 and 1.0.

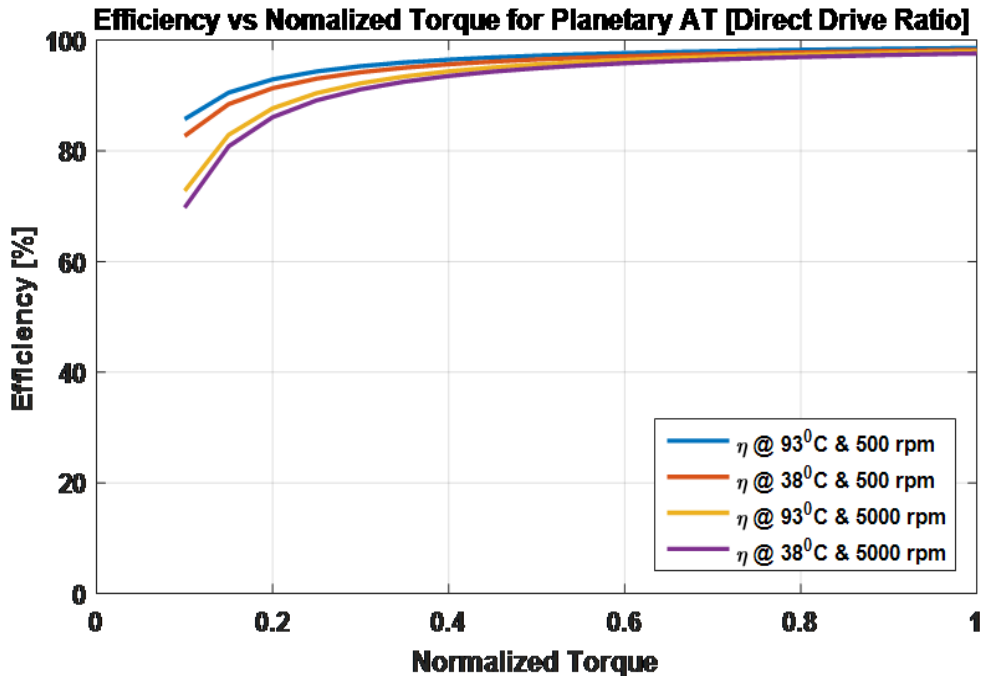


Figure 141. Efficiency for direct drive, for the range of temperatures and speeds considered

Dual-Clutch Transmission Efficiency Rule

The efficiency of the DCT is broken down into a speed-dependent term (spin loss) and a load dependent term (gear train mechanical efficiency).

For the speed-dependent part, the turning torque (Nm) is given by the following equations through curve fit as a function of the overall gear ratio R.

At 93° C and 500 rpm:

$$(4) T = 4.89 \times \left(\frac{1}{R}\right)^2 + 0.135 \times \left(\frac{1}{R}\right) + 0.21$$

At 93° C and 5,000 rpm:

$$(5) T = 23.5 \times \left(\frac{1}{R}\right)^2 + 1.4 \times \left(\frac{1}{R}\right) + 1.7$$

The turning torque is approximately linear between 500 and 5,000 rpm.

The gear mechanical efficiency is very high and can be assumed to be in the range of 99 to 99.5 percent per gear mesh. The mesh efficiency is higher when the meshing gears are of a similar size.

The efficiency data is generated by the following steps.

- The torque loss is subtracted from the input torque.
- The additional torque loss due to constant mechanical efficiency is calculated by multiplying the difference between the input torque and the torque loss by 1 minus the efficiency.
- The efficiency is calculated by taking the sum of the (spin) torque loss and the loss due to mechanical efficiency and dividing it by the input torque.

The data set is based on a DCT with a rated input torque of up to 250 Nm.

Transmission Attributes

Light-Duty Vehicles

Gear Span

Figure 142 shows the analysis on the existing vehicle attributes to determine the gear span of a 6-speed automatic transmission.

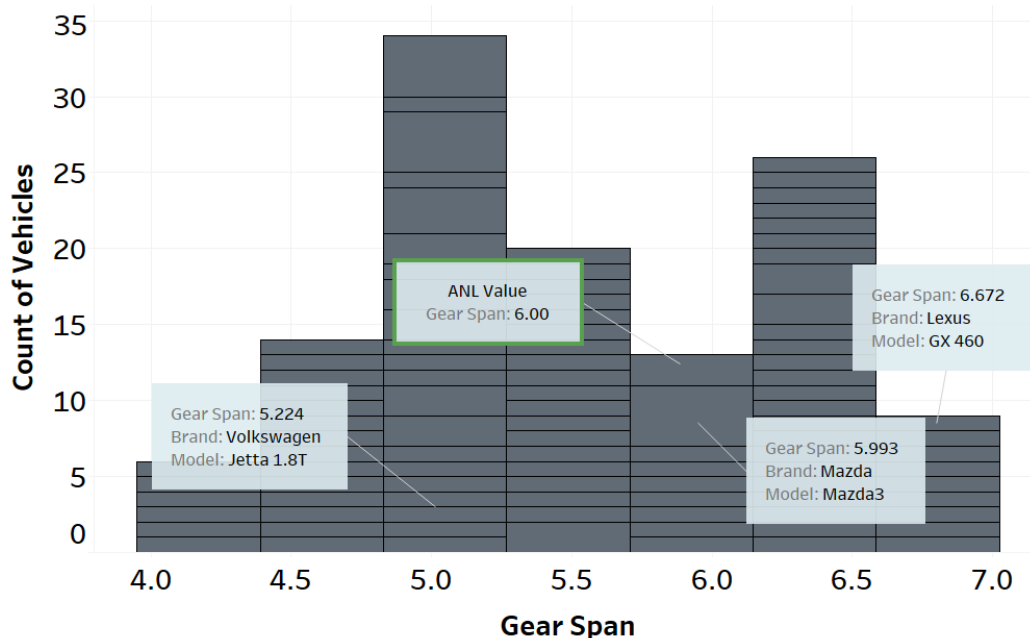


Figure 142. Vehicle attribute analysis for gear span of 6AU (Source: Argonne Vehicle Database)

A similar analysis was conducted on other transmission types and numbers of gears considered for the study. Table 59 summarizes the gear span values implemented across the different transmission types and gear numbers.

While we recognize that some transmissions currently in the market have a higher gear span, the study focuses on selecting assumptions based on the overall market. Separate studies will be conducted to quantify the impact of uncertainties related to variations of the assumptions.

Final Drive Ratio

Figure 143 shows the analysis done on the existing vehicle attributes to determine the final drive ratio of the different number of gears of automatic transmission across the different vehicle classes and engine types (NA and turbocharged).

Descriptive Summary of Final Drive Ratio

vehicle_class	transmission speed	air aspiration method	count	mean	std	min	25%	50%	75%	max	ci95_low	ci95_high
Compact	6	Naturally Aspirated	16.0	3.65	0.38	2.94	3.44	3.63	3.82	4.33	3.44	3.82
		Turbocharged	4.0	3.23	0.00	3.23	3.23	3.23	3.23	3.23	3.23	3.23
	8	Naturally Aspirated	1.0	2.94	NaN	2.94	2.94	2.94	2.94	2.94	NaN	NaN
		Turbocharged	37.0	3.12	0.30	2.81	2.85	3.08	3.32	3.87	2.98	3.18
	9	Naturally Aspirated	10.0	3.52	0.00	3.52	3.52	3.52	3.52	3.52	3.52	3.52
		Other	1.0	3.27	NaN	3.27	3.27	3.27	3.27	3.27	NaN	NaN
	Turbocharged	7.0	2.87	0.30	2.47	2.74	2.82	3.04	3.27	2.60	3.04	
	10	Turbocharged	1.0	2.85	NaN	2.85	2.85	2.85	2.85	NaN	NaN	
Midsize	6	Naturally Aspirated	19.0	3.31	0.38	2.77	2.88	3.42	3.63	3.77	3.25	3.59
		Turbocharged	18.0	3.30	0.37	2.77	3.09	3.21	3.36	3.88	3.04	3.38
	7	Turbocharged	11.0	2.95	0.12	2.65	2.94	2.94	2.94	3.13	2.87	3.01
		Naturally Aspirated	55.0	2.91	0.35	2.56	2.62	2.80	3.07	3.91	2.71	2.89
	8	Turbocharged	97.0	3.16	0.28	2.62	2.93	3.15	3.42	3.73	3.09	3.21
		Turbocharged	8.0	2.63	0.16	2.47	2.47	2.65	2.69	2.89	2.54	2.76
10	Naturally Aspirated	3.0	3.38	0.20	3.27	3.27	3.27	3.44	3.61	3.04	3.50	
	Turbocharged	14.0	3.02	0.35	2.76	2.79	2.85	2.94	3.84	2.67	3.03	
Midsize SUV	5	Naturally Aspirated	12.0	3.73	0.00	3.73	3.73	3.73	3.73	3.73	3.73	3.73
		Turbocharged	16.0	4.00	0.37	3.50	3.50	4.30	4.30	4.30	4.12	4.48
	6	Turbocharged	16.0	3.61	0.16	3.50	3.50	3.53	3.62	3.87	3.45	3.61
		Naturally Aspirated	9.0	2.94	0.00	2.94	2.94	2.94	2.94	2.94	2.94	2.94
	8	Naturally Aspirated	43.0	3.41	0.20	3.09	3.27	3.45	3.60	3.70	3.39	3.51
		Turbocharged	66.0	3.35	0.24	2.85	3.21	3.31	3.39	4.10	3.25	3.37
9	Naturally Aspirated	37.0	3.51	0.07	3.49	3.49	3.49	3.49	3.80	3.47	3.51	
	Turbocharged	27.0	3.36	0.14	3.17	3.17	3.47	3.47	3.47	3.42	3.52	
10	Naturally Aspirated	8.0	3.23	0.00	3.23	3.23	3.23	3.23	3.23	3.23	3.23	
	Turbocharged	45.0	3.43	0.23	3.15	3.15	3.31	3.58	3.73	3.24	3.38	
Pickup	6	Naturally Aspirated	55.0	4.03	0.30	3.42	3.91	3.91	4.30	4.30	3.83	3.99
		Turbocharged	16.0	3.64	0.09	3.55	3.55	3.64	3.73	3.73	3.60	3.68
	8	Naturally Aspirated	13.0	3.44	0.09	3.42	3.42	3.42	3.42	3.73	3.37	3.47
		Turbocharged	0.0	NaN	NaN	NaN	NaN	NaN	NaN	NaN	NaN	NaN
	9	Naturally Aspirated	19.0	3.89	0.31	3.69	3.69	3.69	4.33	4.33	3.55	3.83
		Turbocharged	13.0	3.73	0.00	3.73	3.73	3.73	3.73	3.73	3.73	3.73
Small SUV	4	Naturally Aspirated	2.0	4.28	0.00	4.28	4.28	4.28	4.28	4.28	4.28	4.28
		Turbocharged	60.0	3.66	0.45	3.06	3.46	3.51	3.91	4.62	3.40	3.62
	6	Turbocharged	22.0	3.87	0.47	3.32	3.51	3.53	4.41	4.41	3.33	3.73
		Naturally Aspirated	61.0	3.43	0.29	3.00	3.18	3.51	3.60	4.08	3.44	3.58
	8	Turbocharged	116.0	3.55	0.20	3.20	3.33	3.60	3.73	3.81	3.56	3.64
		Naturally Aspirated	59.0	3.88	0.47	1.68	3.73	3.73	4.33	4.33	3.61	3.85
9	Turbocharged	32.0	3.84	0.52	3.17	3.47	3.73	4.54	4.58	3.55	3.91	
	Turbocharged	8.0	4.17	0.00	4.17	4.17	4.17	4.17	4.17	4.17	4.17	

Figure 143. Vehicle attribute analysis for final drive ratio of 6AU (Source: Argonne Vehicle Database)

A similar analysis was conducted on other transmission types and numbers of gears considered for the study. Table 59 summarizes the final drive ratio values implemented across the different transmission types and gear numbers.

The final drive ratios had been adjusted for the different tech classes across the NA and turbocharged engines. The values used for the NA engines are shown in Table 57 and those for turbocharged engines in Table 58.

Table 57. Final drive ratios for NA engines

Vehicle Class	Performance Category	5-AU	6-AU	7-AU	8-AU	9-AU	10-AU	10-Aupp	6-DCT	8-DCT	Prius	Volt	Single Gear	CVT	CVTp
Compact	Base	3.41	3.31	3.01	3.07	3.26	3.26	3.21	3.65	3.6	3.947	3.02	3.5	4.44	4.44
	Premium	3.41	3.31	3.01	3.07	3.26	3.26	3.21	3.65	3.6	3.947	3.02	3.5	4.44	4.44
Midsize	Base	3.41	3.31	3.01	3.07	3.26	3.26	3.21	3.65	3.6	3.947	3.02	3.5	4.44	4.44
	Premium	3.41	3.31	3.01	3.07	3.26	3.26	3.21	3.65	3.6	3.947	3.02	3.5	4.44	4.44
Small SUV	Base	3.41	3.51	3.01	3.45	3.49	3.59	3.61	3.65	3.6	3.947	3.02	3.5	4.44	4.44
	Premium	3.41	3.51	3.01	3.45	3.49	3.59	3.61	3.65	3.6	3.947	3.02	3.5	4.44	4.44
Midsize SUV	Base	3.41	3.51	3.01	3.45	3.49	3.59	3.61	3.65	3.6	3.947	3.02	3.5	4.44	4.44
	Premium	3.41	3.51	3.01	3.45	3.49	3.59	3.61	3.65	3.6	3.947	3.02	3.5	4.44	4.44
Pickup	Base	3.41	3.51	3.01	3.45	3.49	3.59	3.61	3.65	3.6	3.947	3.02	3.5	4.44	4.44
	Premium	3.41	3.51	3.01	3.45	3.49	3.59	3.61	3.65	3.6	3.947	3.02	3.5	4.44	4.44

Table 58. Final drive ratios for turbocharged engines

Vehicle Class	Performance Category	5-AU	6-AU	7-AU	8-AU	9-AU	10-AU	10-Aupp	6-DCT	8-DCT	Prius	Volt	Single Gear	CVT	CVTp
Compact	Base	3.41	3.63	3.13	3.23	3.47	3.59	3.61	3.65	3.6	3.267	3.02	3.5	4.44	4.44
	Premium	3.41	3.63	3.13	3.23	3.47	3.59	3.61	3.65	3.6	3.267	3.02	3.5	4.44	4.44
Midsize	Base	3.41	3.63	3.13	3.23	3.47	3.59	3.61	3.65	3.6	3.267	3.02	3.5	4.44	4.44
	Premium	3.41	3.63	3.13	3.23	3.47	3.59	3.61	3.65	3.6	3.267	3.02	3.5	4.44	4.44
Small SUV	Base	3.41	3.63	3.13	3.78	3.83	4.03	4.17	3.65	3.6	3.267	3.02	3.5	4.44	4.44
	Premium	3.41	3.63	3.13	3.78	3.83	4.03	4.17	3.65	3.6	3.267	3.02	3.5	4.44	4.44
Midsize SUV	Base	3.41	3.63	3.13	3.78	3.83	4.03	4.17	3.65	3.6	3.267	3.02	3.5	4.44	4.44
	Premium	3.41	3.63	3.13	3.78	3.83	4.03	4.17	3.65	3.6	3.267	3.02	3.5	4.44	4.44
Pickup	Base	3.41	3.63	3.13	3.78	3.83	4.03	4.17	3.65	3.6	3.267	3.02	3.5	4.44	4.44
	Premium	3.41	3.63	3.13	3.78	3.83	4.03	4.17	3.65	3.6	3.267	3.02	3.5	4.44	4.44

Gear Ratio Selected for Each Transmission

Table 59 summarizes the gear ratios selected for the different transmissions for the study.

Table 59. Gear ratios, gear span and final drive ratio selected for different transmissions

Simulation Name	Gear										Gear Span
	1	2	3	4	5	6	7	8	9	10	
5AU	3.85	2.3262	1.5039	1.0403	0.77						5
6AU	4.074	2.4867	1.6241	1.135	0.8487	0.679					6
6DCT	4.074	2.4867	1.6241	1.135	0.8487	0.679					6
7AU+	4.78	3.10	1.98	1.37	1.00	0.87	0.78				6.16
8AU/+/++	4.71	3.14	2.11	1.67	1.28	1	0.84	0.67			7.03
8DCT	4.284	2.6593	1.7763	1.2553	0.9546	0.7768	0.6763	0.63			6.8
9AU+	4.69	3.31	3.01	2.44	1.92	1.44	1	0.75	0.62		7.56
10AU+	4.7	2.99	2.15	1.8	1.52	1.28	1	0.85	0.69	0.64	7.34
10AU++	5.25	3.27	2.19	1.6	1.3	1	0.78	0.65	0.58	0.52	10.10
CVT	Ratios from 0.529 to 3.172										
CVTp	Ratios from 0.45 to 3.6										
Planetary Gear	Sun = 30, Ring = 78										
Voltec	Sun = 37, Ring = 83										

Heavy-Duty Pickups and Vans

Table 60 summarizes the gear span values implemented across the different gear numbers, based on the existing vehicle.

Table 60. Gear span and final drive ratio selected for different transmissions

Simulation Name	Purpose Category	1st Gear Ratio x FD Ratio	Top Gear Ratio x FD Ratio	Gear Span	Source Model
5AU	Van	13.17	2.63	5.00	-
5AU	Pickup	14.36	2.87	5.00	-
6AU	Van	13.78	2.29	6.01	Express (6L90)
6AU	Pickup	15.03	2.50	6.01	Silverado (6L90)
8AU	Van	15.60	2.22	7.02	Express (8L90)
8AU	Pickup	17.01	2.42	7.02	Silverado (8L90)
9AU _p	Van/Pickup	19.22	1.96	9.81	ProMaster (948TE)
10AU _p	Van/Pickup	17.52	2.37	7.38	Transit (10R80) F-250 (10R80)

Table 61 also summarizes the gear ratios selected for the different transmissions for the study.

Table 61. Gear ratios, gear span and final drive ratio selected for different transmissions

Simulation Name	Purpose Category	Gear										Final Drive	
		1	2	3	4	5	6	7	8	9	10		
5AU	Van	3.85	2.33	1.50	1.04	0.77							3.42
5AU	Pickup	3.85	2.33	1.50	1.04	0.77							3.73
6AU	Van	4.03	2.36	1.53	1.15	0.85	0.67						3.42
6AU	Pickup	4.03	2.36	1.53	1.15	0.85	0.67						3.73
8AU	Van	4.56	2.97	2.08	1.69	1.27	1.00	0.85	0.65				3.42
8AU	Pickup	4.56	2.97	2.08	1.69	1.27	1.00	0.85	0.65				3.73
9AU _p	Van/Pickup	4.71	2.84	1.91	1.38	1.00	0.81	0.70	0.58	0.48			4.08
10AU _p	Van/Pickup	4.70	2.99	2.15	1.77	1.52	1.28	1.00	0.85	0.69	0.64		3.73

Transmission Weights

Light-Duty Vehicles

Like the vehicle component weights, the weights for transmission system components have been evaluated from the A2Mac1 database for different transmission types and numbers of gears for the different vehicle classes and performance categories.

Final Drive Weight

Figure 144 shows the distribution of final drive weights for 6-speed automatic transmissions for different vehicle classes.

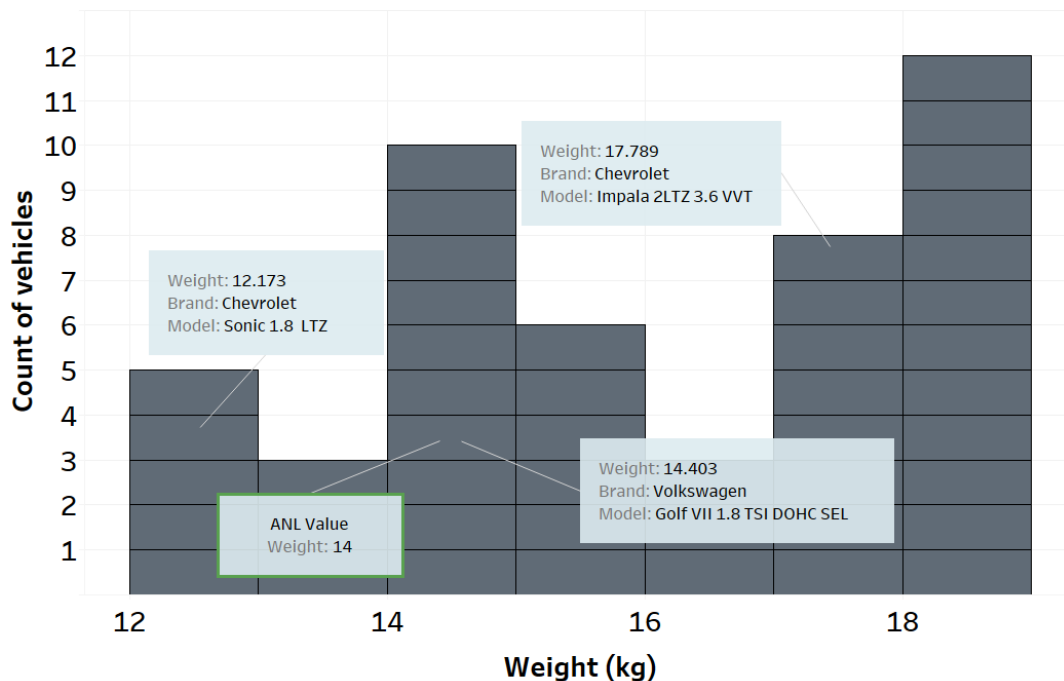


Figure 144. Final drive weight selection for 6AU

Similar analyses were performed across different transmissions, numbers of gears, vehicle classes, and performance categories, and the values for the reference vehicles were defined.

Table 62 summarizes the values defined for the final drive weights of the reference vehicles with different transmissions across different numbers of gears, vehicle classes, and performance categories.

Gearbox Weight

Gearbox weights have been re-evaluated from the A2Mac1 database and have been assigned across the different vehicle classifications and performance categories for the different transmission types and numbers of gears.

Figure 145 shows the distribution of gearbox weight for 6-speed automatic transmissions for the midsize vehicle class.

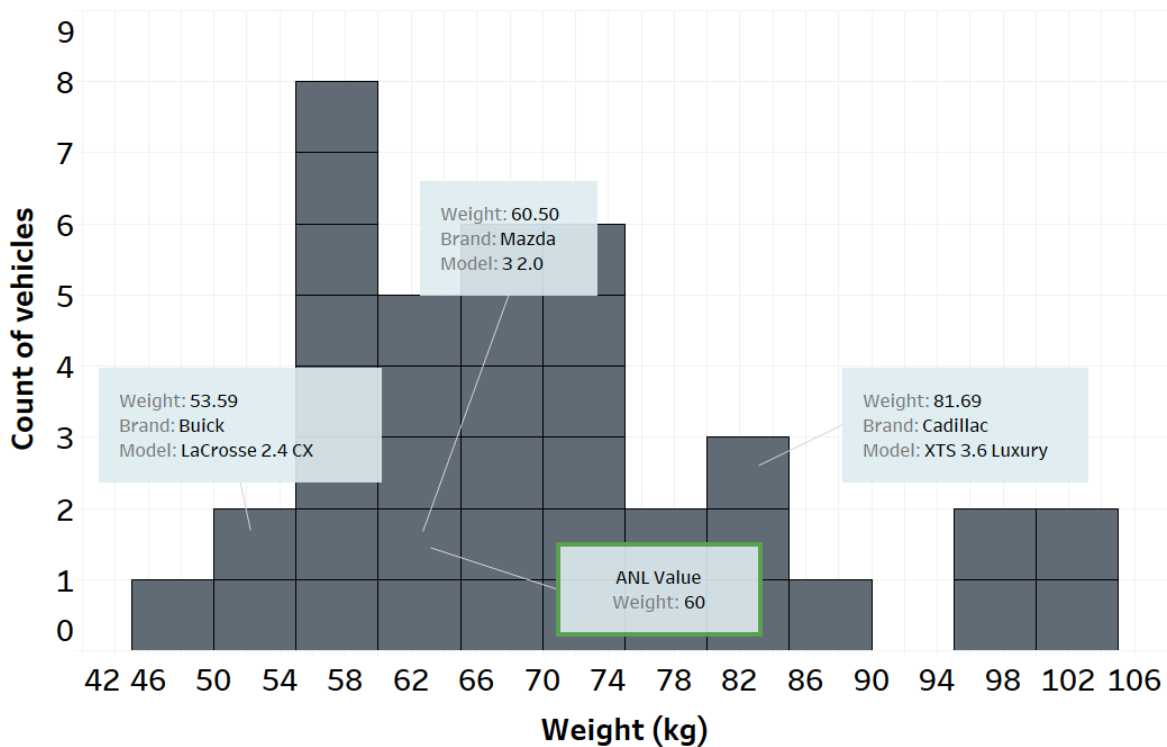


Figure 145. Gearbox weight selection for 6AU for midsize vehicles

Similar analyses are performed across different transmissions, number of gears, vehicle classes and performance categories, and the values for the reference vehicles are defined. Table 63 summarizes the gearbox weights for different transmissions across the different number of gears for the different vehicle classes and performance categories.

Table 62. Final drive weight summary for all transmission types

Vehicle Class	Performance Category	Reference Value (kg)													
		5AU	6AU	7AU	8AU	9AU	10AU	5DM	6DM	7DM	6DCT	8DCT	CVT/+	Power-Split	EREV
Compact	Base/Premium	14	14	14	14	14	14	12	14	14	14	14	14	14	14
Midsize	Base/Premium	17	17	17	17	17	17	12	14	14	14	14	14	14	14
Small SUV	Base/Premium	20	22	22	22	22	22	24	24	24	24	24	24	24	24
Midsize SUV	Base/Premium	25	30	30	30	30	30	35	35	35	35	35	35	35	35
Pickup	Base/Premium	60	70	72	75	75	75	60	65	65	65	65	65	65	65

Table 63. Gearbox weight summary for all transmission types

Vehicle Class	Performance Category	Reference Value (kg)													
		5AU	6AU	7AU	8AU	9AU	10AU	5DM	6DM	7DM	6DCT	8DCT	CVT/+	Power-Split	EREV
Compact	Base/Premium	60	50	60	65	70	40	30	40	50	65	80	41	40	50
Midsize	Base/Premium	65	60	70	80	85	50	35	45	50	70	90	51	40	50
Small SUV	Base/Premium	70	65	72	80	90	55	45	50	50	75	90	56	50	60
Midsize SUV	Base/Premium	80	65	72	80	90	75	45	50	70	80	90	56	50	60
Pickup	Base/Premium	80	75	80	90	95	85	50	60	70	90	100	65	50	60

Heavy-Duty Pickups and Vans

Transmission weights have been evaluated from the Autonomie database for automatic transmission types. Figure 146 shows the distribution of transmission weights for automatic transmissions.

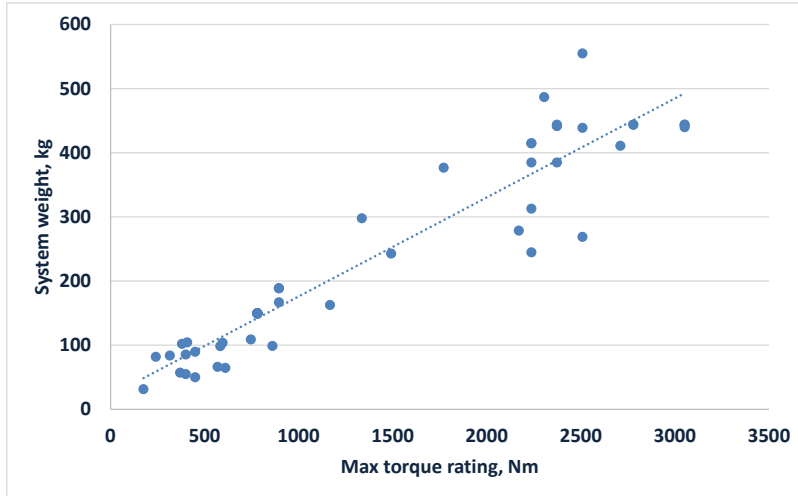


Figure 146. Transmission weight (kg) versus gearbox peak torque (Nm) of automatic transmission

Argonne uses the following equation for the current set of runs.

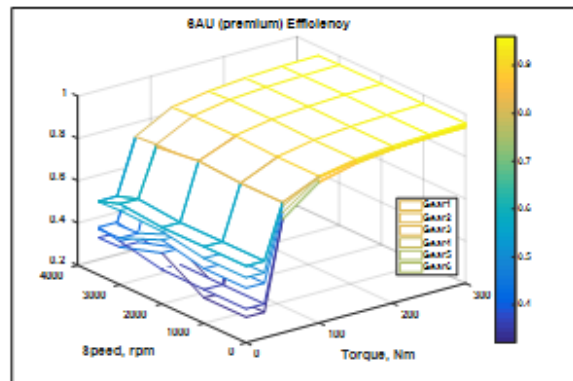
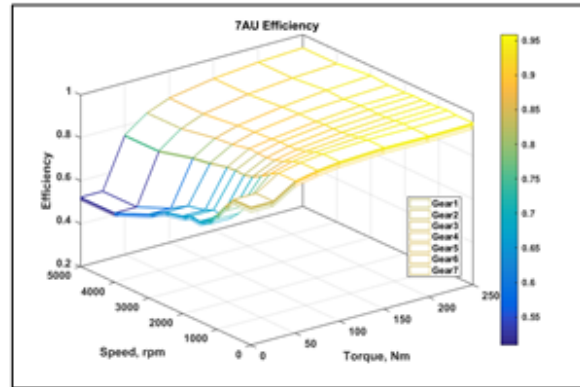
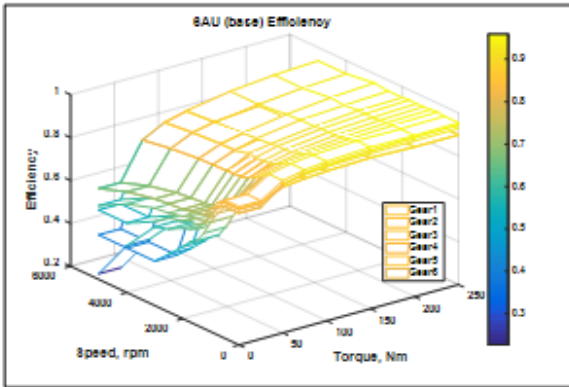
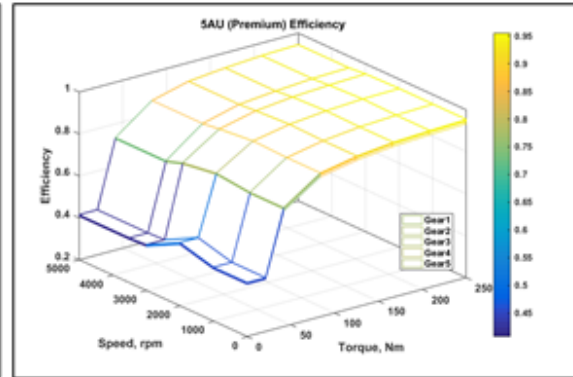
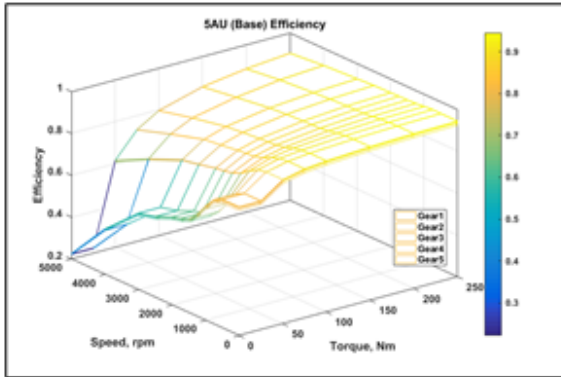
- Automatic gearbox:
Weight (kg) = $0.1544 \times (\text{Gearbox Torque [Nm]}) + 21.612$

Transmission Performance Data

This section details the transmission losses for different ratios for each transmission type considered in the study.

Automatic Transmission

Figure 147 (next two pages) shows the transmission efficiency maps for different numbers of gears for automatic (AU/AU+/AU++) transmissions.



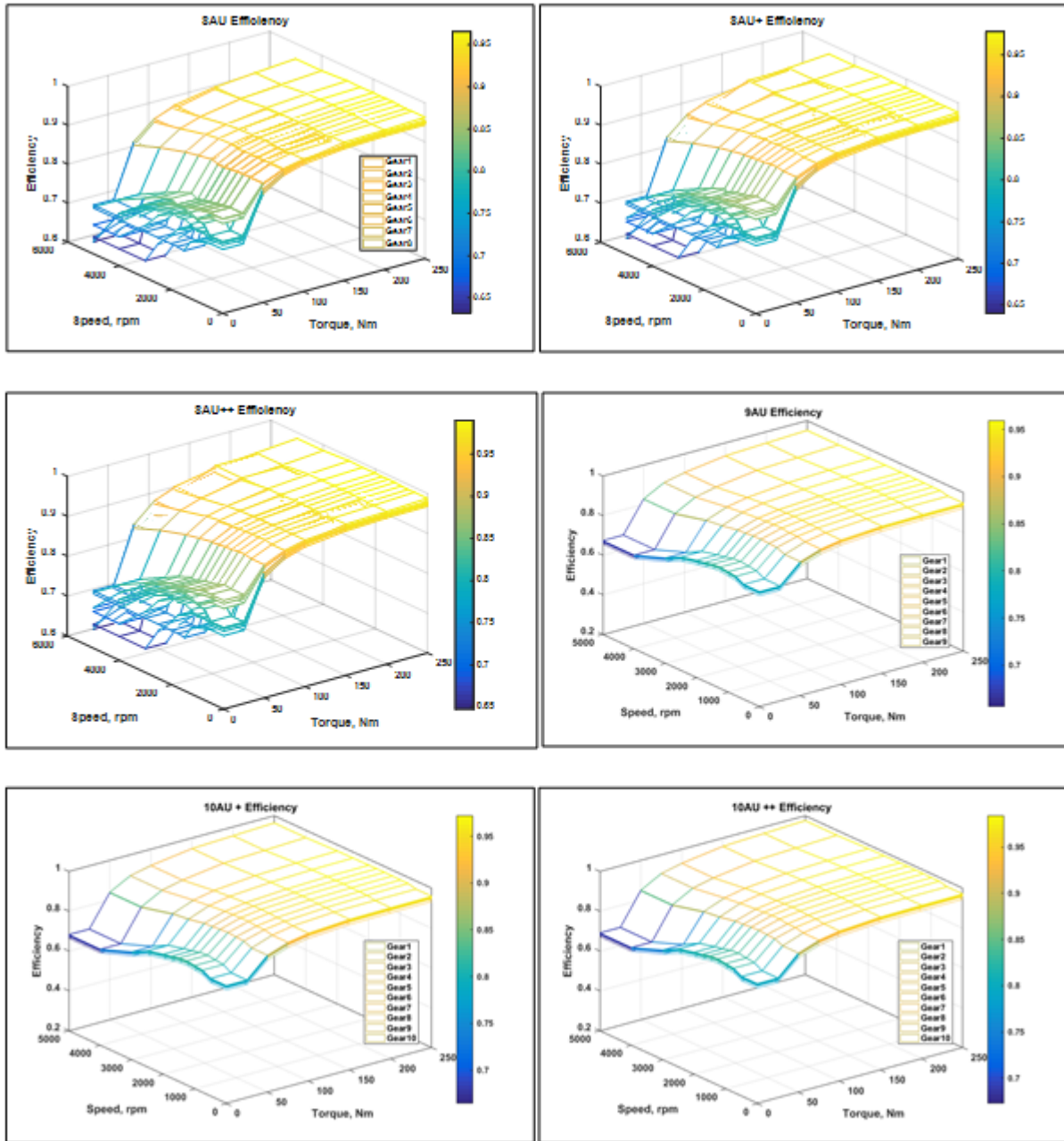


Figure 147. Automatic (AU/AU+/AU++) transmission efficiency maps for different numbers of gears

Dual-Clutch Transmission

Figure 148 shows the transmission efficiency maps for different numbers of gears for DCTs.

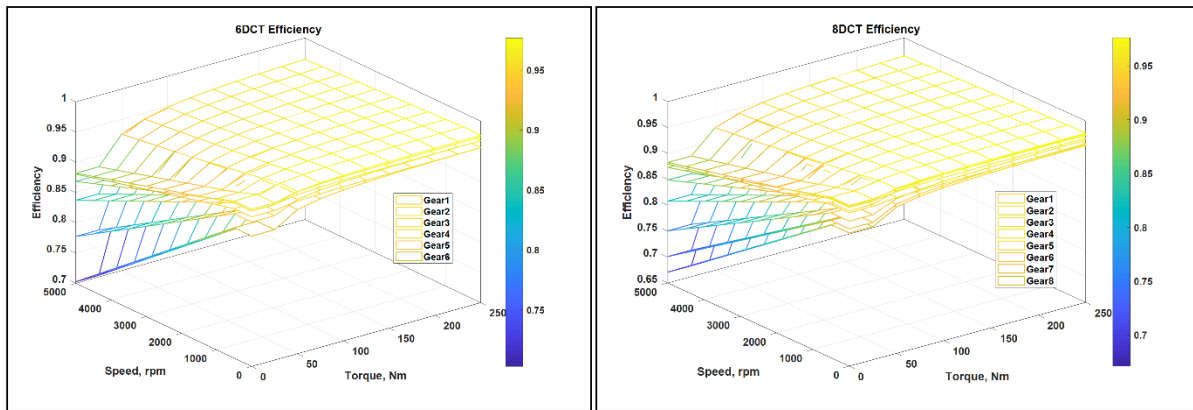


Figure 148. DCT efficiency maps for different numbers of gears

Continuously Variable Transmission

Continuously variable transmission system loss consists of hydraulic and mechanical loss, using experiment-based map data. The hydraulic loss comes from the pump loss in providing the CVT with clamping force when the pump generates line pressure. The mechanical loss is caused by the torque loss from the slip between pulley and belt. The hydraulic loss has a dominant influence on the total CVT system efficiency when the vehicle is driving at low speed, while the mechanical loss is the main part of the CVT system loss at high speed.

CVT Efficiency Maps

Figure 149 shows the oil pump efficiency map and the mechanical efficiency maps for different vehicle speeds for the CVT transmission type.

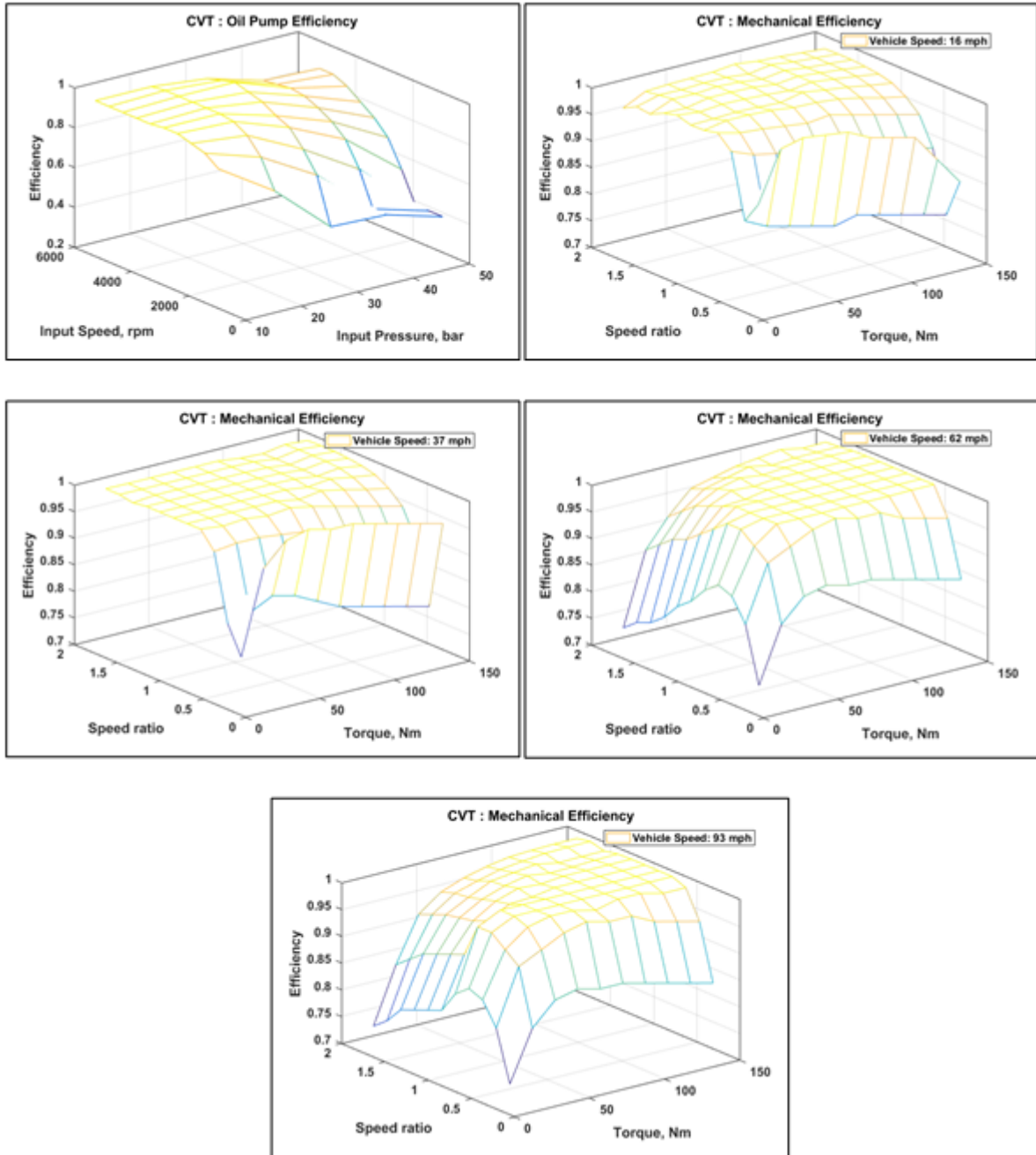


Figure 149. CVT oil pump and mechanical efficiency maps

CVT+ Efficiency Maps

Figure 150 shows the oil pump efficiency map and the mechanical efficiency maps for different vehicle speeds for the CVT+ transmission type.

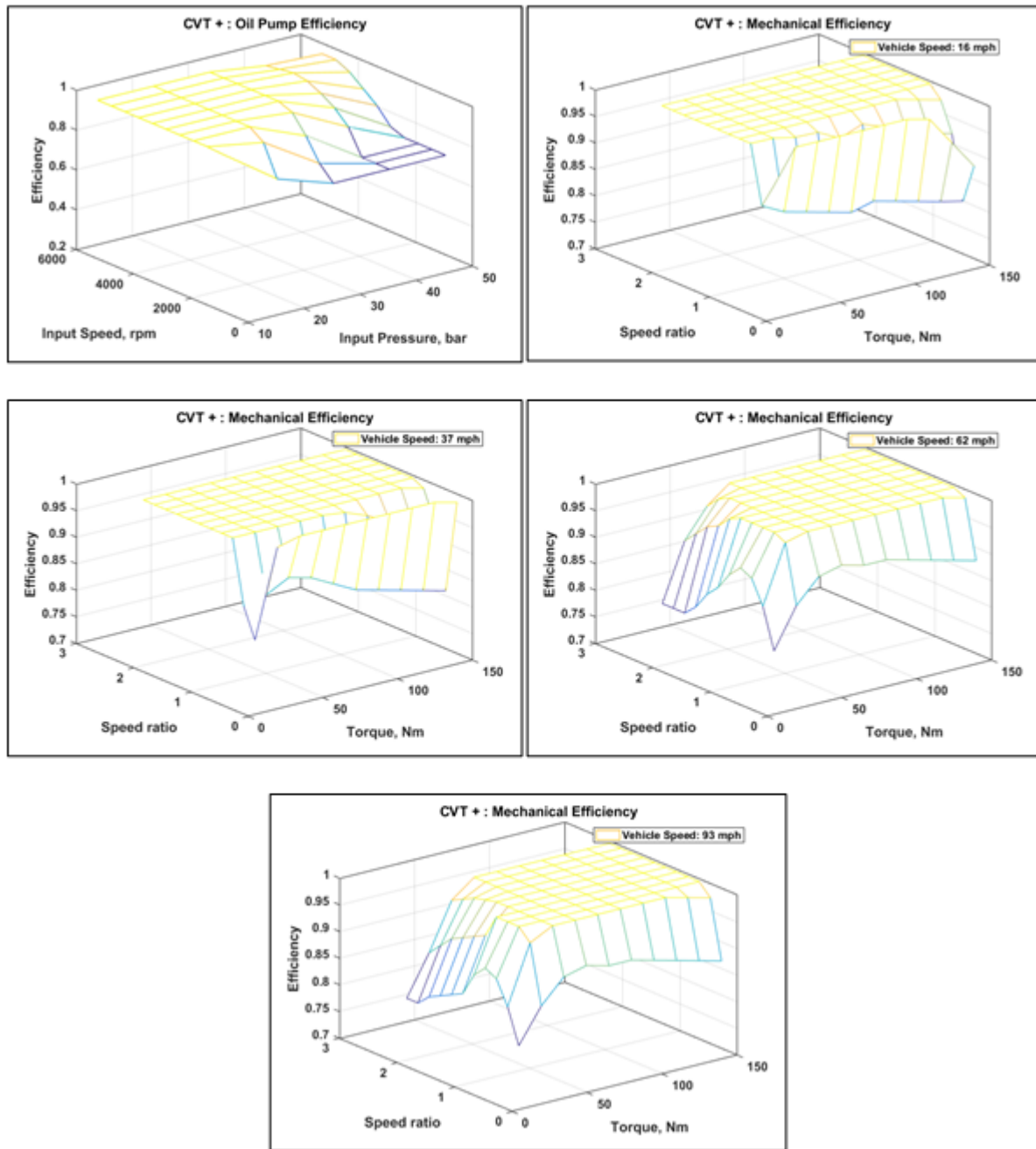


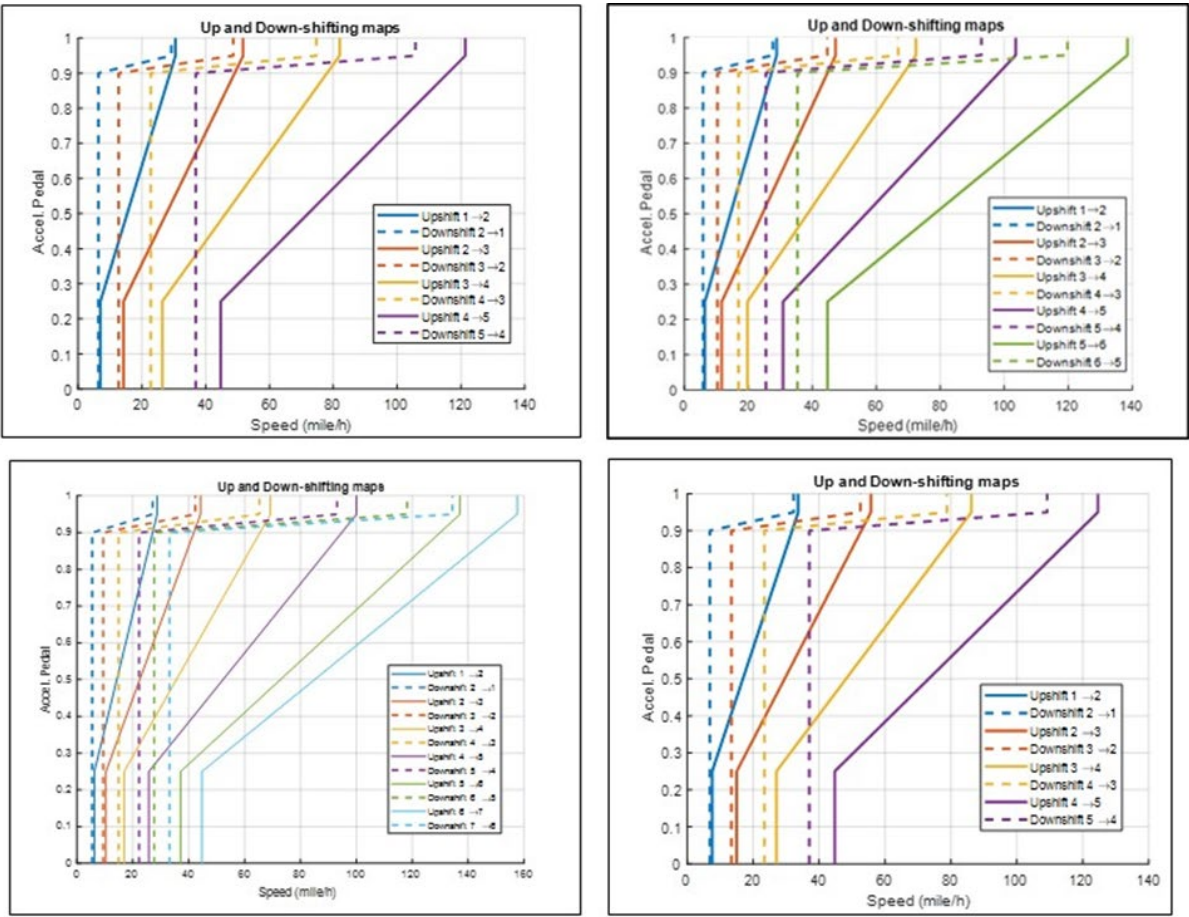
Figure 150. CVT+ oil pump and mechanical efficiency maps

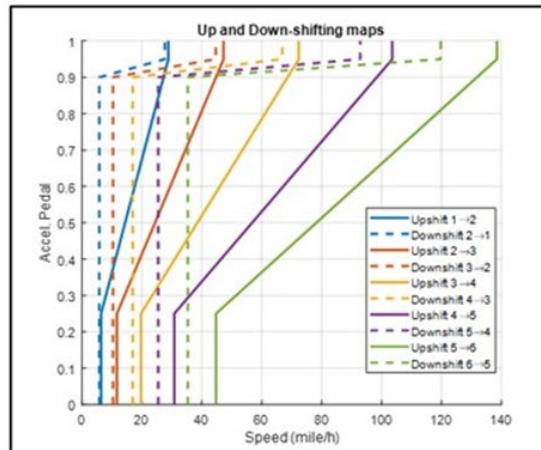
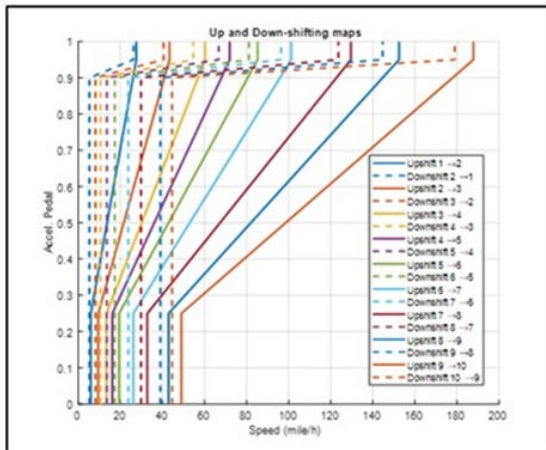
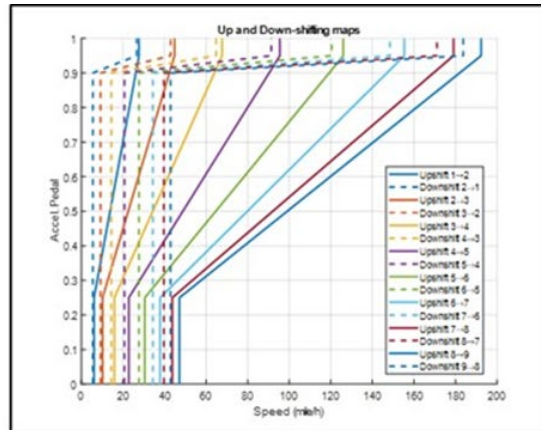
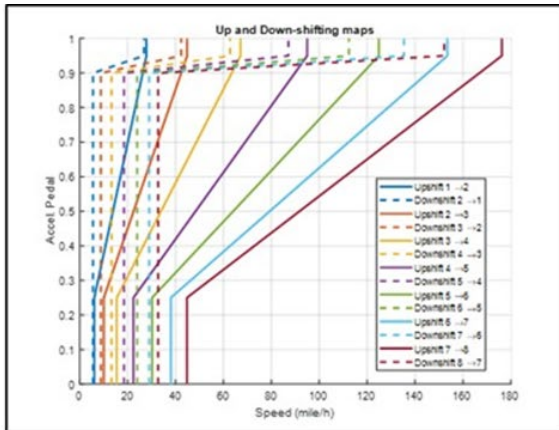
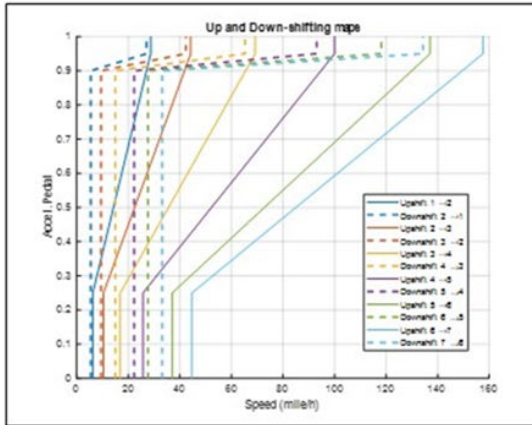
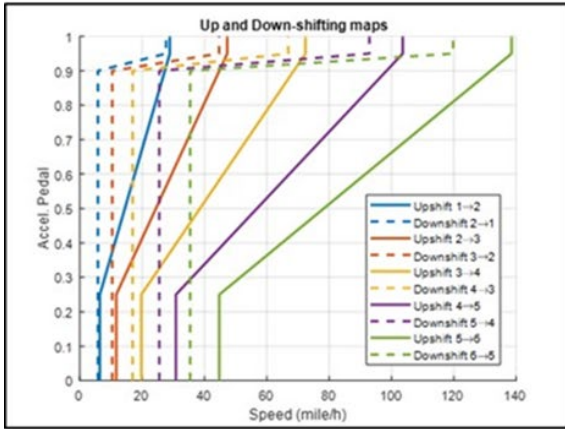
Transmission Gear-Shifting Maps

Light-Duty Vehicles

The development of shifting maps ensures minimum energy consumption across all transmissions while maintaining an acceptable drivability. While plant models with a higher degree of fidelity would most accurately model the impact of each technology on drivability, using such models was not appropriate for the current study, given the complexity and magnitude of the study without individual calibration. The work related to drive quality is focused on the number of shifting events, time between shifting events, engine time response, and engine torque reserve.

Figure 151 shows the upshifting and downshifting maps for the different transmission types and numbers of gears for conventional gasoline powertrains in midsize (base) vehicles.





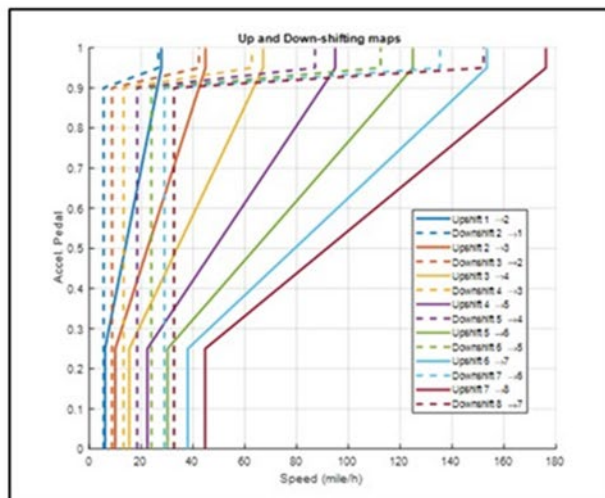
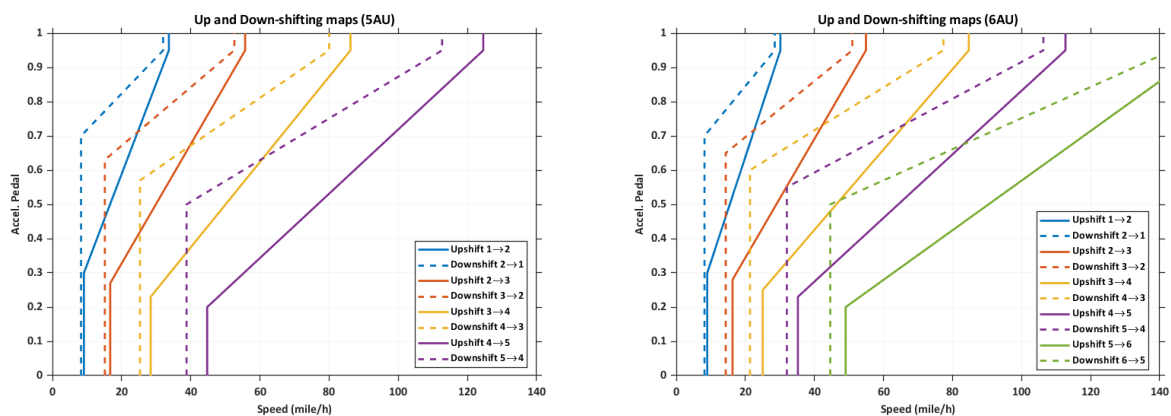


Figure 151. Maps of transmission upshifting (solid lines) and downshifting (dotted lines)

Heavy-Duty Pickups and Vans

Shifting maps have been developed to ensure minimum energy consumption across all transmissions while maintaining an acceptable drivability. While plant models with a higher degree of fidelity would most accurately model the impact of each technology on drivability, using such models was not appropriate for the current study. The work related to drive quality focused on the number of shifting events, time between shifting events, engine time response, and engine torque reserve.

Figure 152 shows the upshifting and downshifting maps for the different transmission types and numbers of gears for conventional gasoline powertrains in HDV (Class 2b van) vehicles.



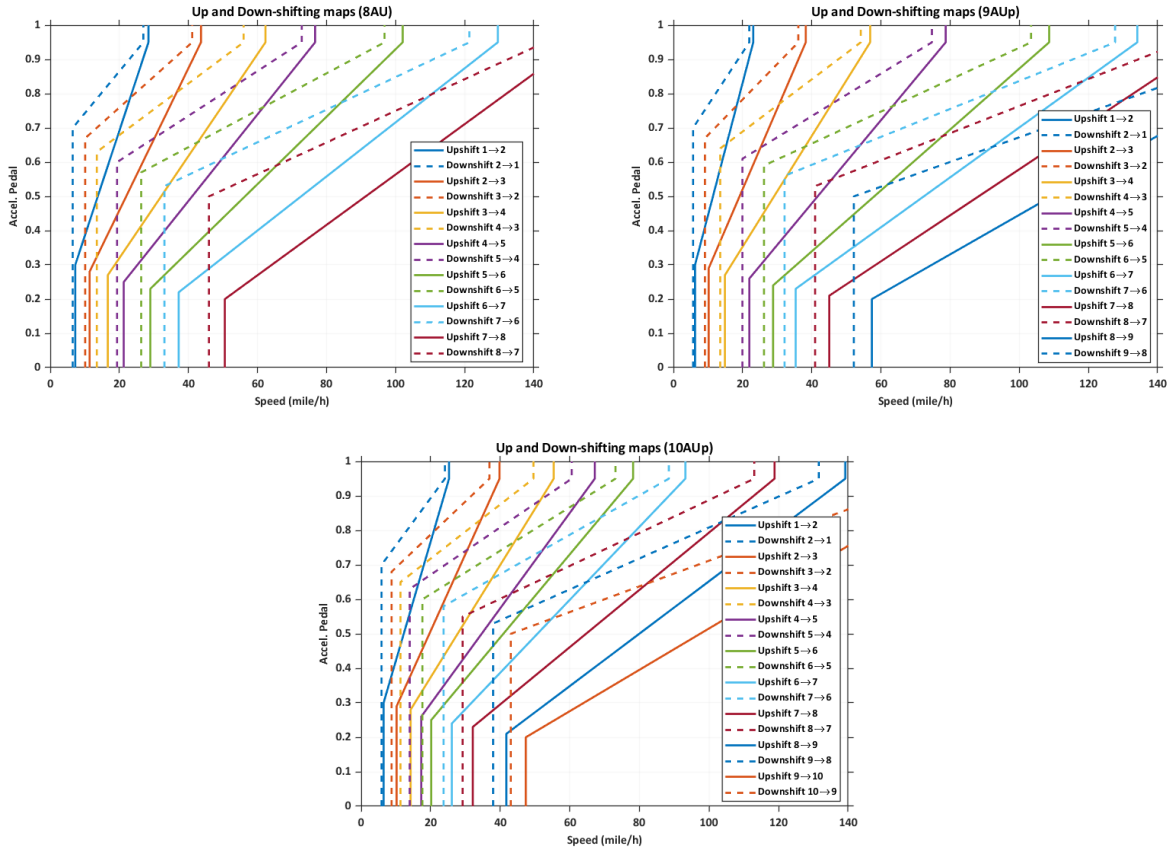


Figure 152. Maps of transmission upshifting (solid lines) and downshifting (dotted lines)

Torque Converter Assumptions

Argonne received torque converter data for different performance and vehicle classes for automatic transmissions. Since there are distinct differences in the data across vehicle classes, Argonne generated an average torque converter characteristic map for each vehicle class. Figure 153 shows the characteristic map for the torque converter data for the different LDV classes.

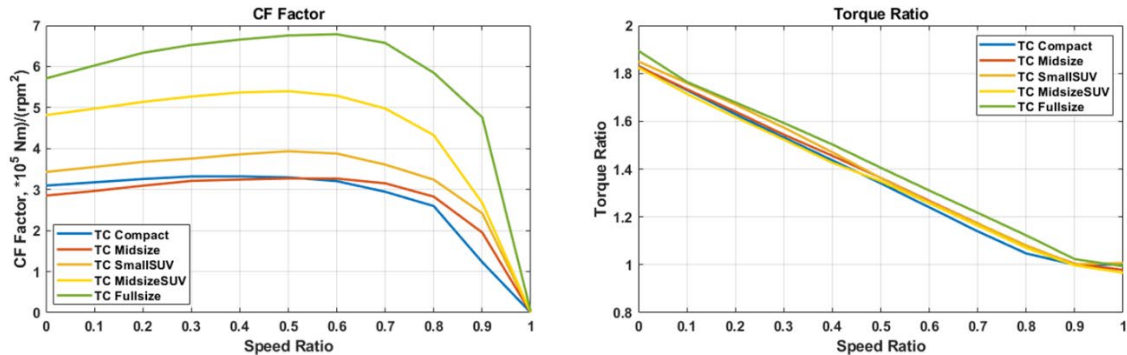


Figure 153. Autonomie torque converter characteristic map (LDV)

Figure 154 shows the characteristic map for the torque converter data for the HDPUV classes.

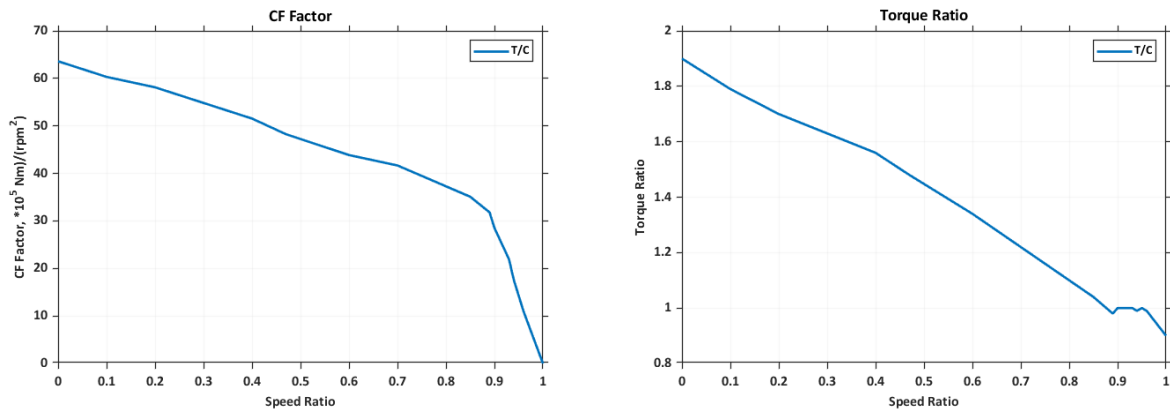


Figure 154. Autonomie torque converter characteristic map (HDPUV)

The relationships of the different factors are as follows.

$$\text{Speed ratio} = \frac{\text{output speed}}{\text{input speed}}$$

$$\text{Torque ratio} = \frac{\text{output torque}}{\text{input torque}}$$

$$\text{CF factor} = \frac{\text{input torque}}{\text{input speed}}$$

Engine Technologies

Light-Duty Vehicles

Engine Technology Definitions

Table 64 shows the different engine technologies studied, along with the associated simulation names and the reference peak power. The engine performance values were provided by IAV Automotive Engineering, Inc., Southwest Research Institute (SwRI), and eng26 values derived from Argonne AMTL test data.

Table 64. Engine technologies with reference peak power and reference displacement

Engine Simulation Name	Engine Technology	Engine Reference Peak Power (kW)	Engine Reference Displacement (L)	Engine Turbo Max Boost Level
eng01	Dual overhead camshaft valvetrain (DOHC) VVT	108	2.0	
eng02	DOHC VVT+VVL	108	2.0	
eng03	DOHC VVT+VVL+GDI	113	2.0	
eng04	DOHC VVT+VVL+GDI+DEAC	113	2.0	
eng5b	SOHC VVT (level 1 reduced friction)	109	2.0	

Engine Simulation Name	Engine Technology	Engine Reference Peak Power (kW)	Engine Reference Displacement (L)	Engine Turbo Max Boost Level
eng6a	SOHC VVT+VVL (level 1 reduced friction)	109	2.0	
eng7a	SOHC VVT+VVL+GDI (level 1 reduced friction)	114	2.0	
eng8a	SOHC VVT+VVL+GDI+DEAC (level 1 reduced friction)	114	2.0	
eng12	DOHC Turbo 1.6l 18bar	132	1.6	1.53
eng13	DOHC Turbo 1.2l 24bar	133	1.2	2.04
eng14	DOHC Turbo 1.2l 24bar + cooled EGR	133	1.2	2.04
eng17	Diesel	140	2.2	
eng18	DOHC VVT + SGDI	113	2.0	
eng19	DOHC VVT + DEAC	113	2.0	
eng20	DOHC VVT + VVL + DEAC	113	2.0	
eng21	DOHC VVT + SGDI + DEAC	113	2.0	
eng26	Atkinson – PSHEV and PSPHEV only	73	1.8	
eng12Deac	DOHC Turbo 1.6l 18bar + DEAC	132	1.6	1.53
eng22b	Atkinson 2.5L VVT PFI CR14	132	2.5	
eng23b	2.0 Miller VTG + VVT + VVL + DI + cEGR + CR12	139	2.0	
eng23c	Miller eCharger + VVT + DI + eEGR + CR12	139	2.0	
eng26a	VCR VVT + DI + Turbo + cEGR + CR9/12	180	2.0	2.09
eng32	2.5L NA, Atkinson DOHC CR13 DI	132	2.5	
eng33	2.5L NA Atkinson DOHC CR13 DI LP-EGR	132	2.5	
eng34	2.5L NA Atkinson DOHC CR13 DI + Deac	132	2.5	
eng36	1.6L Turbo VVT DOHC DI CR10.5	144	1.6	1.67
eng37	1.6L Turbo VVT DOHC DI CR10.5 LP-EGR	144	1.6	1.67
eng38	1.6L Turbo VVT DOHC DI CR10.5 + Deac	113	1.6	1.67
eng39	1.6L Turbo VVT DOHC DI CR10.5 + ADEAC	110	1.6	1.67
eng40	2.0L NA VVT DOHC DI CR11 + ADEAC	110	2.0	
eng45	3.0L Duramax Diesel	213	3.0	
eng46	3.0L Duramax Diesel + DEAC	213	3.0	

Engine Efficiency Maps

IAV Automotive Engineering modeled gasoline engine maps in GT-POWER and supplied those maps to Argonne for use in Autonomie. SwRI provided the diesel engine to be used in the LDV simulations.

IAV also provided wide-open-throttle engine performance values and BSFC maps for future engine concepts. To quantify the benefits of individual technologies, each incremental technology was modeled using GT-POWER and validated with existing dynamometer measurements for several engines. GT-POWER is used to predict engine performance quantities such as power, torque, airflow, volumetric efficiency, fuel consumption, turbocharger performance, and matching and pumping losses. The models were trained over the entire engine operating range and have predictive combustion capability. This is essential, since the BSFC prediction needs to be accurate, while the engine setup is subject to change.

Relevant engine geometries and parameters were measured and modeled with friction/flow losses, heat transfer, and other parameters and calibrated to match measurements. Displacement-normalized mechanical friction was modeled as a function of engine speed and specific load. A combustion model was trained to predict fuel heat release rates in response to physical effects such as cylinder geometries, pressure, temperature, turbulence, residual gas concentration, and other parameters. A knock correlation based on in-cylinder conditions and fuel octane rating predicts whether knock will occur and at what intensity. A combustion stability threshold prediction was trained using covariance of indicated mean effective pressure data and is used for understanding exhaust gas recirculation tolerance, especially at low loads. Load controllers were developed for fuel/air path actuators and targeting controllers to drive optimal and knock-limited combustion phasing, just as in a physical engine. Careful modeling practice provided confidence that calibrations will scale and predict reasonable and reliable results as parameters are changed throughout the various technology concept studies.

IAV provided 27 engine maps in total, for 18 NA gasoline engines and 9 turbocharged gasoline engines. The diesel engine was provided by SwRI based on the test benchmarking of a General Motors Duramax 3.0-liter diesel engine. Finally, one Atkinson engine map, generated using Argonne test data, was used for electrified vehicles with power-split architecture. This gave us a total of 19 engine maps for this study.

For all IAV engines, the engine speed, BMEP, brake torque, fuel flow rate, pumping mean effective pressure (PMEP), and FMEP data were provided to Argonne in a standardized format and ranged from 1,000 rpm to the maximum engine speed and from 0 bar BMEP to full load to provide a full operation map. Fuel flow rates at zero output torque were provided separately and ranged from 650 rpm (defined idle) to 6,000 rpm.

The following fuel specifications are used by IAV when modeling the engines in GT-POWER.

- Gasoline lower heating value (LHV) = 41.58 MJ/kg
- $(R+M)/2 = 87$
- Fuel density = 0.7464 kg/L
- Ambient temperature, $T_{amb} = 25^{\circ} \text{C}$
- Ambient pressure, $P_{amb} = 990 \text{ mbar}$

Table 65 lists the characteristics of fuel used by IAV when modeling the engines in GT-POWER.

Table 65. Characteristics of Fuel Used for Modeling Engines

Type of Fluid	Composition	Molecular Formula			Density	LHV
		C	H	O		
	Mass fraction	C	H	O	kg/m ³	MJ/kg
Hydrocarbon	0.903712493	8	14.851265	0	741.9	43.19
Ethanol	0.094801493	2	6	1	785	26.9
Water	0.001486014	0	2	1	1002.5	0

Engine (eng01) 2L_pfi_dohc_vvt_engine1_baseline

Engine 1 is an NA PFI 2.0-liter gasoline engine from a MY 2013 vehicle with variable valve timing (VVT) engine technology. A BSFC engine map was generated from dynamometer testing of the existing engine, which then served as the baseline BSFC map for all simulated NA engines (Engines 1–8a, 18–21). The engine calibrations are fully optimized for best BSFC and maximum torque. Figure 155 shows the BSFC map for engine 1.

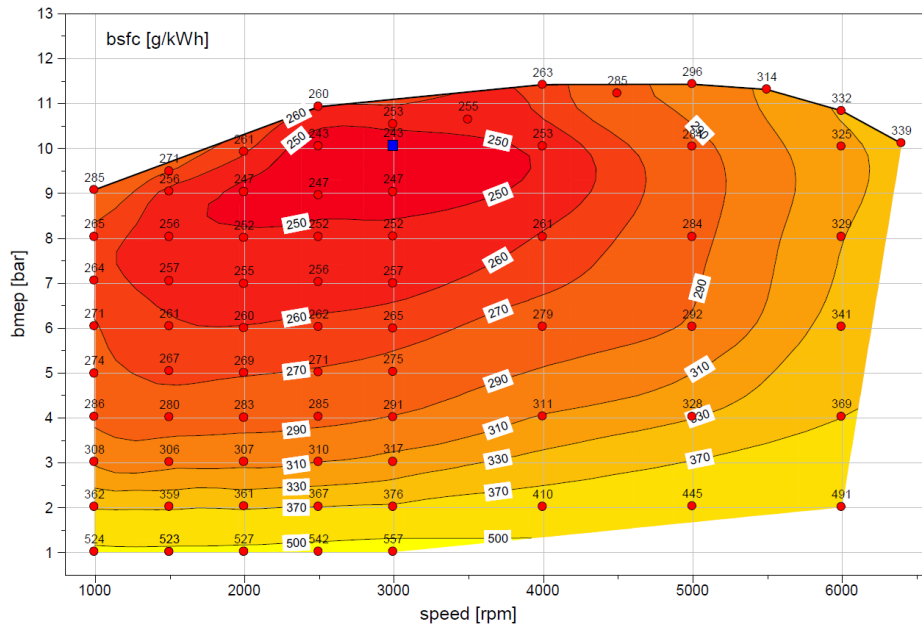


Figure 155. Engine 1 BSFC map

Engine (eng02) 2L_pfi_dohc_vvt_vvl_engine2

For engine 2, a VVL system was added to the intake valves on engine 1 with optimized valve lift and timing. The additional benefit includes reduced pumping work at low torques and more torque at low speeds from reduced intake duration. Figure 156 shows the BSFC map for engine 2.

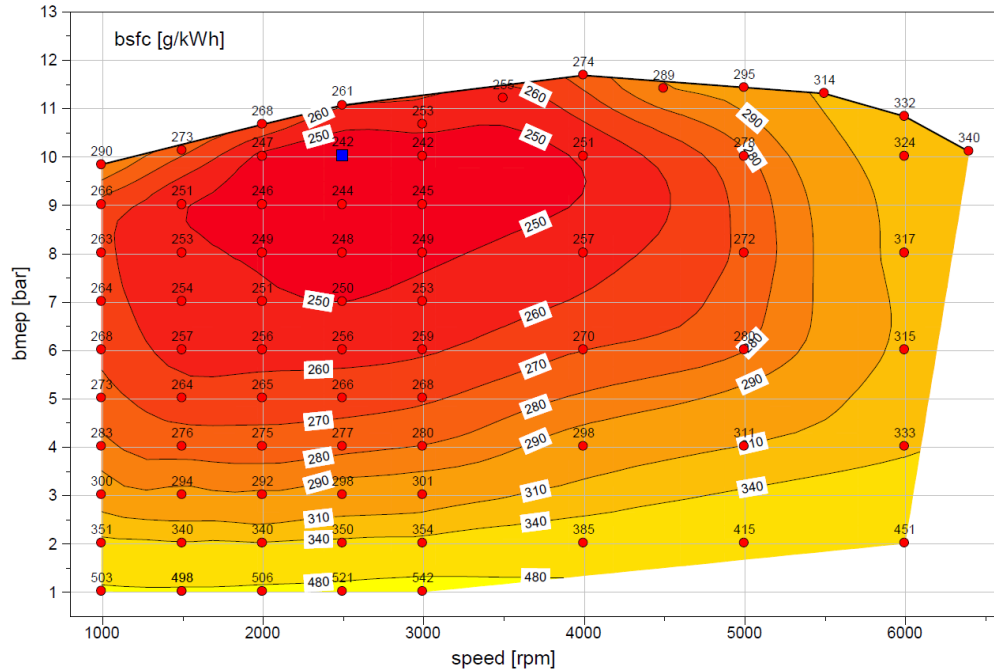


Figure 156. Engine 2 BSFC map

Engine (eng03) 2L_di_engine3

For engine 3, the PFI from engine 2 was converted to direct injection, and the compression ratio was raised from 10.2 to 11.0, with injection timing optimized. The benefit of this technology is that DI provides greater knock tolerance, allowing higher compression ratios and increased efficiency over the entire map. Figure 157 shows the BSFC map for engine 3.

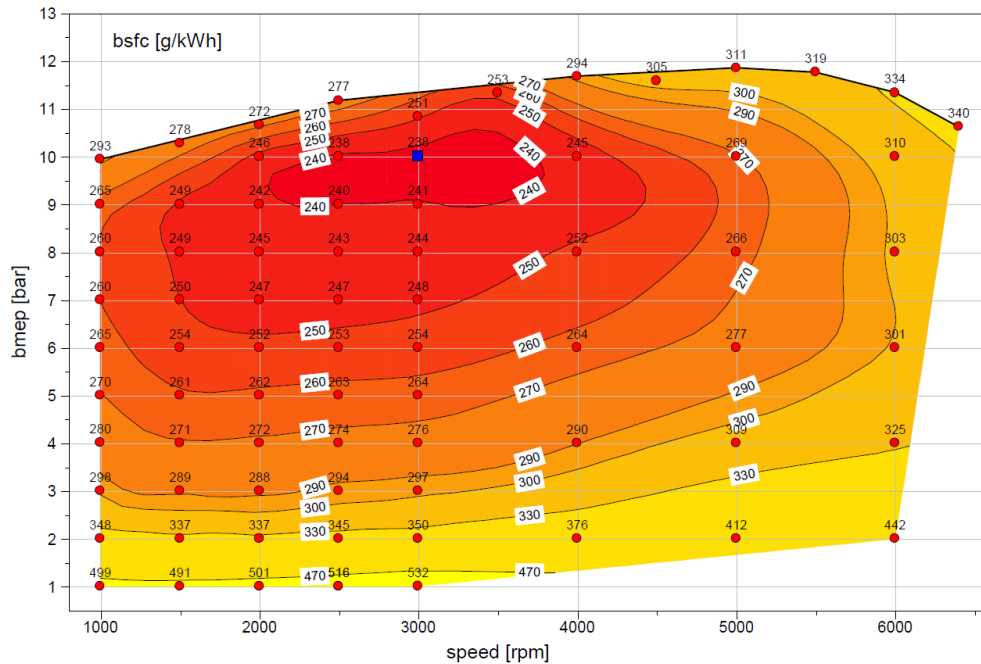


Figure 157. Engine 3 BSFC map

Engine (eng04) 2L_cylinder_deac_engine4

For engine 4, cylinder deactivation capabilities were added to engine 3. The engine fires only two cylinders at low loads and speeds below 3,000 rpm by deactivating the valves on two cylinders. The benefit of this technology is that the effective load doubles on two cylinders, providing less pumping work and higher efficiency. Figure 158 shows the BSFC map for engine 4.

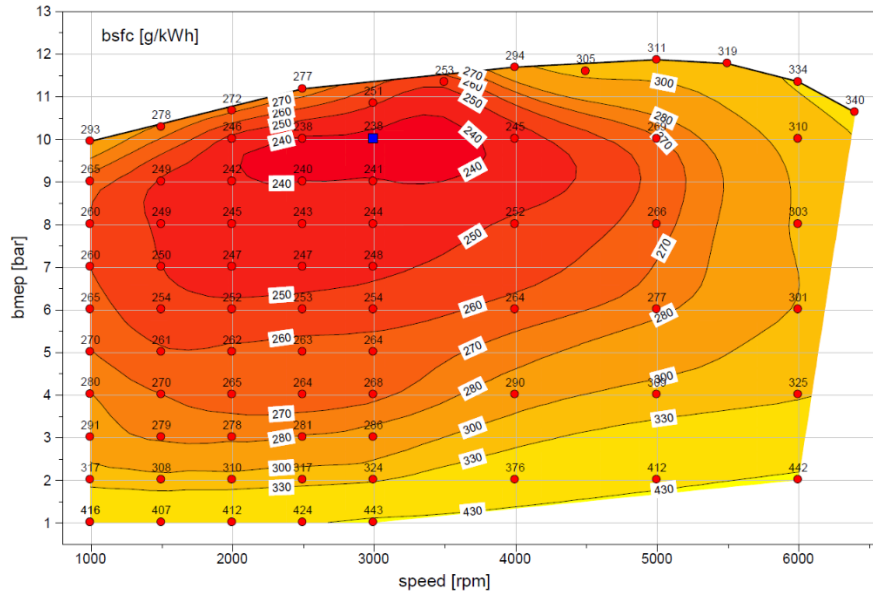


Figure 158. Engine 4 BSFC map

Engine (eng5b) 2L_engine5b_SOHC_low_friction

For engine 5b, the valve timing was optimized for a fixed-overlap camshaft with a standard friction model from DOHC concepts. The engine FMEP was reduced by 0.1 bar over the entire operation range to evaluate the friction benefit from a single overhead camshaft. The benefit of this technology is reduced friction, which improves efficiency at all load points and raises the full-load line. Figure 159 shows the BSFC map for engine 5b.

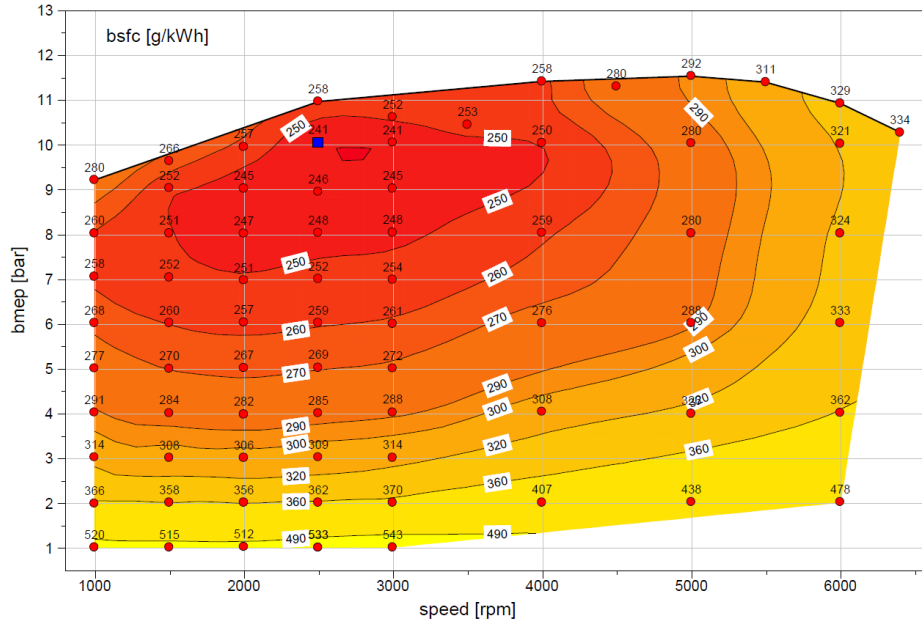


Figure 159. Engine 5b BSFC map

Engine (eng6a) 2L_engine6a_VVL_low_friction

For engine 6a, the engine 2 FMEP was reduced by 0.1 bar over the entire operation range. The benefit of this change is similar to that for engine 5b, with improved efficiency at all load points and the full-load line raised over that of engine 2. Figure 160 shows the BSFC map for engine 6a.

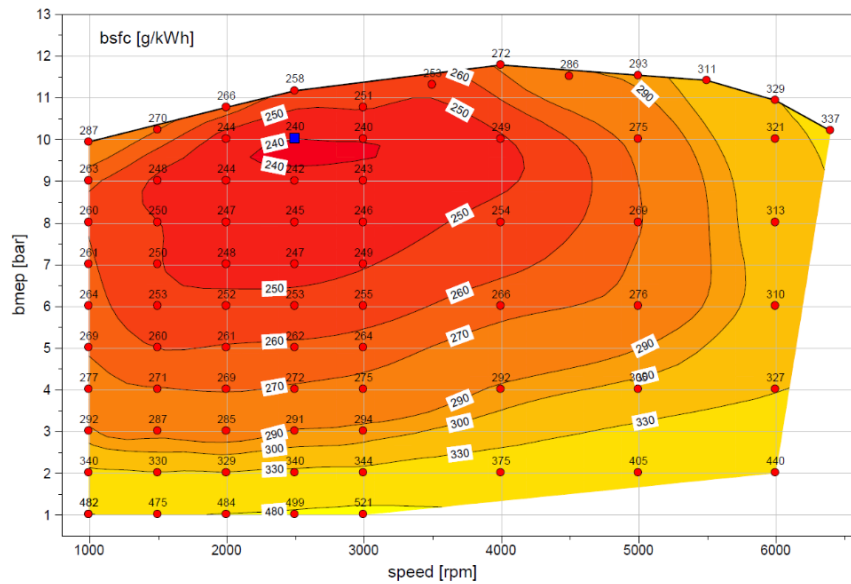


Figure 160. Engine 6a BSFC map

Engine (eng7a) 2L_engine7a_DI_low_friction

For engine 7a, the engine 3 FMEP was reduced by 0.1 bar over the entire operation range. The reduced friction improves efficiency at all load points and raises the full-load line. Figure 161 shows the BSFC map for engine 7a.

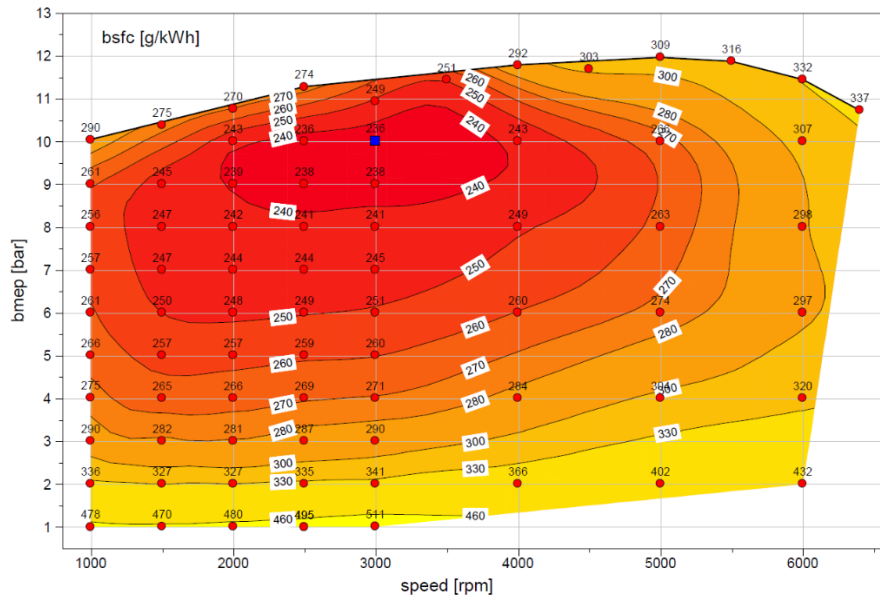


Figure 161. Engine 7a BSFC map

Engine (eng8a) 2L_engine8a_cylinder_deac_low_friction

For engine 8a, the engine 4 FMEP was reduced by 0.1 bar over the entire operation range. The reduced friction improves efficiency at all loads and raises the full-load line. Figure 162 shows the BSFC map for engine 8a.

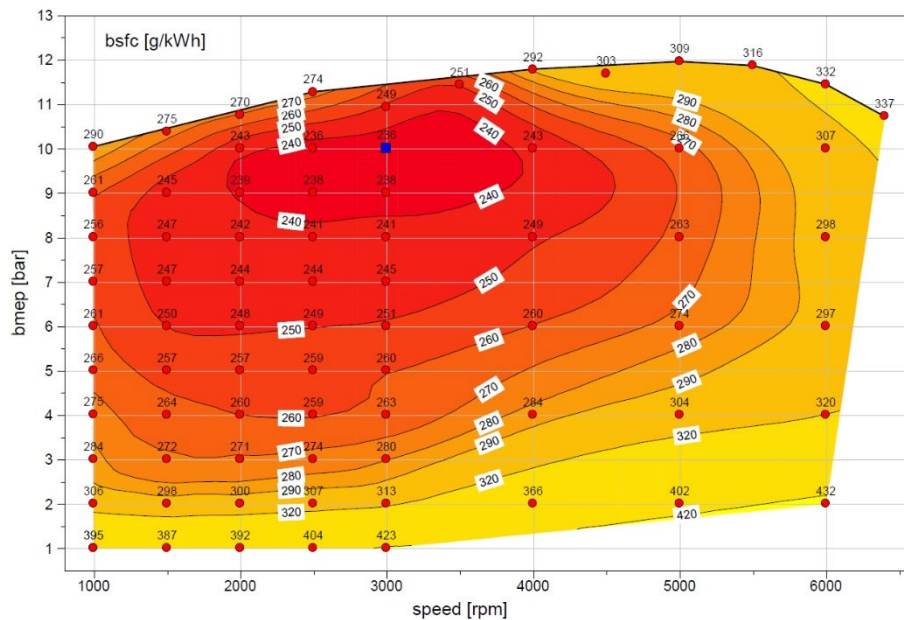


Figure 162. Engine 8a BSFC map

Engine (eng12) 1pt6L_engine12_turbo_DI_DOHC_VVT_VVL

Engine 12 is a 1.6-liter, 4-cylinder, turbocharged gasoline engine with DI, DOHC, dual-cam VVT, and intake variable valve lift. The calibrations for the engine are fully optimized for the best BSFC. Figure 163 shows the BSFC map for engine 12.

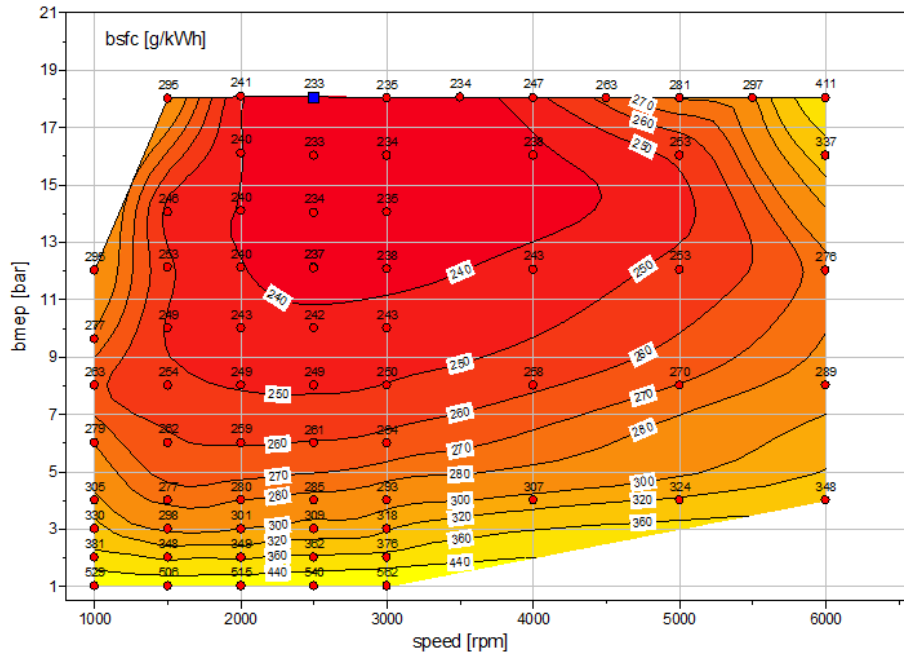


Figure 163. Engine 12 BSFC map

Engine (eng13) 1pt2L_engine13_turbo_DI_DOHC_VVT_VVL

For engine 13, engine 12 was downsized to 1.2-liter. The turbocharger maps were scaled to improve torque at low engine speeds. The downsizing allows for operation at a higher engine load point (increased efficiency) at a given vehicle torque demand. Figure 164 shows the BSFC map for engine 13.

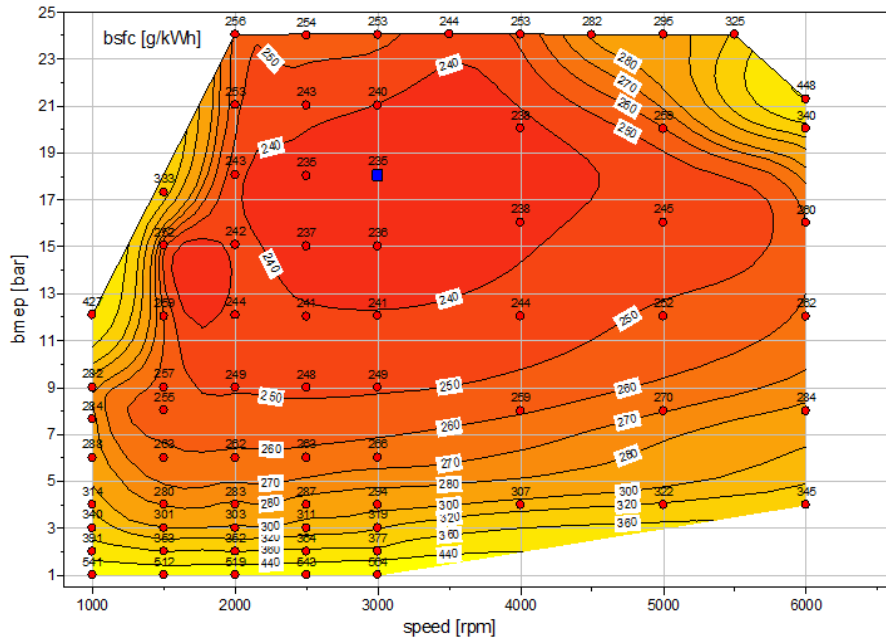


Figure 164. Engine 13 BSFC map

Engine (eng14) 1pt2L_engine14_turbo_external_cool_EGR

For engine 14, high-pressure cooled exhaust gas recirculation was added to engine 13 (Bonkoski, et al., 2014). The cooled EGR target set points were further optimized. There are multiple benefits from the application of cooled EGR.

- The cooled burned gas lowers the in-cylinder temperatures, reducing the knock tendency and thus improving combustion phasing.
- Reduced in-cylinder temperatures lead to reduced exhaust temperatures and therefore a reduced need for enrichment to protect exhaust components.

Figure 165 shows the BSFC map for engine 14.

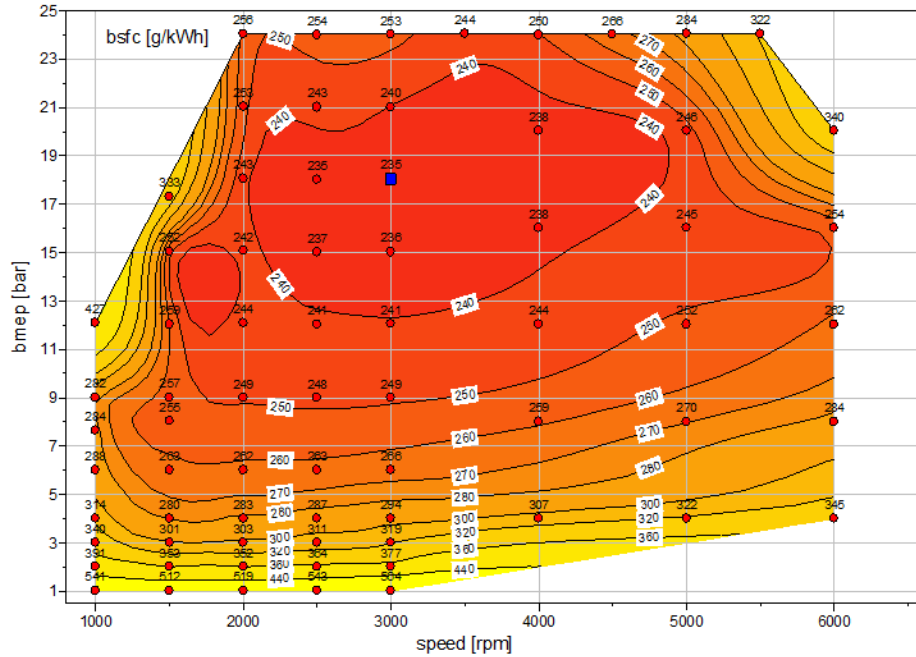


Figure 165. Engine 14 BSFC map

Engine (eng18) 2L_di_dohc_vvt_engine18

Engine 18 is a 2.0-liter, 4-cylinder, naturally aspirated gasoline engine with DOHC, dual VVT, and DI. The engine was developed from engine 1, with increased knock resistance and volumetric efficiency due to in-cylinder vaporization of the fuel. Open-valve injection and homogeneous operation were assumed. Figure 166 shows the BSFC map for engine 18.

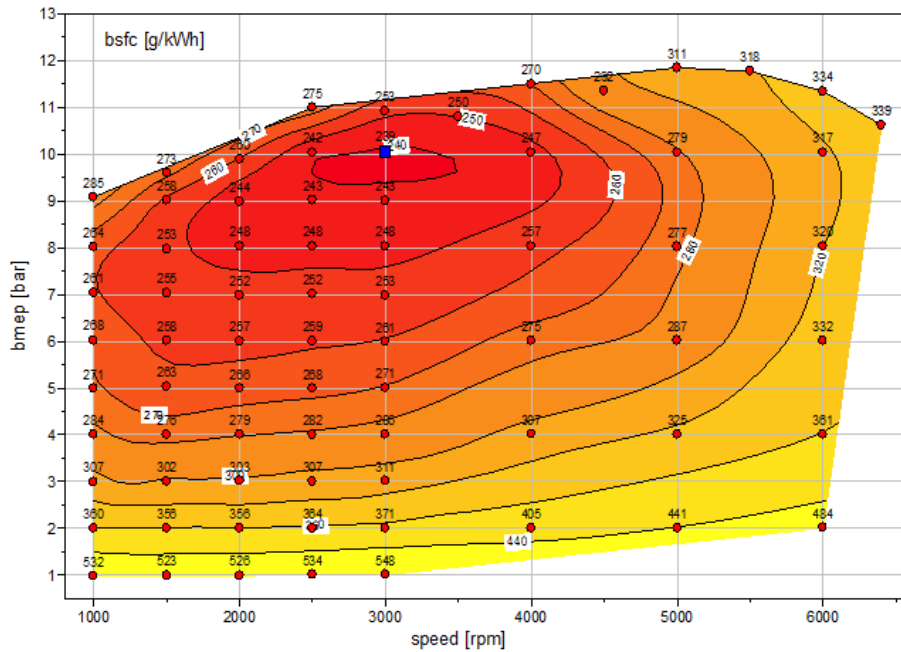


Figure 166. Engine 18 BSFC map

Engine (eng19) 2L_cylinder_deac_engine19

Engine 19 is a 2.0-liter, 4-cylinder, naturally aspirated PFI gasoline engine with DOHC, dual VVT, and cylinder deactivation (DEAC) capability. The engine was developed from engine 1, with the VVT timing map of active cylinders based on the cylinder IMEP of engine 1. Figure 167 shows the BSFC map for engine 19.

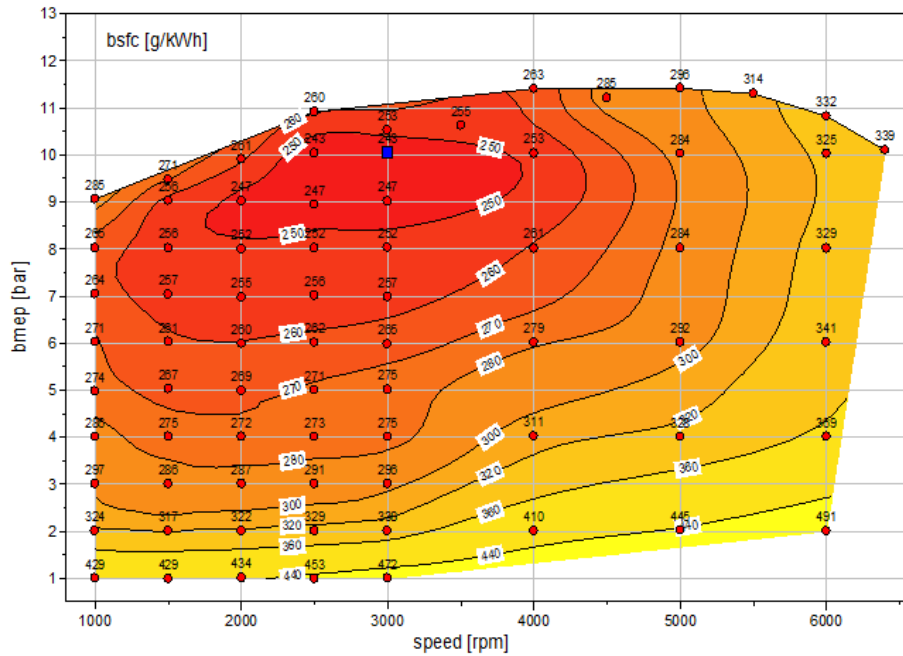


Figure 167. Engine 19 BSFC map

Engine (eng20) 2L_cylinder_deac_engine20

Engine 20 is a 2.0-liter, 4-cylinder, naturally aspirated PFI engine with DOHC, dual VVT, intake VVL, and DEAC abilities. The engine was developed from engine 2. The VVT maps and intake valve map lift of active cylinders are based on the cylinder IMEP of engine 2 (IAV Automotive Engineering, Inc., 2016). Figure 168 shows the BSFC map for engine 20.

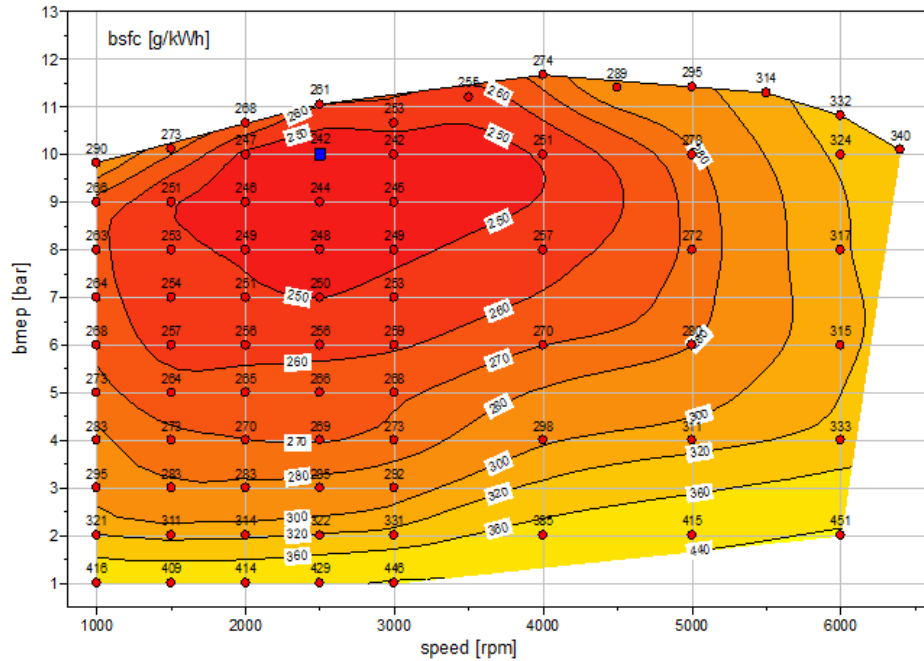


Figure 168. Engine 20 BSFC map

Engine (eng21) 2L_cylinder_deac_engine21

Engine 21 is a 2.0-liter, 4-cylinder, naturally aspirated engine with DOHC, dual-cam VVT, DI and DEAC abilities. The engine was developed from engine 18. The VVT timing map of active cylinders is based on the cylinder IMEP of engine 18 (IAV Automotive Engineering, Inc., 2016). Figure 169 shows the BSFC map for engine 21.

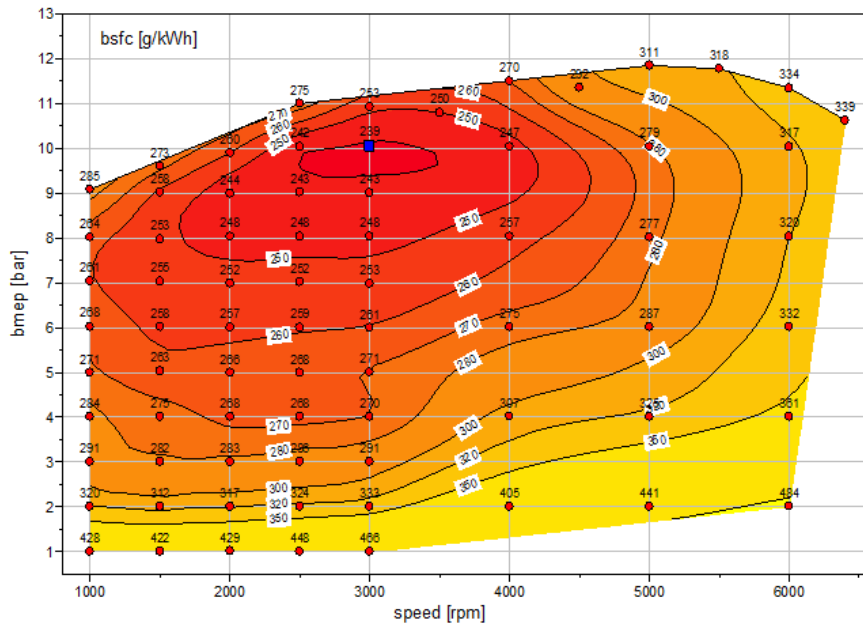


Figure 169. Engine 21 BSFC map

Engine (eng23b) 2L_engine23b_VVT_VVL_DI_cEGR_CR12

Engine 23b is a 2.0-liter, 4-cylinder, turbocharged DI engine with DOHC, dual-cam VVT, intake VVL, and cooled EGR capabilities. The engine has a compression ratio of 12. Figure 170 shows the BSFC map for engine 23b.

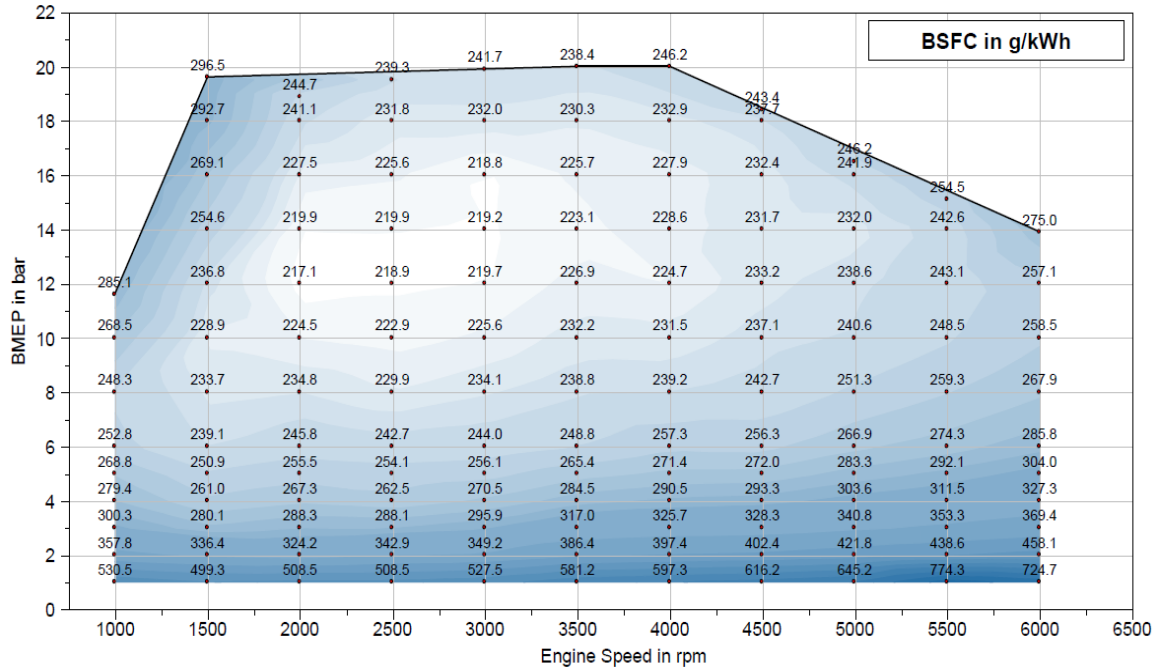


Figure 170. Engine 23b BSFC map

Engine (eng23c) 2L_engine23c_Miller_eCharger_VVT_DI_eEGR_CR12

Engine 23c is a 2.0-liter, 4-cylinder, turbocharged DI engine with DOHC, dual-cam VVT, and cooled EGR capabilities. The engine has a compression ratio of 12. The turbocharging technology has an e-charger to enhance e-boost. Figure 171 shows the engine BSFC map for engine 23c.

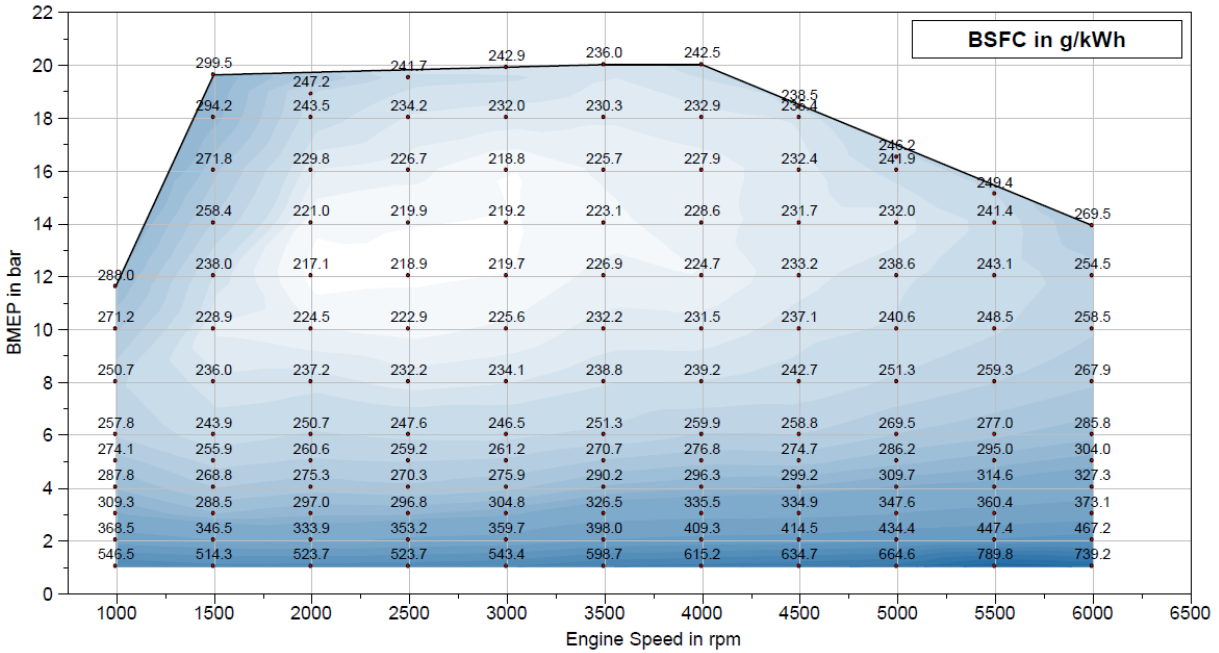


Figure 171. Engine 23c BSFC map

Engine (eng26) Atkinson

Engine 26 is a 1.8-liter, 4-cylinder, 73kW full Atkinson engine. The data for the engine comes from MY 2010 Toyota Prius AMTL test data, but for this analysis the thermal efficiency was scaled up to match the MY 2017 Toyota Prius. Figure 172 shows the BSFC map for engine 26.

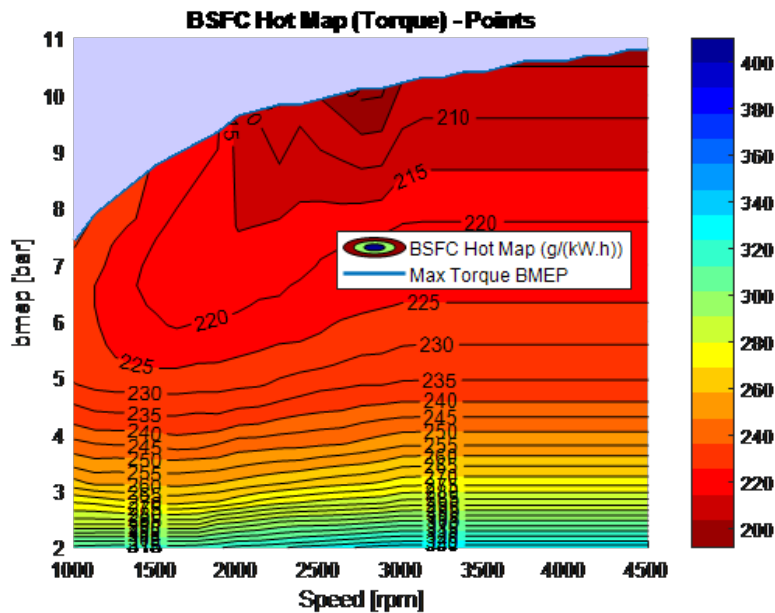


Figure 172. Engine 26 BSFC map

Engine (eng26a) 2L_engine26a_VCR_VVT_DI_Turbo_cEGR_CR9/12

Engine 26a is a 2.0-liter, 4-cylinder, turbocharged DI engine with DOHC, dual-cam VVT, and cooled EGR capabilities. The engine has a variable compression ratio of 9:12. Figure 173 shows the engine BSFC map for engine 26a, which shows the fuel map resulting from merging the two separate maps of individual compression ratios.

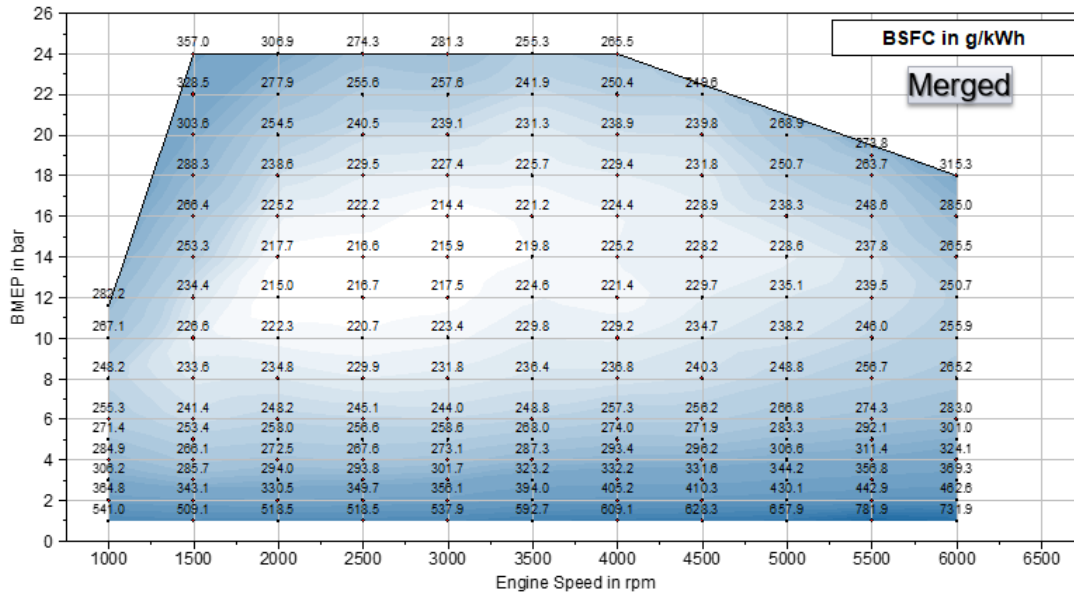


Figure 173. Engine 26a BSFC map

Engine (eng32) 2.5L_NA_Atkinson_DOHC_CR13_DI

Engine 32 is a 2.5-liter, 4-cylinder, NA DI Atkinson engine with DOHC and VVT. The engine has a compression ratio of 13. Figure 174 shows the engine BSFC map for engine 32.

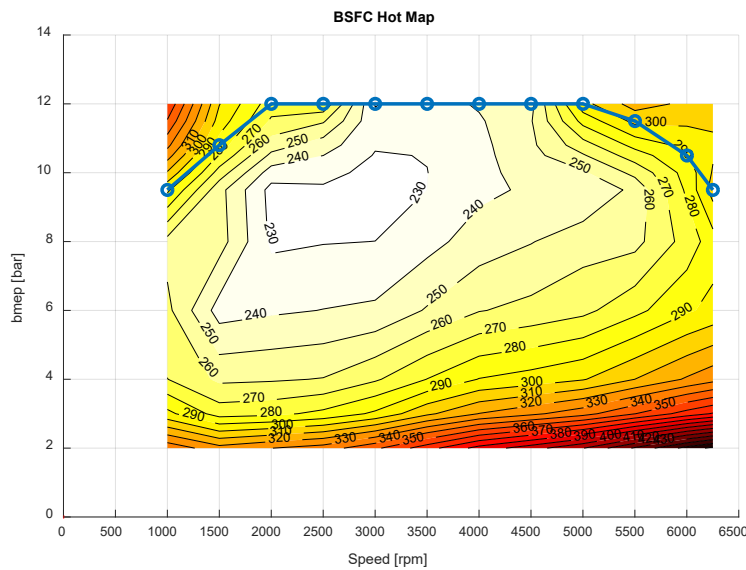


Figure 174. Engine 32 BSFC map

Engine (eng33) 2.5L_NA_Atkinson_DOHC_CR13_DI_With_EGR

Engine 33 is a 2.5-liter, 4-cylinder, NA DI Atkinson engine with DOHC and VVT. The engine has a compression ratio of 13 along with EGR capabilities. Figure 175 shows the engine BSFC map for engine 33.

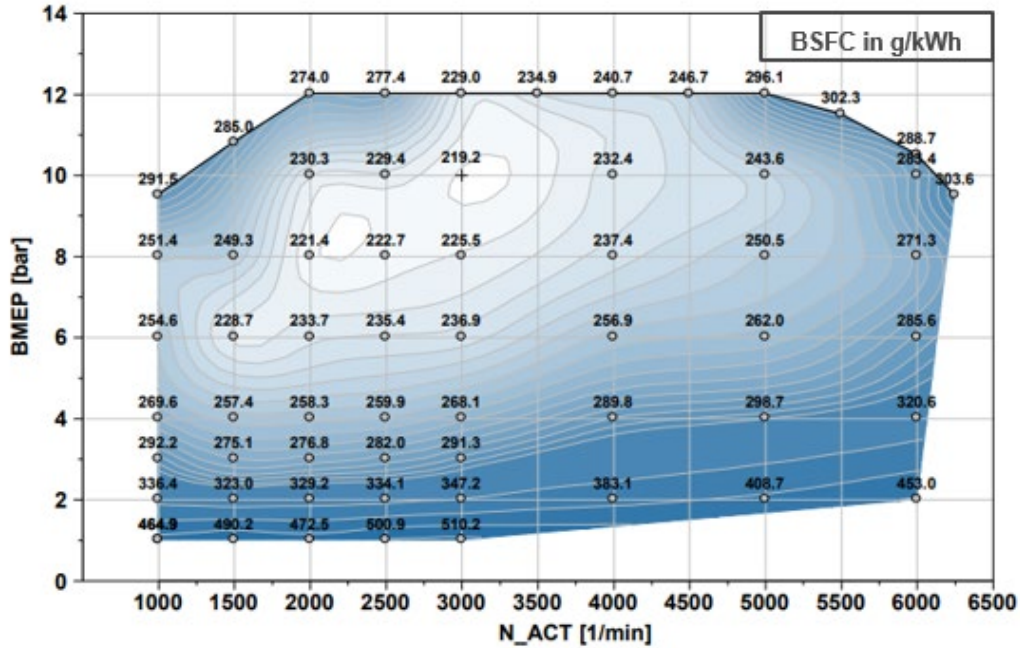


Figure 175. Engine 33 BSFC Map

Engine (eng34) 2.5L_NA_Atkinson_DOHC_CR13_DI_With_Cylinder Deactivation

Engine 34 is a 2.5-liter, 4-cylinder, NA DI Atkinson engine with DOHC and VVT. The engine has a compression ratio of 13 along with cylinder deactivation abilities. Figure 176 shows the engine BSFC map for engine 34 with both the 4-cylinder and the 2-cylinder engine operations.

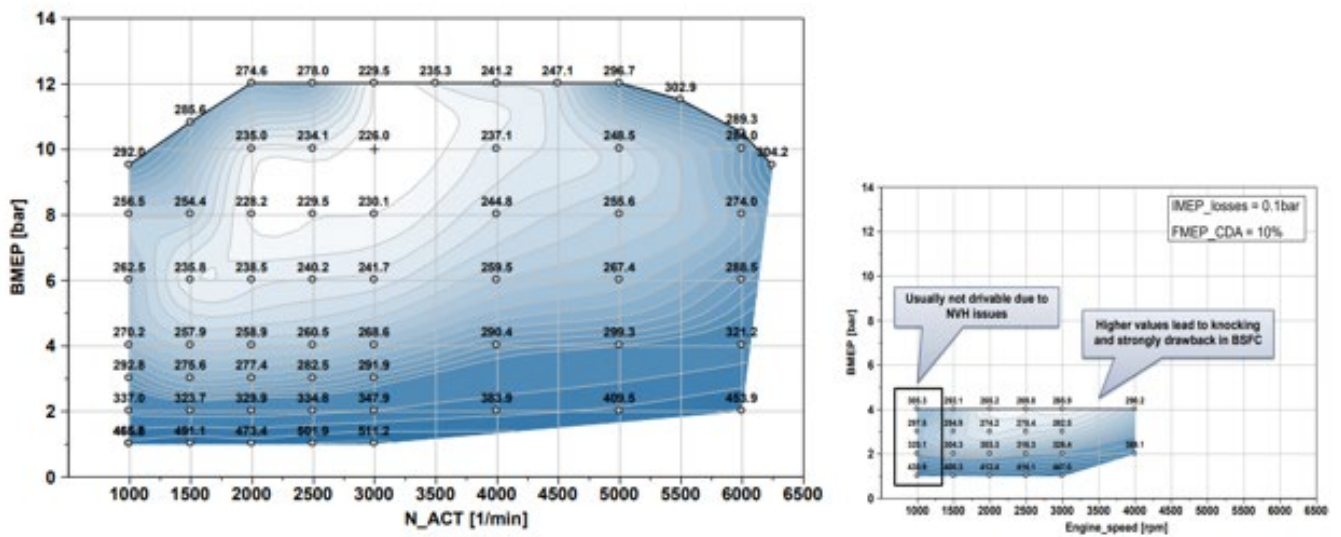


Figure 176. Engine 34 BSFC map

Engine (eng36) 1.6L_Turbocharged_VVT_DOHC_DI_CR 10.5

Engine 36 is a 1.6-liter, 4-cylinder, turbocharged engine with DOHC and VVT. The engine has a compression ratio of 10.5. Figure 177 shows the engine BSFC map for engine 36.

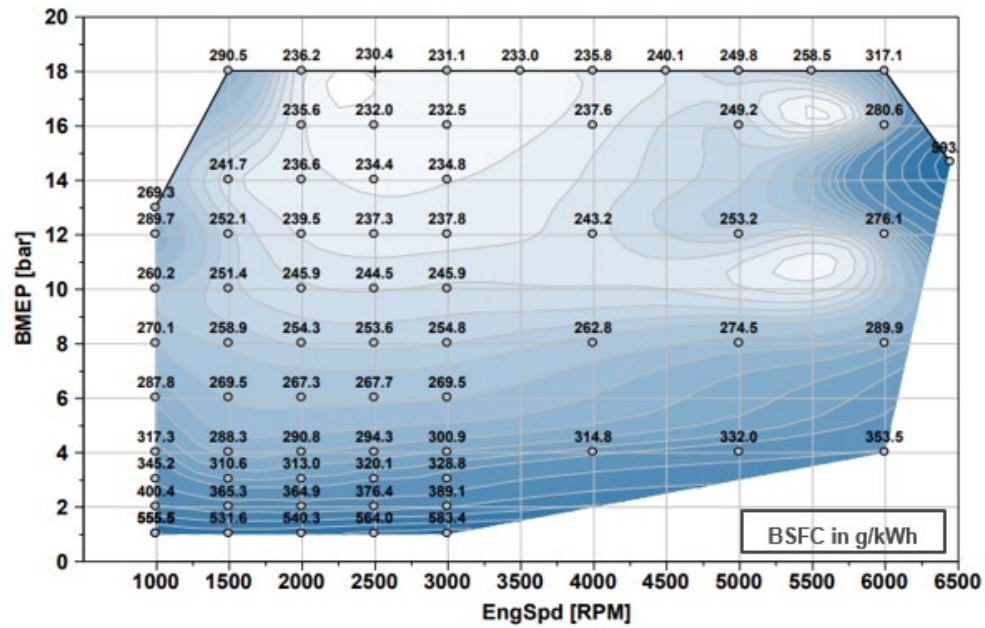


Figure 177. Engine 36 BSFC map

Engine (eng37) 1.6-Liter Turbocharged VVT_DOHC_DI_CR 10.5 With EGR

Engine 37 is a 1.6L, 4-cylinder, turbocharged engine with DOHC and VVT. The engine has a compression ratio of 10.5. The engine also has cooled EGR capabilities. Figure 178 shows the engine BSFC map for engine 37.

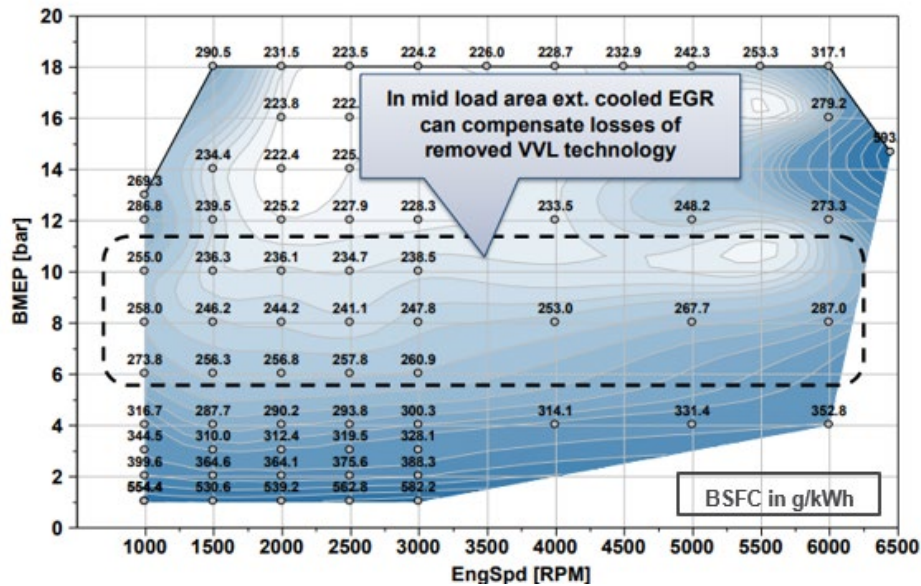


Figure 178. Engine 37 BSFC map

Engine (eng38) 1.6-Liter Turbocharged VVT_DOHC_DI_CR 10.5 With Cylinder Deactivation

Engine 38 is a 1.6-liter, 4-cylinder, turbocharged engine with DOHC and VVT. The engine has a compression ratio of 10.5 with cylinder deactivation abilities. Figure 179 shows the engine BSFC map for engine 38.

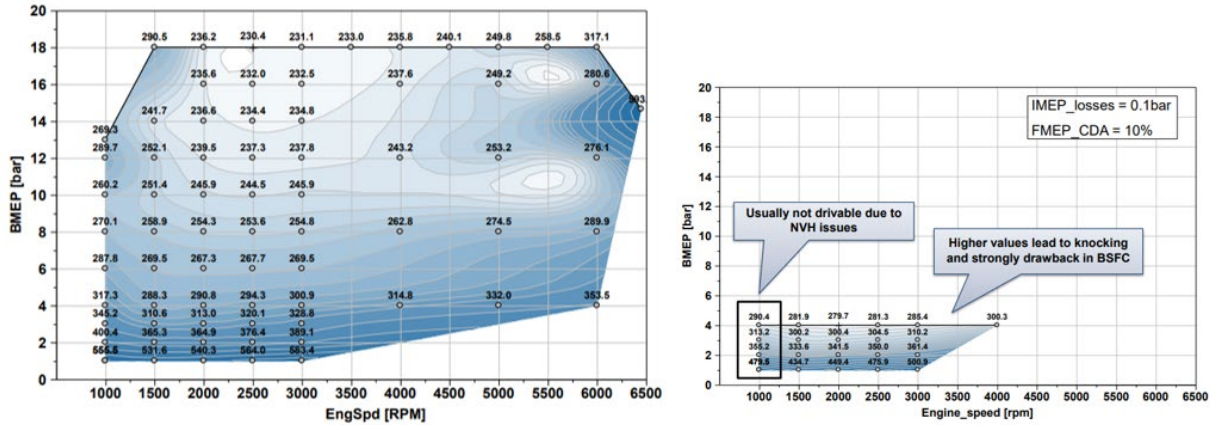


Figure 179. Engine 38 BSFC map

Engine (eng39) 1.6-Liter Turbocharged VVT_DOHC_DI_CR 10.5 With Advanced Cylinder Deactivation

Engine 39 is a 1.6-liter, 4-cylinder, turbocharged engine with DOHC and VVT. The engine has a compression ratio of 10.5 with advanced cylinder deactivation abilities. Figure 180 shows the engine BSFC map for engine 39. The final BSFC map for the engine was developed after merging the optimum engine operating conditions for the individual cylinder operations (1, 2, 3, and 4).

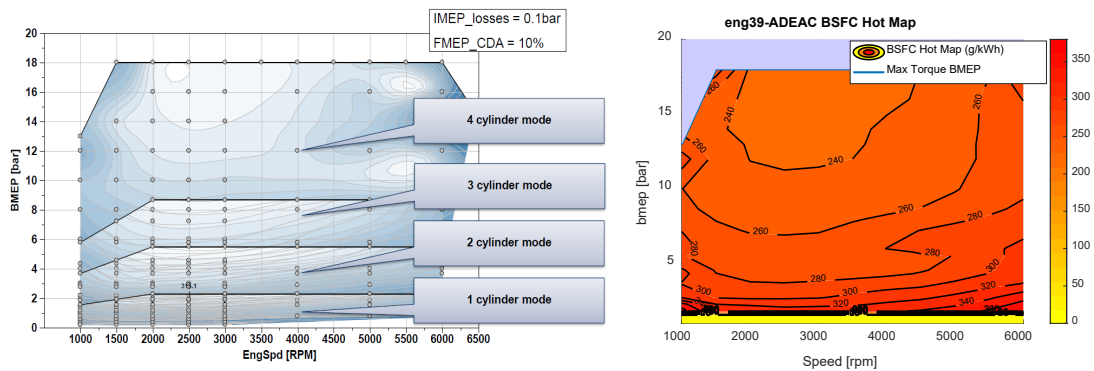


Figure 180. Engine 39 BSFC maps

Engine (eng40) 2L_DI_DOHC_VVT_CR11 With Advanced Cylinder Deactivation

Engine 40 is a 2.0-liter, 4-cylinder, naturally aspired gasoline engine with DOHC and SGDI. The engine was developed from engine 18, with the additional advanced cylinder deactivation abilities. Figure 181 shows the BSFC map for engine 40.

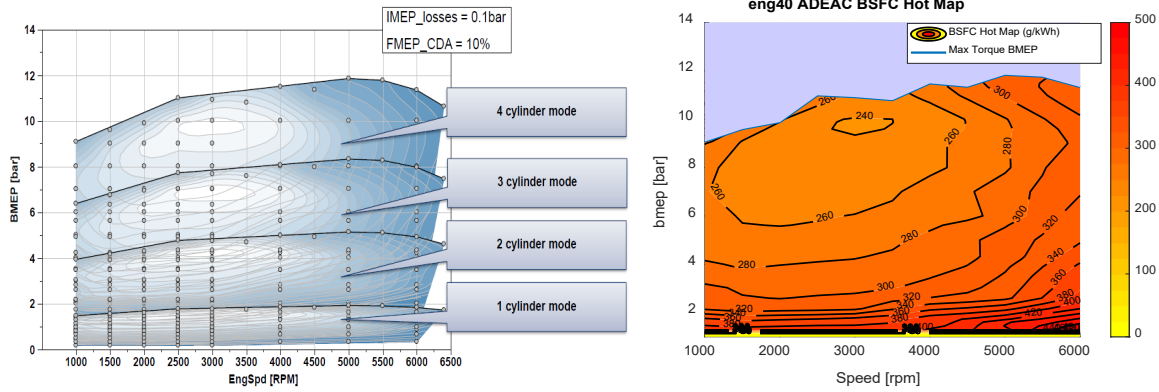


Figure 181. Engine 40 BSFC map

Engine (eng45) 3L_diesel_engine45

Engine 45 is the General Motors Duramax 3.0-liter model from SwRI. It is an in-line 6-cylinder, 4-stroke engine with an 84 mm bore and 90 mm stroke. The engine uses cooled low-pressure loop and un-cooled high-pressure loop EGR systems with a variable geometry turbine, water-to-air charge air cooling that uses a separate low-temperature coolant loop, and a variable intake manifold with dual air intake paths. The torque curve is relatively flat from 1,500 to 3,000 rpm, and the engine has a compression ratio of 15:1. This compression ratio is low by medium- and HD engine standards but is common in high BMEP light-duty diesels. The lower compression ratio allows high BMEP with relatively modest peak cylinder pressure, at the expense of some efficiency. Figure 182 shows the BSFC map for engine 45.

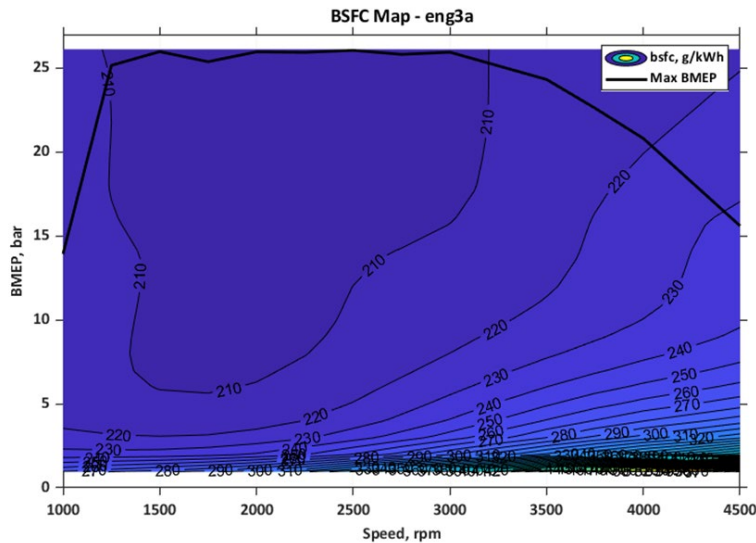


Figure 182. Engine 45 BSFC map

Engine (eng46) 3L_diesel_cylinder_deac_engin46

For engine 46, cylinder deactivation capabilities were added to engine 45. The cylinder deactivation study was conducted using 3-cylinder deactivation at light loads, then switching to normal 6-cylinder operation at higher loads. The approach was to operate three cylinders and gradually increase fueling at each speed, from no-load until either the engine was not able to

meet the BMEP target or the BSFC was higher than baseline. Minimum air fuel ratio was limited to 20:1. Figure 183 shows the BSFC map for engine 46.

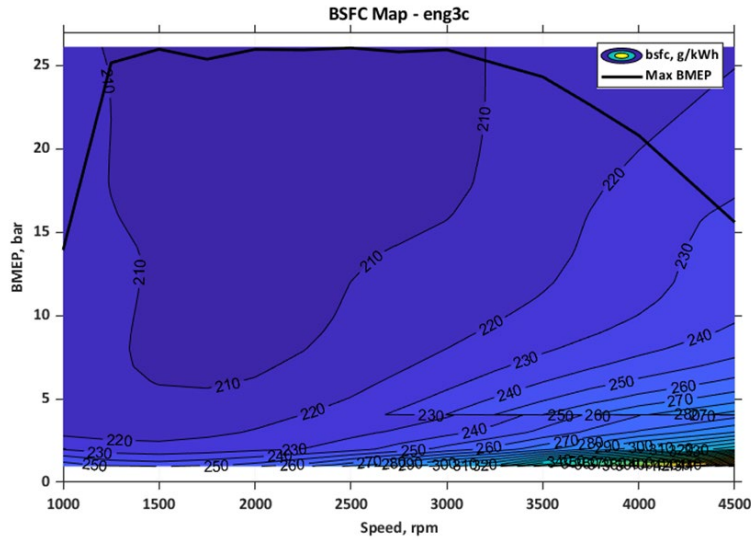
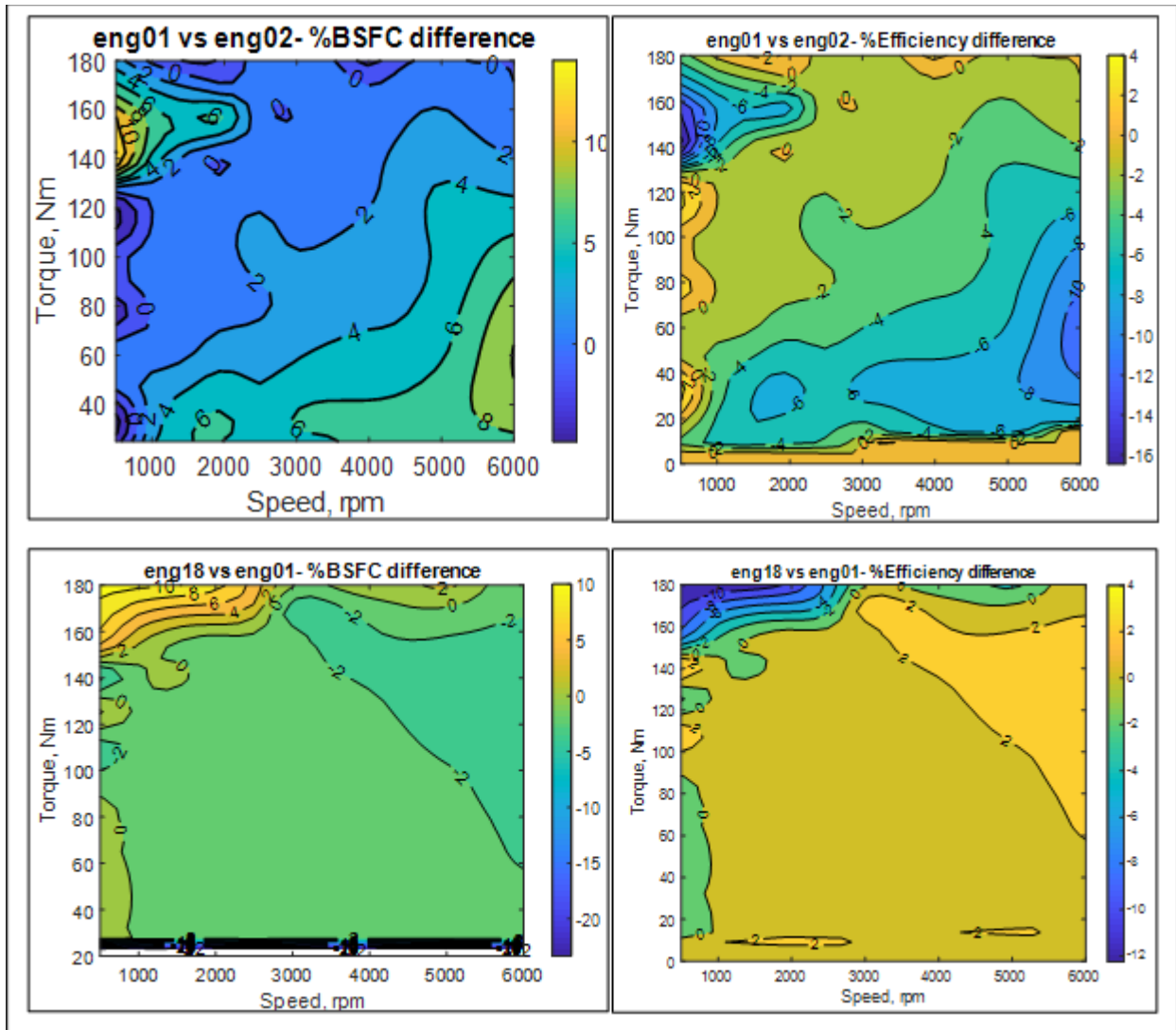
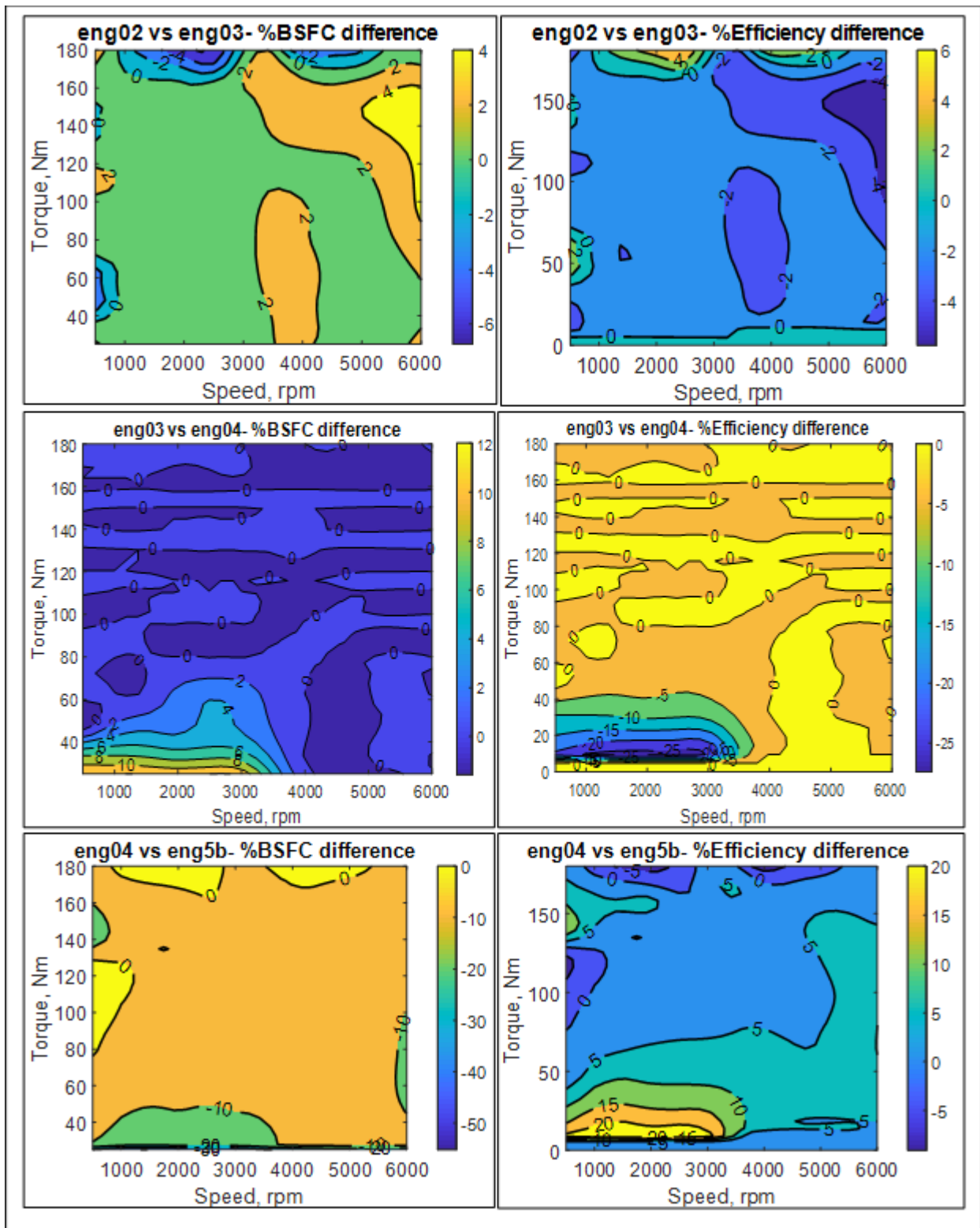


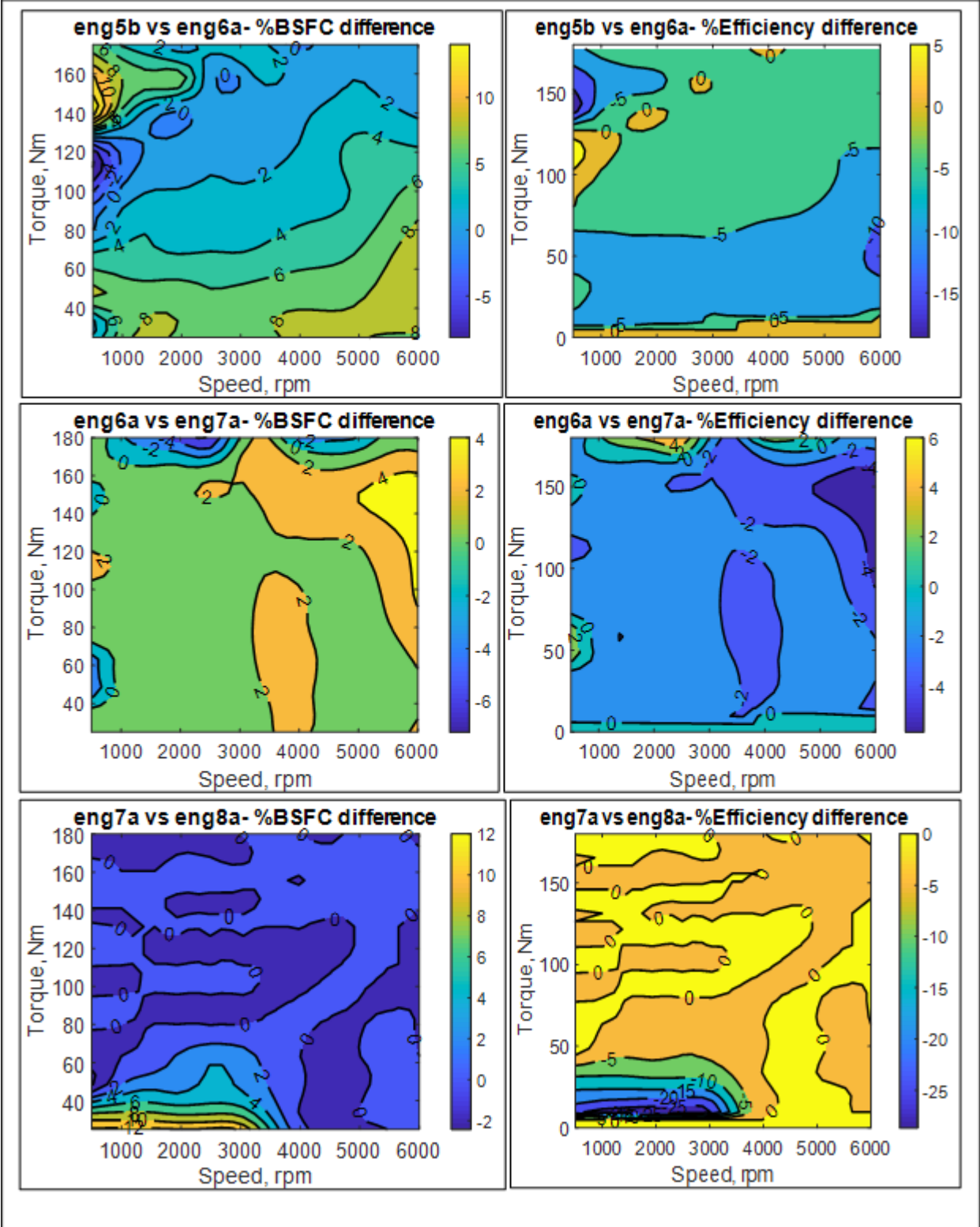
Figure 183. Engine 46 BSFC map

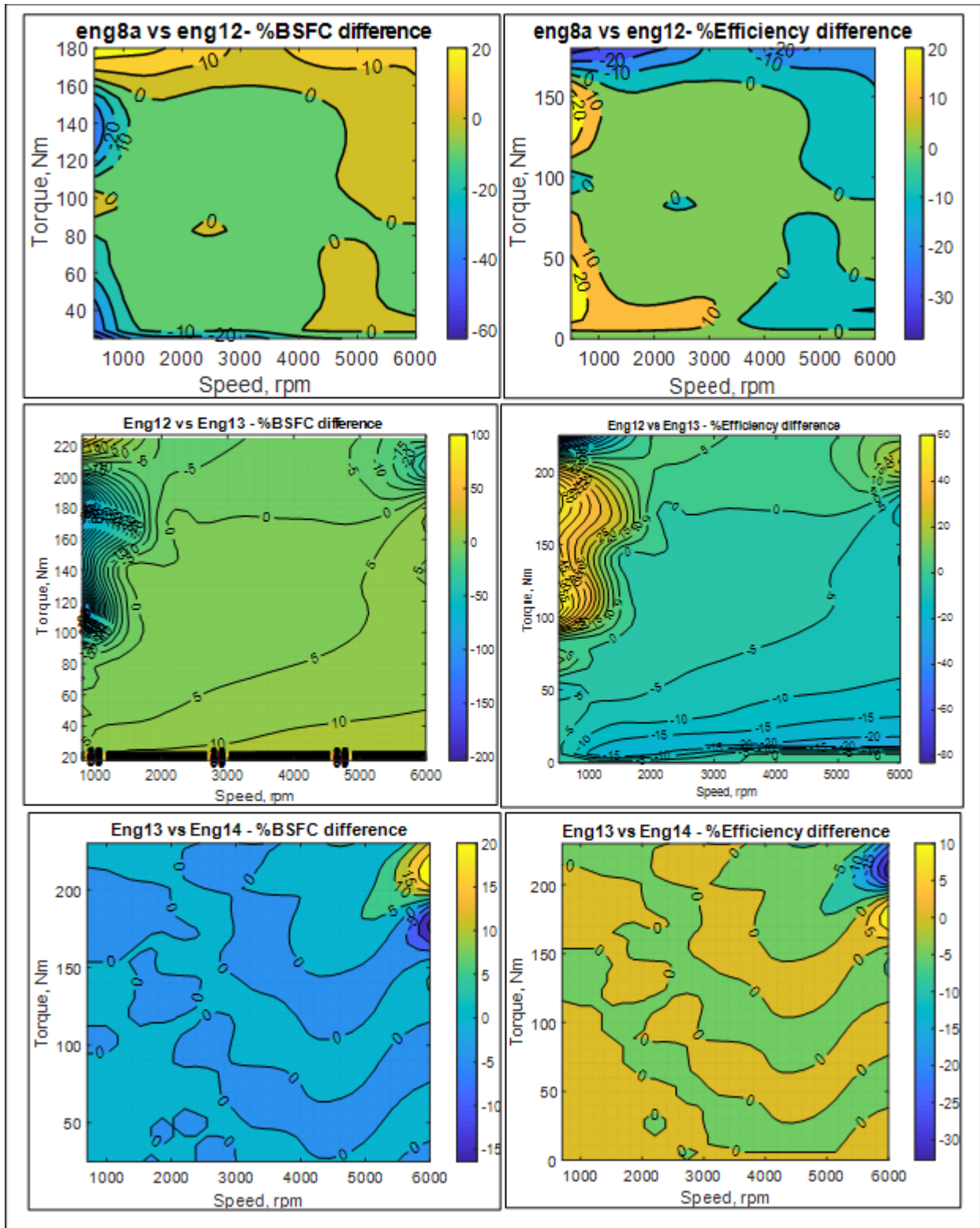
Incremental BSFC and Thermal Efficiency Difference of Engines

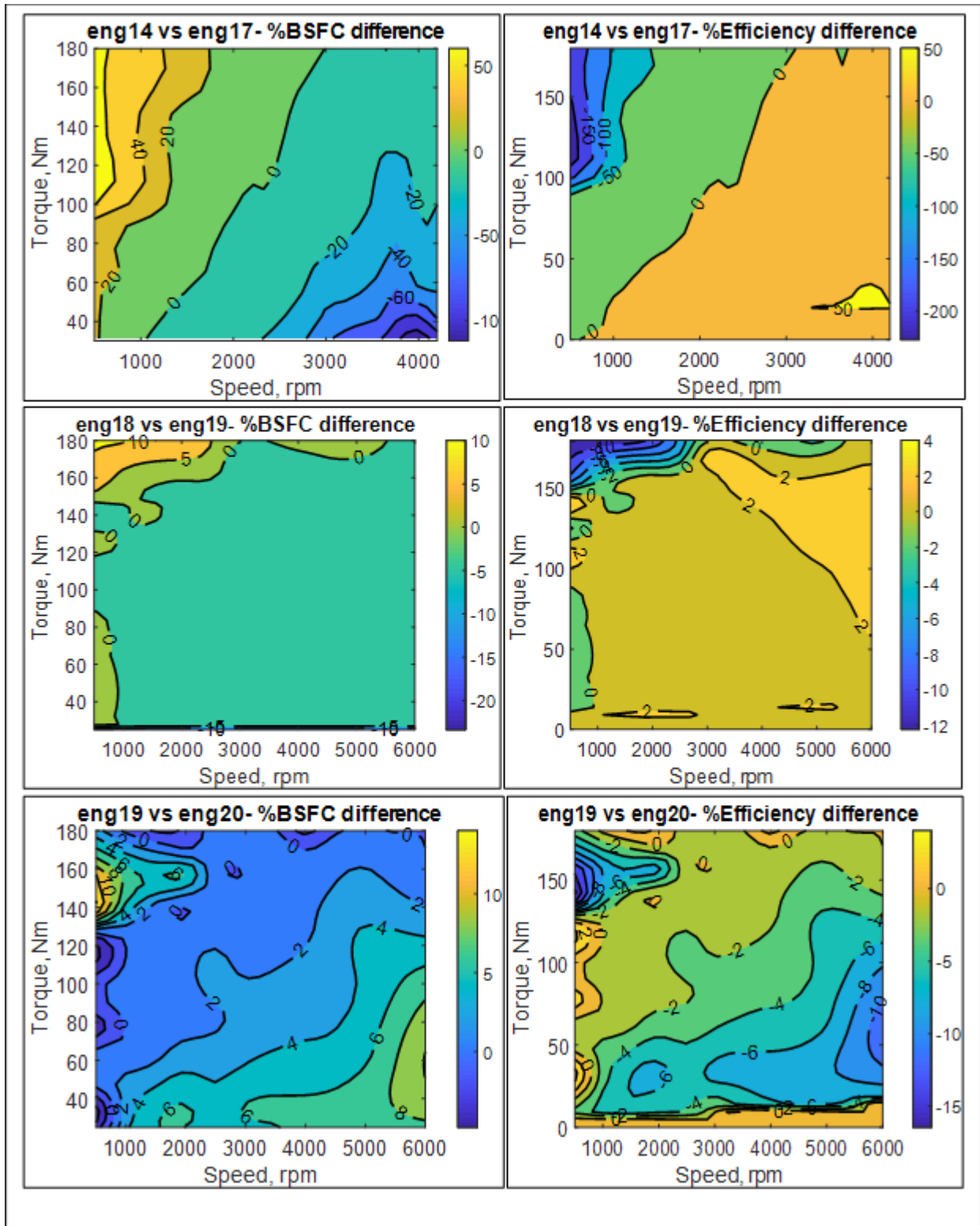
Figure 184 shows the incremental differences (in percentages) in BSFC and thermal efficiency among the different engines.











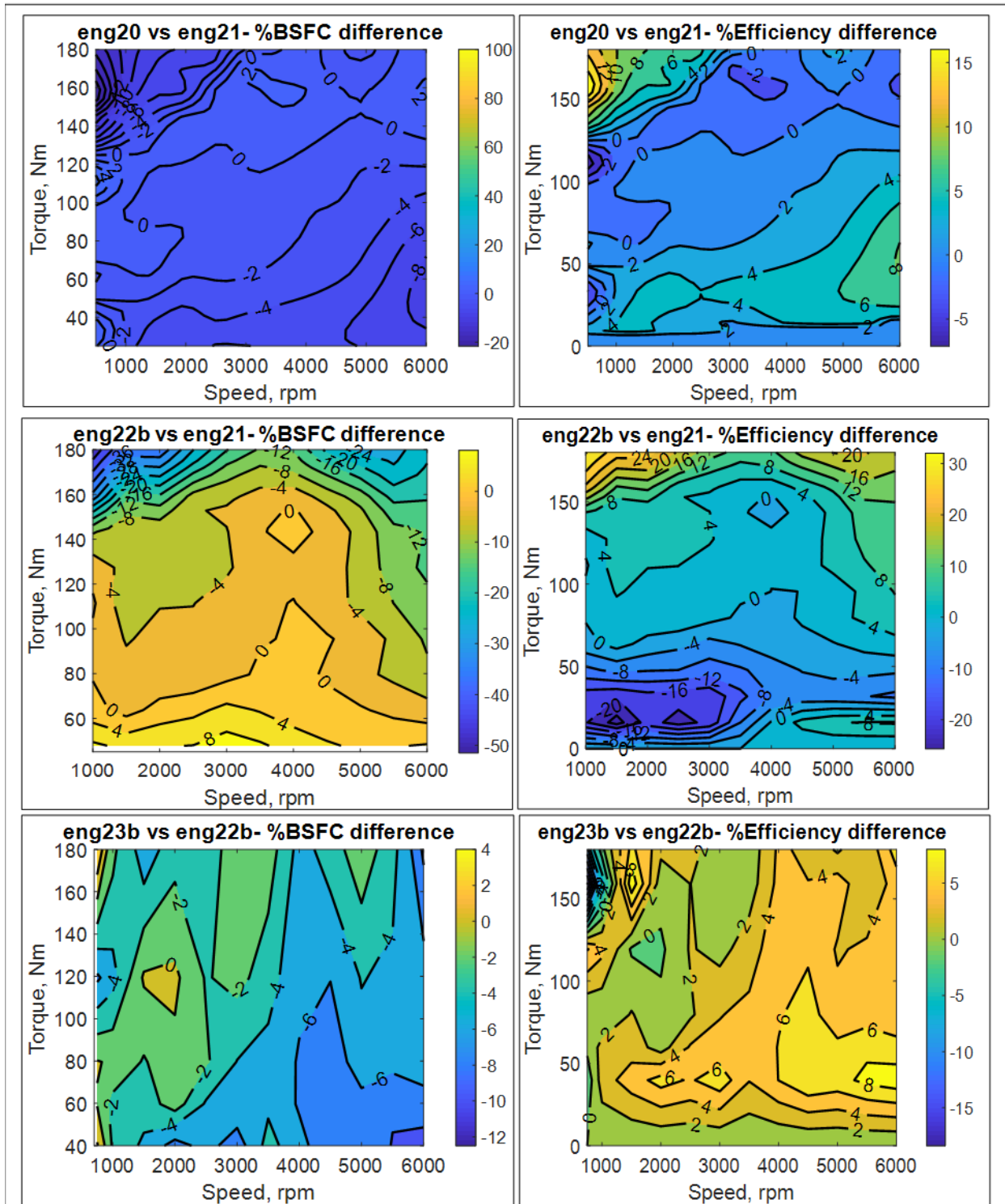


Figure 184. Incremental BSFC and efficiency differences among engines

Idle Fuel Rate Update

For the current set of runs, the specific values for the idle fuel flow rates have been provided by IAV. Table 66 summarizes the specific values for the idle fuel flow rates.

Table 66. IAV idle fuel rate for all engines

Engine List	Comments	Fuel Flow (kg/hr) 650 – 700 rpm Warm Idle
Eng1	Gasoline, 2.0 l, 4 cyl, NA, PFI, DOHC, VVT	0.364
Eng2	VVL added to Eng1	0.355
Eng3	DI added to Eng2	0.350
Eng4	Cylinder deactivation ability added to Eng3	0.270/0.380
Eng5b	Eng5a with valvetrain friction reduction (small friction reduction)	0.339
Eng6a	Eng2 with valvetrain friction reduction (small friction reduction)	0.315
Eng7a	Eng3 with valvetrain friction reduction (small friction reduction)	0.308
Eng8a	Eng4 with valvetrain friction reduction (small friction reduction)	0.216
Eng12	Gasoline, 1.6 l, 4 cyl, turbocharged, DI, DOHC, VVT, VVL	0.230
Eng12Deac	Cylinder deactivation ability added to Eng12	0.230
Eng13	Eng12 downsized to 1.2 l	0.200
Eng14	Cooled external EGR added to Eng13	0.200
Eng18	Gasoline, 2.0 l, 4 cyl, NA, DI, DOHC, VVT	0.380
Eng19	Cylinder deactivation ability added to Eng1	0.270/0.380
Eng20	Cylinder deactivation ability added to Eng2	0.270/0.380
Eng21	Cylinder deactivation ability added to Eng18	0.270/0.380
Eng23b	2.0liter VVL Miller + VTG + EGR	0.229
Eng23c	2.0liter VVT Miller echarge + EGR	0.229
Eng26a	2.0liter variable compression ratio + EGR	0.229
eng32	2.5L NA, Atkinson DOHC CR13 DI	0.328
eng33	2.5L NA Atkinson DOHC CR13 DI LP-EGR	0.328
eng34	2.5L NA Atkinson DOHC CR13 DI + Deac	0.328
eng36	1.6L Turbo VVT DOHC DI CR10.5	0.236
eng37	1.6L Turbo VVT DOHC DI CR10.5 LP-EGR	0.236
eng38	1.6L Turbo VVT DOHC DI CR10.5 + Deac	0.236
eng39	1.6L Turbo VVT DOHC DI CR10.5 + ADEAC	0.236
eng40	2.0L NA VVT DOHC DI CR11 + ADEAC	0.380

Heavy-Duty Pickups and Vans

Table 67 shows the different engine technologies studied, along with the associated simulation names and the reference peak power. SwRI provided the engine performance values.

Table 67. Engine technologies with reference peak power and reference displacement

Engine Simulation Name	Engine Technology	Engine Reference Peak Power (kW)	Engine Reference Displacement (L)
eng4a	DOHC VVT (CR 10.5)	324	7.3
eng4b	DOHC VVT + GDI (CR11.5)	324	7.3
eng4c	DOHC VVT + GDI + CDA (CR11.5)	324	7.3
eng4d	Turbo VVT DOHC DI (CR9.5)	256	7.3
eng3a	Diesel baseline for VAN	213	3.0
eng3c	Diesel baseline + cylinder deactivation for VAN	213	3.0
eng1a	Diesel baseline for Pickup	199	6.7
eng1c	Diesel baseline + cylinder deactivation for Pickup	199	6.7

Engine Performance Maps [9]

SwRI modeled gasoline and diesel engine maps in GT-POWER and supplied those maps to Argonne for use in Autonomie. SwRI evaluated a range of potential efficiency technologies that could be applied to light and medium-duty truck engines. The following three engines were studied.

- Ford 7.3-liter, medium-duty gasoline V8 engine
- General Motors Duramax 3.0-liter, light-duty diesel engine for Class 2a pickup trucks
- Cummins B6.7 medium-duty truck diesel engine

Each engine was modeled in GT-Power, and the models were calibrated and validated against test data available at SwRI or provided by OEMs. Once the models achieved satisfactory results, the technology evaluation began. SwRI provided the engine performance map over the speed and load range as well as fuel maps suitable for use with Autonomie.

The Ford 7.3-liter gasoline engine was exercised over the widest range of technologies in both NA and turbocharged form. The baseline engine is NA with PFI and a two-valve head. The addition of gasoline direct injection allowed the engine to increase the compression ratio from 10.5 to 11.5, which provided a benefit of about 2 percent over much of the map. Adding cylinder deactivation to the 11.5 compression ratio GDI engine provides significant benefits below 4 bar BMEP, and double-digit percentage fuel consumption reductions below about 3 bar BMEP. However, cylinder deactivation has no effect above 4 bar BMEP, where it cannot be used.

The turbocharged option was evaluated in a 4-valve form. A minimum compression ratio of 9.5 was selected to minimize the efficiency penalty of the boosted engines. The potential benefit of boosted engines is that with their narrower speed range, they will run at a lower engine rpm and

a higher BMEP level. Under light load conditions, this pushes the boosted engine BMEP up into a more efficient portion of the map than the NA baseline.

The General Motors Duramax 3.0-liter diesel is a new light-duty diesel that shares design features with many high-BMEP light-duty diesels sold in Europe. One of these features is the combination of high-pressure loop EGR with low-pressure loop EGR, which reduces the pumping work required to flow EGR. The engine also uses little EGR at high load, which helps it run a high 26 bar BMEP at a relatively modest cylinder pressure limit of 180 bar BMEP. The Duramax also has very low friction for a diesel engine, limiting the potential for further FMEP reduction. The CDA technology combination was added to the 30 bar BMEP variant. This provides a significant additional benefit at loads below about 3 bar BMEP.

The Cummins B6.7 engine was evaluated with the 2019 baseline configuration and with eight additional technology options. CDA provided fuel consumption reductions at a light load of 7 percent, and at a low speed to 12 percent at high speed. The maximum load where CDA could be used ranged from just under 2 bar BMEP at low and high speeds, up to about 3.5 bar BMEP in the middle of the speed range.

SwRI provided eight engine maps in total, for three NA gasoline engines, one turbocharged gasoline engine, and four diesel engines. SwRI used the following fuel specifications when modeling the engines in GT-POWER.

- Gasoline LHV = 41.67 MJ/kg, gasoline density = 752.3 kg/m³
- Diesel LHV = 43.08 MJ/kg, diesel density = 835.0 kg/m³
- Ambient temperature, $T_{amb} = 25^{\circ} \text{C}$
- Ambient pressure, $P_{amb} = 990 \text{ mbar}$

Engine (eng4a) 7p3L_pfi_ohv_vvt_engine4a_baseline

Engine 4a, provided by Ford, was the 7.3-liter Godzillan NA pfi gasoline engine in a Ricardo WAVE format. Gamma Technologies converted the WAVE model into a GT-Power model. The baseline model provided was only configured to simulate wide-open throttle operation with power enrichment. Ford also provided steady state experimental data to validate the model. The model used a Wiebe function for describing the combustion. Figure 185 shows the BSFC map for engine 4a.

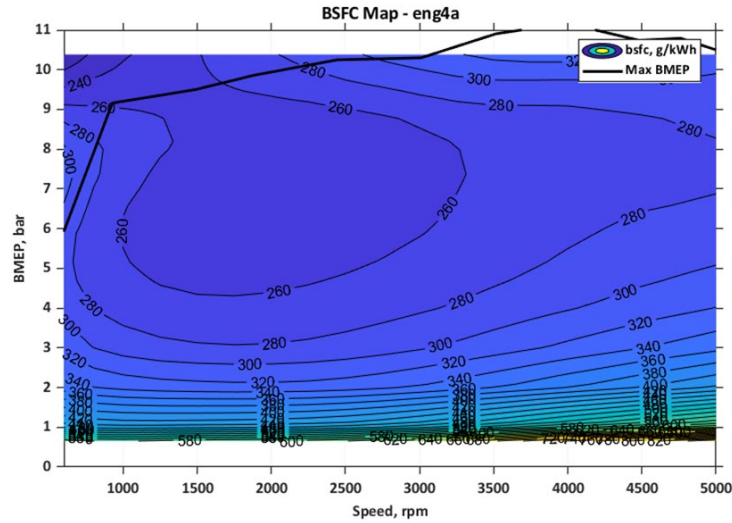


Figure 185. Engine 4a BSFC map

Engine (eng4b) 7p3L_di_ohv_vvt_engine4b

For engine 4b, GDI replaced the standard port injection used on the production 7.3 V8. DI provides better volumetric efficiency, since only air is flowing through the ports. The injection timing can be optimized to provide a degree of charge cooling, which provides a knock benefit. In addition, the GDI model was converted again with a one-point compression ratio increase from the baseline. With a compression ratio of 11.5, the combustion phasing of the knock-limited loads was retarded to nearly the same as the baseline simulation, to match the knock performance of the base engine. The higher compression ratio provides additional efficiency, especially at medium and low loads. Figure 186 shows the BSFC map for engine 4b.

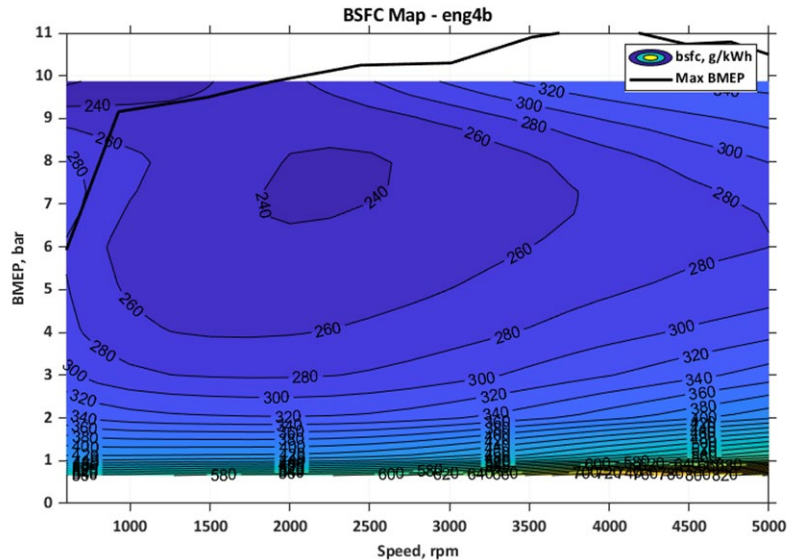


Figure 186. Engine 4b BSFC map

Engine (eng4c) 7p3L_cyclinder_deac_engine4c

For engine 4c, cylinder deactivation capabilities were added to engine 4b. Cylinder deactivation is used at loads up to 4 bar BMEP. One bank of four cylinders was deactivated for simplicity rather than employing a dynamic skip-fire approach. The intake and exhaust valves were deactivated for the deactivated bank to minimize the pumping work. The firing cylinders benefit from operating at a higher IMEP. The manifold pressures are also much higher, which significantly reduces the pumping loss. Figure 187 shows the BSFC map for engine 4c.

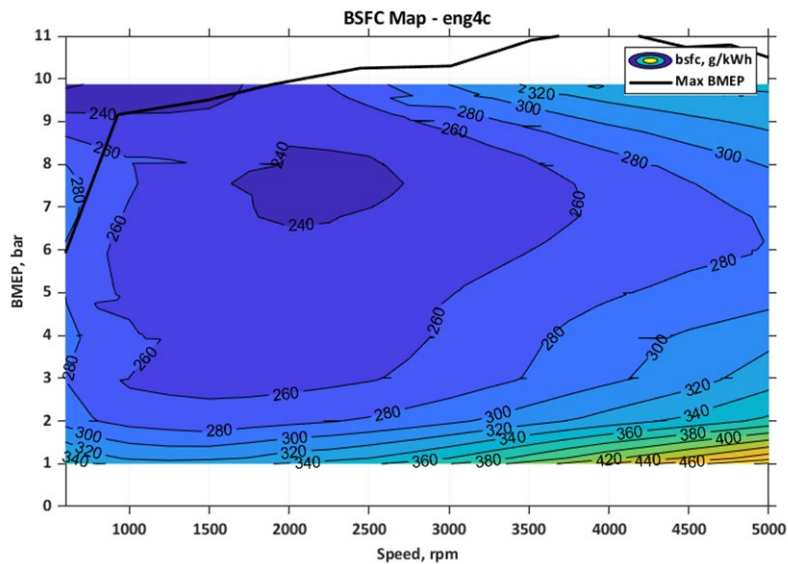


Figure 187. Engine 4c BSFC map

Engine (eng4d) 7p3L_turbo_di_engine4d

Engine 4d is a 7.3-liter turbocharged gasoline engine with DI, OHV and with independent cam phasers. The base engine had a power rating of 260 kW with the rated power near 3,900 rpm. To keep the same vehicle performance, the same power was needed within the narrower speed range. As a practical limitation, a minimum compression ratio of 9.5 was set. Based on the knock model, the results showed that down-speeding to achieve a peak torque of 16 bar BMEP was too aggressive—it would require a compression ratio below 9. It was determined that with a compression ratio of 9.5:1, the 4-valve engine could achieve the power targets at a BMEP of 14.5 bar. Figure 188 shows the BSFC map for the turbocharged GDI 4V engine with independent cam phasers.

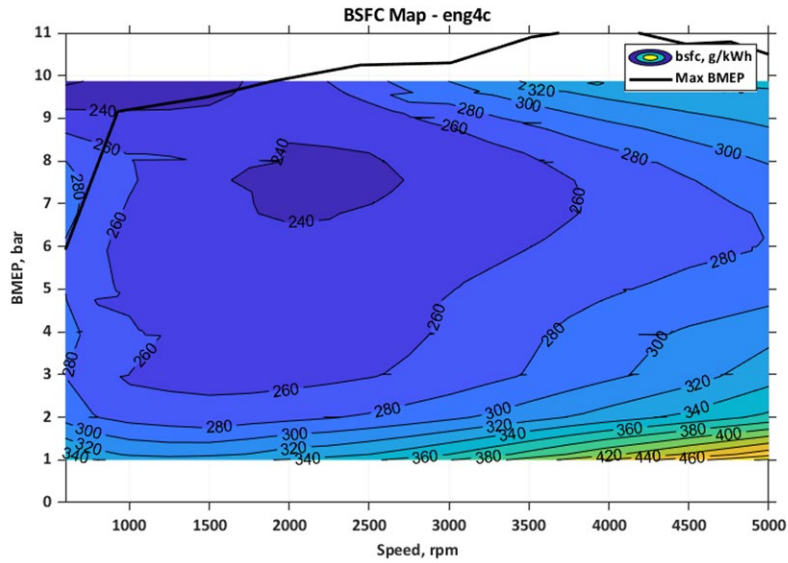


Figure 188. Engine 4d BSFC map

Engine (eng3a) 3L_diesel_engine3a

Engine 3a is the General Motors Duramax 3.0-L. It is an in-line 6-cylinder, 4-stroke engine with an 84 mm bore and 90 mm stroke. The engine uses cooled low-pressure loop and uncooled high-pressure loop EGR systems with a variable geometry turbine, water-to-air charge air cooling that uses a separate low-temperature coolant loop, and a variable intake manifold with dual air intake paths. The torque curve is relatively flat from 1,500 to 3,000 rpm, and the engine has a compression ratio of 15:1. This compression ratio is low by medium- and HD engine standards but is common in high BMEP light-duty diesels. The lower compression ratio allows high BMEP with relatively modest peak cylinder pressure at the expense of some efficiency. Figure 189 shows the BSFC map for engine 3a.

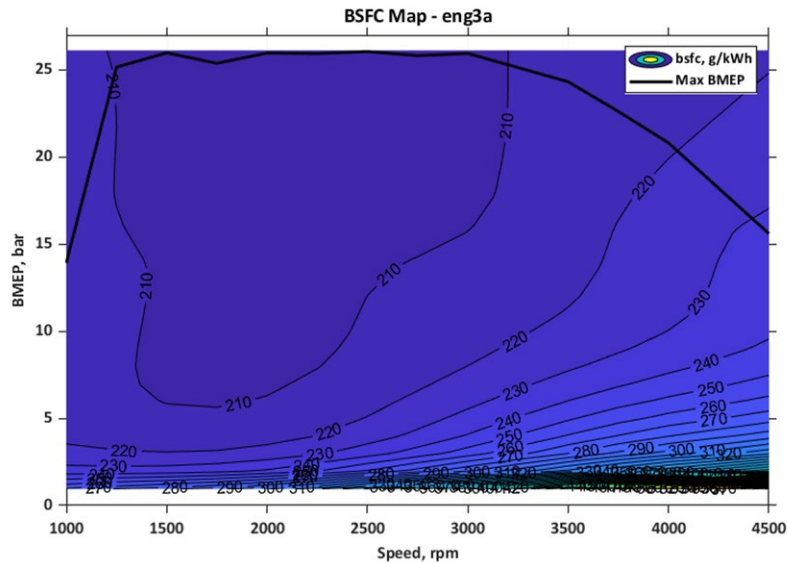


Figure 189. Engine 3a BSFC map

Engine (eng3c) 3L_diesel_cylinder_deac_engin3c

For engine 3c, cylinder deactivation capabilities were added to engine 3a. The cylinder deactivation study was conducted using 3-cylinder deactivation at light loads and then switching to normal 6-cylinder operation at higher loads. The approach was to operate three cylinders and gradually increase fueling at each speed, from no-load until either the engine was not able to meet the BMEP target or the BSFC was higher than baseline. Minimum air fuel ratio was limited to 20:1. Figure 190 shows the BSFC map for engine 3c.

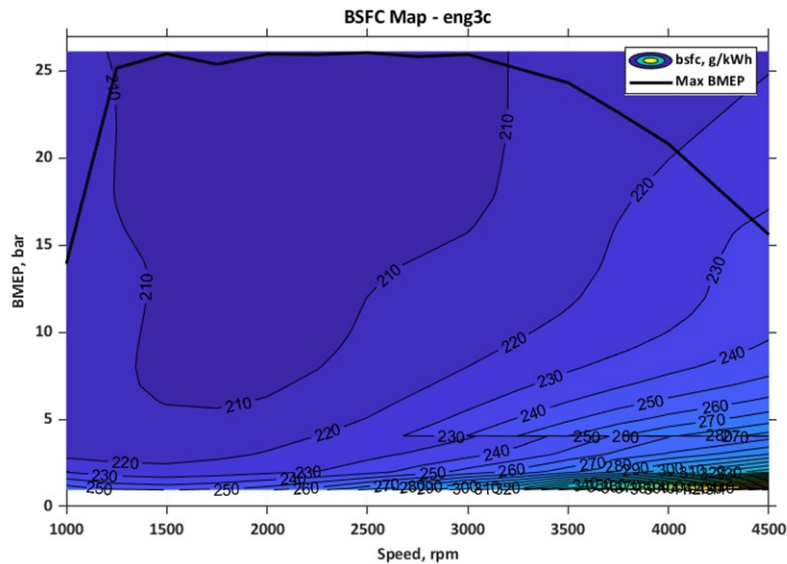


Figure 190. Engine 3c BSFC map

Engine (eng1a) 6p7L_diesel_engine1a

Engine 1a is the Cummins 6.7-liter ISB series. The engine uses a high-pressure loop EGR system with a variable geometry turbine turbocharger and air-to-air charge cooling. The engine is produced in a variety of ratings for different vehicle applications, with torque curves optimized for manual and automatic transmissions, and with two sets of hardware and controls for either maximum fuel efficiency or maximum power emphases. The rating chosen for this project produces 200 kW at 2,400 rpm and maximum torque of 920 Nm at 1,600 rpm. The torque curve is relatively flat from 1,900 to 1,300 rpm and is tailored for automatic transmission installations. This is the highest rating available in the Cummins “fuel efficiency” series and has a compression ratio of 19:1. Figure 191 shows the BSFC map for engine 1a.

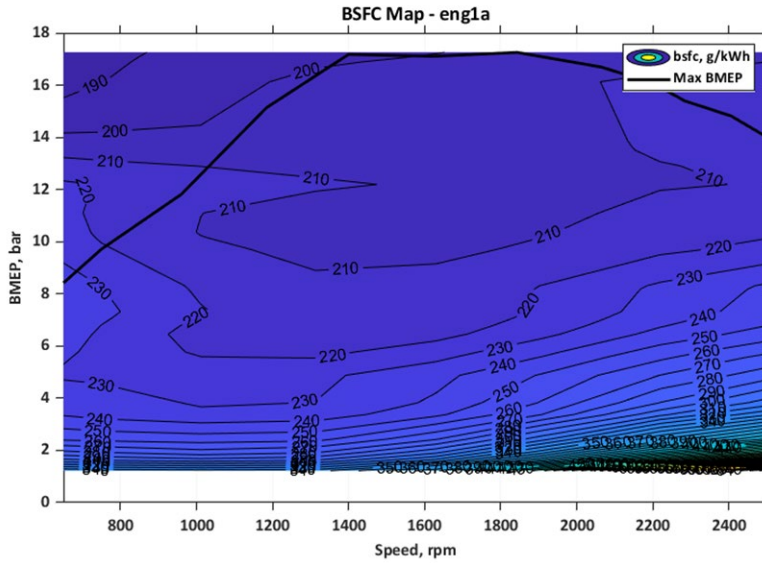


Figure 191. Engine 1a BSFC map

Engine (eng1c) 6p7L_diesel_cylinder_deac_engine1c

For engine 1c, cylinder deactivation capabilities were added to engine 1a. The cylinder deactivation study was conducted using 3-cylinder deactivation at light loads and switching to a normal 6-cylinder operation at higher loads. An intermediate step of four firing cylinders was considered but was ruled out, since further gains would be minimal, and vibration could be problematic with an in-line 6-cylinder engine configuration. The approach taken was to operate three cylinders and incrementally increase fueling at each engine speed, from no load until the air-fuel ratio dropped below 20:1. At this load, operation shifted to six cylinders. Figure 192 shows the resulting light-load fuel efficiency.

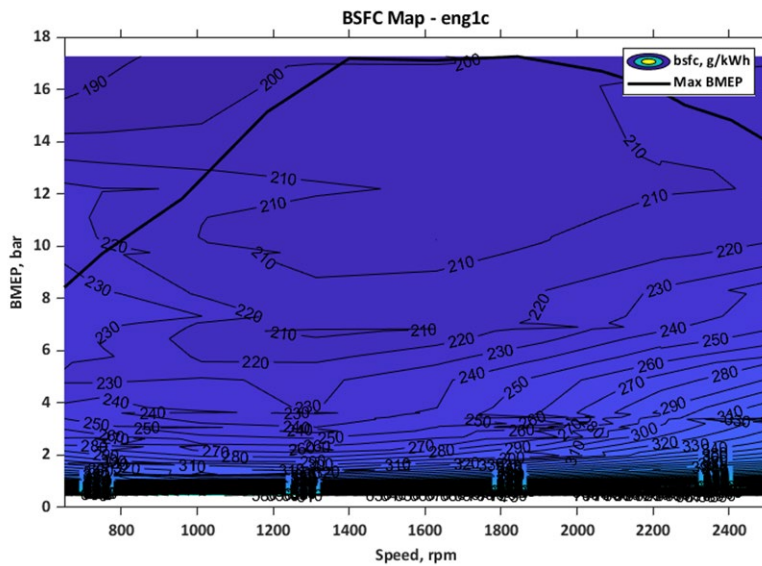
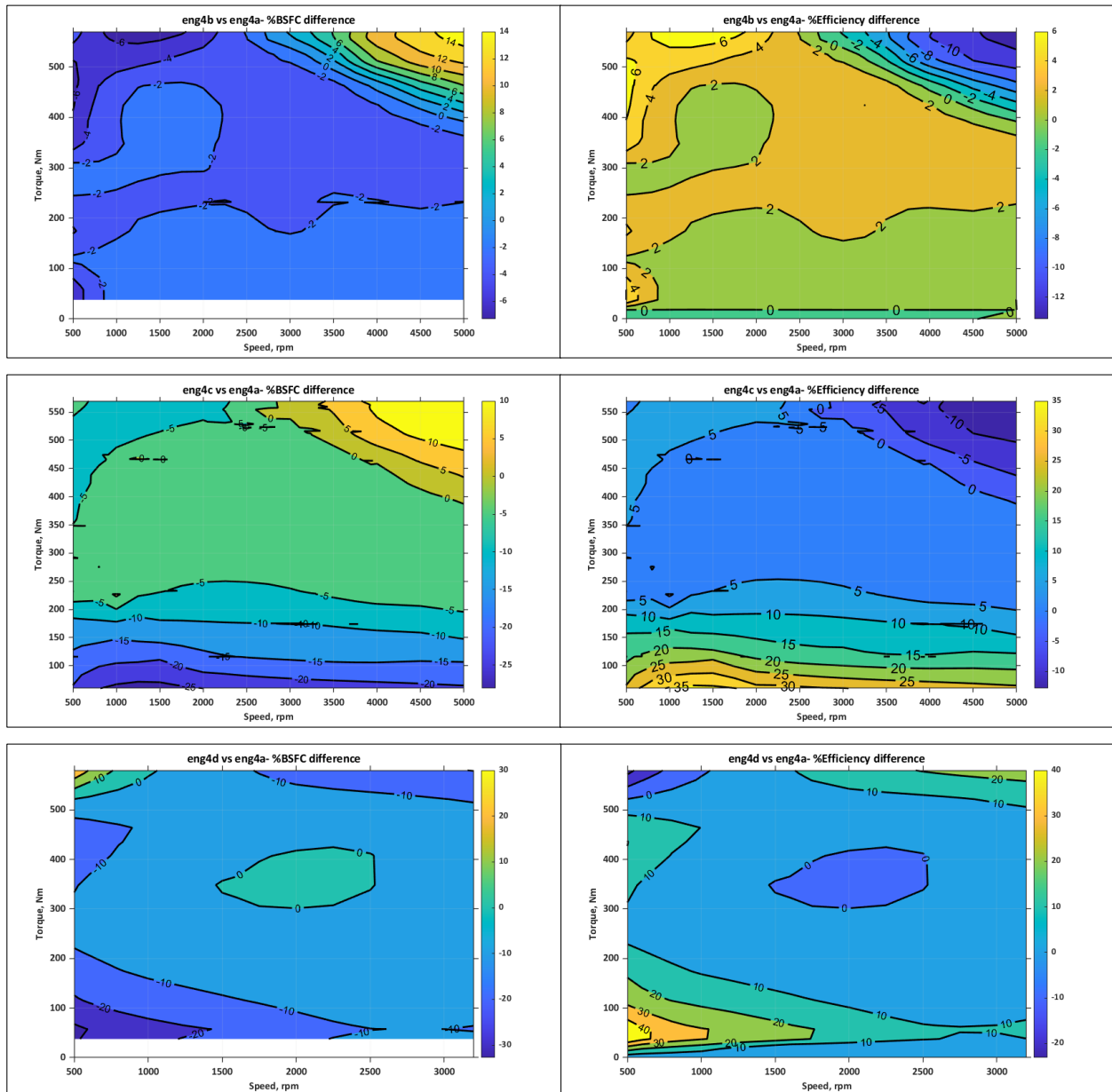


Figure 192. Engine 1c BSFC map

Incremental BSFC and Thermal Efficiency Difference of Engine

Figure 193 shows the incremental differences (in percentage) in BSFC and thermal efficiency among the different engines.



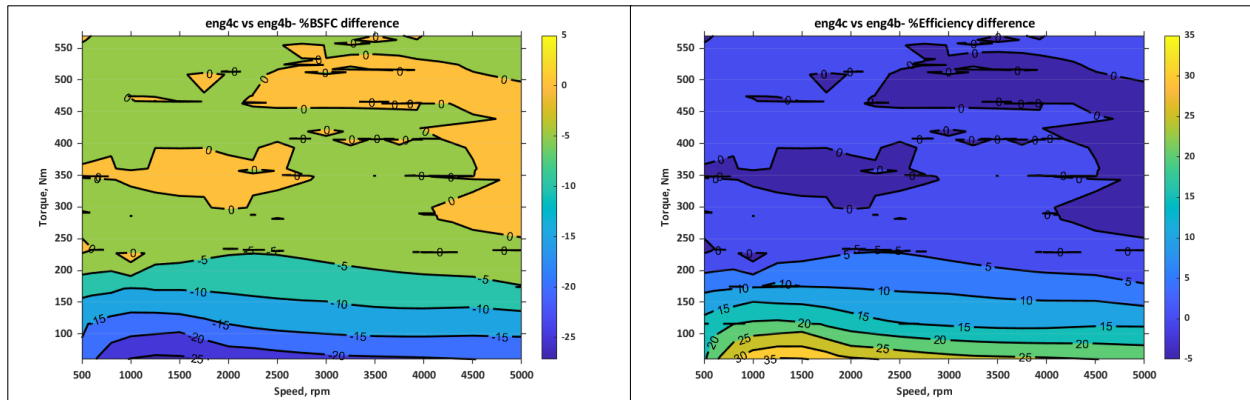


Figure 193. Incremental BSFC and efficiency differences among engines

Electric Machines

The electric machine in BISG hybrid vehicles captures regenerative braking energy and minimally assists the engine during high-transient operating modes. Because the electric machine is linked to the engine through a belt, its power is usually limited. A value of 10 kW peak power was assigned to the BISG electric machine for this study. The micro 12-V hybrid vehicles use a 5-kW peak power electric machine with no regenerative braking capabilities.

The maps in “Electric Machine Efficiency Maps” - shown below were developed assuming normal temperature operating conditions. Electric machine inverter losses are included. The electric machine’s power, like the engine’s, is sized for the reference-sized powertrains. Table 68 details the electric machine efficiency map sources for the different powertrain configurations.

Table 68. Electric machine efficiency map sources for different powertrain configurations

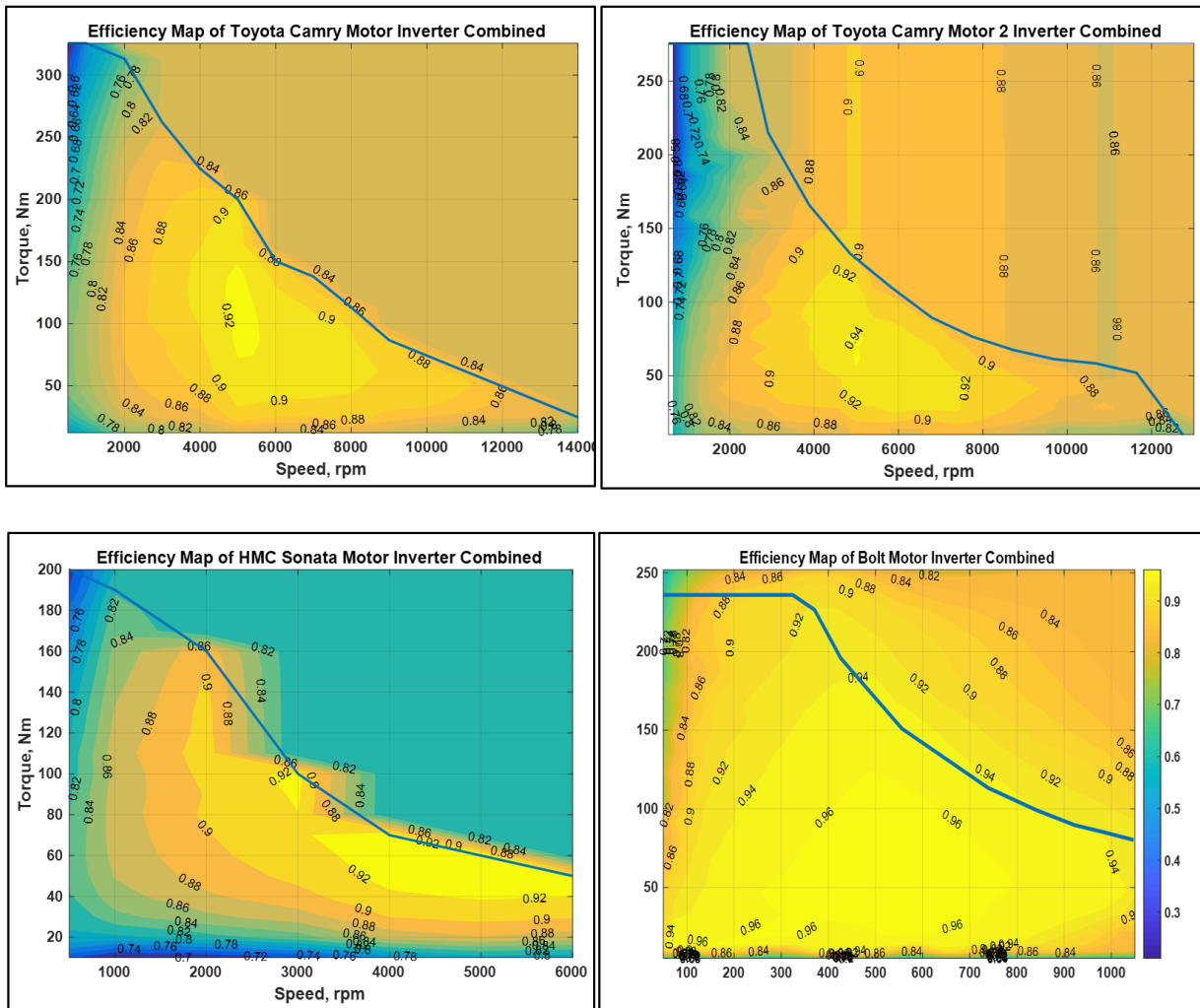
Powertrain Type	Source of Efficiency Map for Motor1 (Traction Motor) + Inverter	Source of Efficiency Map for Motor2 (Motor/Generator) + Inverter
Micro 12-V HEV, BISG	EM1 – Camry HEV Electric Machine Data (Bures, 2012)	
Parallel HEV	EM2 – Sonata HEV Electric Machine Data (Olszewski, 2011)	
Split HEV and Blended PHEV	EM1 – Camry HEV Electric Machine Data (Burrese et al., 2008)	EM3 – Camry HEV Electric Machine 2 Data (Burrese et al., 2008)
EREV PHEV	EM1 – Camry HEV Electric Machine Data (Burrese et al., 2008)	EM2 – Sonata HEV Electric Machine Data (Olszewski, 2011)
Fuel Cell HEV & BEV (LDV)	EM4 – Chevrolet Bolt Electric Machine Data (Momen et al., 2016)	

Powertrain Type	Source of Efficiency Map for Motor1 (Traction Motor) + Inverter	Source of Efficiency Map for Motor2 (Motor/Generator) + Inverter
Fuel Cell HEV & BEV (HDPUV)	EM5 – BorgWarner Electric Machine data (BorgWarner Inc., n.d.)	

- EM1 - Permanent magnet (high speed) for hybrid systems
- EM2 - Permanent magnet (low speed) for hybrid systems
- EM3 - Permanent magnet (high speed) for hybrid systems
- EM4 - Permanent magnet (low speed) for full electric systems
- EM5 - Permanent magnet (low speed) for full electric systems

Electric Machine Efficiency Maps

Figure 194 shows the electric machine efficiency maps for different powertrains.



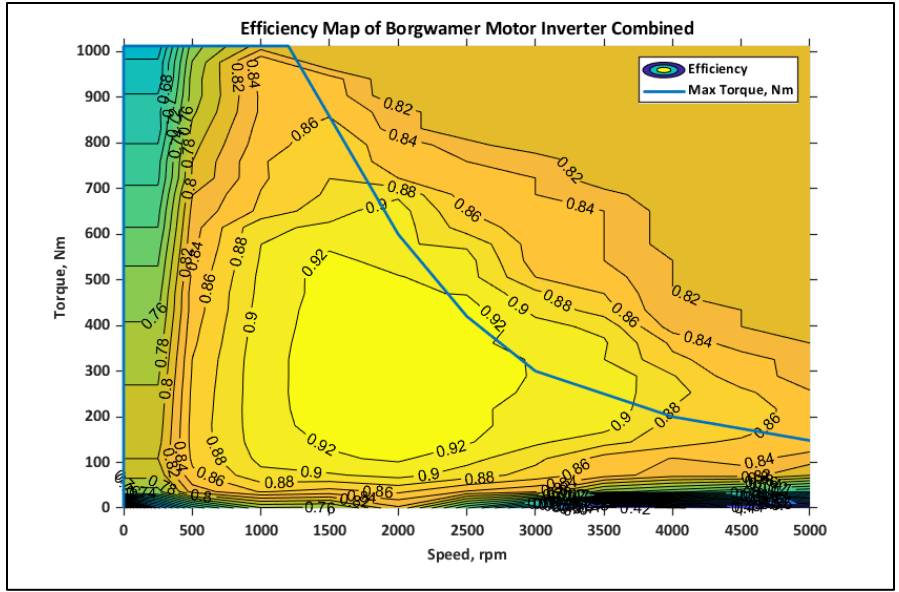


Figure 194. Electric machines efficiency maps for different powertrains

Electric Machine Peak Efficiency Scaling

Light-Duty Vehicles

For the current set of runs, the peak efficiency of electric machines for different powertrains is scaled as shown in Table 69.

Table 69. Efficiency scaling of electric machines

Vehicle Powertrain	Peak Efficiency Scaled (%)
Micro-HEV, Mild Hybrid BISG, Split HEV, Par HEV	96
Split PHEV20, EREV PHEV50, Par PHEV20, Par PHEV50	96
BEV and FCEV	98

A constant ratio was assumed between the continuous and peak torque curves, as follows.

- 2 for micro-HEV and BISG
- 2 for motor 1 and 1.5 for motor 2 of the power-split HEV, blended PHEV, and Voltec PHEV
- 1 for BEVs and fuel cell HEV

Heavy-Duty Pickups and Vans

For the current set of runs, the peak efficiency of electric machines for different powertrains is scaled as shown in Table 70.

Table 70. Efficiency scaling of electric machines

Powertrain Type	Peak Efficiency Scaled (%)
Micro-HEV, Mild Hybrid BISG	93
Parallel HEV & PHEV	93
FC HEV & BEV	93

A constant ratio was assumed between the continuous and peak torque curves, as follows.

- 1.6 for micro-HEV and BISG
- 2 for parallel HEV and PHEV
- 1.4 for BEVs and FC HEV

Fuel Cell System

The fuel cell system was modeled to represent hydrogen consumption as a function of produced power. For the current analysis, Argonne implemented the latest values from *DOE Hydrogen and Fuel Cells Program Record #20005: Automotive Fuel Cell Targets and Status* (Padgett & Kleen, 2020). According to that record, the status of fuel cell system power density is 860 W/kg with a peak system efficiency of 64 percent. For the hydrogen storage weight, Argonne used a value of 0.044 kg per kg usable H₂ fuel mass, based on the latest HFTO assumptions (Islam et al., 2020).

The hydrogen storage technology selected is a high-pressure tank with a specific weight of 0.044 kg H₂/kg for LDV simulations and 1.7 kWh/kg for HDPUV simulations, sized to provide a 360-mile range on the combined cycle (UDDS + HWFET), based on adjusted energy values for LDV simulations, and a 300-mile range for HDPUV based on adjusted energy values.

Figure 195 shows fuel cell efficiency versus fuel cell power. The fuel cell efficiency curve was derived from 2017 Toyota Mirai vehicle benchmarking data in a technology assessment report (Lohse-Busch et al., 2018).

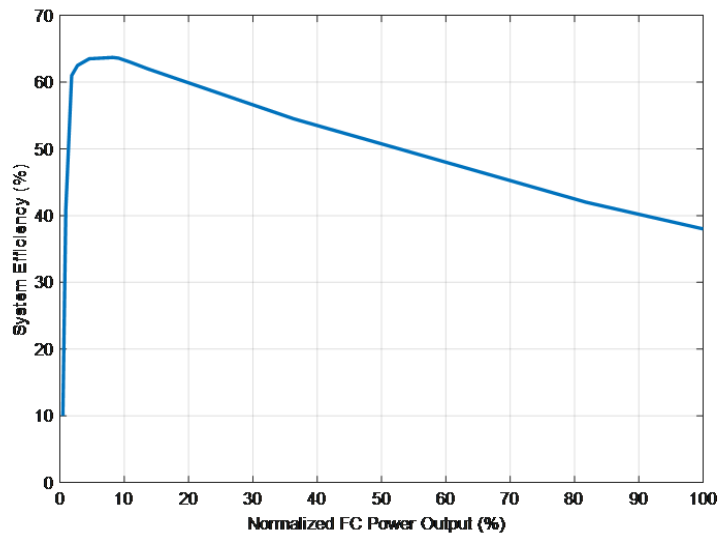


Figure 195. Fuel cell efficiency versus power

Energy Storage System

Lithium-ion batteries are used for all hybrid powertrains. The following are different useable SOC ranges based on the powertrain configuration.

- 10 percent SOC range for micro and mild HEVs
- 20 percent SOC range for full HEVs
- 70 percent SOC range for PHEVs
- 90 percent SOC range for BEVs

Vehicle test data have shown that for the U.S. standard drive cycles and test conditions considered, battery cooling does not draw a significant amount of energy for most vehicle powertrain architectures (Son et al., 2015). The exception is high-energy PHEVs (Kim et al., 2018) and BEVs (Jeong et al., 2017), for which an additional constant power draw is used for battery cooling.

For the current set of runs, the mass, capacities, and voltages of the batteries across different vehicle classes and powertrains are computed using the BatPaC model described a below.

Accessory Loads (LDV)

The electrical and mechanical accessory base load is assumed to be constant over the drive cycles, with values varying by powertrain type. Derived from AMTL data, this value is used to represent the average accessory load consumed during the standard urban Federal Test Procedure and EPA’s HWFET drive-cycle dynamometer testing. For the current set of runs, NHTSA directed Argonne to vary the base accessory loads for different vehicle classes and performance categories across the different vehicle powertrains. Table 71 shows the base accessory load assumptions by vehicle class and performance category across the different vehicle powertrains.

Table 71. Base accessory load assumptions

Vehicle Class	Performance Category	Vehicle Powertrain			
		Conventional	HEVs	PHEVs	BEVs
Compact	Base	250	275	275	225
Compact	Premium	300	325	325	275
Midsized	Base	250	275	275	225
Midsized	Premium	300	325	325	275
Small SUV	Base	275	300	300	250
Small SUV	Premium	325	350	350	300
Midsized SUV	Base	275	300	300	250
Midsized SUV	Premium	325	350	350	300
Pickup	Base	275	300	300	250
Pickup	Premium	325	350	350	300

Lightweighting Technologies

Light-Duty Vehicles

For light-duty vehicles, glider weight defined by the following systems.

- Body
- Chassis
- Interior
- Safety system
- Brake mechanism
- Steering system
- Mechanical accessories
- Electrical accessories
- Wheels

Lightweighting is applied across all glider systems except for those related to safety.

The secondary effects of lightweighting (such as downsizing) are considered as part of the vehicle sizing algorithm. To emphasize technology platform sharing in the study, vehicles with lower levels of mass reduction (5 and 7.5%) inherit the sizing characteristics of the reference vehicle (0% MR). Vehicles with higher levels of MR are resized to meet the vehicle technical specifications.

The percentages of MR s selected for the study are as follows.

- Lightweighting level 0 (MR0): 0 percent (reference vehicle is sized)
- Lightweighting level 1 (MR1): 5 percent (inherited from reference vehicle)
- Lightweighting level 2 (MR2): 7.5 percent (inherited from reference vehicle)
- Lightweighting level 3 (MR3): 10 percent (vehicle is sized)
- Lightweighting level 4 (MR4): 15 percent (vehicle is sized)
- Lightweighting level 5 (MR5): 20 percent (vehicle is sized)

Heavy-Duty Pickups and Vans

For HDPUVs, lightweighting is applied to the reference glider weight specified earlier. The secondary effects of lightweighting (such as downsizing) are considered as part of the vehicle sizing algorithm. The percentages of MR s selected for the study are as follows.

- Lightweighting level 0 (MR0): 0 percent (reference vehicle is sized)
- Lightweighting level 1 (MR1): 1.4 percent (vehicle is sized)
- Lightweighting level 2 (MR2): 13.0 percent (vehicle is sized)

Aerodynamic Drag Reduction Technologies

Along with different levels of lightweighting, five levels of aerodynamic drag reduction have been applied. The percentages of aerodynamic drag reduction selected for the study are as follows for the LDV simulations.

- Aerodynamic drag reduction level 0 (AERO0): 0 percent
- Aerodynamic drag reduction level 1 (AERO1): 5 percent

- Aerodynamic drag reduction level 2 (AERO2): 10 percent
- Aerodynamic drag reduction level 3 (AERO3): 15 percent
- Aerodynamic drag reduction level 4 (AERO4): 20 percent

For the HDPUV simulations, the following aerodynamic drag reduction levels have been applied.

- Aerodynamic drag reduction level 0 (AERO0): 0 percent
- Aerodynamic drag reduction level 1 (AERO1): 10 percent
- Aerodynamic drag reduction level 2 (AERO2): 20 percent

Rolling Resistance Reduction Technologies

For this study, three levels of rolling resistance reduction have been applied for each vehicle configuration. The percentages of rolling resistance reduction selected for the study are as follows for LDV simulations.

- Rolling resistance reduction level 0 (ROLL0): 0 percent
- Rolling resistance reduction level 1 (ROLL1): 10 percent
- Rolling resistance reduction level 2 (ROLL2): 20 percent
- Rolling resistance reduction level 3 (ROLL3): 30 percent

For the HDPUV simulations, the following rolling resistance reduction levels have been applied.

- Rolling resistance reduction level 0 (ROLL0): 0 percent
- Rolling resistance reduction level 1 (ROLL1): 10 percent
- Rolling resistance reduction level 2 (ROLL2): 20 percent

Test Procedure and Energy Consumption Calculations

All simulations were performed in hot conditions. Cold-start penalties were assessed after the simulations, based on test data collected at AMTL and EPA published values. A two-cycle test procedure, based on the UDDS and HWFET drive cycles (EPA, 2023), was used.

Conventional Vehicles

The conventional vehicle test procedure follows the current EPA two-cycle test procedure (Southwest Research Institute, 2022).

The urban cycle for a non-hybrid vehicle (Figure 196) has four parts.

1. Bag 1: Cold start
2. Bag 2: Stop and go
3. Engine OFF
4. Bag 3: Hot start

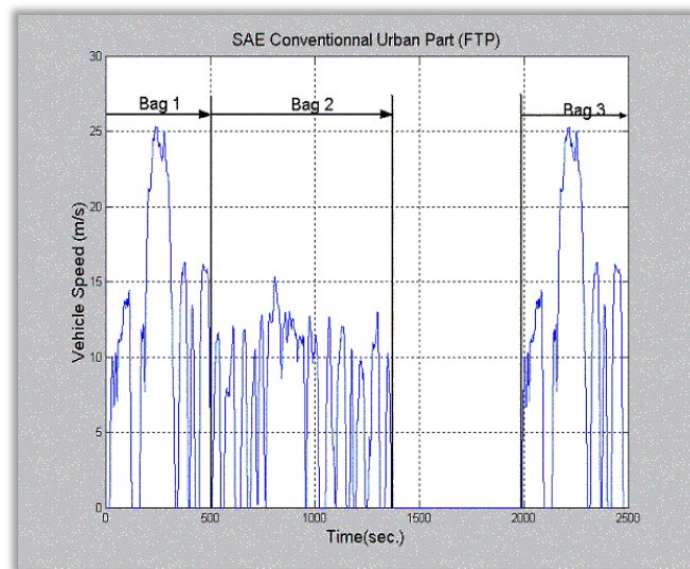


Figure 196. Urban cycle for a non-hybrid vehicle

The highway cycle for a non-hybrid vehicle has the HWFET (Figure 197).

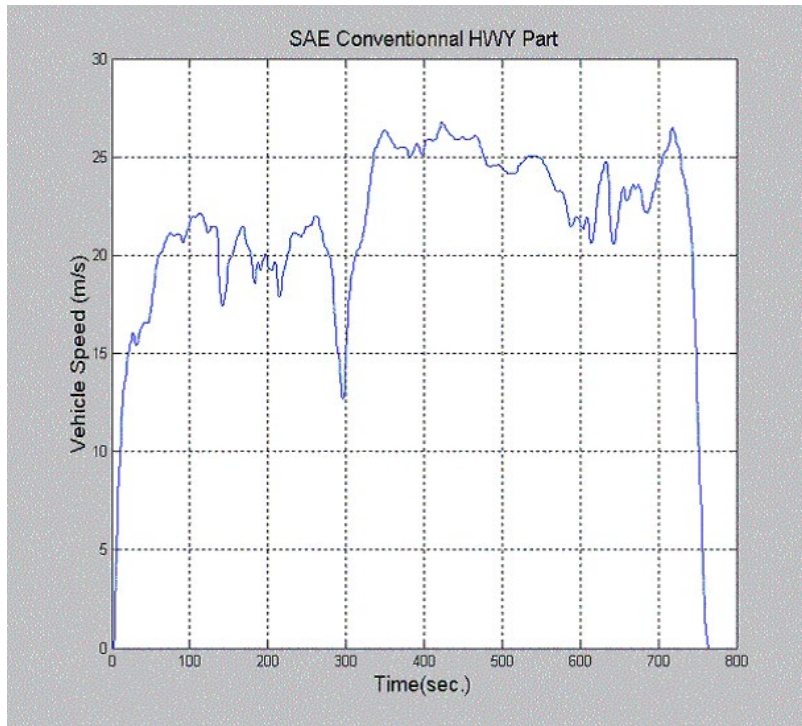


Figure 197. Highway cycle for a non-hybrid vehicle

Hybrid EVs

The HEV procedure is similar to the conventional vehicle procedure except that the drive cycles are repeated until the initial and final battery SOCs are within a tolerance of 0.5 percent (see Figure 198 and Figure 199), based on the SAE J1711 procedure (Douba, 2009). This procedure is used for mild hybrid BISG, split HEV, par HEV, and FC HEV vehicle powertrains.

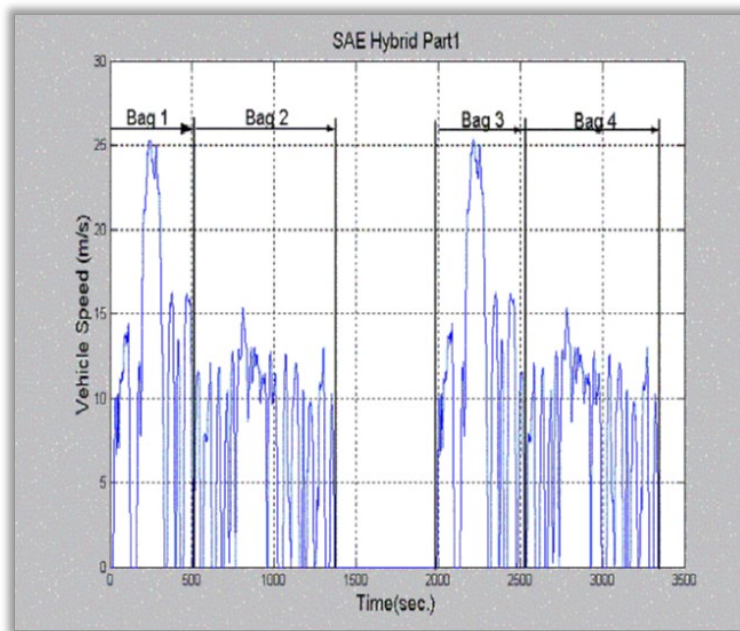


Figure 198. Urban cycle for a hybrid vehicle

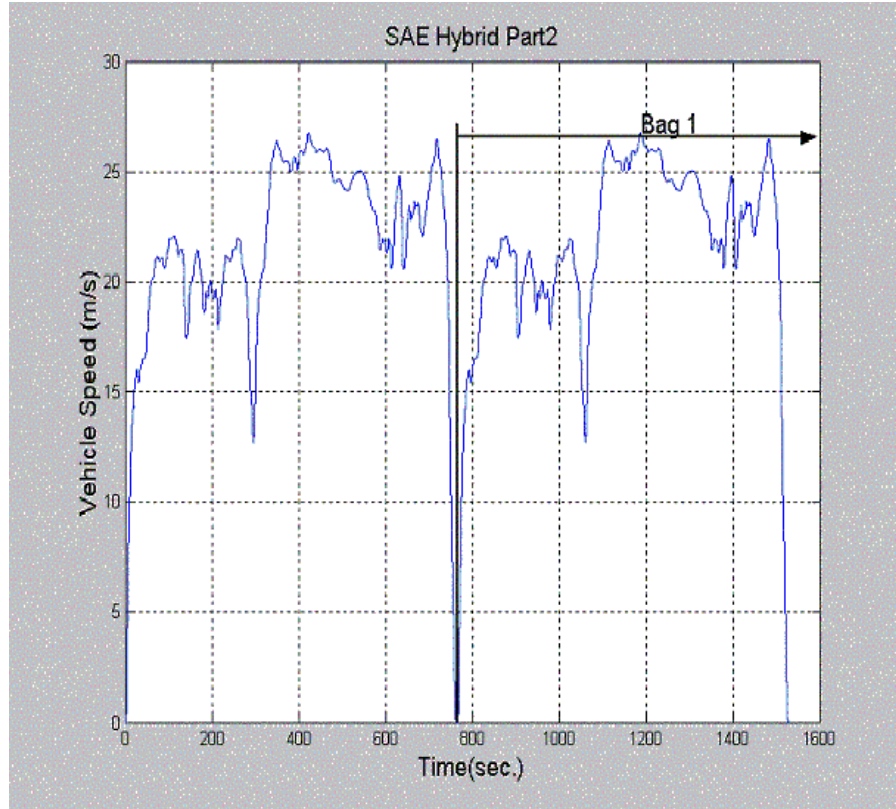


Figure 199. Highway cycle for a hybrid vehicle
(only the results from the second cycle were used)

Fuel Consumption

For the urban cycle, fuel consumption was computed using Equation 1.

$$(1) \text{ Fuel Consumption} = 0.43 \frac{V_{Fuel}^1 + V_{Fuel}^2}{Dist_1 + Dist_2} + 0.57 \frac{V_{Fuel}^3 + V_{Fuel}^Z}{Dist_3 + Dist_Z}$$

where:

V_{Fuel}^y = volume of fuel from Bag y

$Dist_y$ = distance driven by the vehicle for the Bag y part of the cycle

Z = Bag 2 for a non-hybrid vehicle and Bag 4 for a hybrid

The same equation was used to compute the gas-equivalent fuel consumption as well as the SOC-adjusted fuel consumption by replacing V_{Fuel} with the corresponding physical quantity.

The highway cycle results were the same as for an urban cycle, except for the hybrid case, in which only the results from Bag 1 were used to compute the values.

$$(2) \text{ Fuel Consumption} = \frac{V_{Fuel}^2}{Dist}$$

Combined Fuel Consumption

The combined fuel consumption is a weighted value lying between the urban and highway cycles.

$$(3) FC^{combined} = 0.55 \times FC^{urban} + 0.45 \times FC^{highway}$$

Plug-In HEVs

This section describes the methodology currently implemented in Autonomie for PHEVs. This procedure is used for split PHEV20, EREV PHEV50, par PHEV20, and par PHEV50 vehicle powertrains.

Charge Sustaining on the UDDS Cycle

The implementation is based on the J1711 procedure and is divided into several phases, as described below.

- Set battery SOC to charge sustaining (CS) value
- Run UDDS
- 10-minute soak with the key OFF
- Run UDDS
- Assume the cycle charge is balanced. Display warning if it does not meet 1 percent.

Weightings and Cold Factor Correction

The following equations show the cold compensation.

$$(4) M_{0-505}^* = \frac{M_{0-505}}{1 - CF_{75F}}$$

where:

M_{0-505} = fuel mass consumed during the time window between 0 and 505 s

CF_{75F} = cold-factor correction at 75 °F

M_{0-505}^* = cold-corrected mass of fuel

$$(5) Vol_{0-505}^* = \frac{M_{0-505}^*}{\delta_{gasoline}}$$

where:

Vol_{0-505}^* = volume of fuel consumed during the time window between 0 and 505 s

$\delta_{gasoline}$ = density of gasoline

Then FC^{UDDS} , the fuel consumed on the UDDS cycle, can be calculated:

$$(6) FC^{UDDS} = 0.43 \times \left(\frac{Vol_{0-505}^* + Vol_{506-1372}}{D_{0-505} + D_{506-1372}} \right) + 0.57 \times \left(\frac{Vol_{1972-2477} + Vol_{2478-3340}}{D_{1972-2477} + D_{2478-3340}} \right)$$

Charge Sustaining on the HWFET Cycle

- Set battery SOC to CS value
- Run HWFET
- Wait four seconds
- Run HWFET
- Assume the cycle is charge balanced
- Perform calculations on the second HWFET cycle

$$(7) FC^{HWFET} = \frac{Vol_{765-1529}}{D_{765-1529}}$$

where:

$Vol_{765-1529}$ = volume of fuel consumed during the time window between 765 and 1,529 s

$D_{765-1529}$ = distance traveled during the time window between 765 and 1,529 s

FC^{HWFET} = highway fuel consumption

Charge Depleting on the UDDS and HWFET Cycles

- The charge-depleting (CD) calculations are identical for the UDDS and HWFET cycles.
- Set battery SOC to full charge test initial SOC.
- Run UDDS (HWFET).
- Ten-minute soak with the key OFF (15-second pause with key ON).
- Run UDDS (HWFET).
- Ten-minute soak with the key off (15-second pause with key ON).
- Repeat until SOC reaches the CD/CS crossover point, and the last cycle is completed.
- Round down the number of cycles unless the CD range is less than one cycle. In that case, round up the number of cycles. At least one CD cycle is required to run the analysis.

Cold Weighting Calculation

The user specifies the number of cycles over which to apply the cold correction factor.

$$(8) N_{cold} = \min(N_{cold}^{user}, N_{cd})$$

$$(9) N_{hot} = N_{cd} - N_{cold}$$

where:

N_{cold} = number of cold cycles

N_{hot} = number of hot cycles

N_{cold}^{user} = number of user-specified cold cycles

N_{cd} = total number of CD cycles

$$(10) M_{cd} = \left[\frac{\alpha_{cold} M_{cd-cold}^1}{1-CF_{75F}}, \dots, \frac{\alpha_{cold} M_{cd-cold}^{N_{cold}}}{1-CF_{75F}}, \alpha_{hot} M_{cd-hot}^1, \dots, \alpha_{hot} M_{cd-hot}^{N_{hot}} \right]^T$$

where:

$M_{cd-cold}^1$ = mass of fuel consumed during the first cold CD cycle

$M_{cd-cold}^{N_{cold}}$ = mass of fuel consumed during the last cold CD cycle

CF_{75F} = cold-start fuel economy penalty at 75 °F

M_{cd-hot}^1 = mass of fuel consumed during the first hot CD cycle

$M_{cd-hot}^{N_{hot}}$ = mass of fuel consumed during the last hot CD cycle

α_{cold} = user-specified cold weighting factor (default value = 0.43)

α_{hot} = user-specified hot weighting factor (default value = 0.57)

M_{cd} = column vector of cold-corrected fuel mass

$$(11) Vol_{cd} = \frac{M_{cd}}{\delta_{gasoline}}$$

where:

Vol_{cd} = column vector of cold-corrected fuel volumes

Note that each element in the Vol_{cd} vector is divided by its respective distance:

$$(12) FC_{cd} = \frac{Vol_{cd}}{D_{udds}}$$

where:

FC_{cd} = column vector of cold-corrected fuel consumption

The net battery energy used was calculated for each cycle using the open-circuit voltage and the current:

$$(13) \text{ for } i = 1, \dots, N_{cd}; E_{cd}^i = \int_{(i-1)T_{udds}}^{(i)T_{udds}+t} V_{oc}(\tau) \times I(\tau) d\tau$$

where:

E_{cd}^i = net battery energy used during the i^{th} CD cycle

T_{udds} = duration of the UDDS cycle + soak time or (HWFET + 15 s)

i = index of the CD cycle

N_{cd} = total number of CD cycles

V_{oc} = open-circuit voltage as a function of time during the cycle

I = battery current as a function of time during the cycle

$$(14) E_{cd} = [E_{cd}^1, \dots, E_{cd}^{N_{cd}}]^T$$

where:

E_{cd} = column vector of net battery energy used on each cycle

Note that each element in the E_{cd} vector is divided by its respective distance.

$$(15) EC_{cd} = \frac{E_{cd}}{D_{udds} \times \eta_{chg}^{ess} \times \eta_{charger}}$$

where:

EC_{cd} = column vector of electrical energy consumption in AC-Joules (wall outlet)

D_{udds} = distance traveled on a UDDS (or $HWFET - D_{HWFET}$) cycle

η_{chg}^{ess} = user-definable efficiency of the battery during charging (default value = 0.99)

$\eta_{charger}$ = user-definable efficiency of the charger (wall or in-vehicle) (default value = 0.88)

$$(16) \text{ for } i = 1, \dots, N_{cd}; \mu_i = \mu(i \times D_{udds}^i) - \mu(i - 1) \times D_{udds}^i$$

$$\mu_{cd} = [\mu_1, \dots, \mu_{N_{cd}}]$$

where:

μ_{cd} = row vector of utility factors

μ_1 = utility factor on the first CD cycle

μ_i = utility factor on the i^{th} CD cycle

$\mu_{N_{cd}}$ = utility factor on the last CD cycle

μ = fleet mileage fraction utility factor as a function of distance

$$(17) FC = \mu_{cd}FC_{cd} + (1 - \sum_i^{N_{cd}} \mu_i)FC_{cs}$$

where:

FC = fuel consumed on the city or highway portion of the PHEV procedure

$$(18) EC = \mu_{cd}EC_{cd}$$

where:

EC = electrical energy consumed during the city or highway portion of the PHEV procedure

Battery Electric Vehicles

For BEVs the SAE J1634 test procedure (Pasquier et al., 2001) is followed: start the battery at full SOC and run until minimum SOC is reached. The electric consumption is then computed.

$$(19) \text{ Electric Consumption} = \frac{\int V_{oc} \times I_{ess}}{\eta_{ess} \eta_{charger}}$$

where:

η_{ess} = efficiency of the battery while charging

$\eta_{charger}$ = average efficiency of the charger while charging

V_{oc} = open-circuit voltage as a function of time over the cycle

I_{ess} = current as a function of time over the cycle

The SAE J1634 multi-cycle test consists of repeated UDDS and HWFET cycles combined with constant-speed driving phases. The drive cycles aided in determining the energy consumption

and range associated with specific and established driving patterns. The constant-speed driving schedules in the middle and the end of the test are intended to (1) reduce test duration by depleting the battery more rapidly than the established certification drive schedules, (2) improve the robustness of the energy determination by minimizing the impact of drive style variation, and (3) prevent inconsistent triggering of end-of-test criteria that can occur at high power demand points when a BEV is following a dynamic drive schedule at a low SOC.

Figure 200 illustrates how several drive cycles (i.e., UDDS, HFET, and constant-speed cycle) are combined in the combo MCT test.

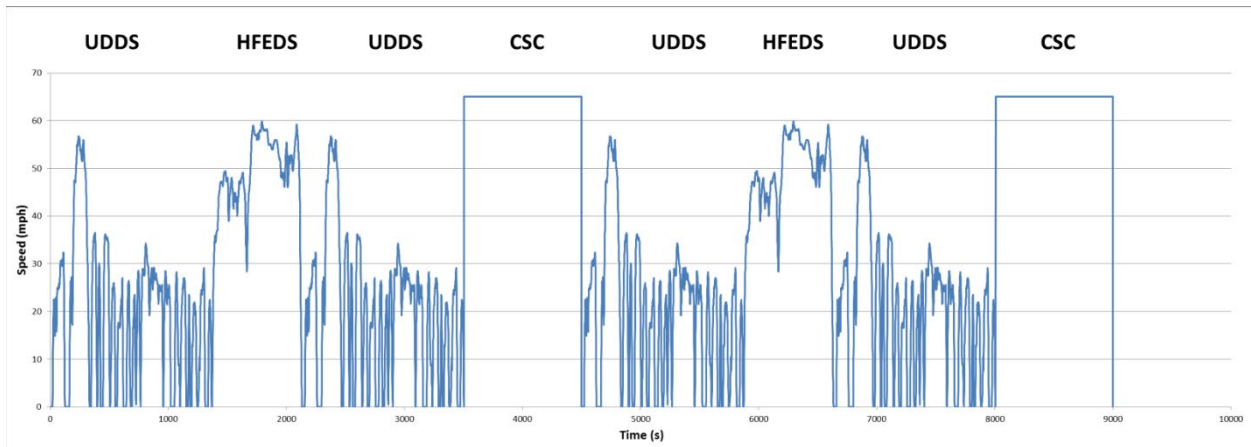


Figure 200. Multi-cycle test

The multi-cycle test enables the determination of the cycle-specific range as well as the measurement of the cycle-specific energy consumption. The range of the driving cycle is determined using both the energy consumption of the cycle and the usable battery energy of the vehicle.

Cold-Start Penalty

The EPA database of MY 2022 light-duty vehicles (EPA, 2019a) was analyzed for fuel economy values reported for the different bags. Following an average of the ratio of Bag 3 fuel economy to Bag 1 fuel economy, an appropriate cold-start penalty was selected. Figure 201 shows the ratio of Bag 3 fuel economy to Bag 1 fuel economy across different engine technologies for MY 2022 vehicles.

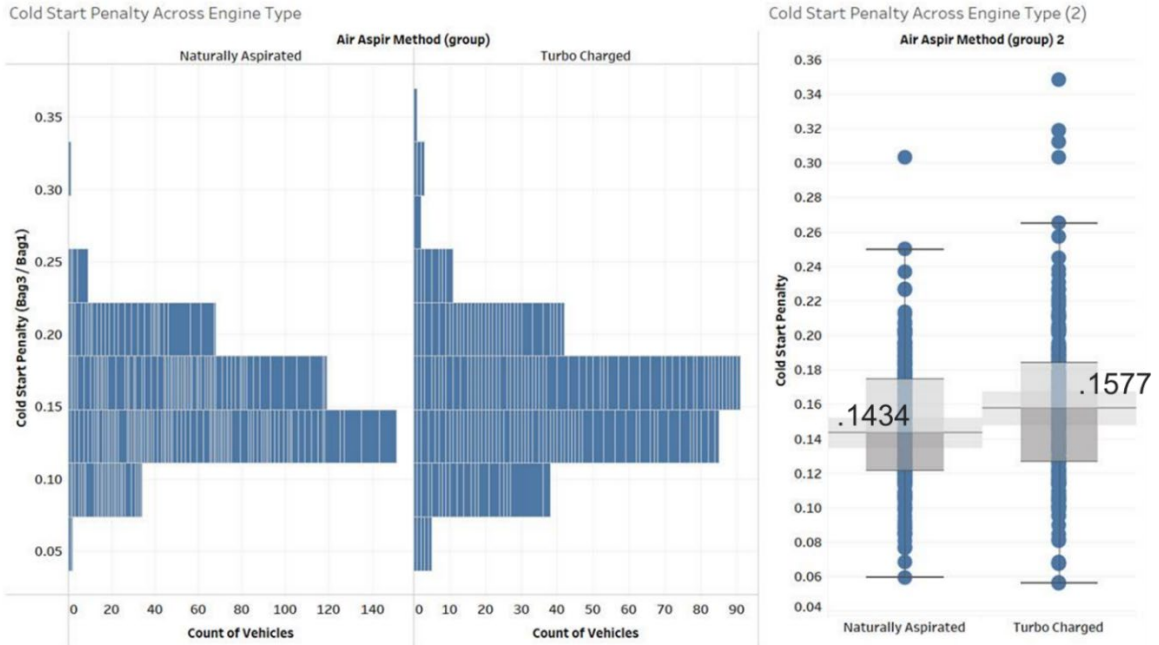


Figure 201. Cold-start penalty on Bag 1 across different engine types

The figure shows that different engine aspiration methods influence the cold-start penalty on Bag 1. We decided to separate out the cold-start penalty on Bag 1 fuel economy associated with the different engine types. In the same way, we evaluated the effect of the cold-start penalty on Bag 2, as shown in Figure 202.

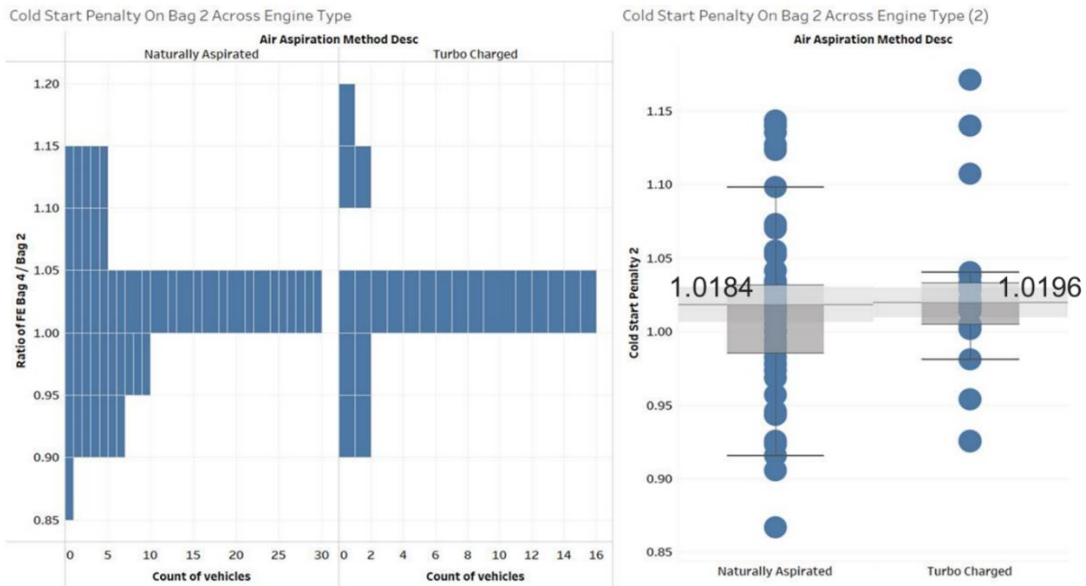


Figure 202. Cold-start penalty on Bag 2 across engine types

As with the case of the Bag 1 cold-start penalty, Figure 202 shows the influence of the different engine types on the additional cold-start penalty on Bag 2. Based on our detailed analysis, we

determined that we would use the combinations of cold-start penalties shown in Table 72 in FY22 runs for both light-duty vehicles and HDPUV.

Table 72. Cold-start penalty combinations

NA/TC	Bag	Penalty (%)
Naturally Aspirated	Bag 1	14.34
	Bag 2	1.84
Turbo-Charged	Bag 1	15.77
	Bag 2	1.96

The cold-start penalty was applied to fuel consumption during the FTP for conventional vehicles, HEVs, and PHEVs; 0 percent was applied for BEVs.

Vehicle Simulation Setup Process

Argonne’s large-scale simulation process was developed to run a very large number of vehicle simulations quickly and effectively, allowing Argonne to quickly respond to DOT requests by simulating any technology combination in any vehicle class. The following subsections describe the steps in the process.

Powertrain Template (LDV)

Powertrain templates contain basic information such as name, class, and technology, as well as component information such as battery technology, engine technology, and transmission type. To automate the differentiated process of the different powertrain options, three different templates are defined: conventional, parallel hybrids, and other hybrids (power-split HEV/PHEV, EREV, fuel cell, and BEV).

Each template contains seven tabs: Vehicle, Parameter, Control, Sizing, Run, Translation, and Assumptions. In each tab columns outline vehicle configurations.

Vehicle Tab

The Vehicle tab defines the initialization files, the component models required for each vehicle, and the vehicle configuration selected. The initialization files selected will depend on the CAFE decision tree selected and the technological combination nominated for that vehicle. Figure 203 shows the Vehicle tab of the conventional template.

	A	B	C	D
1				
2			Conventional	Micro Hybrid
3		Run Number	1	4
4		Template Vehicle (*_a_vehicle)	conv_a_vehicle	micro_a_vehicle
5		AUTONOMIE Vehicle File (*_b_vehicle)	conv_ClassName_EngName_TransName_Mrname_AEROName_RollName_a_vehicle	micro_ClassName_EngName_TransName_Mrname_AEROName_RollName_a_vehicle
6	drv_ctrl	model		
7	drv_ctrl	init		
8	env	model		
9	env	init		
10	vpb	init		
11	vpb	preproc		
12	str_ctrl	model		
13	str_ctrl	init		
14	str_plant	model		
15	str_plant	init		
16	eng_ctrl	model		
17	eng_ctrl	init		
18	eng_ctrl	preproc		
19	eng_ctrl.dmd	model		
20	eng_ctrl.dmd	init		
21	eng_ctrl.dmd	preproc		
22	eng_ctrl.cstr	model		
23	eng_ctrl.cstr	init		
24	eng_ctrl.cstr	preproc		
25	eng_ctrl.trn	model		
26	eng_ctrl.trn	init		
27	eng_ctrl.trn	preproc		
28	eng_ctrl.cmd	model		
29	eng_ctrl.cmd	init		
30	eng_ctrl.cmd	preproc		
31	eng_plant	model		
32	eng_plant	init	EngFile	EngFile
33	eng_plant	scale		
34	eng_plant	preproc		
35	exh_plant	model		
36	exh_plant	init		
37	exh_plant	preproc		
38	accmech_plant	model		
39	accmech_plant	init		

Figure 203. Vehicle tab of conventional template

Parameter Tab

The Parameter tab of the template defines the values of the components specific to the vehicle designated (e.g., power, weight, and performance constraints). Figure 204 shows the Parameter tab of the conventional template.

	A	B	C	D	E	F
7						
8						
9			Conventional	Micro Hybrid	Mild Hybrid BISG	Mild Hybrid CISG
10		Run Number	1	4	10	13
11						
12	Configuration					
13	Specific Comments (i.e. FC files, high case,...)					
14			Mrname	Mrname	Mrname	Mrname
15	AUTONOMIE Vehicle File (*.a_vehicle)					
16			conv_EngName_TransName_Mrname_AEROname_RollName.a_vehicle	micro_EngName_TransName_Mrname_AEROname_RollName.a_vehicle	bisg_EngName_TransName_Mrname_AEROname_RollName.a_vehicle	cisg_EngName_TransName_Mrname_AEROname_RollName.a_vehicle
17	Sizing					
18	AutoSizing		SizingType	Inherited	Inherited	Inherited
19	PerfoCategory		PerfoCategory	PerfoCategory	PerfoCategory	PerfoCategory
20	Vehicle Class		ClassName	ClassName	ClassName	ClassName
21	Vehicle Config		Conventional	Micro Hybrid	Mild Hybrid BISG	Mild Hybrid CISG
22	Engine Type		EngName	EngName	EngName	EngName
23	Mass Reduction Type		Mrname	Mrname	Mrname	Mrname
24	Mass Reduction Percentage		MRValue	MRValue	MRValue	MRValue
25	AERO Type		AEROname	AEROname	AEROname	AEROname
26	AERO Reduction Percentage		AEROValue	AEROValue	AEROValue	AEROValue
27	Rolling Resistance Type		RollName	RollName	RollName	RollName
28	Rolling Resistance Reduction Percentage		ROLLValue	ROLLValue	ROLLValue	ROLLValue
29	Constraints					
30	Acceleration					
31	From	mph	0	0	0	0
32	To	mph	60	60	60	60
33	In	sec	p_time	p_time	p_time	p_time
34	Shifting Time	sec	0.45	0.45	0.45	0.45
35	Constraints					
36	Passing Acceleration					
37	Passing From	mph	50	50	50	50
38	Passing To	mph	80	80	80	80
39	Passing In	sec	p_time	p_time	p_time	p_time
40	Perc. of peak power required to meet VTS					
41	Engine or fuel cell sized to meet X%	%	70	70	70	70
42	Grade					
43	Minimum	%	6	6	6	6
44	At Speed	mph	65	65	65	65
45	Use Grade Mass equation		Yes	Yes	Yes	Yes
46	Maximum Payload	kg	payload_mass	payload_mass	payload_mass	payload_mass
47	Maximum Towing	kg	towing_mass	towing_mass	towing_mass	towing_mass
48	Max Vehicle Speed must be at least	mph	110	110	110	110
49	Range					
50	UDDS Fuel Range	miles	320	320	320	320
51	UDDS EV Range	miles				

Figure 204. Parameter tab of conventional template

Control Tab

The Control tab selects the appropriate controller for the designated vehicle. Figure 205 shows the Control tab of the hybrid template.

	A	B	G	I	L
			Split SI	Split SI - 20mi AER	Erev SI - 50mi AER
1		Run Number	16	22	29
4	conso	vpc_prop		vpc_prop.init.ev_only	vpc_prop.init.ev_only
5	conso	vpc_prop		0	0
6	conso	vpc_prop		vpc_prop.init.stop_at_low_soc	vpc_prop.init.stop_at_low_soc
7	conso	vpc_prop		1	1
8	conso	vpc_prop		vpc_prop.init.whl_pwr_above_eng_turn_on_map_pwr6	vpc_prop.init.whl_pwr_above_eng_turn_on_map_pwr6
9	conso	vpc_prop		20000	20000
10	conso	vpc_prop		vpc_prop.init.whl_pwr_below_eng_turn_off_multiplier	vpc_prop.init.whl_pwr_below_eng_turn_off_multiplier
11	conso	vpc_prop		0.25	0.25
12	conso	vpc_prop		vpc_prop.init.whl_pwr_above_eng_turn_on_map_pwr	vpc_prop.init.whl_pwr_above_eng_turn_on_map_pwr7
13	conso	vpc_prop		20000	20000
14	conso	gb.ctrl.trns			
15	conso	gb.ctrl.trns			
16	conso	gb.ctrl.dmd			
17	conso	gb.ctrl.dmd			
18	conso	gb.ctrl.dmd			
19	conso	gb.ctrl.dmd			
20	conso	gb.ctrl.dmd			
21	conso	gb.ctrl.dmd			
22	ev_only	vpc_prop		vpc_prop.init.ev_only	vpc_prop.init.ev_only
23	ev_only	vpc_prop		1	1
24	ev_only	vpc_prop		vpc_prop.init.stop_at_low_soc	vpc_prop.init.stop_at_low_soc
25	ev_only	vpc_prop		1	1
26	ev_only	vpc_prop			
27	ev_only	vpc_prop			
28	ev_only	vpc_prop			
29	ev_only	vpc_prop			
30	ev_only	gb.ctrl.trns			
31	ev_only	gb.ctrl.trns			
32	ev_only	gb.ctrl.trns			
33	ev_only	gb.ctrl.trns			
34	ev_only	gb.ctrl.trns			
35	ev_only	gb.ctrl.trns			
36	ev_only	gb.ctrl.trns			
37	ev_only	gb.ctrl.trns			
38	ev_only	gb.ctrl.dmd			
39	ev_only	gb.ctrl.dmd			
40	perfo	vpc_prop		vpc_prop.init.ev_only	vpc_prop.init.ev_only
41	perfo	vpc_prop		0	0
42	perfo	vpc_prop			
43	perfo	vpc_prop			
44	perfo	vpc_prop			
45	perfo	vpc_prop			
46	perfo	gb.ctrl.trns			
47	perfo	gb.ctrl.trns			
48	perfo	gb.ctrl.trns			
49	perfo	gb.ctrl.trns			
50	perfo	gb.ctrl.trns			
51	perfo	gb.ctrl.trns			
52	perfo	gb.ctrl.dmd			
53	perfo	gb.ctrl.dmd			
54	perfo	gb.ctrl.dmd			
55	perfo	gb.ctrl.dmd			

Figure 205. Control tab of hybrid template

Sizing Tab

The Sizing tab selects the appropriate sizing rule to size each component to match the required vehicle technical specifications. Figure 206 shows the Sizing tab of the hybrid template.

	A	B	G	J	L	M	N	O
1			Split SI	Split SI - 30mi AER	Erev SI - 50mi AER	FC HEV	BEV - 100	
2		Run Number	16	25	29	75	93	
3	AUTONOMIE Vehicle File (*.a_vehicle)							
4	Rule							
5	rule file	rule_file	_split_IVM_60mph_mot_70p_of_peak_eng_pEVXX_simu_test_70p_of_pei_PHEVXX_simu_70p_of_pei_fc_IVM_60mph_mot_70p_of_pesr_elec_simu_passing					
6	Power							
7	Grade	grade_compo	eng	eng	eng	fc	mot_ess	
8	Acceleration	accel_compo	mot_eng	mot_eng	mot_eng	mot_fc	mot_ess	
9	Regen	regen_compo	mot_ess			mot_ess		
10	EV Only	ev_only_compo		mot_ess	mot_ess		mot_ess	
11	Energy							
12	Range	range_compo		ess	ess		ess	
13	Sizing Cycle for Regen / EV Only / Range							
14	Name	cycle_pwr_name	UDDS	UDDS	US06	US06	US06	
15	File	cycle_pwr_file	fuds1.mat	fuds1.mat	us06.mat	us06.mat	us06.mat	
16	Repair	cycle_pwr_number	1	1	1	1	1	
17	Scale	cycle_pwr_scale	1	1	1	1	1	
18	Grade	cycle_pwr_grade	0	0	0	0	0	
19	Sizing Cycle for EV Only Energy / Fuel Range							
20	Name	cycle_nrg_name	UDDS	UDDS	UDDS	UDDS	UDDS	
21	File	cycle_nrg_file	fuds1.mat	fuds1.mat	fuds1.mat	fuds1.mat	fuds1.mat	
22	Repair	cycle_nrg_number	1	1	1	1	1	
23	Scale	cycle_nrg_scale	1	1	1	1	1	
24	Grade	cycle_nrg_grade	0	0	0	0	0	
25	Control							
26	CD Range	ctrl_tuning		yes	yes			
27								

Figure 206. Sizing tab of hybrid template

Run Tab

The Run tab selects the drive cycle/procedure to be simulated for each powertrain option. Figure 207 shows the Run tab of the hybrid template.

	A	B	C	H	J	M	N	O
1				Split SI	Split SI - 30mi AER	Erev SI - 50mi AER	FC HEV	BEV - 100
2		Run Number		16	22	29	75	93
3		Cycle 1						
4		cycle1	name	US06	US06	US06	US06	US06
5		cycle1	file	us06.mat	us06.mat	us06.mat	us06.mat	us06.mat
6		cycle1	number	1	1	1	1	1
7		cycle1	scale	1	1	1	1	1
8		cycle1	grade	0	0	0	0	0
9		Cycle 2						
10		cycle2	name	Accel	Accel	Accel	Accel	Accel
11		cycle2	file	accel.mat	accel.mat	accel.mat	accel.mat	accel.mat
12		cycle2	number	1	1	1	1	1
13		cycle2	scale	1	1	1	1	1
14		cycle2	grade	0	0	0	0	0
15		Cycle 3						
16		cycle3	name					
17		cycle3	file					
18		cycle3	number					
19		cycle3	scale					
20		cycle3	grade					
21		Cycle 4						
22		cycle4	name					
23		cycle4	file					
24		cycle4	number					
25		cycle4	scale					
26		cycle4	grade					
27		Cycle 5						
28		cycle5	name					
29		cycle5	file					
30		cycle5	number					
31		cycle5	scale					
32		cycle5	grade					
33		Procedure						
34		test_procedure	name	lined Procedure (FTP+HWFT) with 1	PHEV Preliminary Procedures	PHEV Preliminary Procedures	lined Procedure (FTP+HWFT) with 1	BEV Procedure
35		test_procedure	cold_start_penalty_mvnet	15	15	15	15	0
36		test_procedure	cold_start_penalty_udds					
37		test_procedure	cold_start_penalty_nbr_cycle					
38		test_procedure	charger_eff		96	96		96
39								
40								
41								
42								
43								
44								

Figure 207. Run tab of hybrid template

Translation Tab

The Translation tab, shown in Figure 208, translates and transfers inputs into Autonomie to build the vehicle model.

	location	component	variable type	variable name	location	component	variable type	variable name
Sizing								
AutoSizing	drivetrain	vpa	param_var	vpa.init.isSized	sizing	struct	isSized	
PerfoCategory	drivetrain	vpa	param_var	vpa.init.veh_PerfoCategory				
Vehicle Class	drivetrain	vpa	param_var	vpa.init.veh_class_name				
Vehicle Config	drivetrain	vpa	param_var	vpa.init.veh_config_type				
Engine Type	drivetrain	eng.plant	param_var	eng.plant.init.type				
Mass Reduction Type	drivetrain	vpa	param_var	vpa.init.veh_MR				
Mass Reduction Percentage	drivetrain	vpa	param_var	vpa.init.veh_MR_percentage_reduc				
AERO Type	drivetrain	vpa	param_var	vpa.init.veh_AERO				
AERO Reduction Percentage	drivetrain	vpa	param_var	vpa.init.veh_AERO_percentage_reduc				
Rolling Resistance Type	drivetrain	vpa	param_var	vpa.init.veh_ROLL				
Rolling Resistance Reduction Percentage	drivetrain	vpa	param_var	vpa.init.veh_ROLL_percentage_reduc				
Constraints								
Acceleration								
From	sizing	accel	from					
To	sizing	accel	to					
In	sizing	accel	time					
Shifting Time	sizing	accel	shift_time					
Constraints								
Passing Acceleration								
Passing From	sizing	passing	from					
Passing To	sizing	passing	to					
Passing In	sizing	passing	time					
Perc of peak power required to meet VTS								
Engine or fuel cell sized to meet X%	sizing	constraints	peak_pwr_perc					
Grade								
Minimum	sizing	grade	percent					
At Speed	sizing	grade	speed					
Use Grade Mass equation	sizing	grade	use_gvw_equation					
Maximum Payload	drivetrain	vpa	param_var	veh.plant.init.payload_mass	sizing	grade	max_payload	
Maximum Towing	drivetrain	vpa	param_var	veh.plant.init.towing_mass	sizing	grade	max_towing	
Max Vehicle Speed must be at least	sizing	speed	max					
Range								
UDDS Fuel Range	sizing	range	fuel					
UDDS EV Range	sizing	range	ev					
SOC								
Electrical Only								
EV SOC Init ESS #1	sizing	soc	ev_max					
EV SOC Final ESS #1	sizing	soc	ev_min					
Charge Depleting / Blending Mode								
CD SOC Init ESS #1	sizing	soc	cd_max					

Figure 208. Translation tab of template

Vehicle Assumption Template (HDPUV)

Vehicle assumption templates contain basic information such as name, class, and technology, as well as component information such as battery technology, engine technology, and transmission type. An automated process has been developed to read and write vehicle attributes and performance assumptions into reference vehicle files to minimize manual inputs. The code reads the different vehicle attributes and weight and updates the reference vehicle file for each powertrain and each vehicle class.

The assumption template has seven tabs: Vehicle, Parameter, Control, Sizing, Run, Translation, and Assumptions. In each tab, columns outline vehicle configurations.

Baseline Specs Tab

The Baseline Specs tab defines the values of vehicle characteristics for the vehicle designated (e.g., drag coefficient, frontal area, and wheel rolling resistance). Figure 209 shows the Baseline Specs tab of the assumption template sheet.

	A	B	C	D	E	F	G	H	I	J
1	Class		Purpose	Regulatory Code	Frontal Area (square m)	Drag Coefficient (Cd)	Acc Load (W)	Rolling Resistance (Effective)	Payload (kg)	Glider Mass (kg)
2	2b	Van	Medium		5.38	0.50	1000	0.009	2200	1600
3	2b	Pickup	Medium		3.95	0.50	1000	0.009	1800	2000
4	3	Van	Medium		5.60	0.60	1000	0.009	3400	1900
5	3	Pickup	Medium		3.95	0.50	1000	0.009	3200	2100

Figure 209. Baseline specs tab of assumption template

Sizing Tab

The Sizing tab defines the specific vehicle performance requirements for each vehicle class and purpose. The vehicle models are sized to targets specified in this tab. Figure 210 shows the Sizing tab of the assumption template.

	A	B	C	D	E	F	G	H	I	J	K	L	M	N	O	P	Q	R	S	T
1	Class		Purpose	Regulatory Code	Powertrain	0-30mph (s)	0-60mph (s)	Grade Speed (mph)	Parcom Grade	Cruise Speed (mph)	Cruise Grade (%)	Max Speed (mph)	Stability (%)	Taxi Weight (lb)	Towing Weight (lb)	EV Range (mi/eq)	Daily Driving Range (mi/eq)	Range Cycle		
2	2b	Van	Medium	Conv	7	16	50	6	70	1.5	75	20	10000	6000	0	250	EPA_Phase2_55mph_rep5.a_cycle			
3	2b	Van	Medium	Micro	7	16	50	6	70	1.5	75	20	10000	6000	0	250	EPA_Phase2_55mph_rep5.a_cycle			
4	2b	Van	Medium	ISG	7	16	50	6	70	1.5	75	20	10000	6000	0	250	EPA_Phase2_55mph_rep5.a_cycle			
5	2b	Van	Medium	ParHEV	7	16	50	6	70	1.5	75	20	10000	6000	0	250	EPA_Phase2_55mph_rep5.a_cycle			
6	2b	Van	Medium	ParPHEV	7	16	50	6	70	1.5	75	20	10000	6000	50	250	EPA_Phase2_55mph_rep5.a_cycle			
7	2b	Van	Medium	FCV	7	16	50	6	70	1.5	75	20	10000	6000	250	250	EPA_Phase2_55mph_rep5.a_cycle			
8	2b	Van	Medium	BEV1	7	16	50	6	70	1.5	75	20	10000	6000	150	150	EPA_Phase2_55mph_rep5.a_cycle			
9	2b	Van	Medium	BEV2	7	16	50	6	70	1.5	75	20	10000	6000	250	250	EPA_Phase2_55mph_rep5.a_cycle			
10	2b	Pickup	Medium	Conv	7	13	65	6	70	1.5	75	20	10000	15000	0	300	EPA_Phase2_55mph_rep5.a_cycle			
11	2b	Pickup	Medium	Micro	7	13	65	6	70	1.5	75	20	10000	15000	0	300	EPA_Phase2_55mph_rep5.a_cycle			
12	2b	Pickup	Medium	ISG	7	13	65	6	70	1.5	75	20	10000	15000	0	300	EPA_Phase2_55mph_rep5.a_cycle			
13	2b	Pickup	Medium	ParHEV	7	13	65	6	70	1.5	75	20	10000	15000	0	300	EPA_Phase2_55mph_rep5.a_cycle			
14	2b	Pickup	Medium	ParPHEV	7	13	65	6	70	1.5	75	20	10000	15000	50	300	EPA_Phase2_55mph_rep5.a_cycle			
15	2b	Pickup	Medium	FCV	7	13	65	6	70	1.5	75	20	10000	15000	300	300	EPA_Phase2_55mph_rep5.a_cycle			
16	2b	Pickup	Medium	BEV1	7	13	65	6	70	1.5	75	20	10000	15000	200	200	EPA_Phase2_55mph_rep5.a_cycle			
17	2b	Pickup	Medium	BEV2	7	13	65	6	70	1.5	75	20	10000	15000	300	300	EPA_Phase2_55mph_rep5.a_cycle			
18	3	Van	Medium	Conv	7	20	50	6	65	1.5	70	20	14000	6500	0	250	EPA_Phase2_55mph_rep5.a_cycle			
19	3	Van	Medium	Micro	7	20	50	6	65	1.5	70	20	14000	6500	0	250	EPA_Phase2_55mph_rep5.a_cycle			
20	3	Van	Medium	ISG	7	20	50	6	65	1.5	70	20	14000	6500	0	250	EPA_Phase2_55mph_rep5.a_cycle			
21	3	Van	Medium	ParHEV	7	20	50	6	65	1.5	70	20	14000	6500	0	250	EPA_Phase2_55mph_rep5.a_cycle			
22	3	Van	Medium	ParPHEV	7	20	50	6	65	1.5	70	20	14000	6500	50	250	EPA_Phase2_55mph_rep5.a_cycle			
23	3	Van	Medium	FCV	7	20	50	6	65	1.5	70	20	14000	6500	250	250	EPA_Phase2_55mph_rep5.a_cycle			
24	3	Van	Medium	BEV1	7	20	50	6	65	1.5	70	20	14000	6500	150	150	EPA_Phase2_55mph_rep5.a_cycle			
25	3	Van	Medium	BEV2	7	20	50	6	65	1.5	70	20	14000	6500	250	250	EPA_Phase2_55mph_rep5.a_cycle			

Figure 210. Sizing tab of assumption template

Engine Tab

The Engine tab provides the engine data files according to the technology selection. Similarly, in the Driveline, Motor, Wheel, and Battery tabs, the data/information for each component is provided for the purpose of vehicle model building. The initialization files selected will depend on the CAFE or HDPUV decision tree selected and the technological combination for that vehicle.

Figure 211 shows the Engine tab of the assumption template.

	A	B	C	D	E	F	G
1	Class	Purpose	Regulatory Code	Powertrain	Engine Type	Fuel	Engine Init Files
2	2b	Van	Medium	Conv	eng4a	Gasoline	eng_plant_swri_gasoline_7pt3L_HD7pt3_Baseline_2020_Ford
3	2b	Van	Medium	Conv	eng4b	Gasoline	eng_plant_swri_gasoline_7pt3L_HD7pt3_GDI_CR11p5_2020_Ford
4	2b	Van	Medium	Conv	eng4c	Gasoline	eng_plant_swri_gasoline_7pt3L_HD7pt3_GDI_CR11p5_CDA_2020_Ford
5	2b	Van	Medium	Conv	eng4d	Gasoline	eng_plant_swri_gasoline_7pt3L_HD7pt3_GDI_turbo_VVA_4V_2020_Ford
6	2b	Van	Medium	Conv	eng3a	Diesel	eng_plant_swri_diesel_3L_MDHD3_Duramax_LM2
7	2b	Van	Medium	Conv	eng3c	Diesel	eng_plant_swri_diesel_3L_MDHD3_Duramax_LM2_cylinderdeac
8	2b	Van	Medium	Micro	eng4a	Gasoline	eng_plant_swri_gasoline_7pt3L_HD7pt3_Baseline_2020_Ford
9	2b	Van	Medium	Micro	eng4b	Gasoline	eng_plant_swri_gasoline_7pt3L_HD7pt3_GDI_CR11p5_2020_Ford
10	2b	Van	Medium	Micro	eng4c	Gasoline	eng_plant_swri_gasoline_7pt3L_HD7pt3_GDI_CR11p5_CDA_2020_Ford
11	2b	Van	Medium	Micro	eng4d	Gasoline	eng_plant_swri_gasoline_7pt3L_HD7pt3_GDI_turbo_VVA_4V_2020_Ford
12	2b	Van	Medium	Micro	eng3a	Diesel	eng_plant_swri_diesel_3L_MDHD3_Duramax_LM2
13	2b	Van	Medium	Micro	eng3c	Diesel	eng_plant_swri_diesel_3L_MDHD3_Duramax_LM2_cylinderdeac
14	2b	Van	Medium	ISG	eng4a	Gasoline	eng_plant_swri_gasoline_7pt3L_HD7pt3_Baseline_2020_Ford
15	2b	Van	Medium	ISG	eng4b	Gasoline	eng_plant_swri_gasoline_7pt3L_HD7pt3_GDI_CR11p5_2020_Ford
16	2b	Van	Medium	ISG	eng4c	Gasoline	eng_plant_swri_gasoline_7pt3L_HD7pt3_GDI_CR11p5_CDA_2020_Ford
17	2b	Van	Medium	ISG	eng4d	Gasoline	eng_plant_swri_gasoline_7pt3L_HD7pt3_GDI_turbo_VVA_4V_2020_Ford
18	2b	Van	Medium	ISG	eng3a	Diesel	eng_plant_swri_diesel_3L_MDHD3_Duramax_LM2
19	2b	Van	Medium	ISG	eng3c	Diesel	eng_plant_swri_diesel_3L_MDHD3_Duramax_LM2_cylinderdeac
20	2b	Van	Medium	ParHEV	eng4b	Gasoline	eng_plant_swri_gasoline_7pt3L_HD7pt3_GDI_CR11p5_2020_Ford
21	2b	Van	Medium	ParPHEV	eng4b	Gasoline	eng_plant_swri_gasoline_7pt3L_HD7pt3_GDI_CR11p5_2020_Ford
22	2b	Van	Medium	FCV	NA	NA	NA
23	2b	Van	Medium	BEV1	NA	NA	NA
24	2b	Van	Medium	BEV2	NA	NA	NA
25	2b	Pickup	Medium	Conv	eng4a	Gasoline	eng_plant_swri_gasoline_7pt3L_HD7pt3_Baseline_2020_Ford

Figure 211. Engine tab of assumption template

Reference Vehicles Tab

The Reference Vehicle tab provides the basic model and “a_vehicle” files used for each technology selection. Figure 212 shows the the Reference Vehicles tab of the assumption template.

	A	B	C	D	E	F	G	H	I	J	K
1	Class	Purpose	Powertrain	Regulatory Code	Engine Type	Fuel	Autonomie rad vehicle	Procedure	Initfile	Is Inherited	Include p
2	2b	Van	Conv	Medium	eng4a	Gasoline	conv_si_au_su_volpe.a_vehicle	EPA_MDHD_Phase2.a_process	Sizing_Init_HD_Conv_volpe	No	Yes
3	2b	Van	Conv	Medium	eng4b	Gasoline	conv_si_au_su_volpe.a_vehicle	EPA_MDHD_Phase2.a_process	Sizing_Init_HD_Conv_volpe	No	Yes
4	2b	Van	Conv	Medium	eng4c	Gasoline	conv_si_au_su_deac_volpe.a_vehicle	EPA_MDHD_Phase2.a_process	Sizing_Init_HD_Conv_volpe	No	Yes
5	2b	Van	Conv	Medium	eng4d	Gasoline	conv_si_au_su_turbo_volpe.a_vehicle	EPA_MDHD_Phase2.a_process	Sizing_Init_HD_Conv_volpe	No	Yes
6	2b	Van	Conv	Medium	eng3a	Diesel	conv_su_au_volpe.a_vehicle	EPA_MDHD_Phase2.a_process	Sizing_Init_HD_Conv_volpe	No	Yes
7	2b	Van	Conv	Medium	eng3c	Diesel	conv_su_au_deac_volpe.a_vehicle	EPA_MDHD_Phase2.a_process	Sizing_Init_HD_Conv_volpe	No	Yes
8	2b	Pickup	Conv	Medium	eng4a	Gasoline	conv_si_au_su_volpe.a_vehicle	EPA_MDHD_Phase2.a_process	Sizing_Init_HD_Conv_volpe	No	Yes
9	2b	Pickup	Conv	Medium	eng4b	Gasoline	conv_si_au_su_volpe.a_vehicle	EPA_MDHD_Phase2.a_process	Sizing_Init_HD_Conv_volpe	No	Yes
10	2b	Pickup	Conv	Medium	eng4c	Gasoline	conv_si_au_su_deac_volpe.a_vehicle	EPA_MDHD_Phase2.a_process	Sizing_Init_HD_Conv_volpe	No	Yes
11	2b	Pickup	Conv	Medium	eng4d	Gasoline	conv_si_au_su_turbo_volpe.a_vehicle	EPA_MDHD_Phase2.a_process	Sizing_Init_HD_Conv_volpe	No	Yes
12	2b	Pickup	Conv	Medium	eng1a	Diesel	conv_su_au_volpe.a_vehicle	EPA_MDHD_Phase2.a_process	Sizing_Init_HD_Conv_volpe	No	Yes
13	2b	Pickup	Conv	Medium	eng1c	Diesel	conv_su_au_deac_volpe.a_vehicle	EPA_MDHD_Phase2.a_process	Sizing_Init_HD_Conv_volpe	No	Yes
14	3	Van	Conv	Medium	eng4a	Gasoline	conv_si_au_su_volpe.a_vehicle	EPA_MDHD_Phase2.a_process	Sizing_Init_HD_Conv_volpe	No	Yes
15	3	Van	Conv	Medium	eng4b	Gasoline	conv_si_au_su_volpe.a_vehicle	EPA_MDHD_Phase2.a_process	Sizing_Init_HD_Conv_volpe	No	Yes
16	3	Van	Conv	Medium	eng4c	Gasoline	conv_si_au_su_deac_volpe.a_vehicle	EPA_MDHD_Phase2.a_process	Sizing_Init_HD_Conv_volpe	No	Yes
17	3	Van	Conv	Medium	eng4d	Gasoline	conv_si_au_su_turbo_volpe.a_vehicle	EPA_MDHD_Phase2.a_process	Sizing_Init_HD_Conv_volpe	No	Yes
18	3	Van	Conv	Medium	eng3a	Diesel	conv_su_au_volpe.a_vehicle	EPA_MDHD_Phase2.a_process	Sizing_Init_HD_Conv_volpe	No	Yes
19	3	Van	Conv	Medium	eng3c	Diesel	conv_su_au_deac_volpe.a_vehicle	EPA_MDHD_Phase2.a_process	Sizing_Init_HD_Conv_volpe	No	Yes
20	3	Pickup	Conv	Medium	eng4a	Gasoline	conv_si_au_su_volpe.a_vehicle	EPA_MDHD_Phase2.a_process	Sizing_Init_HD_Conv_volpe	No	Yes
21	3	Pickup	Conv	Medium	eng4b	Gasoline	conv_si_au_su_volpe.a_vehicle	EPA_MDHD_Phase2.a_process	Sizing_Init_HD_Conv_volpe	No	Yes
22	3	Pickup	Conv	Medium	eng4c	Gasoline	conv_si_au_su_deac_volpe.a_vehicle	EPA_MDHD_Phase2.a_process	Sizing_Init_HD_Conv_volpe	No	Yes
23	3	Pickup	Conv	Medium	eng4d	Gasoline	conv_si_au_su_turbo_volpe.a_vehicle	EPA_MDHD_Phase2.a_process	Sizing_Init_HD_Conv_volpe	No	Yes
24	3	Pickup	Conv	Medium	eng1a	Diesel	conv_su_au_volpe.a_vehicle	EPA_MDHD_Phase2.a_process	Sizing_Init_HD_Conv_volpe	No	Yes
25	3	Pickup	Conv	Medium	eng1c	Diesel	conv_su_au_deac_volpe.a_vehicle	EPA_MDHD_Phase2.a_process	Sizing_Init_HD_Conv_volpe	No	Yes
26	2b	Van	Micro	Medium	eng4a	Gasoline	micro_si_au_su_volpe.a_vehicle	EPA_MDHD_Phase2.a_process	Sizing_Init_HD_Micro_Inherited_volpe	Yes	Yes

Figure 212. Reference Vehicle tab of assumption template

Translation Tab

The Translation tab, shown in Figure 213, translates and transfers inputs into Autonomie to build the vehicle model.

	A	B	C
1	DisplayName	TableVariable	AuVariable
2	Year	Year	vpa.init.veh_year
3	Case	Case	vpa.init.veh_case
4	Class	Class	vpa.init.veh_class_name
5	Lightweighting	Lightweighting	vpa.init.veh_MR
6	Aerodynamics	Aerodynamics	vpa.init.veh_AERO
7	Rolling Resistance	RollingResistance	vpa.init.veh_ROLL
8	Purpose	Purpose	vpa.init.vocation
9	RegulatoryCode	RegulatoryCode	vpa.init.reg_code
10	Powertrain	Powertrain	vpa.init.veh_config_type
11	Engine Type	EngineType	eng.plant.init.type
12	Frontal Area (square m)	FrontalArea_squareM	chas.plant.init.frontal_area
13	Drag Coefficient (Cd)	DragCoefficient_Cd	chas.plant.init.coeff_drag
14	Rolling Resistance (Effective)	RollingResistance_Effective	whl.plant.init.coeff_roll1
15	Rolling Resistance 2nd order	RollingResistance2ndorder	whl.plant.init.coeff_roll2
16	Wheel Radius	WheelRadius	whl.plant.init.radius
17	Acc Load (W)	AccLoad_W	acelec.plant.init.pwr
18	Payload (kg)	Payload_kg	chas.plant.init.mass.cargo
19	Glider Mass (kg)	GliderMass_kg	chas.plant.init.mass.body
20	Glider Weight Reduction(%)	GliderWeightReduction	vpa.init.veh_MR_percentage_reduc
21	Cd reduction (%)	CdReduction	vpa.init.veh_AERO_percentage_reduc
22	Cr reduction (%)	CrReduction	vpa.init.veh_ROLL_percentage_reduc
23	Peak Eff (%)	PeakEff	eng.plant.scale.eff_max_des
24	#Gears	x_Gears	gb.plant.init.nb_ratio
25	Final Drive Ratio	FinalDriveRatio	fd.plant.init.ratio
26	Fixed Ratio: Motor	FixedRatio_Motor	tc.plant.init.ratio
27	Final Drive Eff (%)	FinalDriveEff	fd.plant.scale.eff_max_des
28	Transfer Case Eff	TransferCaseEff	trc.plant.init.eff_max
29	Starting Gear	StartingGear	gb.ctrl.dmd.init.gear_min
30	Motor Controller SpPwr (W/kg)	BoostConverterSpecificPower_W_kg	mot.plant.scale.specific_power_controller
31	Motor SpPwr (W/kg)	HighVoltageSystemSpecificPower_withoutBoost_W_kg	mot.plant.scale.specific_power_motor
32	Motor Peak Eff (%)	ElectricMachinePeakEff	mot.plant.scale.eff_max_des
33	Motor Controller Eff (%)	BoostConverterEfficiency	pc.plant.init.eff

Figure 213. Translation tab of assumption template

Multi-Vehicle Template Expansion and Duplication

After the large-scale simulation process defines the list of all component and vehicle inputs, a multiplier code expands the reference/template file into as many as needed to define the vehicle's technological combinations based on the decision tree inputs. This step stores all the template files in the folders for each vehicle class and performance category.

Figure 214 shows the vehicle template files for the different vehicle classes and performance categories in their respective folders.

The image shows a file explorer window with a list of files. The files are organized into folders and sub-folders. The main folder contains 34,490 items. A sub-folder contains 34,110 items. Another sub-folder contains 32,490 items. The files are named with a consistent pattern: `Compact_Perfo_CONV_eng01_5AU_MR0_AERO0_ROLL0`, `Compact_Perfo_CONV_eng01_5AU_MR0_AERO0_ROLL1`, `Compact_Perfo_CONV_eng01_5AU_MR0_AERO0_ROLL2`, `Compact_Perfo_CONV_eng01_5AU_MR0_AERO1_ROLL0`, `Compact_Perfo_CONV_eng01_5AU_MR0_AERO1_ROLL1`, `Compact_Perfo_CONV_eng01_5AU_MR0_AERO1_ROLL2`, `Compact_Perfo_CONV_eng01_5AU_MR0_AERO2_ROLL0`, `Compact_Perfo_CONV_eng01_5AU_MR0_AERO2_ROLL1`, `Compact_Perfo_CONV_eng01_5AU_MR0_AERO2_ROLL2`, `Compact_Perfo_CONV_eng01_5AU_MR0_AERO3_ROLL0`, `Compact_Perfo_CONV_eng01_5AU_MR0_AERO3_ROLL1`, `Compact_Perfo_CONV_eng01_5AU_MR0_AERO3_ROLL2`, `Compact_Perfo_CONV_eng01_5AU_MR0_AERO4_ROLL0`, `Compact_Perfo_CONV_eng01_5AU_MR0_AERO4_ROLL1`, `Compact_Perfo_CONV_eng01_5AU_MR0_AERO4_ROLL2`, `Compact_Perfo_CONV_eng01_5AU_MR1_AERO0_ROLL0`, `Compact_Perfo_CONV_eng01_5AU_MR1_AERO0_ROLL1`, `Compact_Perfo_CONV_eng01_5AU_MR1_AERO0_ROLL2`, `Compact_Perfo_CONV_eng01_5AU_MR1_AERO1_ROLL0`, `Compact_Perfo_CONV_eng01_5AU_MR1_AERO1_ROLL1`, `Compact_Perfo_CONV_eng01_5AU_MR1_AERO1_ROLL2`, `Compact_Perfo_CONV_eng01_5AU_MR1_AERO2_ROLL0`, `Compact_Perfo_CONV_eng01_5AU_MR1_AERO2_ROLL1`, `Compact_Perfo_CONV_eng01_5AU_MR1_AERO2_ROLL2`. The files are all Microsoft Excel Workbooks and are 125 KB in size. The dates modified range from 11/7/2017 10:49 PM to 11/9/2017 1:02 AM.

Name	Date modified	Type	Size
Compact_Perfo_CONV_eng01_5AU_MR0_AERO0_ROLL0	11/8/2017 7:01 PM	Microsoft Excel W...	125 KB
Compact_Perfo_CONV_eng01_5AU_MR0_AERO0_ROLL1	11/9/2017 1:02 AM	Microsoft Excel W...	125 KB
Compact_Perfo_CONV_eng01_5AU_MR0_AERO0_ROLL2	11/9/2017 1:02 AM	Microsoft Excel W...	125 KB
Compact_Perfo_CONV_eng01_5AU_MR0_AERO1_ROLL0	11/7/2017 10:49 PM	Microsoft Exc...	125 KB
Compact_Perfo_CONV_eng01_5AU_MR0_AERO1_ROLL1	11/7/2017 10:49 PM	Microsoft Exc...	125 KB
Compact_Perfo_CONV_eng01_5AU_MR0_AERO1_ROLL2	11/7/2017 10:49 PM	Microsoft Exc...	125 KB
Compact_Perfo_CONV_eng01_5AU_MR0_AERO2_ROLL0	11/7/2017 10:49 PM	Microsoft Exc...	125 KB
Compact_Perfo_CONV_eng01_5AU_MR0_AERO2_ROLL1	11/7/2017 10:49 PM	Microsoft Exc...	125 KB
Compact_Perfo_CONV_eng01_5AU_MR0_AERO2_ROLL2	11/7/2017 10:49 PM	Microsoft Exc...	125 KB
Compact_Perfo_CONV_eng01_5AU_MR0_AERO3_ROLL0	11/7/2017 10:49 PM	Microsoft Exc...	125 KB
Compact_Perfo_CONV_eng01_5AU_MR0_AERO3_ROLL1	11/7/2017 10:49 PM	Microsoft Exc...	125 KB
Compact_Perfo_CONV_eng01_5AU_MR0_AERO3_ROLL2	11/7/2017 10:49 PM	Microsoft Exc...	125 KB
Compact_Perfo_CONV_eng01_5AU_MR0_AERO4_ROLL0	11/7/2017 10:50 PM	Microsoft Exc...	125 KB
Compact_Perfo_CONV_eng01_5AU_MR0_AERO4_ROLL1	11/7/2017 10:50 PM	Microsoft Exc...	125 KB
Compact_Perfo_CONV_eng01_5AU_MR0_AERO4_ROLL2	11/7/2017 10:50 PM	Microsoft Exc...	125 KB
Compact_Perfo_CONV_eng01_5AU_MR1_AERO0_ROLL0	11/7/2017 10:50 PM	Microsoft Exc...	125 KB
Compact_Perfo_CONV_eng01_5AU_MR1_AERO0_ROLL1	11/7/2017 10:50 PM	Microsoft Exc...	125 KB
Compact_Perfo_CONV_eng01_5AU_MR1_AERO0_ROLL2	11/7/2017 10:50 PM	Microsoft Exc...	125 KB
Compact_Perfo_CONV_eng01_5AU_MR1_AERO1_ROLL0	11/7/2017 10:50 PM	Microsoft Exc...	125 KB
Compact_Perfo_CONV_eng01_5AU_MR1_AERO1_ROLL1	11/7/2017 10:50 PM	Microsoft Exc...	125 KB
Compact_Perfo_CONV_eng01_5AU_MR1_AERO1_ROLL2	11/7/2017 10:50 PM	Microsoft Exc...	125 KB
Compact_Perfo_CONV_eng01_5AU_MR1_AERO2_ROLL0	11/7/2017 10:50 PM	Microsoft Exc...	125 KB
Compact_Perfo_CONV_eng01_5AU_MR1_AERO2_ROLL1	11/7/2017 10:50 PM	Microsoft Exc...	125 KB
Compact_Perfo_CONV_eng01_5AU_MR1_AERO2_ROLL2	11/7/2017 10:50 PM	Microsoft Exc...	125 KB

Figure 214. Multiple vehicle template files

Vehicle Assumptions Definition

An automated process has been developed to read and write vehicle attributes and weight assumptions into template files to minimize manual inputs. Figure 215 shows the vehicle assumption inputs for different vehicle attributes and the weights for different vehicle classes and performance categories. The code reads the different vehicle attributes and weights and updates the template file for each vehicle class and performance category folder.

Vehicle Sizing Process

A unique approach to sizing the vehicle powertrain components ensures platform sharing among vehicles. While the reference baseline vehicles are sized to meet specific sets of performance criteria, the rest of the vehicles inherit their properties from the baseline reference vehicle and may have variations in performance. This approach represents real-world platform sharing (i.e., OEMs have a limited number of engines that are used across classes). A vehicle with inherited properties is referred to as an inherited vehicle.

Inheritance

The process of inheritance retrieves the values of different vehicle parameters of interest (engine power, engine weights, etc.) from the respective baseline reference vehicle and updates the inherited vehicle with the inherited value.

Conventional Powertrain (Conventional/Micro-12V/Mild Hybrid BISG)

Figure 216 shows the conventional powertrain inheritance flowchart for the range of vehicles using eng01 and the baseline vehicles from which they inherit.

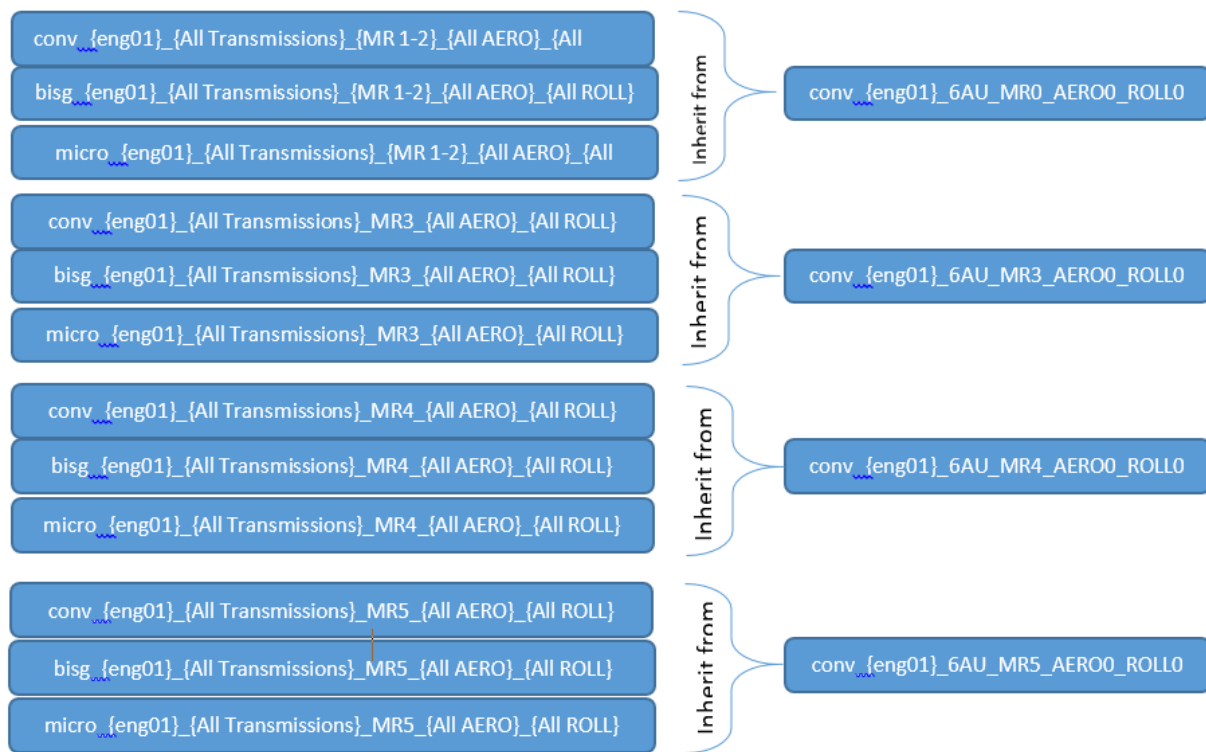


Figure 216. Conventional powertrain inheritance flowchart for eng01

For a given engine, all transmissions, AERO and ROLL combinations would inherit the engine power and mass from conventional/6AU/AERO0/ROLL0 for a given MR combination. The micro-hybrid and mild hybrid powertrains inherit from conventional vehicles as well.

For each conventional inherited vehicle, the algorithm shown in Figure 217 is implemented.

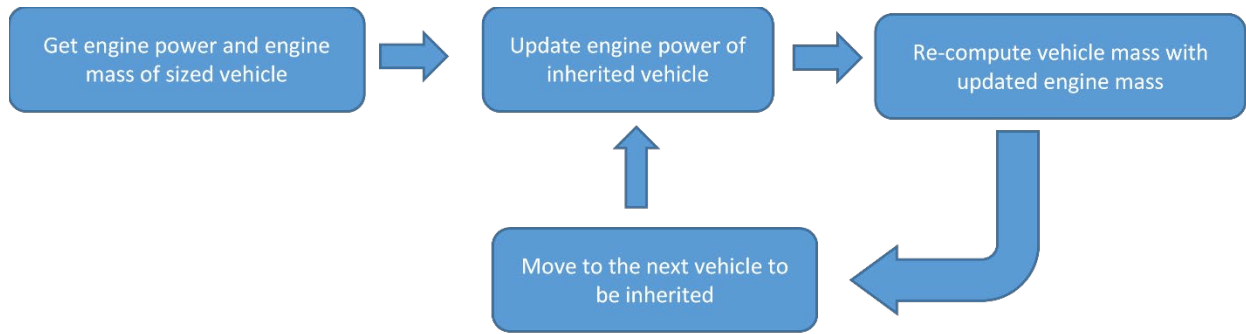


Figure 217. Inheritance algorithm for conventional vehicle

Hybrid Powertrains (Split HEV/Split PHEV/EREV PHEV/Fuel Cell HEV/BEV)

Figure 218 shows the hybrid powertrain inheritance flowchart for the range of vehicles studied and the respective baseline vehicle to inherit from for each of the respective hybrid powertrains.

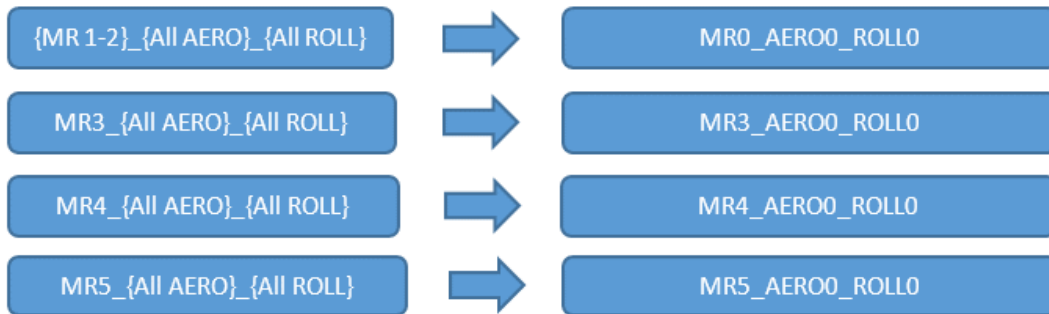


Figure 218. Hybrid powertrain vehicle inheritance flowchart

Inheritance for BEVs

For each inherited BEV, the algorithm shown in Figure 219 is implemented.

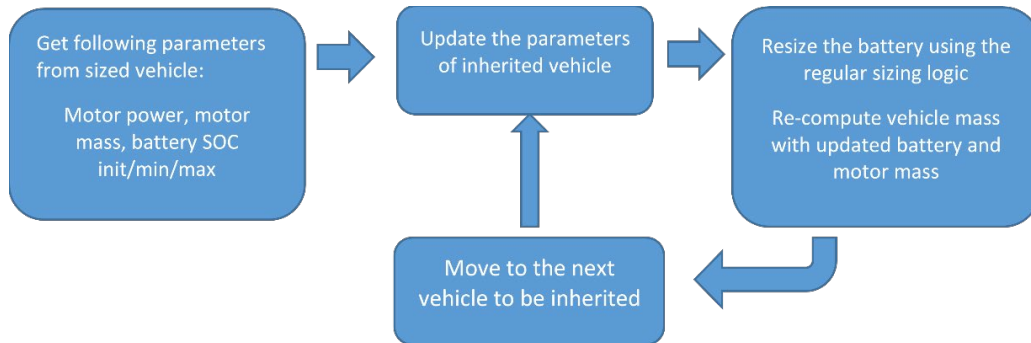


Figure 219. Inheritance algorithm for BEVs

Inheritance for Fuel Cell HEVs

For each inherited fuel-cell HEV, the algorithm shown in Figure 220 is implemented.

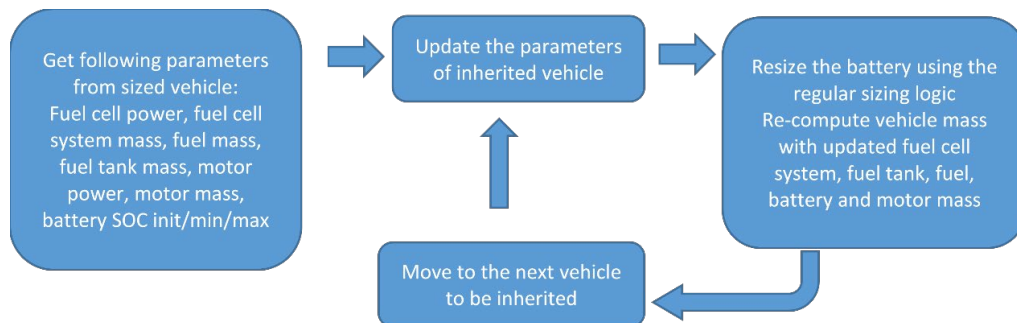


Figure 220. Inheritance algorithm for fuel cell HEVs

Inheritance for EREVs

For each inherited EREV, the algorithm shown in Figure 221 is implemented.

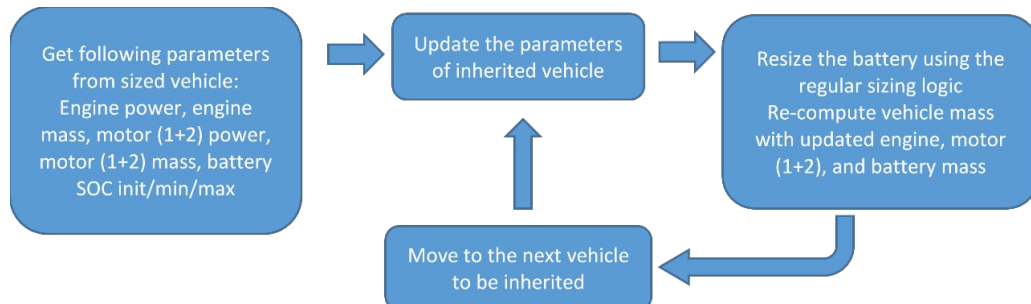


Figure 221. Inheritance algorithm for EREVs

Inheritance for Split PHEVs

For each inherited split PHEV, the algorithm interpreted in Figure 222 is implemented.

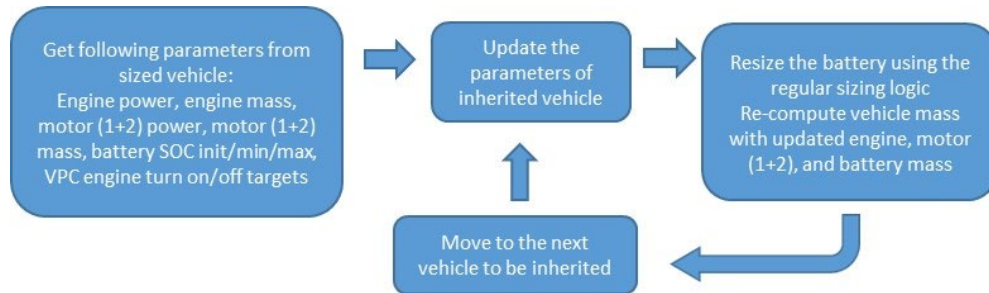


Figure 222. Inheritance algorithm for split PHEVs

Inheritance for Split HEVs

For each inherited split HEV, the algorithm shown in Figure 223 is implemented.

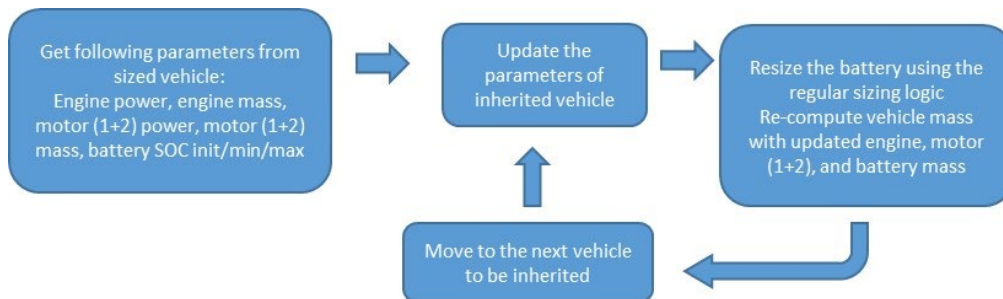


Figure 223. Inheritance algorithm for split HEVs

Parallel Hybrid Powertrains

Inheritance for Parallel HEVs

The flowchart in Figure 224 shows the range of inherited parallel hybrid vehicles and the reference baseline vehicles that the vehicles inherit from.

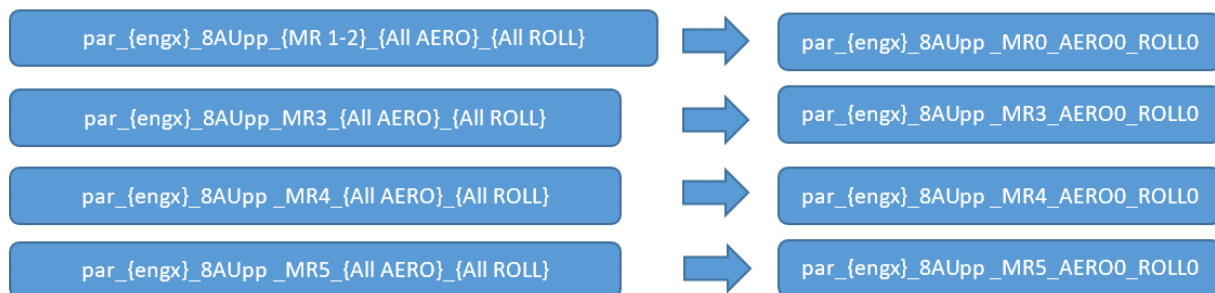


Figure 224. Parallel HEVs: Inheritance from reference baseline vehicles

For each inherited parallel HEV, the algorithm shown in Figure 225 is implemented.

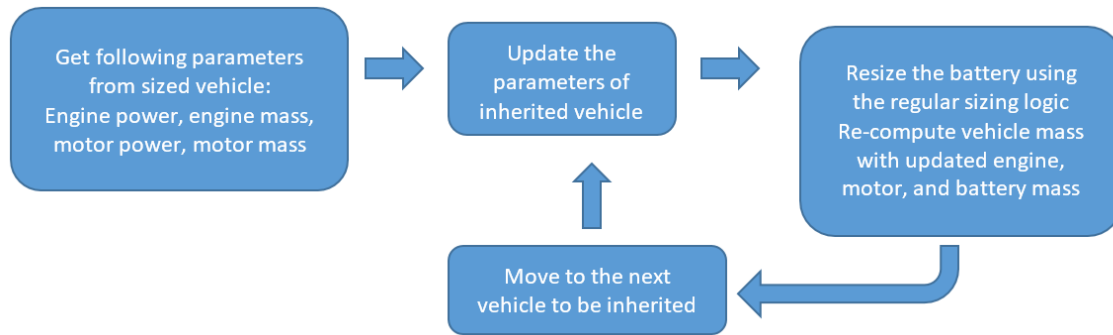


Figure 225. Inheritance algorithm for parallel HEVs

Inheritance for Parallel PHEVs

The flowchart in Figure 226 shows the range of inherited parallel PHEVs and the reference baseline vehicles that the vehicles inherit from.

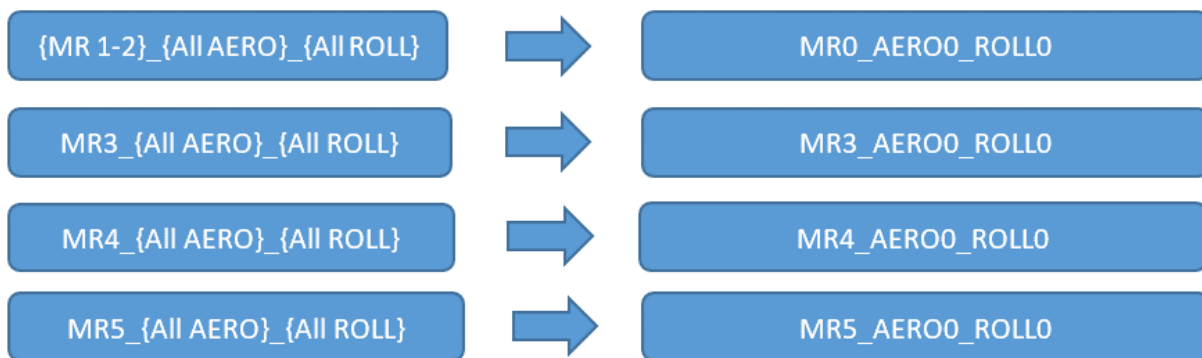


Figure 226. Parallel PHEVs: Inheritance from reference baseline vehicles

For each inherited parallel PHEV, the algorithm presented in Figure 227 is implemented.

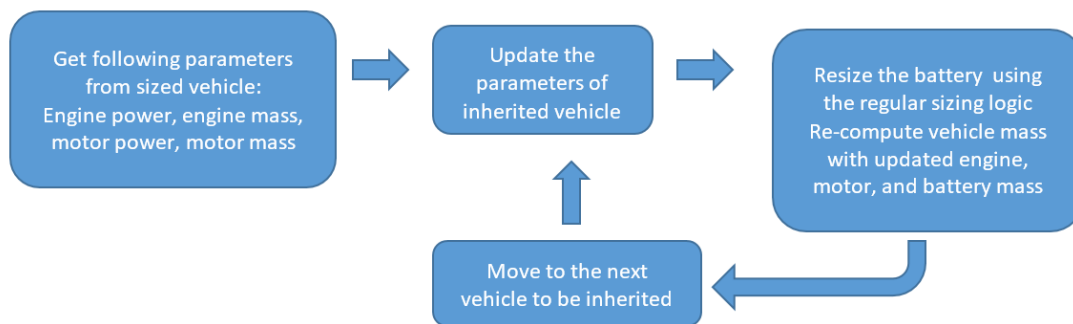


Figure 227. Inheritance algorithm for parallel PHEVs

Vehicle Technical Specifications

Light-Duty Vehicles

Each vehicle class and performance type has specific vehicle performance requirements. Table 73 details the different vehicle classifications and the corresponding performance times used to size the vehicles. The vehicles can exceed specific performance targets (e.g., to 60 mph time) owing to other constraints (e.g., EV range and EV mode).

Table 73. Vehicle class performance times

Vehicle Class	Performance Category	0–60 mph Time (s)	50–80 mph Time (s)
Compact	Non-Performance (Base)	10	10
Compact	Performance (Premium)	8	8
Midsize	Non-Performance (Base)	9	9
Midsize	Performance (Premium)	6	6
Small SUV	Non-Performance (Base)	9	9
Small SUV	Performance (Premium)	7	7
Midsize SUV	Non-Performance (Base)	10	10
Midsize SUV	Performance (Premium)	7	7
Pickup	Non-Performance (Base)	7	7
Pickup	Performance (Premium)	7	7

Along with the initial vehicle acceleration time to 60 mph, all vehicles are sized to meet the following requirements at minimum.

- Maximum grade (gradeability): 6 percent at 65 mph at GVW
- Maximum vehicle speed: >100 mph
- Payload: 900 kg (pickup base/premium only)
- Towing: 3,000 kg (pickup base) and 4,500 kg (pickup premium)

The relationship between curb weight and GVW for current technology-configuration-powertrain combinations is modeled from the existing vehicles in the market, and it forms the basis for estimating the GVWs of future vehicle scenarios. Figure 228 shows the GVWR versus curb weight relationship.

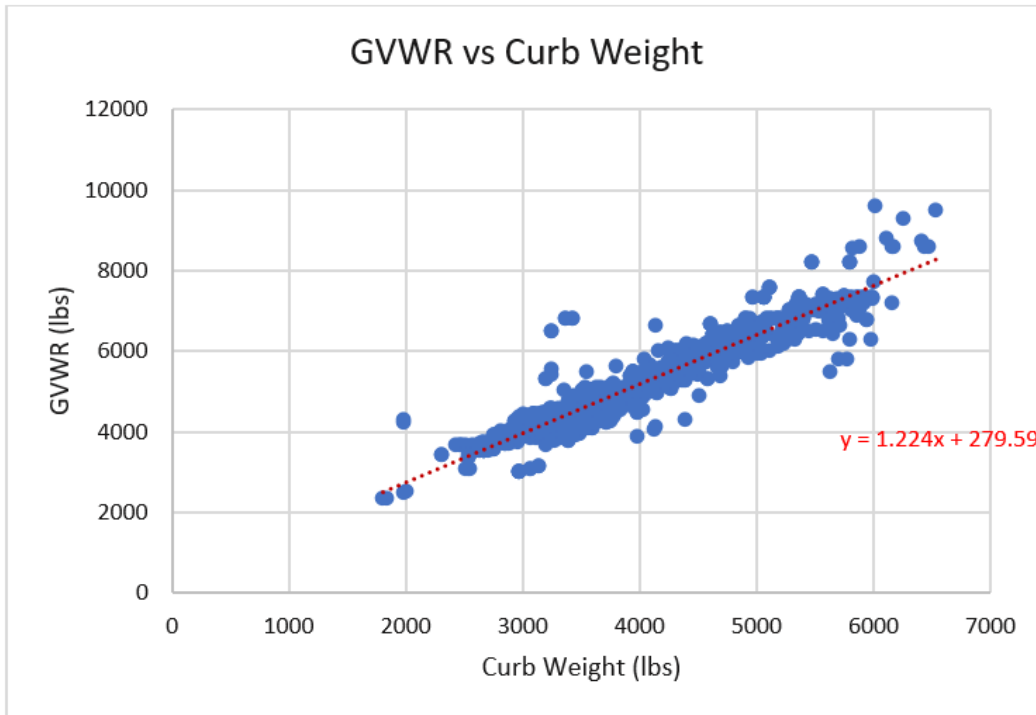


Figure 228. Curb weight versus GVWR

Using the equation derived from Figure 228, the relationship is determined as follows.

$$\text{GVWR} = 1.224 \times (\text{curb weight}) + 279.59$$

Heavy-Duty Pickups and Vans

The sizing process scales and resizes critical powertrain components, such as the engine, motors/generators, and batteries, to ensure that the smallest components are used while still meeting or exceeding all performance requirements. This performance-based sizing process ensures that the alternate powertrains proposed in this work can meet or exceed the cargo carrying capacity, acceleration, and grade climbing capabilities of the vehicles they are expected to replace. Thus, in examining the results, it is important to emphasize that all powertrains meet the same technical performance requirements. Table 74 shows the technical requirements assumed for these vehicles.

Table 74. Cold-start penalty combinations

Class	Purpose	0–30 mph Time(S)	0–60 mph Time (S)	6% Grade Speed (mph)	Cruise Speed (mph)	Cruise Grade (%)	Max Speed (mph)	Start-Ability (%)	Towing Weight (lb)
HD (2b)	Van	7	16	50	70	1.5	75	20	6,000
HD (2b)	Pickup	7	13	65	70	1.5	75	20	15,000
HD (3)	Van	7	20	50	65	1.5	70	20	6,500
HD (3)	Pickup	7	16	65	70	1.5	75	20	18,000

Additional performance metrics have been developed, as follows.

- Test weight for sizing: 10,000 lb (HDPUV class 2b) and 14,000 lb (HDPUV class 3)
- Payload: Calculated as 50 percent of the maximum loading of baseline vehicle
- EV range (miles): BEV1 ranges of 150 and 250 (van) and BEV2 ranges of 200 and 300 (pickup)

In general, the acceleration performance targets (0 to 30 and 0 to 60 mph) are aimed at negotiating typical driving in urban and suburban conditions. In contrast, the 6 percent grade criteria is associated with negotiating the grades allowed on highways. A steady climb at a specific speed at 6 percent grade is considered to be a proxy for the Davis Dam (an actual stretch of road in the western United States) test.

Vehicle Powertrain Sizing Algorithms

Improperly sized components will lead to differences in energy consumption and influence the effectiveness results. Therefore, we have developed several automated sizing algorithms to provide a fair comparison between technologies. Algorithms have been defined for powertrains (e.g., conventional, power-split, and series, electric) and applications (e.g., HEV, and PHEV).

All algorithms are based on the same concept: the vehicle is built from the bottom up, meaning each component assumption (e.g., specific power, and efficiency) defines the entire set of vehicle attributes (e.g., weight). This process is iterative, as the main component characteristics (e.g., maximum power, and vehicle weight) are modified until all vehicle technical specifications are met. The transmission gear span or ratios are currently not modified to be optimized with specific engine technologies. On average, the algorithms take between five and 10 iterations to converge.

Light-Duty Vehicles

Conventional Vehicle Sizing Algorithm

A conventional vehicle is mainly defined by its ICE. Its ability to follow a cycle or meet acceleration performance is directly linked to its power density. Therefore, the sizing algorithm focuses on calculating the mechanical power needed to meet the requirements. Figure 229 illustrates the steps in the sizing process. After a default vehicle is created, a simulation determines the engine peak power and vehicle weight.

First, the desired power to meet the gradeability and acceleration performance requirements is estimated, and engine power is updated with the maximum value.

Then, the sizing enters an acceleration loop to verify the performance (e.g., initial vehicle movement to 60 mph). The definition of IVM is that the vehicle must move 1 ft (about 1/3 m) before the clock starts to record the performance time. This metric provides a more consistent result and removes phenomena that are difficult to model at initial acceleration—such as tire and clutch slip—from consideration.

Finally, acceleration performance for passing (i.e., time to accelerate from 50 to 80 mph) is measured with the vehicle's updated parameters. At the end, the times to reach the targets (0 to 60 and 50 to 80 mph) are compared with the simulated data, which is the main condition to exit the routine. Figure 229 shows the detailed steps of the conventional vehicle sizing algorithm.

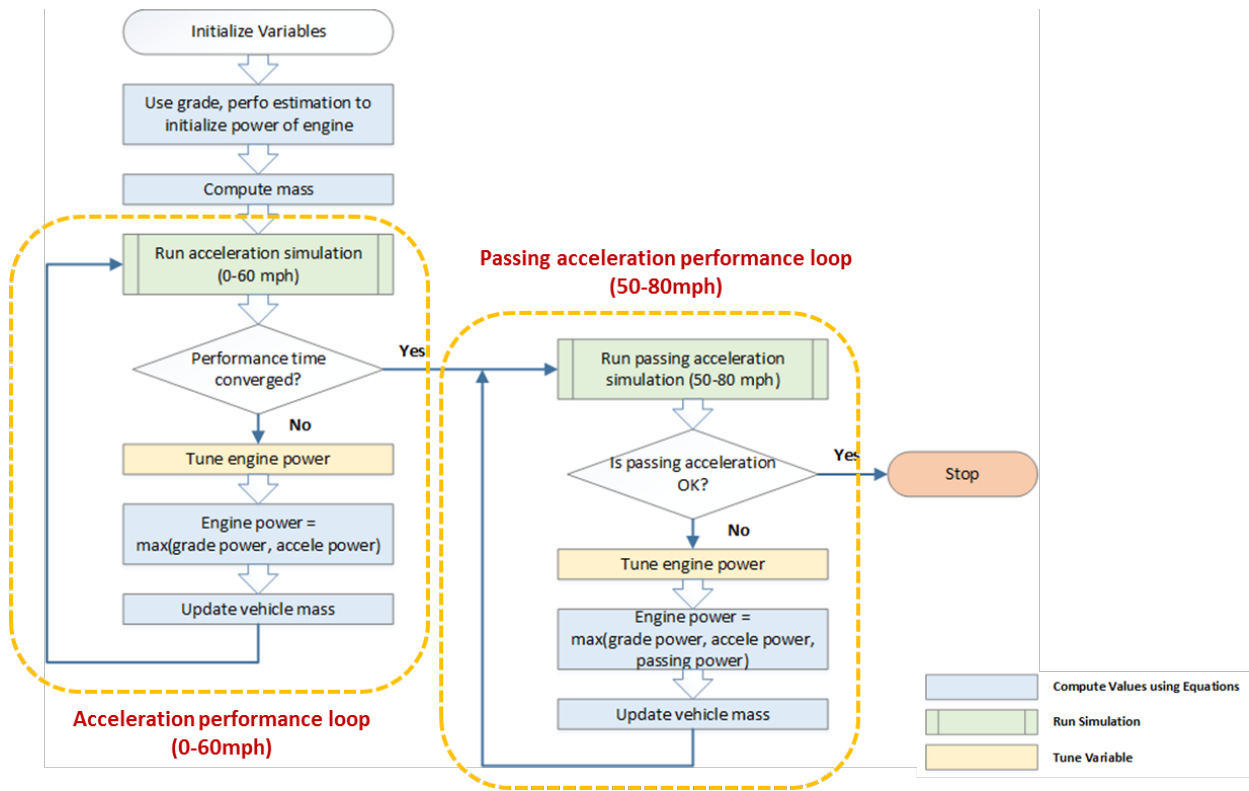


Figure 229. Conventional powertrain sizing algorithm

Split HEV Sizing Algorithm

Figure 230 shows the detailed steps of the split HEV sizing algorithm.

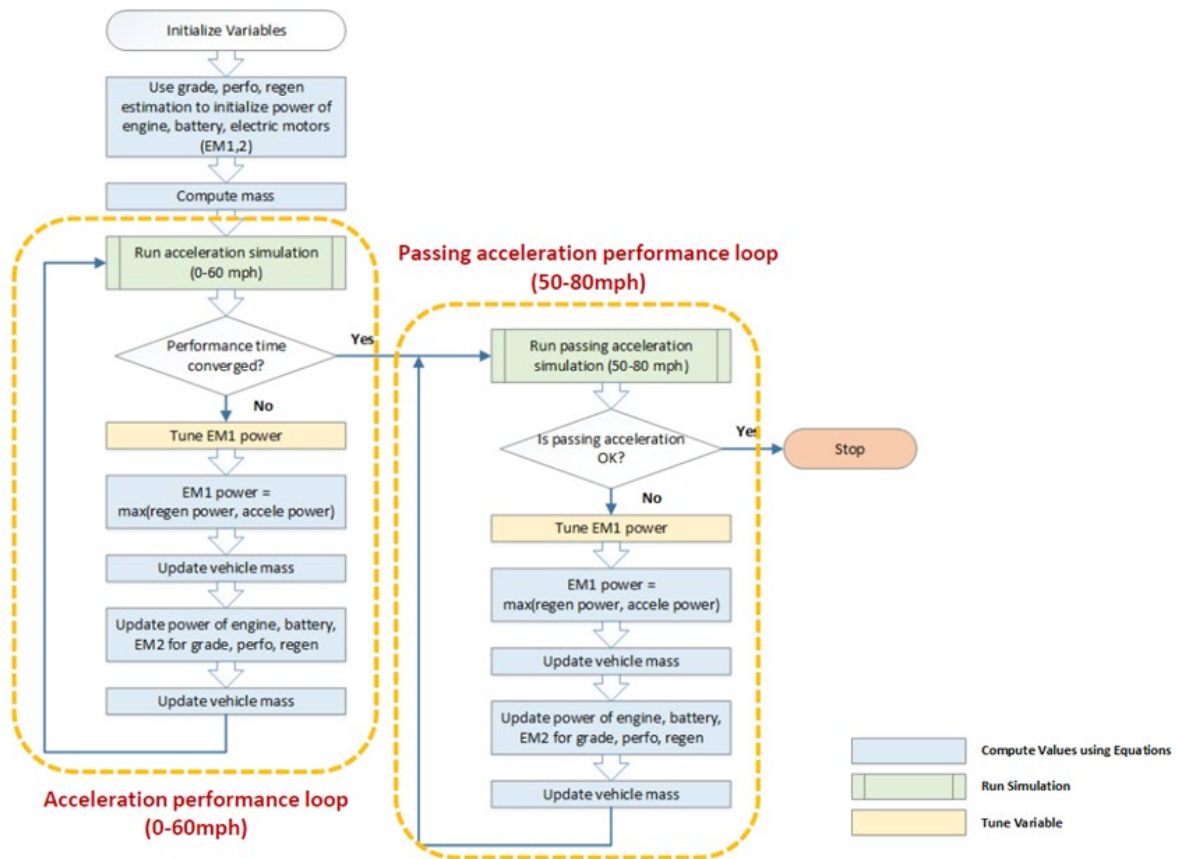


Figure 230. Split hybrid electric powertrain sizing algorithm

The main algorithm for split-HEV is as follows.

- The engine size achieves at least 55 percent of the peak power required to meet VTS (acceleration performance or gradeability).
- The battery and electric machine (EM1) powers are sized for maximum regenerative braking.
- The vehicle weight is updated based on the engine peak power, electric machine (EM1 and EM2) peak power, and battery power.
- The electric machine (EM2) is sized as follows.
 - Start ICE at V_{max} (~57 mph for UDDS cycle). ICE should be ON (i.e., EM2 peak power for engine start at top speed on UDDS cycle).
 - Control maximum power of engine at $V_{spd} = 0$ (i.e., EM2 peak power for engine control on performance).
 - Control ICE at maximum grade (i.e., EM2 continuous power for engine control on grade, and engine power fraction going through electromechanical power path).

Parallel HEV (Par HEV) Sizing Algorithm

Figure 231 shows the detailed steps of the parallel HEV sizing algorithm.

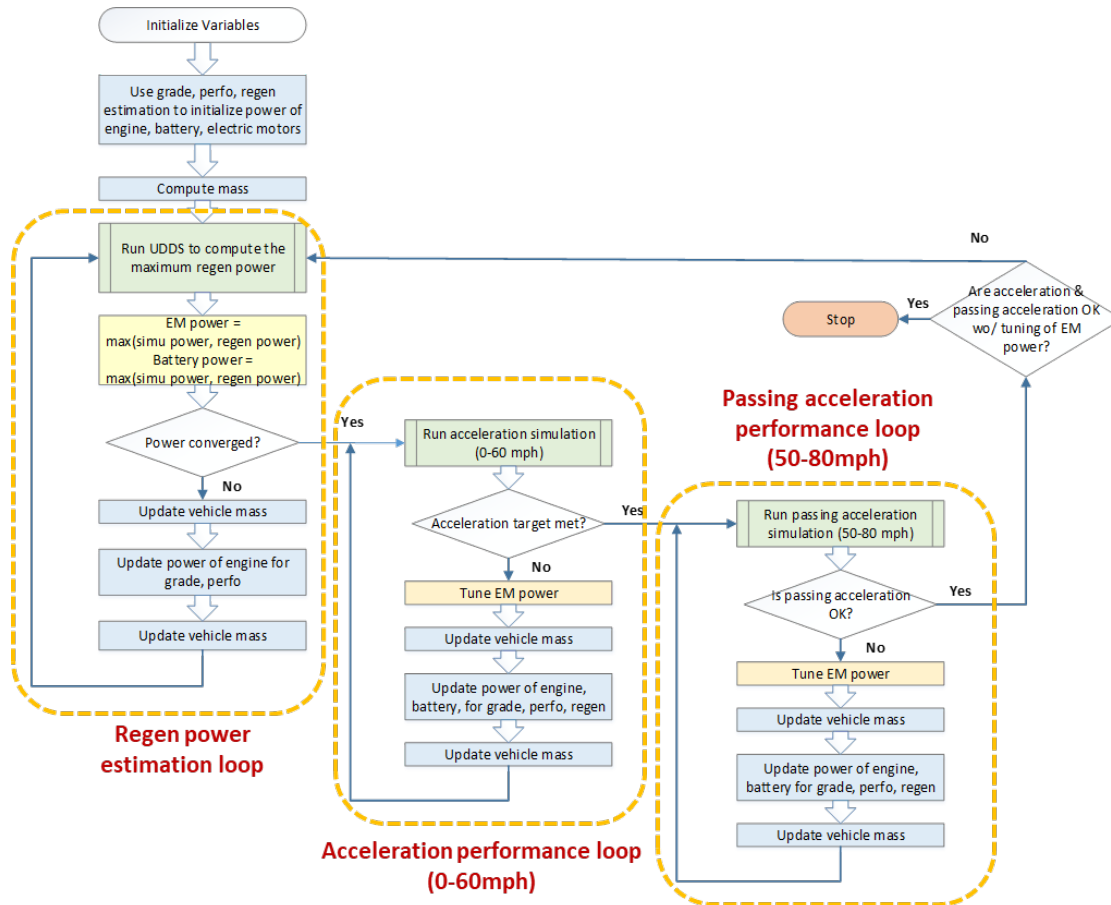


Figure 231. Parallel hybrid electric powertrain sizing algorithm

The main algorithm for parallel HEV sizing is as follows.

- The engine size achieves at least 70 percent of the peak power required to meet VTS (acceleration performance or gradeability).
- The battery and electric machine (EM1) powers are sized for maximum regenerative braking.
- The vehicle weight is updated based on the engine peak power, electric machine (EM1) peak power, and battery power.

Parallel PHEV Sizing Algorithm

Figure 232 shows the detailed steps for the parallel PHEV (par PHEV20) sizing algorithm.

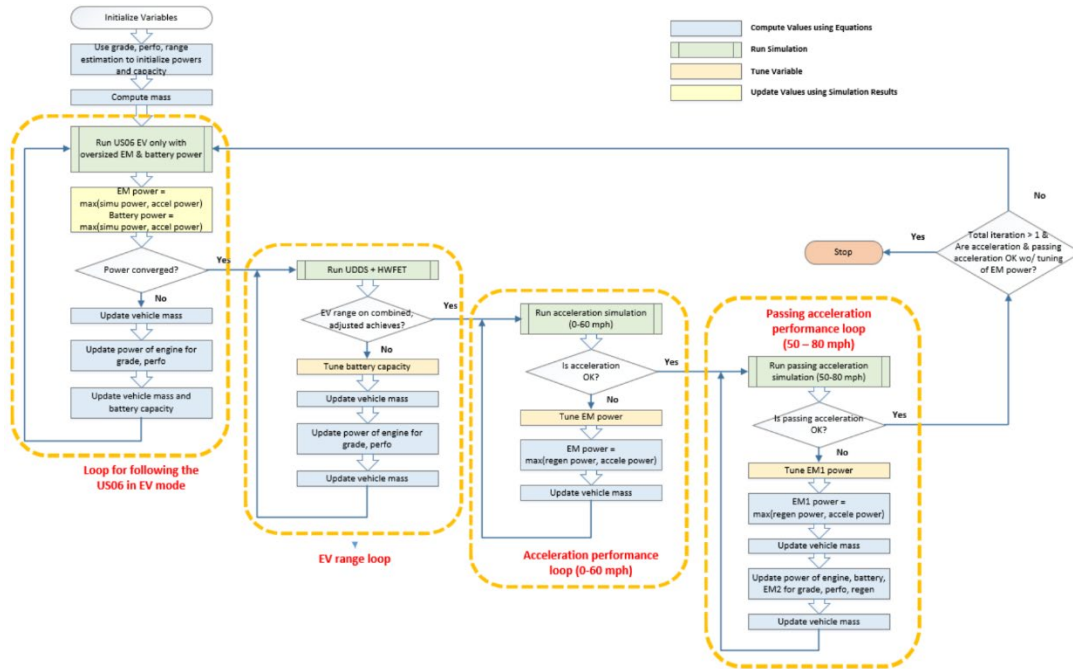


Figure 232. Parallel plug-in hybrid (Par PHEV20) EV powertrain sizing

Figure 233 shows the detailed steps for the parallel PHEV (par PHEV50) sizing algorithm.

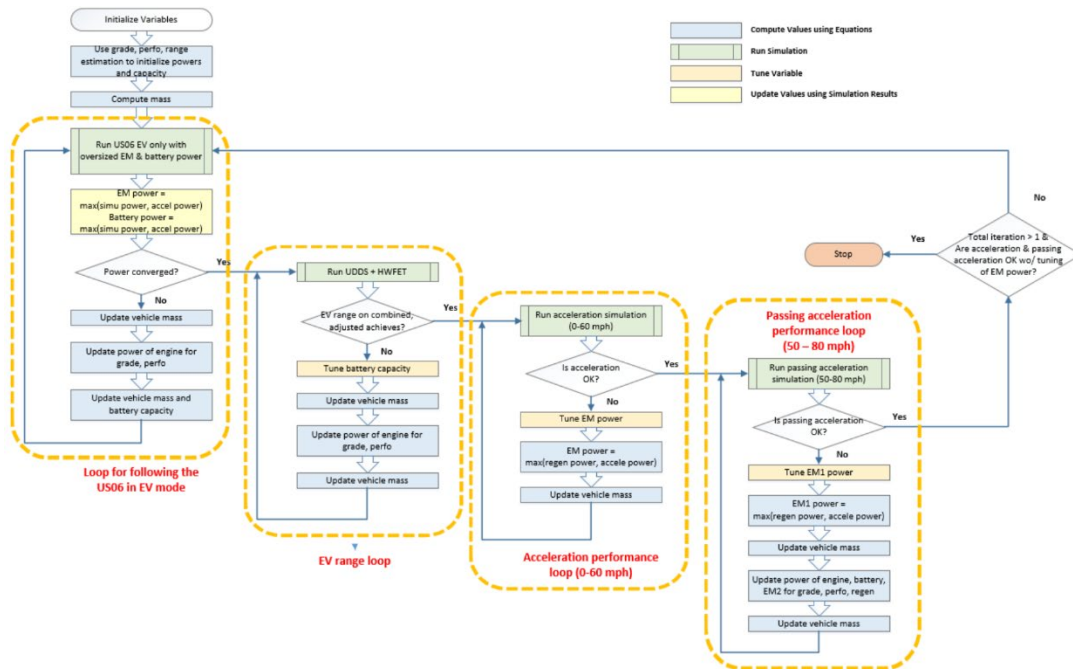


Figure 233. Parallel plug-in hybrid (Par PHEV50) EV powertrain sizing

The main sizing algorithm for parallel PHEV sizing is as follows.

- The engine size achieves at least 70 percent of the peak power required to meet VTS (acceleration performance or gradeability).
- The battery energy size achieves the specified AER on the combined cycle (UDDS + HWFET), based on the adjusted energy values.
- The battery and electric machine (EM) powers are sized to follow the US06 cycle in EV mode for Par PHEV20 and US06 cycle in EV mode for Par PHEV50 at low SOC (beginning of CS mode) or to meet the acceleration performance requirement.
- The vehicle weight is updated based on the engine peak power, electric machine (EM) peak power, and battery energy.

Split-PHEV Sizing Algorithm

Figure 234 shows the detailed steps of the split-PHEV (split PHEV20) sizing algorithm.

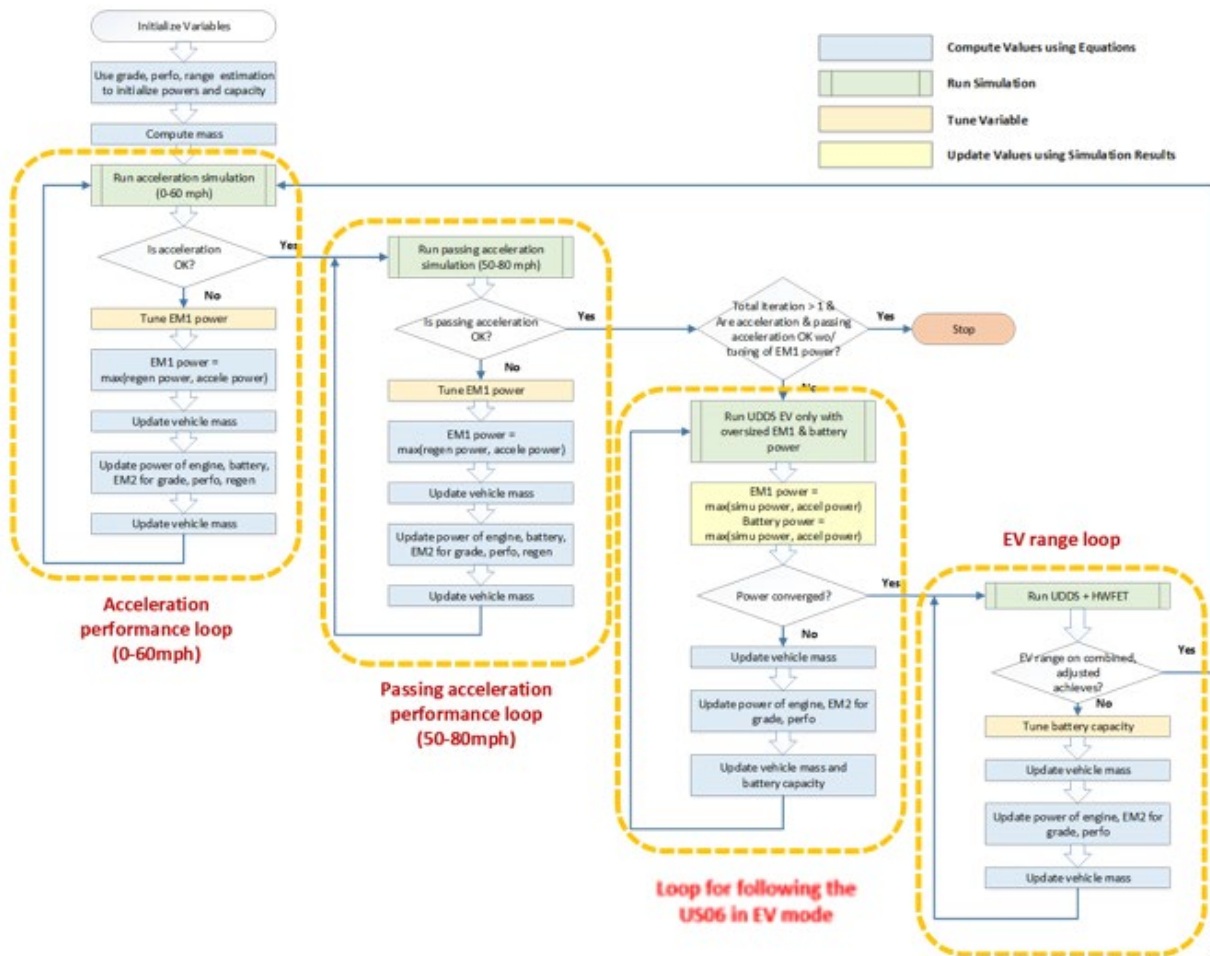


Figure 234. Split PHEV sizing algorithm

The main sizing algorithm for split-PHEV sizing is as follows.

- The engine size achieves at least 55 percent of the peak power required to meet VTS (acceleration performance or gradeability).

- The battery energy size achieves the specified AER on the combined cycle (UDDS + HWFET), based on the adjusted energy values.
- The battery and electric machine (EM1) powers are sized to follow the US06 cycle in EV mode at low SOC (beginning of CS mode) or to meet the acceleration performance requirement.
- The vehicle weight is updated based on the engine peak power, electric machine (EM1, EM2) peak power, and battery energy.
- The electric machine (EM2) is sized as follows.
 - Start ICE at Vmax (~57 mph for UDDS cycle). ICE should be ON (i.e., EM2 peak power for engine start at top speed on UDDS cycle).
 - Control maximum power of engine at Vspd = 0 (i.e., EM2 peak power for engine control on performance).
 - Control ICE at maximum grade (i.e., EM2 continuous power for engine control on grade, engine power fraction going through electromechanical power path).

Voltec PHEV (Extended Range) Vehicle Sizing Algorithm

Figure 235 shows the detailed steps for the Voltec PHEV vehicle sizing algorithm, used for the EREV PHEV50 vehicle powertrain.

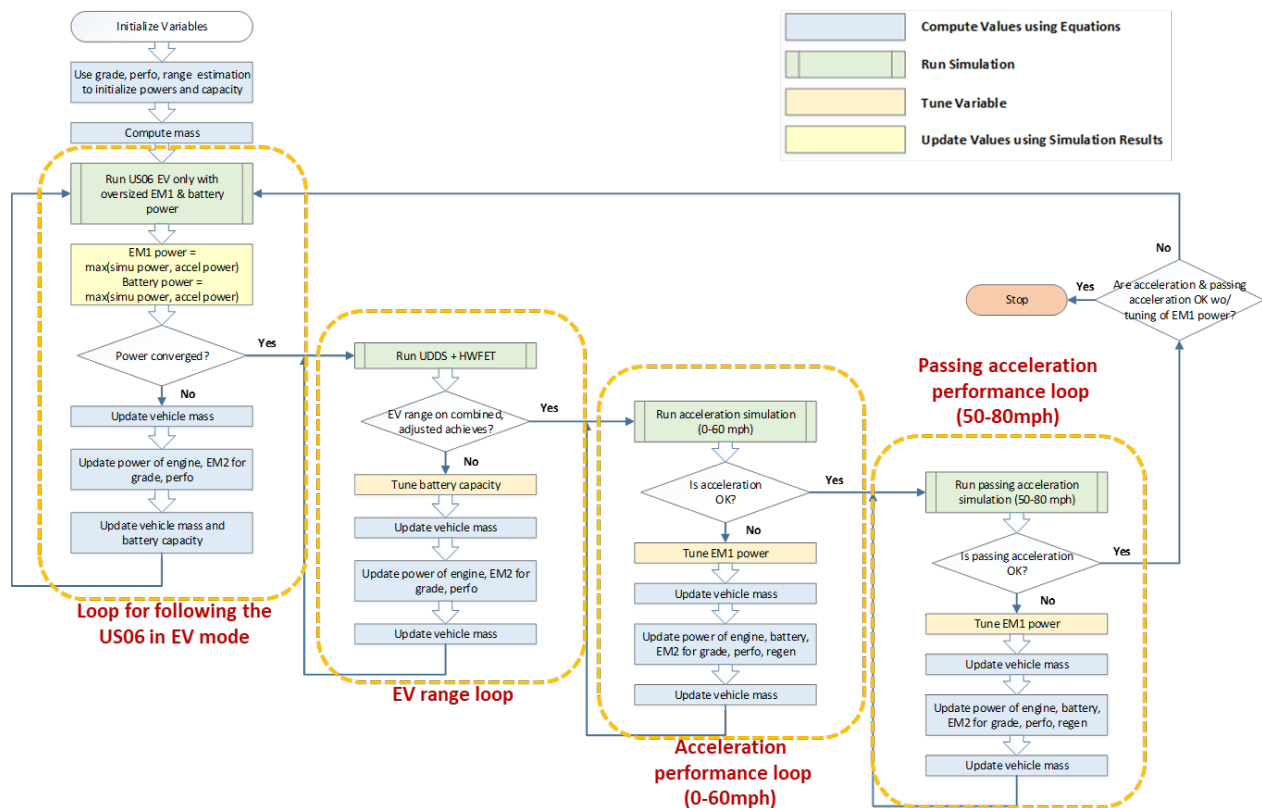


Figure 235. Voltec PHEV vehicle sizing algorithm

The main sizing algorithm for Voltec extended-range PHEV sizing is as follows.

- The engine size achieves at least 55 percent of the peak power required to meet VTS (acceleration performance or gradeability).

- The battery energy size achieves the specified AER on the combined cycle (UDDS + HWFET), based on the adjusted energy values.
- The battery and electric machine (EM1) powers are sized to follow the US06 cycle in EV mode at low SOC (beginning of CS mode) or to meet the acceleration performance requirement.
- The vehicle weight is updated with respect to the engine peak power, electric machine (EM1, EM2) peak power, and battery energy.
- The electric machine (EM2) is sized as follows.
 - Start ICE at Vmax (~57 mph for UDDS cycle). ICE should be ON (i.e., EM2 peak power for engine start at top speed on UDDS cycle)
 - Control maximum power of engine at Vspd = 0 (i.e., EM2 peak power for engine control on performance)
 - Control ICE at max grade (i.e., EM2 continuous power for engine control on grade, and engine power fraction going through an electromechanical power path).

BEV Sizing Algorithm

Figure 236 shows the detailed steps of the BEV sizing algorithm, used for BEV200 and BEV300 vehicle powertrains.

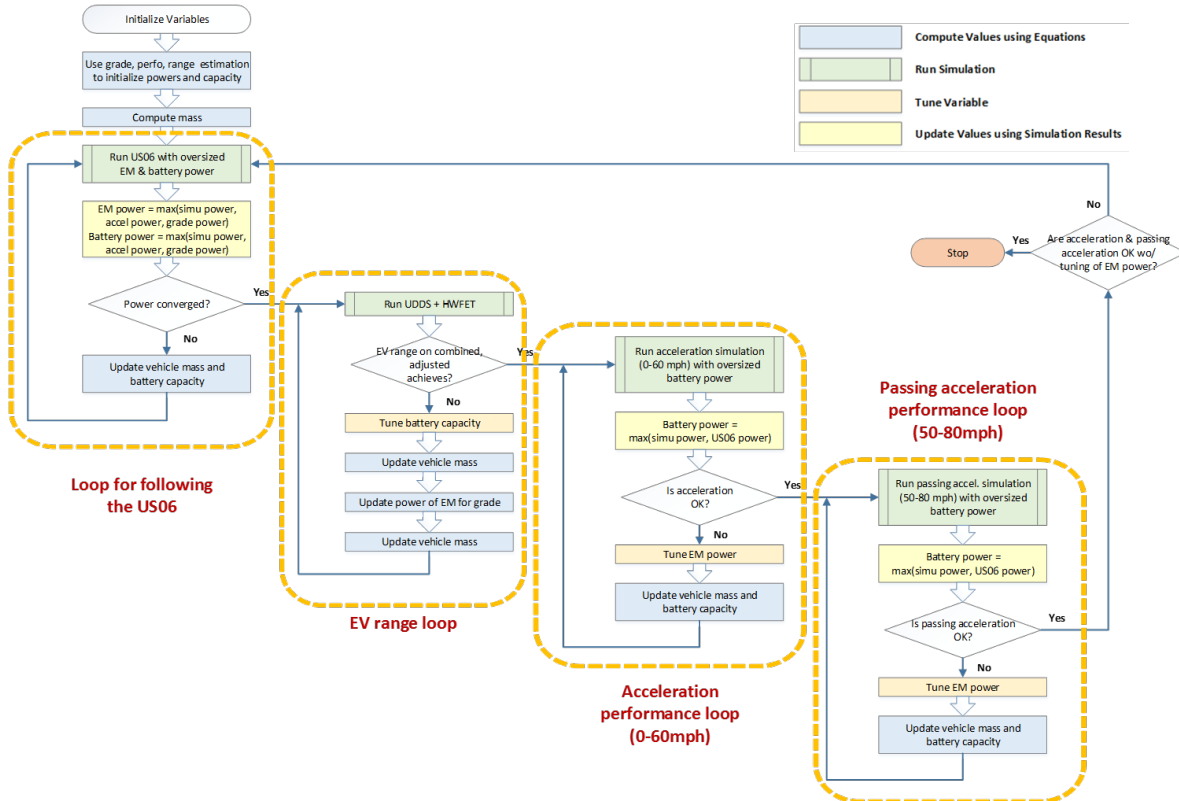


Figure 236. BEV sizing algorithm

The main sizing algorithm for BEV sizing is as follows.

- Battery and electric machine (EM) powers are sized to follow the US06 cycle at low SOC (beginning of CS mode) or to meet the acceleration performance requirement.
- The battery energy size achieves the specified AER on the combined cycle (UDDS + HWFET), based on the adjusted energy values.
- The vehicle weight is a function of the electric machine (EM) peak power and battery energy.

Fuel Cell Series HEV Sizing Algorithm

Figure 237 shows the detailed steps of the fuel cell HEV sizing algorithm.

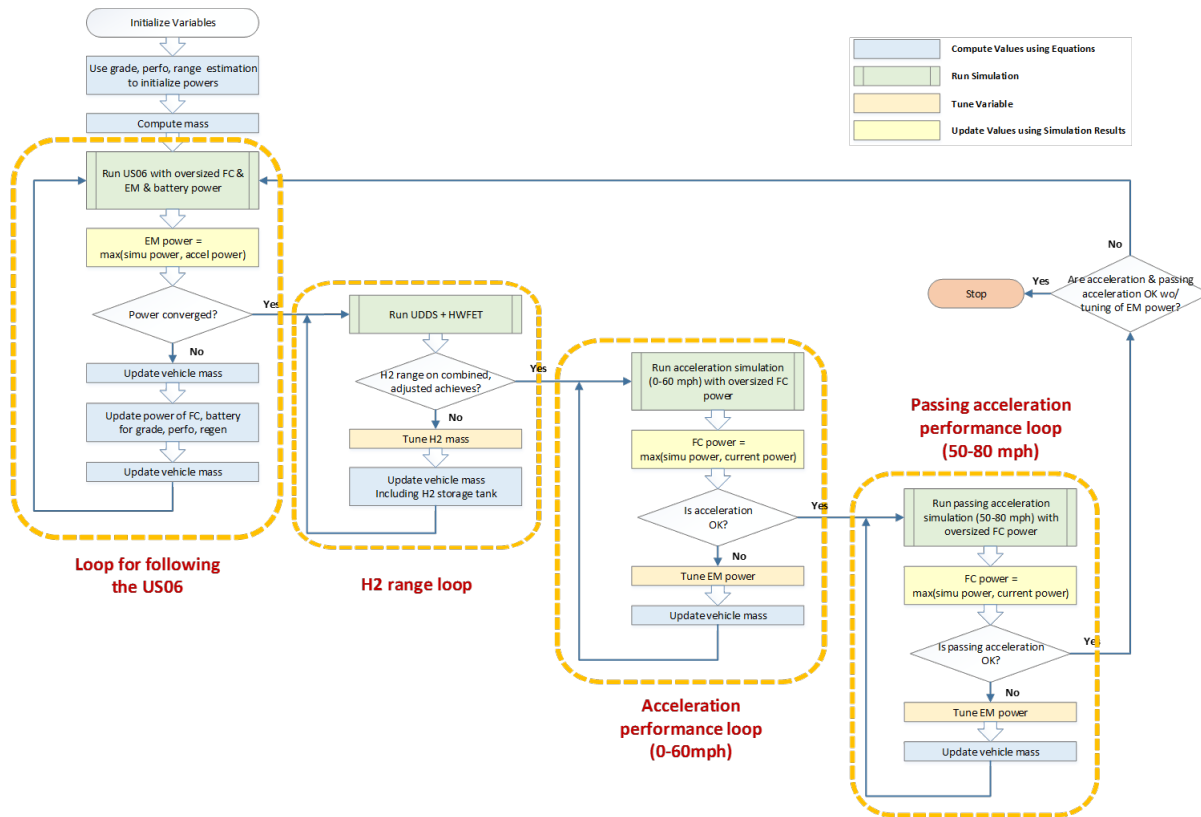


Figure 237. Fuel cell series HEV sizing algorithm

The main sizing algorithm for fuel cell HEV sizing is as follows.

- The fuel cell size achieves at least 70 percent of the peak power required to meet the VTS (acceleration performance or gradeability).
- The hydrogen storage capacity size achieves the specified AER on the combined cycle (UDDS + HWFET), based on the adjusted values.
- The vehicle weight is a function of the fuel cell peak power, electric machine peak power, and battery cell number.

Heavy-Duty Pickups and Vans

Conventional Vehicle Sizing Algorithm

A conventional vehicle is defined by its ICE. Its ability to follow a sustainable maximum speed at grade cycle or meet acceleration performance is directly linked to its power density. Therefore, the sizing algorithm focuses on calculating the mechanical power needed to meet the requirements. Figure 238 illustrates the steps in the sizing process. After a default vehicle is created, a simulation determines the engine peak power.

First, the desired power to meet the gradeability and acceleration performance requirements is estimated, and engine power is updated with the maximum value. Next, the sizing algorithm enters gradeability loops to verify the performance (e.g., sustainable maximum speed at 6 percent grade, start/launch capability on grade, and maximum sustainable grade at highway cruising speed).

Then, the sizing algorithm enters an acceleration loop to verify the performance (e.g., IVM to 30 mph or 60 mph). The definition of IVM is that the vehicle must move 1 ft (about 1/3 m) before the clock starts to record the performance time. This metric provides a more consistent result and removes phenomena that are difficult to model at initial acceleration—such as tire and clutch slip—from consideration. At the end, the times to reach the targets (0 to 30 and 0 to 60 mph) are compared with the simulated data, which is the main condition to exit the routine.

Finally, the sizing algorithm enters a towing capability loop to look for the maximum possible vehicle weight over 40 mph in gradeability. This sizing process ensures that the vehicle can satisfy the gradeability requirement (over 40 mph) with additional payload mass to the curb weight. Figure 238 shows the detailed steps of the conventional vehicle sizing algorithm.

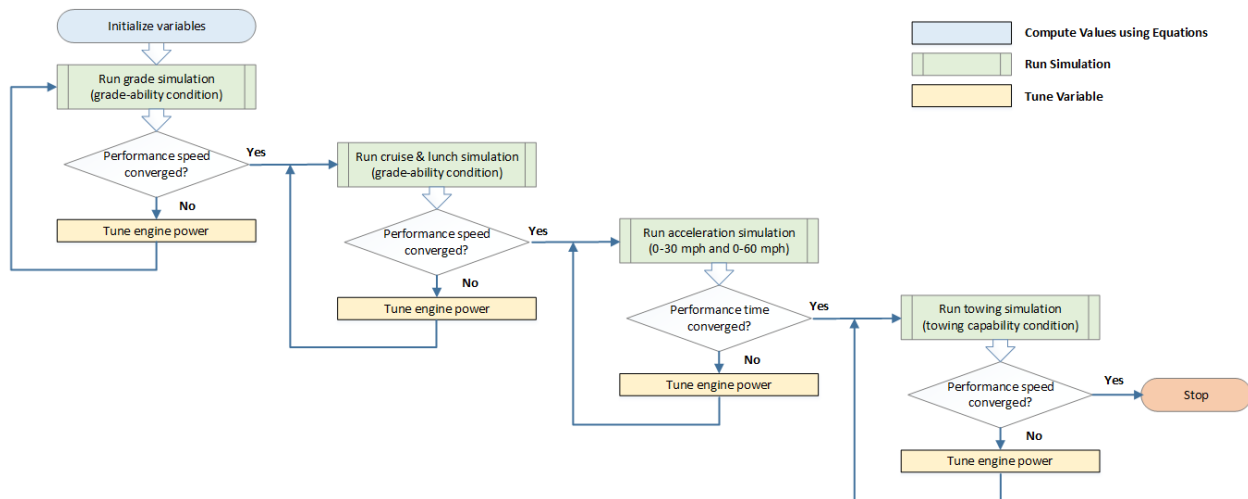


Figure 238. Conventional powertrain sizing algorithm

Parallel HEV Sizing Algorithm

Figure 239 shows the detailed steps of the parallel HEV sizing algorithm.

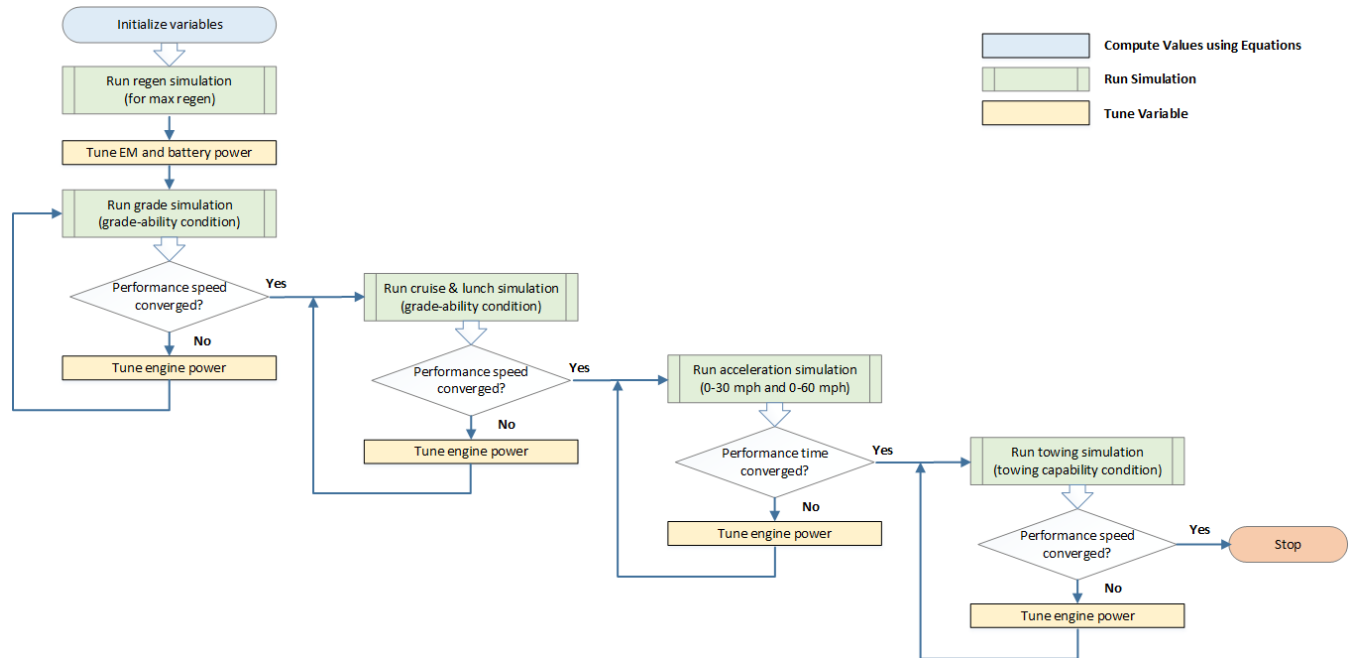


Figure 239. Parallel hybrid electric powertrain sizing algorithm

The main algorithm for parallel HEV sizing is as follows.

- The battery and EM powers are sized for maximum regenerative braking.
- The engine size achieves the peak power required to meet all performance requirements (e.g., acceleration performance, gradeability, or towing).
- The powertrain weight is updated based on the engine peak power, electric machine (EM) peak power, and battery power.

Parallel PHEV Sizing Algorithm

Figure 240 shows the detailed steps of the parallel PHEV sizing algorithm.

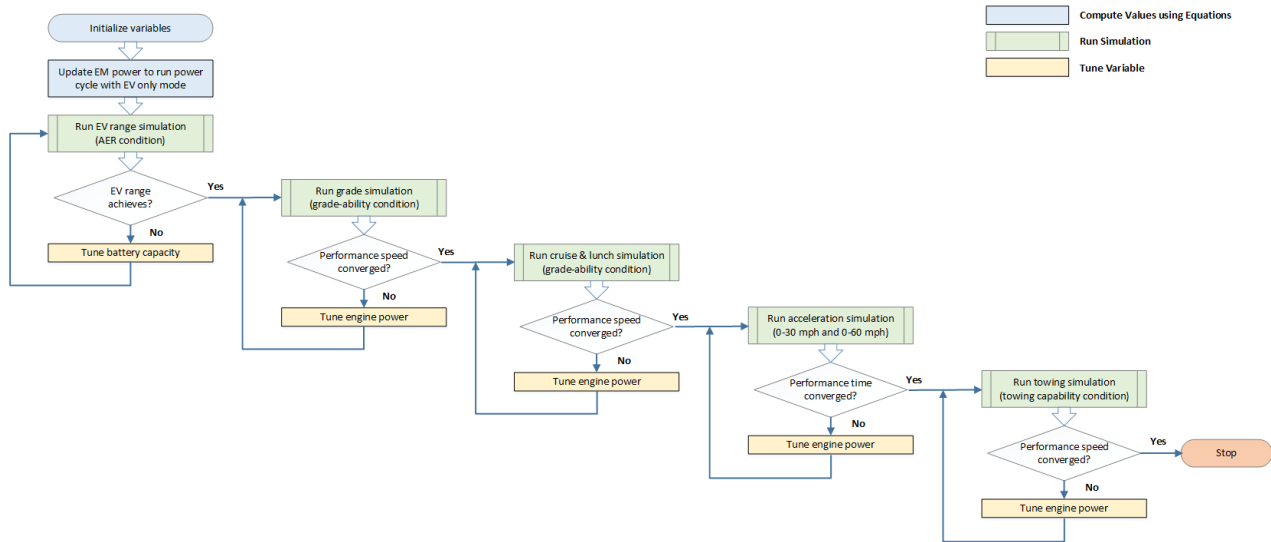


Figure 240. Parallel plug-in hybrid electric powertrain sizing algorithm

The main algorithm for parallel PHEV sizing is as follows.

- The engine size achieves the peak power required to meet all performance requirements (e.g., acceleration performance, gradeability, or towing).
- The battery energy size achieves the specified AER on the EPA phase 2 55-mph cycle based on the adjusted energy values.
- The battery and EM powers are sized to follow the UDDS cycle in EV mode at low SOC (beginning of CS mode) or to meet the acceleration performance requirement.
- The powertrain weight is updated based on the engine peak power, EM peak power, and battery energy.

Fuel Cell Series HEV Sizing Algorithm

Figure 241 shows the detailed steps of the fuel cell HEV sizing algorithm.

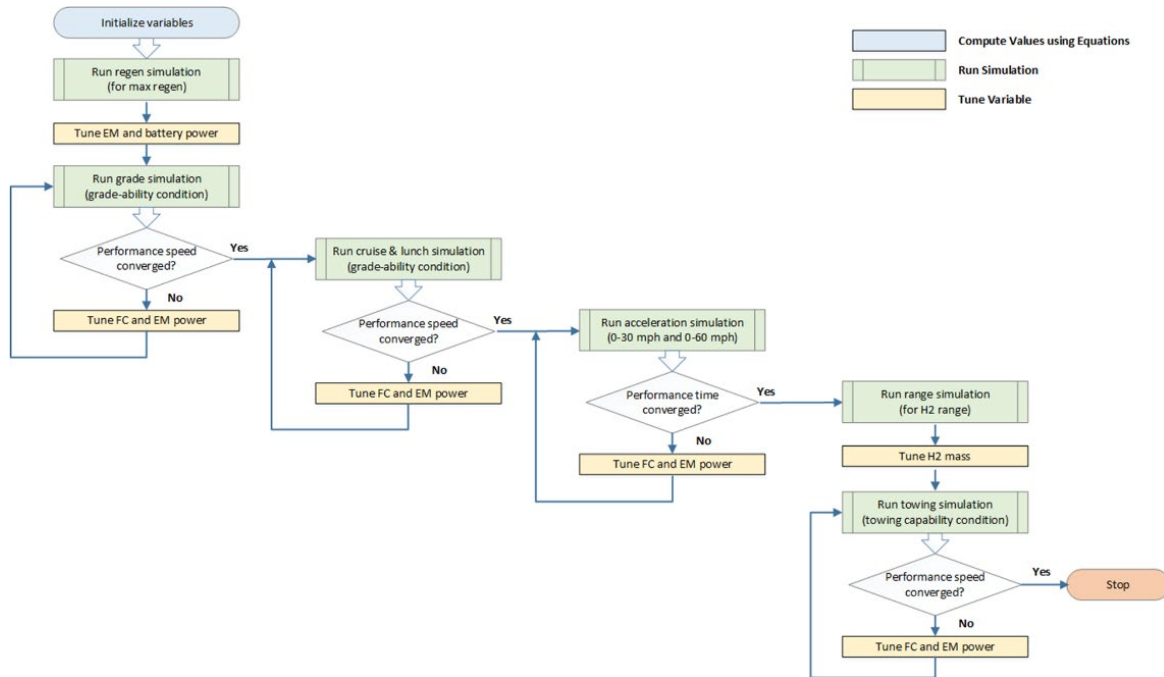


Figure 241. Parallel plug-in hybrid electric powertrain sizing algorithm

The main algorithm for fuel cell HEV sizing is as follows.

- The fuel cell and electric machine size achieves the peak power required to meet all performance requirements (e.g., acceleration performance, gradeability, or towing).
- The hydrogen storage capacity size achieves the specified AER on the EPA phase 2 55-mph cycle, based on the adjusted energy values.
- The battery power is sized to follow the UDDS cycle in EV mode at low SOC (beginning of CS mode) or to meet the acceleration performance requirement.
- The powertrain weight is a function of the fuel cell peak power, electric machine peak power, and number of battery cells.

BEV Sizing Algorithm

Figure 242 shows the detailed steps of the BEV sizing algorithm, used for BEV1 and BEV2 vehicle powertrains.

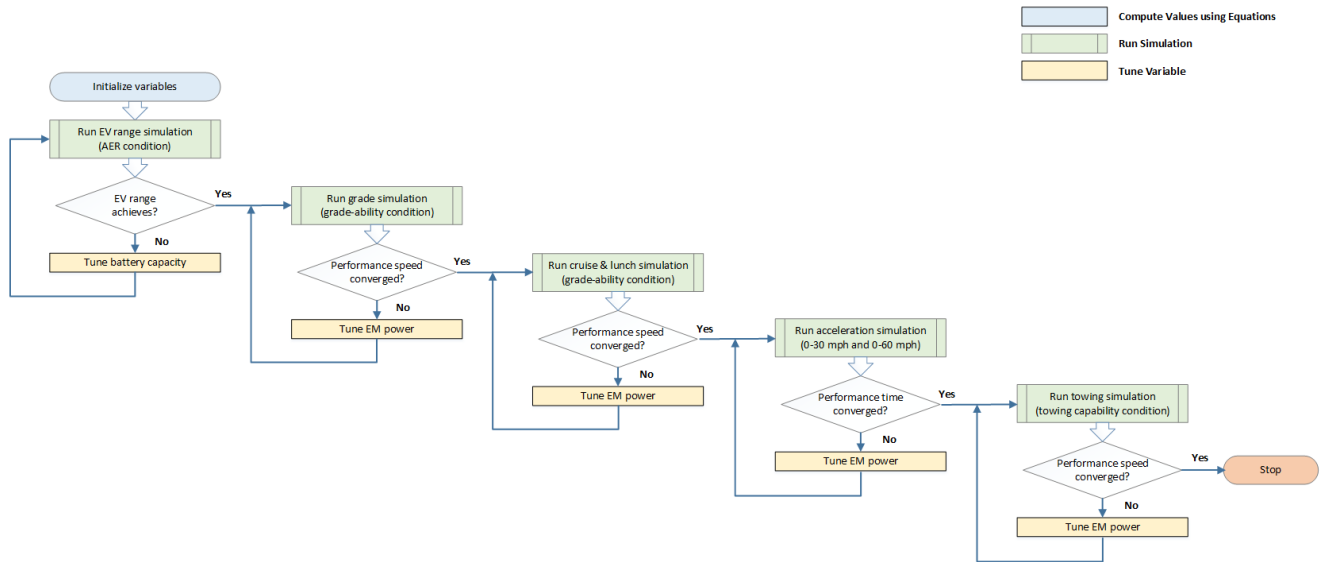


Figure 242. BEV sizing algorithm

The main algorithm for BEV sizing is as follows.

- Battery and EM powers are sized to achieve the peak power required to meet all performance requirements (e.g., acceleration performance, gradeability, or towing).
- The battery energy size achieves the specified AER on the EPA phase 2 55-mph cycle based on the adjusted energy values.
- The powertrain weight is a function of the electric machine (EM) peak power and battery energy.

Determining the Relationship Between Engine Displacement and Number of Cylinders (LDV)

Previously, we evaluated different engine displacements available across the number of engine cylinders to update the relationship used in previous analysis runs. We further evaluated the influence of major manufacturers on engine displacement. Figure 243 shows the relationship between the number of engine cylinders and engine displacement for existing vehicles in the U.S. market and MY 2020 vehicles from EPA test car data (EPA, 2016).

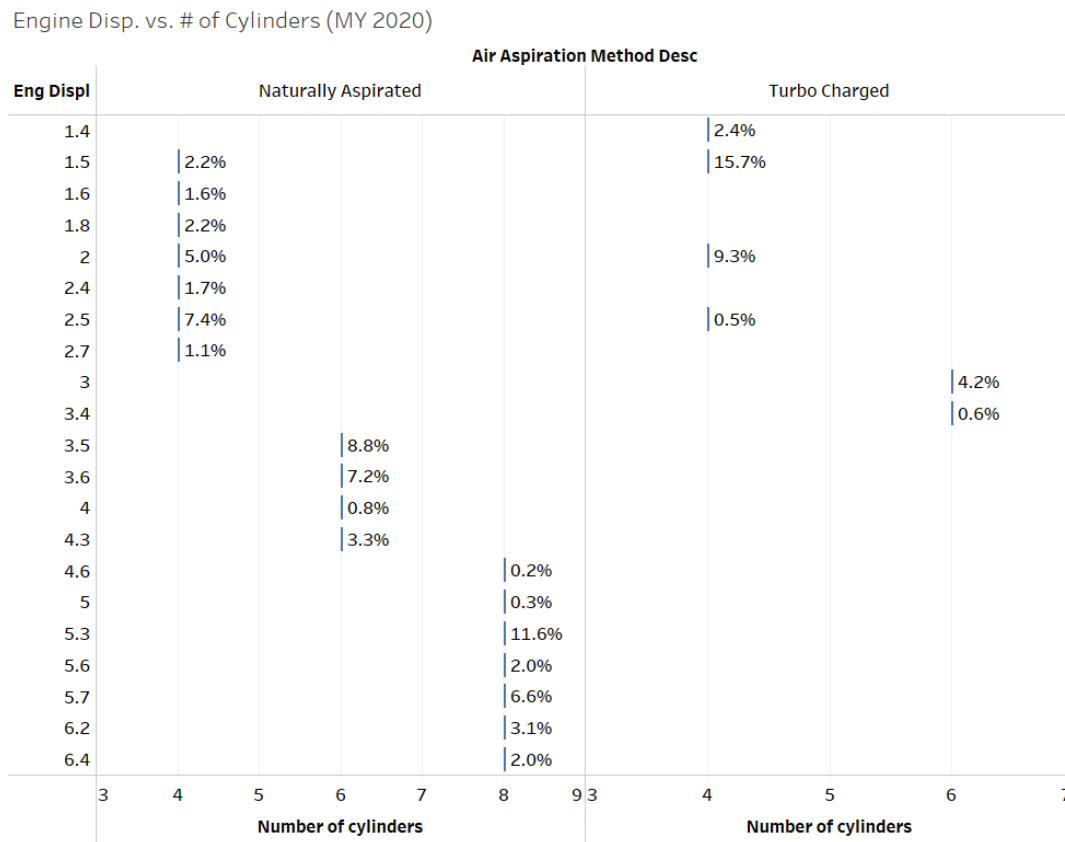


Figure 243. Relationship between engine displacement and number of engine cylinders

Using this relationship, thresholds were created to define the number (and type) of engine cylinders for given engine displacements across different engine configurations. These 15 different engine displacements cover about 93.2 percent of the conventional market in MY 2020. Table 75 shows the thresholds.

Table 75. Thresholds for engine displacement versus number of engine cylinders

Number and Configuration of Engine Cylinders	Engine Displacement (L)		Total
	NA	TC	
4-cylinder, in-line (I4)	NA	1.5, 1.6, 1.8, 2, 2.5	6
	TC	1.4, 1.5, 2	
6-cylinder, V6	NA	3.5, 3.6, 4, 4.3	5
	TC	3	
8-cylinder, V8	NA	5.3, 5.6, 5.7, 6.2	4

The flowchart in Figure 244 shows the detailed method used to calculate the engine displacement and number of cylinders from the initial engine size derived from the engine map.

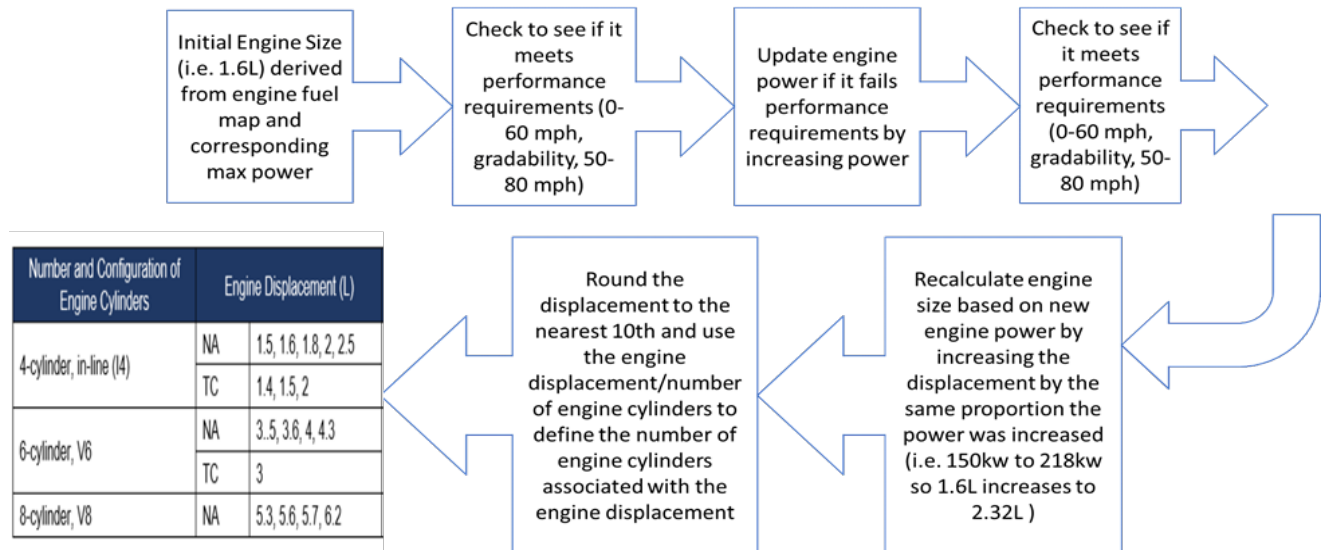


Figure 244. Method for computing engine displacement and number of cylinders

Distributed Computing Process

At this stage of the large-scale simulation process, all the vehicles are created and ready to be sized and simulated in Autonomie. Running millions of vehicles requires more than 5 million simulations, from sizing algorithms—imposing recurrence and iteration/looping—to vehicle simulation on cycles and combined or PHEV procedures.

With a multitude of technology combinations to simulate, and the objective of providing direct inputs from Autonomie to the CAFE model, the usual computing resources are no longer practical. Running all the simulations on one computer would take several months or years to complete. However, thanks to advances in distributed computing, simulation time can be greatly reduced. Among the computing resources available at Argonne is a cluster of several thousand worker nodes dedicated to the Vehicle & Mobility Systems Group. A larger high-performance computing facility will be used in the future to further accelerate the simulations.

Setup

Autonomie is used as the simulation framework, synchronized by a cluster head node computer. The head computer extracts the data describing the different technology pathways from the vehicle files and distributes it, as diagrammed in Figure 245. An algorithm optimizes the distribution of jobs for vehicle simulations.

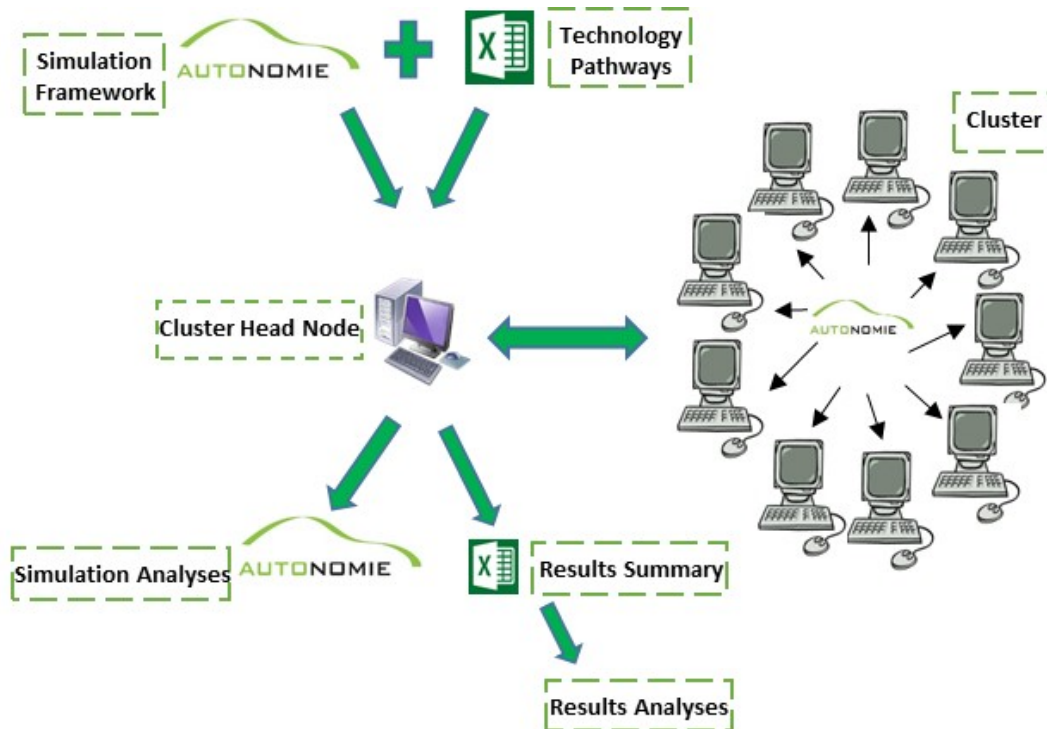


Figure 245. Distributed computing process

Distributed Computing Flexibility

One of the biggest advantages of distributed computing is that it aids in the quick reruns of simulations that occur many times during any study. This enabled Argonne to develop a new process: an ultimate large-scale simulation process that is functional, smooth, and flexible, with the ability to easily and quickly add and rerun as many vehicles and new technologies as needed. The generic process can automatically handle additional technologies without any code modification. As a result, the CAFE model's future technological needs can be easily and quickly integrated at any time, and new runs can be implemented to directly feed the model for CAFE rulemaking analyses.

Vehicle Simulation Process

Once the vehicles are sized or inherited to meet the desired vehicle technical specifications, they are simulated following the appropriate standard driving cycles and run procedures. It is important to properly store individual results as structured data because they will be reused to support database generation and easy browsing. Figure 246 shows the folder organization for each individual simulation.

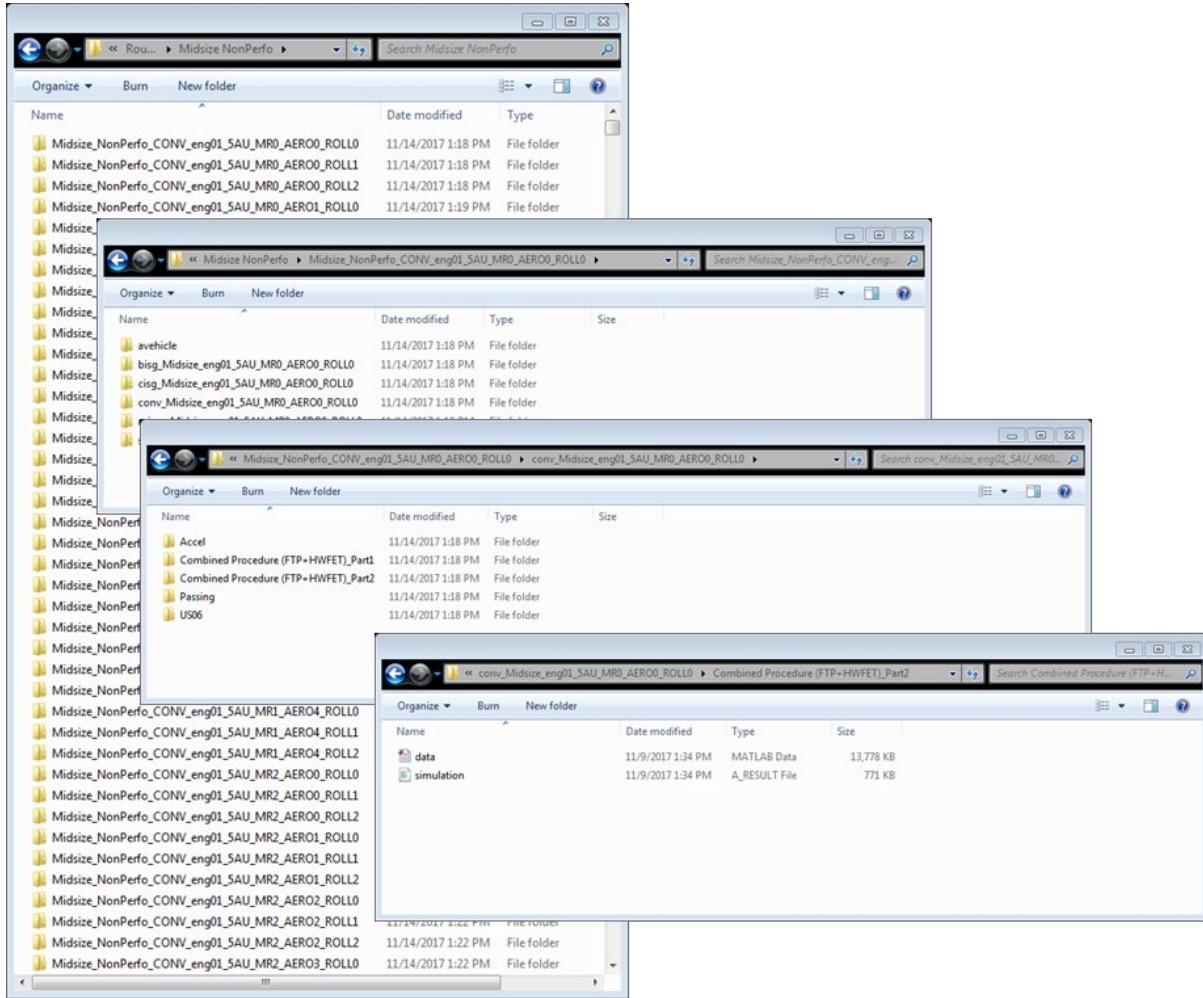
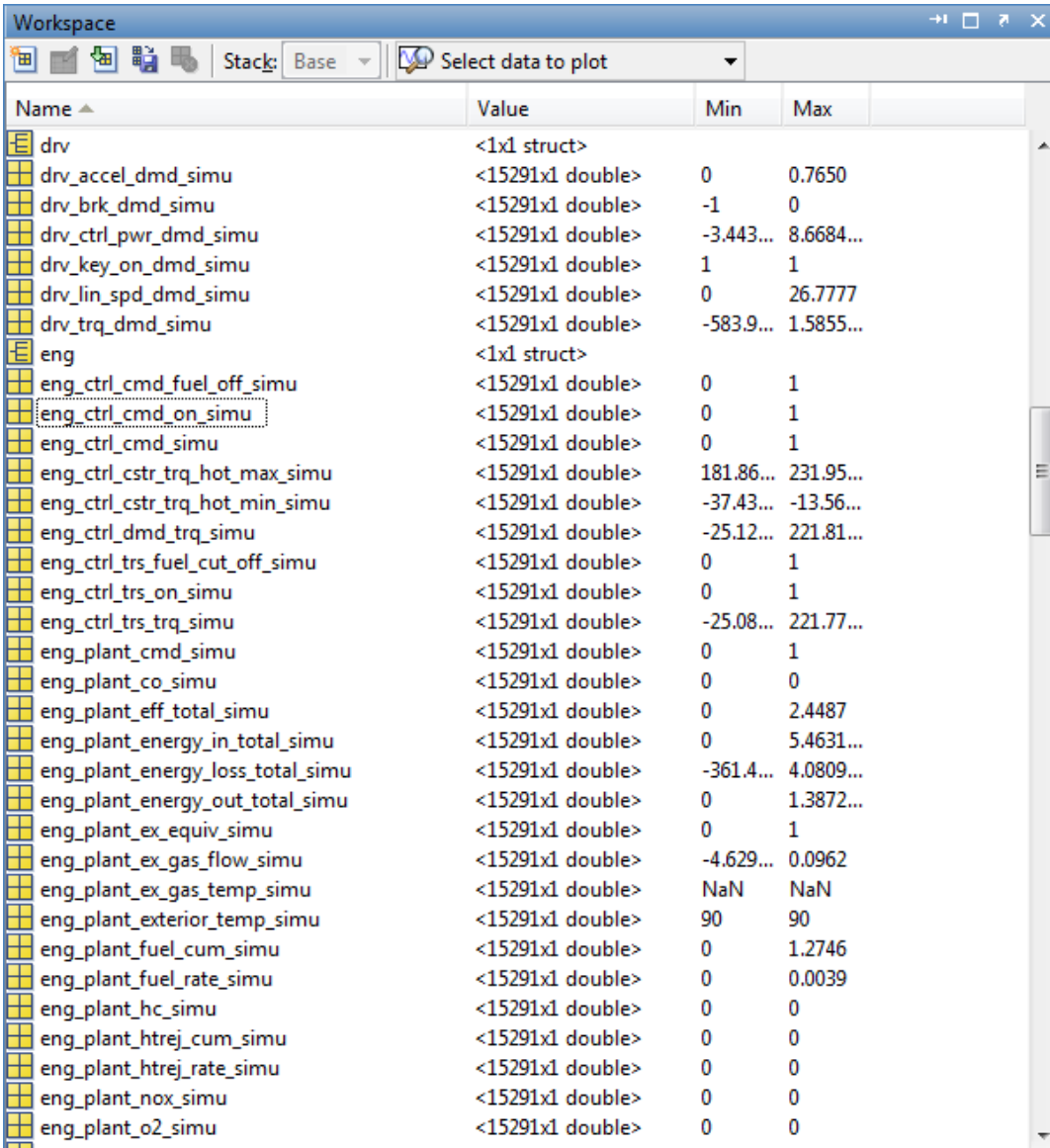


Figure 246. Vehicle simulation folder organization

Each folder contains the results for one combination and characterizes one branch/path of the tree. Folders can contain up to five directories, depending on the vehicle technology and the type of run performed. Results are divided into directories representing the cycle or procedure simulated. For example, the combined procedure for conventional vehicles has two folders, containing the FTP and HWFET runs, and the PHEV procedure has four folders, for the FTP and HWFET runs plus the CS and CD modes. The last directory is the sizing structure (performance test).

Data.mat File

Data.mat contains the results of all the vehicle parameters and the time-based signals. Figure 247 shows a sample of signals and parameters included in data.mat.

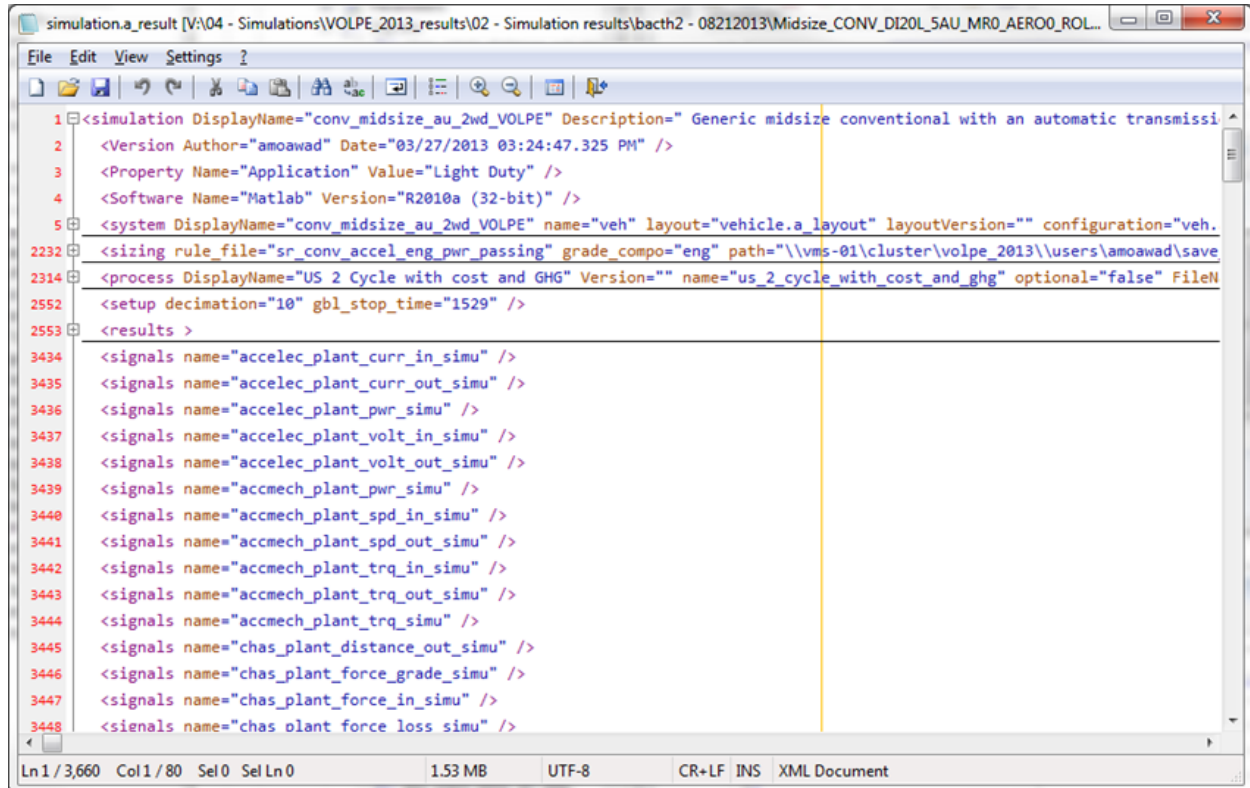


Name	Value	Min	Max
drv	<1x1 struct>		
drv_accel_dmd_simu	<15291x1 double>	0	0.7650
drv_brk_dmd_simu	<15291x1 double>	-1	0
drv_ctrl_pwr_dmd_simu	<15291x1 double>	-3.443...	8.6684...
drv_key_on_dmd_simu	<15291x1 double>	1	1
drv_lin_spd_dmd_simu	<15291x1 double>	0	26.7777
drv_trq_dmd_simu	<15291x1 double>	-583.9...	1.5855...
eng	<1x1 struct>		
eng_ctrl_cmd_fuel_off_simu	<15291x1 double>	0	1
eng_ctrl_cmd_on_simu	<15291x1 double>	0	1
eng_ctrl_cmd_simu	<15291x1 double>	0	1
eng_ctrl_cstr_trq_hot_max_simu	<15291x1 double>	181.86...	231.95...
eng_ctrl_cstr_trq_hot_min_simu	<15291x1 double>	-37.43...	-13.56...
eng_ctrl_dmd_trq_simu	<15291x1 double>	-25.12...	221.81...
eng_ctrl_trs_fuel_cut_off_simu	<15291x1 double>	0	1
eng_ctrl_trs_on_simu	<15291x1 double>	0	1
eng_ctrl_trs_trq_simu	<15291x1 double>	-25.08...	221.77...
eng_plant_cmd_simu	<15291x1 double>	0	1
eng_plant_co_simu	<15291x1 double>	0	0
eng_plant_eff_total_simu	<15291x1 double>	0	2.4487
eng_plant_energy_in_total_simu	<15291x1 double>	0	5.4631...
eng_plant_energy_loss_total_simu	<15291x1 double>	-361.4...	4.0809...
eng_plant_energy_out_total_simu	<15291x1 double>	0	1.3872...
eng_plant_ex_equiv_simu	<15291x1 double>	0	1
eng_plant_ex_gas_flow_simu	<15291x1 double>	-4.629...	0.0962
eng_plant_ex_gas_temp_simu	<15291x1 double>	NaN	NaN
eng_plant_exterior_temp_simu	<15291x1 double>	90	90
eng_plant_fuel_cum_simu	<15291x1 double>	0	1.2746
eng_plant_fuel_rate_simu	<15291x1 double>	0	0.0039
eng_plant_hc_simu	<15291x1 double>	0	0
eng_plant_htrej_cum_simu	<15291x1 double>	0	0
eng_plant_htrej_rate_simu	<15291x1 double>	0	0
eng_plant_nox_simu	<15291x1 double>	0	0
eng_plant_o2_simu	<15291x1 double>	0	0

Figure 247. Sample Autonomie result (data.mat)

XML Results File

As shown in Figure 248, the simulation.a result is an XML version of the results file that includes the main simulation inputs and outputs. This file is later used to generate the complete database.



```
1 <simulation DisplayName="conv_midsize_au_2wd_VOLPE" Description=" Generic midsize conventional with an automatic transmissi
2 <Version Author="amoawad" Date="03/27/2013 03:24:47.325 PM" />
3 <Property Name="Application" Value="Light Duty" />
4 <Software Name="Matlab" Version="R2010a (32-bit)" />
5 <system DisplayName="conv_midsize_au_2wd_VOLPE" name="veh" layout="vehicle.a_layout" layoutVersion="" configuration="veh.
2232 <sizing rule_file="sr_conv_accel_eng_pwr_passing" grade_compo="eng" path="//vms-01\cluster\volpe_2013\users\amoawad\save
2314 <process DisplayName="US 2 Cycle with cost and GHG" Version="" name="us_2_cycle_with_cost_and_ghg" optional="false" FileN
2552 <setup decimation="10" gbl_stop_time="1529" />
2553 <results >
3434 <signals name="accelec_plant_curr_in_simu" />
3435 <signals name="accelec_plant_curr_out_simu" />
3436 <signals name="accelec_plant_pwr_simu" />
3437 <signals name="accelec_plant_volt_in_simu" />
3438 <signals name="accelec_plant_volt_out_simu" />
3439 <signals name="accmech_plant_pwr_simu" />
3440 <signals name="accmech_plant_spd_in_simu" />
3441 <signals name="accmech_plant_spd_out_simu" />
3442 <signals name="accmech_plant_trq_in_simu" />
3443 <signals name="accmech_plant_trq_out_simu" />
3444 <signals name="accmech_plant_trq_simu" />
3445 <signals name="chas_plant_distance_out_simu" />
3446 <signals name="chas_plant_force_grade_simu" />
3447 <signals name="chas_plant_force_in_simu" />
3448 <signals name="chas plant force loss simu" />
```

Figure 248. XML Autonomie results file (simulation.a_result)

Simulation Results Analysis and Detailed Validation Processes

An analysis of the simulation results database is performed using Tableau and MATLAB. This section highlights some examples of these analyses with the objective of automatically detecting potential outliers.

Engine Operating Points Across Transmissions

Light-Duty Vehicle

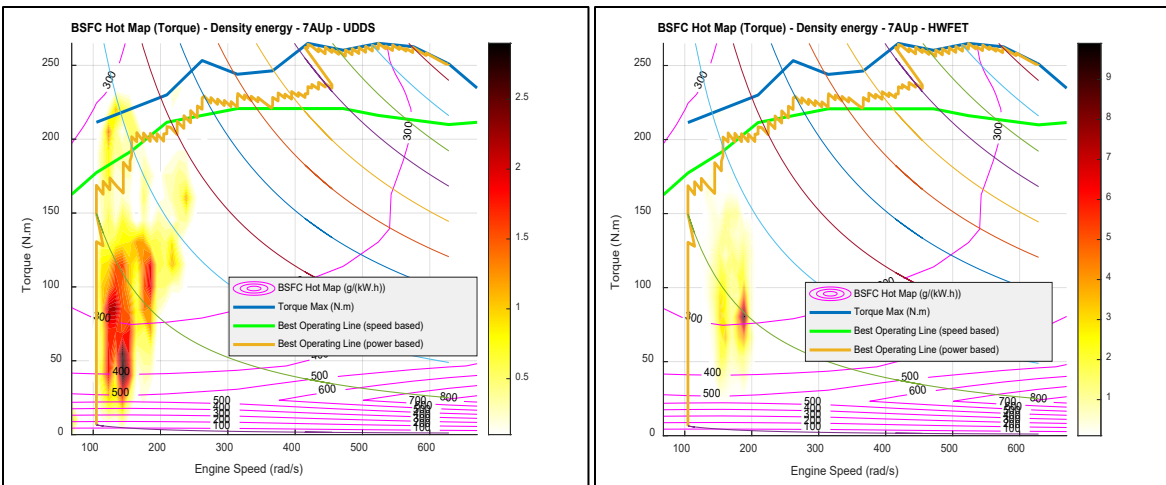
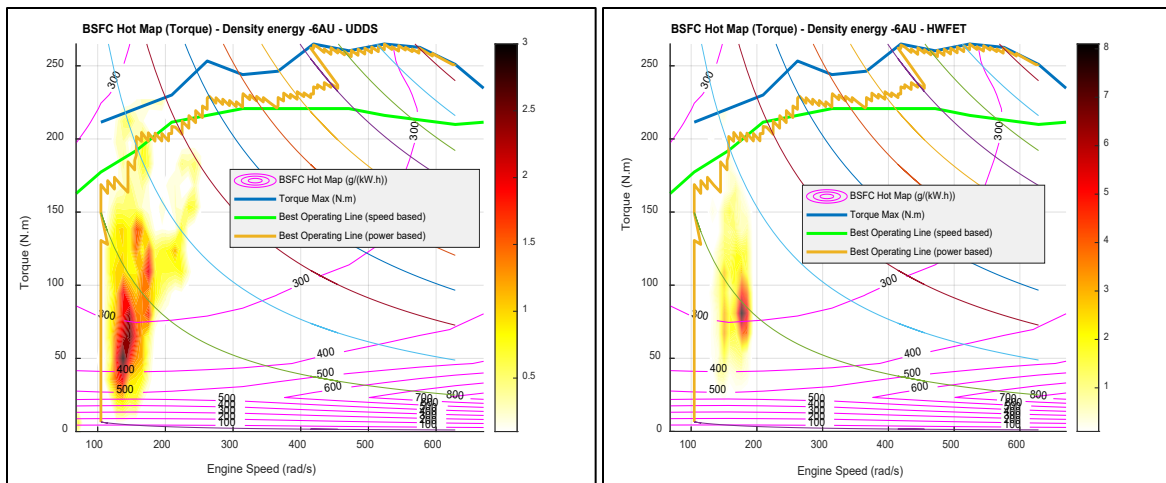
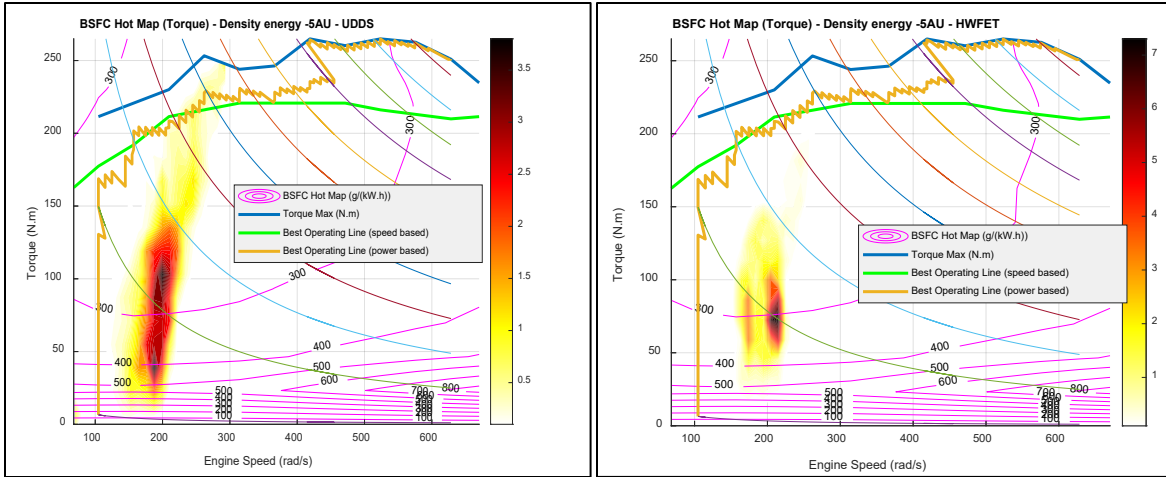
Evaluating the engine density (i.e., operating points) across different transmission types and numbers of gears would help us evaluate the impact of improved transmissions. The vehicle selected for this analysis is as follows.

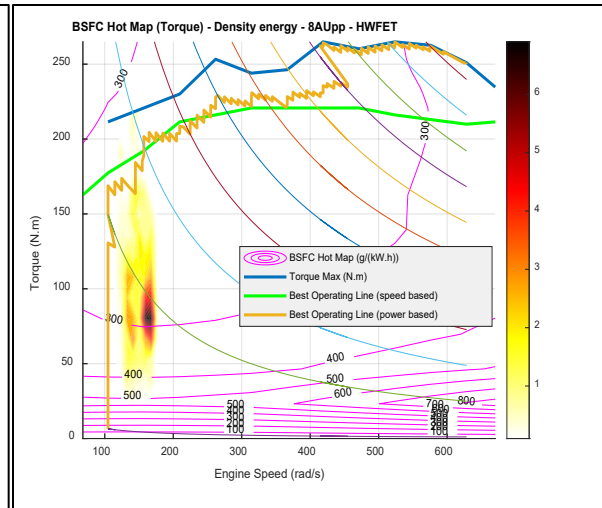
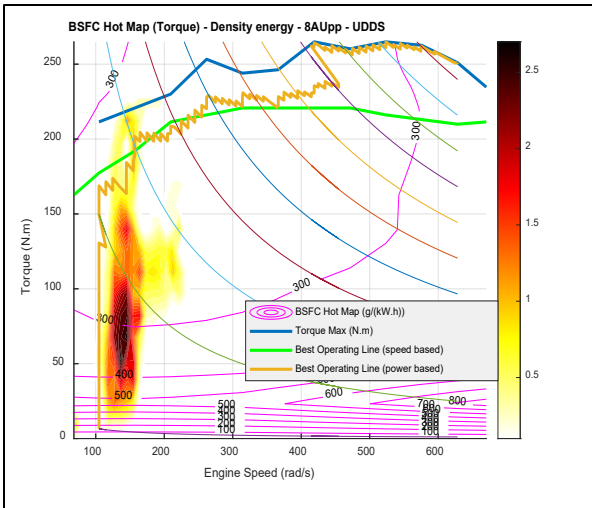
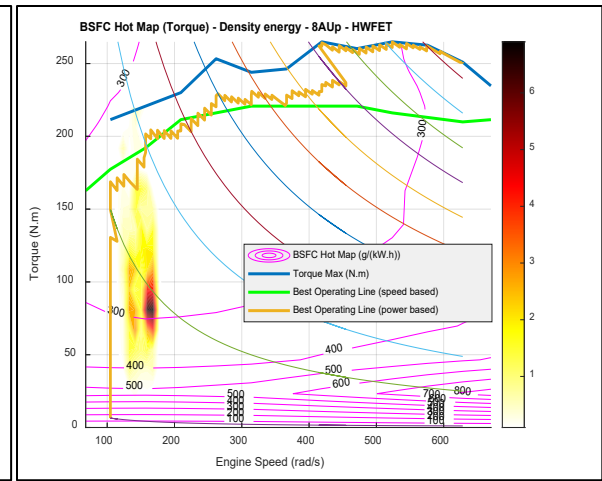
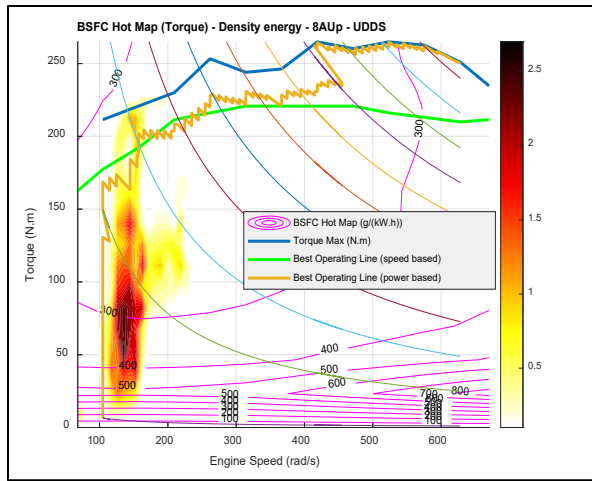
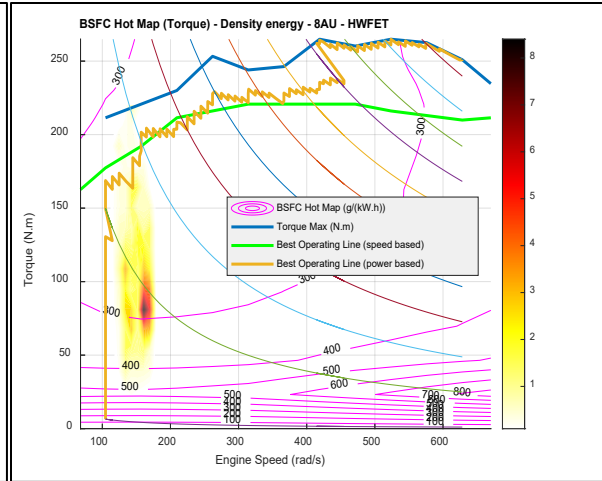
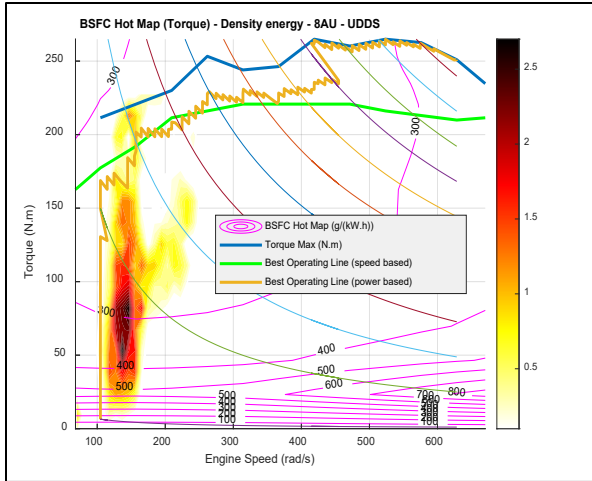
- Vehicle class: Midsize
- Performance category: Non-performance
- Vehicle powertrain: Conventional
- Engine: Engine 01
- Mass reduction: MR Level 0 (MR0)
- Aerodynamic drag reduction: AERO Level 0 (AERO0)
- Rolling-resistance reduction: ROLL Level 0 (ROLL0)

As expected, the average engine speed decreases with more gears and increased gear span.

Automatic Transmission

Figure 249 (next three pages) shows the engine operating points for automatic transmission types with different numbers of gears.





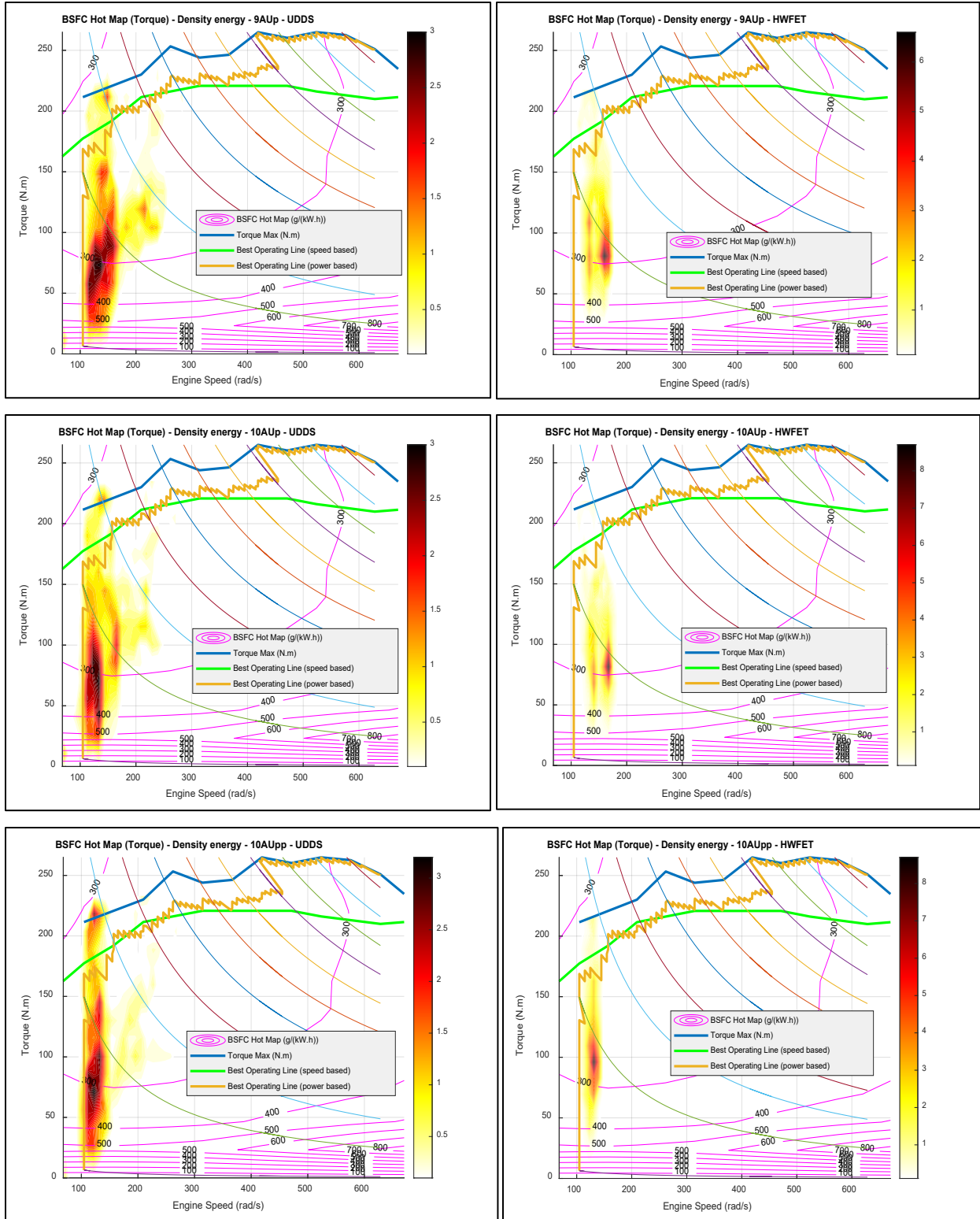


Figure 249. Engine operating points for automatic transmissions

Dual-Clutch Transmissions

Figure 250 shows the engine operating points for 6- and 8-speed DCTs.

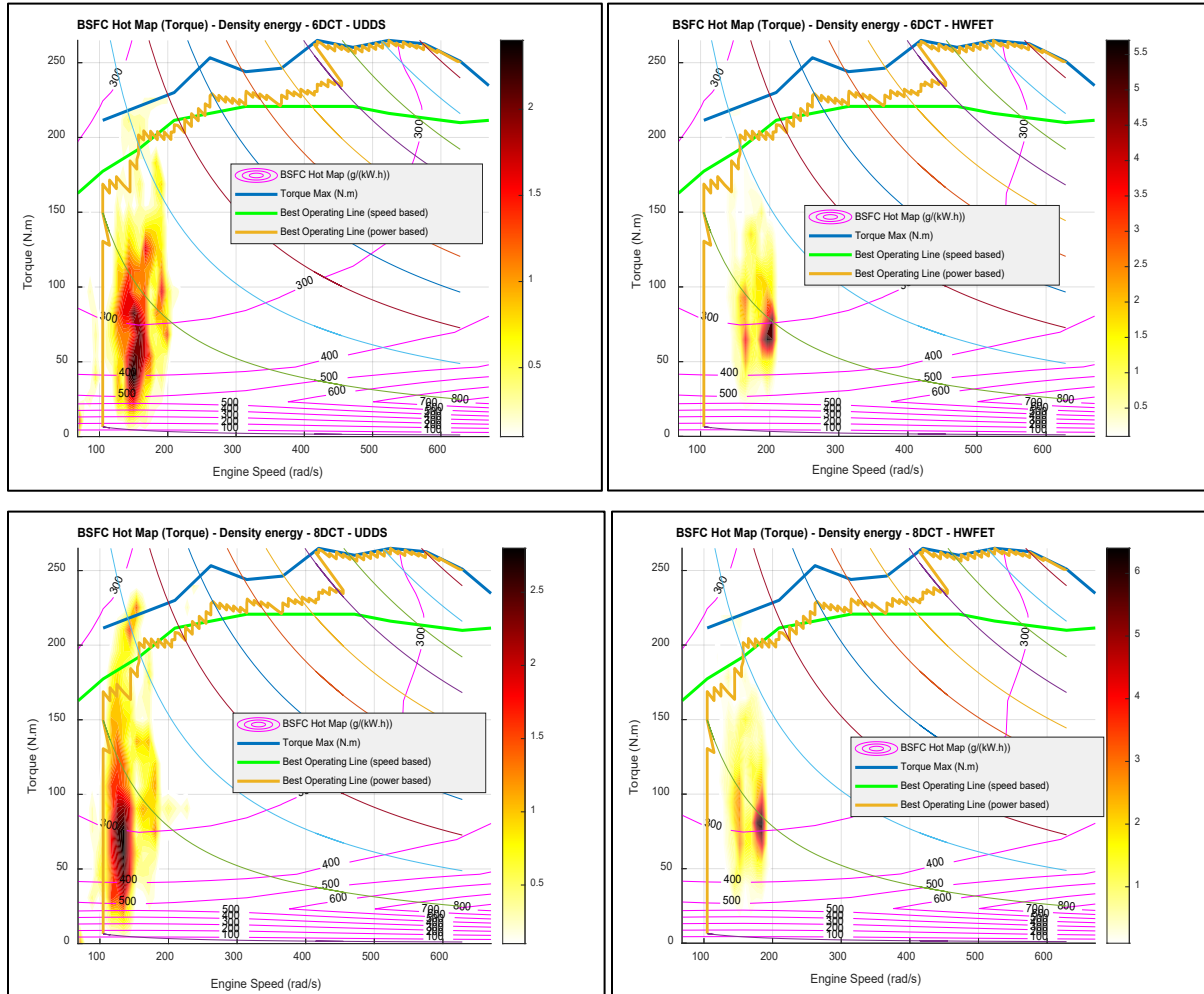


Figure 250. Engine operating points for 6- and 8-speed DCT transmissions

CVT Transmission

Figure 251 shows the engine operating points for two CVT types.

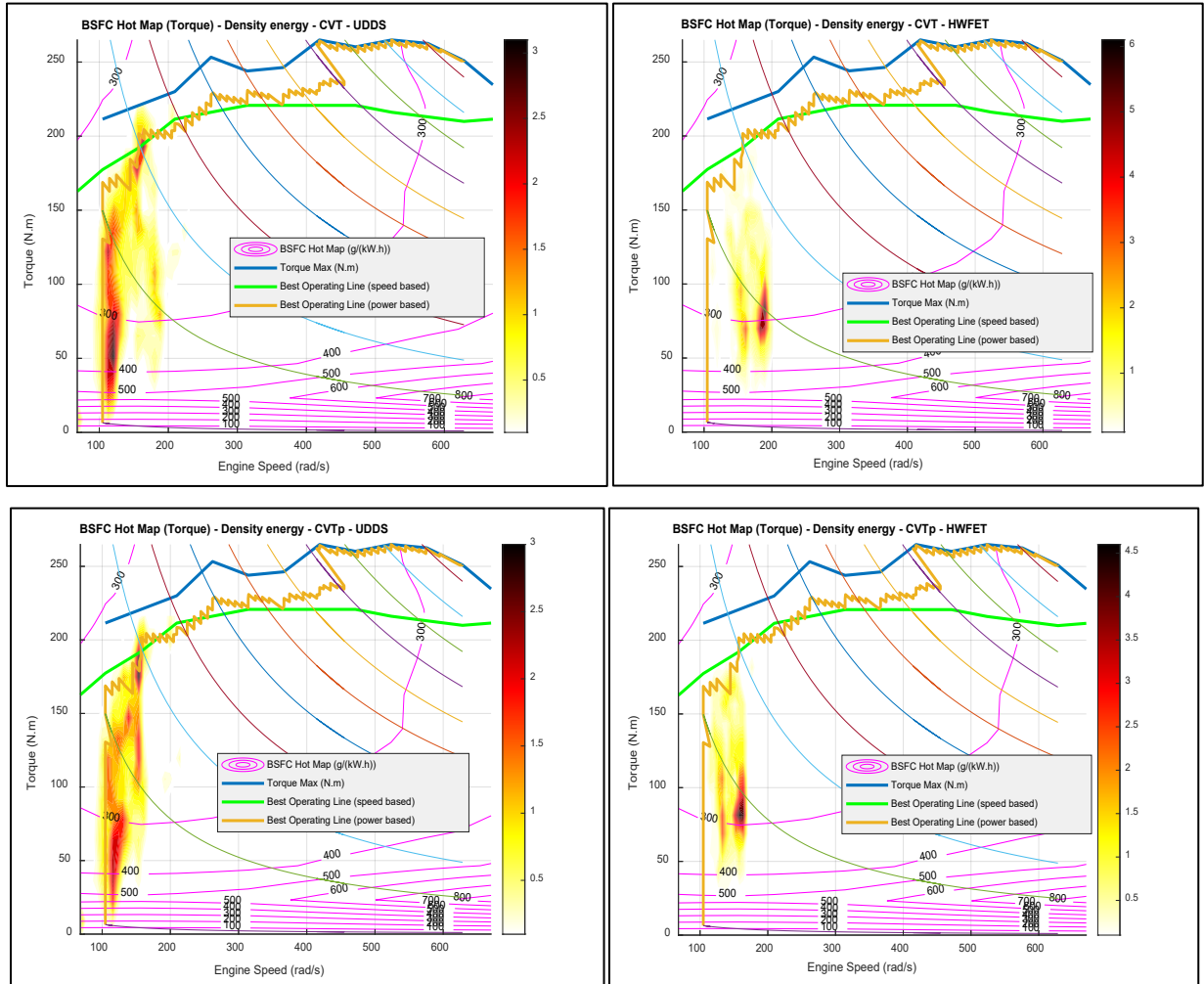


Figure 251. Engine operating points for CVTs

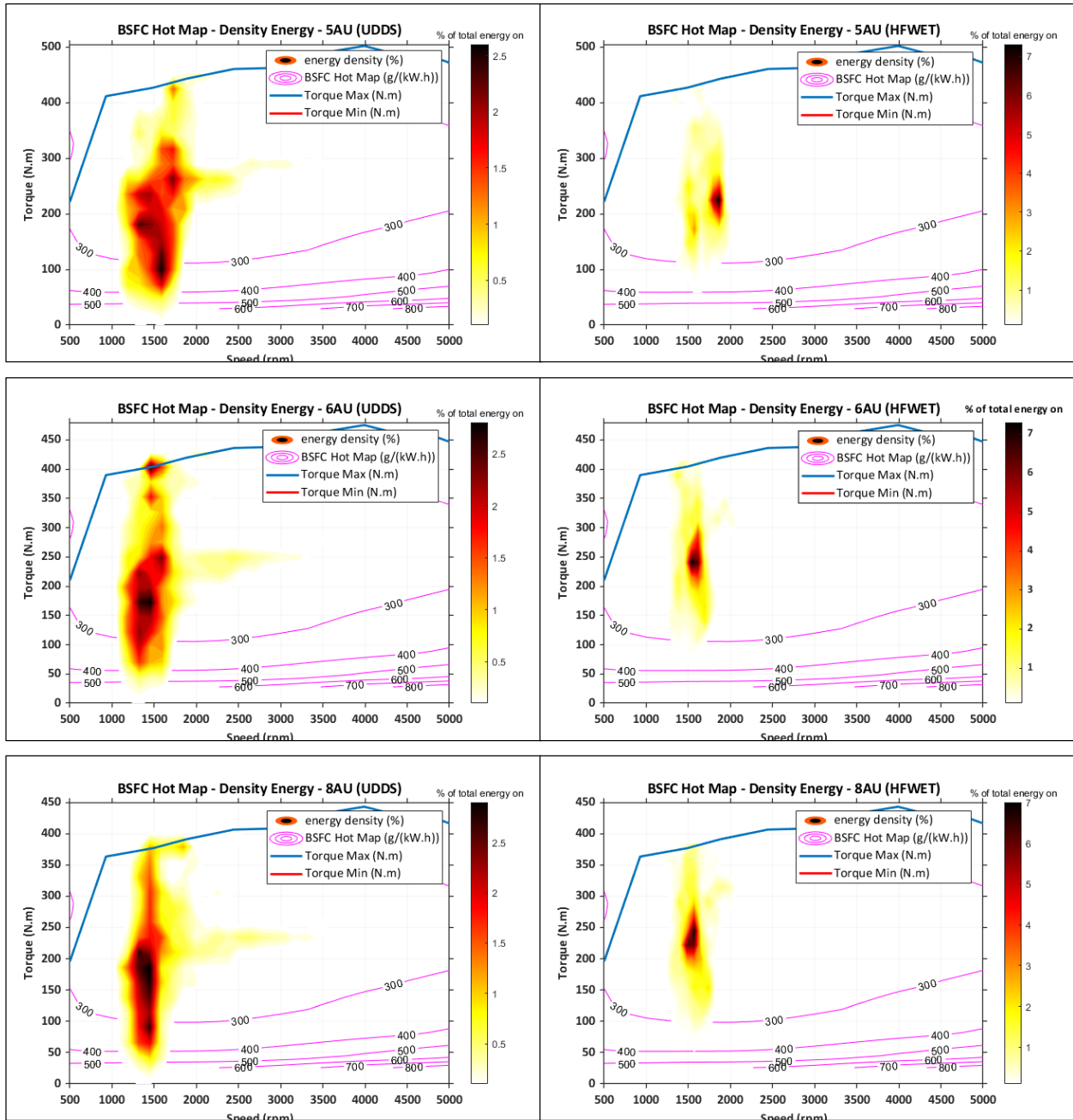
Heavy-Duty Pickups and Vans

Evaluating the engine density (i.e., operating points) across different transmission types and numbers of gears would help us evaluate the impact of improved transmissions. The vehicle selected for this analysis is as follows.

- Vehicle class: HD Class 2b
- Vehicle purpose: Van
- Engine: Engine 4a
- Mass reduction: MR Level 0 (MR0)
- Aerodynamic drag reduction: AERO Level 0 (AERO0)
- Rolling-resistance reduction: ROLL Level 0 (ROLL0)

As expected, the average engine speed decreases with more gears and increased gear span.

Figure 252 shows the engine operating points for automatic transmission types with different numbers of gears.



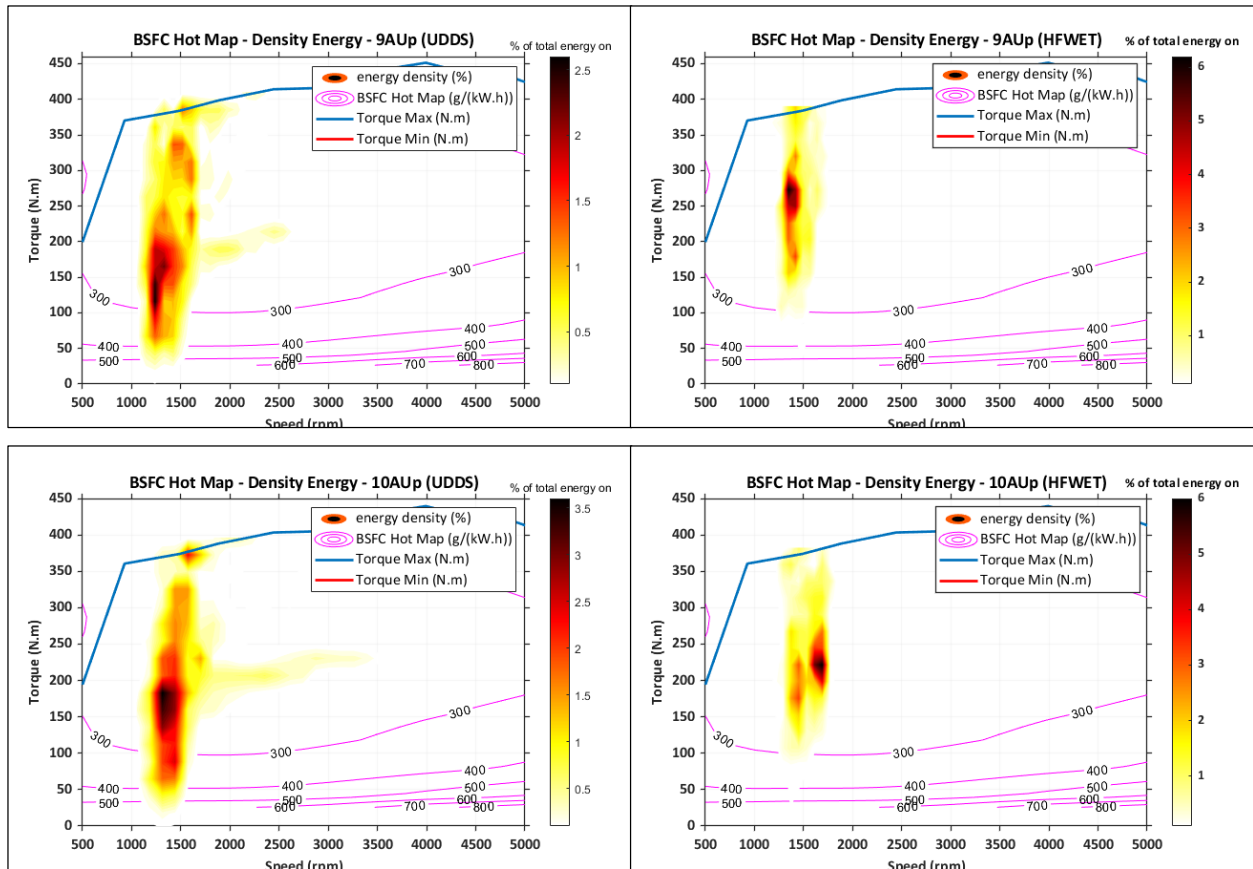


Figure 252. Engine operating points for automatic transmissions

Powertrain Efficiency Analysis

Light-Duty Vehicle

Evaluating powertrain efficiency across different transmission types and numbers of gears as well as individual powertrains would help us evaluate the impact of improved technologies. In this section, the vehicle combination selected for this analysis is as follows.

- Vehicle class: Midsize
- Vehicle powertrain: Conventional
- Performance category: Non-performance
- Aerodynamic drag reduction: AERO Level 0 (AERO0)
- Rolling-resistance reduction: ROLL Level 0 (ROLL0)

Figure 253 shows the powertrain efficiency values for both UDDS and HWFET cycles for different engine types with automatic transmission and different numbers of gears.

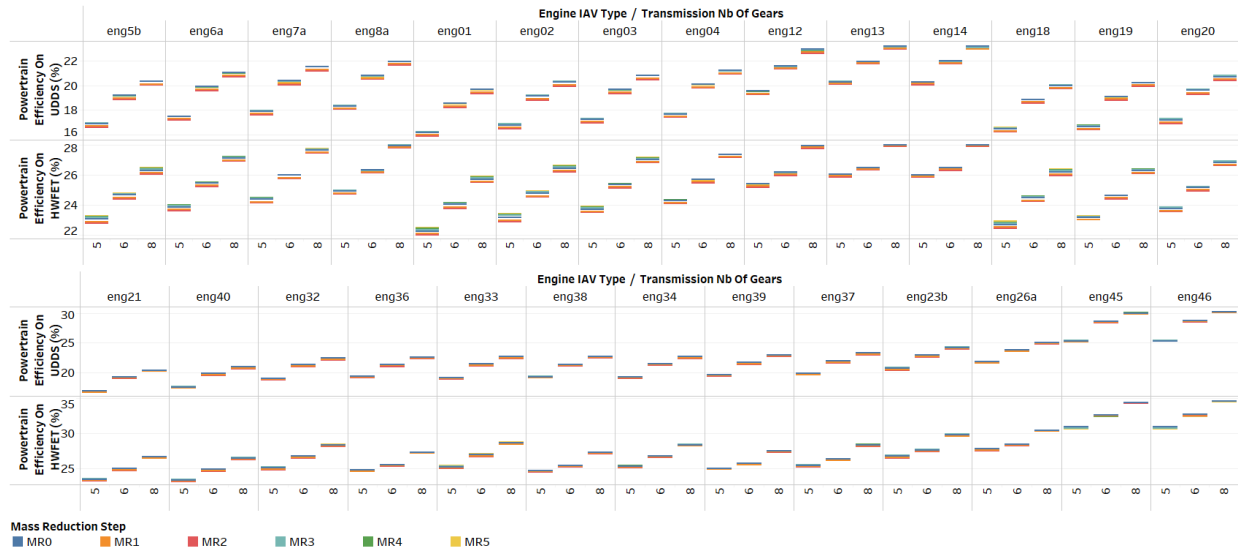


Figure 253. Powertrain efficiency values of different engine types with automatic transmissions and different numbers of gears

Note that with an increasing number of gears, the powertrain efficiency increases for both UDDS and HWFET. This increase is more pronounced with engines demonstrating higher efficiencies (e.g., eng01 versus eng26a).

Figure 254 shows the powertrain efficiency values for UDDS and HWFET for different engine types with automatic+ (AU+) transmissions with different numbers of gears.

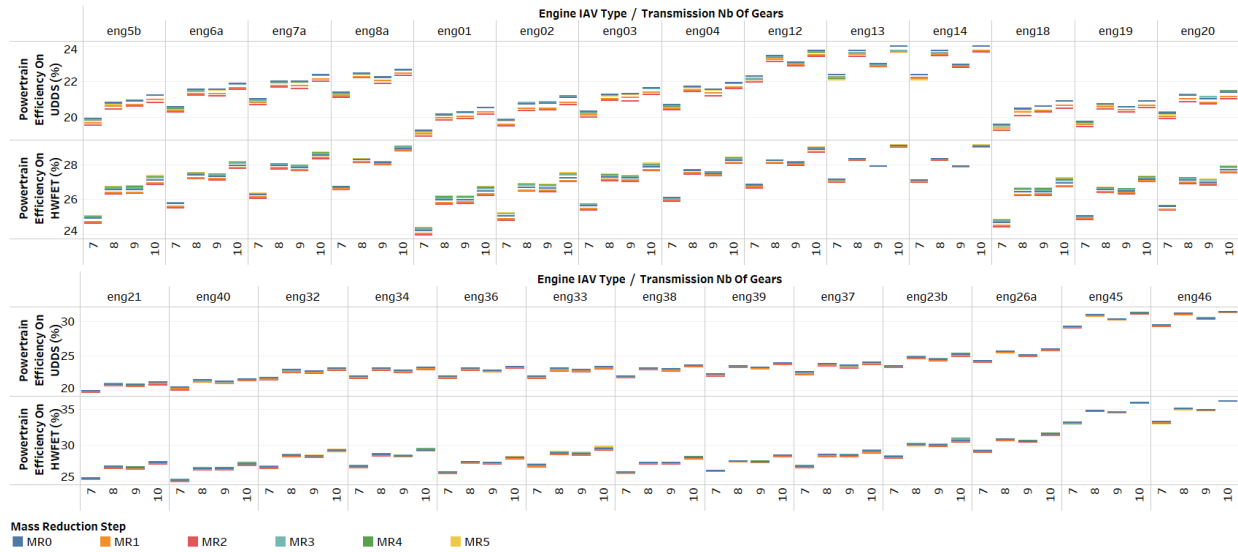


Figure 254. Powertrain efficiency values of different engine types with AU+ transmissions with different numbers of gears

From the figure, going from 8-speed to 9-speed AU+ causes powertrain efficiency to decrease slightly for UDDS, due to increased shifting, as well as a drop in gearbox efficiency. However, for HWFET runs, powertrain efficiency increases with the number of gears.

Figure 255 shows the powertrain efficiency values for different engine types with automatic++ (AU++) transmissions and different numbers of gears.

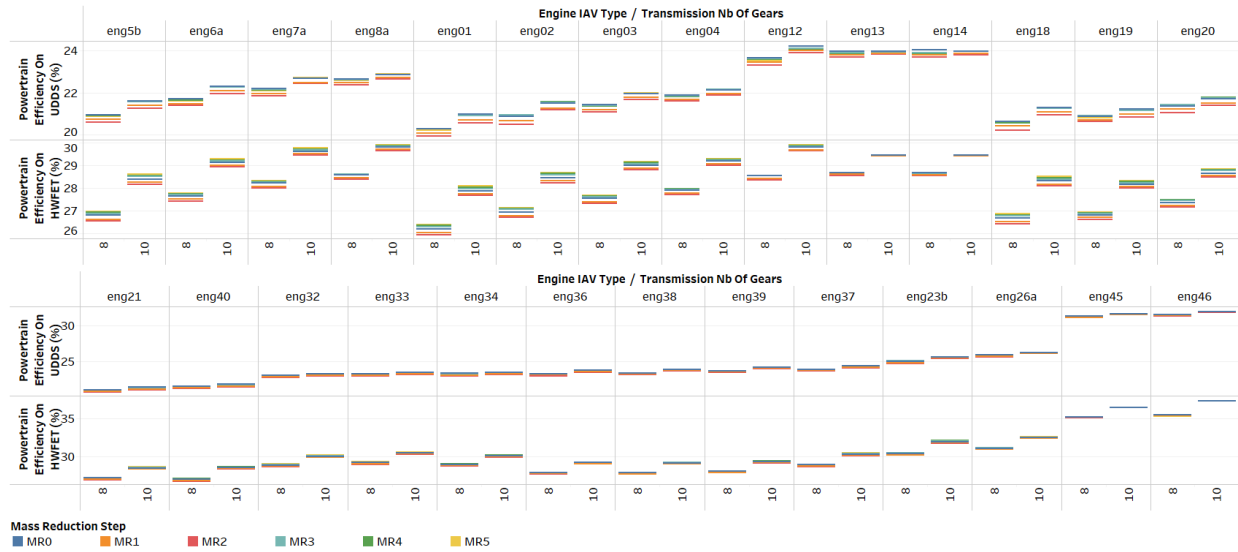


Figure 255. Powertrain efficiency values of different engine types with AU++ transmissions with different numbers of gears

For AU++ transmission, powertrain efficiency increases with an increased number of gears for UDDS and HWFET runs. Values also improve for engines demonstrating higher technology effectiveness (e.g., eng01 versus eng26a).

Figure 256 shows the powertrain efficiency values for the different engine types with DCTs and different numbers of gears.

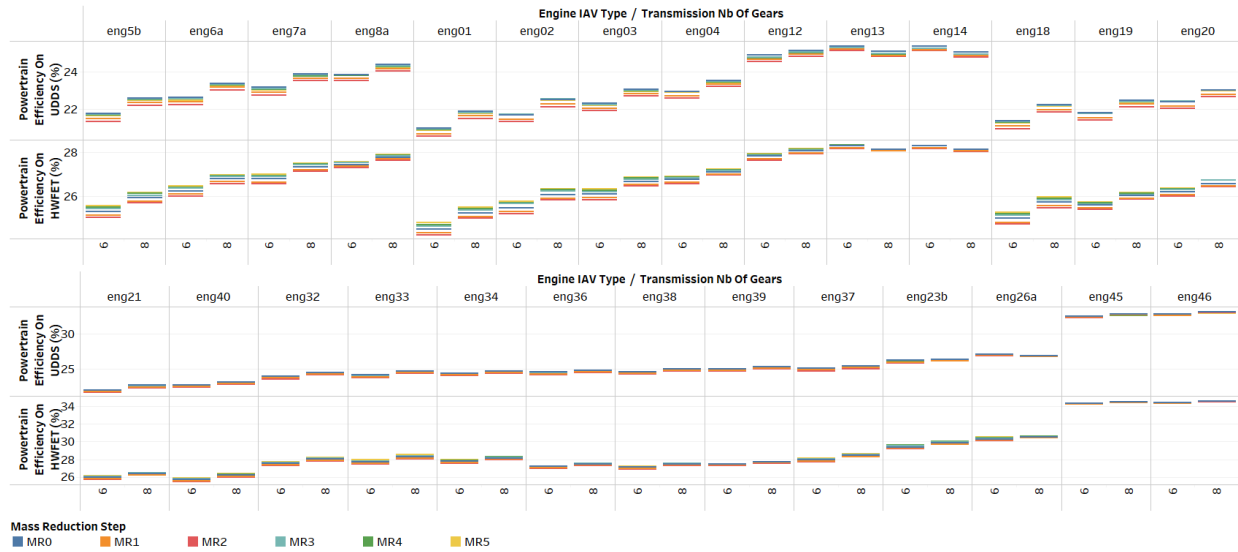


Figure 256. Powertrain efficiency values of different engine types with DCTs with different numbers of gears

The powertrain efficiency of DCT transmissions increases with the number of gears for both UDDS and HWFET runs. Values also improve for engines demonstrating higher technology effectiveness (e.g., eng01 versus eng26a).

Figure 257 shows the powertrain efficiency values for different engine types with CVTs.



Figure 257. Powertrain efficiency values of different engine types with CVT

For CVTs the powertrain efficiency increases with higher engine efficiencies (e.g., eng01 versus eng26a).

Figure 258 shows the powertrain efficiency values for different engine types with CVT+.

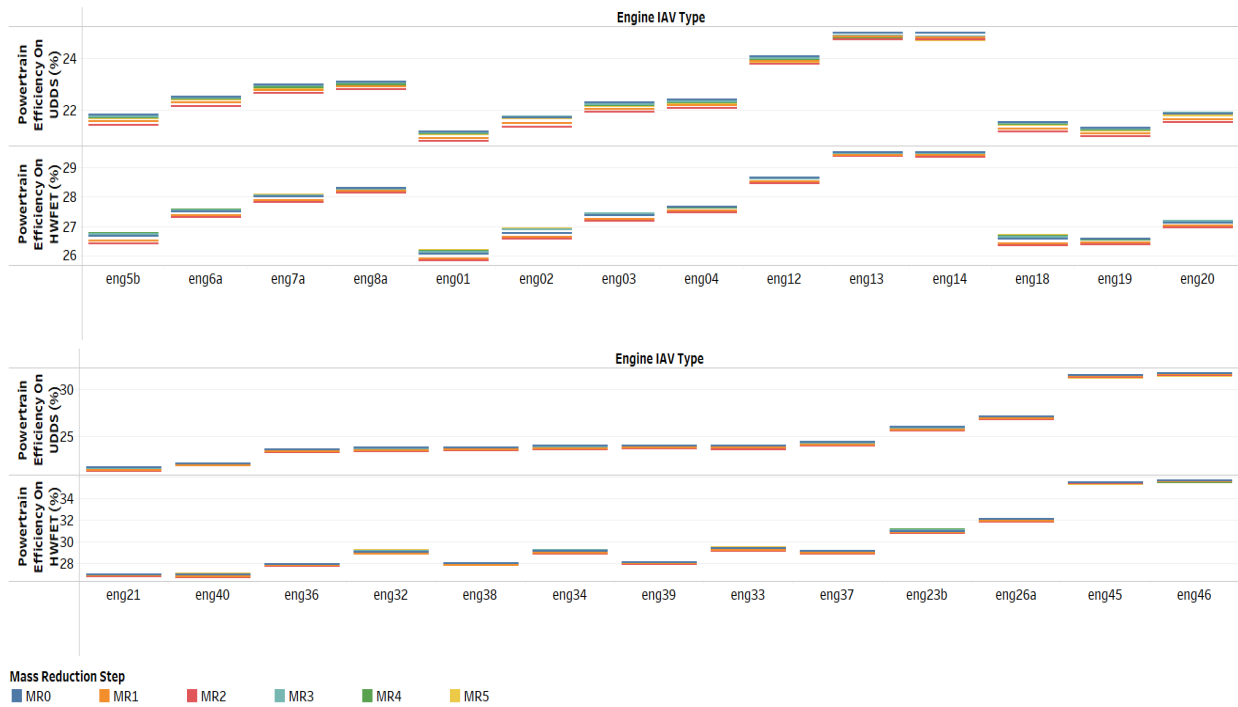


Figure 258. Powertrain efficiency values of different engine types with CVT+

The CVT+, the powertrain efficiency increases with higher engine efficiencies (e.g., eng01 versus eng26a).

Heavy-Duty Pickups and Vans

Evaluating powertrain efficiency across different transmission types and numbers of gears as well as individual powertrains would help us evaluate the impact of improved technologies. In this section, the vehicle combination selected for this analysis is as follows.

- Vehicle class: HD Class 2b
- Vehicle purpose: Van
- Vehicle powertrain: Conventional
- Aerodynamic drag reduction: AERO Level 0 (AERO0)
- Rolling-resistance reduction: ROLL Level 0 (ROLL0)

Figure 259 shows the powertrain efficiency values for both UDDS and HWFET cycles for different engine types with automatic transmission and different numbers of gears. With an increasing number of gears, the powertrain efficiency increases for both UDDS and HWFET.

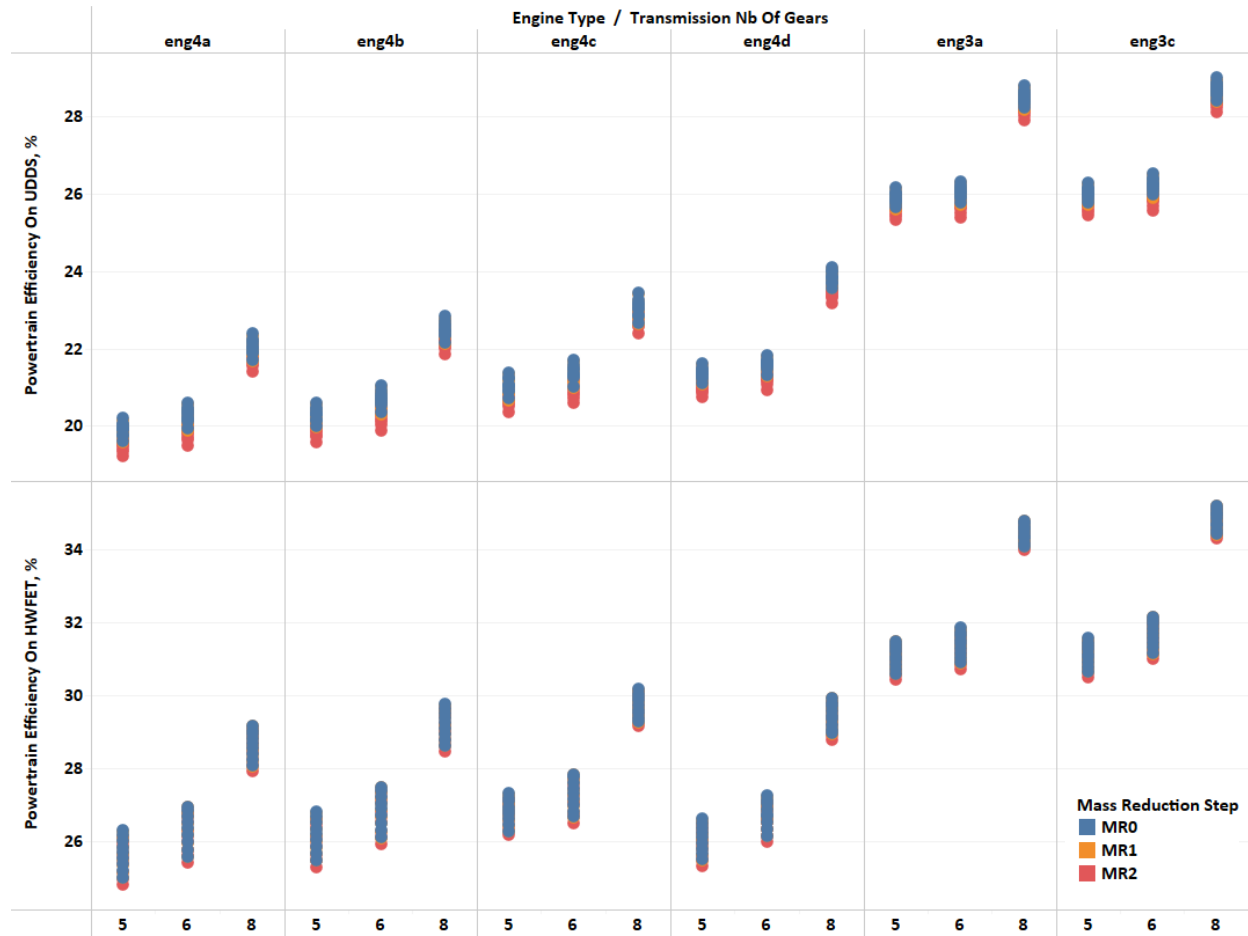


Figure 259. Powertrain efficiency values of different engine types with automatic transmissions and different numbers of gears

Figure 260 shows the powertrain efficiency values for UDDS and HWFET for different engine types with automatic+ (AU+) transmissions with different numbers of gears.

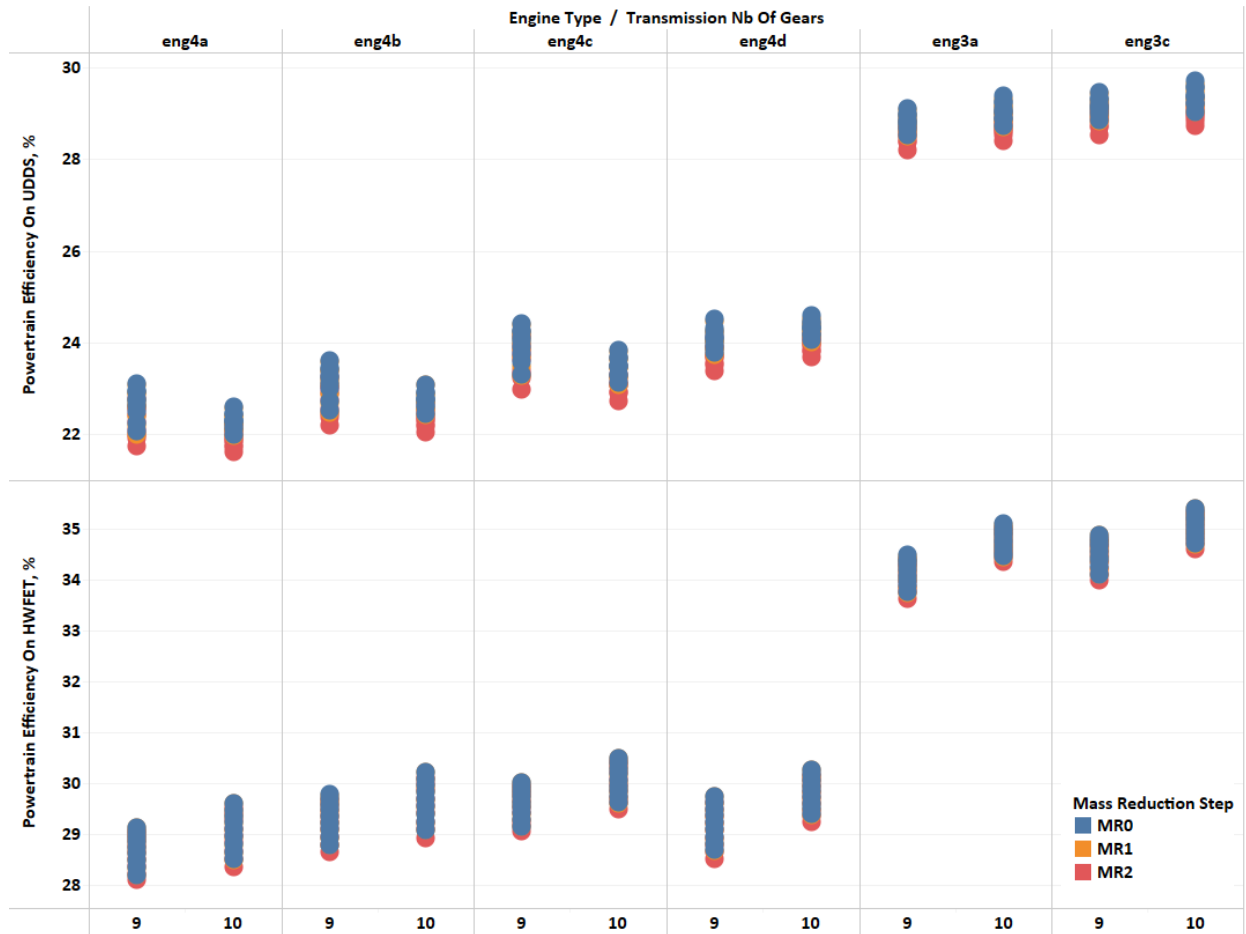


Figure 260. Powertrain efficiency values of different engine types with AU+ transmissions and different numbers of gears

Total Number of Shifting Events With Different Transmission Types and Numbers of Gears

Light-Duty Vehicle

The total number of shifting events (upshift + downshift) determines the drive quality, so it is important to check the total number of shifting events across transmissions and numbers of gears against vehicle test data. Throughout this analysis, the following vehicle was used.

- Vehicle class: Midsize
- Performance category: Non-performance
- Powertrain type: Conventional
- Engine: Engine 01
- Aerodynamic drag reduction: AERO Level 0 (AERO0)
- Rolling-resistance reduction: ROLL Level 0 (ROLL0)

Automatic Transmission Types

Figure 261 shows the total number of shifting events for automatic (AU), automatic+ (AUp), and automatic++ (Aupp) transmissions with different numbers of gears during a UDDS cycle.

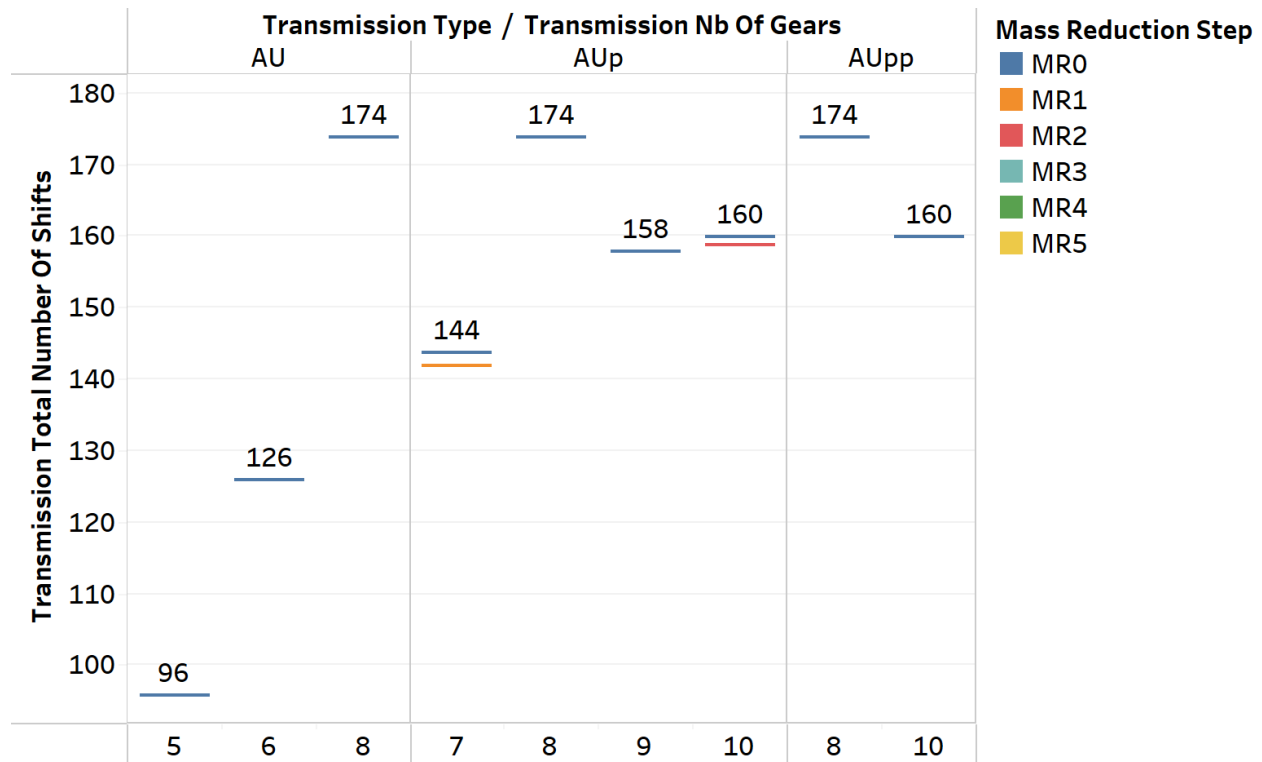


Figure 261. Total number of shifting events for AU/AU+/AU++ transmissions during UDDS cycle

For UDDS runs, the total number of shifting events increases with increasing number of gears. However, for 10-speed transmissions, the total number of shifting events is similar to that of an 8-speed transmission, due to the implementation of gear-skipping methods.

Figure 262 shows the total number of shifting events for automatic (AU), automatic+ (Aup), and automatic++ (Aupp) transmissions with different numbers of gears during a US06 (high acceleration aggressive driving schedule) cycle.

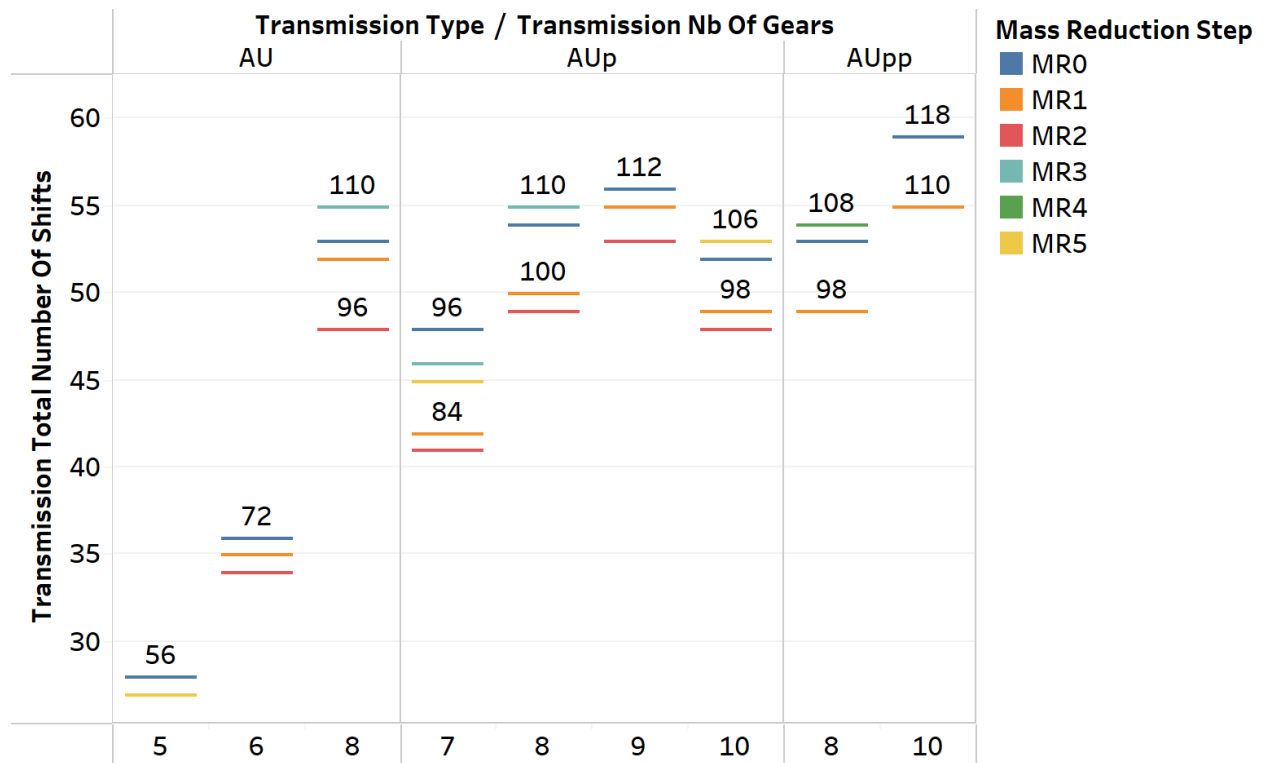


Figure 262. Total number of shifting events for AU/AU+/AU++ transmissions during US06 cycle

For US06 runs, the total number of shifting events increases with an increasing number of gears, except for 10-speed transmissions due to the implementation of gear-skipping methods. The total number of shifting events for US06 runs is lower than for UDDS runs.

Dual-Clutch Transmission Types

Figure 263 shows the total number of shifting events for DCTs with different numbers of gears during a UDDS cycle.

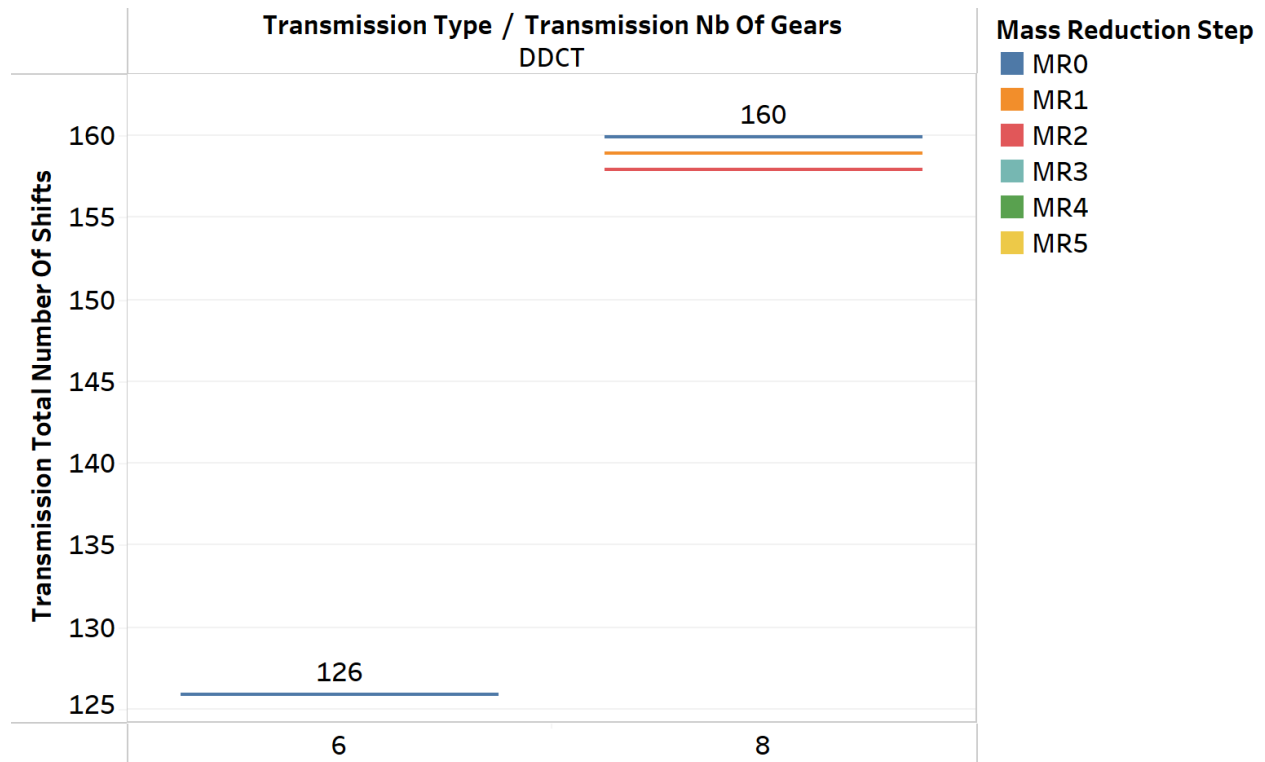


Figure 263. Total number of shifting events for DCTs during UDDS cycle

For DCT transmissions the total number of shifting events increases with an increasing number of gears in UDDS runs, as was observed for AU/DM transmission types.

Figure 264 shows the total number of shifting events for DCTs with different numbers of gears during a US06 cycle.

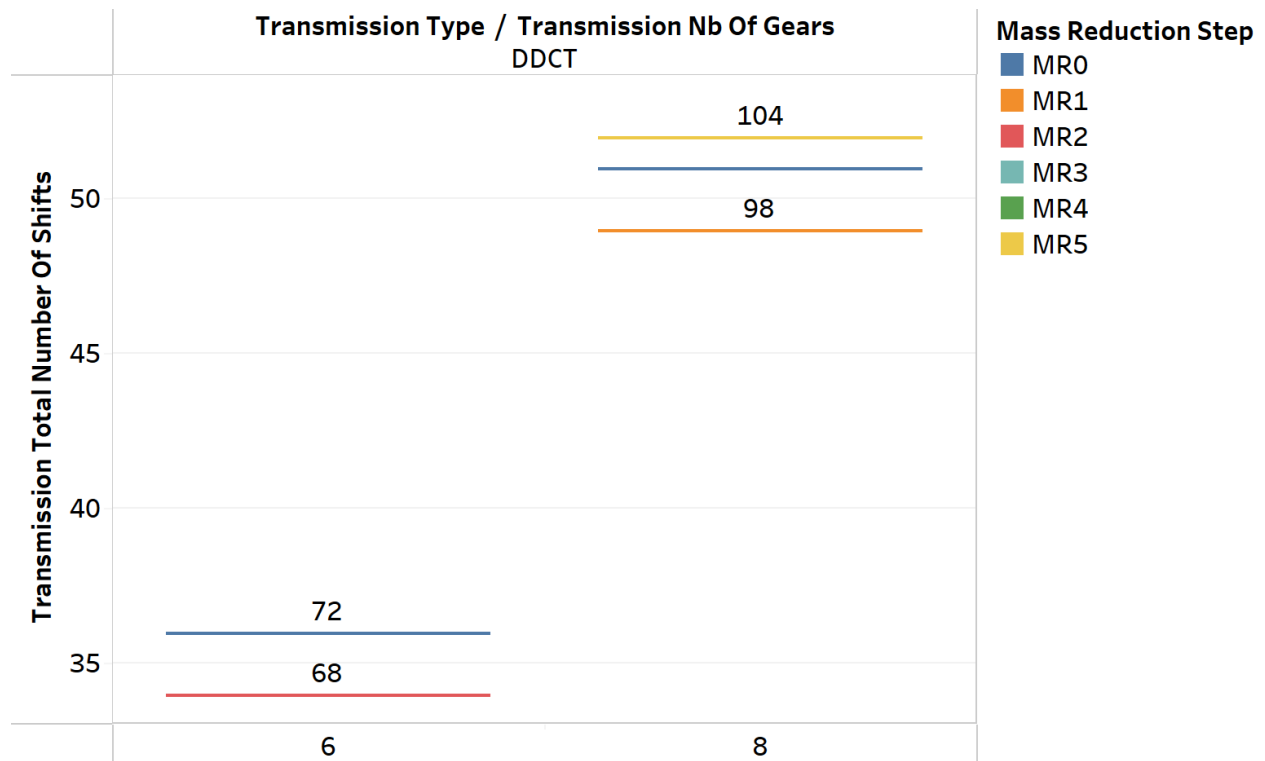


Figure 264. Total number of shifting events for DCTs during US06 cycle

Heavy-Duty Pickups and Vans

The total number of shifting events (upshift + downshift) determines the drive quality, so it is important to check the total number of shifting events across transmissions and numbers of gears against vehicle test data. Throughout this analysis process, the following vehicle was used

- Vehicle class: HD Class 2b
- Vehicle purpose: Van
- Vehicle powertrain: Conventional
- Engine: Engine 4a
- Aerodynamic drag reduction: AERO Level 0 (AERO0)
- Rolling-resistance reduction: ROLL Level 0 (ROLL0)

Figure 265 shows the total number of shifting events for automatic (AU) and automatic+ (Aup) transmissions with different numbers of gears during a UDDS cycle.

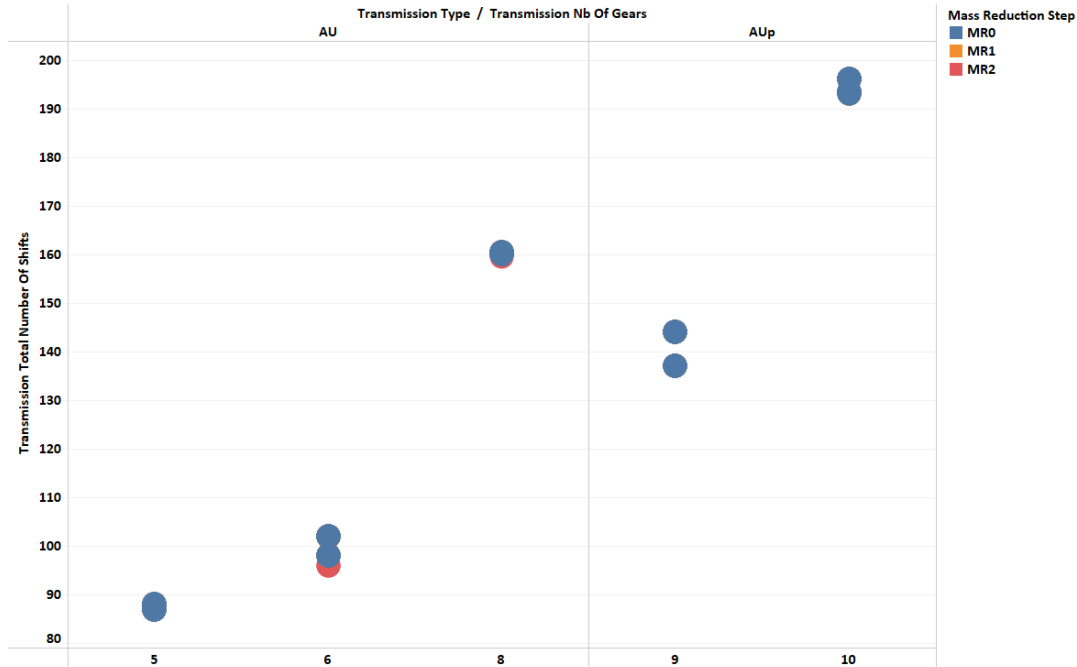


Figure 265. Total number of shifting events for AU/AU+ transmission during UDDS cycle

For UDDS runs, the total number of shifting events increases with increasing number of gears. However, for 9-speed transmissions, the total number of shifting events is smaller than that of an 8-speed transmission, due to the higher gear span of 8-speed transmissions.

Engine Power Inheritance Validation

Light-Duty Vehicle

As part of the vehicle inheritance validation, the engine power of the inherited vehicles was analyzed in comparison to baseline vehicles sized for the conventional powertrain. Figure 266 shows the engine power of the conventional vehicles in the compact vehicle class (non-performance category) in response to the MR step.

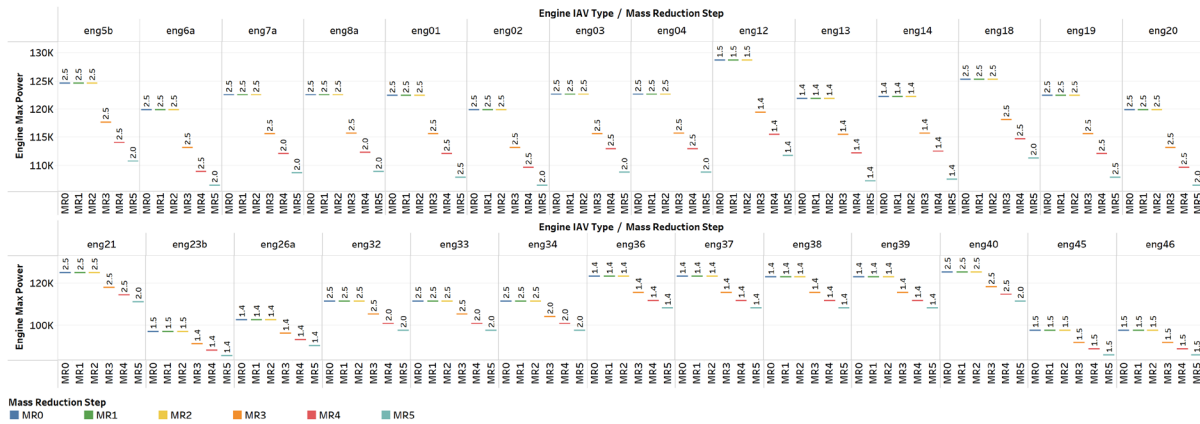


Figure 266. Engine power versus MR step (compact, non-performance)

Figure 267 shows the engine power of the conventional vehicles in the compact vehicle class (performance category) in response to the MR step.

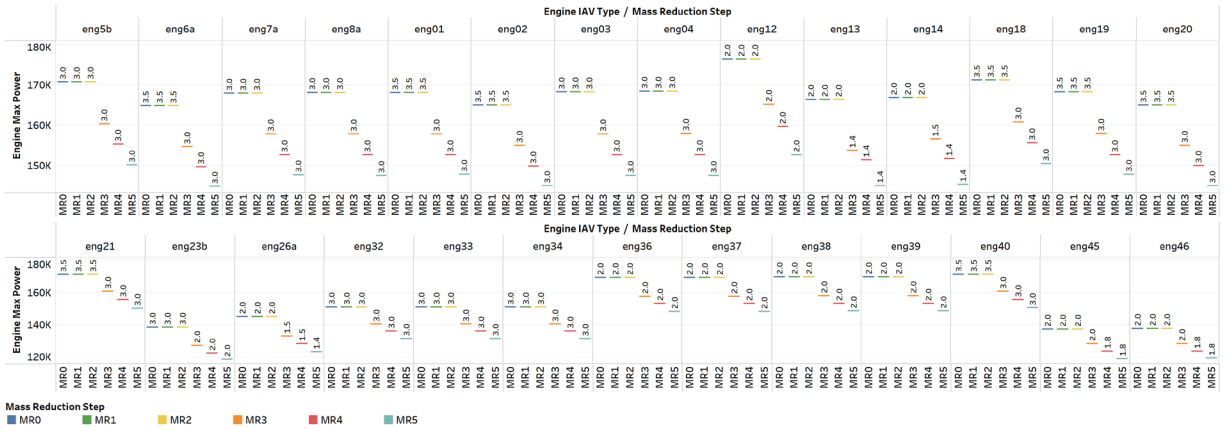


Figure 267. Engine power versus MR step (compact, performance)

Figure 268 shows the engine power of the conventional vehicles in the midsize vehicle class (non-performance category) in response to the MR step.

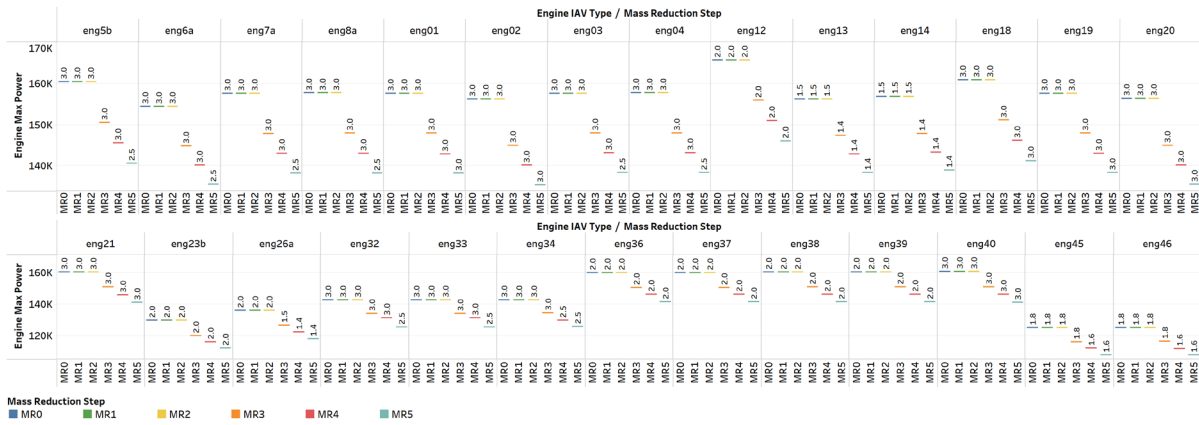


Figure 268. Engine power versus MR step (midsize, non-performance)

Figure 269 shows the engine power of the conventional vehicles in the midsize vehicle class (performance category) in response to the MR step.

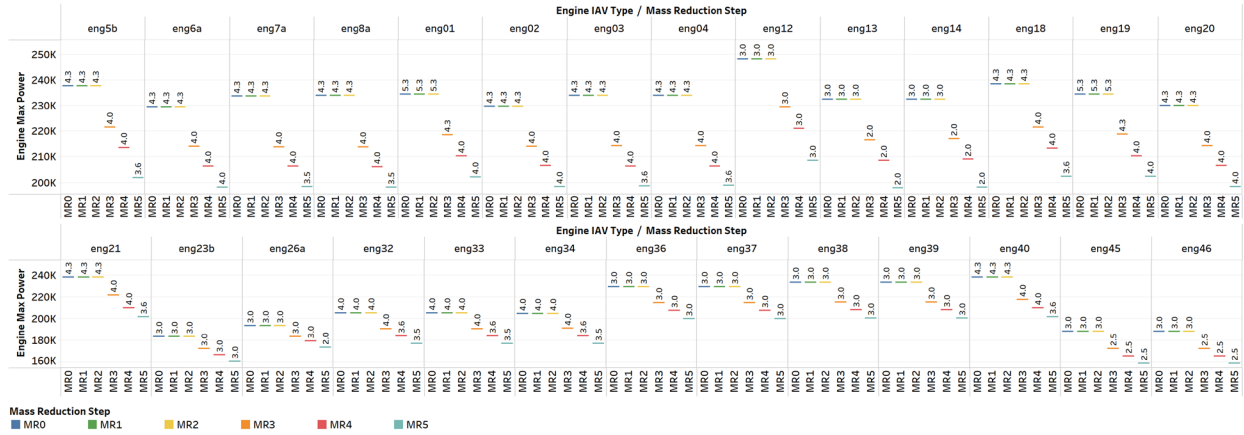


Figure 269. Engine power versus MR step (midsize, performance)

Figure 270 shows the engine power of the conventional vehicles in the small SUV vehicle class (non-performance category) in response to the MR step.

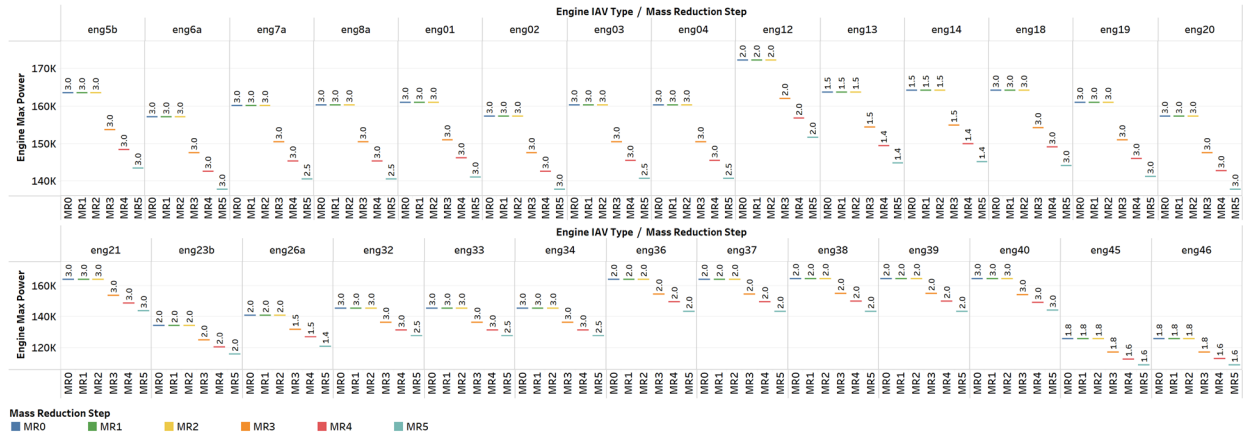


Figure 270. Engine power versus MR step (small SUV, non-performance)

Figure 271 shows the engine power of conventional vehicles in the small SUV vehicle class (performance category) in response to the MR step.

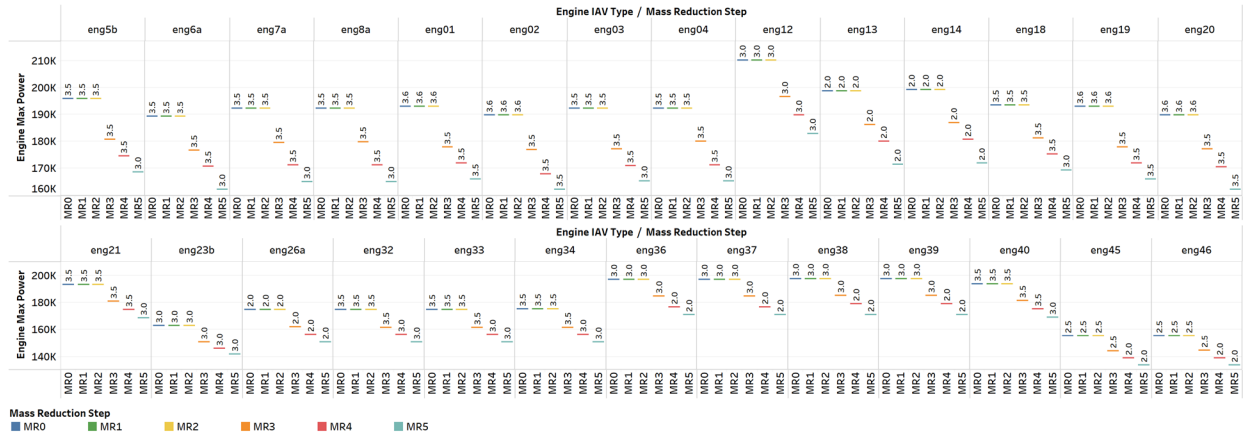


Figure 271. Engine power versus MR step (small SUV, performance)

Figure 272 shows the engine power of the conventional vehicles in the midsize SUV vehicle class (non-performance category) in response to the MR step.

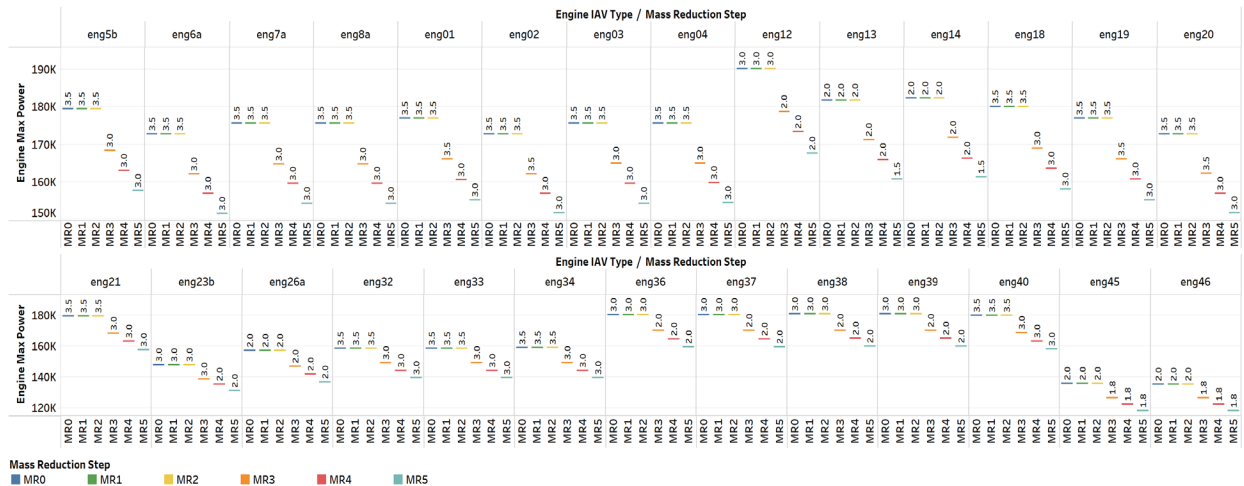


Figure 272. Engine power versus MR step (midsize SUV, non-performance)

Figure 273 shows the engine power of the conventional vehicles in the midsize SUV vehicle class (performance category) in response to the MR step.

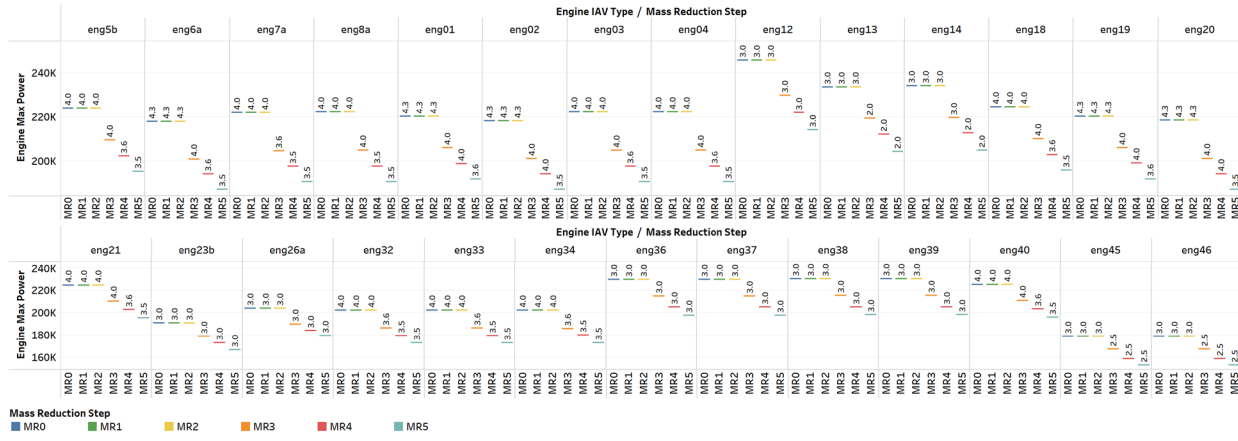


Figure 273. Engine power versus MR step (midsize SUV, performance)

Figure 274 shows the engine power of the conventional vehicles in the pickup vehicle class (performance category) in response to the MR step.

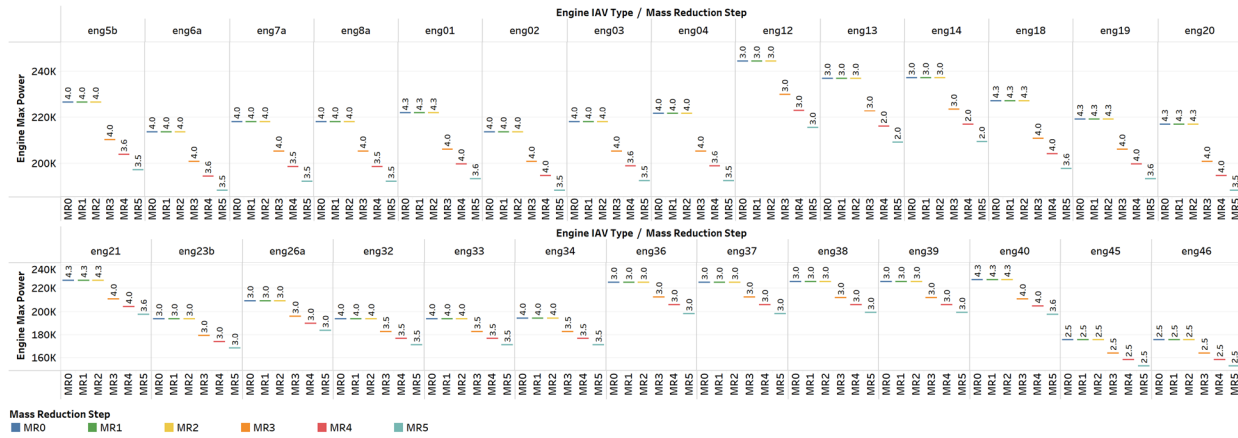


Figure 274. Engine power versus MR step (pickup, non-performance)

Figure 275 shows the engine power of conventional vehicles in the pickup class (performance category) in response to the MR step.

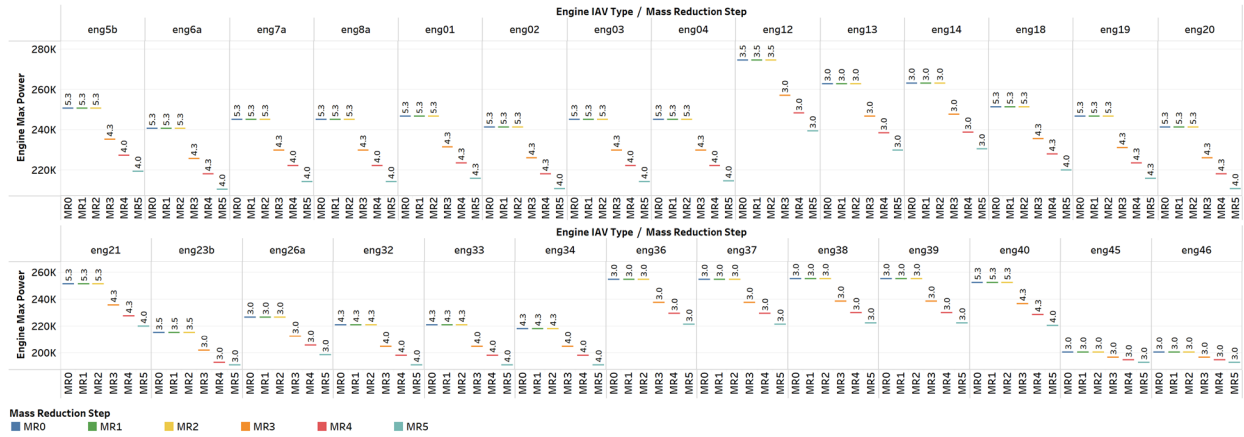


Figure 275. Engine power versus MR step (pickup, performance)

Heavy-Duty Pickups and Vans

As part of the vehicle inheritance validation, the engine power of the inherited vehicles was analyzed in comparison to baseline vehicles sized for the conventional powertrain. Figure 276 shows the engine power of the conventional, micro, and BISG HEVs in the HDV (Class 2b van) vehicle class in response to the powertrain type.

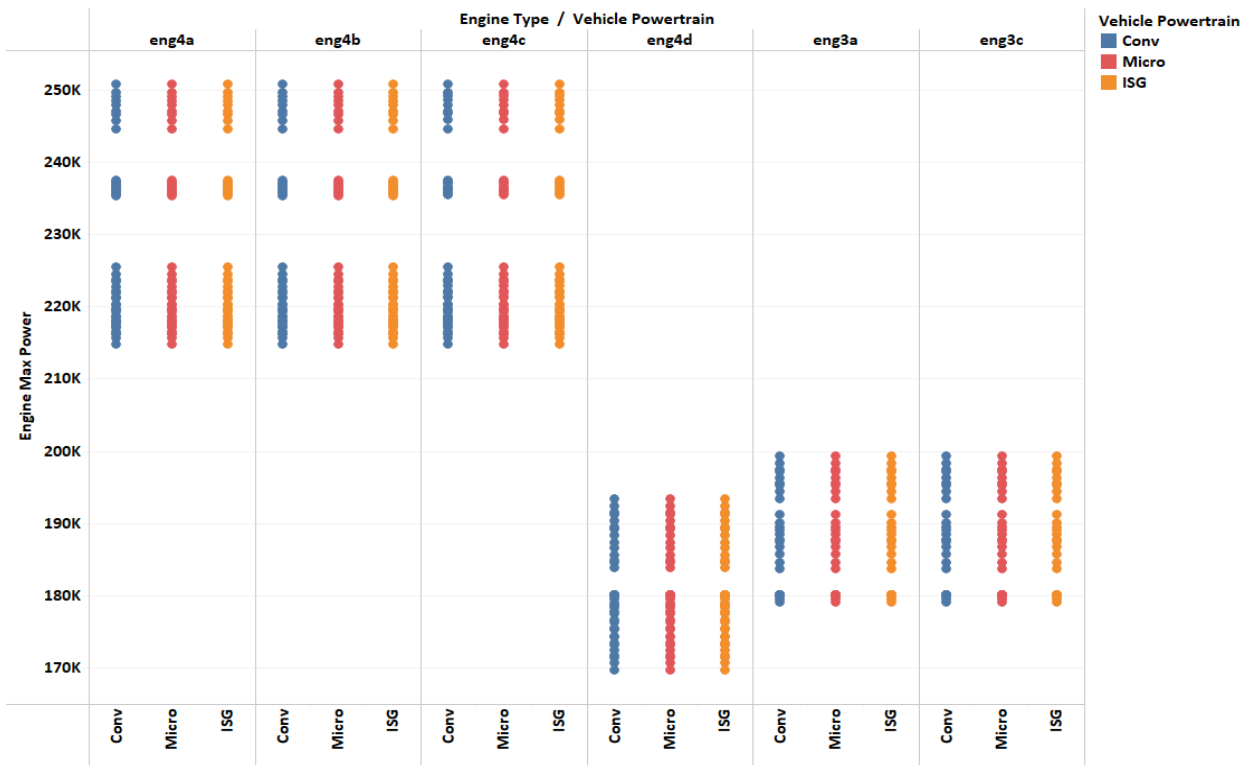


Figure 276. Engine power versus powertrain type (HDV Class 2b van)

Figure 277 shows the engine power of the conventional, micro, and BISG HEVs in the HDPU (Class 2b pickup) vehicle class in response to the powertrain type.

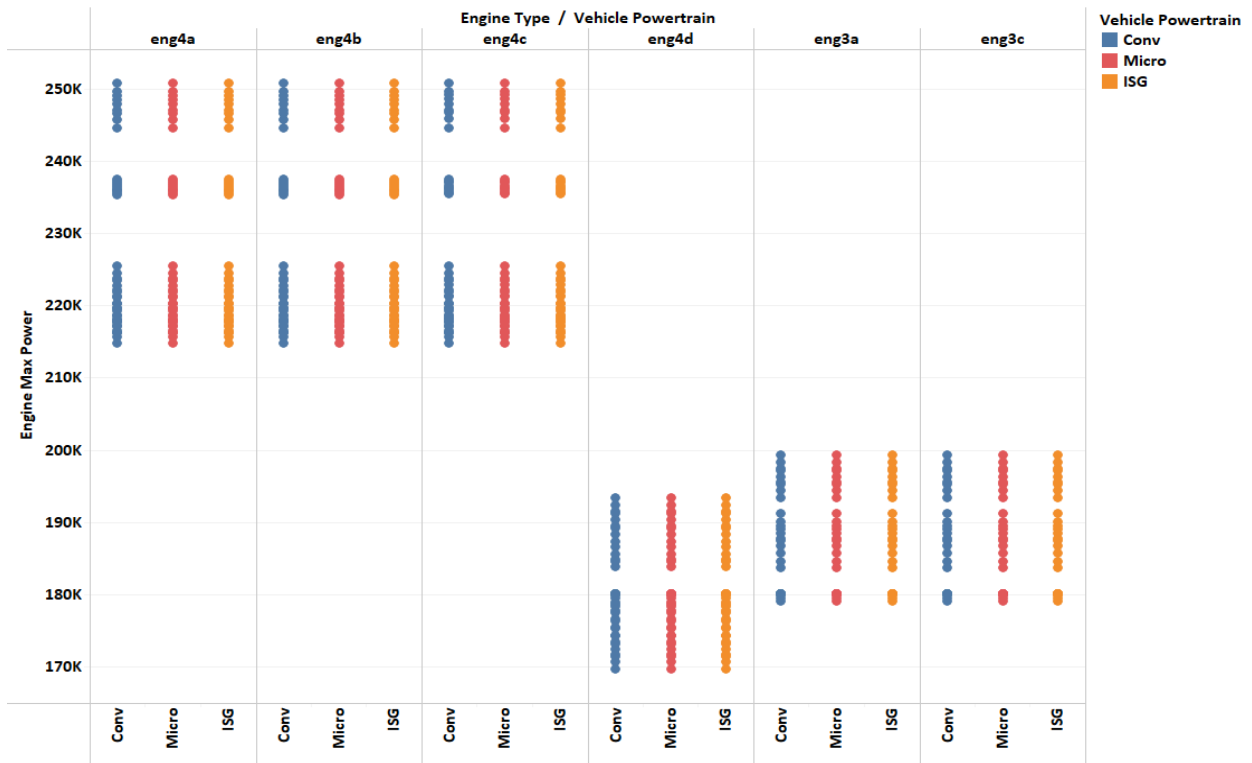


Figure 277. Engine power versus powertrain type (HDPU Class 2b pickup)

Figure 278 shows the engine power of the conventional, micro, and BISG HEVs in the HDV (Class 3 van) vehicle class in response to the powertrain type.

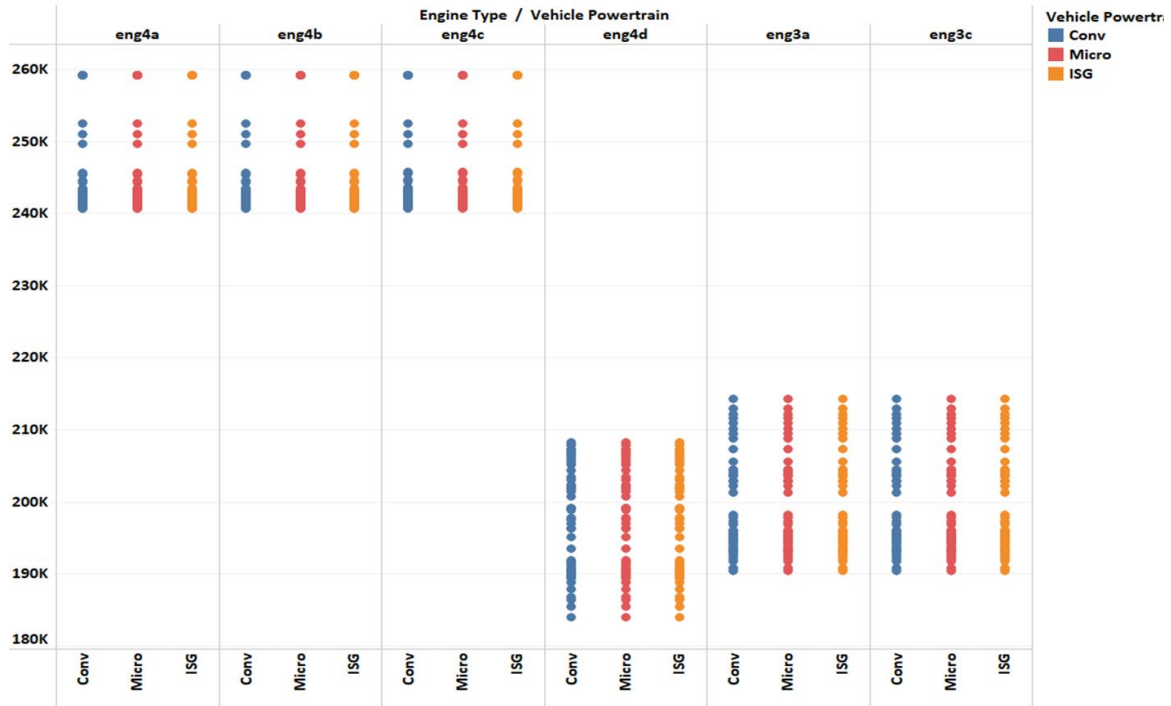


Figure 278. Engine power versus powertrain type (HDV Class 3 van)

Figure 279 shows the engine power of the conventional, micro, and BISG HEVs in the HDPU (Class 3 pickup) vehicle class in response to the powertrain type.

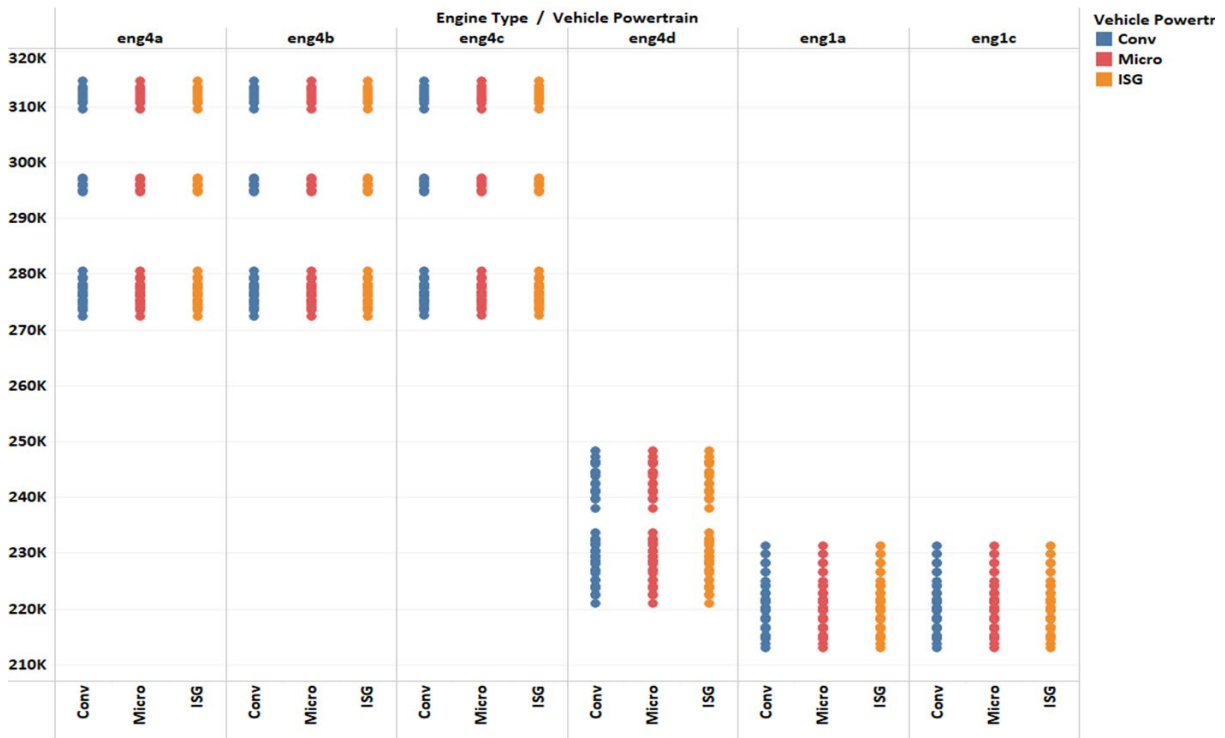


Figure 279. Engine power versus powertrain type (HDPU Class 3 pickup)

Machine Learning for Outlier Detection

A random sample consensus algorithm method validated the simulation results using machine learning. The technique involves iteratively estimating the parameters and best model that fit sufficiently many points (supposed inliers). Outliers will not fit the true model within some error (maximum deviation) attributed to the effect of noise.

For example, Figure 280 shows that most simulation values fit the model within the given confidence interval bands.

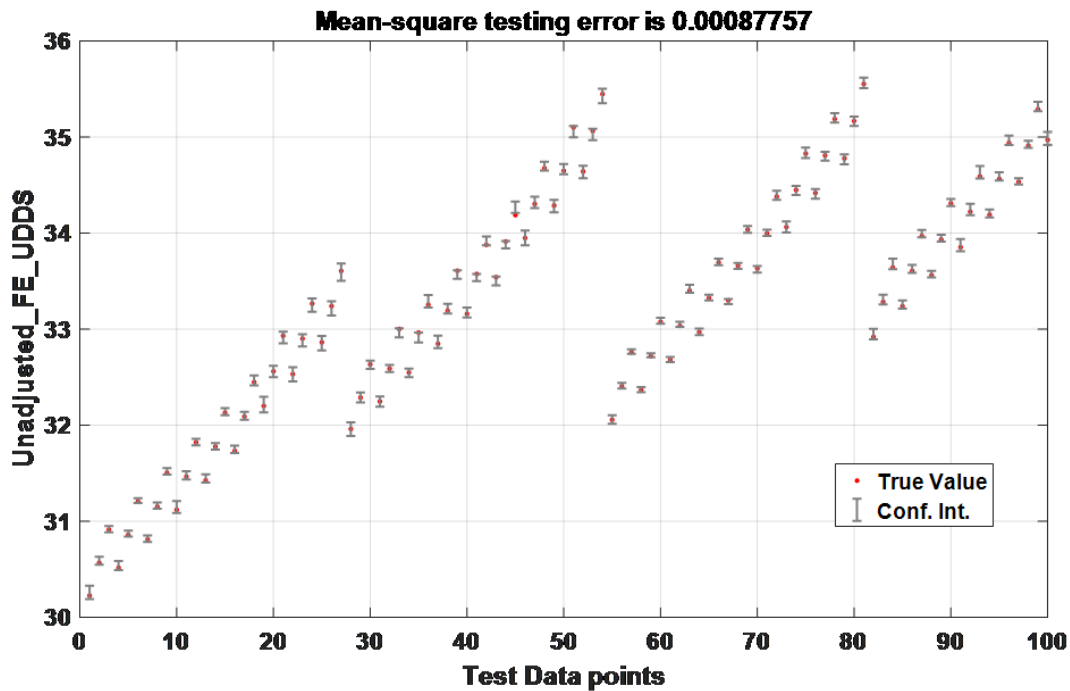


Figure 280. Confidence interval bands of simulation results

Figure 281 shows a situation where some engineering sense is required to conclude that the point detected by the RANSAC method to be an outlier is actually not an outlier. The RANSAC-generated model is a reasonable approximation of the simulation results.

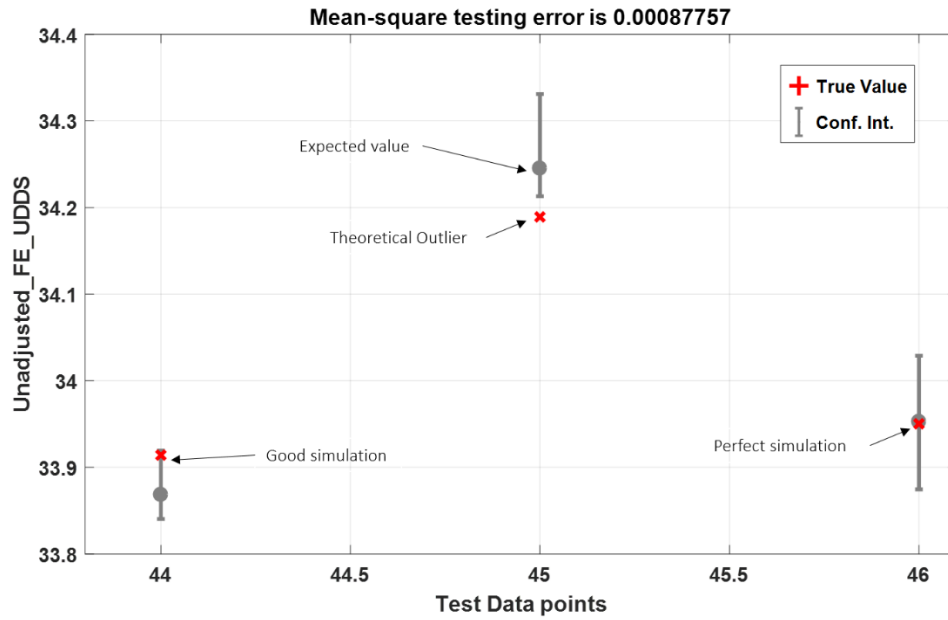


Figure 281. RANSAC validation method

Statistical Methods

Most statistical tests rely on the assumption of normality, so it is crucial to first determine whether the generated data is normally distributed. For results validation, the quantile-quantile plot is a simple way to graphically confirm whether the data comes from a normal distribution. Figure 282 shows the QQ plot of the simulation results.

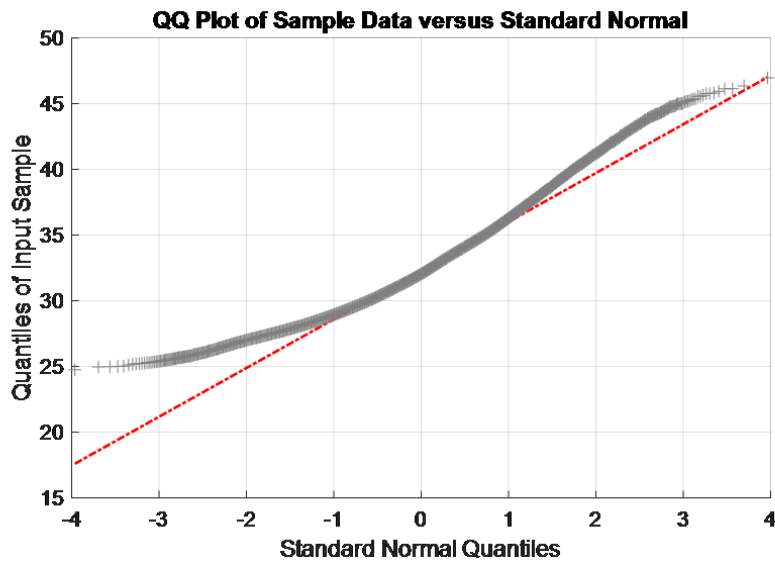


Figure 282. QQ plot to confirm the normal distribution of results

References

- Argonne National Laboratory. (n.d.). *Conventional vehicle testing: Downloadable dynamometer database (D3) testing results for vehicles that run on gasoline or diesel*. [Web page and portal]. www.anl.gov/taps/conventional-vehicle-testing
- Bonkoski, P., & Schilling, H. (2014, February 27). *ANL project final deliverables meeting. GT power study – BSFC maps of multiple engine concepts*. [PowerPoint]. IAV Automotive Engineering, Inc. www.nhtsa.gov/sites/nhtsa.gov/files/140227_anl_gtstudy-finaldelivery.pdf
- BorgWarner, Inc. (n.d.) *Explore our technologies HVH410-150 electric motor*. https://cdn.borgwarner.com/docs/default-source/event-downloads/iaa-cars/borgwarner-hvh410-150.pdf?sfvrsn=34e0153d_7
- Burress, T. (2012, May 9-13). *Benchmarking of competitive technologies*. 2011 U.S. DOE Hydrogen and Fuel Cells Program and Vehicle Technologies Program Annual Merit Review and Peer Evaluation Meeting, Washington, DC. www.energy.gov/sites/-prod/files/2014/03/f10/apec006_burress_2011_o.pdf
- Burress, T. A., Coomer, C. L., Campbell, S. L., Seiber, L. E., Marlino, L. D., Staunton, R. H., & Cunningham, J. P. (2008, April). *Evaluation of the 2007 Toyota Camry Hybrid synergy drive system*. Department of Energy, Office of Scientific and Technical Information. <https://doi.org/10.2172/928684>
- Duoba, M. (2009, May 18-22). *Argonne facilitation of PHEV standard testing procedure SAE J1711*. 2009 DOE Hydrogen Program and Vehicle Technologies Program Annual Merit Review and Peer Evaluation Meeting, Washington, DC.
- Ellies, B., Schenk, C., & Dekraker, P. (2016). *Benchmarking and hardware-in-the-loop operation of a 2014 MAZDA SkyActiv 2.0L 13:1 compression ratio engine* SAE Technical Paper 2016-01-1007). SAE International. <https://doi.org/10.4271/2016-01-1007>
- Environmental Protection Agency. (2023, January 17). *Annual certification data for vehicles, engines, and equipment*. [Web page and portal]. www.epa.gov/compliance-and-fuel-economy-data/annual-certification-data-vehicles-engines-and-equipment
- EPA. (2019a). *Benchmarking advanced low emission light-duty vehicle technology*. [Web page and portal, linking to 2013 GM 6T40 Transmission – Test Data Package – Dated 05-09-19]. www.epa.gov/vehicle-and-fuel-emissions-testing/benchmarking-advanced-low-emission-light-duty-vehicle-technology#test-data
- EPA. (2019b). *Benchmarking Advanced Low Emission Light-Duty Vehicle Technology*. [Web page and portal, linking to 2014 FCA HFE 845RE Transmission – Test Data Package – Dated 04-09-19]. www.epa.gov/vehicle-and-fuel-emissions-testing/benchmarking-advanced-low-emission-light-duty-vehicle-technology#test-data
- EPA. (2016). *Data on cars used for testing fuel economy*. [Web page and portal]. www.epa.gov/compliance-and-fuel-economy-data/data-cars-used-testing-fuel-economy
- EPA. (2016, November 28). *Process for generating engine fuel consumption map (Future Atkinson engine with cooled EGR and cylinder deactivation)*.

www.epa.gov/sites/production/files/2016-11/documents/procs-gen-eng-fuel-cons-map-fut-atkinson-eng.pdf

- EPA & National Highway Traffic Safety Administration. (2016). *Greenhouse gas emissions and fuel efficiency standards for medium- and heavy-duty engines and vehicles phase 2 – Regulatory Impact Analysis* (Report No. EPA-420-R-16-900).
- GM Authority. (n.d.) General Motors Voltec technology. [Web page]. <https://gmauthority.com/blog/gm/general-motors-technology/gm-electric-vehicle-technology/general-motors-voltec-technology/>
- IAV Automotive Engineering, Inc. (2016). *Responses and updates to IAV engine maps*.
- Ide, T., Udagawa, A., & Kataoka, R. (1995). Simulation approach to the effect of the ratio changing speed of a metal V-belt CVT on the vehicle response. *Vehicle System Dynamics*, 24(4–5), 377–388. <https://doi.org/10.1080/00423119508969098>
- Islam, E. S., Moawad, A., Kim, N., & Rousseau, A. (2020). *Energy consumption and cost reduction of future light-duty vehicles through advanced vehicle technologies: A modeling simulation study through 2050*. Department of Energy, Office of Scientific and Technical Information. <https://doi.org/10.2172/1647165>
- Jeong, J., Kim, N., Stutenberg, K., & Rousseau, A. (2019). *Analysis and model validation of the Toyota Prius Prime* (Technical Paper 2019-01-0369). SAE International. <https://doi.org/10.4271/2019-01-0369>
- Jeong, J., Lee, W., Kim, N., Stutenberg, K., & Rousseau, A. (2017). *Control analysis and model validation for BMW i3 range extender* (Technical Paper 2017-01-1152). SAE International. <https://doi.org/10.4271/2017-01-1152>
- Kim, N., Lohse-Busch, H., & Rousseau, A. (2014). Development of a model of the dual clutch transmission in Autonomie and validation with dynamometer test data. *International Journal of Automotive Technology*, 15, 263–271. <http://dx.doi.org/10.1007/s12239-014-0027-5>
- Kim, N., Rousseau, A., & Lohse-Busch, H. (2014). *Advanced automatic transmission model validation using dynamometer test data* (Technical Paper 2014-01-1778). SAE International. <https://doi.org/10.4271/2014-01-1778>
- Kim, N., Choi, S., Jeong, J., Vijayagopal, R., Stutenberg, K., & Rousseau, A. (2018). Vehicle level control analysis for Voltec powertrain. *World Electric Vehicle Journal*, 9(2), 29. <http://dx.doi.org/10.3390/wevj9020029>
- Lohse-Busch, H., Stutenberg, K., Iliev, S., & Duoba, M. (2018). *Laboratory testing of a 2017 Ford F-150 3.5L V6 EcoBoost with a 10-speed transmission* (Report No. DOT HS 812 520). National Highway Traffic Safety Administration. www.nhtsa.gov/sites/nhtsa.gov/files/documents/812520.pdf
- Miller, M., Holmes, A., Conlon, B., & Savagian, P. (2011). The GM Voltec 4ET50 multi-mode electric transaxle. *SAE International Journal of Engines*, 4(1), 1102–1114. <https://doi.org/10.4271/2011-01-0887>

- Meng, Y., Jennings, M., Tsou, P., Brigham, D., Bell, D., & Soto, C. (2011). Test correlation framework for hybrid electric vehicle system model. *SAE International Journal Engines*, 4(1),1046–1057. <https://doi.org/10.4271/2011-01-0881>
- Momen, F., Rahman, K., Son, Y., & Savagian, P. (2016, September 18-22). *Electrical propulsion system design of Chevrolet Bolt battery electric vehicle*. 2016 IEEE Energy Conversion Congress and Exposition, Milwaukee, WI. <https://doi.org/10.1109/ECCE.2016.7855076>
- National Highway Traffic Safety Administration. (2016). Transmission data reporting summary.
- Olszewski, M. (2011). *Oak Ridge National Laboratory annual progress report for the power electronics and electric machinery program*. Department of Transportation, Office of Scientific and Technical Information. <https://doi.org/10.2172/921775>
- Pachernegg, S. (1969, February 1). *A closer look at the Willans-Line* (Technical Paper 690182). SAE International. <https://doi.org/10.4271/690182>
- Padgett, E., & Kleen, G. (2020, October 2). *Automotive fuel cell targets and status* (Record No. 20005). U.S. Department of Energy. www.hydrogen.energy.gov/pdfs/20005-automotive-fuel-cell-targets-status.pdf
- Pasquier, M., Duoba, M. & Rousseau, A. (2001, October 20-24). *Validating simulation tools for vehicle system studies using advanced control and testing procedure*. 18th International Electric Vehicle Symposium EVS18, Berlin. www.autonomie.net/docs/6%20-%20Papers/Validation/validating_simulation_tools.pdf
- SAE International. (2017). *Battery electric vehicle energy consumption and range test procedure J1634_202104*. www.sae.org/standards/content/j1634_202104/
- Son, H., Kim, N., Ko, S., Rousseau, A., & Kim, H. (2015). Development of performance simulator for a HEV with CVT and validation with dynamometer test data. *World Electric Vehicle Journal*, 7(2), 270–277. <http://dx.doi.org/10.3390/wevj7020270>
- Stuhldreher, M. (2016). *Fuel efficiency mapping of a 2014 6-cylinder GM EcoTec 4.3L engine with cylinder deactivation* (Technical Paper 2016-01-0662). SAE International. <https://doi.org/10.4271/2016-01-0662>
- Reinhart, T. E.. (2022, May 6). *Engine efficiency technology study* (SwRI Project No. 03.26457, Revision 1). Argonne National Laboratory. <https://anl.app.box.com/s/nkfasyvmpzituxjx2ntsj2f40iloznzu>
- USCAR Transmission Working Group. (2015). *Inputs to U.S. DRIVE target setting process*.
- van der Sluis, F., van Dongen, T., van Spijk, G., van der velde, A., & van Heeswijk, A. (2007). *Efficiency optimization of the pushbelt CVT*. SAE Technical Paper 2007-01-1457. <https://doi.org/10.4271/2007-01-1457>
- Wileman, C. (2021). *Light-duty vehicle transmission benchmarking, 2017 Ford F-150 with 10R80 and 2018 Honda Accord with Earth Dreams CVT* (Report No. DOT HS 813 163). National Highway Traffic Safety Administration. https://downloads.regulations.gov/NHTSA-2021-0053-0003/attachment_5.pdf

DOT HS 813 431
July 2023



U.S. Department
of Transportation
**National Highway
Traffic Safety
Administration**

